Exploring Holocene Lake Palaeoclimatic records in the Maya Northern Highlands and the central Mayab

Haydar Benyacub Martinez Izquierdo Dyrzo, BChem., MEarthSci.

Thesis submitted to The University of Nottingham

For the degree of Doctor of Philosophy

August, 2021

Approximate word count (excluding references): 82,000 words

This page intentionally left blank

Abstract

The environmental history of the Maya attracts attention since climate changes appear to be linked with the management of resources and, in particular, with the collapse of their civilisation at the end of the Mesoamerican Classic period, (1140-1040 B. P), when, according to palaeorecords from the region, such as lake sediments and speleothems, a series of droughts occurred. However, attention has been focused mostly on the central lowlands and northern Mayab (but barely in the Highlands and other areas) where ca. seventy records have played an important role in our understanding of climate change and the role of drought in societal change, including the Maya Collapse. This includes some stable isotope records, in particular, $\delta^{18}O$ from lake sediments and speleothems as proxies of water balance and precipitation amount, respectively. The most emblematic record comes from Lake Chichancanab, whose sediments contain gypsum deposits at specific points indicating the existence of droughts during crucial moments in Mayan history (e. g. The Maya Abandonment at 1200 years B. P. and the Maya Collapse from 1190 to 1040 B. P). In this thesis, research involves lake core sediments obtained both in the lowlands and the highlands.

First, an isotopic record on bulk carbonate for a site in the highlands (over 1000 m.a.s.l.) was obtained from a sediment core from Lake San Lorenzo in the Lagunas de Montebello Lake Complex. In addition, a density record was developed as well as a record based on the organics, carbonate, and residual content of the loss on ignition. Today, Lake San Lorenzo is hydrologically open. The isotope record $\delta^{18}O$ in Lake San Lorenzo is a proxy of summer rainfall amount, indicating that the lake has always been hydrologically open. Episodes of major organic production appeared after periods when the surroundings were very densely populated, according to Franco Gaviria et al. (2018). Changes in the sedimentation rate through the record, including the abrupt change after 610 – 553 years B. P., as well as changes in the vegetation, are in part linked with changes in the summer rainfall amount but might also be driven by changes in the land use during the Colonial period.

Second, core sediments collected from Lake Esmeralda, a sister lake of Chichancanab, are studied in the lowlands. Isotopic analysis of waters and modern gastropods (family Hydrobiidae) from both lakes (Chichancanab and Esmeralda) were studied, showing that L. Esmeralda is today a more open basin in comparison to L. Chichancanab but still shows an important evaporative effect.

Samples for isotope analyses based on shells of gastropods (*Pyrgophorus coronatus*, family Hydrobiidae) from Holocene aged sediments from Lake Esmeralda were compared with the isotopic composition of samples of carbonate bulk sediment for assessing the quality of the

environmental signal recovered from them. Overall both records should be very similar patterns. Therefore, a complete isotope record based on sieved sediment samples was used as a proxy of effective rainfall (water balance) in Lake Esmeralda (due to its lower cost).

Results based on a multiproxy approach ($CaCO_3$ content, organic content, loss on ignition residuals content, the isotopic composition of bulk sediments, elemental abundance, elemental ratios, density, grey and colour scale) on a sediment core dated by radiocarbon suggest that Lake Esmeralda's sediments are predominantly made up of carbonates from 6500 to 3400 B. P. Lake Esmeralda became a more closed system, after ca. 4200 B. P. After 2500 B. P., there appears to be a further tendency to be a close system. Lake Esmeralda has become more organic-rich in the last 2500 years B. P. This coincides with periods when the human population across the Mayab turned to permanent settlement and developed urban centres. However, settlements (Shaw, 2000) and human impact on vegetation (Bermingham, 2020) near Lake Esmeralda existed practically only during the years of the Terminal Classic Horizon (950 years B. P.), suggesting an increase of the organics in the lake without major direct human disturbance. There is clear evidence for a dramatically increased organic amount in sediments from Lake Esmeralda, mostly produced outside the lake due to the loss of soil cover, during the critical moments of the Maya History, e. g. Maya Abandonment (1800 to 1750 years B. P.), the Maya Hiatus (1360 years B. P) and the Maya Collapse (1190 to 1040 years B. P.) at moments when the $\delta^{18}O$ and the K/Sr show dry periods (at 1140 to 1040 years B. P.). No evidence of gypsum deposit was found before the drought at 167 years B. P., indicating a different catchment and chemistry of Lake Esmeralda compared to Chichancanab.

Finally, records of Lake Esmeralda and Lake San Lorenzo were compared, showing that in both lakes, the terrigenous intake is associated with the rainfall. But in Lake San Lorenzo, this process might also be linked with the erosion enhanced by the abandonment of agriculture. Besides, the $CaCO_3$ precipitation is autogenic in both lakes, but such precipitation increases during dry periods in Lake San Lorenzo, whilst it decreases during dry periods in Lake Esmeralda. An opposite tendency in the hydrobalance at the millennial-scale to the lowlands happens in Lake San Lorenzo, in comparison to Lake Esmeralda. However, at decadal scale, the presence of recurrent droughts as it is registered in Esmeralda is still observed in San Lorenzo, indicating that the droughts during the critical moments of the Maya History were meteorological droughts.

To Dad and Mom

This page intentionally left blank

Contents

List of figures

List of Tables

List of Photos

"Sometimes the rain arrives for cleaning the wounds.
Sometimes only a drop can overcome the drought."
Vivir mi vida, Marc Anthony. 2012

This page intentionally left blank

Preface

"Mexico is a country of inequality.
Nowhere does there exist such
a fearful difference in the distribution
of fortune, civilisation.
cultivation of the soil, and population."
Alexander von Humboldt, 1822

It has been ten years since I have been dealing with a question in my head, how did the Maya collapse happen? This question took me to travel across four continents, and to live in four different countries in Europe. It was clear at the beginning of this journey that my background in chemistry, geology and psychology would not be enough to understand the complexity that the probable answer to this question needed. Therefore, studying a little of archaeology and geography was compulsory. Soon, trying to understand the ancient Maya took me into the deep question of who I am, what makes us human, how do humans change their environment and their way of living? And how the environment can influence humans from their personality to their culture?

I do not remember the first time that I heard about the Maya. Surely, I was a little child. I remember then being conscious that the Aztecs and the Nahua people, in general, were my ancestors. Because this, I have always had perhaps more admiration for Nahuas, even thought I have learnt to admire all Mesoamerican cultures, including the Maya. But my first memory about Maya was the jade mask of the Ahau (King) K'inich Janaab Pakal, which was stolen at that time from the Museo de Antropología e Historia. It was when I was 12 years old when I had to participate in a festival of indigenous cultures when I had to present about the Lacandons, who were hunter-gatherers in the moist forest near to the Guatemalan- Mexican Border. They were few. But their life was so different. They had Maya heritage, and they had forgotten who the ancient Maya were. Then, it happened the unimaginable, when I was 14 years a rebellion composed by Tzetzals, Tzotziles, Tojolabals, Choles, and Mames (people of Maya heritage) and Zoques (people of Olmec heritage) threated the Mexican Government and the new North American Agreement. For a teenager, rebels are always attractive. In the middle of the turbulence of those years, the rebellion pointed out to me that people have had an interest in protecting the Lacandons. Meanwhile, nobody cared about the other Maya people. But the Maya were so far for me. Not until high school did I learn about Caneek and his rebellion in the XVII century. It looked that the Maya have always rebelled. I never was in the Maya Cultural Area before

becoming an adult. I did not have real awareness of the drama that the Maya civilisation suffered until I finished my master's degree in geochemistry. That time I was involved in palaeoclimatology studies when Prof. Gerald Haug was the most famous palaeoclimatologist, and his record from Cariaco was presented as a proof of a climate change during the time of the Maya Collapse.

This thesis is a personal voyage involving one of the most challenging mysteries in human history. The Maya civilisation presents still many questions, but perhaps the most important is the abrupt change of life that they suffered twelve centuries ago.

We have to remember that the Maya cosmovision was very different from our daily conceptions and preconceptions in the western civilisation. Even for me, a Mexican of Nahua and Chichimec heritage, the western civilisation cosmovision is more familiar than the Maya cosmovision of time, spirituality, economy, love, sacrifice, social values and perception of death and life. As an example, war was never undertaken at night in Mesoamerica, and war was performed in a specific season of the year. This is the difficulty when studying a Mesoamerican civilisation; reminding ourselves how different they were.

Another example is that the political cargo systems used between the Maya and other Mesoamericans, was very different from the political and economic systems surged after the French revolution in the western civilisation. This system still survives. In the cargo system, also known as the civil-religious hierarchy, "fiesta" or "mayordomía" system, a collection of secular and religious positions are held by men or households in rural Amerindian communities. These revolving offices, or "cargos", become the unpaid responsibility of men who are active in civic life. They typically hold a given post for a term of one year, and alternate between civic and religious obligations from year to year. Officeholders execute most of the tasks of local governments and churches. In this economy system, merchandise and services are interchanged without transferring money as gifts or favours, where the officeholders have to cover the expenses of the whole population during civic or religious celebrations. This "collective" societal organization might have a role in how ancient Mayas interact with nature.

Concerning religion, the belief that God can give himself as rain, shows in one of the most beautiful human perceptions the value that rain had for Mesoamericans. In this way, the biggest pyramid during the Classic Horizon in Mesoamerica (the pyramid of the Sun in Teotihuacan) was actually dedicated to the God of Rain. For this reason, also, the ancient Maya called God as the "One, whose name is said sighing", thinking in rainfall.

This year is also the 500 anniversary of the first contacts between the Spanish expedition of Hernan Cortes and the Maya people and other Mesoamerican people, which finished with the fall of the Aztec capital city Tenochtitlan, and the surrender of many cities across Mesoamerica, Oasiaamerica and Aridoamerica (USA Archaeological Southwest Area) during the XVI century. Therefore, this is the right moment to look back and remember how life was in the Americas, how the world changed after that, how fair was the balcanization of the Maya Cultural Area by the Spanish and British Empires in three different countries, what is our connection with the past and which debts still exist with the original native people of the Americas. To study how climate impacted society is only an excuse for studying the environmental history of not only the Maya, but of all the people from Mesoamerica, Aridoamerica and Oasisameica, whose ancient people compose the ancestors of Native Americans of today's Mexico, USA and Central American nations as well as the ancestors of whom we identified as Mestizos. (For example, according to my genetics analysis, I am around 70 % Mesoamerican, 20 % Eurasian and 10 % African. This is just as an example of how critical the world migrations into the Americas were).

I focus on the Maya because this is the only civilisation in Mesoamerica whose script has been deciphered. We know more about the Maya than other ancient native people in Mexico because of that. But, you do not think for a minute that when I am studying the Maya, I do not recall the Ñuu Dzahui people (Mixtecs), the Ben' Zaa (Zapotecs), the Totonacs, the Nahuas, the Purepecha, the Soctona(Chiapanec), the Mazahua (Toltecs), the Otomi (Olmecs), the Teenek as well as the other peoples in Aridoamerica and Oasisamerica; the Mayo, the Raramuri (Tarahumara), the Wixarikas (Huichols), the Xi'ui (Pames), the Naayeri (Coras), the Inde (Apaches), the Zacatecs, the Tepecans, the Caxcans, the Guamares, and the Tecuees. I am pretty sure, that someday when scientific research will not be restricted by the financial support of grants, we will be able to do the environmental reconstruction of the sites occupied by these people, which currently have attracted less attention than the Maya, although numerous scientific studies have been done concerning to the environmental stories of the sites of these people.

After working and studying archaeological sciences in Germany, (I promise someday I will graduate). I got the privilege to study at the University of Nottingham under the supervision of Prof. Sarah E. Metcalfe and Prof. Matthew D. Jones, whose guidance really enlightened my path. This research took more than four years from my first travel in the shoreline of Lake Chichancanab until writing the last sentence of this document

As Humboldt said before, Mexico is still today in terms of fortune and richness distribution, unfortunately, a land of inequality. Two hundred years have passed, and we still struggle with that. Shame on us. But concerning the inequality of civilisation, soil cultivation and population, where he observed inequality, I see diversity. This diversity make us rich and proud. (Mexico is perhaps the most diverse land after China, India and Papua New Guinea in terms of cultural landscapes). This diversity took me to study two different sites inside the Maya Cultural Area, whose contrast allows us to assess the differences in the relationship between humans and the environment. The chosen sites are Lake Esmeralda in the Cochuah Region in central Mayab and Lake San Lorenzo in the Lagunas De Montebello Lake Complex in the Northern Maya Highlands.

Another aspect to consider for this thesis is that studies of human and cultural activities present the same problems of objectivity as history and anthropology. For instance, historians readily acknowledge that their perspectives prevent them from ever objectively reconstructing historical events. Similar arguments are applied to the study of environmental history. Although many pieces of evidence speak for themselves, the reconstructed environmental history after linking the different studied samples and variables have almost always a considerable amount of interpretation. Cognitive bias can always be present.

This thesis must meet the rigours of the scientific community, but it also must take into account the reputation of the humans that were settled in the Maya Cultural Area. If we concluded at the end of our studies that the human impact in our sites was important and drove the Maya Classic Collapse in our sites, we would label the Mayan as barbarians. In contrast, it exists the danger to portrait them as beings filled with wisdom if we conclude that they knew how to manage the environment. Even though in this thesis, we do not conduct studies that involve interaction with the modern Maya, any label on their ancestors will emphasis a stereotype of them. The first key to avoid this predicament is to remember that in 4000 years of Maya History, they were not always the same in all the times and all the places, as well as the surrounding environments, was not the same. The second key is to use the parsimony principle known as the Occam's razor during the interpretations. This principle implies that if any phenomenon or observation can be explained without the intervention of humans, it must be explained in that way.

I hope this research contributes to the around 70 palaeoenvironmental studies performed in the Maya Cultural Area, and to the environmental studies performed in the rest of

Mexico. I also hope they contribute to the Maya civilisation studies in general. Luckily, this work will be useful for both palaeoclimatologists and environmental archaeologists. This thesis will not answer definitely how the Maya Collapse happened, but it gives interesting data that will be useful for continuing the discussion on this topic.

Because this research was performed searching to reach a Ph. D. degree, the views, interpretations and conclusions in this thesis are my sole responsibility. Although in scientific literature, where Newton's impersonal view has prevailed for centuries, passive voice is recommended, I write many times in this thesis using the active voice, following the advice of the Metamodel of language precision in Neurolinguistic Programming. I know, saying "I "sounds quite pretentious, I apologise for that.

I also decided to use the Maya ancient names deciphered using epigraphy for sites and historical characters when they are available instead of the common name, e. g. Mutul instead Tikal. But the common name is still given in brackets. I also refer normally as Chichancanab instead Lake Chichancanab, since k'aak'naab means sea or lake.

In this thesis I use "years Before Present (B. P.)" (where the present is 1950) as a time scale for most of the dates with exception of dates in the Modern Era (ca. last 300 years) which are given in the Gregorian calendar. In some occasions some relevant dates are written in both time scales, and few dates are also given in the Maya long count calendar.

Before every chapter, a photo and a famous quote are presented as an artistic way to prepare our mind for the chapter. This is a method used in pedagogy called "previous idea". All photos were taken by me, except the photo at Lake Esmeralda taken by the crew of the University of Nottingham, the photo of Chinkultic downloaded from the travel blog of cityexpress.com (dedicated to the touristic sites of Latin-American), the 1842 Catherwood map, which is in the public domain and can be downloaded from the web page of the Reed College at Oregon, USA and the photo of the Loltun Cave taken by Alexei Genova. Their description is at the foot of them.

This thesis would never have been possible without the support of the Consejo Nacional de Ciencia y Tecnologia CONACYT from the United Mexican States and the scholarship 440756 granted to me for studying abroad, which covered 62% of my fees and expenses for 35 months, including two granted extensions. I am also very thankful for the 30% discount on the fees offered by the University of Nottingham.

I also have a very special thanks to Prof. Melanie Leng, whose invaluable support during the isotopes analyses is the core of this research. I am also very thankful for the people at the British Geological Survey (BGS) that helped me performing the isotope analysis. I thank especially to the chemist Robert D. Burton, who conducted the bulk carbonate analysis.

I am very thankful to Prof Sarah J. Davies for her support and help during the XRF analysis of the cores from lake Esmeralda at Aberystwyth University. I also thank Dr Dai Anthony Grady at Aberystwyth University for his help during the signal processing of this analysis.

I am also thankful to Dr Suzanne Maclachlan, Dr Miros S. J. Charidemou and their team at the British Ocean Sediment Core Research Facility, BOSCORF, for conducting the attenuated Gamma radiation and colour analyses as well as for obtaining the images of the cores collected from Lake Esmeralda.

I thank Dr Luz Maria Cisneros-Dozal at the Radiocarbon Facility of the Natural Environment Research Council, NERC, for conducting the radiocarbon analyses of the samples obtained from sediments from Lake Esmeralda.

This thesis would have also been impossible without help during the fieldwork of the MSc. Roger Medina Gonzales and the Biol. Samuel Calderon from the Universidad Autónoma de Yucatán, UADY.

I am greatly indebted to Dr Alexander Correa Metrio and Dr Felipe Franco Gaviria of the Universidad Nacional Autónoma de México, UNAM for helping us in getting material from Lake San Lorenzo and their help during the research related to Lake San Lorenzo. I am also grateful with Dr Edna Naranjo from UNAM for her invaluable help in the taxonomy of the gastropods studied in this thesis.

My eternal gratitude with the staff of the School of Geography. I am especially in debt to the chemist Teresa Needham, for all the support and discipline in the labs. I also very grate full for all the help that Mr Ian Conway provided me.

I want to express my gratitude with Dr Adam Bermingham, and Dr Bronwen Whitney from the Northumbria University for their help with the charcoal analyses of the Middle Holocene sediment sequence of Lake Esmeralda. I also value their parallel palaeoenvironmental research in the Meghalayan sediment sequence of Lake Esmeralda using pollen and charcoal, whose results help me to establish the human impact in the region.

I would like also to thank to Peter G. Atkinson and Annabel Mellor for most of the analyses of loss of ignition performed on sediments of Lake Esmeralda, as well as Harriet Galley, Nicholas Robinson and Jonathan Dobson for the previous preparation of many of the samples from Lake Esmeralda for the isotope analyses.

I recognise the trust of Dr Socorro Lozano from the UNAM, Dr Isabel Israde from the Universidad Michoacana de San Nicolas de Hidalgo, Dr Gabriel Vazquez and Dr Berenice Solis from UNAM, Prof. Ximena Villagran from the Universidade de São Paulo, Dr Susan M. Mentzer from the Seckenberg Centre of Human Evolution and Palaeoenvironment and Prof. Christopher E. Miller from the Eberhard Karls Universität Tübingen for giving me the required recommendation letter during the application of the scholarship for this project.

I also want to recognise the help provided by Dr Alan Covich from the University of Georgia, Dr Eberhard Gischler from the University of Frankfurt, Dr. Margarita Caballero from UNAM, Dr Holger Weissenberg and MSc. Emmanuel Valencia from the Colegio de la Frontera Sur, Dr Philip van Beyen from the University of South Florida, Prof. Mark Brenner from the University of Florida, Dr Kees Nooren from the University of Utrecht, Dr Eduardo Cejudo Espinosa from the Centro de Investigación Científica de Yucatán, Dr Francisco Gomez from UNAM and Archaeologist Francisco Maury from the City University of New York answering my email messages.

I gratefully remember my friends at the "communist experience group" at the University of Nottingham; Fernando Legarda, Linghan Zeng, Marzhan Baigaliyeva and Ahmad I. AlShdaifat. Their support and friendship in Nottingham made my life in the UK a joyful experience. You will improve the scientific community. You will always be in my heart.

I also would like to thank my friends and colleagues at the University of Nottingham, Karla Hernandez, Jesus Molinar, Fernando Ruiz, William Tonderai Kusena, Hazel Wilson, Jahzeel Aguilera, Neven Tandarić and Jose Daniel Morales.

I also would like to thank Flora Schilt and Alvise Barbier at the Universidade do Algarve whose life has been an inspiration for not giving up during these years. I thank Jonathan Gaytan for his lovely friendship. I thank to Axel Becerril for his love and support. I want to thank my sister Heidy for her help with the references. I thank my grandmother Guadalupe for her prayers. I hope she has seen the face of God by now.

No Ph. D could be finished without the help of all educators that accompanied me during my education from kinder garden to higher education. This acknowledgment is for them. (Including to Mrs Fanny, my high school chemistry teacher, who taught me the skill of observation and Dr Alain Quéré, who taught me the most important lessons in faculty, showing me why chemistry is an exact science). Special thanks to the advisers that I had at different stages of my high education studies; Dr Teresa Condreau, Dr Gustavo Tavizon, Dr Juan Pablo Bernal, Prof. Gerald Haug, Dr Sebastian F. Breitenbach, Dr. Susan M. Mentzer and Prof. Christopher E. Miller.

I would like particularly to thank the help to my advisers Prof. Sarah E. Metcalfe and Prof. Matthew D. Jones. Their patience with this poor student was invaluable, as well as the 38 meetings that we had. Their advice and discussions were blessings from heaven. It was a privilege to be your student. They were also great in getting numerous analysis performed outside the University as well as in reviewing the manuscript of this thesis.

Finally, I thank Prof Suzanne McGowan from the University of Nottingham and Prof Jonathan A. Holmes from the University College London for the examination of this thesis and project in its different stages. I hope they find it enjoyable. I also wish that you, my dear reader, find this research enjoyable and interesting. I tell you like the Maya people dyos bo'otik (thanks).

Sapientia urbs conditur

Haydar B. Martinez Dyrzo

Mexico City, May 23rd, 2021.

Exploring Holocene Lake Palaeoclimatic records in the Maya Northern Highlands and the central Mayab

Chapter 1 Introduction

Photo: Sayil ruins in the Puuc Region

"We sat down on the very edge of the wall, and strove in vain to penetrate the mystery by which we were surrounded. Who were the people that built this city? In the ruined cities of Egypt, even in the long-lost Petra, the stranger knows the story of the people whose vestiges are around him. America, say historians, was peopled by savages; but savages never created these structures, savages never carved the stones. We asked the Indians who made them, and their dull answer was 'who knows?"

John Lloyd Stephens, 1841.

The present scenario of climate change has focused our attention on the relationship between the biosphere, atmosphere, oceans and human settlement; a relationship that still needs exploration. Due to the influence that the climate might have in the development of settlements and the creation of social-economic and political networks in past human societies, this issue has been explored intensively over the last two decades (Mayewski et al., 2004). This is due, in part, to the improvement in resolution of the analytical methods applied to reconstruct palaeoclimates (Gornitz, 2007), as well as a set of new techniques appearing in archaeology (Wagner, 2007). In particular, the reconstruction of such relationships in societies without written historical records, or where the historical record was destroyed, represents a major challenge for completing the global understanding of the behaviour of the atmosphere and oceans and its two-way relationship with human societies.

With the publication of the Great Maya Droughts by Gill (2000), an intense debate about the role of climate in the collapse of an entire civilization, only 1200 years ago, was opened. Since then, numerous works in the fields of palaeoclimatology and Quaternary Studies have identified the existence of a series of droughts from 1140 to 1040 years B. P. over the Maya Cultural Area in the tropical region of the North American continent at the time of the Maya Classic Collapse (also called just the Maya Collapse) at 1190 to 1040 years B. P. (e. g. Gill et al., 2007; Haug et al., 2001; Hodell et al., 2005; Webster et al., 2007).

The research presented in this thesis is a palaeoenvironmental reconstruction using different proxies in lake sediment cores from two different sites in the Maya Cultural Area, one in the Maya Northern Highlands and the other in the Maya Northern Lowlands (Mayab). Data from other reported palaeoclimatic records from the region (e. g. lake cores, speleothems, stratigraphic sequences and corals), archaeological excavations and instrumental records are used to complete and contextualise the obtained information. The results, in particular derived changes in the evaporation precipitation ratio or changes in the rainfall amount, allow further discussion of potential human-ecosystem interactions focussing on the balance between human agency and nature as determining factors in the dynamic of settlement patterns across the Maya Cultural Area in the Holocene. In addition, this research contributes to the study of the differences between palaeoclimatic records from lakes that share the same climate, but have different characteristics, such as the size and morphology of the lake and the surrounding lithology.

1.1 Justification for new research in the Maya region

A not completely understood environmental history of the Maya

The role of climate in the development of culture has been a part of the palaeoclimatic research concerning the Quaternary in different zones across Earth. Some examples of this are: modern anatomical humans and the change to warm periods (Clark et al., 2003; McDougall et al., 2005); the palaeohumidity reconstructions of the Fertile Crescent Zone (Schönwiese, 2013); the collapse of the Old Kingdom in Egypt (Gibbons, 1993); the cultural development on the Atacama desert (Eitel, 2006; Mächtle, 2007); the Little Ice Age and the Renaissance (Fagan, 2000); and drought as a driver of the Russian Revolution at the beginning of the XX century (Urry, 2011).

The Maya Cultural Zone is a zone where the Maya civilisation was developed (see Figure 2.1 in chapter 2). How they interacted with the environment is still not completely understood (Aimers, 2007, 2011). The peculiar geomorphological characteristics of this region, in particular the northern lowlands known as the Mayab, supposes management of resources (principally water and soil), that was different from other advanced civilisations (e. g. ancient Egypt, Mesopotamia, Indus-Valley, among others) (Douglas et al., 2016b, 2015; Faust, 2001; Schreg, 2009). At the end of the IX baktun in the Maya Calendar (circa 1100 years B. P.; see section 3.1), 90% of Maya settlements were reconfigured. Most cities were abandoned, and their cultural production was interrupted (e. g. Culbert, 1973; Gill, 2000; Grube et al., 2012; Haug et al., 2003; Kennett et al., 2012). A series of droughts is described as an important factor of this "collapse". However, this collapse was not experienced equally across all the Maya Cultural Zone (Gill, 2000; Gill et al., 2007) and there is therefore a need for more records from across the entire Maya region, to better understand the variability.

The lack of comparative studies from the different zones in the Maya Cultural Zone

Even though some studies present this perspective (a spatial perspective), e.g. studies on lakes in the Peten (Kennett and Beach, 2013) as well as comparative studies of palaeoclimatic records in the northern Yucatán Peninsula (Asmerom et al., 2012; Islebe, 2012), it is clear that a spatial perspective is required in a cultural area of approximately 300, 000km^2 which has different ecosystems. This has been especially suggested by Beach et al., (2015) and Marchant et al., (2004) based on the fact that the intensity and timing of events of the collapse were not the same in all Maya Cultural Area. Most of the research

has been performed in the lowlands, with only scarce palaeoenvironmental studies in the Northern and Southern Maya Highlands (Díaz et al., 2017; Franco-Gaviria et al., 2018; Islebe, 2012). In this research, we study the environmental changes of Lake San Lorenzo in the Northern Highlands, which will be compared with the other studied site of this thesis from the lowlands, Lake Esmeralda.

The opportunity to study lakes influenced by the same climate but with different characteristics;

The reason for conducting research on Lake Esmeralda is to compare the environmental records developed from its sediments with the published records from its sister lake; Chichancanab. This kind of comparison is important for assessing the variables (e.g. the catchments, the mineral composition, the hydrological balance) involved in recording and preserving the environmental signal (e.g. the evaporation-precipitation signal in $\delta^{18}O$ isotopes, the signals of episodes of severe droughts in gypsum or in the amount of organics) as well as to compare different responses in the commonly applied environmental proxies to a presumed same climatic input mechanism (such as the humidity of the environment or the rainfall amount; Roberts et al., 2016). At the same time, this comparison can potentially separate a regional natural environmental signal from site-specific stochastic "noise" or from site-specific anthropogenic signal (Anderson et al., 2012; Roberts et al., 2016). Finally, assessing the responses of both lakes instead of focussing on single lakes helps to understand the past and present connectivity (if it existed) between both lakes (Moorhouse et al., 2018).

1.2 Problems and suggested solutions in the study of the Environmental History and Collapse of the Maya Civilisation

The idea of drought as the primary driver of the Maya Classic Collapse has been widely debated, not only by archaeologists, who call these ideas deterministic but by palaeoclimatologists, who argue based on the archaeological record, that the droughts happened after the initiation of the Maya Classic Collapse (Douglas et al., 2016b).

Other hypotheses have been suggested for the Maya Classic Collapse. For instance, the hypothesis related to the overuse of ecological and environmental resources (Dunning and Beach, 2000), which would have produced a reduction in productivity and a lack of essential goods for their subsistence (Demarest, 2004). A detailed description of these hypotheses is presented in chapter 3.

In contrast, it has been argued that the Maya were an example of the proper management of resources in many aspects (Faust, 2001).

The hypothesis of the Maya droughts as drivers of the collapse has received the following criticism:

- It flattens the complexity of the archaeological record and ignores the ability of the Maya to react and adapt (Aimers, 2011).
- It has shown an insufficient understanding of the relationship between climate and Maya cultural change during the Terminal Classic (Hodell, 2011).
- It lacks a spatial perspective. Since the intensity, duration and impact of the Maya droughts was different in every local zone of the Maya Cultural Area (Beach et al., 2015).
- It fails to consider that the knowledge about regional changes in vegetation and soils is still little (Douglas et al., 2016a). Therefore, it is difficult to assess how critical the Maya droughts were for changes in vegetation (and perhaps vice versa), and how these changes impacted the human life. In addition, there are only a few studies of human bones, and too few animal bone and shell records for assessing a critical impact of droughts on humans and wild life at the time of the Maya Collapse (Beach et al., 2015).

Consequently, it has been proposed that

- New high-resolution, accurately dated records, preferably records inside the Maya Cultural Area, from both archaeologists and palaeoclimatologists working together, are needed when interpreting the results (Beach et al., 2015; Hodell, 2011).
- It must combine a spatial perspective with site-specific studies that combine archaeology and palaeoecology in situ in order to understand interactions between environments and cultures (Beach et al., 2015; Marchant et al., 2004).
- It must refine the comparison of archaeological and palaeoclimate chronologies (Douglas et al., 2016a).
- It must estimate the drought sensitivity of the ancient Maya (Douglas et al., 2016a).
- It must perform an integrative analysis of the proposed causes of collapse (Douglas et al., 2016a).

1.3 Research Strategy

The present research compares the environmental history of two sites in the Maya Cultural Zone. The first site is Lake Esmeralda in the Cochuah Region in the centre of the Maya Northern Lowlands (Yucatan peninsula or Mayab), which is a relatively small lake near to the bigger, widely studied Chichancanab. These two lakes have been described as twin lakes due to their proximity. The sediments recovered from Lake Chichancanab, as well as the sediments recovered from the Cariaco basin in Venezuela, are reference points in the palaeoclimatic studies conducted in the Maya Cultural Zone, even though the Cariaco basin is not inside the Maya Cultural Area (Haug et al., 2001, 2003). Lake Esmeralda represents an opportunity to study the environmental history of a system that is influenced by the same climate as Chichancanab, but whose recorded environmental signals could be different since it has differing size, biology, trophic status and catchment.

The second site is Lake San Lorenzo, one of the lakes in the Montebello Lake Complex in the Northern Highlands of Chiapas, a lake of similar size to Chichancanab. The geo-context of both lakes will be discussed in chapter 4. Lake San Lorenzo has already been studied for reconstructing an environmental history based on pollen, charcoal, elemental abundances and elemental ratios. However, it lacks other important proxies, such as the percentage of organic matter and isotope records.

The present research studies sediments collected from these two sites to reconstruct the environmental signal recorded using different proxies. In the case of Lake Esmeralda, the sediments were analysed for pollen and charcoal concurrently by Adam Bermingham of the University of Northumbria, generating independent research. His work will be cited for comparison in section 9.6 in chapter 9.

The present thesis developed records for Lake Esmeralda based on elemental abundances, elemental ratios, colour and greyscale reflectance, density, total inorganic and organic carbon content (including the percentage of residuals), and stable isotope analysis ($\delta^{18}O$ ‰). For this latest particular purpose, a complete assessment of the methods for extracting the environmental signal from isotopes was performed using bulk sediment and shells of gastropods. This assessment is a separate strand of research and has some interesting implications in the palaeoclimatic studies using lake sediments, especially in the Mexican Yucatan where isotope records from gastropod shells have been an important proxy in the Mayan drought narrative (Carrillo-Bastos et al., 2010; Curtis et al., 1996; Escobar et al., 2010; Hodell et al., 1995, 2005; Wahl et al., 2014; Whitmore et al., 1996).

In the case of Lake San Lorenzo, the sediments are used to complete the proxies of elemental abundance, and pollen developed by Franco-Gaviria et al. (2018, 2020), analysing the density, the inorganic and organic carbon content as well as their residuals and $\delta^{18}O‰$ and $\delta^{13}C‰$.

1.4 Epistemic Levels in the research

In order to validate the results and interpretation of the environmental history of these two lakes and consequently, the comparison between the two sites, different levels must be addressed (Figure 1. 1). These levels are:

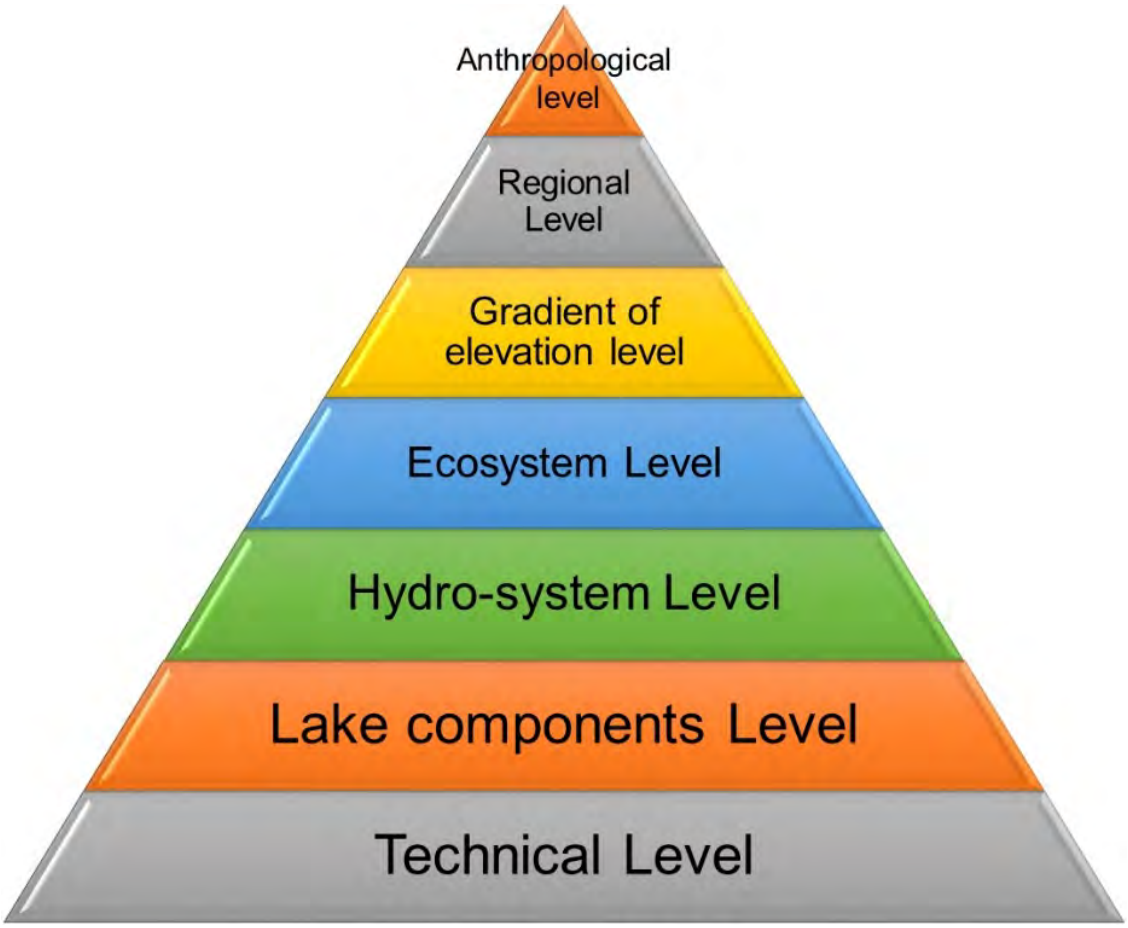

Figure 1.1 Epistemic Levels

Technical level

The tests and results at this level aim to determine the robustness, variation (meaning the lack of resilience of the system), affordability and purity of the environmental signal in a particular proxy (the reasons behind the questions in this level will be expanded upon in later chapters). In the case of Lake Esmeralda examples of such technical questions are:

- Is the grey scale or the colour of the sediment sequence a proxy of textural changes and a tool for determining the number of layers (see section 6.7 in chapter 6)? How different are the records developed from the grey scale and colour of the sediments?
- What is the best strategy for recovering the environmental signal using stable oxygen isotopes ($\delta^{18}O$ ‰) (see chapter 8), to analyse the isotopic composition of bulk carbonate, 'composite' gastropods' shells or individual gastropod shells?

In the case of Lake San Lorenzo

- Is it feasible to use the $\delta^{18}O$ ‰ in carbonates as a proxy of the evaporation-precipitation ratio (see section 7.5 in chapter 7)?

Lake components level

At this level, tests and analysis will determine issues related to the behaviour of the lake as a system. It addresses the following kinds of questions

For Lake Esmeralda

- Is Lake Esmeralda a closed system?
- Has Lake Esmeralda presented changes in the balance of carbonate/organic deposition over the time? If so, what is the cause?
- Were evaporites produced in Lake Esmeralda at some point in time?

For Lake San Lorenzo

- Was Lake San Lorenzo always an open system as it is today?
- Are the carbonates washed in from the surrounding karst, or are they authigenic precipitates?
- Has Lake San Lorenzo presented changes in the balance of carbonate/organic deposition over the time? If so, what is the cause?

- What phenomena were responsible for the changes in the texture of the sedimentary sequence?

Hydro system level

The questions at this level make a comparison between nearby lakes. In the case of Lake Esmeralda, this means comparisons with Chichancanab, while in the case of Lake San Lorenzo, this means comparison with other lakes like Lake Kail 30 km away, since other lakes at Lagunas de Montebello Lake Complex do not have comparable data. Relevant questions at this level are

- Is Lake Esmeralda a twin sister lake of Chichancanab?

Ecosystem level

The questions at this level try to clarify the evolution of the lake and its surroundings. Such questions are the same for Lake Esmeralda and Lake San Lorenzo.

- Was there human impact on the lake?
- How did the vegetation around the lake change?
- Were the changes in vegetation reflected in changes in the sedimentation of the lake?

Gradient of elevation level

At this level, a comparison between the system Esmeralda-Chichancanab (4 m.a.s.l.) and the Montebello Lake Complex (1455 m.a.s.l.) is made. The question to resolve is:

- What were the differences in the environmental history between the lowlands and the highlands according to the records obtained from Lake Esmeralda and Lake San Lorenzo?

Regional level

At this level, a comparison of the two sites with the records produced in the Maya Cultural Zone is made. It addresses the following questions:

- What were the differences in the environmental history of these two sites, in comparison to the records developed across the Maya Cultural Area?

- What are contributions to the environmental history of the Maya Cultural Zone of the studies at Esmeralda and San Lorenzo considering the previous almost seventy sites studied in the Zone?

Anthropological level

On this level, a series of hypothetical cultural scenarios are tested:

- Were the Maya in harmony with the environment or an early example of a unconscious human impact?
- Did the drought make the lake water unsuitable for human needs?
- Did the droughts produce a scarcity of water, making agriculture difficult?

All these different epistemic levels highlight the complex nature of both the palaeoclimate research per se and the integration of the results of the paleoclimate research with the archaeological sets of data for creating a plausible scenario that explains observations in both fields, the geosciences field and the archaeology field. This thesis works through these questions for the two studied sites.

1.5 Thesis outline

This thesis consists of ten chapters:

- Chapter 1 "Introduction" (the present chapter)
- Chapter 2 "The Maya Cultural Area" defines this area as well as describing its geography, geology and climatology. The chapter also describes the subareas present in the zone. Finally, the chapter describes the cultural development and settlement patterns of the Maya People.
- Chapter 3 "The Maya Collapse" presents a general discussion of the different hypotheses of how the Maya Classic Collapse happened related to environmental changes.
- Chapter 4 "Palaeoenvironmental records in the Maya Cultural Area." presents a meta-analysis of the palaeoclimatic and palaeoenvironmental records in the Maya Cultural Zone published until early 2020, providing a spatial-temporal visualisation of the records and their significant conclusions related to the presence of droughts and human impact.
- Chapter 5 "Study sites" describes the areas where the palaeoenvironmental records studied in this thesis were collected, Lake Esmeralda and Lake San Lorenzo. This

chapter also presents the rainfall regime, and previously published water isotope data.

- Chapter 6 "Methodology" describes the fieldwork and laboratory analyses performed on the samples as well as the diverse mathematical algorithms used during the research.
- Chapter 7 "Environmental History of Lake San Lorenzo" presents the research on the sediments of Lake San Lorenzo complementing the environmental reconstructions of Franco-Gaviria et al. (2018, 2020).
- Chapter 8 "Preservation of environmental isotopic signal in gastropods" presents the results and discussions of this thesis related to the best strategy for recovering the environmental signal using oxygen isotopes in Lake Esmeralda.
- Chapter 9 "Environmental History of Lake Esmeralda" presents the research on the sediments of Lake Esmeralda for environmental reconstruction.
- Chapter 10 "Final thoughts and Conclusions" sets out the general conclusions of this thesis. At the same time, it highlights the limitations of the research and the questions developed during this research that remained unanswered. Finally, it recommends further studies on some specific topics.

This page intentionally left blank

Chapter 2 The Maya Cultural Area

Photo: Loltun cave in the Puuc Region

"They were here, because they were here created by the One whose name is said sighing. They were beautiful and brave men and they gave love and mercy. Lord Zamná, the Father of all, was among them; his hand, producer of the wonders of the world, rose high to lead and command them. And He cured them of the ills of their body, and gave them heat from the sun to ignite their spirits, which were thus always clear as the sky. They made the high and shining temples where men near and far come to worship the One who has no name and is above all. They erected the great white houses in which the masters taught wisdom. They built with holy stones the ancient cities where the gods lived with men. They constructed Itzmal, Muutul, T'-Ho and Chichen Itza and around them 307 cities."

Leyendas Mayas: Origenes, XVI Century.

This chapter focuses on describing the geographical, geological and climatic context of the Maya Cultural Area. In addition, the chapter presents a resume of the history of the Maya civilization based upon archaeological and epigraphic research.

2.1 Political Geographic context

The Maya Cultural Area is in a tropical area (low latitude) of the Americas and is part of a cultural region in the world designated as Mesoamerica (Nichols and Pool, 2012). Mesoamerica is known as the fifth civilisational centre of humankind (an independent cradle of civilisation), and one of the civilisational centres in the Americas besides the Andean civilizations (Kirchhoff, 1960). Mesoamerica is composed of nine different cultural zones, where the Maya is the most prominent cultural unit (Figure 2.1) (Vela-Ramirez and Solanes-Carraro, 2000).

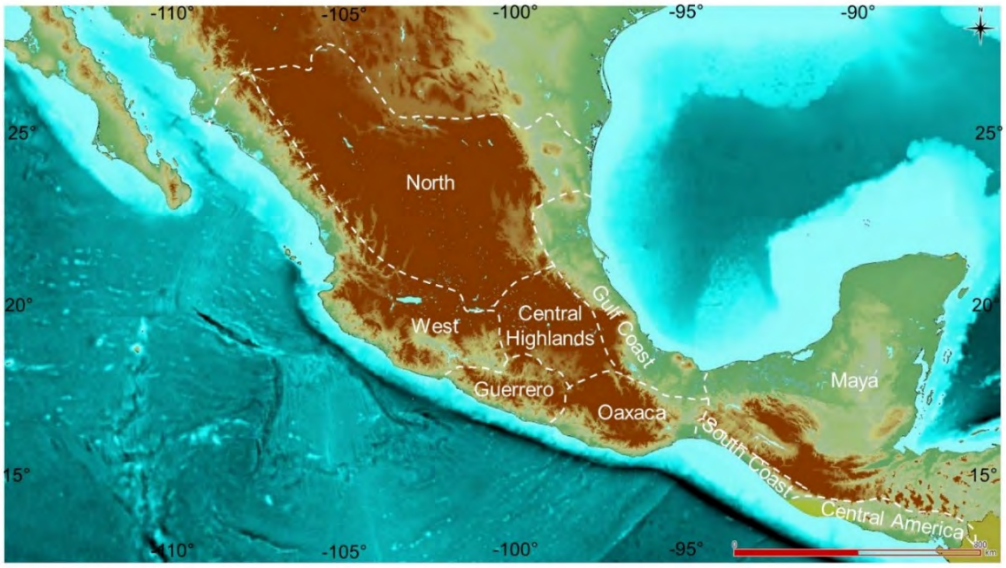

Figure 2.1 Map of the cultural areas of Mesoamerica. The Maya Cultural Area is at the East part of Mesoamerica (denoted as "Maya" in the map). Modified from Vela-Ramirez & Solanes-Carraro (2000) All maps in this thesis use latitude and longitude as the geographic coordinate system.

Despite the difference between its cultural regions, the Mesoamerican Cultural complex is defined as a unity due to the sedentary way of life, the common use of cacao, maize, beans, tomato, avocado, vanilla, squash and chilli, and turkey; the common complex mythological and religious tradition (despite sub-regional differences) a vigesimal numeric system, the use of two complex calendrical

systems, a tradition of ball playing, and a distinct architectural style (Nichols and Pool, 2012).

Among scholars, it is common to define the Maya Cultural Area as a region that contains the modern Mexican states of Campeche, Quintana Roo and Yucatan, most of the Mexican state of Tabasco and the eastern part of the Mexican state of Chiapas, the countries of Guatemala, Belize, and partially the northern departments of Honduras and El Salvador (e. g. Phillips & Jones 2009, Webster et al. 2007). However, this definition is not entirely right, since there are regions belonging to the Zoque-Olmec and Nahua cultures in the area, which are clearly divergent from the Maya (Charles and George, 2010; Grube et al., 2012; McKillop, 2004; Phillips and Jones, 2009; Sabloff, 1994; Thompson, 1966; Wilhelmy, 1981).

It is actually difficult to define the Maya Cultural Area since they did not recognise themselves as a political unit, or as a nation or as a folk (Grube et al., 2012; Thompson, 1966; Wilhelmy, 1981). An attempt at definition could constrain the Maya Cultural Area to the area occupied by the modern Maya people, but this would not correspond entirely to the areas occupied by the ancient Maya since there have been changes in the ethnicities of the population as well as migrations.

The Maya Cultural Area was formed by several political entities called "payolelo'ob" (singular payolel)(Garcia-Capistran, 2019; Tokovinine and Dumbarton, 2013). Other definitions of the Maya Cultural Area tried to limit it to all payolelo'ob which spoke a Mayan language. The problem with this definition is that the Teenek civilisation (called Huastec in the Aztec-Mexica language), also spoke a Maya language (Kaufman, 1976). The Teenek lived at the same latitude as the Maya, but on the western side of the Gulf of Mexico, in a region between the Mexican states of Veracruz, Tamaulipas and San Luis Potosi, in the Gulf Cultural Area of Mesoamerica (Figure 2.1) (Phillips and Jones, 2009).

Sensu stricto the Maya Cultural Area is actually constrained not just to the "payolelo'ob", which spoke a Maya language in the southern and eastern part of Mesoamerica, but to those groups who shared common religious practices and a common cosmovision of the universe. In this way, Zoque-Olmec settlements in the Soconusco and Nahua settlements in the Pipil and Lenca areas, which are designated the South Coast Area and the Centro-American Area of Mesoamerica,

respectively (Figure 2.1), are not part of the Maya Cultural Area (Vela-Ramirez and Solanes-Carraro, 2000). These areas occupied the south zone of the Mexican state of Chiapas, Guatemala and El Salvador. Even though in this thesis I recognise this definition constrained to the area covered by Maya language payolelo'ob (see previous sentences), when I refer to the Mayan Cultural Area, I also include the South Coast and the Central America areas (Figure 2.1) due to their historical interaction and proximity with the Maya people, as many scholars do (Grube et al., 2012).

Scholars tend to divide the Maya Cultural Area into five different regions without considering the South Coast and the Central America area (the Central America area of Mesoamerica does not cover the same territory as the subcontinent Central America)(Figure 2.2) (Sharer and Traxler, 2005). Three of these regions are in a passive tectonic margin, in the lowlands (Perry et al., 2009) and two regions are in the highlands, in a tectonically active margin (Morán Zenteno, 1988a). These regions are:

- The Northern Maya Highlands in the mountains of Guatemala and Chiapas (Mexico).
- The Southern Maya Highlands in south Guatemala and El Salvador.
- The Southern Maya Lowlands in the moist forest from the deltas in Tabasco (Mexico) to the southern moist forest in Guatemala.
- The Central Maya Lowlands composed of the Peten lake complex in northern Guatemala.
- The Northern Maya Lowlands in the dry broadleaf forests in a territory called by Mesoamericans as the Mayab, and by the Spanish as the Yucatan peninsula (Sharer and Traxler, 2005). In this thesis, these terms (the Northern Lowlands, Mayab and Yucatan peninsula) are used as equivalents.

It is common to agglomerate these zones into two super zones, the lowlands and the highlands. The altitude in the lowlands is around 30 m. a. s. l., while the elevation in the highlands is over 800 m. a. s. l. However, the complexity inside these superzones makes the description by zones more accurate.

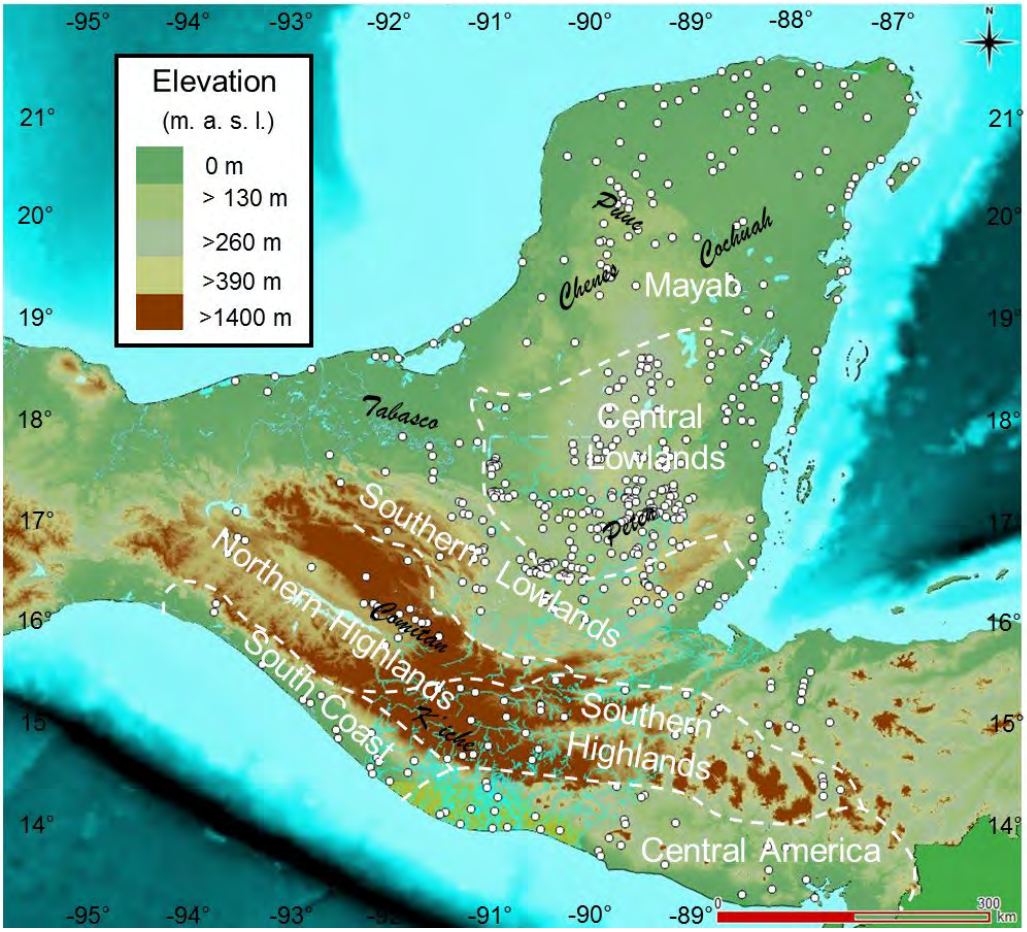

Figure 2.2 Geographic context of the Maya Cultural Area. Borders between regions are suggested based on Sharer and Traxler (2006). The white points are indicative of the Maya settlements according to the archaeological records mapped in the "Archaeological Sites Maya Forest GIS" database developed by the University of California, Santa Barbara (Ford et al., 2009). Relevant subregions named in this thesis are indicated in black letters.

2.2 Geological context

Figure 2.3 shows the geology of the Maya Cultural Area. In the Highlands, Palaeozoic and Mesozoic sequences outcrop mainly as marine sedimentary rocks (Castro et al., 1975), some of them present a low grade of metamorphism (Hernández–García, 1973). Terrigenous sedimentation began during the Paleogene, which is a product of the uplift of the western part of Mexico due to the subduction of the Pacific Plate under the Cocos plate and the movement of North America to the Northwest relative to the Caribbean plateau and the folding of the Sierra Madre oriental (Morán Zenteno, 1988). This tectonic dynamic is also responsible for the existence of volcanoes in the region; both Chiapas and Guatemala have volcanic fields, which are considered active.

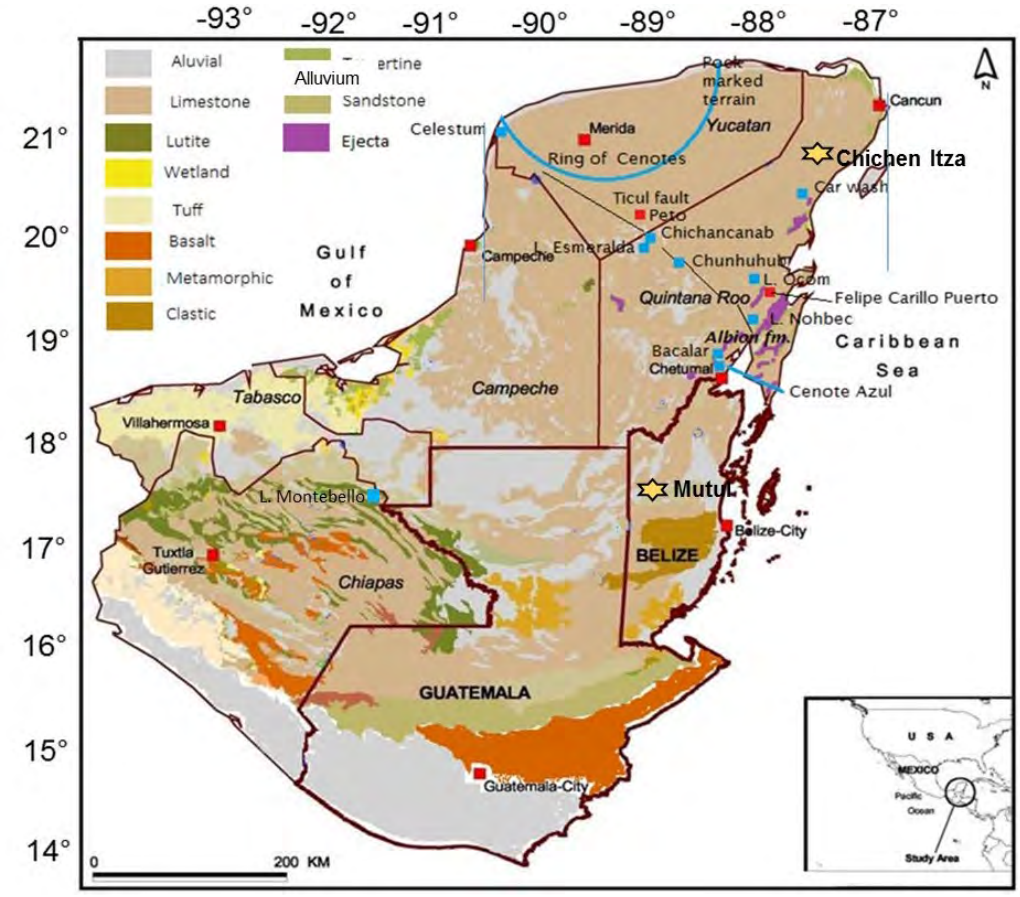

Figure 2.3 Geological context of the Maya Cultural Area. The map incorporates the lithographic units proposed by Perry et al. (2009) for the Maya Cultural Area. The resulting map is a modification of the map designed by Holger Weissenberger, LAIGE, ECOSUR, which pick up the lithography described by Morán Zenteno (1985), where the ejecta produced during the Chicxulub impact was originally described as alluvium. The yellow stars indicate the ancient Maya cities referred in this section. Red and blue squares indicate modern cities and important water bodies, respectively. Borders in Purple delimit the modern countries of Belize and Guatemala and the Mexican states of Chiapas, Tabasco, Campeche, Quintana Roo and Yucatan.

The Mayab was underwater before the Neogene presenting a submarine relief typical of a continental platform on the Gulf of Mexico side, while it was at depths of 4000 m in the Caribbean side (Lugo-Hubp, 1990). The Mesozoic deposits of the Mayab are known due to oil exploration. Under the Cretaceous sequence rest red layers of siltstones and sandstones intercalated with some quartz gravel of quartz, bentonite and dolomitic limestones. These layers cover crystalline rhyolite from the Silurian, which has, at the same time an intrusion of quartz and chlorite. Since the Cretaceous, the Mayab was a place for the deposition of evaporites, mainly of calcite and gypsum (Ramos, 1975). It has been argued that development of the unusual and extended karst in that area could have resulted, in part, from

the dissolution and collapse of a subsurface evaporite as well as from dissolution of carbonate rocks.

That hypothesis is reinforced by strontium isotopes which indicate the existence of a deep evaporite/ejecta layer (the origin of ejecta is explained below) beneath some Cenotes (water sinkholes called cenotes, from Maya *dzonoot*, which means "hole with water") (cenotes Ucil and Xkolac) and by the discovery of evaporite in an observation well on the outskirts of Valladolid (Urrutia et al., 2008).

An extensive region in the central northern part of the Peninsula of Yucatan (Mayab) that is characterised by an exceptionally high concentration of cenotes and other dry sinkholes receives the name of the "Pockmarked terrain". It extends eastward from the Ring of Cenotes (Figure 2.3) (Perry et al., 2009), which allows access to underground waters (see paragraph below related to Figure 2.4).

At the end of the Cretaceous, an asteroid or comet of ca. 10 km diameter hit the north part of the Mayab and the Caribbean Sea, producing a global stratigraphic marker of iridium (Cretaceous-Paleogene boundary), and driving the fifth massive extinction (Alvarez and Zimmer, 1997; Gulick et al., 2008; Kenkmann and Schönian, 2006). The impact produced ejecta, which is dispersed across the peninsula (Perry et al., 2009). This event is called the Chicxulub impact after the village of the same name in the Yucatan State. The Chicxulub impact has possibly contributed to the extensive karstification of the region since there is a dense pattern of radial faults that have been documented offshore in the shallow pre-Palaeogene basement near the pockmarked area. These faults, which are perpendicular to the shoreline and project into the land, may have resulted in exceptional permeability, opening the limestone and evaporites in this zone to extensive groundwater penetration. (Gulick et al., 2008).

In the Cenozoic, the ejecta blanket formed a seal that inhibited the development of a subsurface drainage system. Therefore, a high-sulphate content of groundwater exists in the region east and south of Lake Chichancanab, which is called the Evaporite region. In the west, ejecta, where present, became covered along with the highly irregular contact with the Palaeocene Limestone Formation. The Mayab partially emerged during the Paleogene, presenting its first karstification. The second karstification occurred during the elevation of groundwater due to an increase in sea level during the Pleistocene. The Mountains

(sierra) of Bolonchen-Tikul (also written as Ticul) in the Puuc region is an elevated region (100 m. a. s. l.) produced by a normal fault (Figure 2.3). Puuc means in Yucatecan Mayatan "forested hills", indicating the orography in this region, practically the only mountain system in the Mayab.

The northern and central Mayab does not have any surface rivers, having only underground waters, produced by the filtration of rainfall or the intrusion of the seawater at the coast, which creates a permanent water table. The depth of the phreatic level depends on the elevation and permeability of the terrain (Figure 2.4).

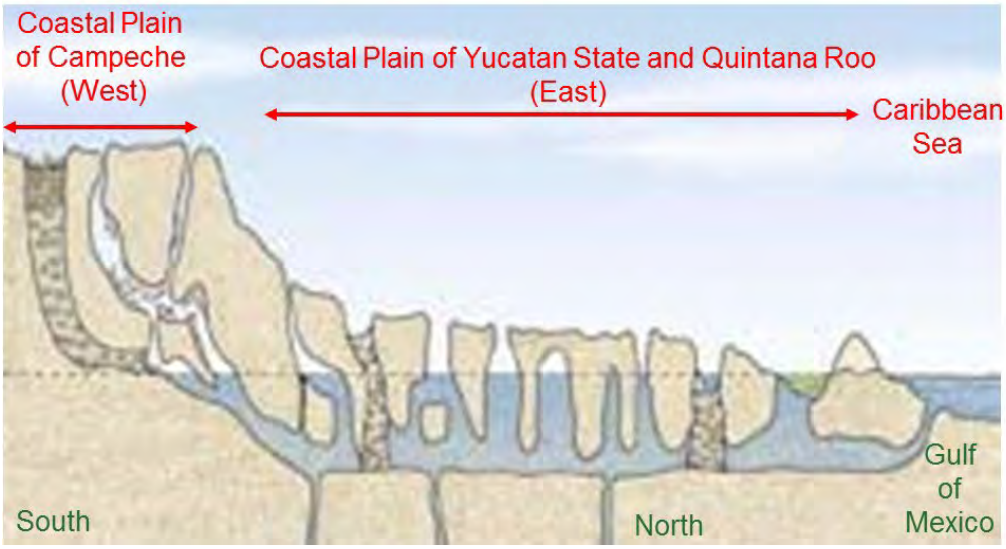

Figure 2.4 Yucutan hydrology scheme taken and edited from (Peterson and Haug, 2006).

In this way, the freshwater depth increases at the rate of 18cm/km as one moves further inland (Gill, 2000). For instance, the water table is reached at 28 m in Chichen Itza in the north (Figure 2.3), but at 130 m at Mutul (Tikal) in the south (Figure 2.3) (Gill, 2000). A similar gradient existed from east to west due to differences in permeability. Therefore lagoons are found on the Caribbean coast, whilst the coastal plain of Campeche presents dry sinkholes (Gill, 2000). The repercussions of the water table's depth for human settlements are discussed at the end of section 3.3 in chapter 3.

The geology of the Southern and Central Maya Lowlands can be described as a transitional zone between the Highlands and the Mayab where surface water flows come from the tributaries of rivers rising in the Highlands (Sharer and Traxler, 2005).

The water sources have shaped the geology of these two regions through weathering, transport and resettlement of materials.

2.3 Climatic context

The climate of the Maya region is determined by the area's position relative to the oceans, latitude, altitude and landscape beside the global atmospheric circulation. In this way, there are essential climatic differences between places, even though they are all at low latitude and in a narrow strip of continent between the Pacific Ocean and the Atlantic Ocean.

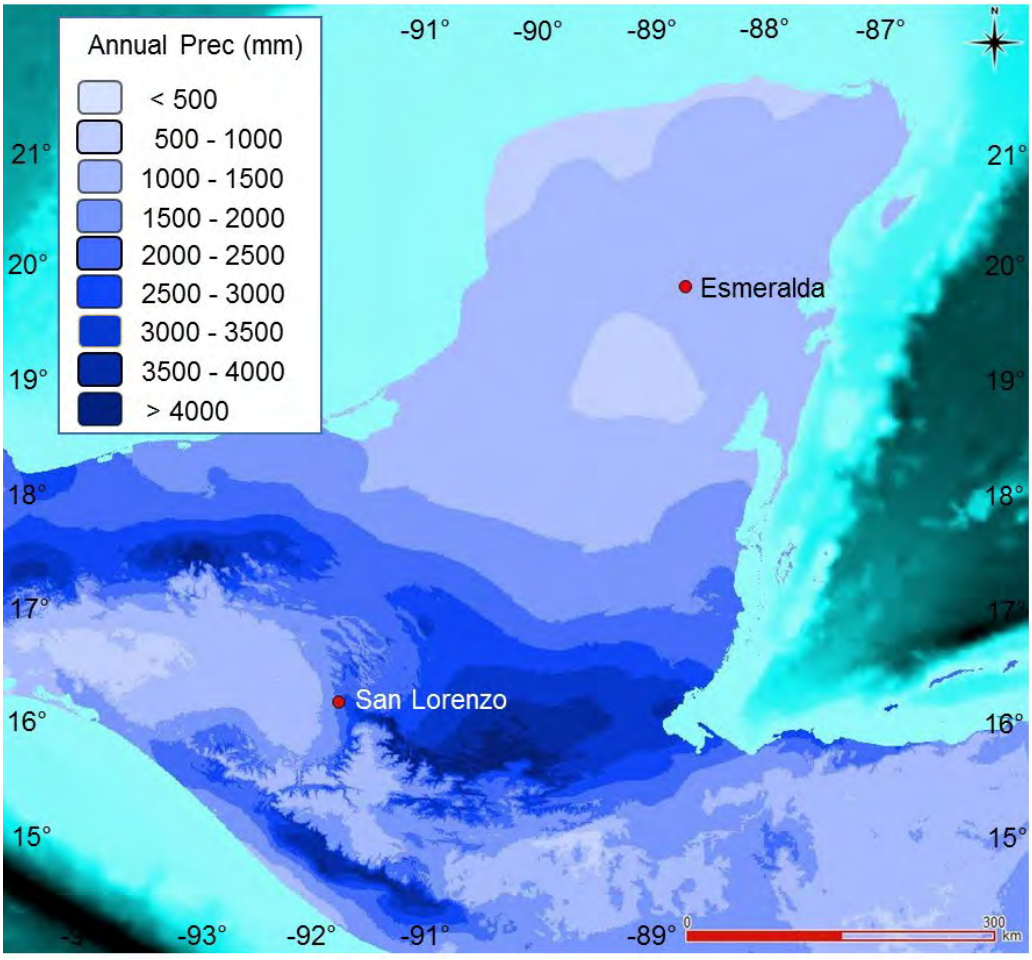

Figure 2.5 Annual precipitation (1950 – 2000) calculated with WorldClim version 1.4 (release3) using the method of Hijmans et al. (2005) by Nooren (2017). The zones present in gradients of 500 mm/year coincide partially with the climatic zones of the modified Koeppen classification for the Mexican states by Garcia-de-Miranda & Falcon-de-Gyves (1986) (not shown). The map indicates the position of our study sites at Lake Esmeralda in the Cochuah Region and Lake San Lorenzo at the Lagunas de Montebello Lake Complex in the Comitan-Chinkultic Region.

The highlands possess a major variation of climates and amount of precipitation (Figure 2.5) in comparison with the lowlands due to the variables mentioned above (Garcia-de-Miranda and Falcon-de-Gyves, 1986)

The Mayab receives less than 1000 annual mm, while the Central Maya lowlands and the Maya Southern lowlands have regions of 1500 to 2000 annual mm and 2000 to 2500 mm depending on the altitude. In the highlands, the regional variations go from 1500 to 2500 annual mm to over 4000 annual mm depending not only on the altitude due but to the collision of different airflows. (Chapter 4 describes the particular rainfall regime in the study sites).

The climate dynamics of the Maya Cultural Area are complex and still not completely understood. In summer, the Bermuda North Atlantic High-Pressure Cell (or subtropical ridge, STR) is at about 35°N and the Trade Winds bring a deep easterly flow over most of Mexico, including the whole Yucatan peninsula (Figure 2.6).

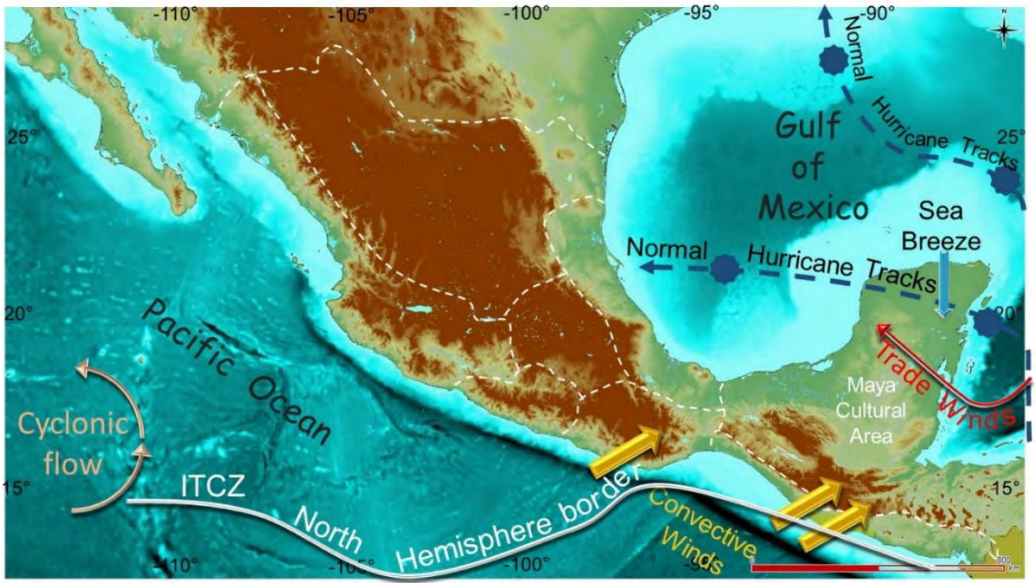

Figure 2.6 Summer Climate Context of the regions of Mesoamerica, including the Maya Cultural. The Bermuda North Atlantic High-Pressure Cell does not appear in the figure since it is located about 35°N.

The Trades blow along the south side of the Bermuda North Atlantic High-Pressure Cell, and a tongue of moist air moves from south-east to the northwest (Figure 2.6) (Kappas, 2009; Metcalfe et al., 2000). When the position of the Bermuda High is constrained to the subtropical North Atlantic, warmer surface

temperatures in the waters of the Atlantic Ocean happen, which allows wetter trade winds from the south-east and sea breeze from the north, bringing more rainfall to the Maya Cultural Area. In contrast, when the Bermuda High spreads to the south of the North Atlantic, cold surface temperatures exist, making the trade winds drier (Montero-Serrano et al., 2011) and reducing the movement of sea breeze (Gunn et al., 1995). The rain brought by this easterly flow is supplemented by convective storms triggered by heating over the continent.

In addition, hurricanes in the Atlantic frequently affect summers over the Yucatan peninsula, adding further moisture (Castro, 2010; Mosiño-Alemán and García-Acosta., 1974). They result from the high sea surface temperatures over the Caribbean and tropical North Atlantic (Kappas, 2009). In contrast, Pacific cyclones are rarely reported to touch the western coast of the Maya Cultural Area (Castro, 2010). On the slope of the mountains on the Pacific Coast, onshore winds are primarily southerly, converging with the easterly Trade Winds near the mountain range crest (Lachniet and Patterson, 2009). In summer also the intertropical convergence zone (ITCZ) moves to its most northern position moving near to the southern part of the state of Chiapas, and Guatemala. (Bernal et al., 2011), also bringing precipition.

The summer rainy season can be disrupted for 2 to 4 weeks by a dry period called the "Canicula", (the heatwave), or midsummer drought (Toledo, 1980). This disruption of easterly flow is caused by the development of an upper airflow. This flow goes down the eastern seaboard of the USA, extending from Florida through Cuba, and extending down to the Yucatan peninsula. However, the canicula is not so pronounced in the Mayab as it is in the centre of Mexico (Magaña et al., 1999).

Long climatic cycles such as the Pacific Decadal Oscillation, PDO or the Atlantic Multi-decadal Oscillation, AMO might have an impact in the Maya Cultural Area (AMO has certainly an impact over the Yucatan peninsula) (Lachniet et al., 2012; Ruiz-Suárez and Núñez, 2004; Stahle et al., 2012). In addition, short climatic cycles, such as the El Niño Southern Oscillation, ENSO have effects on the region (Jones et al., 2015; Lachniet et al., 2012). Signals associated with ENSO have been found in palaeoclimatic records in Panama and Guerrero, Mexico to the south and the north of the Maya Cultural Area, respectively (Lachniet et al., 2012, 2004) but have been not detected directly in most of the records inside the Maya cultural Area

(perhaps due to the lack of resolution, see Chapter 4). It has been suggested that drought events correlate with ENSO events in Chiapas (Franco-Gaviria et al., 2018). Meanwhile, drought events coincide with the negative phase of AMO in the Yucatan peninsula, when the low sea surface temperatures of the Atlantic Ocean prevail (Magaña et al., 1999).

In winter, the North Pacific Subtropical High brings dry conditions to the centre of Mexico and the Maya region, westerly flows from middle latitudes can enter from the northwest to about 19°(Metcalfe et al., 2015) (Figure 2.7). Additionally, outbreaks of cold polar air from the high latitudes penetrate Mexico towards the South (Figure 2.7 white line). These cold air masses produce fronts of "storm lines" along the zone of contact with the warm tropical air. Large areas of cumulous clouds and often rainfall occur in front of and along the cold front. They are called "Nortes" after contact with the tropical air in the Gulf of Mexico (Figure 2.7 red line) (Vivo-Escoto, 1964), which are confined to the eastern coastal margins by the Sierra Madre Oriental. They can bring heavy rain to the eastern slopes of the mountains (Metcalfe et al., 2000), including the eastern slopes of the mountains of Chiapas as well as rain over the Mayab.

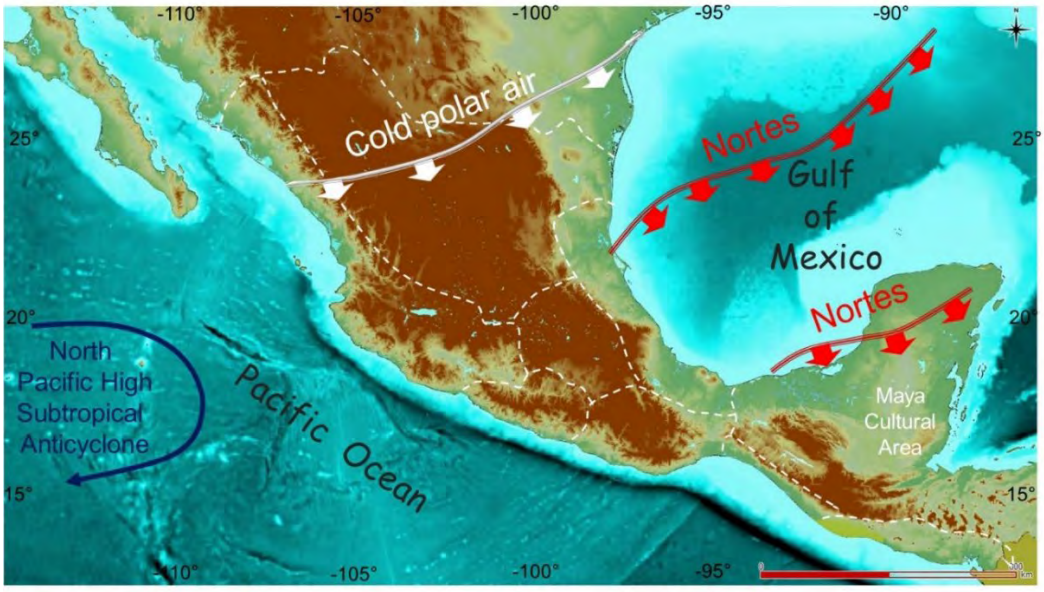

Figure 2.7 Winter Climate context of the regions of Mesoamerica, including the Maya Cultural Area.

2.4 Geography of the Subareas in the Maya Cultural Area

In the next paragraphs, we describe grosso modo the geographical characteristics of the different zones of the Maya Cultural Zone (Figure 2.2), including the Mesoamerican South Coast and Mesoamerican Central America regions, which as I said in the first section are not sensu stricto Maya areas.

The Mayab is formed by a plain with few hills or mountains and a generally low coastline (Sharer and Traxler, 2005). Moist broadleaf evergreen forest covers most of Quintana Roo, southern Campeche, and a portion of the south of the Yucatan state (*Figure 2.8*) (Grube et al., 2012).

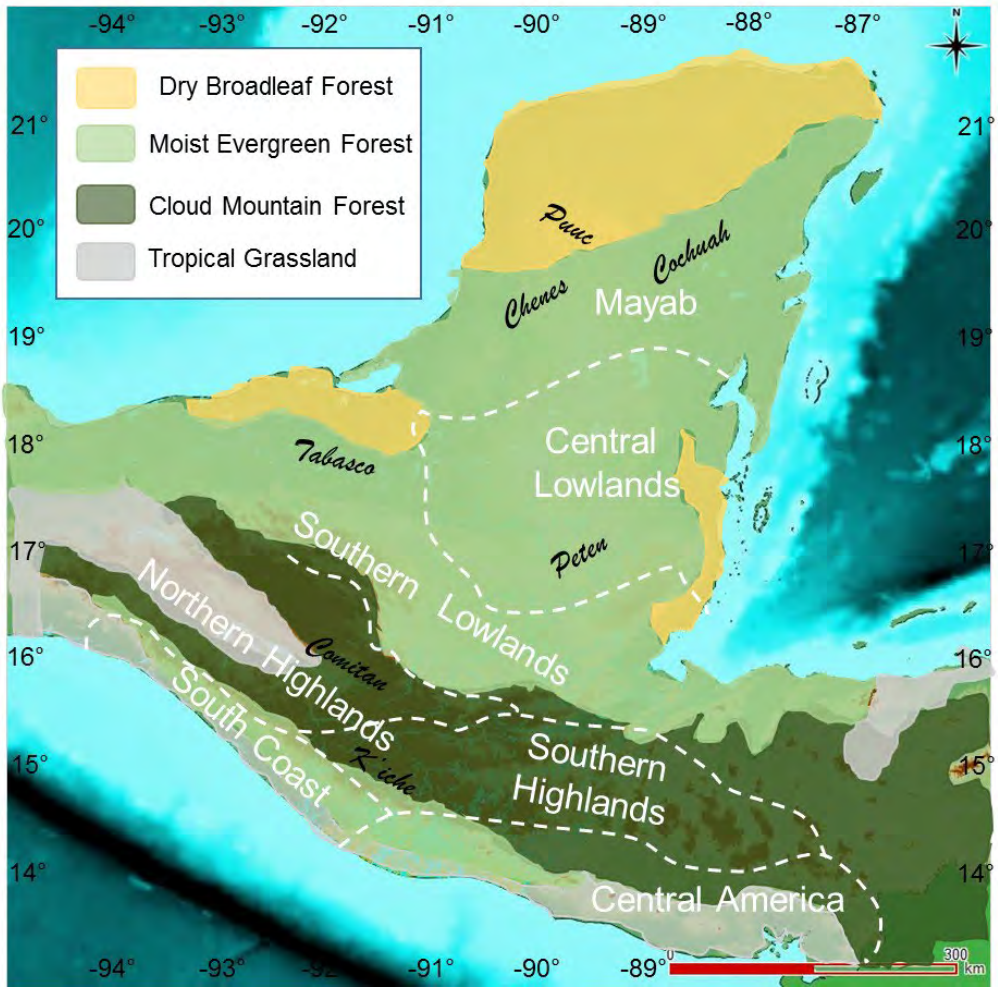

Figure 2.8 Historical General Vegetation in the Maya Cultural Area. (Grube et al., 2012). The map considers only natural vegetation types without human intervention, therefore artificial grasslands are not shown. Relevant subregions named in this thesis are indicated in black letters.

Farther north, the vegetation turns to lower forest consisting of dense scrub which forms the dry broadleaf forests (wrongly commonly described as a savanna, since

this ecosystem has a low forest density, which is not present in the Maya Cultural Area).

As described above, the region has no surface rivers but underground rivers.. The Mayab contain only one hill zone, which is in the western part of the northern lowlands. This zone is the Puuc region (see previous section 2.2). Another region of the Mayab relevant for being one of our study sites is the Cochuah Region (Figure 2.8).

In the Southern Maya Lowlands (Figure 2.2), mangrove and other swamp flora predominate in the low lying and coastal regions (*Figure 2.8*), but the rest of the region is cover by tropical moist broadleaf evergreen forest at an altitude between the 800 to 1000 m. a. s. l. (*Figure 2.8*) (Sharer and Traxler, 2005). Alluvial plains make up the state of Tabasco and Campeche (Sharer and Traxler, 2005). The city of B'aakal (commonly called Palenque or El Tortuguero) is found in this region (Figure 2.9). To the south, the plain gradually rises towards the Guatemalan Highlands (Garcia-de-Miranda and Falcon-de-Gyves, 1986).

The Central Maya Lowlands cover the Petén and Belize (Sharer and Traxler, 2005). The Petén region in Guatemala (Figure 2.2) consists of a natural densely moist broadleaf evergreen forested, low-lying limestone plain (*Figure 2.8*). A chain of fourteen lakes runs across the central drainage basin of Petén (Sharer and Traxler, 2005). The large city of Mutul (commonly known as Tikal) (Figure 2.9) was in this region (Sharer and Traxler, 2005).

The Northern Maya Highlands lie on the north of the continental rift. (Figure 2.2). The highest peaks exceed 3000 m. a. s. l., composed of metamorphic rocks (Grube et al., 2012). The region includes the highlands of Chiapas (Mexico) and northwestern part of Guatemala, where the vegetation is Mountain Cloud Forest (*Figure 2.8*). The slopes are steep, presenting poor soils for agriculture, but more fertile alluvial soils have been deposited in valleys (Sharer and Traxler, 2005). The major pre-Columbian population centres of this region were in the Comitan Valley.

The village of Chinkultic (Figure 2.9) in the Lagunas de Montebello Lake Complex in the Chinkultic-Comitan Region is in this subarea (Sharer and Traxler, 2005). This Lake Complex is one of our study sites.

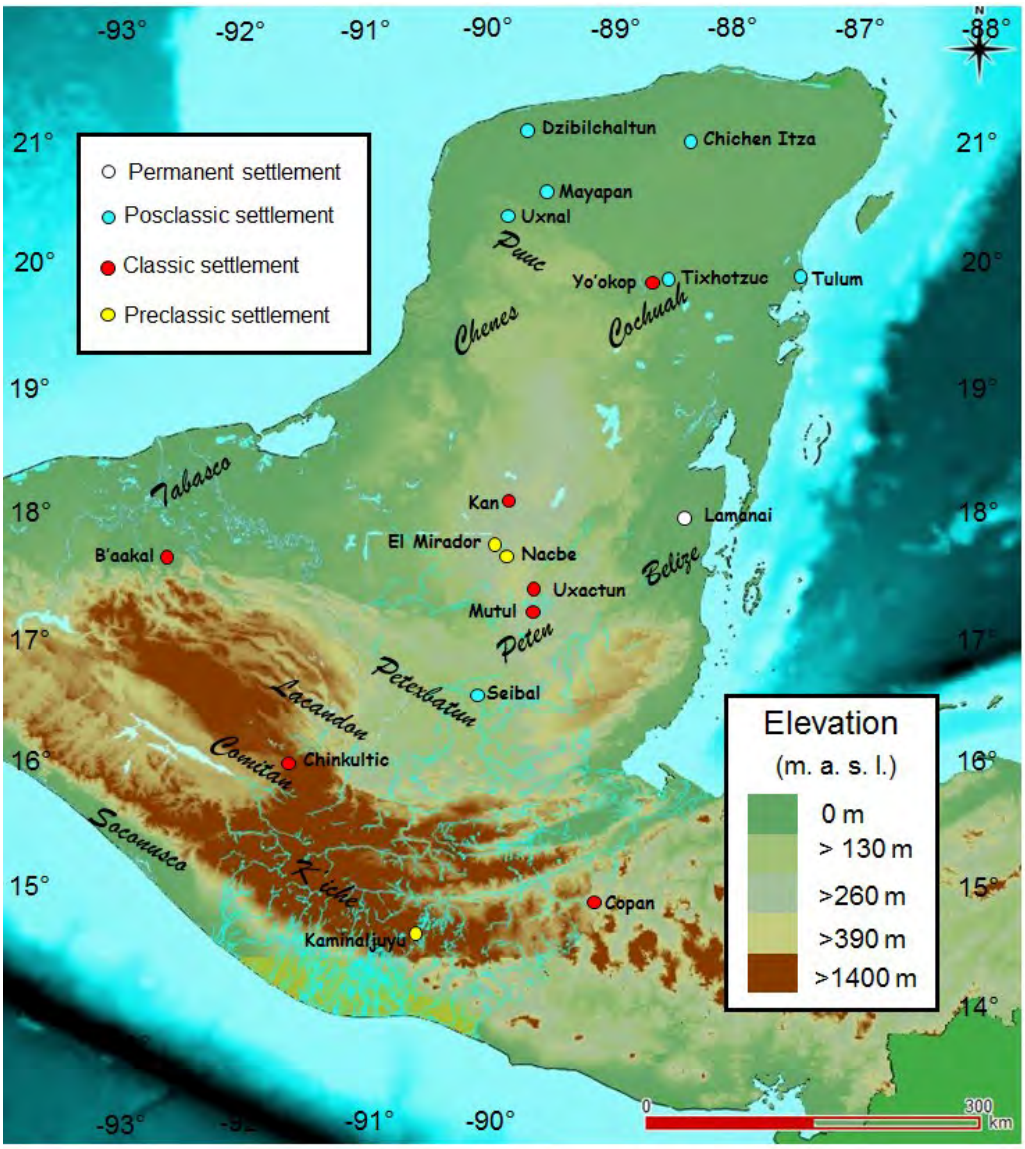

Figure 2.9 Maya settlements and regions named in this chapter, particularly in section 2.5. The map shows named cities which were mainly occupied during the Preclassic horizon (yellow circles), the Classic horizon (red circles), the Postclassic Horizon (pale blue) as well as settlements occupied permanently (white circles). Relevant subregions named in this thesis are indicated in italics.

The southern highlands (Figure 2.2), comprise high mountains and cloud forest (*Figure 2.8*), lying in an east-west orientation between the belt of volcanic cones that parallel the Pacific coast and the great rift valley systems to the north that mark the junction of two tectonic plates; the North American Plate and the Caribbean Plate (Sharer and Traxler, 2005). Therefore, this region is tectonically active and has experienced volcanic eruptions (Ford and Rose, 1995; Macías, 2005; Newhall et al., 1987). The average altitude of the region is 800 m. a. s. l. The major pre-Columbian population centres of the southern highlands were located in the largest

highland valleys, such as the Valley of Guatemala, the Quetzaltenango. The city of Kaminaljuyu (Figure 2.9) was an important centre in the region (Michels, 1979).

The littoral zone of Soconusco (Figure 2.9) in the South Coast Cultural Area (Figure 2.2) lies to the south of the Northern Highlands. It consists of a narrow coastal plain, and the foothills of the Sierra Madre covered primarily by tropical grass and tropical rainforest (*Figure 2.8*) (Nichols and Pool, 2012).

The Central America area lies to the south of the Southern Highlands. It also consists of a narrow coastal plain, covered primarily by tropical grass, tropical rainforest, and contains cloud foster in its north elevated part (*Figure 2.8*) (Nichols and Pool, 2012).

2.5 The Mesoamerican Horizons and the Maya History

During the time of human occupation, the Maya Cultural Area suffered a series of changes in its cultural configuration. The Maya Cultural Area followed the same cultural evolution as Mesoamerica as a whole, so the period of human occupation is divided into five cultural horizons or periods until the arrival of Europeans (Figure 2.10).

The next paragraphs are a resume of the changes in the settlement patterns and political history of the ancient Maya.

During the Palaeoindian Period 12000 to 5450 years B. P., humans arrived in the region as hunter-gatherers. The changes from the nomadic way of life to the first settlements, agriculture and domestication of some animals happens in the Archaic Period between 5450 to 3450 years B. P. (Demarest, 2004). This neolithization process was different, and not synchronous with the process occurring in Eurasia (Drew, 2015). Mesoamericans did not domesticate pack animals or mammals such as cattle; fishing, hunting, and gathering continued to be part of life (Nichols and Pool, 2012). The artificial selection of some grasses developed maize (*Zea mays*) during this period (Drew, 2015). *Zea mexicana* was the wild ancestors of *Zea mays*, which may have originated in the Balsas River, in Guerrero (Figure 2.1) *Zea mays* was already present at Oaxaca 6000 years B. P. Maize cultivation then spread to the Northern Maya Highlands and then to Eastern Mesoamerica, reaching the lowlands at Belize and Honduras 3000 years B. P. (Sharer and Traxler, 2005). This

pattern of development from Highlands to Lowlands in Mesoamerica might be related to the drier climate of the Highlands. It has been suggested that *Zea mays* proliferate in dry environments in contrast to humid ones (Wahl et al., 2014).

The early Preclassic Mesoamerican Horizon also called Formative Horizon between 3450 to 2450 years B. P. (Fig. 2.4) marks the development of the first Maya centres in the northern highlands. These cities were the result of the development of the Maya societies and not the result of an influence of the Olmec-Zoque civilisation (Sharer and Traxler, 2005). It was argued that the Olmec-Zoque civilization was the mother culture of all Mesoamerica by scholars at the beginning of the Mesoamerican studies during the XIX and early XX centuries (Nichols and Pool, 2012).

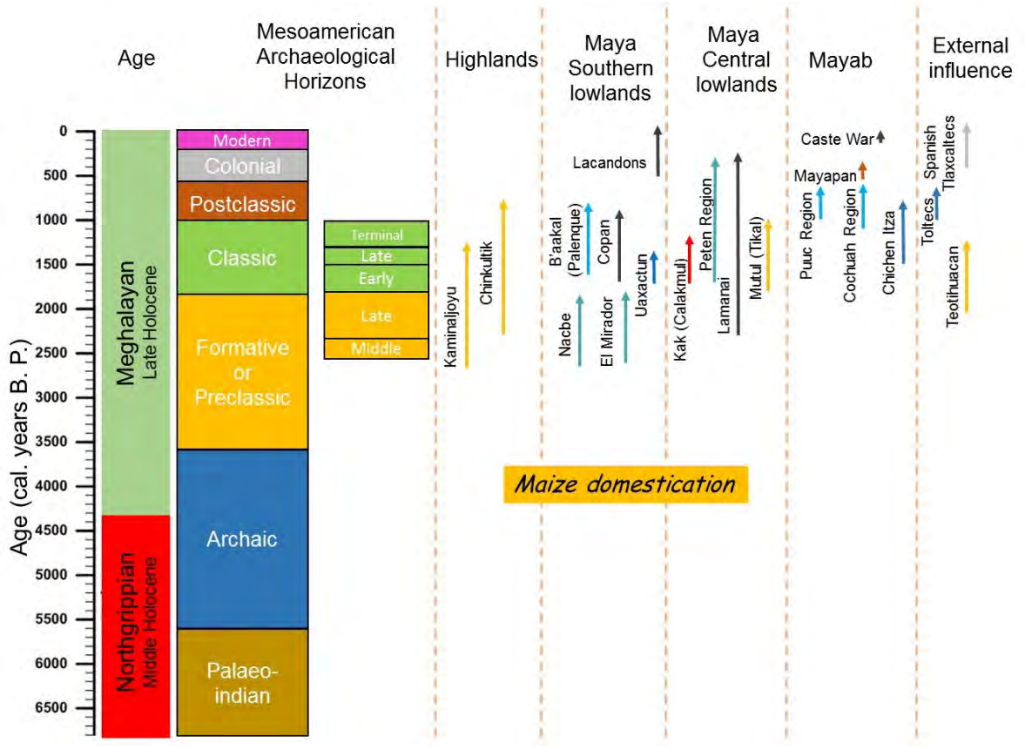

Figure 2.10 Archaeological Horizons and subhorizons in Mesoamerica in years B. P. focused in the last 7000 years according to the time frame established in the CRAS project ((Shaw, 2015a)*) The arrows indicate the active time frame of the different Maya centres and regions as well as the constitutions of the Lacandon people (see text) and the events of the Caste War.*

By the middle Preclassic, 2450 to 2250 B. P., new centres thrived in the southern lowlands due to migration from the northern highlands (Grube et al., 2012). The story of the city of Nacbe (Figure 2.9) started at that time, and the oldest occupation of Mutul (Tikal) (Figure 2.9) also occurs (Drew, 2015)

In the Late Preclassic, 2250 to 1700 B. P., Kaminaljuyu (Figure 2.9) in the southern highlands is established as a significant political power (Michels, 1979), as well as Mutul (Tikal) in the central lowlands. El Mirador (Figure 2.9) turned into the most important centre for trading in the lowlands (Sharer and Traxler, 2005). The Peten region became highly populated, and the city of Lamanai (Figure 2.9) was established in Belize. In this time, the Mayab had a low population density while the other areas were filled with payolelo'ob ruled by family dynasties, which marked the beginning of a new political organization (Schele and Freidel, 1990).

At the end of the Late Preclassic Mesoamerican Horizon between 2250 years B. P.to 1700 years B. P., various cities were abandoned in the southern Lowlands in a critical period in Maya history known as the Maya Abandonment (1800 years B. P.to 1750 years B. P.) (Houston and Inomata, 2009). Kaminaljuyu declined, and El Mirador was abandoned during this period (Drew, 2015).

During the Early Classic Mesoamerican Horizon 1700 years B. P. to 1400 years B. P. Kaminaljuyu recovered its power and Lamanai thrived (Houston and Inomata, 2009). New settlements in the north of the Peten flourished as a result of the diaspora resulting from the destruction of El Mirador (Drew, 2015). The early Classic Period around 1700 years B. P. brings the interference of the political power of the city of Teotihuacan in the centre of Mesoamerica into the Maya Cultural Area. It is unclear what the role of Teotihuacan was in the warfare between Mutul and Uaxactun (Figure 2.9) at 1622 years B. P. (328 A D), but most hypotheses imply some degree of involvement in the conflict (Drew, 2015; Schele and Freidel, 1990). The warfare between the two cities was a story of intermittent battles, revenge and marionette kings controlled by one dynasty or another. This conflict extended for more many decades and finished with the destruction of Uaxactun at 1572 years B. P. (378 A D) (Houston and Inomata, 2009). It looks like Teotihuacan also played an essential role in the recovery of Kaminaljuyu during this period, establishing trade routes and monopolising the green obsidian trade and gaining privileged access to commodities such as jade, quetzal feathers, cacao and other products (Houston and Inomata, 2009). Teotihuacan's political influence might also have been related to the flourishing of another city, the city of Copan (Figure 2.9) (Houston and Inomata, 2009). Chinkultik (Figure 2.9), the biggest centre near to our study site at Lake San Lorenzo in the Laguna de Montebello Lake Complex,

next to the Comitan Valley (Figure 2.9), probably functioned as an outpost of Teotihuacan in the trade routes between Kaminaljuyu and Teotihuacan.

The Late Classic Mesoamerican Horizon between 1400 to 1200 years B. P. started with the Maya Hiatus (1414 years B. P.), a time when Mayan artists stopped producing inscriptions and monuments (Moholy-Nagy, 2003). This phenomenon has been argued to be a local circumstance that happened only in Mutul (Drew, 2015; Foster, 2001), but similar trends might have happened in Kaminaljuyu and Chinkultik. The Maya Hiatus also coincides with the decline of Teotihuacan (Nichols and Pool, 2012). The eruption of the volcano El Llapango in El Salvador at 1414 years B. P. is argued to be responsible for such a calamity (Demarest, 2004). Other explanations involve substantial political and economic changes at Mutul (Tikal) and the Peten region (Figure 2.9) in general (Sharer and Traxler, 2005) and a dry period (Webster et al., 2007). As a result, Chinkultic started a period of decreasing population (See chapters 5 and 7)(Franco-Gaviria et al., 2018).

The Late Classic Horizon showed the settlement of new cities across the Mayab. During this time, Copan thrived, developing new trade routes as a result of the decline of Teotihuacan (Schele and Freidel, 1990). Kan (Calakmul) (Figure 2.9) was established as a centre of some kind of federal political entity, which threated the political power of Mutul (Tikal) after the disappearance of its allies of Teotihuacan (Drew, 2015). Kan (Calakmul) took control of Mutul (Tikal) in 1388 years B. P. (Houston and Inomata, 2009). After 1350 B. P. the dynasty of Pakal ruled B'aakal (Palenque) (Figure 2.9) making the city flourish in the region, taking the city to its peak (Gerardo Aldana, 2007). As we see in the following chapters, in the Cochua Region a period of decreasing population occurred (Table 2.1), where only Yo'okop (Figure 2.9) contained a sizable resident population (see chapter 9) (Shaw, 2015b). During this Horizon, B'aakal (Palenque) started a series of wars with its neighbours. Warfare was more frequently described in the ancient texts for this horizon in different centres of the Maya Southern and Central Lowlands, particularly in the Petexbatun Region (Figure 2.9) and Western Peten Region (Demarest, 2004).

B'aakal (Palenque) survived after the demise of the Pakal dynasty, but is abandoned around 1050 years B. P. (Schele and Freidel, 1990), during the time of what has

been referred to as the Maya Classic Collapse (1190 to 1140 years B. P.) when centres across all the Maya Cultural Zone were abandoned (Gill, 2000).

Table 2.1 presents the relative population sizes in percentages for some regions in the Lowlands for every horizon estimated from the archaeological record (Culbert and Rice, 1990). This table gives an idea of the size of the abandonment that occurred after the Maya Collapse. Most regions had their maximum populations in the Late Classic, presenting a decline at the Terminal Classic Horizon. The regions of Central Peten in the Central Lowlands were those with most loss of population according to Culbert & Rice (1990). It has to be highlighted that models of population based on the discovered sites indicate that the population was far from being homogeneous across the lowlands, and big differences existed in population and density of population between political centres and peasant settlements; and between the different regions (Ford et al., 2009). For instance, the estimate population for central Mutul (Tikal) in the Late Classic was 11300 habitants, whilst the peripheral of Mutul had 50700 habitants (Culbert and Rice, 1990). In comparison, Seibal (Figure 2.9) had 1600 habitants at the political centre and 8000 habitants in the periphery. Unfortunately, archaeological research in the Comitan-Chinkultik Region (Figure 2.9) (Navarrete, 2007), as well as the research in the Cochuah Region (Figure 2.9), started only in this century (Shaw, 2015a), therefore there is not enough conclusive data for giving an absolute estimated number of the population in these regions.

*Table 2.1 Relative population sizes by Mesoamerican horizons, as percentages of maximum population estimates, at selected lowland sites after Culbert & Rice (1990). * Percentages of the maximum population at Cochuah Region were calculated for this thesis based on the total sherd (broken pieces of ceramic material,) counts by horizon studied by Shaw (2015b).*

	Central Peten Lakes							Northern Mayab	
	Mutul/ Yaxha	Macanche/ Salpeten	Quexil/ Petenxil	Yaxha/ Sacnab	Belize Valley	Seibal	Becan/ Kan	Dzibilchaltun	Cochuah*
Late Postclassic	-	10	-	-	21		-	6	3
Early PostClassic	-	19	2	8	-	14	29	5	100
Terminal Classic	92	29	29	11	50	85	59	-	-
Late Classic	100	100	100	100	100	85	100	100	4
Early Classic	84	8	5	46	50	34	94	5	12
Late Preclassic	100	18	10	29	93	100	94	29	22
Middle Preclassic	41	25	34	13	52	28	9	-	6

An overall population density in the Late Classic has been estimated at between 100 and 1000 habitants per square kilometre (Culbert and Rice, 1990). Considering 1000 habitants per square kilometre, it would imply a similar density population to today's Sri Lanka (Ford et al., 2009) or Bangladesh population. A more realistic overall estimation based on the technology managed by the Maya and the environmental resources is 100 habitants per square kilometre, implying a population around 10 to 20 million in the lowlands (Gill, 2000).

The Maya Collapse period is part of the Terminal Classic Horizon. There are discrepancies between the times constrained by this Horizon. Therefore, some authors prefer to call this time and the first years of the Postclassic Horizon, the Epiclassic (Demarest, 2014). In this thesis, we use the time-constrained period between 1190 to 850 years B. P. for designated the Terminal Classic Horizon which was used in the Cochuah Regional Archaeological Survey (Shaw, 2015a), due to the relevance of that region to our research. The Cochuah Region is relevant to this thesis since Lakes Chichancanab and Esmeralda are in this jurisdiction.

During the Terminal Classic Horizon, Uxmal (Figure 2.9), and other cities in the Puuc Region in the Mayab flourished (Grube et al., 2012). Some hypotheses argued that the Puuc Region apparently could be the result of the introduction of Nahua people (from Central Mexico) into the Maya Cultural Area during the times of the Collapse (see section 3.9 in next chapter) (Segura, 2017). The inhabitants of the Puuc region (Figure 2.9) were then threated and finally beaten by the Chenes (Figure 2.2) at 900 years B. P. (Grube et al., 2012; Sharer and Traxler, 2005). The Cochuah region started to be relatively high densely populated (Shaw, 2015b). Lamanai continued existing after the Maya Classic Collapse (Sharer and Traxler, 2005) as well as Chinkultik in the northern highlands (Álvarez, 1993; Navarrete, 2001), while other cities collapsed in the Comitan valley in the Northern Highlands (Álvarez, 1993). Chapter 3 explores the Maya Collapse in greater depth.

The Postclassic Mesoamerican Horizon (850 to 450 years B. P.) was marked by a civilisation which abandoned most of the big cities, returned to small villages and lost literacy (Michels, 1979). A new religion related to the figure of Kukulkan also gained followers (Navarro, 2008). Both these facts were a sign of a great change of life in the Maya Society.

The Later Postclassic was also characterised by the introduction of non-Maya people into the Maya Cultural Area. A new power was exerted by Zoques in the South Pacific Coast of the highlands (Calderón et al., 2006). The northern highlands received the migration of the Soctona, an Oto-Mangue ethnic group from Nicaragua (Navarrete, 1966). While Chichen Itza (Figure 2.9) thrived, and Tulum (Figure 2.9) was established (Sharer and Traxler, 2005), some cities in the Comitan Valley were abandoned (Álvarez, 1993). The influence of Toltecs into the Maya region marks the foundation of the city of Mayapan (Figure 2.9) during this time frame. The Toltecs emerged in the central highlands of Mesoamerica after the Collapse of Teotihuacan, having a strong influence in Chichen Itza. Mayapan started to rule the Mayab after the collapse of Chichen Itza (850 years B. P.) in a superstate, (Sharer and Traxler, 2005) although it has been theorised that this superstate was a later invention of Maya people during the colonial period (Nichols and Pool, 2012). Most of the Maya settlements resisted the bellicose campaigns of the later Aztec Empire (Drew, 2015). The Mayapan superstate ruled the Mayab for a century. Mayapan then enters into a phase of internal disputes (Sabloff, 1994). After its disintegration (509 –489 years B. P.), the Mayab was divided into sixteen independent jurisdictions called "Kuchkabal". Tixhotzuc (Tihosuco) (Figure 2.9) was the capital of the kuchkabal of Cochuah, which was still independent of the Spanish crown during all the XVI century (Riese, 2006).

At 1519 A. D. (431 years B. P.), the Spanish arrived in the Maya Cultural Area. After defeating the Aztec empire in the centre of Mesoamerica, the Spaniards and their Mesoamerican allies, the Tlaxcaltecs started campaigns to incorporate the Maya settlements into the Spanish rule. Most of the cities in the highlands fell under the control of Spaniards during the century after their arrival. Nevertheless, a lot of Maya hid in the moist broadleaf evergreen forest to preserve their freedom and traditions. This behaviour was the case of the Lacandons in the rainforest of Chiapas, which transformed themselves into hunter-gathers to survive in a new ecosystem, where the Spanish could not follow them (Boremanse, 1998; Eroza-Solana, 2006). The city of Lamanai was not abandoned until 1700, two centuries after the arrival of Europeans (Pendergast, 1986).

The Spanish established a series of "encomiendas", where the Maya were incorporated in a regimen of de facto slavery (García de León, 1985; Ruz, 1992).

In 1750 A. D. (200 years B. P.), British pirates and merchants gained control of the area of modern Belize (Bolland and Shoman, 1977). With the foundation of the modern nations of Central America and Mexico around 1821 A. D., the British declared Belize as part of its empire. The onset of the new industrial era converted the Maya Cultural Area into a source of commodities of exotic crops (e. g. rubber, gummy latex, coffee) and textiles, including henequen (Evans, 2013; García de León, 1985; Pérez Domínguez et al., 2001).

After the formation of the modern nations, the Maya people entered into an uprising for decades in the XIX century (Caste wars). The response was the attempted genocide against the Maya (Paoli Bolio, 2015). During the XX century, the regime of de facto slavery imposed by the Spanish slowly disappeared due to the lack of market for and value of the traditional commodities in the new industrial era (Grube et al., 2012). Political reforms resulting from the anticapitalist Mexican revolution of 1910 established a quasi-socialist government in the Mayab region, which helped in the destruction of the facto slavery (Diaz-Bolío, 1998), but similar reforms were never applied in Tabasco and Chiapas. A similar situation to these two states existed in Guatemala and Belize.

For the second part of the XX century, various guerrilla groups started, first in Guatemala and then in Chiapas, fighting for the human rights of the Maya people. Economic inequality persists in the Maya Cultural Area, where the modern Maya are one of the most marginalised population (Bracamonte y Sosa and Lizama-Quijano, 2003).

2.6 Conclusion

This chapter describes the geographical, geological, climatic and historical context of the Maya Cultural Area. This area presents a complex diversity of landscapes reflecting the diverse altitudes, geology, vegetation and climatic agents in the region.

Despite this diversity, Maya people have populated the different ecosystems maintaining a cultural unit. This culture suffered changes over time, mainly associated with the concentration of population in a specific area (population centres). These population centres managed the natural resources not only in the surroundings but in the rest of the territory. These specific areas changed, for

example, during the Preclassic Horizon, the Southern Highlands and the Southern Lowlands concentrated political power, being the most populated regions. During the Classic Horizon, the Central Lowlands was the most populated area, exerting significant political influence over the rest of the zone. During the time of the collapse, the Puuc Region was the most populated area, concentrating political power. Finally, during the Postclassic Horizon, the Mayab became the most densely populated region, becoming the heart of the Maya Culture. All these changes reflect a migration across centuries which cannot be explained only by human agency but responding to changes in the environment.

This chapter also provides a brief introduction to the Cochuah and Lagunas de Montebello regions, which are relevant since our study sites are inside these regions. A more detailed description of our study sites is presented in chapter 5. The next chapter deals with the possible explanation of the most studied change in Maya civilization the 'collapse'.

Chapter 3 The Maya Collapse

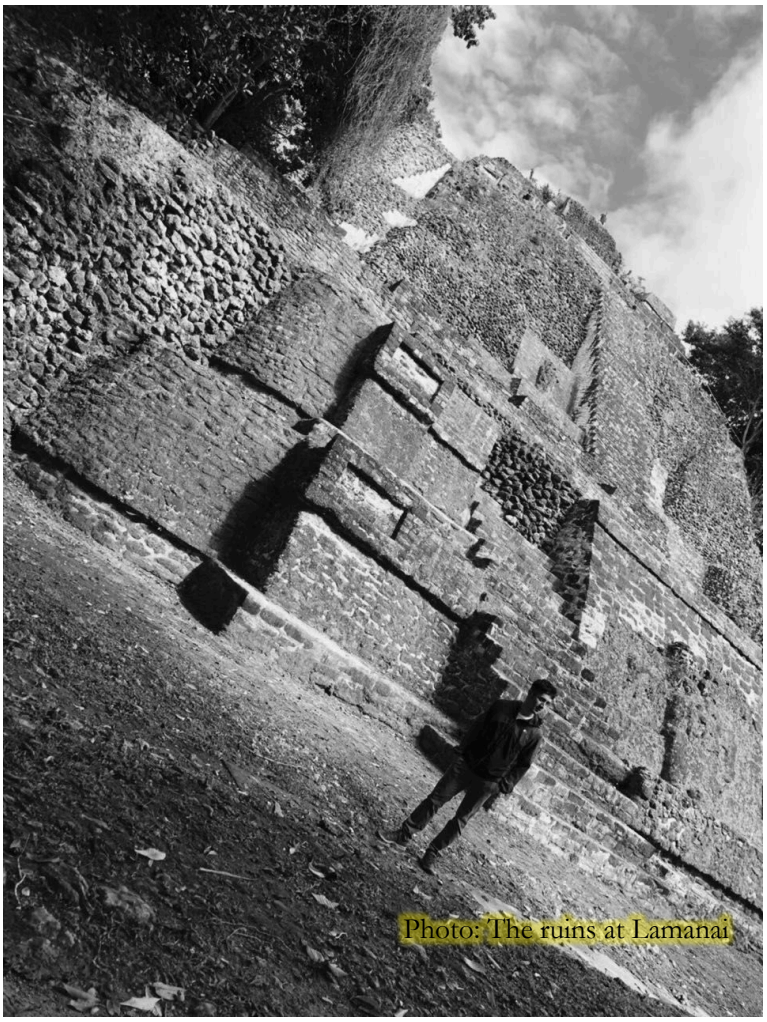

Photo: The ruins at Lamanai

"What induced the Mayas to abandon the enormous capital represented by their sacred cities? Nobody knows. Almost certainly they were not invaded, and there is no sign of their monuments having suffered from destructive earthquakes. Some archaeologists believe that their agricultural methods exhausted the soil and that the population could no longer feed itself; others, that there was an almost sudden change of climate, involving heavier rainfall, a more luxuriant and, for the Mayas, uncontrollable forest growth and an increase of yellow fever and perhaps malaria."

Beyond the Mexican Bay, Aldous Huxley, 1934.

Besides the questions related to the arrival of the anatomically modern human to the American continent (Waters, 2019), the Maya collapse is arguably the most unsolved mystery in the study of past societies in the Americas. At this event, the Maya society suffered deep cultural, political and socioeconomic transformations, when an important number of settlements were abandoned in 150 years (1190 to 1040 years B. P. or 760 to 910 A. D.), including most of the more powerful payolelo' ob. The purpose of this chapter is to show how the concept of the "Maya Collapse" was developed, what its definition is, as well as the theories developed for explaining both the drivers of the collapse and the possible scenarios lived by humans.

3.1 A brief history of the evidence of collapse

Although Diego de Landa, first catholic bishop of Yucatan in the XVI century A. D., attributed the construction of the numerous ruins in the Mayab to the ancestors of his contemporaneous Maya (Drew, 2015), the idea of a civilisation collapse was theorised first by John Lloyd Stephens and Frederick Catherwood after their expedition in the XIX century (Stephens, 1854). They understood that the ruins were constructed by the ancestors of the Maya, but thought that the ruins had been occupied practically until the arrival of the Europeans (Stephens, 1854). In this way, they viewed that a collapse would have been a result of the Spanish conquest. They thought that in the dense moist broadleaf evergreen forest of the XIX century, some Maya settlements with kings ruling and architects constructing new temples would have survived the collapse provoked by the arrival of Spaniards. Nevertheless, such an idea was incorrect, since the last Maya city Noj Peten, fell to Spanish troops in 1697 (Rice and Rice, 2009), more than a century before the expedition of Stephens (Drew, 2015). In addition, the Maya ruins reflected settlements that had been abandoned centuries before the Spanish arrival. For example, the Lacandons, Maya hunter-gatherers in the moist broadleaf evergreen forest in the north part of the Southern Lowlands, venerated the ruins of the city of B'aakal (Palenque or el Tortuguero), attributing its construction to the Gods (Boremanse, 1998; Eroza-Solana, 2006). It is unclear if this veneration existed at the arrival of the Spaniards, although highly probable, but it has been documented since the XVIII A. D. century (Stephens, 1854). This incorporation of the ruins into the Maya mythology reflects that many cities had been abandoned for centuries.

The modern idea of a collapse of the Maya civilisation came from the works of Morley (1946), where he revealed how the use of the Long Count changed during time. The Long Count is the non-repeating Mesoamerican calendar combining a base 20 and a base 18 calendar. One of the units of the Long Count is the k' atun, composed by 20 tuno'ob or years. At the same time, 20 k' atuno'ob forms a b'aktun (Figure 3.1).

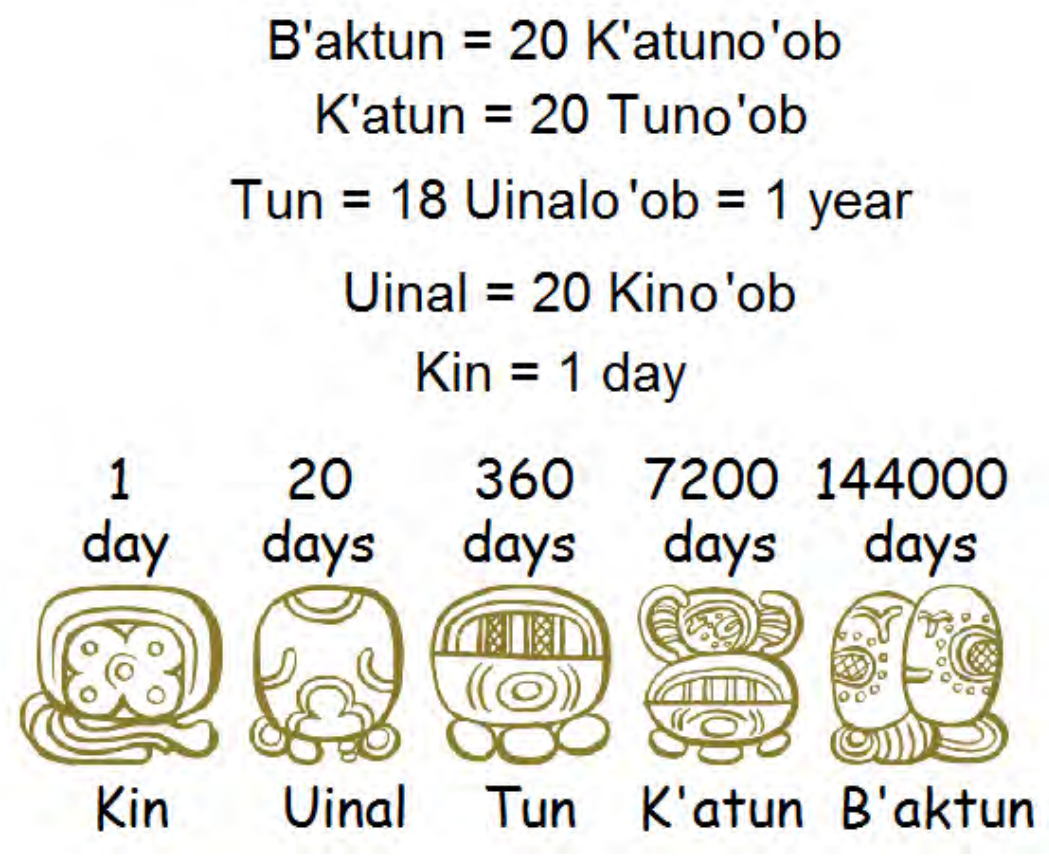

Figure 3.1 Schematics of the long count Maya calendar, which indicates the vigesimal system of countings. Suffix o' ob indicates plural.

The Classic period (see section 2.5 in chapter 2), was between the eighth to tenth b'aktun. Morley (1946) presented a chart of the number of cities with a particular date written on monuments (Figure 3.2). Most of the documented monuments used by Morley (1946) were in the Central and Southern Lowlands (Figure 3.3) because archaeological research was focused in these areas at that time, but the idea of the collapse was extrapolated to the entire Maya Cultural Area. The Central and Southern Lowlands are between the Mayab and the Northern Maya Highlands (see Figure 2.8 in chapter 2), where the study sites of this thesis are located. Therefore, it is sensible to think that our study sites might have been impacted in some way by the changes suffered in the Central and Southern lowlands.

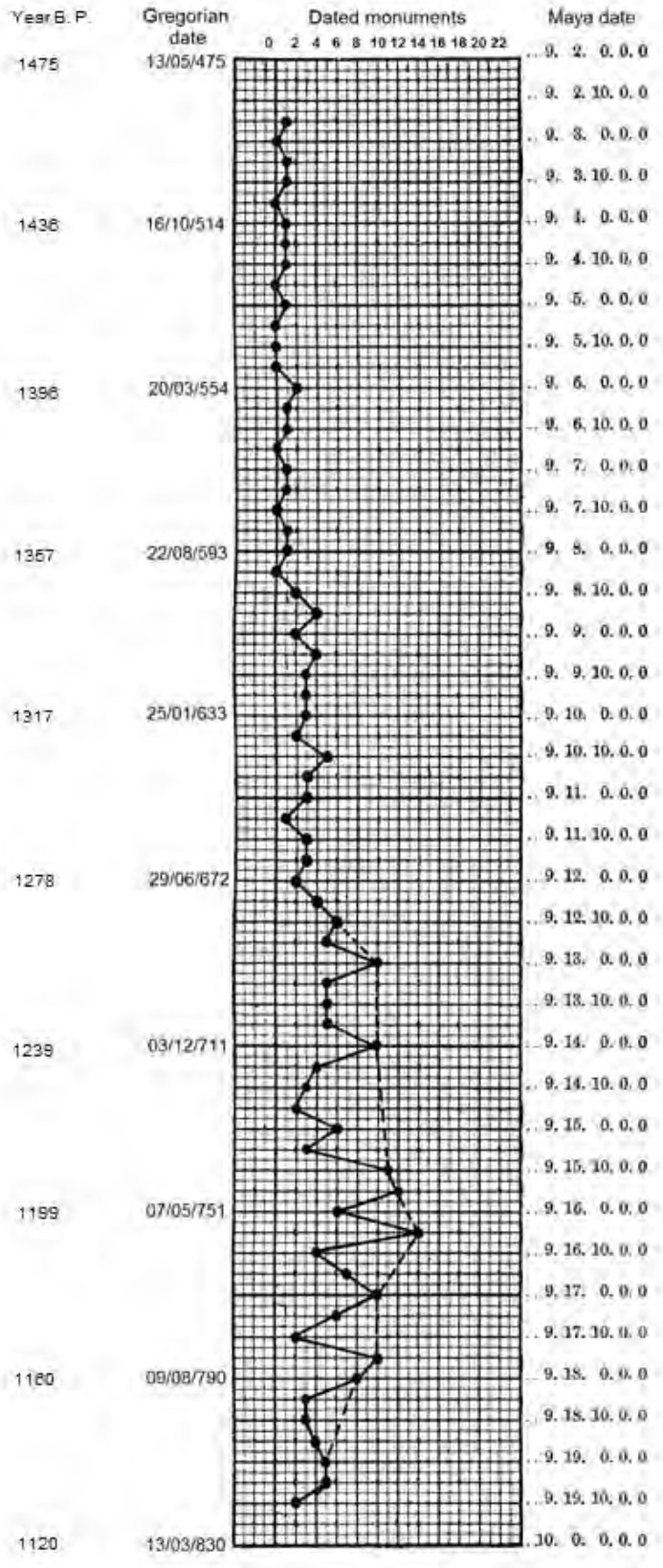

Figure 3.2 Number of dated monuments constructed in the Mesoamerican Classic Period after Morley (1946). The left column indicates the gregorian calendar date (AD/CE) corresponding to the Mayan date calculated by me using the Goodman-Martinez-Thompson correlation of 584,283 days, although the Julian calendar was used during that time in western countries.

The date on a monument usually indicates the date of the construction of it, since any inscription in Classic Mayatan (the languages of ancient maya) started with a date. Few monuments have a date prior to 1317 years B. P. (633 A. D.) After this, the number of monuments starts to accelerate. The production of them reach their highest between 1219 to 1160 years B. P. (731 to 790 A. D.), then, there is a precipitous drop off in monument building, with only some new monuments remaining at 1130 years B. P. (Figure 3.2). This chart (Figure 3.2), produced by Morley (1946), did not take into account many monuments which had an illegible inscription, as well as the many sites without dated monuments (Figure 3.3). In addition, it is clear now that many governments disappeared before the last inscription in a settlement and many survived after the production of the last inscription. Nevertheless, the chart was a good proxy of the trends of cultural production. At the end of the day, the chart gave a date for the collapse (Webster, 2002).

Outside the early documented monuments in the Central and Southern Lowlands, other sites with dated monuments have been found in Chichen Itza, the Puuc Region and in the Northern Highlands (Figure 3.3), including the site of Chinkultic, which is relevant for this thesis (see section 2.5 in chapter 2, section 3.11 in chapter 3 and section 5.8 in chapter 5). Unfortunately, no monuments with dates have been found in the Cochuah Region.

Archaeological excavations showed that in some centres, during the period of the collapse, there were building projects that were abandoned before finishing and local ceramic traditions appear to become less sophisticated or disappear (Webster, 2002). These results and the Morley chart led scholars in the first part of the XX century to postulate a Maya collapse resulting from a demographic catastrophe, that diminished the population within a period of many decades (Thompson, 1966). For Thompson (1973), it was clear that the interval spanned by inscriptions on the monuments bears no relation to the actual last occupation of a site. For him, the Maya common people would not have died but faded away (Thompson, 1966). It was clear from Morley (1946) 's chart that the collapse had been a gradual process. For instance, in some centres, the last monument was raised more than a century before the last monument at Kan (Calakmul) 1141 years B. P. (909 A. D.) (Figure 3.3), where the last monuments with inscriptions in a city that did not survive to the Post Classic Mesoamerican Horizon in the Maya Cultural Region were erected (Webster, 2002).

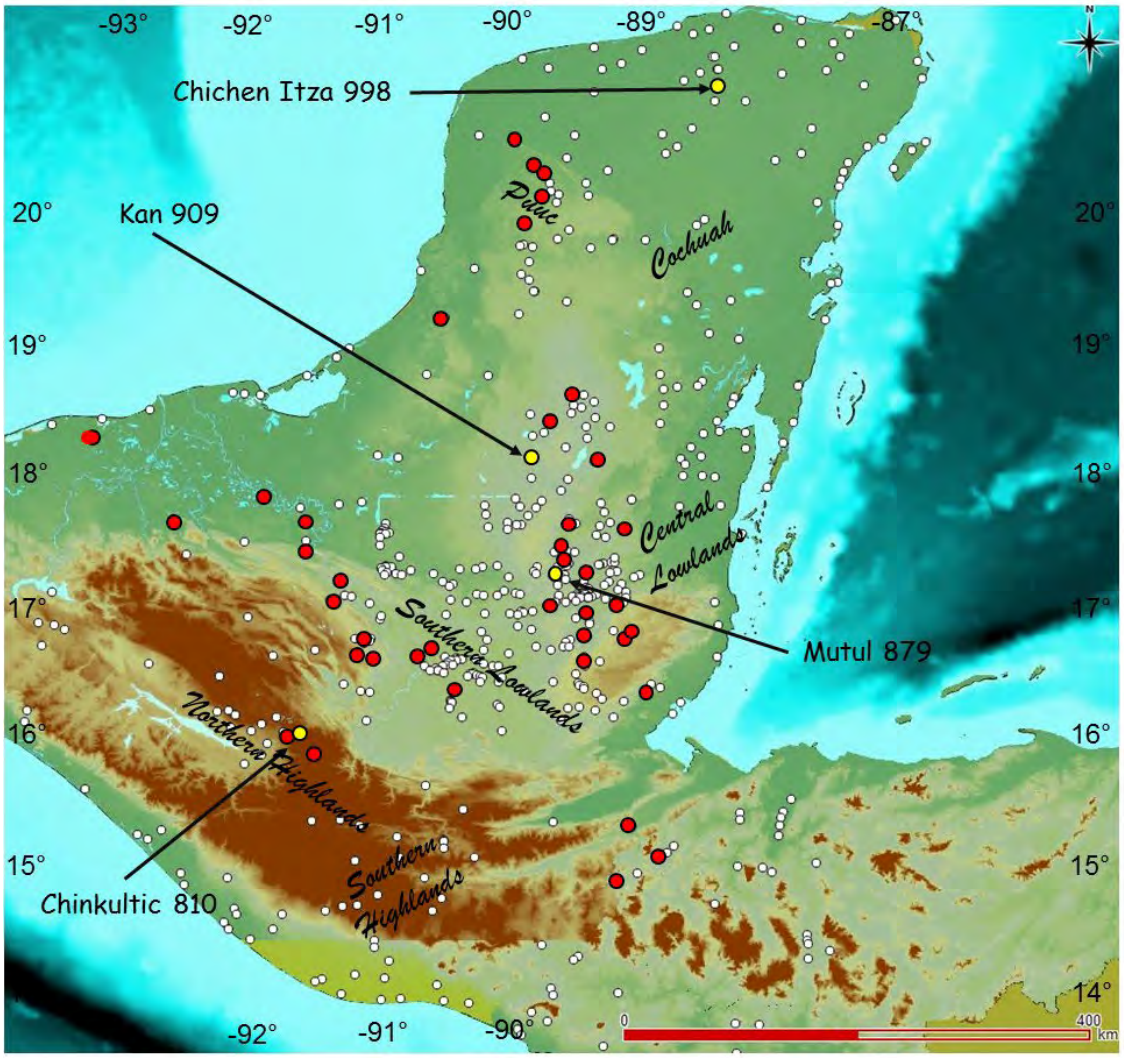

Figure 3.3. Map showing the settlements with the year of their last monument erected (red dots) in contrast to settlements without a date on monuments (white dots). It can be observed that many settlements do not have a date even in the lowlands. In comparison, some cities in the highlands (> 1500 m. a. s. l.) like Chinkultic have dates, which were not considered by Morley (1946) and subsequent works. The years are obtained from the calculated year in the Gregorian calendar from the date sculpted into the monument. The map is based on Grube & Schubert (2015), showing the location of the last monuments presenting a date. Cities highlighted in yellow indicate the sites with monuments presenting a date that are referred to this section. Mutul (Tikal) and Kan (Calakmul) started the collapse after a confrontation in 1190 years B. P. (760 A. D.). However, both cities did not fall until the last stages of collapse. The 530 ancient Maya settlements (white and red circles) presented are based on Ford et al. (2009). Chinkultic is relevant since it is next to Lake San Lorenzo, one of the study sites in this thesis. Unfortunately, no dated monuments have been found in the Cochuah Region, where Lake Esmeralda, the other studied site in this research is.

An update of Morley's (1946) chart (Figure 3.4) using radiocarbon samples of skeletons and charcoal in the Maya Cultural region (Sudrys and Berger, 1979), with samples linked to activities of the Maya elite (Figure 3.5a) pointed to a decline around 1201 to 1041 cal. years B. P. (749 to 909 A. D.) (using Intcal13; ages were calibrated with a different curve

in the original article). A similar trend was found in the radiocarbon samples linked to common people (Figure 3.5b). Samples selected for this purpose are problematic from many angles, such as the criteria of sample selection, contamination issues, and location. However, looking at the radiocarbon dates, a peak can be observed around 1361 to 1201 years B. P., which coincides when the maximum number of inscriptions on monuments (Sudrys and Berger, 1979). Although the chart based on monuments indicates the collapse from 1140 years B. P. (810 A. D.), scholars typically identify the period of the Collapse from 1190 to 1040 years B. P. (760 to 910 A. D), since Kan (Calakmul) started to collapse after 1190 years B. P. (760 A. D.) (see above), being the first major power in the region showing political stress (Grube and Schubert, 2015).

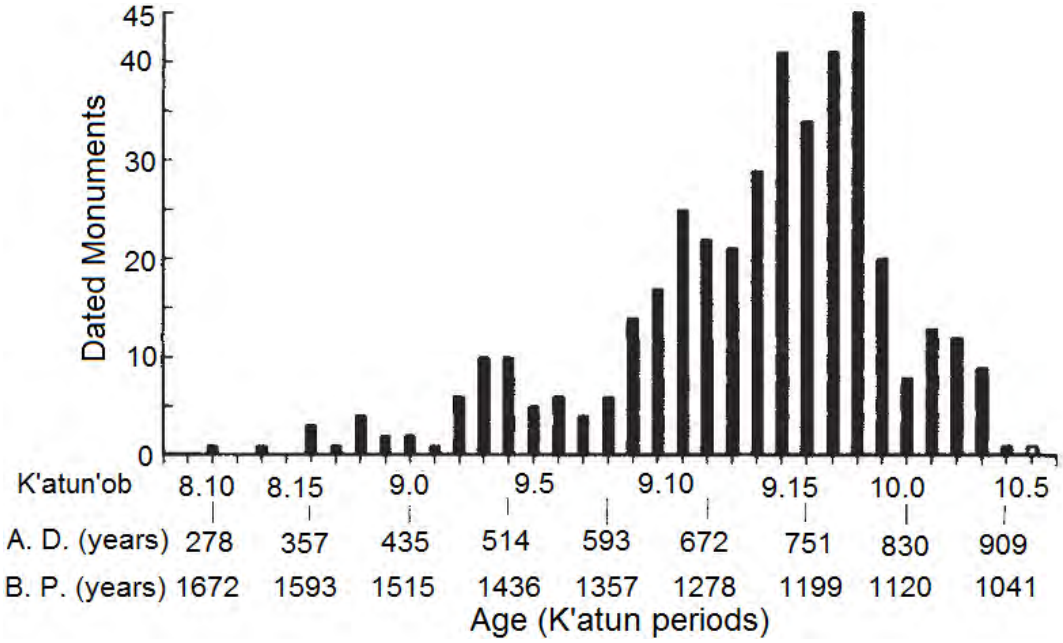

Figure 3.4 Number of dated monuments per k' atun in the Southern Maya Lowlands according to Sudrys & Berger (1979). These authors focused specifically on monuments in the southern lowlands for comparing with radiocarbon dates on samples obtained in that area. The purpose of this comparison was to assess signals of collapse in other materials of the archaeological record in addition to the monuments, as well as to establish differences between the elite and common people contexts (Figure 3.5). Although this study focused on the Lowlands, the idea of the collapse obtained from it has been extrapolated to the entire Maya Cultural Area. The Southern Lowlands are between the Mayab and the Northern Maya Highlands, where the study sites of this thesis are located.

In this way, during the XX century scholars were conceiving a socioeconomic and political phenomenon called a Maya collapse.

Although some monuments with a date have been discovered at sites not considered by Morely (1946) and Sudrys & Berger (1979), a more recent graph has not be produced since

processual archaeologists have prefered to use the number of archaeological finds for the purpose of establishing site occupations instead of dated monuments (Sabloff, 1990). The original concept of the Maya Collapse conceived by Morley (1946), has been observed in many kinds of finds. It is clear that the Maya Collapse, however, was a process of many decades, that was lived in different ways, and it impacted in a different way across the Maya Cultural Area. In this chapter, I explain the Maya Collapse, the different hypotheses and theories that have been proposed and their critics. Due to the nature of the central theme of this thesis, I focus on hypotheses related to changes in the environment, which as I propose in this chapter played a substantial role in the Maya Collapse.

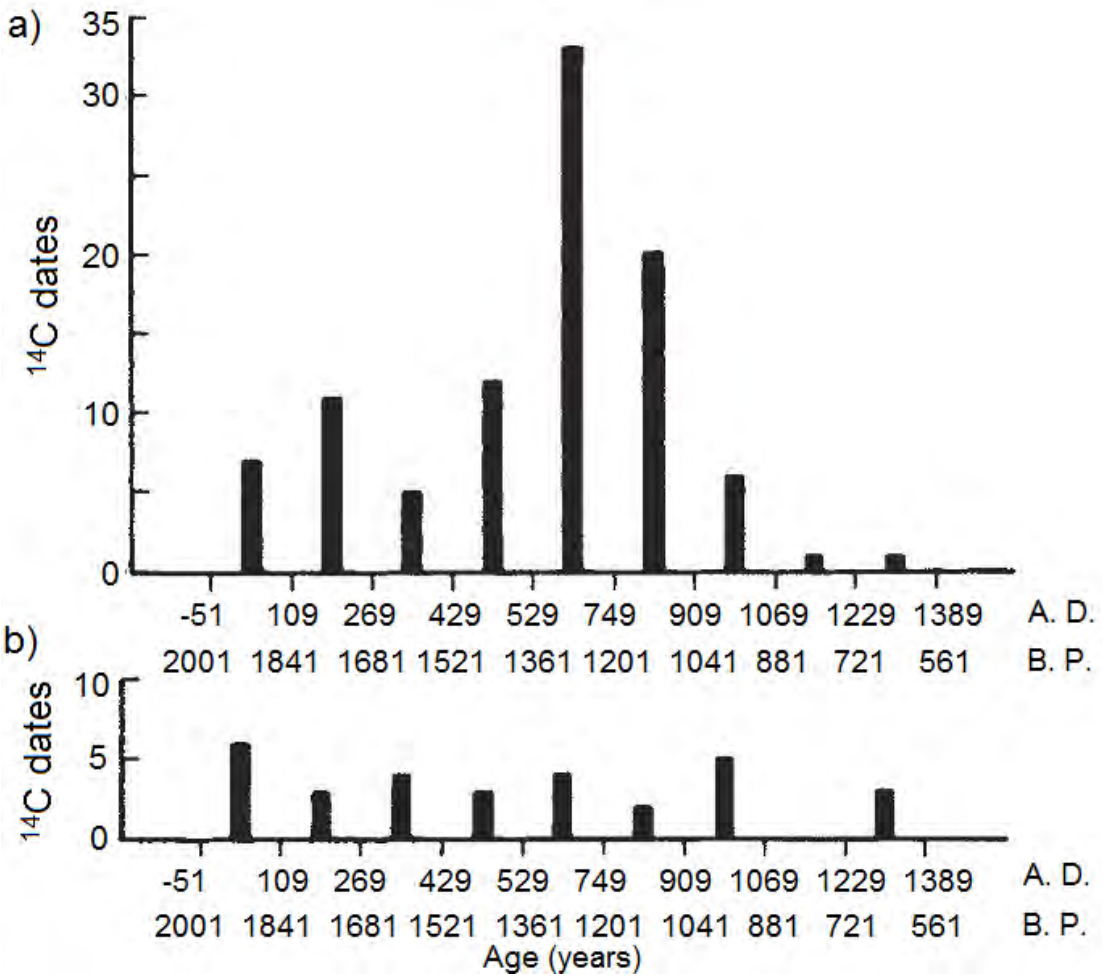

Figure 3.5 a) Number of radiocarbon dates from elite contexts in the Southern Lowlands. b) The number of radiocarbon dates from peasants and handicraftsmen contexts in the Southern lowlands. Data taken from Sudrys and Berger (1979).

3. 2 Maya Collapse or Maya Cultural transformation

Does the political phenomenon that happened in the Terminal Mesoamerican Classic period resemble a collapse like the fall of the old kingdom of Egypt (deMenocal, 2001), or look like just a cultural transformation like the fall of Rome? (Storey and Storey, 2017). Comparisons might be forced, and the event at the beginning of the Terminal Classic (1190 to 1040 years B. P.) might have been very different from any other societal process in the planet, although comparative studies exist elucidating how political entities disappear (Storey and Storey, 2017). So, why do we use the term "Collapse", instead of the words "cultural transformation" for referring to the change that happened at the Terminal Classic period?

First of all, it is worth noting that Mayan studies have been performed in six principal languages besides the Mayatan; Spanish, German, Russian, French, Italian and English. The Spanish word for indicating unusual situations among Mesoamerican cultures, which are linked with the disappearance of a culture (like the Maya Classic Collapse or the "Sunset" of the city of Teotihuacan or the "Sunset" of the Toltec civilisation) is "Ocaso", the same word is used in German "Untergang", which mean "sunset". The term "sunset" does not have necessarily the same meaning as collapse and implies just "ending", and it is used in the Mesoamerican context for indicating "disappearance of a political entity". Although the German literature has used the term “Untergang” for describing Armageddon scenarios for the Maya in the 1190 to 1040 years B. P. (Peterson and Haug, 2006). While the Russian term "Упадок" means "fall". The French term "effondrement", has a similar connotation as "collapse".

It can be argued that "collapse" seems to refer to an Armageddon scenario that leads to the rapid and absolute disappearance of a population, political system or civilisation or some combination of these (Mcanany and Yoffee, 2010), therefore the Maya collapse may not be the correct term to describe the variable, long-term process of Maya decline (Aimers, 2011, 2007). However, the classical political system was indeed reconfigured in the Terminal Classic Period.

A better definition defines collapse as any situation where the rate of change of a system:

- Has a negative effect on human welfare, which in the short or long term, are socially intolerable.

- Is more rapid and usually in the opposite direction to that preferred by at least some members of society.
- Cannot be stopped or controlled via an incremental change in behaviour, resource allocation or institutional values (Young et al., 2007).

In the case of Mesoamerica, continuous occupation and continuity in culture are observed with the Ben'zaa (Zapotec) civilisation in Oaxaca (Phillips and Jones, 2009) or the Mokaya culture (perhaps the last outpost of the Olmec) in the South Coast area in the same Maya Cultural Area (Evans and Webster, 2013). However, this is not the case for most of the payolelo' ob which were abandoned in the Terminal Classic period (Charles and George, 2010; Phillips and Jones, 2009; Thompson, 1966) consequently the cultural productivity of handicrafts and monumental architecture stopped. Only the cities in the Puuc region, e. g. Uxmal, Labna and the cities towards the northern tip of the Mayab, such as Mayapan, Chichen Itza and Coba continued and thrived (Andrews et al., 2003).

The effects of the collapse in the highlands are still less understood. It is known that some payolelo'ob in the highlands also thrived in the Postclassic period until the European incursion (Wilhelmy, 1981), while others were abandoned (Álvarez, 1993; Navarrete, 2001). Some argue that the survival of the settlements in different subareas of the Maya Cultural Zone is sufficient to say that the Maya civilisation as a whole did not collapse, although many zones did experience a profound change in the lowlands (Aimers, 2007). However, even if "collapse" is not the best term, the Maya experienced a colossal human tragedy during those years, which changed them profoundly (Grube et al., 2012; Phillips and Jones, 2009). Therefore, there is no continuity, but disruption in the Maya cultural life. According to the definition of Young et al., (2007), the Maya Cultural Zone as a whole experienced a collapse.

It is the opinion of this author that the term "sunset" should be used instead of the term "collapse" since collapse tends to evocate an Armageddon scenario despite the definition of Young et al. (2007). This term also is appropriate to the Mesoamerican cosmovision, which is based on the sun, moon and star cycles. However, in this thesis, I will use the terminology "Maya Classic collapse" for the event suffered between 1190 to 1040 years B. P. since it is more commonly used in English.

3.3 Evidence of the Mayan Classic Collapse

The event between 1190 to 1040 years B. P. described as the "infamous" Terminal Classic collapse by Iannone (2014) is one of the critical moments of the Maya past. The collapse was well underway by 1120 years B. P. (A. D. 830) (Culbert, 1973). Despite the uncertainties that this phenomenon has around its cause and exact nature, as discussed above, the recent interpretations of the archaeological and historical records according to Grube et al. (2015), Iannone et al. (2014) and Webster (2002) suggest that:

- Royal dynasties disappeared over a region of the southern lowlands. In some payolelo'ob, this happened rapidly, but it took more than a century to affect the complete subarea.
- Royal courts stopped functioning as centres of dynastic power and cultural influence
- Monuments were no longer produced, and royal buildings were no longer constructed or maintained.
- Elaborate burials ceased, as well as the production and exchange of sumptuary goods.
- Major settlements were abandoned (although there were exceptions) without a sign of widespread and severe violence or destruction. In many sites, monuments were subsequently destroyed or defaced. Royal buildings and tombs were robbed.
- At some payolelo'ob, no royal elites and most of the supporting population, including peasants, disappeared at the same time as the kings lost power or very shortly after that. In contrast, payolelo'ob where the royalty and farmers survived, experience a rearrangement of the royal traditions.
- The political disruption happened where there were a larger number of ruling dynasties than at any time before. Thus, court centres were more numerous, and the population reached its maximum size and density. After the collapse, the population never reached its previous size until the conquest of Itza by the Spaniards in 1697.
- The final fact related to the Maya collapse is the existence of a climate change to a dry period (or series of droughts), according to multiple environmental proxies (see chapter 4).

In contrast, there are some unknown critical points which are indispensable for assessing any hypothesis of collapse. For example, we do not know about:

- The social order in the classic Maya society. Three models have been proposed: the linage model, a stratigraphic model, and a house model. A detailed explanation of these models is found in Webster (2002).
- The political and social relationships between Maya people of different ranks, both among and within particular payolelo'ob
- Precisely how the Maya lords, the ahau'ob (some kind of kings) respond, how an ahau managed their territory concerning subjects, subsistence economies and agricultural landscapes
- If ahua'ob controlled essential flows of staple goods such as crops or the production, acquisition and redistribution of goods, and how they manipulated either of these as a political currency.

The relationship between the general people and royalty is critical to understand the probable responses to the possible drivers of the collapse, such as wars, natural disasters, disease, droughts or environmental degradation. At the same time, knowing the royal tasks and power is essential for understanding the response of ahau'ob to the possible scenarios during the collapse.

Most scholars propose that the collapse started with warfare between Mutul (Tikal) and Kan (Calakmul), where the city of Kan was conquered by the warriors of Mutul. This conquest happened 50 years before the first strong drought event at the Terminal Classic Horizon at 1140 years B. P. according Hodell et al., (1995). However, the dry phase started since 1192 years B. P. according the observations in the stalagmite MC01 in Belize (Webster et al., 2007). A series of wars in the southern lowlands were triggered as a result of the defeat of Kan. At the beginning of the drought period, the war stopped, and alliances were created, according to the epigraphy (Grube et al., 2012), showing that the Maya were aware of the difficulties that they had related to environmental issues. The pattern of the last inscribed dates at Maya sites indicates a slight southwest to northeast trend in the collapse sequence (Lowe, 1985). The settlements near to the rivers on the west side were abandoned first. They were followed in the next years by the cities around the Peten lakes (in modern Guatemala). The abandonment of the cities continued toward the north in the following years. During this period, the Puuc region thrived, concentrating the majority of population and density of population in the Maya Cultural region during the collapse and

in the Early Postclassic. Similar migration occurred to the centre and north of the Mayab, where new settlements appeared or increased their size, including more than 100 settlements in the Cochuah Region, near Lake Chichancanab, one of the three biggest lakes in the Mayab (Shaw, 2015a, 2015b).

The details of the Maya collapse used to be explained in terms of the drivers of the collapse, e.g. droughts, pandemic, political instability. But explanations arguing how specific populations, royal families or common people lived during this time frame are less often taken into account, presenting in many circumstances cognitive bias. For example, it has been proposed that the hypotheses and interpretations argued for explaining the Maya Collapse respond to the popular and scientific concerns of the western civilisation societies (Wilk, 1985). For example, according to Wilk, (1985), hypotheses proposing foreign invasion as a driver of the collapse responded to U. S. A.'s bellicose foreign policy in the 1960s and 1970s. When the media were concerned about over population in the 1980s, the collapse was explained by theories stressing demographic pressure. The hypothesis related to the overexploitation of the natural resources surged on the 1980s when the major environmental movements started (Wilk, 1985). Finally, the theory of the great Maya Droughts gained adherents while the scientific community reached a consensus about the certainty of planetary global warming (Webster 2002). These correlations between theories explaining the collapse and modern concerns does not imply that these theories do not have a role in explaining the complexity of the Maya collapse. However, it seems that during the time of particular concern, a related theory tends to predominate, provoking bias, due to the scientific attention, peer acceptance and possibilities of funding (Webster, 2002). The lack of details in the collapse is also produced by not incorporating a regional vision of the collapse. Paradoxically, local observations are often intended to be used as a general explanation of the collapse in all the regions.

The end of the time frame of the Maya Collapse (1040 years B. P or 910 A. D.) is usually considered the end of the Terminal Classic Horizon (but not in this thesis, see below) marked by the last known recorded hieroglyphic date of 1041 years B. P. (909 A. D.) at Kan (Calakmul). This coincides with the societal changes in the Central Highlands of Mesoamerica (Vela-Ramirez and Solanes-Carraro, 2000). However, due to the complex changes during these years, scholars tend to put together the events from 1190 to 750 years B. P. (760 to 1200 A. D.) calling them the Epiclassic Horizon (Nichols and Pool, 2012). As stated in chapter 2 (section 2.5) of this thesis, the chronology proposed by the Cochuah

Archaeological project is used (Shaw, 2015b). Therefore, the end of the Terminal Classic Horizon in this thesis is 850 years B. P. (1100 A. D.) In this way, the Maya Collapse period covers only 150 years of the defined Terminal Classic Horizon for the Cochuah Region.

3.4 The Drought Hypothesis

The link between climate change and the collapse of civilisations has been proposed for different cases through the Holocene (deMenocal, 2001; Mayewski et al., 2004), e. g. the collapse of the Old Kingdom in Egypt (Gibbons, 1993), the collapse of the Akkadian Empire (in modern Iraq) (deMenocal, 2001), the Tiwanaku collapse (in modern Peru) (Thompson et al., 1994), the Anasazi Collapse (modern Southwest USA) (Van West and Dean, 2000), and the collapse of Greenland's Norse colonies (Buckland et al., 1996) as well as the link between climate and cultural transformations e. g. Moche IV-V transformation (modern Peru) (Buckland et al., 1996) and the fall of the Tang civilisation in China (Yancheva et al., 2007). The dissolution of the Roman Empire has also been linked to climate changes (Decker, 2017; McCormick et al., 2012; Schreg and Sirocko, 2009). The link between the Maya Collapse and a dry period has not been the exception.

A scenario where climate change would be the driver of the depopulation of the Peten subarea was first proposed by Huntington et al. (1914), and restated some decades later by Sapper (1931). At that time, both authors thought that the Maya civilisation should have existed in grassland environments, with a prolonged annual dry period of scarce rainfall and contrasting temperatures as well as major differences between summer and winter. This scenario was assumed since the view at that time considered that high civilizations could not have been developed in tropical moist broadleaf evergreen forest type ecosystems. In this way, a climate change to a scenario of increasing rainfall provokes the proliferation of the moist broadleaf evergreen forest, which would be an inhospitable ecosystem for living for any high complex civilisation. Environmental studies showed that the Peten never had a woodland-grassland ecosystem. In the second part of the last century, some theories implying a megadrought were suggested, without presenting conclusive evidence (Webster, 2002).

Lamb (1982) mooted the possibility of drought as the primary cause of the abandonment of many cities during the Mesoamerican Terminal Classic period in the Maya Cultural Area. However, no evidence existed to support the hypothesis. This lack of evidence changed after the works of Hodell et al. (1995) and Curtis et al. (1996) using lake sediment cores.

These studies were used by Gill (2000) to support his theory of the Great Maya droughts. At the beginning of his book, he suggests an Armageddon scenario, imaging famine, destruction and death as consequences of the droughts. Gill (2000) describes the droughts as completely exogenous causes of the collapse, where the Maya were victims, without causing the drought and having few abilities to overcome them. Gill (2000) also discussed that the droughts were the driver, not only of the Maya Collapse at the Terminal Classic Mesoamerican Horizon but other critical moments in the Maya history, for instance, the Maya Preclassic abandonment and the Maya Hiatus (see chapters 2 and 4). He also highlighted the role of volcanic eruptions, some of them outside the Maya Cultural Area, to explain the primary driver of the droughts. Soon after the work of Curtis et al., (1996); Hodell et al., (1995) and the theory of Gill (2000), a marine core extracted from the Cariaco basin in Venezuela supported the existence of droughts during the critical moments of Maya history including the Maya Classic Collapse. The concentration of titanium in the core was a proxy of runoff and hence the movement of the Intertropical Convergence Zone or ITCZ (see section 2.3 in chapter 2 and section 4.8 in chapter 4), whose most northern position provokes humid periods in the study region, coinciding with the most northerly position of the Bermuda North Atlantic High-Pressure Cell. The most northern position of the Bermuda High to the subtropical North Atlantic happens when warmer surface temperatures prevail, which allows wetter trade winds, which bring more rainfall to the Maya Cultural Area. In this way the droughts in the Maya Cultural Zone would have been the result of a failure of the ITCZ to reach its usual northern position close to the south Coast of Mesoamerica (see Figure 2.6 in chapter 2), displacing itself not so far from the equator and allowing the extension of the Bermuda High to the south. The displacements of the ITCZ and the Bermuda High would have also been triggered by changes in the spatial distribution and seasonal intensity of insolation on the planet (Haug et al., 2001; Montero-Serrano et al., 2011).

In the *Great Maya Droughts*, Gill (2000) suggests three distinct phases for the Classic Maya collapse (Figure 3.6). Phase I (A.D. 760–810) led to initial abandonment of the western lowlands, where the groundwater was scarce, and rainfall was the primary source of water for Mayan cities. Phase II (A.D. 811–860) was characterised by the abandonment of the south-eastern lowlands, a region where freshwater lagoons provided at least some surface water supplies. Finally, Phase III (A.D. 861–910) led to a large-scale abandonment of remaining cities in the central lowlands and the north. Availability and management of water greatly influenced human settlement in the Maya Lowlands (Scarborough and

Gallopin, 1991), and much of Maya social innovation was centred on storing excess water for times of need (Freidel and Schele, 1990). However, the drought theory was criticised, because, in this scenario, the cities in the central lowlands should have been the most vulnerable. Therefore they should have been abandoned first (Webster, 2002).

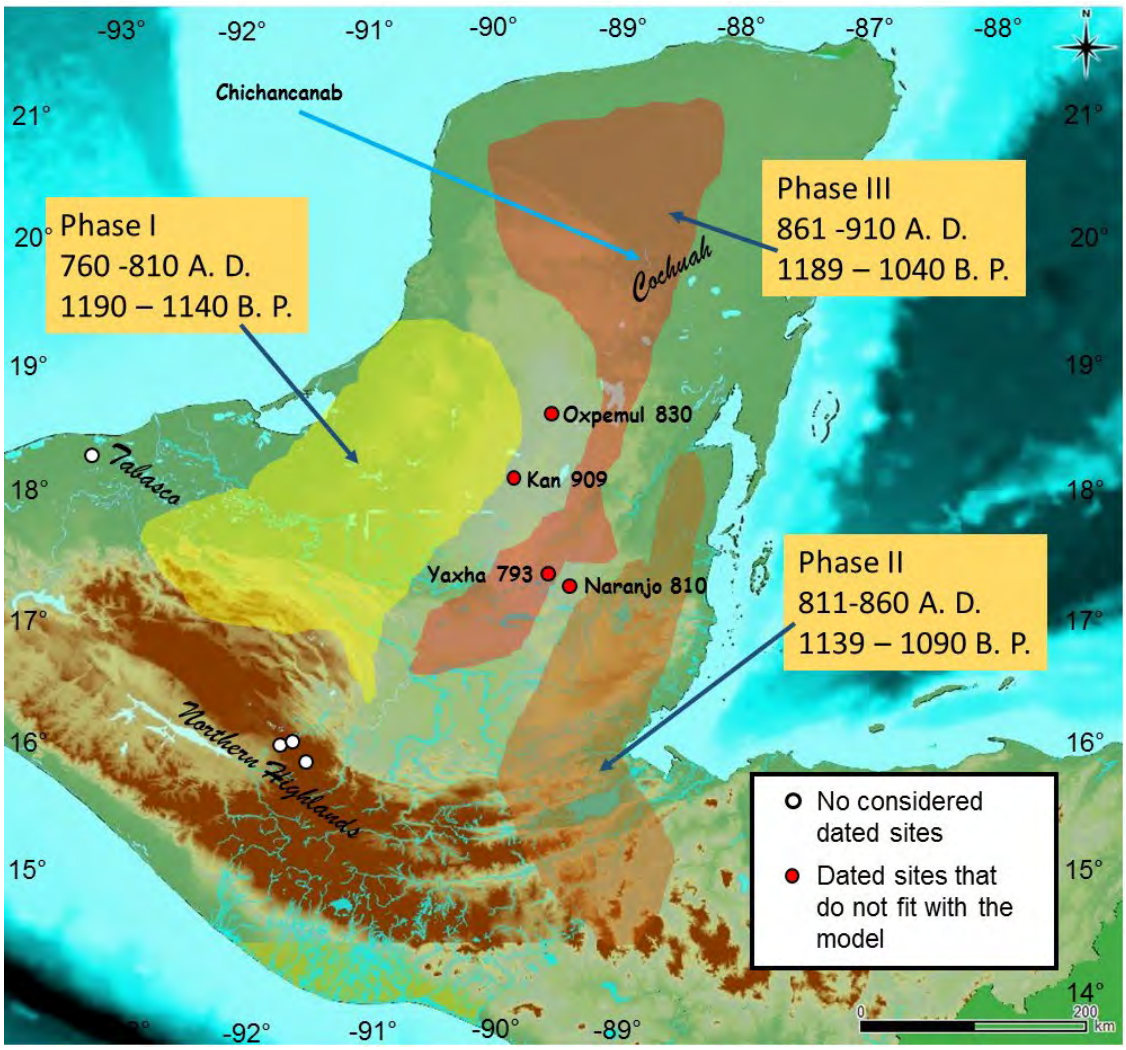

Figure 3.6 Model of the distinctive phases of the Maya Classic Collapse, according to Gill (2000). Sites with last dated monuments which do not fit the model of Gill (2000) (red circles), e. g. Kan (Calakmul) are presented with their date based on Grube & Schubert (2015). The model does not consider the settlements in the Northern Highlands and Tabasco (white circles). Despite being created 20 years ago, there have not been more recent publications on the phasing of collapse modifying substantially the areas described for the model. Gill (2000) and Haug et al. (2001) considered that the Cochuah region was inside the territory of phase III probably based on the palaeoclimatic records of Chichancanab (Hodell et al., 1995). At that time there were not enough data in the Cochuah region for contradicting such an assumption. With new data, the Cochuah Region does not fit in the model, according to the findings of Johnstone (2015); Shaw (2015b,a). Map modified from Haug et al. (2001).

In the northern Mayab, the permanent water table (see section 2.2 in chapter 2) is sufficiently shallow (≤ 20 m below the surface) that it can be accessed by sinkholes, known

as cenotes (Beach et al., 2008; Faust, 2001). However, in the inner lands of the Mayab, near the border between the Mayab and the Central Maya Lowlands, the water table is too deep to have been easily reached (see figure 2.4 in chapter 2). In response, they constructed artificial reservoirs to trap runoff (Freidel and Schele, 1990). Gallopin (1990) estimates that the reservoirs at Mutul (Tikal) could have covered the domestic needs of about 9600 people for a period of 6 to 18 months. Even with elaborate water capture and management systems, the Maya at Mutul were greatly dependent upon adequate rainfall over much of their payolel and were thus susceptible to frequent or prolonged droughts that approached or exceeded the capacity of their reservoirs. Evidence of droughts in the region based on studies of lake sediments in the Maya Cultural Area and shallow ocean sediments in the Cariaco Basin has led many researchers to suspect that climate was responsible for the Classic Maya collapse, creating models which support Gill's pattern of abandonment (Curtis et al. 1996, Haug et al. 2001, Hodell et al. 2005a, 2007, Rosenmeier et al. 2002a). Other studies on speleothems support the existence of droughts in that period (Kennett et al., 2012; Webster et al., 2007).

Another point to criticise in this hypothesis is that the Puuc region thrived during and after the Maya Classic Collapse. In this forest hill territory (see section 2.2 in chapter 2) the water table is at 65 m depth, much too deep to be practically reached without mechanised pumps (Grube et al., 2012). The development of the settlement in the Puuc region was aided by the development of cisterns called *chultunes*, which caught water in the rainy season. This pre-existing system (before the years of the Collapse) may, therefore, have helped to mitigate the impact of drought in this region. A similar situation is inferred in the Cochuah Region, where new settlements thrived after the collapse (Shaw, 2015a), but there is little evidence of cisterns.

After all the evidence accumulated in sixty years from palaeoenvironmental studies (see chapter 4) it can be shown that all the subzones of the Maya Cultural Area, including the highlands (although the number of palaeoclimate records is scarce in the highlands), experienced a series of droughts or low rainfall events during the Terminal Classic Mesoamerican Period. According to Hodell et al. (1995) and Webster et al. (2007), three drought events happened at 1140, 1090 and 1028 years B. P. based on lake sediments from Chichancanab in the Central Mayab or 1196-1152, 1079 and 1057-1028 years B. P. according to the speleothem from the Macal Chasm, at the Central Maya Lowlands (discrepancies fall inside the uncertainty of the age models used in the different records). However, the direct consequences of this series of droughts would not have produced a

collapse directly in the payolelo' ob of the Maya Southern Lowlands, which are more humid. For example, the reduction of rainfall over B'aakal (Palenque) would have never dried the rivers at that time. Water could never have been scarce in the Maya Southern Lowlands (Beach et al., 2008; Gyles Iannone, 2014; Harrison, 1993).

3.5 The Overexploitation of natural resources Hypothesis

The early hypotheses related to the over exploitation of resources come from the works of Cook (1921), Cooke (1931) (not the same author as 1921), and Morley (1946). These scholars proposed that the Maya overexploited the soil with intensive agriculture. Therefore, the first settlements that would have felt the impacts would have been the oldest settlements in the central and southern lowlands in contrast to the Mayab, where settlements were much younger. This hypothesis had the problem that the soil is quite different in the Mayab than in the Maya Central and Southern Lowlands, the soils of the Mayab tend to be easily impoverished since the soil over the karst is very thin. In addition, slopes are steeper in the Maya Central and Southern Lowlands in comparison to the Mayab. In contrast, the ability of soils surrounding Copan to regenerate, for example, is very elevated as any depletion of nutrients created by agriculture could have easily been overcome by the capture of nutrients during floods in this zone (Sapper, 1931). However, the soil in the tropical moist broadleaf evergreen forest is still thin and unproductive after clearance of the forest (Perez-Gil, 1991).

Probably due to these issues, some authors talked not only of the existence of unproductive soils but the erosion of soils (Morley, 1946; Sapper, 1931). Erosion would have been produced by clearance, deforestation and agriculture produced by the exploitation of wood as raw material for construction or as fuel and for the extension of the settlements. It is not easy to assess which of both ecosystems, the tropical evergreen forest moist broadleaf evergreen forest or the dry broadleaf forest (in the Mayab) would be more vulnerable to such overexploitation. The leaching of the soil nutrients and erosion present significant problems in the moist broadleaf evergreen forest forest, while the impact might be lower in the dry broadleaf forest in the North of the Mayab (Sedov et al., 2007). (Erosion also depends on topography). Besides, agriculture in moist broadleaf evergreen forest ecosystems supposed a rapid growth of weeds, which crowd out domestic plants and lock up essential nutrients in their roots (Webster, 2002). The amount of insects, pest and plant pathogens is also relatively more extensive in the moist broadleaf evergreen forest than in

other ecosystems, making the environmental degradation in tropical Evergreen forest moist broadleaf evergreen forest even stronger (Webster, 2002).

Slash and burn agriculture promotes the impoverishment of the soils and in many cases, their erosion if some means are not taken to prevent this (see next paragraph). It is believed that the practice of slash and burn was used in the Classic period in most parts of Mesoamerica. Therefore, the overexploitation of resources hypothesis makes sense. In addition, this hypothesis must also consider the probability of wildfires is more significant in tropical and subtropical ecosystems that have been stressed by agriculture. Therefore, additional zones of moist broadleaf evergreen forest in the central and southern lowlands and the dry broadleaf forest in the northern Mayab might have been deforested due to this phenomenon, which might be caused indirectly by humans (Webster, 2002).

This degradation of the agricultural landscape implies that the Maya could have caused their own destruction, without any external factors such as droughts or other natural disasters such as earthquakes or hurricanes. This view does not take into consideration the possibility of intensified food production from the management of infield forest gardens around structures in the settlements (Ford and Hord, 2018). The familiar gardens ("Huertas") of modern Maya shows the complexity of these agriculture infield systems as well as the management developed to avoid a substantial impact on the environment (Flores et al., 2012).

In the 1960s archaeology underwent a profound revolution in its methods with the emergence of Processual archaeology (Binford, 1968). Processual archaeology started for the first time, having a focus on the common people (peasants) and started to explore the methods of agriculture. After excavation of many settlements in the southern and central lowlands, it was clear that the Maya managed the land (Sabloff, 1994). Processual archaeology also encourages the use of ethnography for reconstructing the past. After observing the guerrilla farmers in Guatemala, whose *milpas* produce beans, maize and banana, among other crops, archaeologist realised that the ancient Maya may have avoided thin and fragile hillside zones (Webster, 2002). They may have chosen the most stable and productive parts of their landscapes, shifting the location of their fields at frequent intervals as the fertility of the old milpas declined (Dunning et al., 1998). They also had controlled fires (Franco-Gaviria et al., 2018). They knew how to minimise human impact. For instance, Dos Pilas, one of the most important sites in the southern lowlands falling during the Maya Collapse, does not present signals of soil leaching or soil erosion(Dunning et al.,

2017). It has been argued that no agricultural activity was performed there due to the lack of phosphate inside the nearest lake (Dunning et al., 1997), but Gramineae (grass), Cyperaceae (sedge), and Z. *mays* are present in the pollen record of the lake (Dunning et al., 2017).

During the last 20 years, probably in response to the drought theory, soil scientists have performed studies across the Maya Cultural Zone. Most works argued for a substantial depletion of nutrients in the soils and increased erosion caused by human impact (Beach et al., 2006). At the same time, other investigations showed artificially enriched soils (Beach et al., 2015). Soil science work tends to support the idea that the Maya caused their own destruction (Roman et al., 2018). However, it has to be highlighted that land degradation is particularly recorded in the Southern and Central Lowlands, where soils are more liable to erosion if vegetation cover is not maintained due to topography and their more acid character. It is possible that despite the high density of population (see section 2.5 in chapter 2) these regions had in comparison to the Mayab, these factors have been crucial in the soil degradation. In contrast, soils in the Mayab are also thin (in northern Mayab extremely thin and patchy), but they have a neutral pH due to the high content of $CaCO_3$ avoiding aluminium toxicity and allowing the stabilization and high accumulation of humus (Sedov et al., 2007), making them more likely to be preserved (but they still present high weathering status).

Many of the soil science studies, taking in consideration the pieces of evidence of droughts during the period of the Maya Collapse (1190 to 1040 years B. P.) consider that the droughts, if not severe, might have increased the environmental crisis caused by the overexploitation of the soil. Some other authors suggested that drought would have been a local phenomenon and could have been caused by the deforestation. This particular explanation can be dismissed following the research on palaeoclimatic records across Mesoamerica (Bernal et al., 2011; Lachniet et al., 2012; Lozano et al., 2015; Metcalfe et al., 2000). This overexploitation of the soil would have been enhanced during the decades prior to the Maya Classic collapse due to the dramatic increase in population compared with the early Classic times (see section 2.5 in chapter 2), which triggered more frequent cultivation. In this way, processual archaeologists indicated that the Maya knew how to minimise their impact, using shifting cultivation, but they would have been unable to apply this method when the demographic explosion was too high (Webster, 2002). For example in the Peten lakes, deforestation caused the soil to erode into lakes, depositing massive amounts of inorganic sediments into the lakes (Anselmetti et al., 2007), including

phosphorus at the time frame of the Collapse (Leyden, 1987; Mueller et al., 2010). This inorganic sediment is a ubiquitous multiphase anthropogenic induced colluvium in the Peten lakes: Tuspan; Quexil; Sacnab; Petenxil; and Peten Itza, which was called the Maya Clay (Vaughan et al., 1985). The Maya Clay has been claimed as a stratigraphic marker of the Mayacene, an early Anthropocene analogue in the region (Beach et al., 2015). As well as in these lakes, it has also been found in wetlands in the Central lowlands e.g. at Los Bajos (Dunning et al., 2002).

Finally, the thriving of the Puuc region during the collapse does not support the overexploitation hypothesis, since this region contains productive soils, and it increased its population dramatically during the Collapse (Grube et al., 2012), a similar situation existed in the Cochuah Region (Shaw, 2015b) (see section 9.8 in chapter 9). The examples of the Puuc and Cochuah Regions, both in the Mayab, proves that the environmental anthropogenic overexploitation if it existed, was not present in all sites. (It is also possible that productive soils were more resilient to exploitation, and therefore they never reached an overexploitation state).

In contrast to the drought hypothesis, where signals of droughts across all the Maya Cultural Area have been seen, the hypothesis of environmental overexploitation focused on the degradation of soils does not have ubiquitous evidence. However, it has been established that agriculture was intense in the Central (Anselmetti et al., 2007) and some parts of the Southern Maya Lowlands (Faust, 2001). In some sites, some degree of soil degradation has been observed (Beach et al., 2006), whilst in other sites, it has been observed that the Maya were aware of the degradation and attempted to stop it (Dunning et al., 2017).

3.6 Chaos Theory and Resilience Systems applied to the role of hurricanes as drivers of the Collapse

The Yucatan peninsula is susceptible to be hit by hurricanes (see chapter 2). Therefore it has been proposed that hurricanes could have had a role during the Maya Classic Collapse (Segura, 2017; Smyth et al., 2017; Webster, 2002). Adams (1973) rejected this hypothesis since these climatic events are localised and sporadic. The delta coast of the Grijalva River in Tabasco on the Gulf of Mexico in the southern lowlands is hardly hit by hurricanes. However, the use of chaos theory can give a new perspective on the role of hurricanes in the Maya Classic collapse. This mathematical theory describes that a small disturbance can

propagate through the system having devastating effects of disruptions in the system (Cvitanović, 1989).

The theory applied to the case of the Maya civilisation proposes that a hurricane would have hit a small (any) settlement near the Caribbean coast. This small settlement would have been a subject of a relatively important payolel (e.g. Yaxha), whose local natural resources would not be sufficient to cover its needs (Segura, 2017). Therefore, the elite of this payolel (e.g. Yaxha) would have conquered other cities, which pay tribute.

After the hurricane strike, the small settlement would have been incapable of paying tribute. Without this tribute, the elite at the important payolel would have been incapable of sustaining their settlement. The workforce of peasants and craftsmen of the important payolel (e. g. Yaxha) would have been dismissed, they would then have suffered from famine, and would have been more susceptible to disease (Segura, 2017). This scenario would have generated a revolt of the humble classes at the important payolel (e.g. Yaxha). Therefore, the elite of the important payolel (e.g. Yaxha) would have escaped to an important powerful city, (like Mutul also called Tikal). The increase of the elite at the powerful city (e.g. Mutul) would have represented a challenge, since the peasants that would have sustained the powerful city were scattered in the region and far from the centre of the city. Then, the ahau (king) of the powerful city (e.g. Jasaw Chan k' awiil II from Mutul) would have decided to conquer another city for getting the tribute, instead increasing the tribute of his own subjects (Segura, 2017). A war expedition would have been organised against one of these satellite cities (e.g. Kan).

The war and the political disorganisation in the powerful city would have disrupted the routes in all the Maya Cultural Area, including the highlands and lowlands. In many settlements, the collapse of the trade routes would have stressed the local political system, where the elite would have been deposed by the peasants when they would have incapable of guaranteeing the availability of goods (Segura, 2017).

A possible criticism of this scenario is that it has been demonstrated that the hurricane activities were negligible during the time of the drought events during Maya Classic Collapse (Medina-Elizalde et al., 2016). Small tropical storms would also have not done significant damage to any coastal vassals. The same argument could be applied to other natural disasters such as floods, for instance a flood have been observed in the palaeoclimatic record at the Puuc Region at 1018 years B. P. (932 A. D.)(Smyth et al., 2017), but the region did not collapse during the time of the Maya Collapse. Medina-Elizalde et

al. (2016) also suggest that tropical storms could be beneficial during these periods of relatively low humidity. We also have to consider the resilience of the system to face any potential damage due to natural resources such as volcanic eruptions, earthquakes and hurricanes.

I use the bases of the Kardashev scale created for measuring the development of hypothetical advanced technological civilisations in a galaxy (Kardashev, 1964) in the context of preindustrial societies in order to explain the requirements that any civilization must have for surviving natural catastrophes. Then, a political entity is more resilient to any natural disaster when

- It has control of a bigger territory in contrast to a small territory. Therefore, empires or political alliances are more resilient than isolated settlements.
- The territory is diverse in its natural resources and much bigger than the area covered by a natural disaster.
- It is capable of managing the bigger territory, redistributing the natural resources, workforce and products across it to subareas where these things are needed. Therefore, scarcity does not happen for a long time.
- It is capable of relocating human population easily. Therefore, migrations can happen inside the territory without causing any important stress
- It has the technology to obtain and store energy to accomplish the task required for maintaining society.

The settlements in the Maya Cultural Zone did not form an empire, but many cities such as Mutul (Tikal), Copan and Chichen Itza controlled extensive territories, in addition, many payolelo' ob had alliances. According to the Maya ancient texts, these alliances were invoked during the dry phase of the Maya Collapse after 1150 B. P. calling for peace possibly to help deal with the consequences of the dry period (Grube and Schubert, 2015). Therefore, the Maya payolelo' ob were resilient to local natural disasters to some degree. The fact that some payolelo' ob survived the collapse is in part explained to the fulfilment of the Kardashev requirements. If the trade routes were disrupted during the Maya Classic Collapse, they would fall for multiple causes, not only due to the war between a powerful city and a satellite city. In the end, chaos theory could also be an oversimplification of the events at that time. However, local environmental disasters might have had a small role in the collapse, although they might not have been able to trigger a collapse per se.

3.7 Catastrophic causes: volcanic activity and earthquakes

Natural disasters such as volcanic eruptions or earthquakes are rarely argued for as drivers of the collapse despite their potential impact and capacity for destruction. As explained in the last section, such events are easy to overcome for political entities that meet the Kardashev requirements. Volcanic eruptions with a volcanic explosivity index smaller than 5, or earthquakes less than 7 in the Richter scale would have been easy to overcome since their destructive power is highly localised (Newhall and Self, 1982). If earthquakes had been a real challenge, the Maya would have adapted their constructions as the Incas did (Hurtado-Casas, 2017). However, many settlements in the Maya Cultural zone, and particularly the settlements in the Mayab are on a passive margin where the effects of the earthquakes have been historically negligible. However, some intraplate earthquakes have affected the Mayab recently since their epicentres are close to the Yucatan Peninsula (Palemón-Arcos et al., 2020). The cities in the highlands are located on metamorphic structures, whose volcanic and metamorphic fields tend to cushion the effects of the earthquakes, even the earthquakes over 8 on the Richter scale.

Small eruptions have destroyed settlements in parts of Mesoamerica, the destruction of Cuicuilco in the centre of Mesoamerica is an emblematic case, or Ceren a Maya settlement in today's El Salvador were buried by volcanic ash during the Maya hiatus at 1360 B. P. (590 A. D.), but these dramatic events destroyed settlements, not civilisations. It can be argued that these small events might have challenged a civilization according to chaos theory (see the section above) but complex civilizations are resilient when they meet the Kardashev requirements.

Volcanic eruptions with an index over five (Newhall and Self, 1982), however, are the only natural disasters that might have potentially challenged the existence of the Maya civilisation. While the Maya Hiatus and the Preclassic Abandonment can be linked to volcanic eruptions, since the geological record shows eruptions of massive volcanoes during this period, e. g. the eruption of the volcano Ilopango in modern El Salvador (Dull et al., 2001), the eruptions of the Tacana (Ford and Rose, 1995) or the eruption of the El Chichon (Macías, 2005), there are no data that support mega volcanic eruption during the period of the collapse. Gill (2000) proposes a possible eruption of El Chichon during the time of the Collapse at 1128 years B. P. based in personal communications with Prof. Claus Siebe (UNAM), but this date was never confirmed. These volcanoes are practically at the

borders of the Maya Cultural Area, the volcanic ashes emitted by them might have caused a drought, since ashes decrease the amount of solar light in the atmosphere.

3.8 Non human ecological disruptions. Pandemics and changes in the ecological niche

In history, pandemics are found to be essential factors in the depopulation of a region. However, some studies suggest that historic pandemics were hardly ever the product of the propagation of a single pathogenic agent, but the confluence of various pathological agents in the right environment that promote a low immunological activity.

Even though it is relatively hard to have all the factors required for a pandemic, this scenario is not entirely impossible. The hypothesis of pandemics inside the Maya Cultural Zone was first proposed by Spinden (1928). This hypothesis is able to explain the demographic catastrophe, as well as why people did not repopulate these subareas. Since some areas in the tropics start to be the habitat of a specific pathogen agent. The effects of the major epidemic are also consistent with the protracted collapse itself since initial episodes of mortality might have been followed by recurrent, less aggressive outbreaks.

The principal implausibility of this hypothesis is that the people of the Americas were healthier than habitants of the high civilizations in Eurasia. This is related not only to the cultural customs, but to the kind of food that they ate. Also, most of the major pandemics in the world, smallpox, influenza, measles, typhus, typhoid, plague and cholera come from the interaction with domestic cattle (Webster, 2002). Since the neolithization process in Mesoamerica never reached the domestication of animals, the Maya, among other ancient Americans never reached the level of interaction with animals that existed in Europe and Asia. Therefore the chances of pathogens jumping from animals to humans were much less (Webster, 2002). Besides, despite its high population, the Maya cultural zone settlements had a lower density in population compared with the cities in Europe and Asia. The final argument against the hypothesis of pandemics is that the villages in the Puuc region and the north of the Mayab in general would have remained immune to the epidemic since they do not collapse. Such immunity cannot be explained. Besides, it is hard to explain why such pandemics would have not propagated to other sites in Mesoamerica. In addition, a pandemic scenario would have required that the disease was greater than that for many other societies and increased over the span of occupation during the Collapse. Works based on palaeopathology studies conclude that this was not the case (Wright et al., 1996).

Finally, the pandemic as a driver of the collapse is difficult to assess, since pandemic could also be a consequence of other drivers of the collapse, such as famine, droughts, or disruption of the trade networks.

Another possible scenario of an environmental non-anthropogenic driver of the collapse could have been the changes in the behaviour of an archaea, bacteria, animal, fungi or plant species with which the Maya had a symbiotic or parasitic relationship. For instance, one of the species that they hunted or fished could have changed its patterns of transit and become unavailable on the zone or just become extinct. It could also be a disruption of the pollinating agents or an increase of the diseases affecting maize (the staple crop). Again, in these scenarios, it is hard to think that the Maya would not have found alternatives. However, this idea has not been explored. A related case of this scenario is the ecology of the apple snails, *Pomacea flagellate*, in the Southern Lowlands during the Maya Abandonment (Sharpe et al., 2020). Its population decrease during the Maya Abandonment had consequences in the ecosystem, allowing that other mollusks occupied its niche (Sharpe et al., 2020). However, it is unknown if this had a critical consequence in the local ecosystem. The depletion of the apple snail can be either explained by a natural ecological disruption or by overexploitation by Maya people, since this taxon was used for trading due to its use as ornament (Sharpe et al. 2020). Therefore, it is not the best example of a biological agent that might have detonated a societal crisis without the intervention of humans.

3.9 Hypothesis of economic causes

Modern western civilisation experiences substantial consequences when the economic system is in crisis, Capitalism functions in this way. Nevertheless, societies with other kinds of economies, such as the cargo system economy used in Mesoamerica, are not easily disrupted by economic issues. To put things in perspective, in the Maya Cosmovision, every family needed to produce its own maize supply for being respectable (Webster, 2002), except for some members of the royalty.

Therefore, the only way to disrupt the economics of the Maya cultural zones is cutting the trade routes. Unfortunately, scholars still ignore trade routes, arguing that the economy of a settlement was local and did not need the exportation and importation of goods at long distances. In section 3.5, we observed that the disruption of the Motul (Tikal) trade net could have caused the collapse of other cities. Nevertheless, this assumption is far from being proved since we do not know if that route provided goods for daily life such as food or textiles, or luxury goods for the elite such as obsidian. Some products, like salt, are an

example of a basic product for daily life, which needs to be produced in specific places in the Mayab and distributed across the lowlands. (Sosa et al., 2014).

3.10 Hypotheses of sociopolitical causes

The hypotheses concerning social or political causes propose different scenarios related to internal wars between payolelo'ob, foreign invasions (from the centre of Mesoamerica or Central America), internecine wars like a fight for the throne or peasants revolts, national decadence, and religious or superstitious causes (Webster, 2002).

Before the decipherment of the Maya scripture by the Soviet Yuri Knorozov (Юрий Кнорозов) in the last years of XX century (ca. 1980 A. D.) archaeologists tended to believe that the Maya were peaceful people. Nevertheless, the ancient texts talk about warfare, conquest, and war rituals. We have to understand that these people did not have permanent armies, agriculture was a preponderant duty, therefore, there was a time during the year for performing warfare. At the same time, nocturnal battles never existed in Mesoamerica, which shows that warfare was a programmed and ritualistic task.

The wars were followed by a strict code of conduct. The wars among payolelo' ob are argued to be the cause of the Maya Classic Collapse since ancient texts describe more confrontations during the Terminal Classic (Demarest, 2004). However, we have more texts about wars in that epoch because we also have more texts (Johnson, 2013). In this way, the increased number of warfare tales cannot be a proxy of the degree of violence during the time. It is also possible that the focus in the ancient texts on wars does not reflect the real bellicosity of the common populations. The ancient texts indicate wars at the moments prior to the royal and artistic collapse in the settlements at the Southern lowlands, which is before the abandonment of these sites according to the archaeological record (Grube and Schubert, 2015). The ancient texts also describe anomalous political situations, like women on the thrones, which may suggest a political crisis that the payolelo' ob had (Martin and Grube, 2000; Nygard et al., 2015).

Nevertheless, the ancient Maya texts also talk about alliances and peace when the effects of the droughts started to be felt after the first drought event at 1140 years B. P. (Grube and Schubert, 2015). For instance, the charcoal accumulation rates and non-carbonate records obtained from Laguna Ek'Naab, which associate peaks of fire events with wars described in an ancient text (Wahl et al., 2019), shows negligible signals of fire events during 1140, 1090 and 1040 years B. P. (the years of the droughts) and a comparatively

much lower number of fire events in general for the Terminal Classic Period defined in this thesis. Wahl et al. (2019) described that the warfare was intense around 1253 years B. P. (697 A. D.), 50 years prior to the Collapse. This supports the observation of Grube & Schubert (2015) of a calling for peace. Therefore, the war between payolelo' ob is hardly the cause of the collapse because the wars were not necessarily destructive; warfare existed during all the classic period. Even if warfare would have been more frequent during the terminal classic, their intensity is not comparable to the warfare exerted by the Aztecs in central Mexico in the next centuries (Phillips and Jones, 2009). The Aztec constant warfare did not cause the collapse of any society in the Central Highlands of Mesoamerica. Following this example, it has to be highlighted that warfare normally implies winners and losers. Scenarios, of pyrrhic victories that would have caused the collapse, are in my opinion almost implausible during history, normally a winner always has the resources to reconstruct its society. Moreover, warfare is not so evident in most of the Maya archaeological records, but sporadic. However, intense warfare has been documented in the Central Maya Lowlands during Late Classic Period (1400 to 1190 years B. P.) (Demarest, 2004). Therefore, warfare would be more a consequence of the collapse than a cause.

This lack of warfare can also be applied to dismiss the hypothesis that implied invasions of foreigners (Sabloff, 1994; Sabloff and Willey, 1967). This hypothesis was proposed since the surviving cities adopted a culture that had more similarities to the Toltecs in Central Mesoamerica than to the classic Maya. However, such influence can also be explained without an invasion scenario (Binford 1968). Despite this, anthropological studies of skeletons show that the people in the Puuc region and the north of the Mayab were still Maya and not from Central Mesoamerica. The variation of the phenotypic characteristics in the Puuc region is one of the lowest in the Maya Cultural Area (Moreno-Estrada et al., 2014), which implies that the groups there were locals suggesting that migration from outside the region was small. In addition, any Toltec invasion could have implied that Nahuatl, the language of the Toltecs would have started to be spoken in the Maya Cultural Zone, in particular in the Puuc region, and the kuchkabalo'ob in the north if the Mayab, but that was not the case.

It has to be highlighted that the genetic difference between Maya and Nahuas, the people that usually lived in Central Mesoamerica, including the Toltecs is more significant than the difference between Caucasian Europeans and Mongoloid Asians (Moreno-Estrada et

al., 2014). DNA studies have not found the presence of Nahua ancestry in the modern Maya population (Moreno-Estrada et al., 2014).

Another hypothesis is the role of revolts during the Collapse. If the revolts of peasants existed they would probably have also been a consequence and not the cause of the collapse. This point is linked to national decadency, which is the common process of many states where political institutions start to be useless (Webster, 2002). It is known that royalty was deposed during the collapse (Iannone et al., 2019). The end of the royal families is argued as one of the most critical drivers of the collapse (Demarest, 2004). The disappearance of dynasties might be just part of the internal process of the civilizations when they are reaching a significant degree of complexity (Iannone et al., 2019). A more complex society implies more diversity of tasks and more access to knowledge and goods (Webster, 2002). This step weakens the power of the Maya rulers and dynasties. For example, Chichen Itza started to be governed by a council instead of a single ruler, which indicates a new way of conceiving the political power (Iannone et al., 2019).

3.11 The Maya Collapse in the study sites of this thesis

This thesis focuses on the environmental history around Lake Esmeralda in the Cochuah Region and Lake San Lorenzo at the Lagunas de Montebello Lake Complex in the Chinkultic Region (see chapter 4). In comparison with the Central and Southern lowlands and other important centres in the Mayab like Chichen Itza, Copan or the Puuc Region, the archaeological record of the ancient Maya settlements that are near our zone of study have been barely studied, even though these places show dynamics that are very different from the sites at the Southern and Central Maya Lowlands. For example, the city of Chinkultic in the Montebello Lakes complex at the Northern Highlands presented a gradual abandonment during the Terminal Mesoamerican Classic period (Álvarez, 1993), which started after the Maya Hiatus, according to the reconstructed Human Impact Index by Franco-Gaviria et al. (2018). The city was finally completely abandoned at 750 years B. P. (Navarrete, 2007), although some authors suggest a permanent occupation until the arrival of the Spaniards-Tlaxcaltecs 400 years B. P. (Álvarez, 1993). In contrast, Jo'otsuuk (Tihosuco), and other settlements in the Cochuah region at the centre of the Mayab increase its population dramatically after the collapse, passing from one settlement to more than 100 settlements dispersed across the region (Shaw, 2015a).

3.12 Conclusion

This chapter explained the principal hypotheses related to the Maya Collapse at the end of the Mesoamerican Period, including the challenges to each hypothesis. As scholars suggest, the scenario of the collapse is complex and cannot be constrained to one driver, but to multifactors that had different regional outcomes (Sharer and Traxler, 2005). What we know about the period of the collapse is:

- It occurred between 1190 to 1040 years B. P.
- The Maya Cultural Area was densely populated, but the distribution of the population was not homogeneous (Sharer and Traxler, 2005).
- At the beginning of the Collapse Period, the Southern Lowlands and Central Lowlands were more populated than other regions inside the Maya Cultural Area (Sharer and Traxler, 2005).
- It starts during warfare in the Central lowlands, where the more important conflict was the victory of Mutul (Tikal) over Kan (Calakmul) (Grube and Schubert, 2015).
- Last monuments with a date were being produced (Sudrys and Berger, 1979).
- Dry conditions were established over all the Maya Cultural Area, having three intense droughts at 1140, 1090 and 1040 years B. P. according to Hodell et al., (1995) or 1196-1152, 1079 and 1057-1028 according to Webster et al., (2007).
- After the first intense droughts (1140 years B. P.), the Maya payolelo' ob tend to create alliances, and there was a significant decrease in warfare (Grube and Schubert, 2015).
- Some zones presented significant soil degradation (Beach et al., 2015).
- There is no evidence of significant disease or famine in the population (Wright et al., 1996). The faunal assemblages do not show stress resulting from lack of water. However some food products were scarce (Iannone, 2014).
- The Mayab started to increase its population dramatically, reaching its historical maximum population at the end of the Collapse Period which is evident in the Puuc Region (Grube et al., 2012).
- The lack of nearby volcanic eruptions during the time of the Collapse (Sharer and Traxler, 2005).
- The lack of ancient texts describing earthquakes (Sharer and Traxler, 2005).
- Most Royal dynasties were deposed (Demarest, 2004).

The critical points that we do not know about the collapse are:

- The power that an ahau can exert for controlling the trade networks (Webster, 2002).
- The goods distributed by the trade networks (Webster, 2002).
- The relationship between peasants and the ahau'ob (Royalty) (Webster, 2002).

Taking these data into consideration, it is clear that hypotheses related to pandemics and catastrophic events cannot be supported. I have discussed that such events would have a role, considering the proposal of Segura (2017) of using the chaos theory. But as I have explained in this chapter, Maya societies covered the Kardashev (1964) requirements to minimize any butterfly effect triggered by a catastrophic event. Ancient texts indicate the formation of alliances during the time frame of the Collapse, which is the most critical Kardashev requirement.

In comparison, the overall dry period and the series of intense droughts inside of it played an important role in the Collapse period. However, as the data suggest, the drought started 50 years after the beginning of the collapse (Grube and Schubert, 2015). As I will discuss in chapter 4, the effects of the droughts were not the same in all the Maya Cultural Area; therefore, the response of the population to the droughts was also diverse. The hypothesis of the overexploitation of natural resources, especially the part concerning soil degradation actually happened in some cities of the Maya Cultural area (Beach et al., 2015). But, as data suggested, that was not always the case due to the management that the Maya have performed in some cities (Dunning et al., 2017) or the resilience of the natural system in other sites (Sedov et al., 2007). In any case, the degradation of the soil was a factor of the Collapse in some places, but it was not a driver. In contrast to droughts for which evidence is extensive in most of the Maya Cultural Area, the degradation of soil was neither ubiquitous nor observed in most places.

Finally, the hypotheses related to socio-political causes play the most important role in explaining the collapse. The collapse was initiated by some kind of political motive, the warfare in the Southern and Central Lowlands suggest that (Grube and Schubert, 2015). However, the dry period after 1140 years B. P. exerted pressure on the political and economic systems, which responded in different ways. Migration was the most evident result. The effects of droughts on politics, e.g. alliances, royal dynasties deposed, is clear, but we know almost nothing about the impact on economics, including the response of

the trade network. In a Marxist interpretation, it might be possible that the changes in the trade network forced the abandonment of the cities, the waves of migration from the Southern Lowlands to the Mayab and the diminishing of the political power of the dynasties. Politics, as an expression of human agency, also played the final role of how populations adapted or not to the series of droughts.

In this Earth Science project, I cannot respond to why or what political changes happened as a result of a new reality imposed by a dry period, but I might be able to discern the impact on the natural system that such dry periods imposed, indicating what were the challenges that the Maya people had in the Cochuah and Chickultic regions as a result of the droughts, or if drought was as widespread as has previously been suggested. Lake sediment analysis also allows the project to test the impact of potential human activity in the lake catchments, for example by studying the organic content and the terrigenous input to the lake. The next chapter enlightens us about the previous studies and methods that have confirmed the presence of a series of droughts, the regional extent of these droughts, as well as the impact in the environment that the Maya exerted due to agriculture.

Photo: Pyramid of the Magician at Uxmal

"The Chac that drops snakes, will raise with drought for everywhere, but its delivered famine will be not so strong, the water in channels will give bread beyond the mountains, beyond the rocky hills. This time will bring horrible famine, but not everywhere."

Chilam Balam de Tizimin, XVII Century.

With the appearance of processual archaeology in the 1970s, environmental reconstruction began to be perceived as necessary for the study of the human past. Archaeo-botany, zooarchaeology and landscape studies started to be widely used fields for understanding the habitats of the Maya. Since then, environmental reconstruction studies have been implicit in archaeology work (Sabloff, 1994).

The first attempt to analyse environmental change in this way was made by Cowgill et al., (1959) in Petenxil Lake, Guatemala, using pollen as a proxy. Since then, until January 2020, around 70 records have been produced for the Holocene, or parts of it, across the Maya Cultural Area, including lake cores, speleothems, corals, tree rings and cave sediments (Figure 4.1). However, before the works of Hodell et al. (1995), Gill (2000) (see section 3.4 in chapter 3), and the decoding of ancient Maya text concerning droughts (Jobbová et al., 2018), palaeoenvironmental studies were not searching for answers related to the connections between the Maya Collapse and events of droughts. In those years, (1960's,70's and 80's) the purpose of palaeoenvironmental reconstruction was to clarify the ecological context where the Maya lived, which meant mainly to know what kind of vegetation and crops existed during the Maya History, since this knowledge was barely covered by the recently decoded ancient Maya texts (Demarest, 1976; Grube et al., 2012; Johnson, 2013).

In this way, detailed palynological and geochemical examination was carried out on sediment cores obtained from several sites in the Peten district in Guatemala, as a part of the Central Peten Historical Ecology Project (CPHEP) initiated under the direction of Edward S. Deevey in the early 1970s. An approximately 8,000-year pollen record from a shallow-water site in Lake Quexil, Guatemala (also called Eckixil) (Figure 4.1 right bottom) demonstrated that tropical forest had dominated the area at least since the early Holocene (Deevey et al., 1979; Deevey, 1977; Vaughan et al., 1985; Wiseman, 1985). A significant decline in forest taxa began before 3000 B. P. The vegetation change generally coincided with a climatic drying detected at Chichancanab using oxygen isotopes ratios (Covich and Stuiver, 1974). Since the inception of the CPHEP, other studies have looked at the regional vegetation history using pollen as a proxy of vegetation in Quexil, Salpeten, Macanche, Yaxha, and Sacnab, and covering the complete Holocene. Most of these studies had centennial or multi-decadal resolution and were dated by radiocarbon (Brenner et al., 2002). These studies confirmed that the change in vegetation between 4000 to 3000 years

B P. coincides not only with a dry period but with early agricultural activities in the Peten area (Rice et al., 1983; Rice and Rice, 1984).

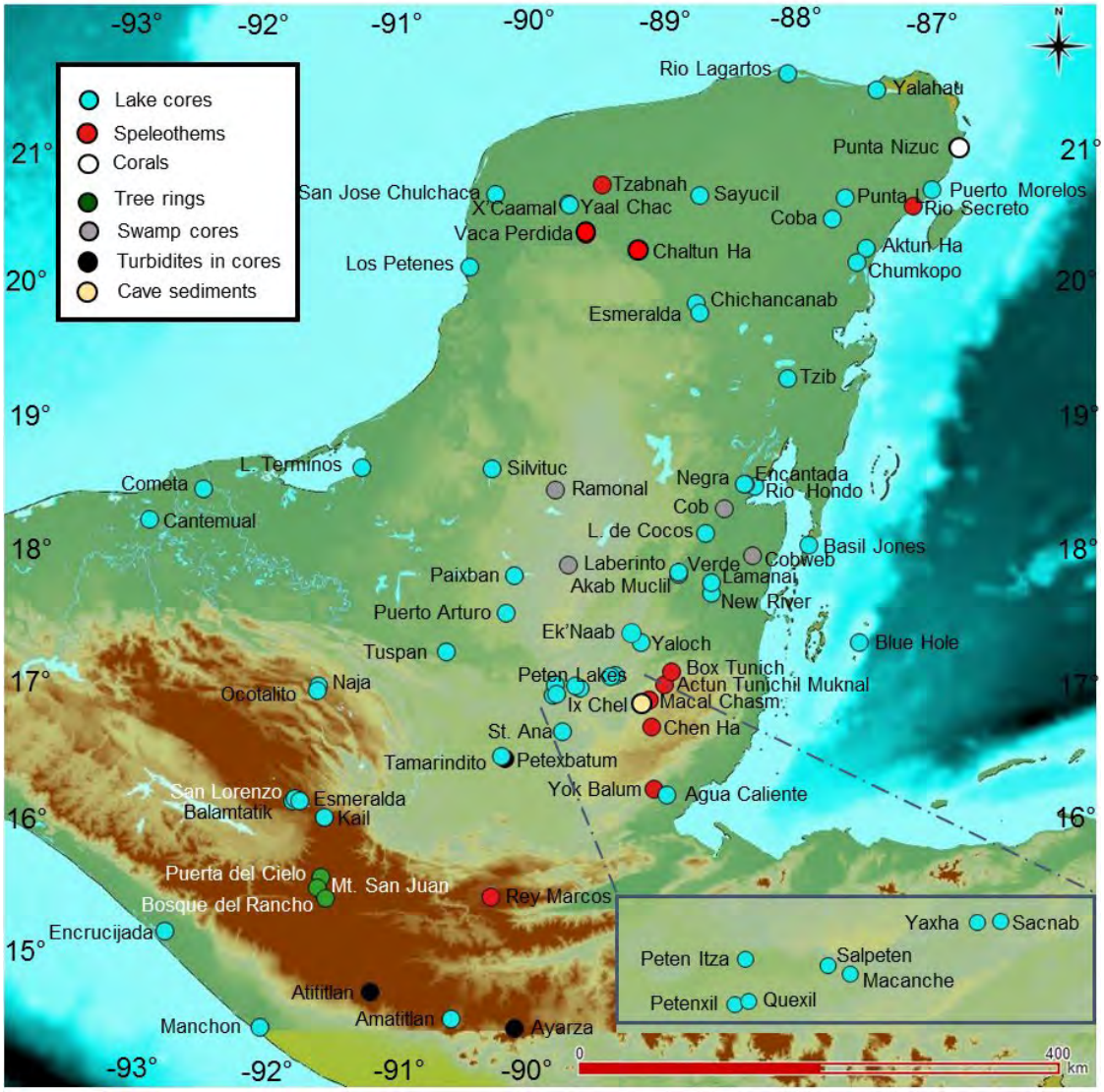

Figure 4.1 Palaeoenvironmental records in the Maya Cultural area for the Holocene. The colour indicates the kind of record; lake sediment cores, speleothems, tree rings, swamp or wetland sediment cores and cave sediments. The map also shows the sites where efforts to develop a palaeoclimatic record failed due to the presence of turbidites in lake sediments or the presence of diagenetic minerals in speleothems. Map produced using QuantumGIS 2.18.11.

The improvements in analytical techniques since the last decades of the XX century allowed a better resolution in the palaeolimnological records. In particular, the advent of new detectors in ICP-QMS and XRF equipment, with its improved precision and smaller sample sizes, began a new era in palaeoclimatology in general (Bernal et al., 2010), e.g. isotopic analysis on *Pyrgophorous coronatus* in Chicancanab and the sinkhole Aguada X'Caamal in the Mayab used these improvements (Hodell et al., 1995, 2005b).

In addition, these improvements found their counterparts in geochronology, when the advent of the Accelerator Mass Spectrometry, AMS allowed the use of a smaller amount of sample for radiocarbon dating. In addition, U-series became a reliable dating method for many carbonate (or evaporite) samples of Quaternary age with unprecedently small uncertainties (Andersen et al., 2004; Bernal, 2003; Mortimer et al., 2002). To date, the U-series method has just been applied to speleothems in the case of the Maya Cultural Area.

In this chapter, I present an assessment of around 70 Holocene palaeoenvironmental studies performed in the Maya Cultural Area since the first studies at Petenxil in 1959 until January 2020 (more recent published records were not considered for this part of the thesis, since the writing process of this thesis started on February 2020). I reviewed the published research and some theses related to this topic in English, German, Spanish and French, which, along with the Italian, Russian and Mayatan are the common languages used in Mayan studies. (Although Mayatan is absent from academic work outside linguistics). In the end, the published research that I could find was mainly presented in English or Spanish, except for some academic books (e.g. Grube et al., 2012; Grube and Schubert, 2015) published in German and science communication articles (which are based on scientific journals published in English) also published in German (e. g. Peterson et al., 2006).

4.1 Types of palaeoclimatic records in the Maya Cultural Area

Although sensu stricto, not all palaeoenvironmental records are palaeoclimatic records, the studies presented here tell us something about climate changes during the Holocene. The kind of palaeoclimatic records used in the Maya cultural area are

- Lake records; which are based on sediment cores.
- Speleothems, which are sedimentary deposits of secondary carbonates developed in caves due to the changes of pressure of CO_2 infiltrating water creating stalagmites, stalactites among other formations.
- Cave sediment records, which are sediments deposited inside a cave and due to the characteristic of caves, are less susceptible to weathering and diagenesis in comparison with sediments in open areas.
- Tree rings which are formed in the trunk according to the seasonal environmental changes of temperature or humidity.

- Seasonal Swamp records, which are similar to the lake sediments, are based on cores taken from seasonal swamps or wetland inland environments.
- Corals, which are marine animals leaving on colonies and developing hard skeletons annually.

Every kind of record, or archive, can potentially be studied using a set of palaeoenvironmental proxies such as pollen, the elemental, ionic and molecular chemical composition, mineral composition, textural composition, charcoal content, the kind and amount of microfauna, the isotopic composition such as $\delta^{18}O$ of bulk carbonates or the exoskeleton of a particular taxon, density changes, magnetic susceptibility (μ) and the colour or response (e.g. reflectance) of the record. It has to be highlighted that the same proxy in two different places can indicate different phenomena depending on the context, and sometimes could indicate different phenomena in the same place if the environmental conditions changed drastically (e.g. Mills et al., 2017), as in the isotope record from Sinkhole Aguada X'Caamal (Hodell et al., 2005b).

Bhattacharya et al., (2017); Bhattacharya and Coats, (2020); Lozano et al., (2015); Metcalfe et al., (2000, 2015), have presented a spatial distribution of the palaeoclimatic records in Mesoamerica including some records of the Maya Cultural Area. In Figure 4.1 I have taken their work much further showing the spatial distribution of the 70 different kinds of records in the Maya Cultural Area. Some records on the Pacific Coast and the Gulf of Mexico are in mangrove zones. Therefore they are classified as permanent swamps, e.g. site Cerritos 2 in the La Encrucijada Biosphere Reserve (Joo-Chang et al., 2015), Manchon (Neff et al., 2006), Los Petenes (Gutiérrez-Ayala et al., 2012); however, due to their characteristics related to palustrine environments, I classified them as lake sediment cores instead of wetlands.

In the case of the seasonal wetlands, the Cobweb Swamp records in Belize were developed in areas inside artificial channels developed by the Maya (Jones, 1994), which are dry today, while the records at Akab Muclil and Cob, are wetlands in flood plains (Kylander et al., 2012; Pohl et al., 1996). In addition, records at El Laberinto and El Ramonal adjacent to Kak (Calakmul) were developed from sediments (colluvium) deposited in what were called seasonal swamps (Gunn et al., 2002). Figure 4.1, also shows the lakes Atitlan (Newhall et al., 1987) (not to be confused with Lake Amatitlan), Ayarza(Poppe et al., 1985) and Petexbatum (Dunning et al., 1997)(black dots) where palaeoclimatic studies were intended, but the presence of turbidites was argued to prevent the development of a reliable

chronology. However, we present these failed records since they help us to understand the spatial distribution of the studies.

Ten records were developed using speleothems (Akers et al., 2016; Asmerom et al., 2012; Frappier et al., 2014, 2007, Medina-Elizalde et al., 2016b, 2016a; Pollock et al., 2016; Smyth et al., 2017, 2011; Webster et al., 2007; Wiseman, 1985), two of the speleothems from the same site at Yok Balum but covering different time periods (Kennett et al., 2012; Lechleitner et al., 2015)

Figure 4.1 also presents other records from tree rings (Anchukaitis et al., 2013), corals (Gischler et al., 2008; Horta-Puga and Carriquiry, 2012) and cave sediments (Polk et al., 2007).

Figure 4.2 presents the palaeoenvironmental records developed in the Maya Cultural area compared to the location of the Maya period archaeological sites. It can be observed that most of the palaeoclimatic studies have been performed in zones of high-density archaeological sites, e. g. the Peten region, the Lamanai region and the Riviera Maya (Figure 4.2). However, there are high-density regions of archaeological sites which have small numbers of palaeoclimatic studies, such as the Chincultic-Comitan region in the Northern Maya Lowlands, the Puuc region in the Mayab and the area of the north coast of the Mayab.

There is also a lack of sufficient studies in regions with a low density of archaeological sites. These regions are the flood plains in Tabasco; the centre of the Mayab (where the kuchkabal of Cochuah was located); the Southern Highlands in Guatemala; and the Southern Lowlands in Guatemala and Honduras.

We have to highlight that the archaeological sites do not necessarily reflect the distribution of the Maya settlements since undiscovered sites may exist. In addition, the Maya settlements were not equally populated, and most of them were just populated during a particular Mesoamerican archaeological horizon. In this way, most of the Maya settlements were located in the Highlands and Southern Lowlands during the Preclassic Horizon, in the Central Lowlands during the Classic Period, and in the Mayab during the Postclassic Period (Sharer and Traxler, 2005) (see section 2.7 in chapter 2).

Lake sediments are well distributed in all the regions where paleoclimatic research has been carried out. However, the major studies are concentrated in the Peten region of northern

Guatemala, probably due to a large number of lakes in that region and the existence of the Peten project (see the section above) in the last quarter of the XX century (Figure 4.2).

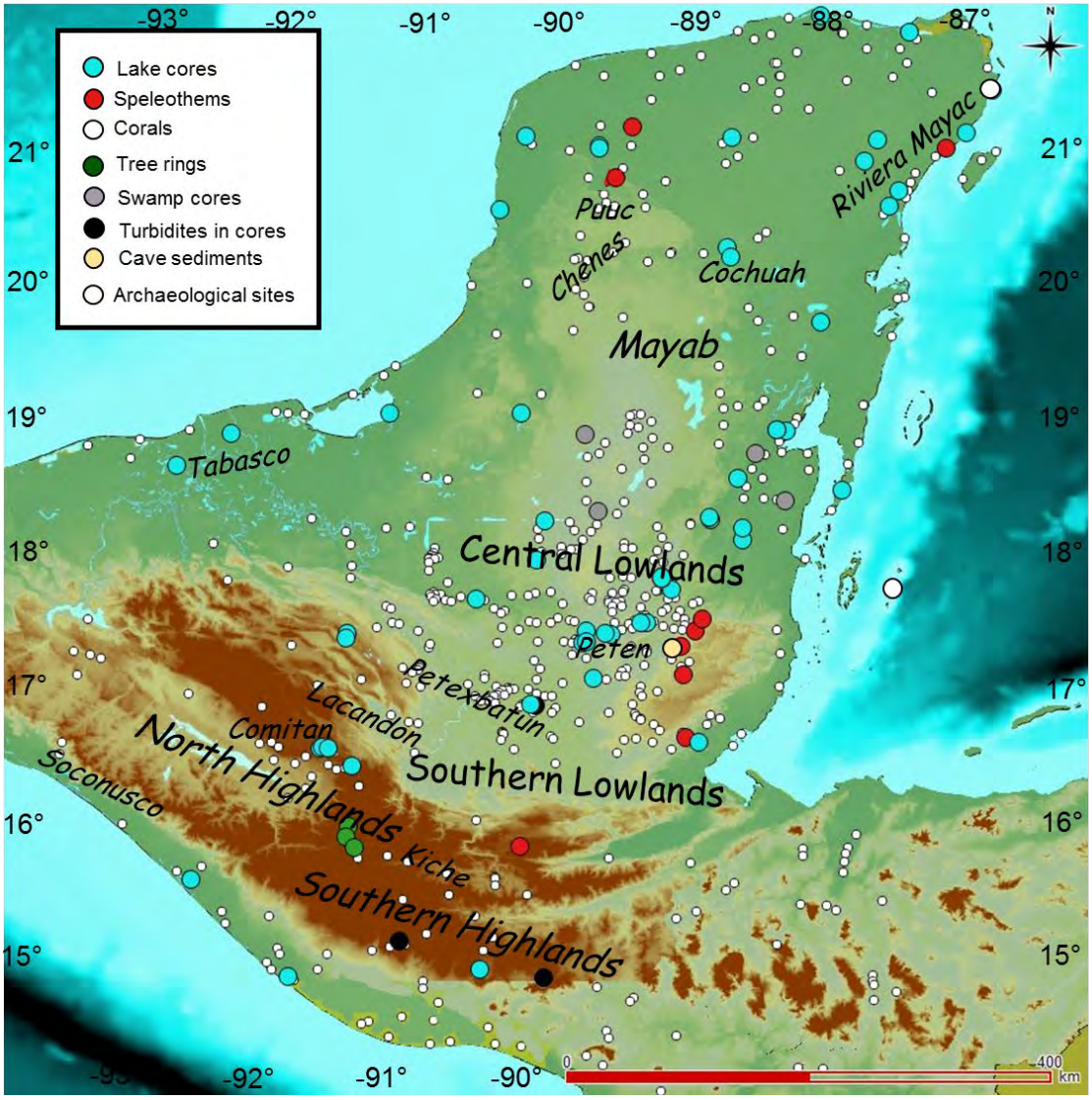

Figure 4.2 Location of the different palaeoclimatic records and archaeological sites . The colour indicates the kind of record; lake sediment cores, speleothems, tree rings, swamp or wetland sediment cores and cave sediments. Map produced using QuantumGIS 2.18.11. The location of archaeological sites is based on Ford et al., (2009).

4.2 Lake sediment records in the Maya Cultural Area

In the Maya Cultural Area, most palaeoenvironmental records have been produced using sediment cores extracted from lakes. All the lakes still have water, and no dry palaeo-lakes have been studied in the area. The Blue Hole (Gischler and Storz, 2009), which is a sinkhole (cenote) in the continental platform merged into the Caribbean Sea, is worthy of note due to the sedimentation process existed there that include the inclusion of coral debris. Lake records contain a range of different proxies.

I developed a database containing these records (Table 4.1), summarising the proxies used and the dating method. The proxies were classified into twelve categories: density; isotopes; fauna; algae; elemental and molecular chemical composition; magnetic susceptibility (μ); in- and organic carbon content; proxies of a trophic index; mineral composition; and texture.

All the proxies related to chemical composition were put into a single category, except for the inorganic and organic carbon content analysed mainly by loss on ignition. In this way, the elemental and molecular composition, mineralogy and proxies of the trophic index were put together. The spatial distribution of these records has been compiled (Figure 4.3.) using the combined version of these chemical proxies.

It can be appreciated that pollen has been the most widely used proxy. Figure 4.3 also shows that the multiproxy approach was applied in most of the records. However, the records with isotopic composition as a proxy usually did not use pollen as proxy, making a comparison between changes in the surrounding vegetation and changes in the amount of rainfall, humidity-evaporation ratio or water balance difficult. A relatively recent exception to this is the research of Wahl et al., (2014).

Figure 4.3 also makes evident that most of the lake records were developed from actual lakes, while a small number of records have been taken from sinkholes with groundwater (cenotes or aguadas). This lack of studies in cenotes is interesting since the sinkholes play an essential role in the theory of the Maya droughts developed by Gill, (2000), but it has to be considered that classic cenotes do not accumulate sediments (Guzmán, 2017). This issue also reflects the fact that despite the critical role of cenotes in the ancient Mayan texts and archaeology, they are present in no more than 33% of the Maya Cultural Area (Perry et al., 2002).

Figure 4.4 shows the number of lakes that have a particular proxy, while Table 4.1 completes Figure 4.4 displaying the material used for dating, isotopic analysis and the kind of chemicals analysed (except in- and organic carbon content).

As I said in the preceding paragraph, pollen is the most used proxy. Therefore, most sites have a record of vegetation changes. It is followed by in- and organic carbon content (%C in Figure 4.4). Therefore, many records are able to indicate carbonate precipitation and productivity changes, respectively. Elemental, ionic and molecular chemical abundances are the third most used proxy.

Table 4.1 Palaeoenvironmental records based on lake sediments. The different kinds of chemicals analysed (in- and organic carbon content are excluded), fauna and algae studied, and material used for isotopic analysis and dating is displayed as well as the name and length of the core, dating method, age model type and mean resolution of the proxy with more samples. Pollen, (including aquatic pollen), charcoal, density and magnetic susceptibility analyses are excluded since this information is in Figure 4.3. The category "No Transformation" indicates the records which do not develop an age model although they were dated, presenting the results against depth.

Location	Isotopes	Fauna	Algae	Chemical	Trophic index proxies	Mineral proxies	Reference	Dating method	Core length (cm)	Number of dates	Age model type	Name of core	Dated material	Mean resolution (years)
Agua Caliente							Walsh et al., 2014	Radiocarbon	123	4	Polynomial	AC07B	Charcoal, single twig	121
Aguada X'Caamal	*Darwinula stevensoni* $\delta^{18}O$ and $\delta^{13}C$, *Pyrgophorus coronatus* spinose $\delta^{18}O$ and $\delta^{13}C$,						Hodell et al., 2005	Radiocarbon	413.5	10	Second-order polynomial equation	XCA 08-VIII-01 MWI	Charcoal, wood, and seeds	8
Aktun Ha	$\delta^{13}Corg$, *Cytheridella ilosvayi* $\delta^{18}O$ and $\delta^{13}C$	Foraminifera, thecamoebians, ostracods					Gabriel et al., 2009	Radiocarbon	61	5	No transformation	No reported	Three twigs, one shell, one charcoal	47
Amatitlan					N%		Velez et al., 2011	Radiocarbon	701	5	Piecewise-linear model	Amatitlán 15-III-00	Charcoal	19
Balamtetik			Diatoms	Al, Ti,Mn, Ca	P		Caballero et a., 2020	^{137}Cs, ^{210}Pb	70	3	Piecewise-linear model	Balam13-GI	Bulk sediments	1
Blue Hole	Bulk sediment $\delta^{18}O$ and $\delta^{13}C$,						Gischler et al., 2008	Radiocarbon	600	11	Piecewise-linear model	No reported	Organic residue	24
Cantemual			Diatoms	Si, Fe, S, Ca, Sr, Br			Nooren, 2017;	Radiocarbon, Tephra layers	325	5	Piecewise-linear model	LCa1		3
Chichancanab	*Pyrgophorus coronatus* $\delta^{18}O$, $\delta^{13}C$ plant wax δD			Plant wax lipids	Wgt % S,	Gypsum	Covich& Stuiver, 1974; Curtis et al., 1996; Douglas et al., 2014; Hodell et al., 1995, 2001, 2005	Radiocarbon	260	14	Polynomial model	CH1 7-III-04, CH-23-V-00, CH-21-V-00, CH1 08-III-04	Wood, plant waxes, terrigenous macroffossils	5
Chumkopo							Brown et al., 2014	Radiocarbon and ^{137}Cs	103	4	No transformation	CKCV2	Leaf, twig, and bulk organic	68

Table 4.1 Continue

Location	Isotopes	Fauna	Algae	Chemical	Trophic index proxies	Mineral proxies	Reference	Dating method	Core length (cm)	Number of dates	Age model type	Name of core	Dated material	Mean resolution (years)
Coba	Ostracods $\delta^{18}O$ and $\delta^{13}C$, Gastropods $\delta^{18}O$ and $\delta^{13}C$		Diatoms	Cl, and Ca, Mg, K, Fe, Na			Leyden et al., 1998; Whitmore et al., 1996	Radiocarbon, TL, OSL	880	8	No transformation	Coba(15-VIII-80)	Ostracods, mud, wood	176
de Cocos		Ostracods, *Pyrgophorus sp.*		Al, Ti, Na			Bradbury et al, 1990	Radiocarbon	500	1	No transformation	No reported	Organic material	117
Cometa							Nooren, 2017;	Radiocarbon, stratigraphic correlation with L. Cometa	425	1		LC1, LC2	No applicable	3
Ek'Naab						Alumino-slicates	Wahl et al., 2019	Radiocarbon	698	6	Piecewise-linear model using CLAM	No reported	non-aquatic plants, wood, and seed	14
La Encantada	Ostracods $\delta^{18}O$			Ca, Ti, Fe			Correa et al., unpublished	Radiocarbon						
Encrucijada						Glass shards identified	Joo-Chang et al., 2015	Radiocarbon	600	4	Linear regression	CERRITOS-02	Wood, leaves remains, bulk organic sediment	52
Esmeralda, Chiapas				Zr, Sr, Fe, Ca			Cordero-Oviedo, 2015; Franco-Gaviria et al. 2019	Radiocarbon	600	4	BACON	ESM12	Pollen extract	21
Kail	Bulk sediment $\delta^{18}O$ and $\delta^{13}C$						Stansell et al., 2020							
Laguna de Terminos/Rio Candelaria				Al, B, Ba, Ca, Cd, Co, Cr, Cu, Fe, K, Mg, Mn, Na, Ni, Pb, S, Si,	P		Gunn et al,. 2012	Radiocarbon	290	8	No transformation	Panlao	Organic	170
Los Petenes							Gutierrez-Ayala et al. 2012	Radiocarbon	220	6	Piecewise-linear model age from Calib© 6.1.1. But no transformation for data	No reported	Bulk organic material	40
Macanche				Ca, Mg, Fe	P		Brenner , 1983; Vaughan et al., 1985	Radiocarbon	420	No reported	No transformation	Mac 80-1	Organic and calcareous material	multidecanal

Table 4.1 Continue

Location	Isotopes	Fauna	Algae	Chemical	Trophic index proxies	Mineral proxies	Reference	Dating method	Core length (cm)	Number of dates	Age model type	Name of core	Dated material	Mean resolution (years)
Manchon Swamp				Mn, Ca, sr, Mg, Na, Sb, As, Sn, K, Rb, Ba, Ni, Co, Zn, V, Fe, U, Alm Th, Ti, Ta, Zr, Hf			Neff at al., 2006	Radiocarbon	620	7	Piecewise-linear model age–depth model tool from Calib© 6.1.1;	MAN015	Macrobotanical constituents	55
Naja							Dominguez & Islebe, 2008	Radiocarbon	340	6	Piecewise-linear model	No reported	Bulk sediments samples	59
La Negra				XRF			Correa et al., in unpublished							
New River Lagoon, Lamanai Hillbank	Bulk sediment $\delta^{18}O$ and $\delta^{13}C$, *Cochliopina sp. & Pyrgophorous sp.* δ18O and δ13C,		Diatoms				Metcalfe et al., 2009; Rushton, 2014	Radiocarbon, ^{210}Pb	1381	8	Polinomial	Hillbank1998, Hillbank2000, lamanai1999, Lamanai1999-II, Outpost2000	Organic material and gastropods	-56
Ocotalito		*C. ilosvayi, D. stevensoni, Potamocypris sp.*		Sr, Ti, Ca, Mg, Na, K and Cl	SO_4^{2-}, N %		Diaz et al.,2017	Radiocarbon	900	8	Piecewise-linear model	Oco-12-II	Organic material, charcial, pollen extract	14
Paixban	$\delta^{13}C$ of Organic material						Wahl et al. 2016							
Peten Itza	$\delta^{18}O$ and $\delta^{13}C$ from *Cochliopina sp.*	*P. coronatus*		Ca %, plant pigments, stanol, Ti, Fe, Al			Anselmetti et al., 2007 Bush et al., 2009; Correa et al., 2012; Curtis et al., 1998; Hillesheim et al.,2005; Hodell et al., 2008, 2012; Mueller et al., 2008; Perez et al., 2014; Schüpbach et al., 2015	Radiocarbon	550	25	Polynomial CLAM 2.2	PI 8-VI-02 11A, PI 5-VI-02 11B, PI 9-VI-02 11C	Leaf, charcoal, wood	108
Petenxil		sponge spicules, Cladocera, Tubellaria, Insects	Diatoms, algae	Na, K, Mg, Ca, Li, Sr,, Al, Si, halogens, Ti, V, Rb, Ce, La, Sa	P		Cowgill et al. 1966	Radiocarbon		4	No transformation	Core 2, Core 3	Organic material	0
Puerto Arturo	*P. coronatus* $\delta^{18}O$,						Wahl et al., 2006,2014; Wahl 2005.	Radiocarbon	728	11	Third orden Polinomial model CLAM 2.2	No reported	Charcoal, macroscopic plant fragments, wood, and macroscopic insect	28

Table 4.1 Continue

Location	Isotopes	Fauna	Algae	Chemical	Trophic index proxies	Mineral proxies	Reference	Dating method	Core length (cm)	Number of dates	Age model type	Name of core	Dated material	Mean resolution (years)
Puerto Morelos							Islebe & Sanchez, 2002	Radiocarbon	190	2	Piecewise-linear model	MPM-1	Unidentified organic material	22
Punta Laguna	Cytheridella ilosvayi $\delta^{18}O$, Pyrgophorus coronatus $\delta 18O$						Curtis et al., 1996	Radiocarbon	630	9	Piecewise-linear model	No reported	Wood, aquatic gastropods	14
Quexil	Bulk Sediment $\delta^{18}O$ and $\delta^{13}C$,			Ca, Mg, Fe,	P		Leyden, 1984; Rice and Rice 1983, 1990; Vaughan et al., 1985	Radiocarbon	904	6	No transformation	Three cores no reported	Organic mud, lacustrine organism	-71
Rio Lagartos							Aragon-Moreno et al.,2012; Carillo-bastos et al., 2013	Radiocarbon	190	4	Piecewise-linear model	No reported	Bulk organic material	60
Rio Hondo				Ca, Fe, Ti			Aragon-Moreno et al.,2018	Radiocarbon	797	7	Piecewise-linear model	No reported	Bulk organic material	14
Sacnab					P	SiO_2, $Al_x(SiO_2)_x$	Rice & Rice, 1983; Vaughan et al., 1985	Radiocarbon	630	3	No transformation	No reported	Organic material	204
Salpeten	*Physocypria globula* $\delta^{18}O$, Plant wax $\delta^{13}C$ and δO			Ca, Mg, Fe, plant wax lipids	P		Brenner et al., 2002; Leyden, 1984, 1987; Rosenmeier et al., 2002, 2016	Radiocarbon	350	17	Fourth-order polynomial model	Sal 80-1, SP1-17-VIII-99, SP1-17-VIII-99	Wood, charcoal, sees	10
San Jose Chulchaca	Ostracods $\delta^{18}O$ and $\delta^{13}C$, Gastropods $\delta^{18}O$ and $\delta^{13}C$		Diatoms	Cl, and Ca, Mg, K,	P		Whitmore et al., 1996; Hodell et al, 2005.	Radiocarbon	110	8	No transformation	SJC(9-VII-92)	Mud	196
San Lorenzo		Cladocea		Ti, Ca, Sr, Fe, Mn, Zr, Rb, K			Franco-Gaviria et al., 2019, 2020	Radiocarbon	670	4	BACON 2.2	LIQ13	Plant remains, charcoal, wood	5
Santa Ana Vieja							Cowgill and Hutchinson 1966	Indirect stratigraphy correlation with Pentexil	23	0	No transformation	No reported	No apply	multidecanal

Table 4.1 Continue

Location	Isotopes	Fauna	Algae	Chemical	Trophic index proxies	Mineral proxies	Reference	Dating method	Core length (cm)	Number of dates	Age model type	Name of core	Dated material	Mean resolution (years)
Sayaucil	Ostracods $\delta^{18}O$ and $\delta^{13}C$, Gastropods $\delta^{18}O$ and $\delta^{13}C$		Diatoms	Cl, Ca, Mg, K	P		Whitmore et al., 1996	Radiocarbon	613	5	No transformation	Sayucil(26-VII-89)	Mud	206
Silvituc (Noh)							Torrescano-Valle et al., 2012, 2015	Radiocarbon	135	6	Piecewise-linear model age–depth model tool from Calib© 6.1.1;	No reported	Bulk organic material	152
Tamarindito		Gastropods			P	Fe_2O_3, SiO_2	Dunning et al., 1998	Radiocarbon	235	5	Piecewise-linear model	No reported	Organic material	676
Tuspan	Cytheridella ilosvayi $\delta^{18}O$ and $\delta^{13}C$, $\delta^{13}Corg$,	*Cytheridella sp.* *Candonopsis sp.*	Diatoms	Ca %, Ti%, Si, S, K, Ca, Ti, Mn, Fe, Al		Smectite, chlorite, halloysite	Fleury et al., 2015; Nooren et al., 2018	Radiocarbon	975	14	CLAM model	Tuspan A, Tuspan B, Tuspan C	Vegetal macro remains, charcoal, wood	6
Tzib	*Pyrgophorus sp.* $\delta^{18}O$ *Assiminea sp.* $\delta^{18}O$						Carillo-Bostezano et al., 2010, 2012	Radiocarbon	250	2	Extrapolated line with an additional CALIB 5.0.2 date	No reported	Bulk organic material	322
Verde							Morse, 2009	Radiocarbon	365	3	No transformation	No reported	Organic material	127
Yalahau				S			Correa et al.unpublished	Radiocarbon						
Yaloch	$\delta^{13}Corg$,					Alumino silicate %,	Wahl et al. 2013	Radiocarbon	397	10	Composite of two polynomial regressions	No reported	Organic material	8
Yaal Chack				Fe, Ti, Br, Ca			Primmer, 2018	Radiocarbon			Piecewise-linear model	YC11, YC14, YC16	Organic material	
Yaxha					P	SiO_2, $Al_x(SiO_2)_x$	Brenner, 1983; Rice & Rice, 1983	Radiocarbon	630	3	No transformation	No reported	Organic material	204

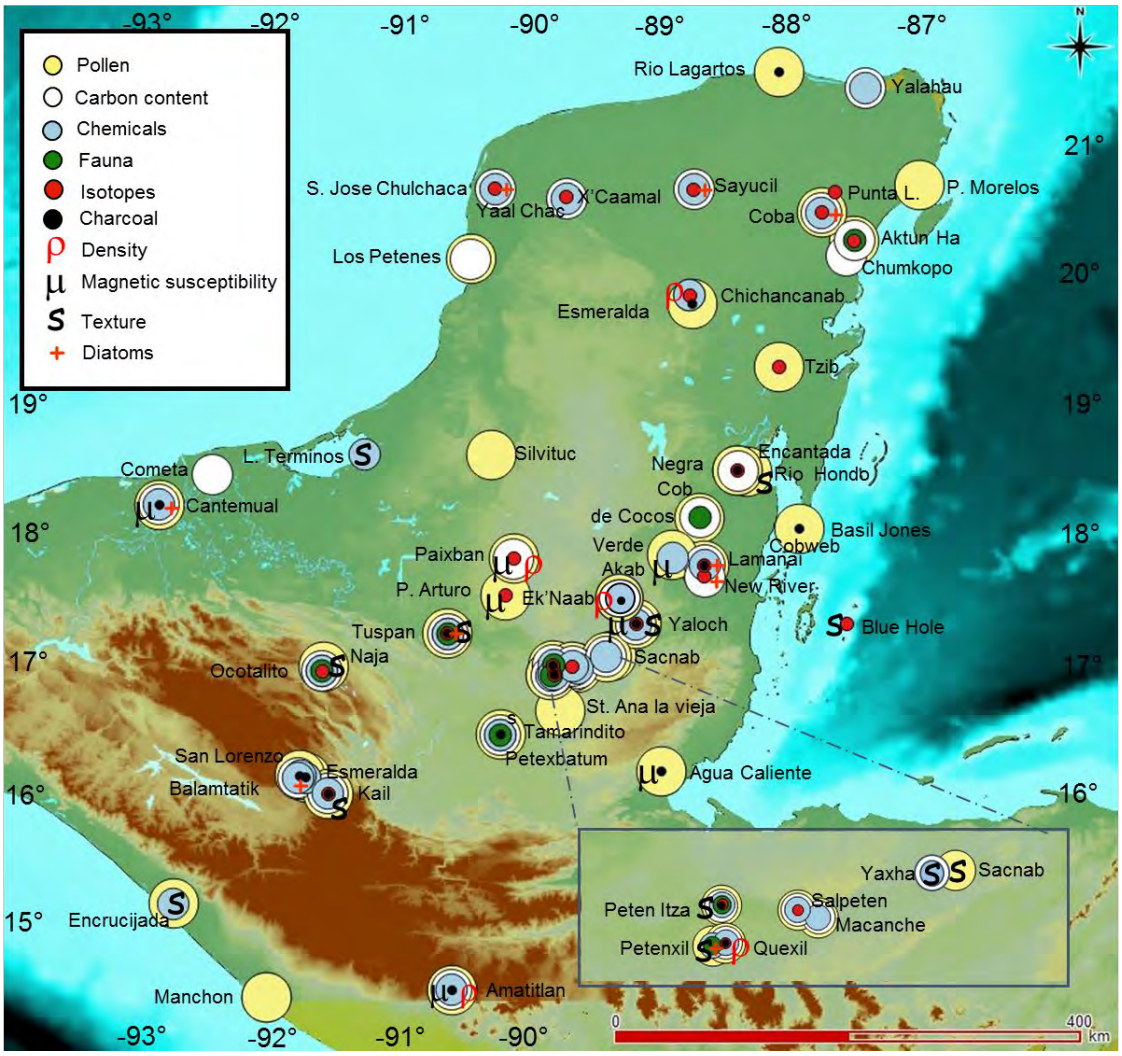

Figure 4.3 Location of studies which used lake sediments as environmental records indicating the different kinds of proxies involved. Although we divided the different chemical proxies into various categories (see Table 4.1), we unified all in a single category for presenting their spatial distribution. Map produced using QuantumGIS 2.18.11.

Depending on the specific chemical entity used, these proxies usually gave information about the terrigenous input into the lakes and the degree of erosion around the lake among other properties (see third paragraph in this section). In the case of the texture as a proxy, only a number of the records are listed where the publication actually discusses changes in the texture, e. g. Encrucijada, (Joo-Chang et al., 2015) Laguna de Terminos (Gunn et al., 2012), Yaxha (Brenner, 1983), Yaloch (Mueller et al., 2009; Wahl et al., 2013) Peten Itza (Curtis et al., 1998; Mueller et al., 2010, 2009), but it is possible that some records indirectly present such changes although they do not discuss them. These textural changes normally indicate changes in the source of the sediments or the energy of the flow.

Along with texture, density is a less used proxy. This might be due to the difficulties of finding a direct environmental driver of the changes in density. The case of Chichancanab is a particular exception, where the changes in density are substantial and linked with major precipitation of evaporites (specifically gypsum), which implies the presence of dry periods (Hodell et al., 2005a).

Finally, another aspect to consider is the low number of records that contain charcoal as a proxy in comparison with a large number of pollen records. This issue might be related to the potentially poor preservation of charcoal in hard water (Braadbaart et al., 2009) which is present in many of the lakes in the Maya Cultural Area (Cervantes-Martìnez et al., 2002; Gondwe et al., 2010; Pérez-Ceballos et al., 2012). However, no major challenges have been reported in the records that have used charcoal as an environmental proxy.

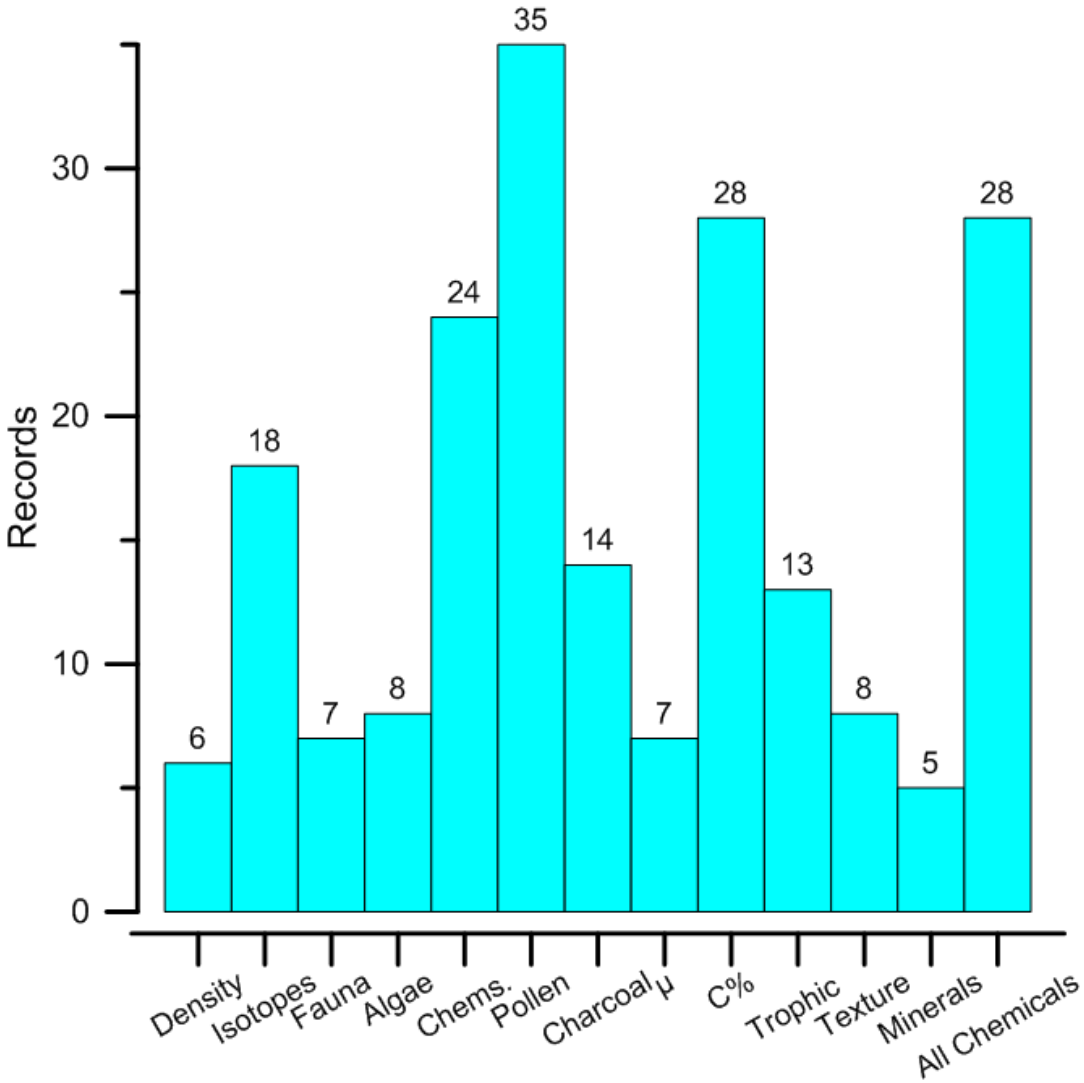

Figure 4.4 Bar chart showing the number of studies using a particular environmental proxy on lake sediments in the Maya Cultural Area. Percentage of organic carbon and magnetic susceptibility are denoted by C% and μ, respectively.

4.3 Speleothem records in the Maya Cultural Area

Only eleven records have been developed in the Maya Cultural Area based on speleothems (Table 4.2) (Figure 4.5). These records are invaluable since they can be dated by uranium-series which can potentially have very small uncertainties and does not need to be calibrated like radiocarbon since the parental nuclides are not cosmogenic, often allowing a very reliable chronology to be developed (Bernal et al., 2010), which has been valuable considering the issue of old carbon in karstic lakes for ^{14}C dating.

Some speleothems have a chronology established with numerous dated points, which posess relatively very small uncertainties e. g. the speleothems at Macal Chasm (Akers et al., 2016; Webster et al., 2007) and Rey Marcos (Winter et al., 2020), although correction for the presence of detrital material is typically applied (Bernal, 2003; Bernal et al., 2010). Speleothems can also potentially be annually layered, allowing high-resolution chronologies to be established, similar to those using varves in lakes. Unfortunately, only the speleothem at Actun Tunich Muknal cave had continuous layers, but it does not cover the period of the Maya civilisation (Frappier et al., 2007).

In contrast, speleothems can present some degree of diagenesis, which is evident by the presence of aragonite (Domínguez-Villar et al., 2017). In this case, the speleothems are functioning as an open system which loses nuclides, resulting in unreliable dates.

Although practically any kind of speleothem could be used for environmental reconstruction (Fairchild et al., 2006), stalagmites are the only kind of speleothem used for this purpose in the Maya Cultural Area. All the speleothems were studied using stable isotopes, and all of them used $\delta^{18}O$ except for the stalagmite Yok-G which used the $\delta^{13}C$ as a proxy. Figure 4.5 shows the proxies used on speleothems. Only the speleothems found at Macal Chasm (Webster et al., 2007) and Chen Ha (Pollock et al., 2016) used both carbon and oxygen isotopes as environmental proxies. In the case of Yok Balum, both isotopes are referred to but were used in different stalagmites (Jamieson et al., 2016; Kennett et al., 2012; Lechleitner et al., 2015).

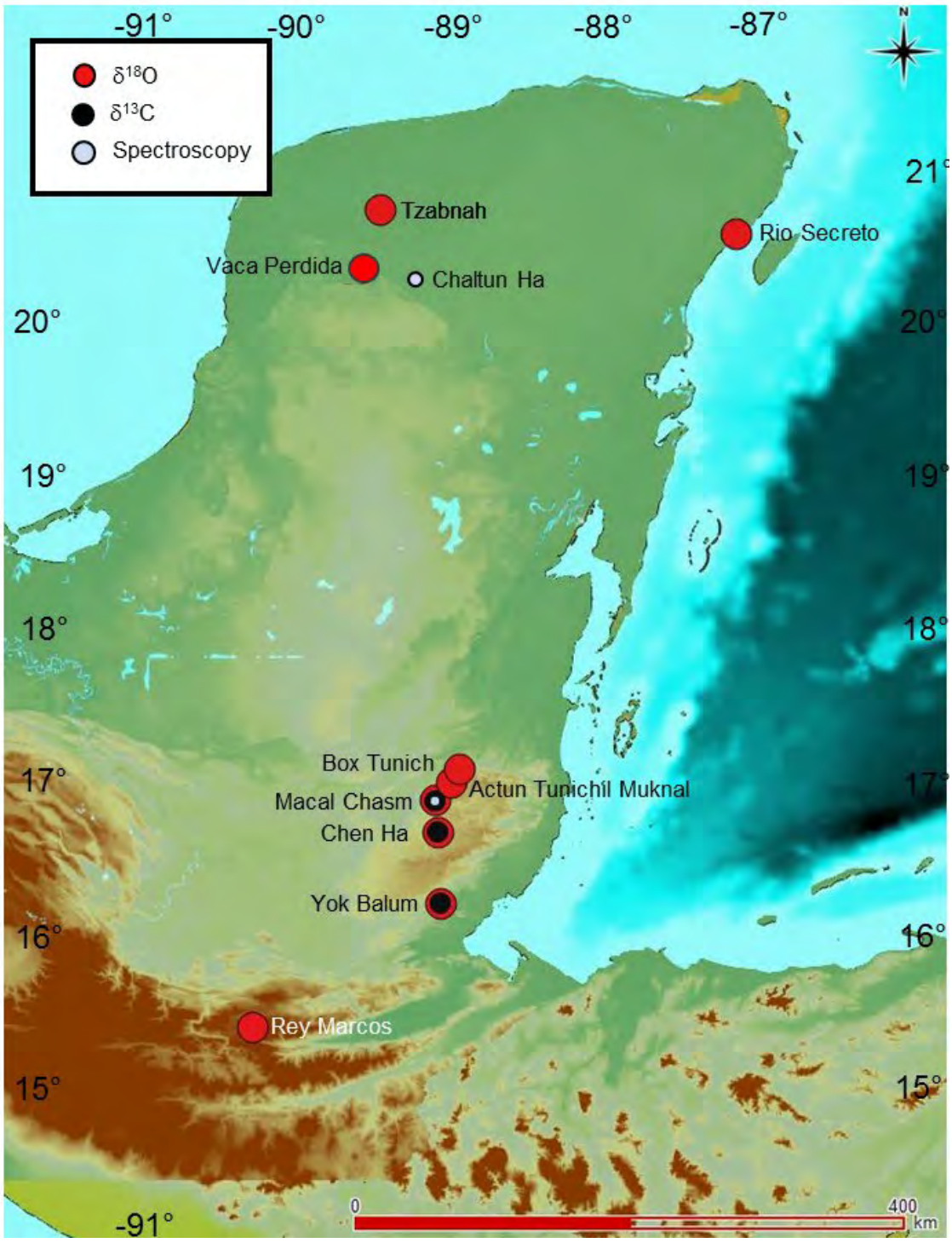

Figure 4.5 Location of studies which used speleothems as environmental records. The map also shows the spatial distribution of the proxies studied in each speleothem.

Table 4.2 Palaeoenvironmental records based on speleothems presenting the proxy studied, its temporal resolution, the name of the rock and the environmental signal recovered (a proxy of). The table also shows information related to the age model, such as the dating method, number of dating samples, age model type and dated material.

Location	Proxy	Reference	Dating method	Size of speleothem (cm)	Number of dating samples	Resolution	Age model type	Name of rock sample	Dated material	Proxy of
Actun Tunichil Muknal cave	$\delta^{18}O$	Frappier, 2002; Frappier et al., 2007	^{137}Cs, layer counting	2.6	12	Subseasonal	Piecewise-linear model	ATM7	Organic material	ENSO, hurracanes
Box Tunich cave	$\delta^{18}O$	Akers et al., 2019	U-series, ^{14}C, ^{210}Pb	9.3	9	8 years	Piecewise-linear model Chronoloical Tunning	BZBT	Calcite, Organic Material	Palaeoprecipitation
Chaltun Ha Sinkhole	Fluorescence	Frappier et al., 2014	layers counting	16.9	layers counting	annual	Piecewise-linear model	CH-1	Calcite	Flooding events
Chen Ha cave	$\delta^{13}C$, $\delta^{18}O$	Pollock et al., 2016	U-series	100	11	Subannual	Linear interpolation model	CH04-02	Calcite	PalAeoprecipitation , carbonate rate
Macal Chasm cave	$\delta^{18}O$,$\delta^{13}C$, luminescence, reflectance	Akers et al., 2016; Webster et al., 2007	U-series, Radiocarbon	93.6	16 of U-Th, 8 of ^{14}C, 2 of ^{210}Pb	Byannual TCP, 4 & 15 years modern, 20 years paleoindian & pre-classic	Piecewise-linear model, Bacon age-depth model	MC-01	Calcite	Palaeoprecipitation, cultivation and soil use
Rey Marcos cave	$\delta^{18}O$	Winter et al., 2020	U-series		20	Decadal	COPRA	GU-RM1	Calcite	Palaeoprecipitation
Rio Secreto Cave	$\delta^{18}O$	Medina-Elizalde et al., 2016	U-series	31	13	8 years	Piecewise-linear model	Itzamna	Calcite	Palaeoprecipitation
Vaca Perdida Cave	$\delta^{18}O$	Smyth et al., 2017, 2011, 2010	U-series	45	14	16.6 years	Piecewise-linear model	VP-10-1	Calcite	Palaeohumidity
Yok Balum cave	$\delta^{13}C$	Ridley, 2014; Ridley et al., 2015	cycles of $\delta^{13}C$, U-series	365	18	Monthly	Piecewise-linear model	Yok-G	Aragonite	Hurricanes
Yok Balum cave	$\delta^{18}O$	Kennett et al., 2012; Lechleitner et al., 2015; Maya et al., 2012; Ridley et al., 2015	U-series	41.5	40	Subannual	Piecewise-linear model	Yok-1	Calcite	Palaeoprecipitation
Tzabnah cave	$\delta^{18}O$	Medina-Elizalde et al., 2010; Medina-Elizalde and Rohling, 2012	U-series and laminae counting	44.1	12	2.3 years	Piecewise-linear model	Chaac	Calcite	Palaeohumidity

$\delta^{18}O$ is a rainfall amount proxy in the speleothems at low latitudes because inside a cave the gradient temperature between seasons is negligible, precipitation amount is generally considered the biggest driver of rainfall $\delta^{18}O$ values (Fairchild et al., 2006; Lachniet and Patterson, 2009). In this way, compared with modern instrumental records, it was possible in some cases to estimate the amount of ancient rainfall for the stalagmite, as at Tzabnah (Medina-Elizalde et al., 2010), as well as to reconstruct the occurrence of hurricanes (Medina-Elizalde et al., 2016b).

The speleothem at Macal Chasm was the only one where other kinds of proxies were used. In this case, the greyscale (reflectance) and U. V. stimulated luminescence were used as proxies of humidity (Akers et al., 2016) since the density of the precipitate carbonated is driven by the humidity and the incorporation of detrital material (Webster et al., 2007).

It has to be highlighted that the speleothems have in most of the cases a very high resolution in the environmental isotopic signal. This kind of resolution is only also achieved in tree rings (Douglas et al., 2016), varved sediments (Primmer, 2019) or lake sediment records studied by XRF (Davies et al., 2015). In the case of lakes, a series of factors do not allow a high-resolution isotopic signal, where the most important factor is that lakes are very resilient systems due to their residence time. An isotopic signal tends to reflect the signal of a period of 10 years in small-medium hydrologically closed lakes (e.g. Lake Tilo Ethiopia, Lake Golhisar, Turkey) and 100's years in large lakes (e.g. Lake Malawi, Lake Turkana, Turkey) (Leng et al., 1999). Is still unknown the residence time in many of the closed lakes of the Maya Cultural Area (Pérez et al., 2013).

Finally, Figure 4.5 shows that palaeoclimatic studies involving speleothems have been performed mainly in Belize. The stalagmite collected at Rey Marcos cave is the only record in the Highlands and in Guatemala **(**Winter et al., 2020**).**

4.4 Additional records in the Maya Cultural Area

Figure 4.6 and Table 4.3 show records based on dendroclimatology. The only research that has used tree rings in the Maya Cultural Area was performed in Puerta del Cielo, San Juan Mountain and Bosque del Rancho in the Southern Highlands in Guatemala. This small number of records is probably a consequence of several factors. First of all, there have been few studies on trees in the region, because it has generally been assumed that trees in the lowland tropics do not form annual rings, unlike trees in higher-latitude or higher-altitude regions that cease growth completely in winter (Douglas et al., 2016).

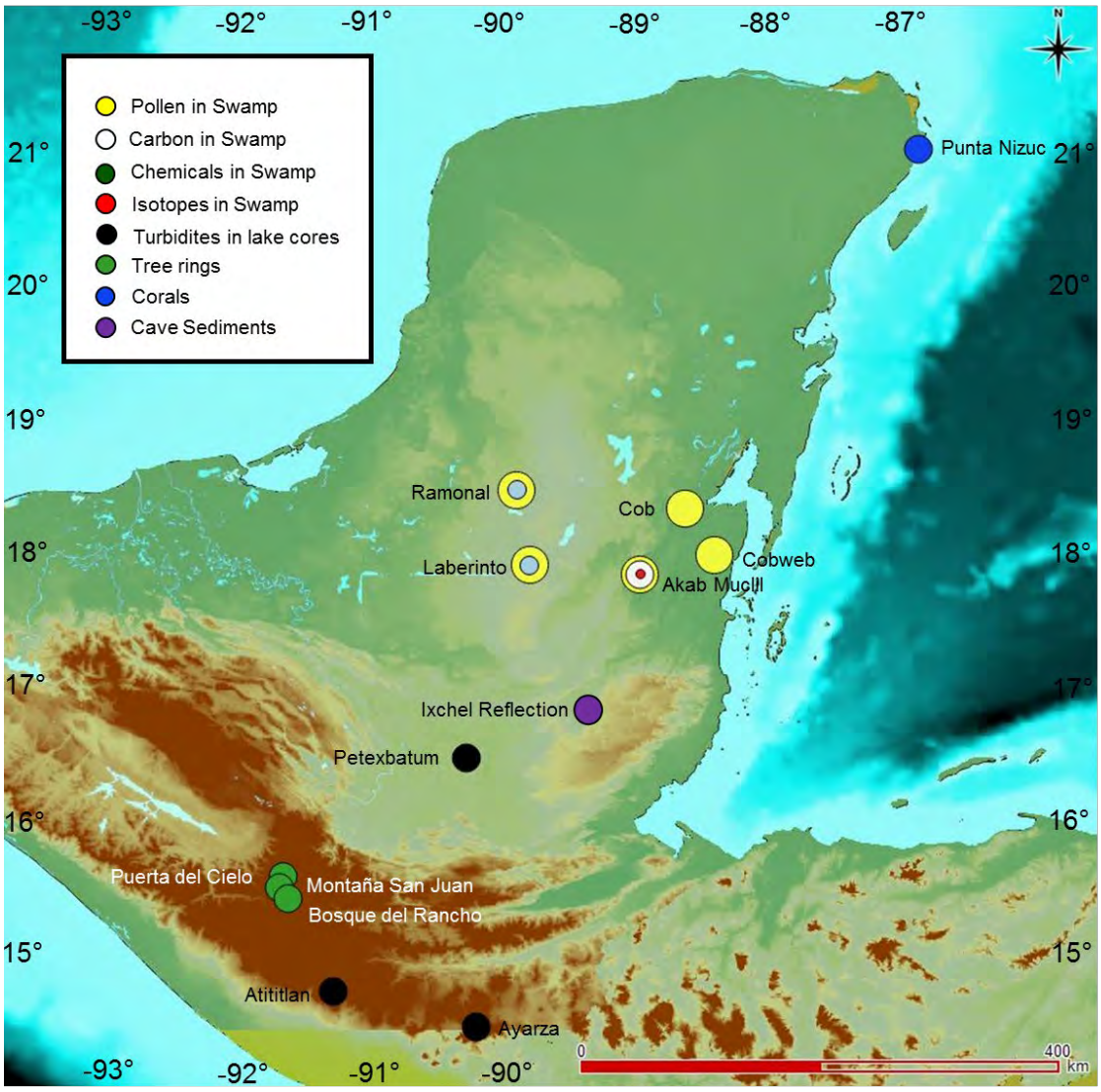

Figure 4.6 Location of dendrochronological records, swamp or wetland sediment core records as well as corals. The map shows the different proxies used in the seasonal wetland sediment records. The map also presents the sites where palaeoenvironmental studies in lakes were attempted but failed since a chronology could not be developed due to the presence of turbidites. The map also shows the location of the cave sediment record. Map produced using QuantumGIS 2.18.11.

This assumption is because there is not a significant gradient of temperature between winter and summer, therefore the rings reflect seasonal changes in precipitation. However, it has been shown that trees still produce rings at low latitudes. Besides, as in other parts of North America, the vegetation in the highlands is composed of the cloud forest of coniferous trees due to the high elevation that produces more temperate climates. The issue with the dendroclimatological records is not the lack of tree rings but the preservation of the old trees (Douglas et al., 2016).

Second, it is unlikely that many living trees in the Maya area are older than a few hundred years (the same applies in general for tropical ecosystems), restricting the time frame over which climate variability in the region could be studied by this method (Douglas et al., 2016). Therefore, the chance to find dendroclimatological records contemporary with the Mesoamerican Horizons is very low.

The current stage of dendroclimatology research in the Maya cultural area, make this kind of records an unsuitable option for reconstructing climates during the Mesoamerican periods. Some drendrochronological archives in the Cultural Archaeological Areas of Aridoamerica, Southwest and the centre of Mesoamerica, evidently outside the Maya Cultural area, has been used to sustain the hypothesis of the Maya Droughts (Stahle et al., 2011). However, the location of these records makes them very problematic since they were exposed to different climate regimes. However, if the climate dynamics between them is known, it might be possible to link the different areas.

Table 4.3 Palaeoenvironmental records not based-on speleothems or lake sediments. The table also shows information related to the resolution of the proxies studied (see Figure 4.6) as well as the age model, (dating method, age model type and dated material).

Location	Kind of Record	Reference	Dating method	Age model type	Dated material	Mean resolution (years)
Punta Nizuc Reef	Coral	Horta-Puga & Carriquirry, 2012	Layer counts	Linear regression	Coral	Annual
Ix Chel Reflection cave	Cave sediments	Polk et al., 2007	Radiocarbon	Piecewise-linear model	organic material	Centennal
Bosque del Rancho	Dendroclimatology	Anchukaitis et al., 2013	Crossdating	Piecewise-linear model	Trees	Annual
Puerta del cielo	Dendroclimatology	Anchukaitis et al., 2014	Crossdating	Piecewise-linear model	Trees	Annual
San Juan Mountain	Dendroclimatology	Anchukaitis et al., 2015	Crossdating	Piecewise-linear model	Trees	Annual
Akab Muclil	Seasonal swamp	Krause et al. 1919	Radiocarbon	Piecewise-linear model	Organics	Cenntennal
Cob Swamp	Seasonal swamp	Pohl et al., 1996	Radiocarbon	No transformation	Organics	Cenntennal
Cobweb	Seasonal swamp	Jones et al., 1991	Radiocarbon	No transformation	Organics	Cenntennal
Laberinto	Seasonal swamp	Gunn et al., 2012	Radiocarbon	No transformation	Organics	Cenntennal
Ramonal	Seasonal swamp	Gunn et al., 2002	Radiocarbon	No transformation	Organics	Cenntennal

Figure 4.6 also shows the records based on sediment cores or discrete sediment samples from profiles from seasonal wetlands (e. g. sediments from archaeological profiles). All wetland records used pollen as a proxy for vegetation, while three of them, Ramonal, Laberinto (Gunn et al., 2002) and Akab Muclil (Krause et al., 2019) used the elemental

composition of the sediments. The record at Akab Muclil is the only record to use an isotopic proxy, $\delta^{13}C_{organic}$.

All wetland records are located in the southern part of the Mayab near to the border of Central Lowlands. Another record shown in Figure 4.6 is the one based on cave sediments at Ixchel Reflection Cave where $\delta^{13}C$ was compared to a similar record in the speleothem of Macal Chasm (Webster et al., 2007) showing similar trends interpreted as variations of humid and dry conditions (Polk et al., 2007). Table 4.3 shows additional information related to these records that is not shown on the map.

Figure 4.6 also shows the lake records that failed in making an environmental reconstruction, since the presence of turbidites did not allow an age model to be established. These records, however, contain pollen records and faunal assemblages. In the case of the cores extracted at Atitlan and Ayarza, the lakes are in a volcanic crater. Considering that both volcanos are in an active margin, the presence of turbidites might be explained by earthquakes (Poppe et al., 1985). The hydraulic system at Petexbatum is connected with lake Tamarindito, which has a well-established record. In this way, the lack of dates at Petexbatum could be compensated for. Figure 4.6 also shows a record based on studying corals (Horta-Puga and Carriquiry, 2012).

4.5 Temporal framework of palaeoclimatic records in the Maya Cultural Area

I developed a comparison of the chronologies of all the records in the Maya Cultural area. As the chronology of the lake sediment records are mainly based on radiocarbon dating I created a list of the calibrated ages assigned to the oldest and youngest measured points, as well as a list of the assigned age for the bottom and top points of the full record extrapolated from the applied age model (we used the extreme assigned ages of this interval, instead of the median ages). The sources of material for dating are mentioned, as well as the number of dates obtained (Table 4.1). I did not mention if a record's age model used a hard water error correction since this step is not always described even in records with high carbonate content in karst areas. This issue is more commonly addressed in the records produced in the Maya Cultural Area for the last 15 years, normally searching terrestrial material for dating, which is not influenced by old carbon.

The method used for establishing the age model of each point in the record is also shown, including the records where no age model is really assigned, leaving the measured ages as a point of comparison besides the depth. Age models were assigned by multiple methods

by the authors of the respective research, including linear and polynomial regression, piecewise-linear models, and Bayesian statistics-based models.

Many records attributed the date of the core collection to the top of the core, without assuming any removal of material and a continuous sedimentation process. Many records attribute an age of 0 years B. P. at the top even though the discrepancies between the year of collection and the assigned age 0 B. P., (1950 A D), were not always negligible.

Only some records had the opportunity to use an actual tephra layer of known provenance for dating, e. g. records at Guatemala, Tabasco and Campeche (Nooren, 2017; Stansell et al., 2020). Other dating methods used, such as ^{210}Pb, are also specified in Table 4.1. For the records published before the 1990s, the published radiocarbon dates were uncalibrated. Therefore, I calibrated these dates using the IntCal13 calibration Curve in OxCal.

The assigned name of the core, year of coring, length of the record and spatial sampling interval of the proxy with most samples is also noted. The temporal resolution of the record was calculated using these two last parameters and the chronology, following the formula

$$R = SD\,\frac{(Om - Ya)}{Do}$$ *Equation 4.1*

where *R* is the obtained resolution, *SD* is the sampling distance of the proxy with most samples, *Om* oldest measured date, *Ya* assigned date at the top, *Do* depth of the oldest date.

Figure 4.7 shows the time frame covered by every palaeoenvironmental record in the Maya Cultural Area. The records are displayed first by groups (colour indicates the type of record), the wetland records, lake sediment records, speleothems, cave sediments, corals and tree rings, and second by alphabetical order.

Unpublished records that have been presented only as postgraduate research theses are also presented. However, where records have longer chronologies, e.g. Chichancanab (Covich and Stuiver, 1974), Yaal Chack (Primmer, 2019), we constrained the period of the record to the time frame that has been studied using a group of proxies. Figure 4.7 also shows a dotted line for the major part of the period studied at Aguada X'Caamal, representing the time when this sinkhole functioned as an open system, making its studied proxy (δ^{18}O) unreliable as a proxy of evaporation-precipitation ratio (Hodell et al., 2005b).

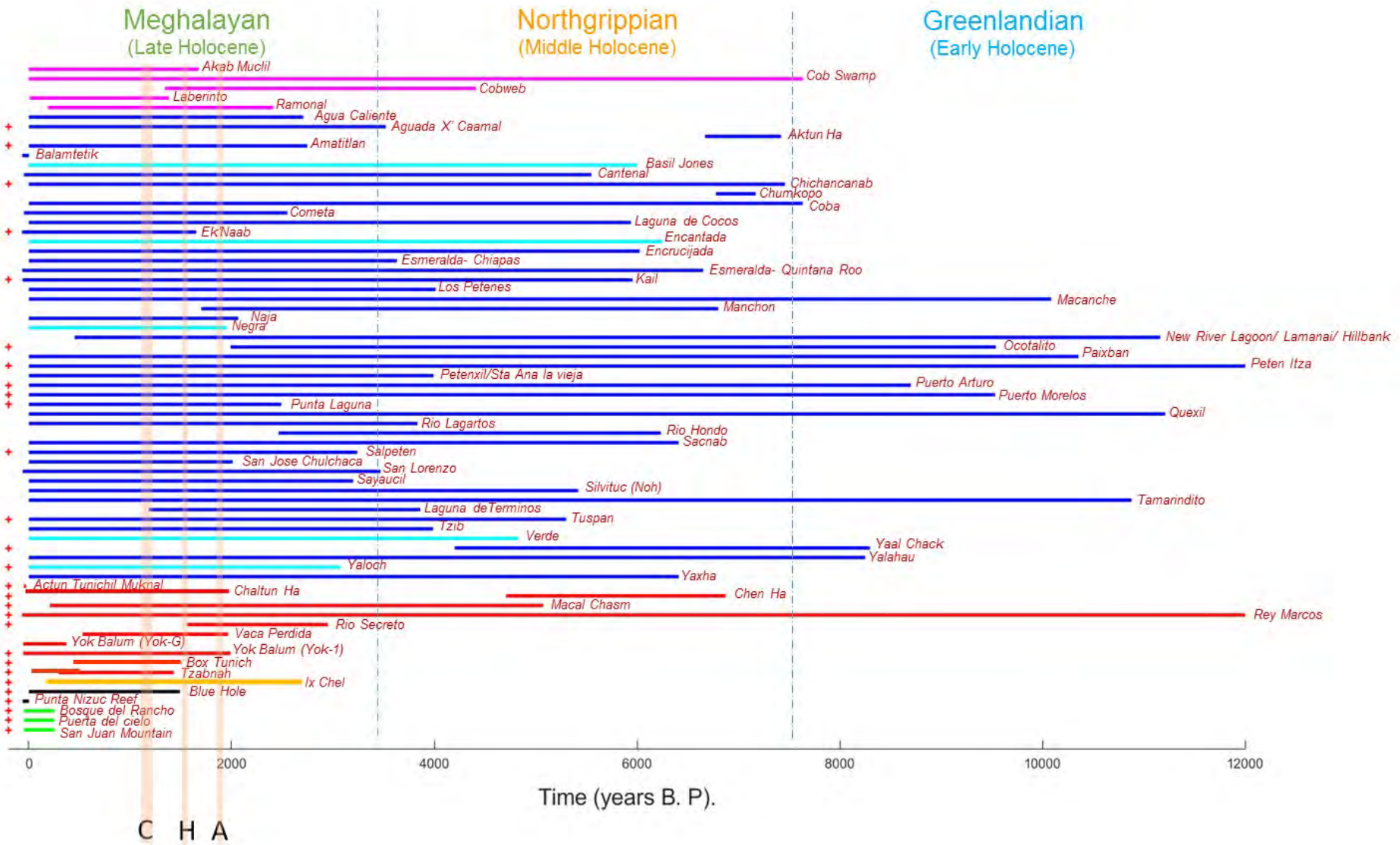

Figure 4.7 Time frame of the different records of the Maya Cultural Area; temporal swamp (pink), lake (blue), spelethems (red), cave sediments (yellow), corals (black) and tree rings (green). Unpiblished lake records are in pale blue. The letter indicates the critical periods during Maya History (see section 2.5, chapter 2), the Maya Abandonment (A), the Maya Hiatus (h) and the Maya Collapse (C). The symbol (+) indicates the records which have at least one proxy with a resolution better than 20 years.

Some records share the same chronology, for instance, the records at Santa Ana La Vieja and Petenxil (Cowgill et al., 1966).

Figure 4.7 shows that most of the records cover only a part of the Holocene. Only ten records cover the Greenlandian Stage. The number increases to 40 for the Northgrippian Stage, while the Meghalayan stage is the time frame that contains most records; 66. Forty-eight records also highlight the three critical points in the Maya History, the Maya Abandonment at the end of the Preclassic Mesoamerican horizon, the Maya Hiatus and the Maya Collapse at the end of the Mesoamerican Classic period.

In this way, it can be observed that not all records cover these critical historical moments. Finally, the additional sign (red crosses) in Figure 4.7 represents the records that have at least one proxy with a resolution better than 20 years. Speleothem, coral and tree rings tend to have a better resolution than lake sediments. However, these records only cover a small fraction of the Holocene. The exception is the speleothem in the Rey Marcos cave, which covers all the Holocene **(**Winter et al., 2020**)**, however, this record is in the Highlands. In summary, despite the relatively large number of records, the Maya Cultural area still needs to have records that cover longer time frames, that have high resolution and that have more of a multiproxy approach.

4.6 Historical Evaporation-Rainfall conditions in the Maya Cultural Area based on high-resolution records.

Figure 4.8 presents the $\delta^{18}O$ records for the Maya Cultural Area. Two of these records do not cover the period of the Maya Civilisation, while eleven records have a low resolution. Only thirteen $\delta^{18}O$ records have a resolution better than 20 years and cover the period of the Maya civilisation. Seven of these records are lake sediments, including the core collected at Blue Hole (Gischler and Storz, 2009).

Figure 4.9 presents five of these $\delta^{18}O$ records, selected because they cover a time frame of 7000 years, covering most of the Meghalayan and the whole Northgrippian. The Meghalayan in the Maya lowlands is described as a transition phase from wetter to drier conditions (Aragón-Moreno et al., 2018; Carrillo-Bastos et al., 2010; Metcalfe et al., 2000; Wahl et al., 2016, 2014). It can be observed that the relatively humid phase until 4700 years B. P. (Figure 4.9 right blue zone) followed by a dry phase until the 4.2 event (Figure 4.9 right yellow zone) do not coincide entirely with the humid and drought trends in every

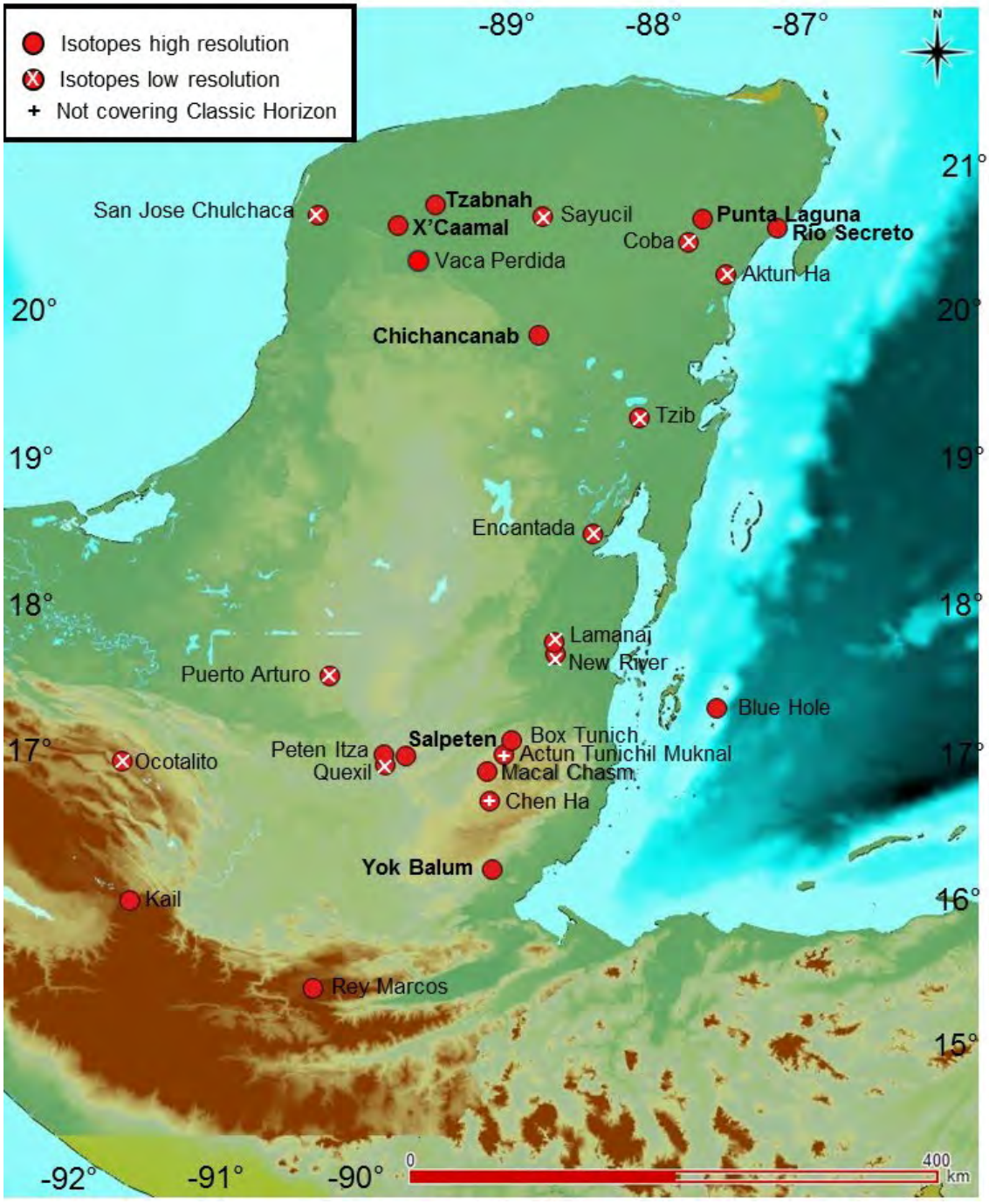

Figure 4.8 Location of the palaeoclimatic records that used the $\delta^{18}O$ as a proxy of rainfall, evaporation-rainfall ratio, humidity or water balance in lake sediments and speleothems. The map indicates the records which have a resolution better than 20 years and cover the period of the Maya civilisation. These records are plotted in Figure 4.9 and Figure 4.10. Map produced using QuantumGIS 2.18.11.

displayed record. For instance, these humid and dry phases of the Meghalayan coincide in the speleothem record at Rey Marcos and the lake records at Chichancanab (Hodell et al., 1995, 2001, 2005) and Kail (Stansel et al., 2020) but have the opposite trend to the lake record at Peten Itza (Curtis et al., 1998). It has to be highlighted that the newly developed

records at Kail (Stansell et al., 2020) and Rey Marcos (Winter et al., 2020) in the Maya Highlands have matched with the observed humid-drought trends observed in the Maya Lowlands at decadal scale, although they have opposite trends at the millennial-scale (see chapter 7 related to our studies in Lake San Lorenzo).

In Figure 4.9 (grey band left) a pattern that might be related to the 4.2 ky Rapid Climate Change event proposed by Mayewski et al., (2004) can be seen in every record, although the signal appears a little offset in the Kail record (Stansell et al., 2020). After this event, the Meghalayan is marked by the return of a short period of humid conditions (Figure 4.9 left blue zone) mainly in the highlands. Figure 4.9 shows that wetter conditions were indeed presented in all the displayed records. This humid phase in the Meghalayan is supported in other pollen records at the Northern Mayab (Leyden, 2002).

For example, the palynology record from Rio Lagartos, displays high proportions of taxa characteristic of stable wet, tropical forest environments, such as *Brosimum alicastrum*, Moraceae and *Ficus* sp, until 3,500 cal years B. P. (Aragón-Moreno et al., 2012). In contrast, records in the southern lowlands indicate a long term drying trend at Puerto Arturo (Wahl et al., 2014), Tzib (Carrillo-Bastos et al., 2010), Silvituc (Torrescano-Valle and Islebe, 2015), and the same palynological record at Peten Itza (Mueller et al., 2009). However, Peten Itza's isotopes describe a different panorama (Curtis et al., 1998), which might be related to the difference between records obtained in shallow (isotopes) and deep (pollen) water.

Conditions are dry in the lowlands after 3500 years B. P. (prevailing a millennium), this tendency is clear in the shift to drier conditions in Lake Chichancanab (Hodell et al., 1995, 2001, 2005), Peten Itza (Curtis et al., 1998), Salpeten (Rosenmeier et al., 2002, 2016) and Rey Marcos (Winter et al., 2020). The record at Lake Kail at the Maya Highlands also presents dry decadal periods during this phase, although conditions at centennial scale are humid (Stansell et al., 2020). This millennial-scale wetting pattern at Kail might be the result of insolation forcing; however; the persistence of wetter conditions is the opposite to what is expected during this period of decreased convective activity in the northern tropics (Stansell et al., 2020). This dry period is constrained to the 2.5-3.5 Rapid Climate Change interval (Mayewski et al., 2004), which ends at 2500 years B. P. A relatively humid period is established after the 2.5-3.5 Ky interval until 1700 years B. P.

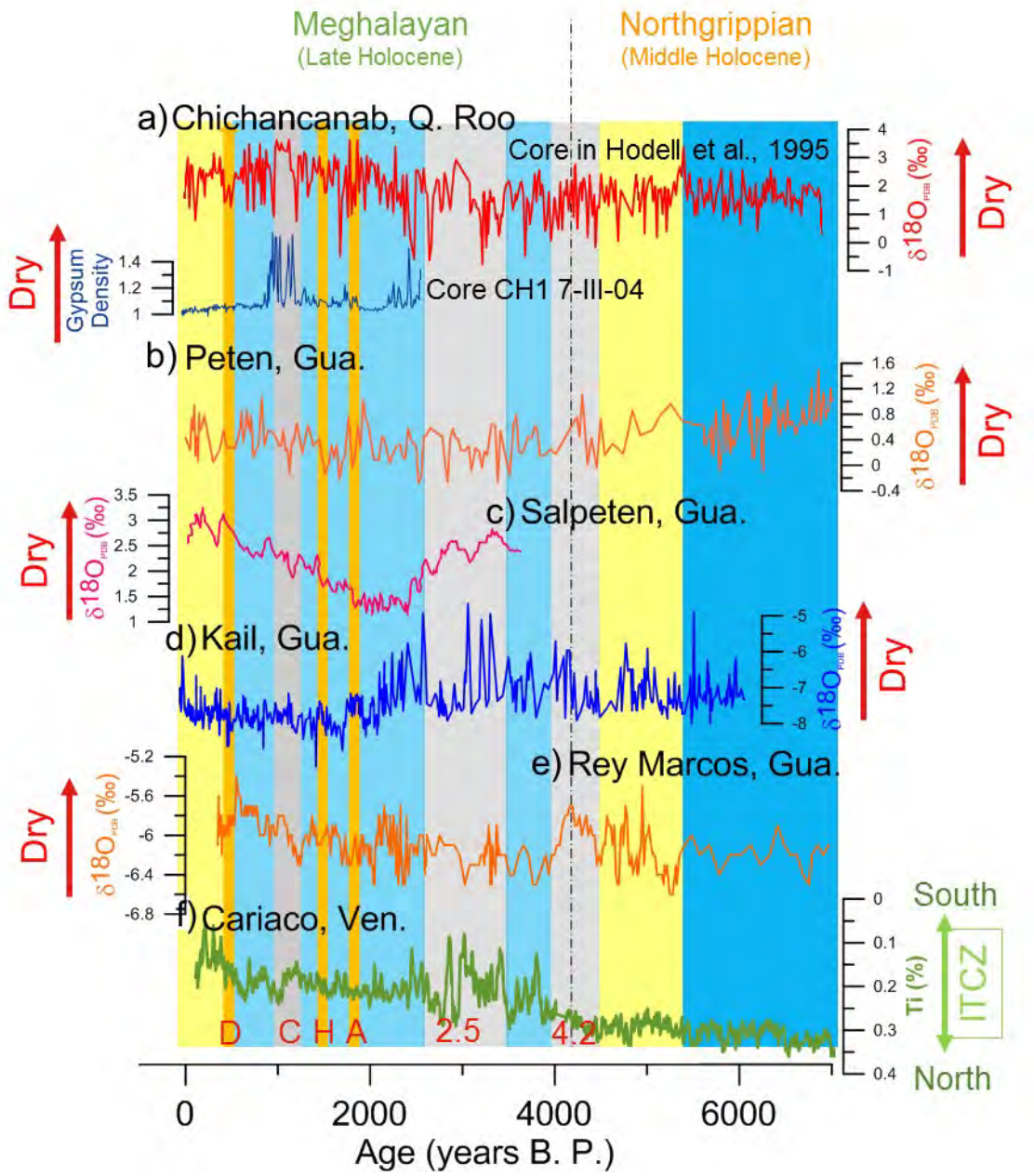

Figure 4.9 High-resolution records of the Maya Cultural Area based on $\delta^{18}O$ indicating the relative changes between dry and humid conditions for the last 7000 years; a) Lake Chichancanab, displaying the core collected by Hodell et al., (1995), and core CH17-III-04 (Hodell et al., 2005a), b) Lake Peten Itza (Curtis et al., 1998), c) Lake Salpeten (Rosenmeier et al., 2002, 2016), d) Lake Kail (Stansell et al., 2020) and e) Speleothem at Rey Marcos (Winter et al., 2020). The percentage of Titanium of the Cariaco marine record is also shown, indicating the movement of the ITCZ (Haugh et al., 2003), which is argued as the primary driven of humid conditions in the area, although the ITCZ does not reach the Maya Cultural Area entirely. The grey bands highlight the dry periods linked to the 4.2 and 2.5 Holocene Events (Mayewski et al., 2004) *and the Maya Collapse (C), while the orange bands indicate climatic stress (droughts) related to the Maya Abandonment (A), the Maya Hiatus (H) and the Destruction of the League of Mayapan (D) (see section 2.5, chapter 2). Humid periods are indicated by blue, (more intense blue colour indicates more intense humid conditions) and dry centennial periods are indicated by yellow.*

For example, the pollen record identified taxa related to humid conditions at Tzib according to Carrillo-Bastos et al., (2010). The $\delta^{18}O$ records at Punta Laguna, Salpeten (Rosenmeier et al., 2002, 2016), Rio Secreto (Medina-Elizalde et al., 2016) and Macal Chasm (Webster et al., 2007) indicate such relatively wet conditions (Figure 4.10).

These low evaporation-rainfall ratio conditions (more effective rainfall) were apparently favourable to the development of the Maya Culture in the southern and central lowlands during the Preclassic Period, probably due to the challenge that an excess of water represented, making them create new technologies to manage it (Kennett et al., 2012).

Low evaporation-rainfall ratio conditions also prevailed during the Classic Mesoamerican Horizon (ca. 1850 years B. P.), having decadal periods of drought during the Maya Abandonment (orange band A in Figure 4.9 and Figure 4.10) and the Maya Hiatus (orange band H) (see section 2.5, chapter 2). Both dry periods are apparent in the $\delta^{18}O$ records of the Highlands (Figure 4.9 d and e) and in Chichancanab, where the density record shows the precipitation of gypsum during the time of the Abandonment. Both periods are also shown at the speleothem records at Punta Laguna (Curtis et al., 1996, c), Rio Secreto (Medina-Elizalde et al., 2016), Macal Chasm (Webster et al., 2007) and Yok Balum (Kennett et al., 2012) The next section in this chapter reviews the spatial distribution of the environmental signal related to droughts or vegetation change during these two periods in more detail. Neither dry period is observed in lakes Peten Itza (Curtis et al., 1998) and Salpeten (Rosenmeier et al., 2002, 2016) (Figure 4.9c and d).

After the Maya Hiatus, relatively humid conditions are established until a series of droughts at the end of the Classic period happened, which is the period of the Maya Collapse (grey band H) (see section 2.5, chapter 2). The drought signal is relatively strong in the speleothem record at Rey Marcos (Winter et al., 2020) but is weak at Lake Kail (Stansell et al., 2020) (Figure 4.9 d and e). The signals are not present either in the Peten Itza (Curtis et al., 1998) and Salpeten lakes (Rosenmeier et al., 2002, 2016, but see below) (Figure 4.9b and c), while the signal is clearly observed not only in the oxygen isotope record in Chichancanab but in its density record, presenting intense precipitation of gypsum, which changed the density of the sediments (Figure 4.9a) dramatically. The presence of dry conditions during the time of the Maya Collapse is observed in the speleothem records at Tzabnah (Medina-Elizalde et al., 2010), Box Tunich (Akers et al., 2019), Macal Chasm (Webster et al., 2007) and Yok Balum (Kennett et al., 2012). Another important point has been the calibration done in the Tzabnah record, which infers a decrease in rainfall during

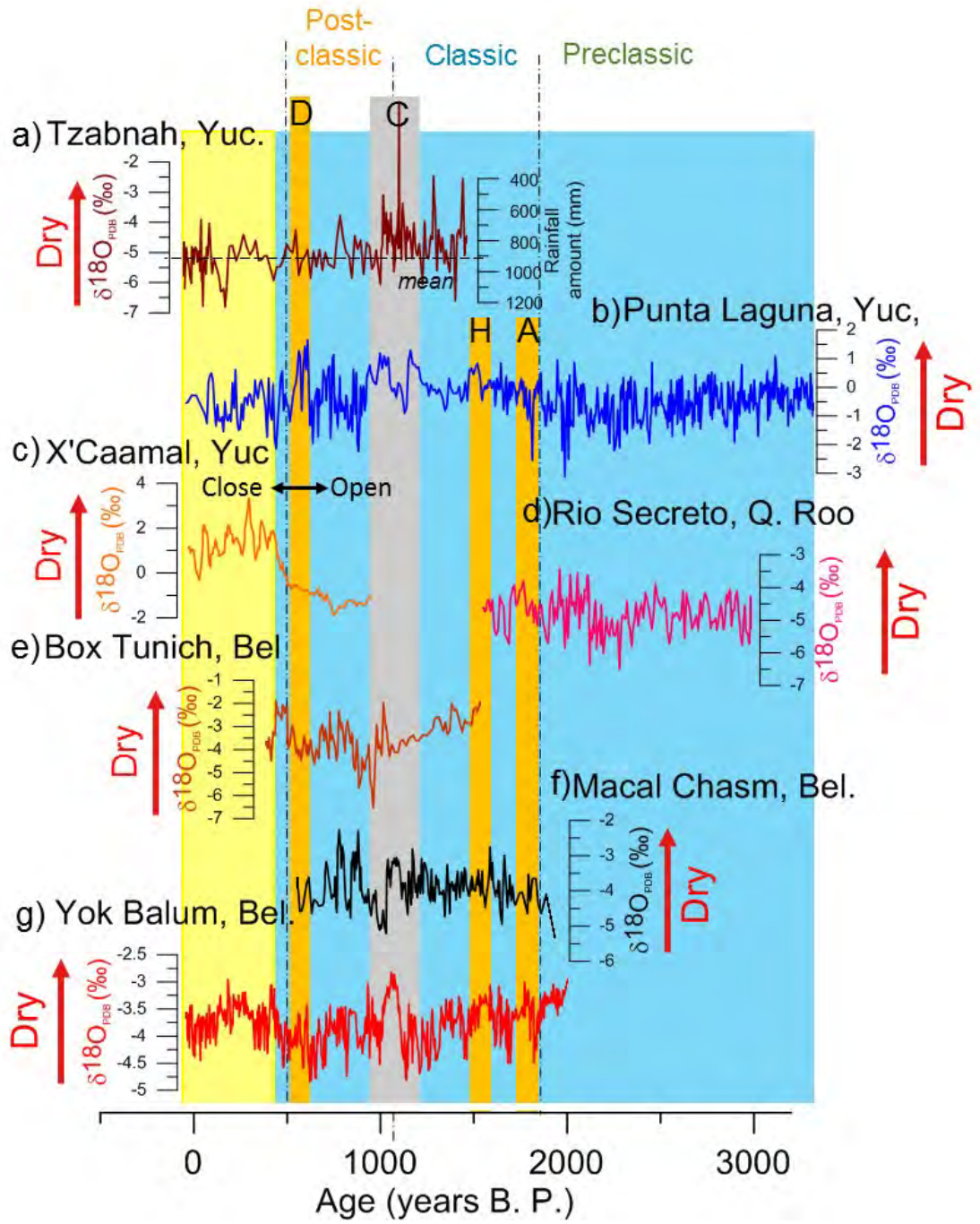

Figure 4.10. High-resolution records of the Maya Cultural Area based on $\delta^{18}O$ indicating the relative changes between dry and humid conditions for the last 3500 years; a) Speleothem at Tzabnah (Medina-Elizalde et al., 2010), b) Lake Punta Laguna (Curtis et al., 1996, c) Waterbody Aguada X'Caamal (Hodell et al., 2005), d) Speleothem at Rio Secreto (Medina-Elizalde et al., 2016), e) Speleothem at Box Tunich (Akers et al., 2019), f) Speleothem at Macal Chasm (Webster et al., 2007) and Spelethem at Yok Balum (Kennett et al., 2012). The grey band highlight the dry period linked to the Maya Collapse (C), while the orange bands indicate climatic stress (droughts) related to the Maya Abandonment (A), the Maya Hiatus (H) and the Destruction of the League of Mayapan (D). Humid periods are indicated by blue and dry centennial periods are indicated by yellow.

the Mesoamerican Terminal Classic period to 600 mm, when the average during the Mesoamerican Classic period was around 1000 mm, confirming a dry period (Medina-Elizalde et al., 2010).

Another rainfall amount reconstruction has been performed using the $\delta^{18}O$, and δD isotopes found in the gypsum precipitated during the Terminal Classic Mesoamerican Horizon in Chichancanab (Evans et al., 2018). Using a model capable of reproducing the ^{17}O excess in gypsum samples, their calculations point out an average decrease of around 47% compared to the present amount. The most severe dry periods, had a reduction of up to 70 %, meaning a reduction between 400 to 500 mm of rainfall per year. The present amount is around 1200 mm (see next chapter 5). According to this amount, Chichancanab would have decreased its average water depth of 15 to 11 m. (Evans et al., 2018). This is in part congruent with the calculations obtained from the stalagmite Chaac at Tzabnah cave, where there was a reduction of rainfall up to 35% during the most severe dry periods at 1125 years B. P. (825 A. D.) and 1020 years B. P. (930 A. D.). Both records in the Mayab are in an area that receive less than 1200 mm of precipitation per year today (see Figure 2.5 in chapter 2). However, since Chichancanab is more far away from oceans than the Tzabnah cave, a slightly continental effect might have impacted the amount of ^{18}O in the records, which would explain the discrepancy between the calculated values.

Finally, the apparent lack of a clear climate change signal during that time in Salpeten is attributed not only to changes in the rainfall amount but the impact of deforestation on inflowing water (Rosenmeier et al., 2016, 2002). The impact of the size of Lake Salpeten on the signal of the $\delta^{18}O$ was not discussed. The next section presents the spatial distribution of the drought signal during the time of the Collapse in detail.

After the Collapse, Humid conditions are re-established for the rest of the Postclassic Mesoamerican Horizon. The last strong drought in Maya History (orange band D) appeared during the destruction of the League of Mayapan (500 years B. P. or 1450 A. D., see section 2.5) a political superpower that existed in the Mayab. The existence of the Mayapan alliance registered in the Chilam Balam books (Chilam-Balam, 1966), written during the Spanish colonisation, is argued mythical by many scholars (see section 2.5, chapter 2). However, the constitutions of the political entities, the Kuchkabalo'ob started during this particular epoch. Unfortunately, the link between environmental changes and the destruction of the League of Mayapan has been barely studied. This dry period coincides with the expansion of the Aztec empire in central Mesoamerica and the

introduction of the Soctona (a Zoque Olmec ethnicity) in the Maya Northern Highlands. The intensity of this dry period might have been similar to the droughts presented during the Maya Hiatus or even the Maya Abandonment.

The signal of the drought linked to the League of Mayapan destruction is the one with the most positive values in the $\delta^{18}O$ Punta Laguna record (Figure 4.10b) (Curtis et al., 1996, c). The record at Aguada X'Caamal presents the existence of this dry period, which apparently promoted a change in the basin hydrology, including its salinity. It has to be highlighted that the absence of variation in the record of X'Caamal for the previous Mesoamerican Horizons has been explained due to changes in the influx of external water resources, arguing a more hydrologically open water body at that time (Hodell et al., 2005b). General dry conditions are present for the Maya Lowlands after the drought linked to the League of Mayapan until the present time (Figure 4.9 and Figure 4.10).

4.7 The critical periods of the Maya Environmental History in the palaeoclimatic records

Three critical events in Maya environmental history were compared among all the records based on published lake sediment cores and speleothems: the Maya Abandonment at the end of Formative period (ca. 1750 B. P.), the Maya Hiatus (ca 1414 years B. P..) and the Maya Collapse (ca. 1140 B. P.) (see Figure 2.10 in chapter 2), in order to assess the existence of droughts during these periods in the available records.

Figure 4.11 shows the spatial distribution of the palaeoclimatic records that cover the period of the Maya Abandonment at the end of the Preclassic Mesoamerican Horizon (see section 2.5, chapter 2), showing the records that register the presence of a climatic stressing event (a drought, a change to more dry forest or a change in vegetation that cannot be explained by anthropogenic forcing), and the records that show any signal related to it (even anthropogenic). This stressing event is a drought in a proxy related to rainfall, a change of the anthropogenic signal in some taxa of the pollen or charcoal records, or changes in the precipitation of secondary carbonates or evaporites.

Figure 4.11 also shows records that possibly suggest a climatic stressing event. For example, this is the case at Lake Sayucil, Laguna de Cocos, Macanche and Petenxil, where at least one proxy related to rainfall or anthropogenic activity suggests a drought or/and

Figure 4.11 Spatial distribution of the environmental signal at the moment of the Maya Abandonment (1800 to 1750 years B. P.). The records indicating a possible drought are not conclusive and have an insufficient temporal sampling resolution for observing decadal variations. The asterisk indicates that a stressing climatic event is observed in the record, but it is not discussed by the authors.

lack of anthropogenic activity respectively (e. g. no presence of *Zea mays*). The problem of these records is their lack of resolution. For instance, the pollen record at Lake Yaloch did not record any *Zea mays* and has a decrease in Poaceae, but such crops reappear after the period of the Maya Hiatus, indicating that the region was not abandoned at all or re-occupied (Wahl et al., 2013). The asterisk symbol indicates that the existence or possible existence of climatic stressing event appears in the record but is not discussed by the authors.

Records that do not show a signal of a stressing climatic event are found in the central Lowlands of the Peten region and relatively near to the Caribbean coast (Figure 4.11). Naja

is the only record that does not present a stressing signal in the inland area. In contrast, most of the records show a stressing climatic signal at the Maya Abandonment, including records in the highlands e. g. Lake Esmeralda in Chiapas (Franco-Gaviria et al., 2018)(see Section 5.8 in Chapter 5), Lake Kail (Stansell et al., 2020) or Lake Amatitlan (Velez et al., 2011), while all the speleothems indicate a very dry period.

Figure 4.12 shows the spatial distribution of the palaeoclimatic records at the moment of the Maya Hiatus according to the presence or absence of a stressing climatic event.

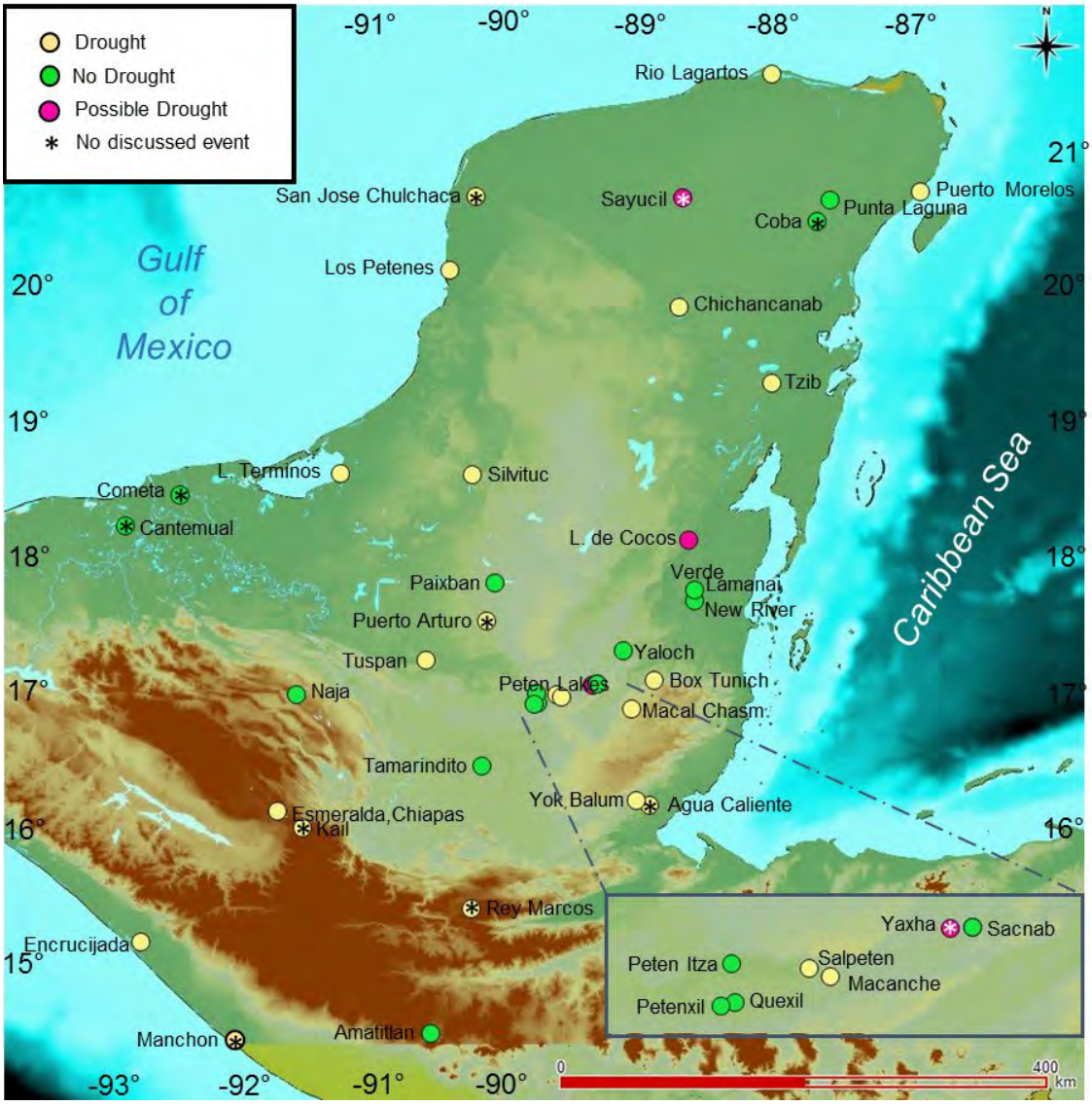

Figure 4.12 Spatial distribution of the environmental signal at the time of the Maya Hiatus (1414 years B. P.). The records indicating a possible drought are not conclusive and have an insufficient temporal resolution for observing decadal variations. The asterisk indicates that a stressing climatic event is observed in the record, but it is not discussed by the authors.

The map also includes the records where the signal is ambiguous but could indicate a possible drought, e. g. Sayucil $\delta^{18}O$ ((Whitmore et al., 1996) or absence of anthropogenic activity, e. g. Laguna de Cocos (Bradbury et al., 1990), Lake Yaxha (Brenner, 1983). All records based on speleothems suggest a drought at the moment of the Maya Hiatus (see section 2.5, chapter 2).

Lake records in the central Lowlands, however, do not register signals of a climatic stressing event, including records at Paixban and Lamanai. Paradoxically, the concept of the Maya Hiatus was conceived based on the story of monuments and stelae constructions at Motul (Tikal) (Drew, 2015), which is a city in this region. Records in the Northern Mayab near the Caribbean Sea and near the flood lands of Tabasco near the Gulf of Mexico also do not show signals of a climatic stressing event. The fact that fewer lake records show the presence of a climatic stressing event during the Hiatus also implies that the drought was less intense in comparison to the previous dry period at the end of the Preclassic period, which is in agreement with the observations in the stalagmites. Another interesting point is the presence of a stressing climate event in the records at the Highlands except for the record at Amatitlan (Velez et al., 2011). The asterisk symbol again indicates that the existence or possible existence of climatic stressing event appears in the record but is not discussed by the authors.

Figure 4.13 shows the spatial distribution of the palaeoclimatic records based on speleothems and lake sediments that cover the period of the Maya Collapse at the end of the Classic Mesoamerican Archaeological Horizon (see Figure 2.10 and section 2.5 in chapter 2). The spatial distribution of the records that do not register a drought or a change of vegetation at the time of the Collapse is again concentrated in the central lowlands Peten lakes (Cowgill et al.,1966, Leyden et al.,1993, Mueller et al., 2009, Schüpbach et al., 2015, Vaughan et al.,1985), Paixban (Wahl et al., 2016), the region of Lamanai (Metcalfe et al., 2009) and in the flood plains of Tabasco (Cometa and Cantemual (Nooren, 2017).

The number of records that do not register a drought event or a change in vegetation is six. In contrast, twenty-nine records recognise a stressing climatic signal meaning a drought event or a change of vegetation. The asterisk again indicates an apparent stressing climatic event in the record that is not discussed. At Tuspan its chronology ends at the moment of the Collapse.

Other than a pollen-based record, the other records that show a drought is based on a tendency to relatively high values in the $\delta^{18}O$, significant precipitation of evaporates, or changes in sedimentation rate. All the speleothems indicate dry period between the 1140 to 1040 B. P. (810 – 910 years A. D.). The drought started around a half-century after the first step of the Collapse, the invasion of Motul (Tikal) over Kak (Calakmul) (Grube and Schubert, 2015).

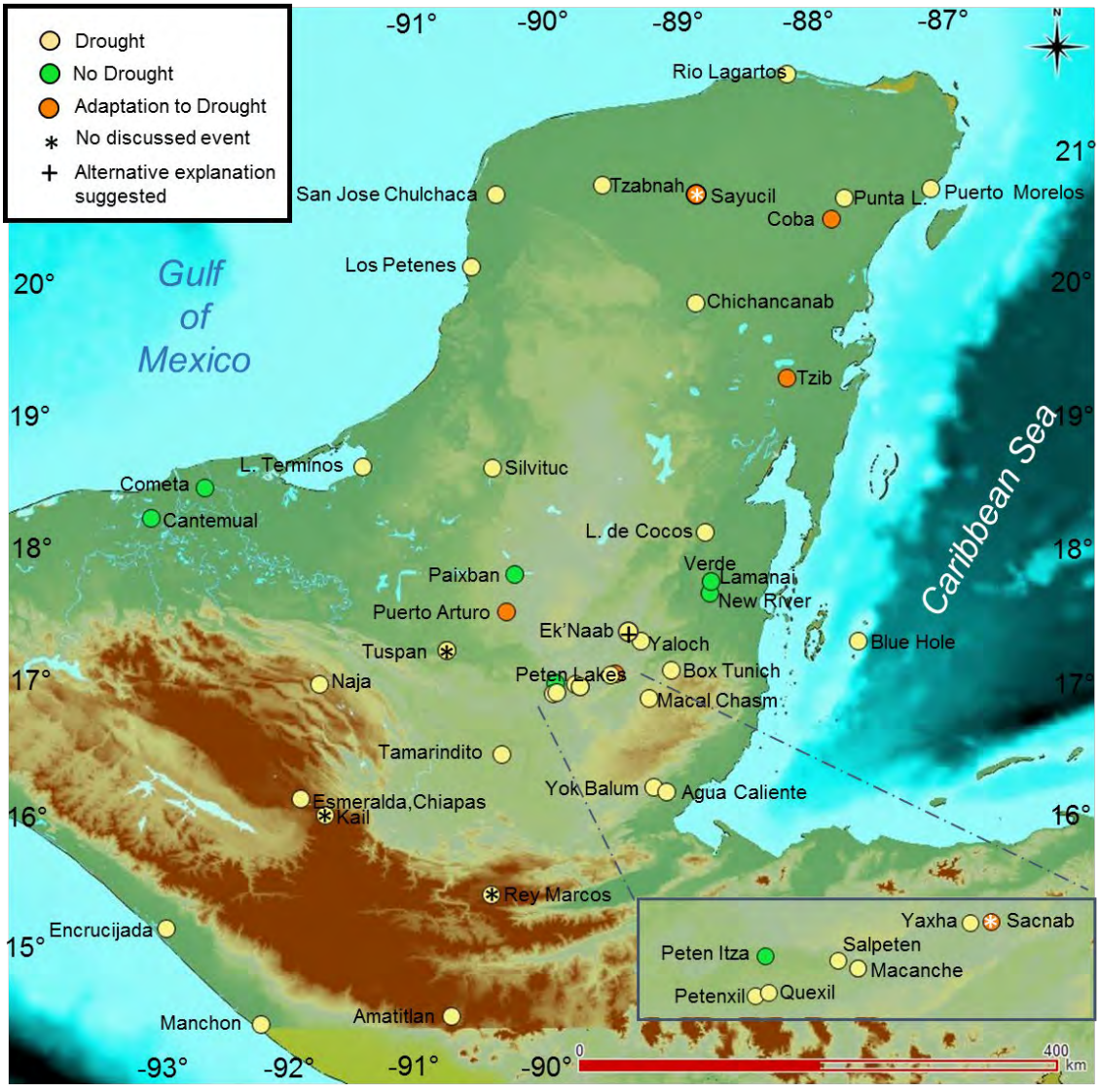

Figure 4.13 Spatial distribution of the environmental signal at the time of the Maya Collapse (1140 to 1040 years B. P.). The asterisk indicates that a stressing climatic event is observed in the record, but it is not discussed by the authors. The label "Adaptation to droughts" indicate sites where the physical proxies indicate the presence of droughts, but the pollen record does not show a change in vegetation, including the preservation of crops like Z. mays.

If the droughts were not the primary drivers of the Collapse, the insights provided by the 29 records indicate that the drought existed during the times of the Maya Collapse and

may, therefore, have played a role in it. Therefore, the hypothesis of the Mayan droughts has reached the status of a theory. However, at the same time, the existence of records that do not show any signal related to a drought indicates that regional variables were able to cushion the effect of a drought (which depends of the sensitivity of the system). Another separate issue is if the drying was sufficient to disrupt agricultural and other human activities, from which some particular proxies depends (e. g. charcoal production, pollen, sedimentation rate).

Figure 4.13 also shows the records where a proxy marks the existence of drought, but the pollen record does not apparently indicate changes in vegetation. For example, in the lake sediment record of Coba, physical proxies indicate lower lake level and an increase in salinity, suggesting a drought. However, the pollen record indicates a presence of *Zea mays* during and after the Collapse during the Terminal Classic Mesoamerican Horizon (Leyden et al., 1998; Whitmore et al., 1996). Thus perseverance of *Zea mays* is congruent with the archaeological and historical record that shows that the city of Coba did not have a collapse. Dry conditions might have offered favourable conditions for agriculture of *Zea mays* in subareas of the Maya Cultural Area that used to suffer severe floods e.g. Puerto Arturo (Wahl et al., 2014). However, this was not the case around Coba (Leyden et al., 1993). Thus, the perseverance of *Zea mays* here might suggest an adaptation to the droughts.

It has to be highlighted that changes in vegetation occur not only in response to climate change and human activity, but to changes in other non-human populations. The introduction of a new species, the disappearance of an adapted species, or drastic changes in the amount of population of a species could affect an ecosystem completely, changing the vegetation. For example, changes in the amount of population of arthropods like bees might have altered the vegetation in the area. Therefore, changes in vegetation and charcoal are not necessarily linked to changes in the temperature, humidity, or wind flows. In the Maya Cultural Area, changes in the vegetation are commonly linked to anthropogenic activity besides climate change, since agriculture promotes the clearance of extensive hectares of forest, the introduction of species like *Zea mays* (e.g. Carrillo-Bastos et al., 2010; Wright et al., 1996) or proliferation of the genus Cucurbita or Poaceae (e.g. Aragón-Moreno et al., 2012; Gutiérrez-Ayala et al., 2012; Kennett and Beach, 2013; Pohl et al., 1996), or the diminishing of some particular kind of forest for obtaining wood (Franco-

Gaviria et al., 2018). Therefore, the interpretation of changes in the vegetation surrounding a lake has to be undertaken very carefully, and it has to be supported by additional proxies.

In summary, we can be sure that there were dry conditions during these three critical events of the Maya History. The dry period had different intensities, the drought at the Maya Hiatus being the least severe. The intensity of the drought might also have had a different intensity and different impact on each subregion.

The zone of the Centra Lowlands (see Figure 2.2 in Chapter 2). is the region that experiences the least drought impact based on the lack of environmental signals that imply a disruption, followed by the flood plains of Tabasco (see Figure 2.2 in Chapter 2). The droughts' effect not only happened at the lowlands, contrary to what has been argued, but also in the highlands, where the impact was also severe. Finally, from a spatial perspective, there is a need to develop more records that increase our perspective of the impacts of the droughts in the subregions of the Maya Cultural Area.

4.8 Relevant palaeoclimatic records outside the Maya Cultural Area

The Maya Cultural Area covers an extension of approximately 400,000 km^2, comparable to twice the area of Great Britain. Therefore, the use of palaeoclimatic records outside this area to indicate the presence of a drought presents major challenges and is problematic from the epistemic point of view. The use of external palaeoclimatic records for supporting the Mayan drought is more complicated when they come from Southern Central America, e. g. the speleothem recovered at Chilibrillo Cave in eastern Panama (Lachniet et al.,2004) or central Mesoamerica, e. g. the speleothem collected at Juxtlahauca Cave in Guerrero at Mesoamerica (Lachniet et al., 2012). For example, the use of records in central Mesoamerica to support the Mayan drought hypothesis is problematic since they are immersed in different kind of climates, although they are all in the same summer rainfall regime, so a shift in the overall drivers of this could give a coherent signal. For instance, substantial changes in settlement patterns also happened there at the time of the Maya Collapse at the end of the Mesoamerican Classic Period (Carrasco, 2001; González-José et al., 2007).

Most of the palaeoclimatic records in central Mesoamerica indeed register recurrent droughts through the Mesoamerican horizons, but they are not linked to societal Collapse on the same scale that occurred in the Maya Region. The drought is not seen as a driver of the societal Collapse in central Mesoamerica, although it has been established that drought

played a role at some degree in the decline of Teotihuacan as a major power, one of the most populated cities in the world at that time (Lachniet et al., 2017).

The use of palaeoclimatic records outside the Maya cultural area for supporting the drought hypothesis is only justified if the drought was a manifestation of a climate event of planetary or transoceanic proportions. The fact that a series of civilisations in north-western South America presented a collapse, e. g. the Mochica, Tiwanaku culture a similar time around 1000 years B. P. (deMenocal, 2001), supports the idea of subplanetary climate event. The end of the Tang dynasty in imperial China at the time of the Maya classic Collapse could be connected to the same climatic event. (Yancheva et al., 2007).

The most accepted explanation of a climatic event of subplanetary proportions that could have caused droughts in parts of Mexico, Central America, the northern part of South America and an increase in the intensity of monsoons in China, which impacted the Tang dynasty is the displacement of the Intertropical convergence zone (see chapter 4).

Related to this, the most cited record outside the Maya Cultural Area presented linked to the droughts during the Maya Collapse at the Terminal Mesoamerican Classic Horizon is the titanium record of the marine sediments collected from the Cariaco basin off the coast of Venezuela (Haug et al., 2003, 2001). The titanium content through the record is a proxy of the displacement of the Intertropical Convergence, Zone, ITCZ (Figure 4.9f). Since the movement of the ITCZ responds to solar insolation in a similar way that the Bermuda High, a displacement to the south of the highest north latitude position of the ITCZ might have coincided with a displacement to the south of the Bermuda High, causing drier trade winds over the Maya Cultural Area (see section 2.3 in Chapter 2). The Cariaco record is frequently used to compare with local studies in the Maya Cultural Area for distinguishing between regional patterns and sub-planetary patterns of the hydrological balance in spite of its considerable distance from the Maya area and lack of correlation in terms of modern climatology.

4.9 Conclusions

This chapter has presented an assessment of the palaeoenvironmental records in the Maya Cultural Area. The spatial and temporal areas covered by records have been presented graphically. In this way, it was possible to highlight the gaps of information related to the absence of records or lack of proxies in a particular area. An example of information gaps is that the highlands have a comparatively lower number of records in comparison with

the central lowlands. Another example is the fact that most isotope records developed on lake sediments are in Northern Mayab.

Failed efforts to develop palaeoclimatic records have also been presented to explain the absence of records in some particular areas and contexts, e.g. tree rings in the Maya Cultural Area.

In addition, I presented the spatial distribution of the environmental signal recorded in the different records across the Maya Cultural Area in three critical time frames of the Maya history: The Abandonment; the Hiatus; and the Collapse.

This comparison supports the idea that these historical events are linked to dry regional environmental conditions. However, the intensity of the dry conditions was different in specific areas. Some of these areas might have specific conditions to cushion the dry conditions. During the three critical points, the Maya Central Lowlands was the area with more resources for cushioning the dry events. One of the purposes of this thesis is to fill some of the information gaps. Therefore, new palaeorecords from the Northern Highlands and Central Mayab were developed.

In the next chapter, we will be introduced in the study sites of this thesis; Lake Esmeralda and its neighbour Chichancanab in the Cochuah Region and Lake San Lorenzo at the Lagunas de Montebello Lake Complex in the Chinkultic Region. We will also know about their present rainfall regime and we will do a review of the palaeohumidity conditions of these study sites

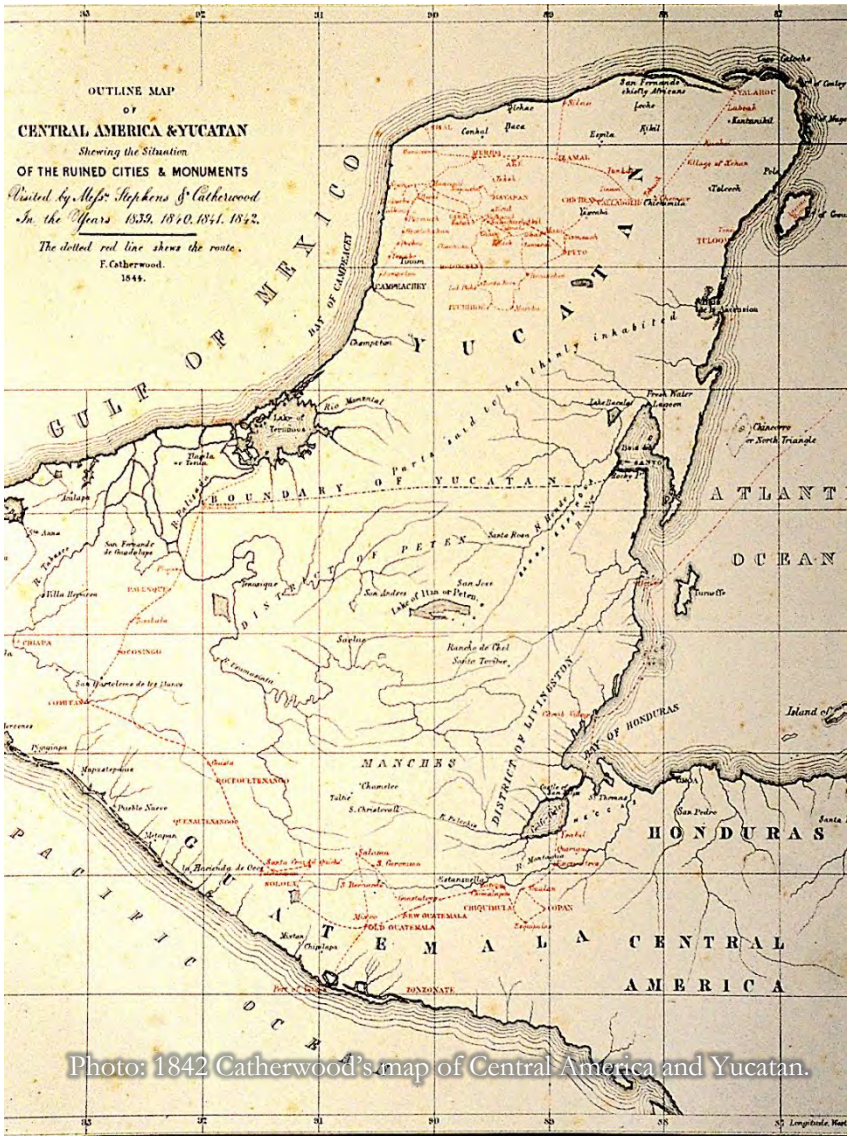

"… it means deep water, and we Spaniards call them -sonot (cenote)- because we hear calling them so, and there are many of them in this land, and because the land is so flat, without rivers, it is inferred that through concavities running rivers arrive to the far away mountain ranges. And they appear through the pit that these cenotes by themselves have opened without have been made by any men"

Relaciones Histórico Geográficas de la Gobernación de Yucatán, XVI Century.

In this thesis sites selected in the Maya Lowlands and the Maya Highlands are studied, as a response of the suggestion of Beach et al. (2015); and Marchant et al. (2004) (see section 1.1 in chapter 1 and section 4.9 in chapter 4), to add to the spatial perspective of the environmental history studies of the Maya people, in particular, adding to the small number of previous palaeoenvironmental studies in the Maya Highlands. This chapter focuses on describing these study areas; one related to the site called Lake Esmeralda in the Cochuah Region in the Lowlands and the other related to the site named Lake San Lorenzo in the Lagunas de Montebello Lake Complex in the Highlands. The chapter includes discussion of the rainfall regime and previous work on the isotopic composition of waters in these areas.

5.1 Location of Lake San Lorenzo

The study site in the Maya Highlands is a lake in the Lagunas de Montebello National Park, which is located in the municipalities of La Trinitaria and Independencia in the state of Chiapas, near the Comitan Valley (Figure 5.1). The National Park covers 65.25 km^2 and is located in the physiographic province of Altos de Chiapas, which is also known as the Macizo Central Chiapas near the border with Guatemala (Calderón et al., 2014).

Lithologically, the entire area of interest is covered by a lower Cretaceous limestone that is associated with the formation of a lake complex of karst origin; it includes solution lakes (Hutchinson, 1975) with dolines, uvalas and poljes (Durán-Calderón et al., 2014). More than 50 lakes are present in the area (Oseguera and Alcocer, 2015).

The selected lake called Lake San Lorenzo (1455 m a.s.l., zmax 67m, zmean 11 m) (Figure 5.1) is the second biggest lake (180ha) in that lake complex (Alcocer et al., 2016). Hydrologically, the basin has been described as endorheic by Alcocer et al., 2018, being part of the sub-basin of the Comitán River, and is fed by the Grande River (Alcocer et al., 2018; Calderón et al., 2014). Lake San Lorenzo has a maximum depth of 67 m. This fact makes San Lorenzo the fifth deepest lake in Lagunas de Montebello Lake Complex, and the sixth deepest in Mexico (Alcocer et al., 2016) and one of the ten deepest lakes in the Maya Cultural Area. Lake San Lorenzo is a freshwater system (conductivity of 617 ± 14 µS /cm), a pH of 9.7± 0.03. It is considered a Ca – Mg SO_4 lake (Palomino et al., 2017). This characteristic is due to the limestone and dolostone rocks and the gypsum block present in the basin.

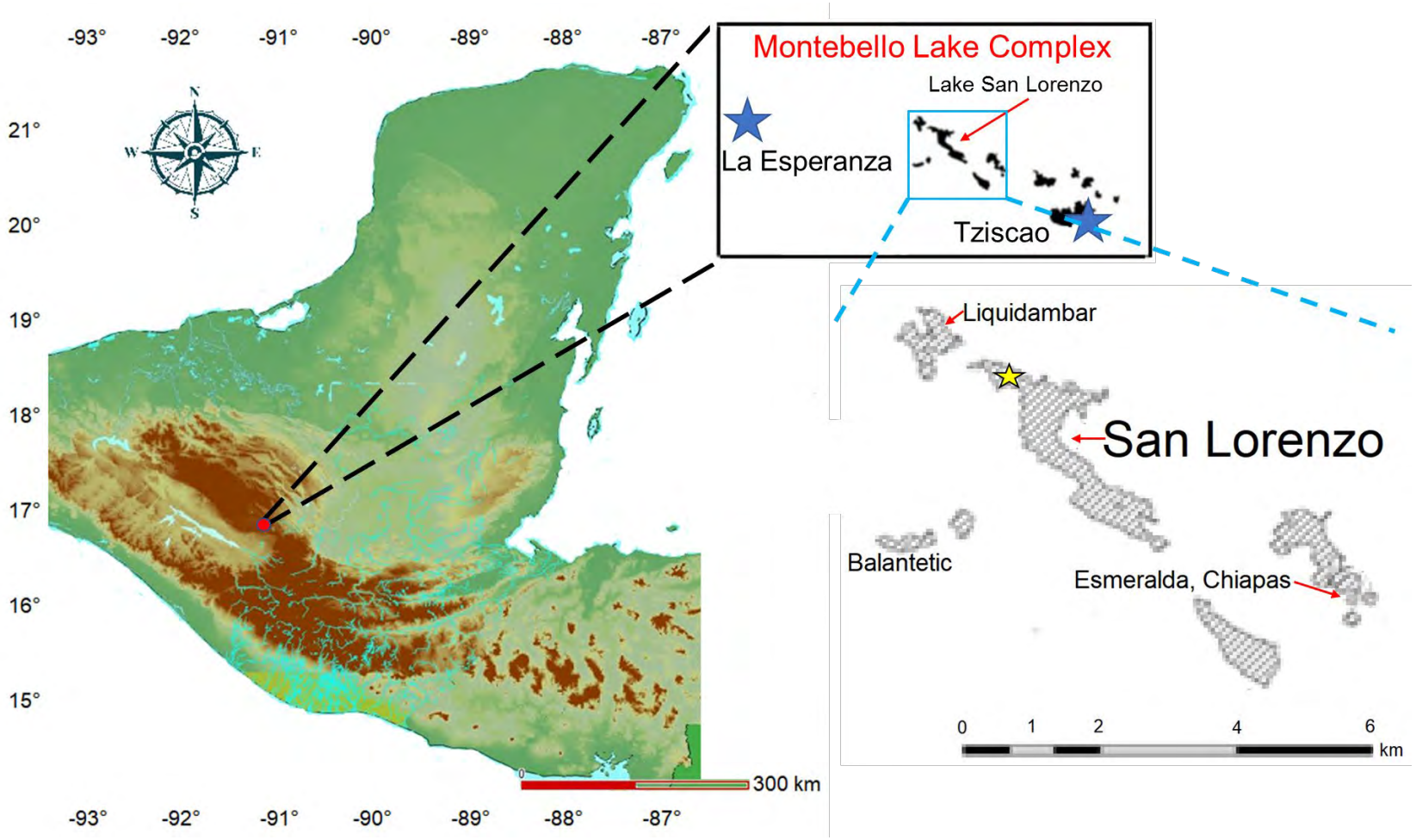

Figure 5.1 Location of Lake San Lorenzo. The map shows Lake San Lorenzo in relation to the Laguna de Montebello Lake complex. The map shows the lakes that are named in this thesis at different stages (chapter 4 and 7). The blue stars indicate the location of meteorological stations in relation to the Montebello Lake Complex and particularly to Lake San Lorenzo (upper). The yellow star indicates the coring site.

5.2 Rainfall regime at Lake San Lorenzo

The climate of this region is marked by a long relatively cool summer that is humid and has a typical summer precipitation regime (Oseguera and Alcocer, 2015). Figure 5.2 shows average monthly precipitation measured from 1950 to 2010 in the meteorological stations of la Esperanza and Tziscao, which are near the Montebello Lakes Complex (Figure 5.1).

There is a large difference (1281 mm per year) in the annual rainfall amount received at the station at Tziscao (2490 mm) (CONAGUA, 2010c) compared to the amount of rainfall received in La Esperanza (1209 mm) (CONAGUA, 2010d). Both stations are 20 km from one to another and have practically the same elevation, (1470 m. a. s. l. for La Esperanza and 1500 m. a. s. l. for Tziscao). Therefore, this difference cannot be explained by a difference in the elevation, but by the pattern of the air flows in the East of Chiapas moulded by the topography, which can be observed in Nooren et al. (2018). I must highlight that the massive amount of rainfall, 2490 mm per year received at the station inside the Lake complex (Tziscao) (CONAGUA, 2010c), might also be influenced by the natural vegetation (dense cloud forest) that has prevailed in Montebello, meanwhile the precipitation at La Esperanza might be influenced by the artificial vegetation (agriculture lands and grass plains) in the deforested part.

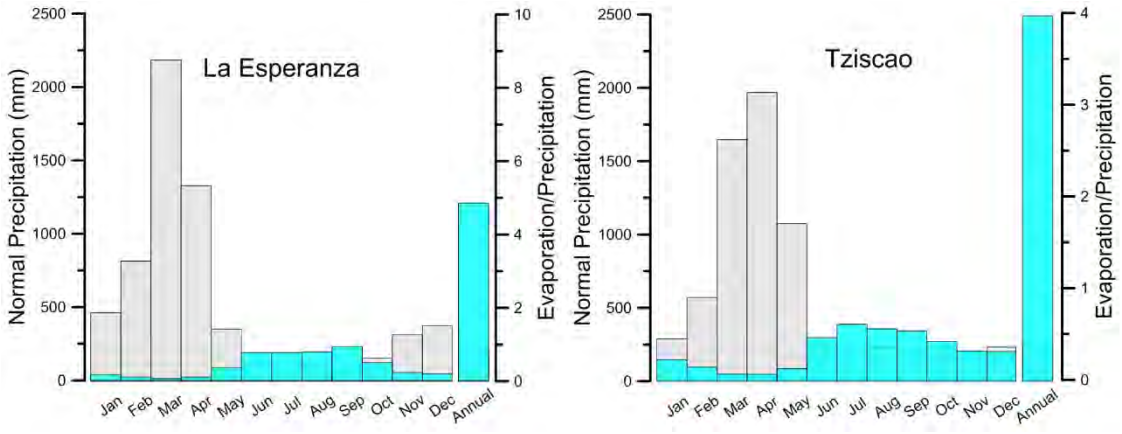

Figure 5.2 Average monthly precipitation measured for the period from 1950 to 2010 A. D. in meteorological stations near to Lake San Lorenzo. Data collected at la Esperanza CONAGUA (2010c) is indicative of the grasslands at the eastern part near lake San Lorenzo, while the data collected at Tziscao CONAGUA (2010d) reflect the rainfall trends in a year in Lagunas de Montebello Lake Complex (blue). The annual rainfall is presented at the end. Calculated evaporation/precipitation is presented for monthly variation (grey), which was calculated from meterorological data measured from 1950 to 2000 A. D. in Tziscao meanwhile calculated evaporation/precipitation was calculated from 2011 to 2018 for La Esperanza.

It can also be argued that the geomorphology of the park of surrounding hills might create local differences in rainfall due to the interaction of the wind with the foothills. For instance, the nearby Lacandon rainforest, which has a very contrasting topography, has similar rainfall values (Domínguez-Vázquez and Islebe, 2008). Data from the meteorological station in Tziscao indicate that the mean annual temperature is 17.3°C, and the mean annual evaporation is 948 mm (CONAGUA, 2010c). Therefore, the evaporation is much lower than precipitation. While in the Maya lowlands the lowest precipitation is recorded in February and March, March and April are the months with the lowest values of precipitation in the Highlands.

Another peculiar difference happens when we look at the precipitation at Tziscao (CONAGUA, 2010c), where the month with the highest precipitation occurs in July and not at September as at La Esperanza and the other station near Chichancanab and Esmeralda. Rainfall is still high in November and December in Tziscao.

5.3 Isotopic composition of water in the Lagunas de Montebello Lake Complex

Figure 5.3 shows the isotopic composition of water samples from Lake San Lorenzo, collected by Dr. Alexander Correa from the UNAM. The samples fall near the calculated local meteoric water line based on isoscapes (Wassenaar et al., 2009). This composition confirms that the lake functions as an open basin. The lake also receives intake from underground flows (Alcocer et al., 2018).

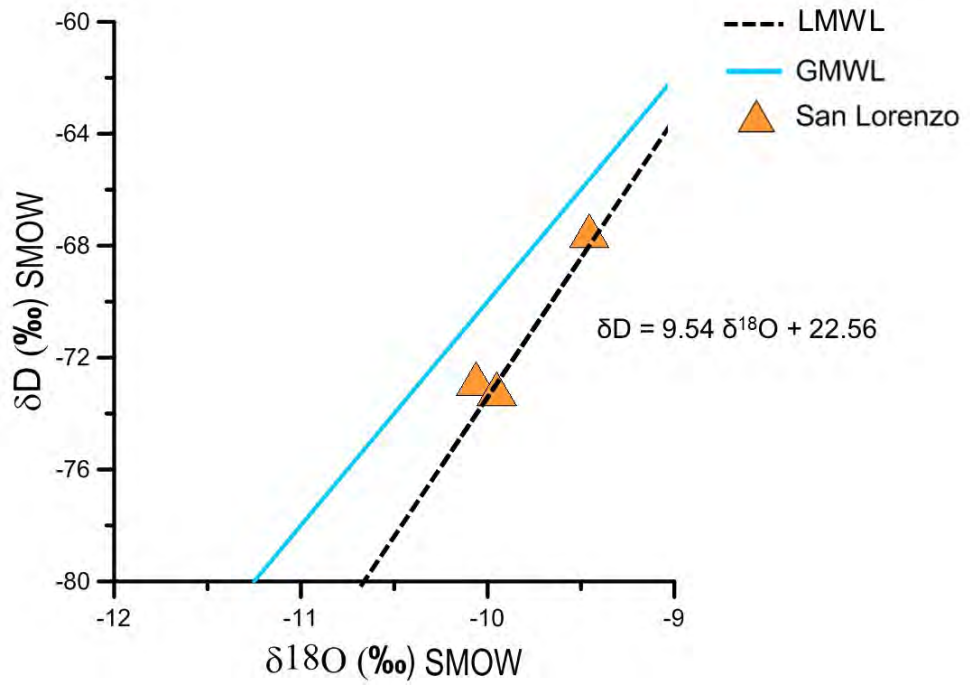

Figure 5.3 Isotopic compositions of water samples taken from Lake San Lorenzo. The equation corresponds to the Local Meteoric Water Line (LMWL).

5.4 Previous Environmental studies at Lake San Lorenzo

Lake San Lorenzo has been studied previously by Franco-Gaviria et al. (2018, 2020). They extracted a core named LIQ13 (after Liquidambar, because initially, it was thought they were in that lake) (Alcocer et al., 2016; Calderón et al., 2014). The 670 cm core was taken using a Livingstone type corer from a platform in 3.66m of water in 2012. They created an age model (Franco-Gaviria, 2018) using the algorithms programmed in BACON (Blaauw and Christen, 2011) based on four radiocarbon dates.

Franco-Gaviria et al. (2018, 2020) performed μXRF, cladoceran, pollen, and charcoal analysis on core LIQ13, and identified three distinctive environmental stages and four eco-facies using these data (Figure 5.4). The first stage constrains two eco-facies. The next paragraph is a summary of the results obtained by Franco-Gaviria et al. (2018):

The record revealed a long-term trend towards drier conditions with superimposed centennial-scale droughts according to the Ti record, which is similar to the records at the lowlands. Based on this proxy (Ti), they argued a tendency of declining precipitation from 3400 B. P. until the Maya Hiatus. Stage 1 is described as the beginning of the existence of the lake as a shallow water body based on an alga associated with fluvial environments (*Concentrycistis* sp.) (Christopher, 1976). From 3400 to 2400 years B. P., the pollen record is characterised by grains of *Pinus-Quercus* forests and open vegetation. The charcoal record for this stage indicates a predominance of recurring regional fires. The Cladoceran assemblage is dominated by littoral-benthic species from 3400 to1500 years, B. P.

During stage 2 from 2400 to1500 years, B. P. the records show an increase of disturbance taxa, including repeated occurrences of *Z. mays*, which implies the existence of agricultural activities. A high human impact index is calculated for this stage (Franco-Gaviria et al., 2018). Paradoxically, the amount of charcoal indicates fire suppression, which might indicate management of natural resources. The presence of *Pinus* was reduced significantly. An explanation is found in the use of this taxon as a material for construction and fuel. The highest amount of input of terrigenous elements is found in this period according to the Ti and Ti/Sr records interpreted as a consequence of human impact and a period of higher humidity in comparison with the previous stage. Stage 3 from 1500 to 600 years B. P. is marked by a decrease in disturbance taxa and a decline of the human activities according to the calculated Human Impact Index. From 1500 to 1000 cal. years B. P., littoral Cladoceran communities remained dominant, suggesting adverse environmental conditions for the aquatic community, associated with dry climates.

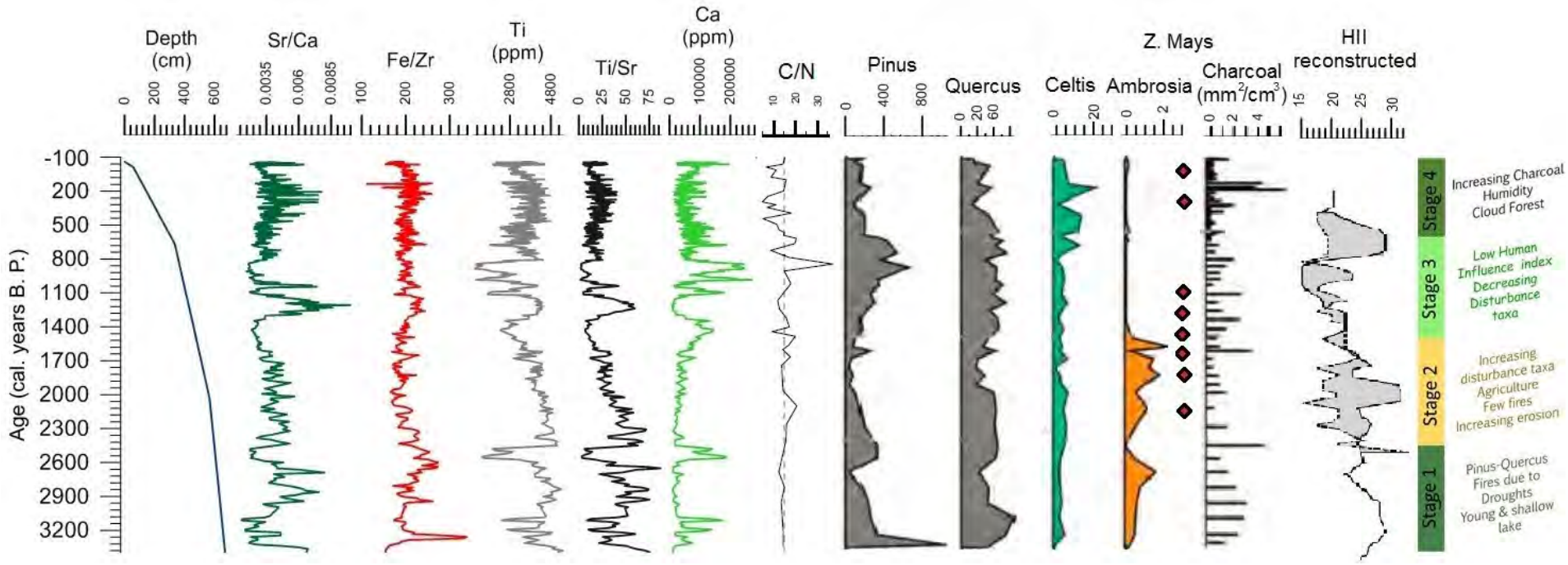

Figure 5.4 Environmental history of Lake San Lorenzo based on the records developed by Franco-Gaviria et al. (2018, 2020). Rhombohedral represent the presence of Z. mays. The grey coloured zone in the human impact index HII reconstructed record shows the difference in the human impact index between Lake San Lorenzo (continuous line) from the human impact index (HII) at Lake Esmeralda in the Montebello Lake Complex according to Franco-Gaviria et al. (2018). T/C record developed by Franco-Gaviria et al. (2020) is relevant for the origin of organic material (see section 7.4 in chapter 7).

From 1500 to 1200 years the palynological archive shows a predominance of *Quercus*, *Alchornea* and *Pinus*, while the period from 1200 to 600 years B. P. is marked by an abrupt increase in Mountain Cloud Forest (e. g. *Celtis*). The absence of *Z mays* from 1200 to 600 and the low Human Impact Index supposed that human activities were minimal in the region. This absence is after the Maya Classic Collapse. The final stage, between 600 years to the present, is characterised by declines of *Alchornea* and *Pinus*, at the same time it looks as if the Mountain Cloud forest expanded. According to the age model, after 600 years, B. P. the sedimentation rate increases dramatically from ca. 0.11 cm/year to ca. 0.47 cm/year.

The sedimentation rates then accelerate again after -50 years B. P. reaching 0.9 cm/year (Franco-Gaviria et al., 2020). Apparently, the human population was not resettled in the region until colonial times, according to the human disturbance in the palynological record (Franco-Gaviria et al., 2018). During the last 800 years, planktonic taxa of Cladocera become dominant, which means a substantial deepening and enlargement of the lake (Franco-Gaviria et al., 2020).

5.5 Location of Lake Esmeralda

Lake Esmeralda is a circa 1 km long narrow lake located at N 19° 46' 58.2", W 88° 44' 13.5", 4 m. a. s. l. in the municipality of Jose Maria Morelos in the state of Quintana Roo in Mexico (Figure 5.5). It is located near to the town of Dziuche, and it has a north-south orientation (depth = ~4 m). It is the southern extension of its twin lake Chichancanab, which it might join with at periods of high water level (Hodell et al., 2005), but no evidence of this has been found. The eastern shore of both lakes is a 20 m high ridge which marks the south part of the Tikul fault (see Figure 2.3 in chapter 2) (Hodell et al., 2005; Perry et al., 2009).

The average temperature of the area around Esmeralda is 25.4°C (Hodell, 2001). Lake Esmeralda has a geochemical environment slightly different from Chichancanab, even though both derive their mineralogy mainly from the Albion formation of northern Belize and Southeastern Quintana Roo, which could be Chicxulub impact breccia or a Tertiary evaporite (Kenkmann and Schönian, 2006; Perry et al., 2009), according to the value of $^{87}Sr/^{86}Sr$ (0.70776) (Perry et al., 2009); which is the same for both lakes.

Slight geochemical differences between the lakes might be caused by their relative position within the Albion formation and the permeability of the surroundings. Both lakes have exceptionally low values of 1000 Sr/Cl, which is an index for quantifying the contribution

of sea water in a water body, which indicates a lack of saline intrusions (Perry et al., 2009). At the same time, both lakes have about 70 times the SO_4/Cl ratio in comparison with seawater, where the levels of Cl^- and SO_4^{2-} are 0.180 mmol/kg and 7.43 mmol/kg for Chichancanab and 0.127 mmol/kg and 3.76 mmol/kg for Esmeralda, respectively (Perry et al., 2009). Lake Chichancanab effectively has a closed hydrology (Hodell et al., 2005) as does Lake Esmeralda, but isotopically Esmeralda sits closer to the Meteoric Water Line, suggesting it is a little more hydrologically open than Chichancanab (see section 5.3), it is less evaporative (Hodell et al., 2005). The lake is a freshwater system (conductivity of 3200 to 3400 µS/cm, according the measurements performed by us in 2018), with a pH between 7.2 and 7.5 (Perry et al., 2002) (comparing with pH of 8.3 to 9.3 of measurements performed on 2018). The water in Lake Esmeralda is undersaturated in relation to gypsum and celestite (Perry et al., 2009), which is a significant difference compared to the over-saturation of these minerals in Chichancanab. The surrounding vegetation is composed of low-stature vegetation (Leyden, 2002; Rosenmeier et al., 2002); similar to the dry broadleaf forest zone (figure 2.3 in chapter 2).

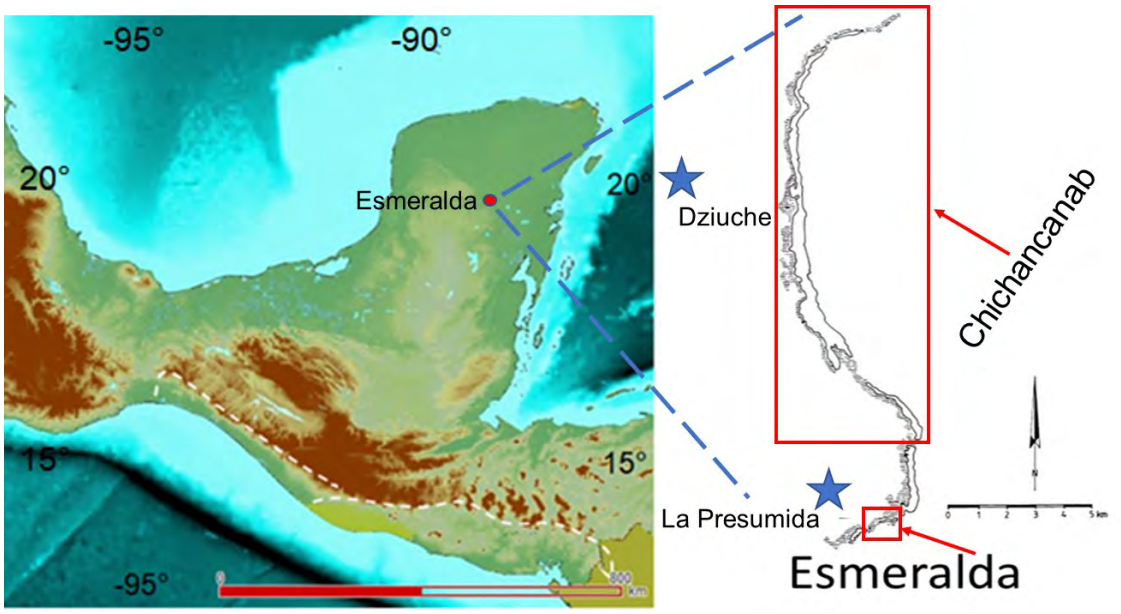

Figure 5.5 Location of Lake Esmeralda and its sister Lake Chichancanab. The red rectangles indicate the area of each lake. The blue stars indicate the meteorological stations.

5.6 Rainfall regime at Lake Esmeralda

Figure 5.6 shows average monthly precipitation measured from 1950 to 2010 in meteorological stations near to Lake Esmeralda. The stations at Dziuche and La Presumida are near to the Lakes Chichancanab and Esmeralda respectively (Figure 5.5). The rainfall at Dziuche (CONAGUA, 2010a) is very similar to the precipitation measured at La

Presumida, 1191 annual mm to 1339 annual mm, respectively (CONAGUA, 2010b), which is congruent with the mean annual precipitation levels of 1300 mm reported by Hodell et al., (2001). It can be observed that the months with a more elevated amount of rainfall are between June to October. The massive increase during these months is explained by the humid flow of the Trade winds from north to the east when the Bermuda High is constrained to the North Atlantic (see chapter 2). Another possible contributor to the increase of rainfall during these months is the formation of hurricanes in the Atlantic and the convective storms triggered by heating over the continent (see section 2.3 in chapter 2). The pattern observed at La Presumida (CONAGUA, 2010b) presents a sub-annual period known as the Canicula, which is a tendency of moderate rainfall during two weeks in a season of intense rainfall (see chapter 2). This feature is not clear in the average conditions at Dziuche, but it occurs in some individual years (CONAGUA, 2010a). Both plots show that September is the month with the greatest amount of rainfall. Evaporation-rainfall ratio is also presented since it is relevant for this thesis (see section 8.10 in chapter 8). It can be observed that this ratio is higher during the months that have relatively small amounts of rainfall (Figure 5.6).

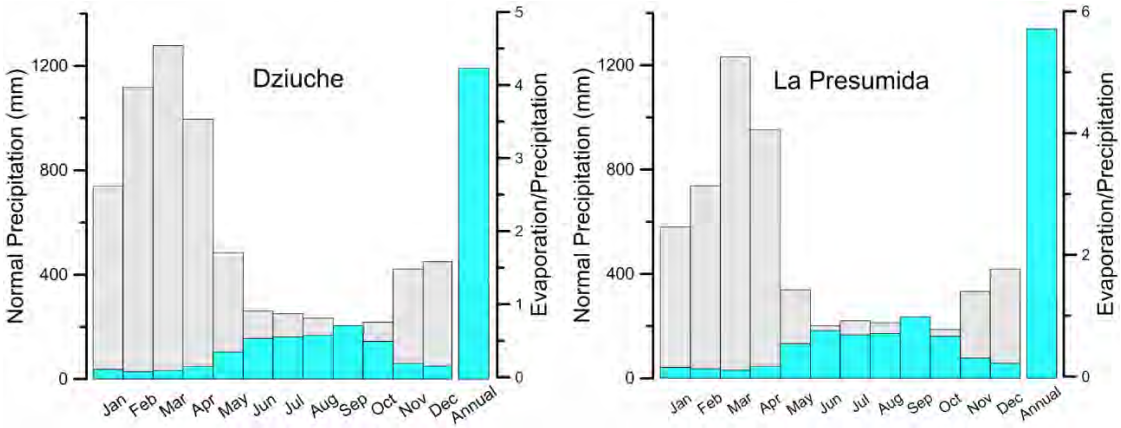

Figure 5.6 Average monthly precipitation measured for the period from 1950 to 2010 A. D. (0 to -60 years B. P. in meteorological stations near Lake Esmeralda. Data collected at Dziuche CONAGUA (2010a) and La Presumida CONAGUA (2010b) represents the rainfall in Lake Chichancanab and Lake Esmeralda respectively (blue). The annual rainfall is presented at the end. Calculated evaporation/precipitation is presented for monthly variation (grey), which was calculated from meteorological data measured from 1950 to 2010 A. D. in each station.

5.7 Isotopic composition of water in the northern Mayab

In this thesis, the isotopic composition of water plays an important role, since it might reflect the effective rainfall conditions in evaporative water bodies and rainfall amount in open lakes. This signature can be recovered from some components in sediments. For this reason, it is important to know the isotopic context of the water bodies in the Mayab.

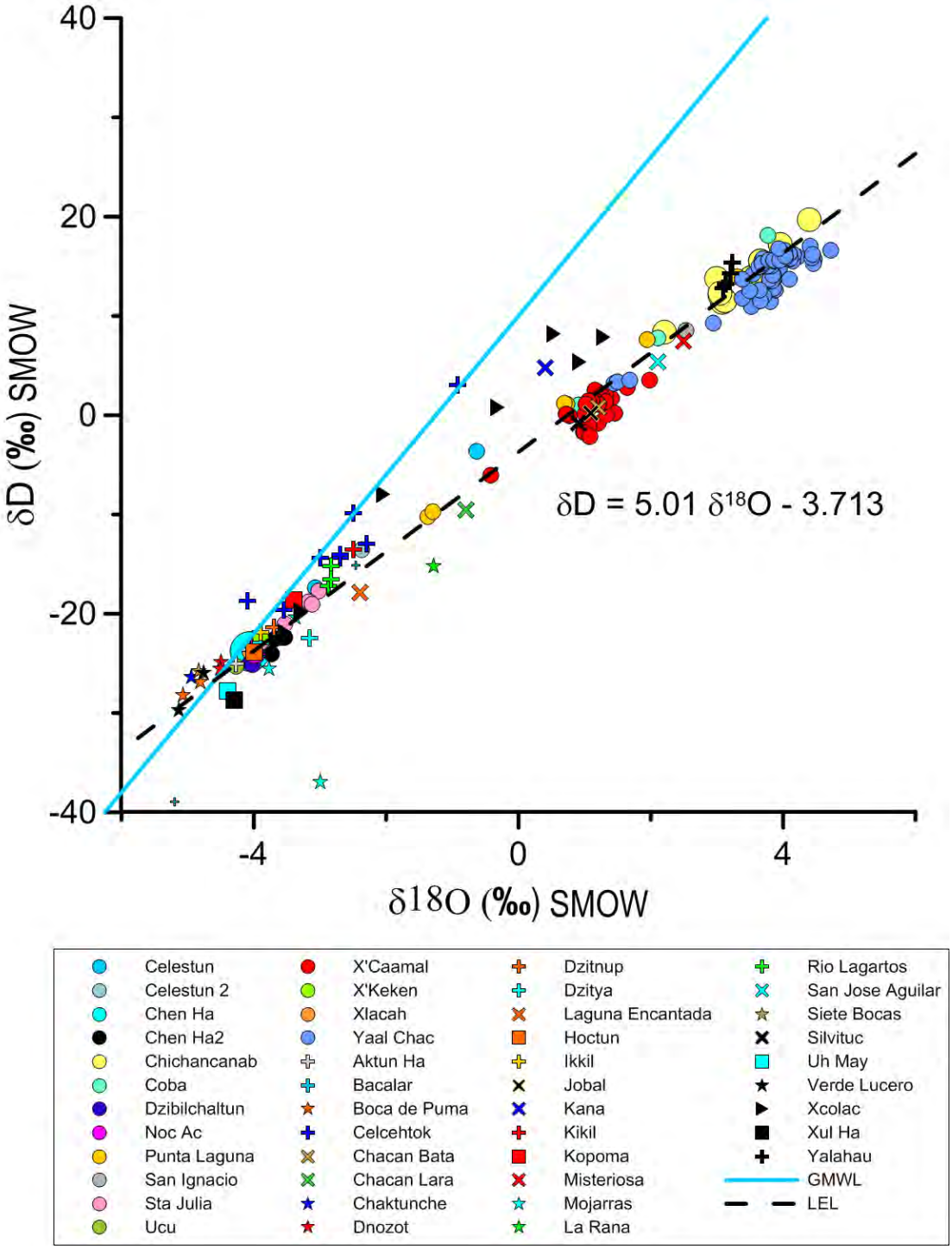

Figure 5.7 Isotopic composition of water bodies in the Mayab. Data obtained by undergraduate students of the University of Nottingham from 2010 to 2018 under the supervision of Prof. Sarah E. Metcalfe (circles). Published results of water analyses of isotopes performed by Evans et al., (2018) (crosses); by Lases-Hernandez et al. (2019)(stars); by Perez et al., (2011) (exes); by Socki et al. (2002)(triangles) and by Wassenaar et al. (2009)(squares). A similar plot with older samples(2001 to 2011) is presented by Perry et al. (2003). All published results of the isotopic composition of water from water bodies from the Mayab have been taken from the database developed by Cejudo et al. (2020). The equation corresponds to the Local Evaporation Line (LEL) proposed by Primmer (2019).

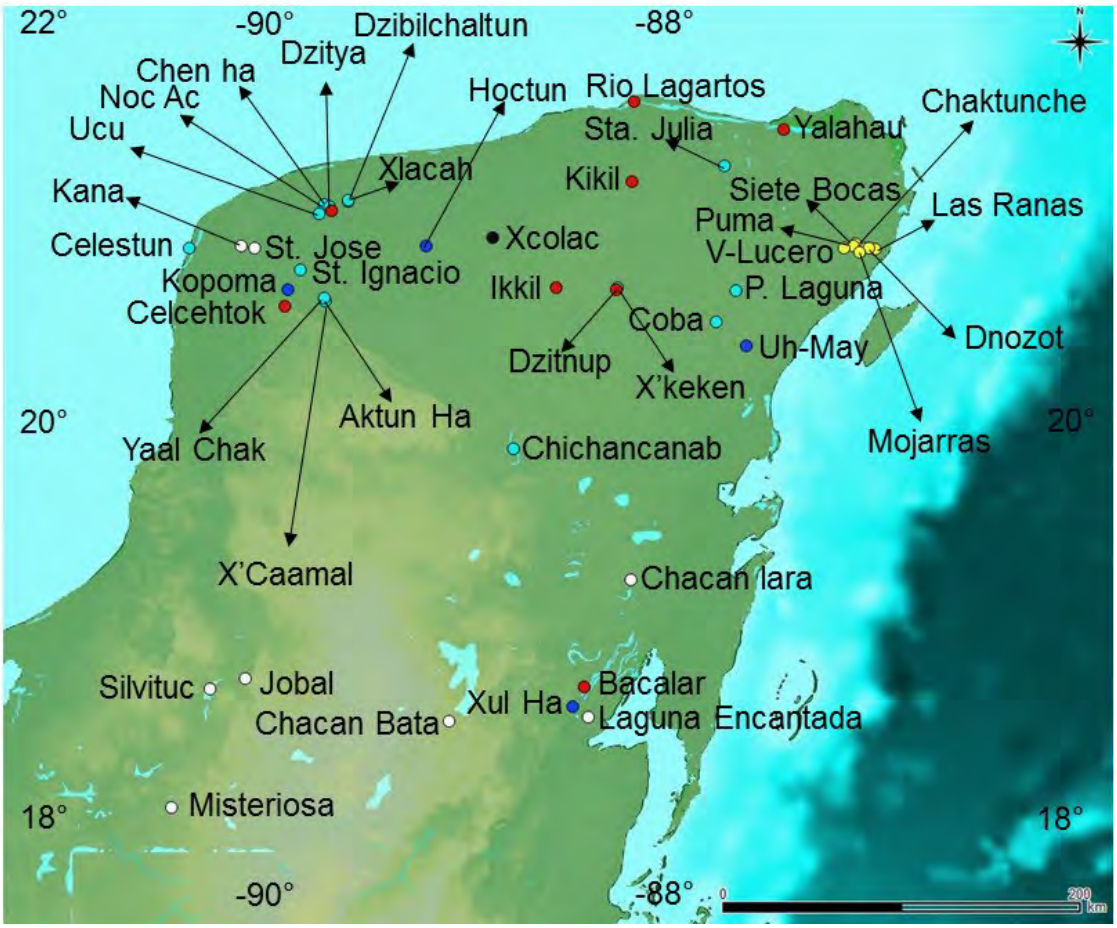

Figure 5.8 Location of water bodies (lakes and cenotes) sampled for water isotope analysis (results shown in Figure 5.7). The colour of the circles indicates the scientific team that took the samples; Metcalfe (unpublished data) (pale blue); Evans et al., (2018) (red); Lases-Hernandez et al. (2019)(yellow); by Perez et al., (2011) (white); by Socki et al. (2002)(black) and by Wassenaar et al. (2009)(dark blue).

It would also be desirable to know the isotopic composition of meteoric water for the Mayab, however only some data have been obtained from peninsula, mostly around the cities of Merida, Cancun and Kantunikin (not shown) (Cejudo et al., 2020; Lases-Hernandez et al., 2019). Figure 5.7 shows the isotopic signature of water bodies (lakes and cenotes) in the Mayab. Meanwhile, Figure 5.8 shows the location of these water bodies. Their composition falls inside the local evaporation line (excepting Celcehtok, sometimes called Calcehtok, which is groundwater inside a cave), which implies that most water bodies are a relatively closed system. Therefore, the evaporation in the region overcomes the rainfall, which is congruent with the instrumental record from 1981 to 2010 at the stations of La Presumida and Dziuche, where evaporation values are 1,605.3 mm/year and 1,509.6 mm/year, respectively meanwhile the values of rainfall are 1,347.2 mm/year and 1,201.4 mm/year, respectively (CONAGUA, 2010a, b).

5.8 Previous environmental studies at Lake Esmeralda and Lake Chichancanab

Palaeoclimatic studies in Chichancanab have developed some high-resolution (sub centennial resolution) records such as:

- Carbonate and sulphur content records, which are proxies of $CaCO_3$ and gypsum (or celestite) precipitation, respectively (Hodell et al., 1995).
- an oxygen isotope record on shells of gastropods Hydrobiidae *P. coronatus* which are proxies of the effective rainfall (Hodell et al., 1995).
- a density record, which highlights zones of gypsum deposition linked to dry periods (Hodell et al., 2005).
- oxygen and deuterium isotopes records on plant waxes, which are proxies of amount of rainfall (Douglas et al., 2014).
- oxygen and deuterium isotopes records on gypsum, which are proxies of the amount of rainfall and lake water level (Evans et al., 2018). This record is constrained to the gypsum layers, so it is not a continuous high resolution record.
- a pollen record indicating changes in vegetation was developed by Leyden (2002) for a short period and updated and amplified by Bermingham (2020) for Chichancanab.

A low-resolution organic content and a C/N records have also been developed, which might be a proxy of productivity or oxidative conditions in the lake (Covich and Stuiver, 1974).

Lake Chichancanab began to fill about 8200 ^{14}C years ago as worldwide sea level was rising and then proceeded to fill rapidly (Brenner et al., 2003; Hodell et al., 1995). It can be suggested that the lake has responded closely to changing sea level since the Pleistocene. According to Covich and Stuiver (1974), there are lake sediments with ages as old as ca. 29,100 uncalibrated radiocarbon years suggesting there was open water in the basin before the Last Glacial Maximum as well.

Figure 5.9 shows the different records obtained from Lake Chichancanab for the time frame studied in this thesis, the last 7000 years B. P. It has to be highlighted that most records developed in Chichancanab, including those studied on core CH1 7- II- 04 comes from the middle of Chichancanab (see Figure 6.1 in chapter 6), while the records developed by Covich and Stuiver (1974) were developed in a core collected in the south of Chichcancanab.

The core obtained in 1995 had its highest percentage of gypsum (circa 30%) at 7000 years B. P. when the lake was filling according to the percentage of sulphur (Hodell et al., 1995). During this time (7000 years B. P.) the record reached a low value of calcium carbonate around 2 % (Hodell et al., 1995). After 7000 B. P., the levels of carbonates increase abruptly, becoming the predominant component of the cores from 7000 to 6100 years B. P (Hodell et al., 1995). The environmental conditions are more humid according to the $\delta^{18}O$ after 7000 years B. P. (Hodell et al., 1995). At this point, the lake appears to be unsaturated in sulphates since the percentage of sulphur falls to values near zero (Hodell et al., 1995). After 6100 years B. P., the amount of carbonate has a decreasing tendency until 3500 years B. P. Occasional precipitation of sulphates happens during this period during circa 3300 to 3200 years B. P. (Covich and Stuiver, 1974). Chichancanab enters into a phase of high precipitation of carbonates in a moment of relatively high rainfall precipitation according to the $\delta^{18}O$ of *P. coronatus* from circa 3300 to 3200 years B. P. After this point, the evaporation rainfall ratio starts to increase (Hodell et al., 1995).

We can observe signals of drought in the core obtained in 1995 at the time of the Maya Abandonment (with a value up to 15 % of sulphur and a small amount of precipitation of carbonates, since calcium carbonates are not forming due to the capture of calcium by sulphates). A low percentage of carbonates indeed records the Maya Hiatus. However, the amount of precipitated sulphates (gypsum) is not so high as in other moments of droughts (e. g, around 7000 years B. P, the Maya Preclassic Abandonment or the Maya Collapse).

In the Maya Classic Collapse, the density record on core *CH1 -II-04* registered an increase due to the precipitation of gypsum (Hodell et al., 2005). Therefore, we can observe the highest content of sulphur since the 7000 years B. P. period in the core obtained in 1995. The $\delta^{18}O$ also registers the longest period of high evaporation precipitation ratio since the 7200 years B. P. at this moment in this core *(*Hodell et al., 1995*).*

As was discussed in chapter 4, the rainfall amount reconstruction performed using the $\delta^{18}O$, and δD isotopes in gypsum precipitated on core *CH1 -II-04* during the Terminal Classic Mesoamerican Horizon in Chichancanab modelled a rainfall decrease of around 47% compared to the present amount (Evans et al., 2018), while the most severe dry periods had a reduction of up to 70 %, meaning a reduction between 400 to 500 mm of rainfall per year (Evans et al., 2018). The δD of the plant waxes obtained also from core *CH1 -II-04*, also record a dry environment (Douglas et al., 2014). After the Maya Classic Collapse period, the percentage of carbonates starts to increase and the percentage of sulphur decreases (core obtained in 1995) *(*Hodell et al., 1995*).*

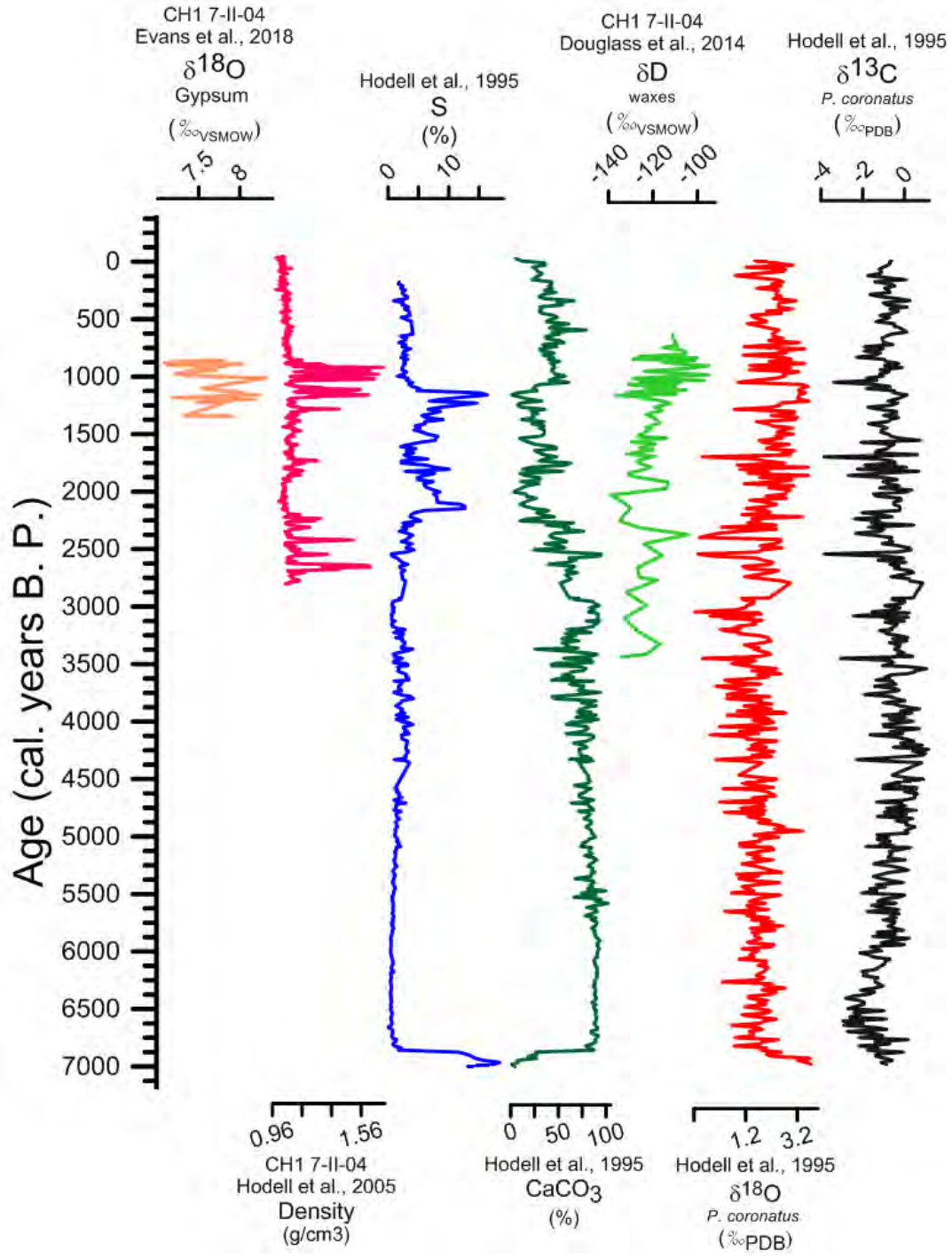

Figure 5.9 Environmental History based on records produced from sediments of the core CH1 7- II-04 from the middle of Chichancanab, studied by Douglas et al., (2014), Evans et al., (2018) and Hodell et al., (2005) and from the core obtained in 1995 in the middle of Chichancanab collected by Hodell et al., (1995). (Figure 6.1 in chapter 6 shows the coring sites in the Lake). All the presented records have been updated to a new age model by Douglas et al., 2015 and Evans et al., (2018) including the core of Hodell et al., 1995.

The next two proxies, percentage of organic carbon and C/N ratio based on the core obtained by Covich and Stuiver, (1974) are problematic not only due to their low resolution but the lack of stratigraphic data that makes it impossible to establish an age model based

on calibrated ages. However, both proxies are used for giving a general tendency (they are not shown in a plot). In this way, the amount of organic material obtained from the core in 1974 has a general tendency of increasing, having its highest level during the Classic period (remember the age model is based in uncalibrated ages) (Covich and Stuiver, 1974). The low C/N ratio (12:1) also obtained from the core in 1974 is interpreted as a signal that the organic material is autochthonously produced and decomposed (Covich and Stuiver, 1974). However, it has been demonstrated that the lake catches exogenous material, at least the plant waxes, which were retained by soils for several decades according the research done on core *CH1 -II-04* (Douglas et al., 2014).

Disturbance vegetation and maize cultivation has been found in the pollen record from Chichancanab for the Classic Mesoamerican Horizon (Leyden, 2002).

In conclusion, Lake Chichancanab proxies suggest a period of intense droughts not only during the time of the Maya Collapse but during most of the Terminal Classic Horizon.

The only palaeoenvironmental study performed in Lake Esmeralda has been the pollen and charcoal records developed in the doctoral thesis of Bermingham (2020), which was conducted in parallel to this research. He used the same cores analysed in this thesis. This record has a high resolution for the period covered by the Preclassic, Classic and Postclassic Mesoamerican Horizons. Bermingham (2020) has established three ecozones which marked vegetation transitions (see section 9.6 chapter 9). In addition, he describes disturbance taxa at the end of the Archaic Horizon and the beginning of the Formative Horizon, 4200 -3400 years B. P. linked to an early human occupation near the lake. A second occupation is inferred by Bermingham (2020) for disturbance taxa during the second part of the Terminal Classic Period after the Collapse ca. 1000 years B. P.

5.9 Conclusion

This chapter described the study sites and the previous palaeoenvironmental studies performed on them. I have explained the importance of having study sites in these contrasting regions, the Northern Highlands, and the Mayab (Northern Lowlands) in the Maya Cultural Area, for having a complete perception of how the Maya people interacted with their environment. The research that is presented in the next chapters attempts to perform new palaeoclimatic reconstructions in these areas, complementing the studies performed until now.

Chapter 6 Methodology


Photo: South part of Lake Chichancanab

"Science is a game—but a game with reality, a game with sharpened knives … If a man cuts a picture carefully into 1000 pieces, you solve the puzzle when you reassemble the pieces into a picture; in the success or failure, both your intelligences compete. In the presentation of a scientific problem, the other player is the good Lord. He has not only set the problem but also has devised the rules of the game—but they are not completely known, half of them are left for you to discover or to deduce. The experiment is the tempered blade which you wield with success against the spirits of darkness—or which defeats you shamefully. The uncertainty is how many of the rules God himself has permanently ordained, and how many apparently are caused by your own mental inertia, while the solution generally becomes possible only through freedom from its limitations."

Erwin Schrödinger, 1887 -1961.

The purpose of this chapter is to describe the fieldwork, laboratory work and mathematical analyses performed during this research. All the tasks described in the chapter were carried out by the author unless otherwise noted.

Due to logistics at the British Geological Survey (BGS) and the British Ocean Sediment Core Research Facility (BOSCORF), the author was not present during the analyses performed in these institutions. In contrast, the author performed the charcoal analyses of samples obtained from the sediments of Lake Esmeralda corresponding to the Middle Holocene (Northgrippian), which were used in parallel research by Adam Bermingham under the supervision of Dr. Bronwen Whitney at the University of Northumbria. Any discussion related to this charcoal analysis is treated as independent research, and it is cited as any other reference.

6.1 Fieldwork concerning core extraction, water chemistry and modern gastropod sampling

In January 2014, a 6.88 m core was collected by undergraduate and PhD students from the University of Nottingham from the southern part of Lake Esmeralda (Figure 6.1) in a water depth of 3.66 m, using a Livingstone type corer with a 1 m core barrel. Four drives were taken from the point of first resistance, an 87cm water-surface sediment interface drive was also taken. Two years later, a modified piston corer was used by other students, Prof. Matthew Jones from the University of Nottingham and M. Sc Roger Medina from the Universidad Autónoma de Yucatán to collect overlapping cores (Figure 6.2) ES-16-01 consisting of four drives and ES-16-02 consisting of three drives (Figure 6.3). In this way, full stratigraphic recovery was ensured. Cores ES-16-01 and -02 were taken from 19° 46' 59.9" N, 88° 44' 10.7" W at 2.63 m of depth (Figure 6.1). Additionally, a Glew core was also taken. The cores were transferred to the University of Nottingham and stored at < 4°C.

In January 2018 I performed the collection of water samples and the sampling of gastropods in lakes Esmeralda and Chichancanab. Water samples were collected from the surface of Lake Esmeralda for the isotopic composition of water and dissolved inorganic carbon at nine sites designated as E1 to E9 (Figure 6.1). Additional water samples were collected at E7, E8 and E9 to identify major ions (see section 6.2 below). At E8 samples were taken from the surface and at 270

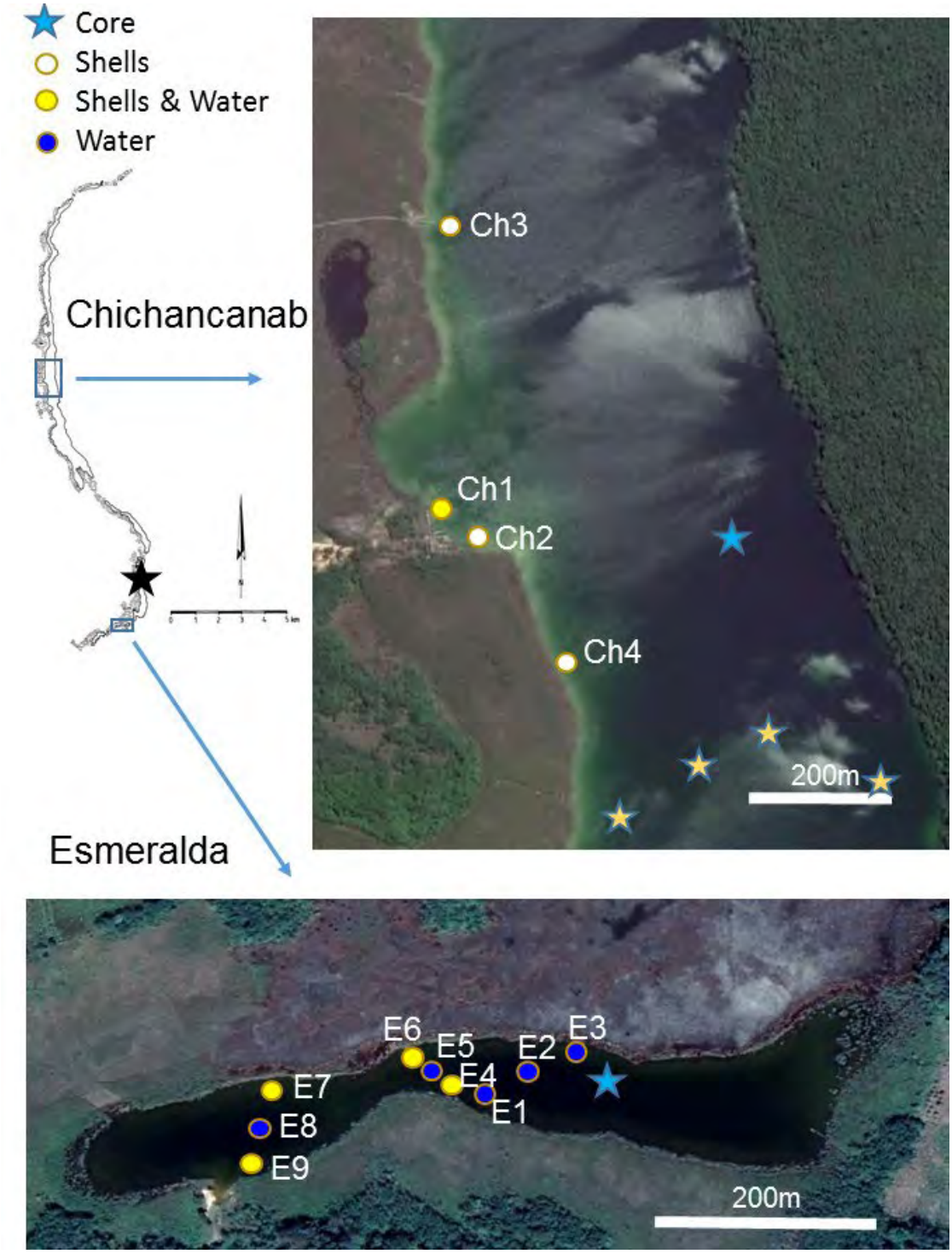

Figure 6.1 Sites sampled during the fieldwork at Lakes Esmeralda and Chichancanab. Blue rectangles on the Chichancanab-Esmeralda map indicate the areas were the fieldwork was performed. Colour of circles indicates where shells were collected (white), shells and water samples were collected (yellow), and only water samples were collected (dark blue). The stars indicate where cores were collected. The coring site (blue star) at Chichancanab refers to the site used for the research performed by Hodell et al., (1995) meanwhile the coring locations (yellow stars) are related to the research performed by Hodell et al., (2005) including the collection of core CH1 .7-III-04 (see section 5.4 in chapter 5 and section 9.7 in chapter 9). The approximate coring site (black star) of Covich et Stuiver (1974) is presented in the general map of both lakes (upper left).

Figure 6.2 Collection of cores ES-16-I and ES-16-II at Lake Esmeralda during the fieldwork in January 2016. Photo courtesy of Sarah E. Metcalfe.

Figure 6.3 Drives of the core ES-16 after collection during fieldwork in January 2016.Photo courtesy of Sarah E. Metcalfe.

cm depth. At the same time, two more water samples were collected from deep water at site E5 (315 cm) and site E8 (270 cm). Temperature, conductivity and pH were measured at these nine sites (E1 to E9) in Lake Esmeralda (Figure 6.1) using Hannah HI-98129 stick meters (EC/TDS and pH) previously calibrated with saline solutions of 1600 and 500 µS for the conductivity and two buffers at pH = 7 and pH = 4.

A similar collection of samples was performed next to the west shore of Chichancanab (Figure 6.1) in order to compare results with samples from Lake Esmeralda, collecting water samples for analysis of $\delta^{18}O/\delta D$ and $\delta^{13}C$ of the dissolved inorganic carbon.

Samples of modern gastropod shells were collected at four sites in Lake Esmeralda (E6 to E9), and four sites in Chichancanab designated consecutively Ch1 to Ch4 (Figure 6.1). In addition, some gastropods were collected at the cenote Chen Ha 2, and the Aguada X'Caamal. The initial purpose of this collection was to identify the different taxa of gastropods of genus *Hydrobiidae* present in the lakes, as well as to compare the isotopic signature in specimens of different taxa, and between lakes.

The collection of a core of 670 cm at Lake San Lorenzo is described in Franco-Gaviria et al. (2018). The core was split every centimetre, and 614 resulting samples were sent to the University of Nottingham for this research.

6.2 Chemical analysis of water

To determine the content of major ions in Lake Esmeralda, a Metrohm 883 basic ion-exchange chromatography unit was used with suppression for anion analysis and without suppression for cation analysis. The anion analysis was carried out using metrosep A Supp 5-250/4.0 column. The eluent was a carbonate/bicarbonate solution with a flow rate was 0.7 ml/min. The cation analysis was done using a metrosep C 6-250/4.0 column. The eluent was 1.7 mmol of HNO_3/0.7 mmol/L of dipicolinic acid ($C_7H_5NO_4$). The analytical time was 30 minutes per sample. A tablet count method for testing alkalinity (HCO_3/CO_3) was performed in a close cell titration in the field using Bromcresol Green-Methyl Red tablets.

6.3 Textural analysis of the core

The drives that composed the three Livingstone/piston cores were cut in half vertically using a wire by the undergraduate students of the University of Nottingham (see Figure 9.1 in chapter 9).

Each half of the drives was cleaned using a spatula, then, a general description of the cores obtained from Lake Esmeralda was performed by undergraduate students, noting the different layers of sediment, organic matter and presence of biota. The cores were also described using a Munsell colour chart to obtain a relatively accurate description of colour changes between and within lithostratigraphic units by Jonathan Dobson. Finally, the three core sequences (ES-14, ES-16-01 and ES-16-02) were stratigraphically correlated using fourteen strata as tie points in order to construct a combined core sequence called "master sequence" (see Figure 9.1 in Chapter 9).

6.4 X-Ray Diffraction analysis

Two different analyses were performed involving the use of X-Ray powder diffraction, XRD in order to identify the mineral composition of crystalline phases in sediments and shells. A standard XRD analysis was performed on sediment samples from Lake San Lorenzo and Esmeralda, while a particular analysis on shells of gastropods from Lake Esmeralda was performed (Figure 6.4).

Eleven samples and seven samples were taken for XRD analysis across the Lake Esmeralda and Lake San Lorenzo records, respectively, using the powder method in a PANalytical MPD- X-ray diffractometer B15 CHB, which has a Bragg-Brentano geometry configuration and CuK_{α} source. The analyses were performed from 5° to 70° 2θ. The samples were selected according to observed variations in Ca/Ti in Lake San Lorenzo mainly for assessing the presence and purity of enough calcium carbonate material for isotope analysis. Ti/Sr was interpreted as a record of the nature of the sedimentary input into the lake (Franco-Gaviria et al., 2018). Figure 7.3 in chapter 7 shows the stratigraphic layers where the samples for XRD analyses were taken. Analyses of bulk sediment were performed every 6 cm in the upper ES-14 core from Lake Esmeralda (see Figure 9.9 in chapter 9).

An XRD analysis of modern single shells from Lake Esmeralda was performed to establish their mineralogy for calculating the isotopic fractionation (see section 6.11 below) during the isotope analyses of shells, which is different depending on the mineral composition (Leng and Marshall, 2004). A set of five individuals, previously cleaned in an ultrasonic bath (see table 8.2 in Chapter 8) was mounted using melted adhesive from tape and pasted on a plate. The plate was settled vertical inside a Bruker D8 Advance diffractometer, and the beam was fixed at the beam size and level that allowed the maximal level of diffracted rays (Figure 6.4). This equipment also has a Bragg-Brentano geometry configuration and

CuK_{α} source. Due to these characteristics, lengthy analyses of around 5 hours were performed in order to achieve a high resolution that can get a better crystalline diffractogram.

The diffractograms resulting from both kinds of methodologies were analysed using Match! V.2.3.2, the Open Crystallographic Database and the International Centre for Diffraction Data database, ICDD version 2, searching for minerals that contain only Si, C, O, P, S, Cl, H, Na, Mg, K or Ca.

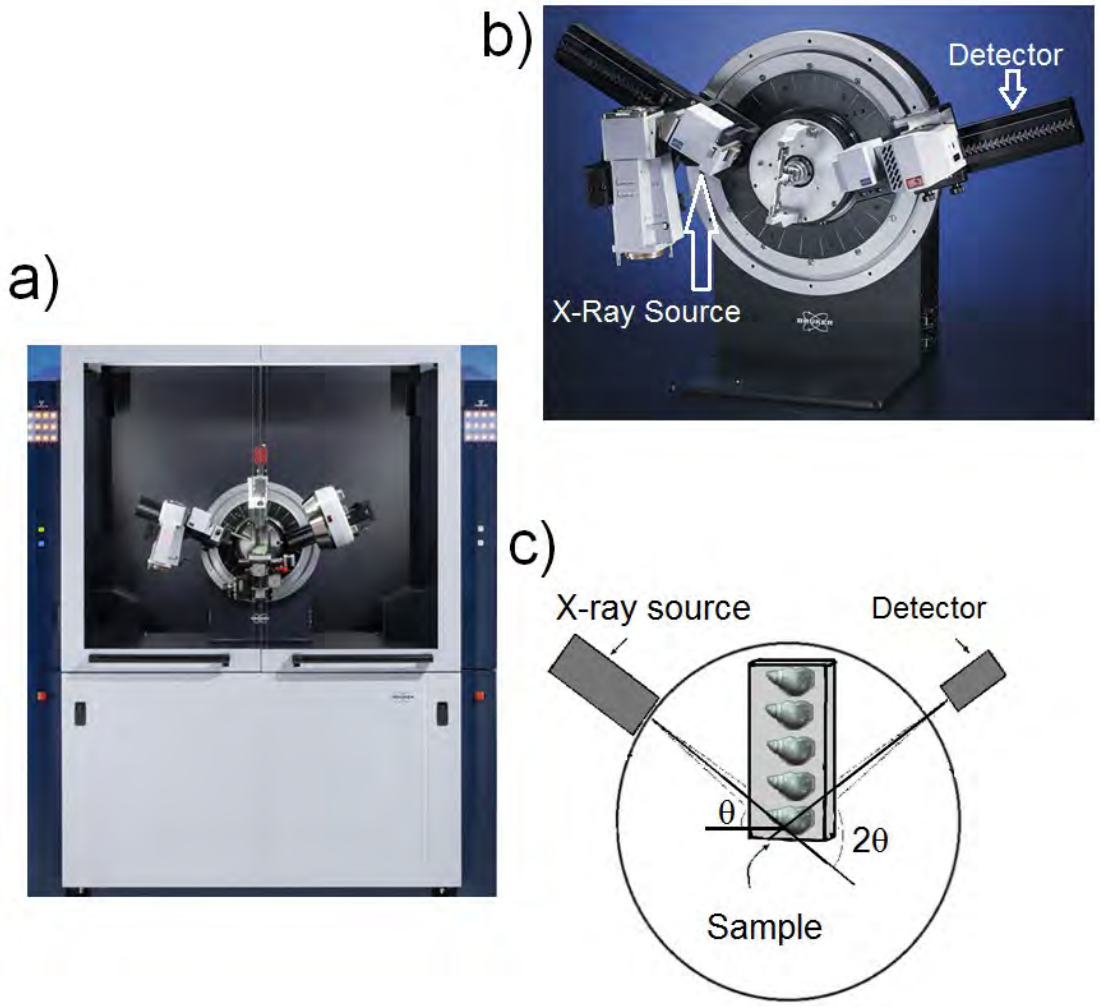

Figure 6.4 X-Ray analyses of shells of Hydrobiidae from Lake Esmeralda. Each shell was measured separately, constraining the analytical area. a) The Bruker D8 Advance diffractometer. b) Main parts of the X-ray equipment with a typical Bragg-Brentano geometry configuration, including the X-Ray source and detector. c) Schematics of the Bragg-Brentano geometry configuration in a diffractometer showing the position of the shells for the analyses in relation to the X-Ray source and the detector. It can be observed that the beam touched specific parts of a shell according the angle θ used. Shells were mounted on a wood block using melted adhesive from tape, therefore some shells (samples 17 and 153, see Table 8.2 in chapter 8) were slowly slid by their own weight by gravity, moving themselves for their original mounting position.

6.5 Generation of the Age Model

Since the core obtained from Lake San Lorenzo already had an age model (Franco-Gaviria et al., 2018), I describe only the steps to obtain an age model for the cores from Lake Esmeralda.

We sampled five levels for radiocarbon analysis on bulk sediment from Lake Esmeralda to establish a chronology for the combined core sequence and to establish an age model for further analysis (see Figure 9.1 in Chapter 9). Radiocarbon analysis on sample taken at the sediment-water interface layer from the Glew core (taken in 2016) (see Table 9.1 in Chapter 9) allowed to assess the hard water error in Esmeralda, since it is assumed that the age of this layer is the year of coring (ca. -66 years B. P. or 2016 A. D.) because the lake is still catching or producing organic material. Any other date will be a consequence of the hard water effect. The radiocarbon dates on the rest of the samples helped to establish an initial chronology for the whole sequence. The hard water effect was corrected subtracting the difference between the radiocarbon age at the sediment-water interface layer and the core collection date -66 years B. P. (2016 A. D.) to every radiocarbon age.

Calibrated dates were calculated from conventional radiocarbon dates after correcting for the hard water effect using OxCal v 4.3 with the standard parameters for continental archives, in the northern hemisphere and employing IntCal13 as a calibration curve.
An alternative calculation using the corrected conventional radiocarbon ages was performed in the program CLAM (Blaauw, 2010) run in R for comparison to the ages produced in OxCal v 4.3, with the same parameters used in OxCal v 4.3. At the same time, an age model was also generated, fixing the age at the interface as -66 B. P in CLAM.

Since the age model calculated for Lake San Lorenzo by Franco-Gaviria et al. (2018) and the model calculated for Lake Esmeralda by Adam Bermingham were calculated using BACON v2.1.0, I also developed an age model for the cores of Lake Esmeralda using BACON v2.3.3. The same parameters used for OxCal v 4.3 and CLAM were applied. However, instead of using the radiocarbon dates after considering the hard water effect, an offset of 330 years B. P. was considered, assuming a concentration of pMC of 100.83 at the interface, which is equivalent to an age of -66 years B. P (the date of coring). The age model in BACON is actually a collection of probable models based on the calibrated ages and the Bayesian statistics of the accumulation rate every 5 cm assuming that dramatic environmental changes did not exist, applying a Bayesian model-based in a beta distribution whose accumulation shape parameter for default is 1.54 for this purpose

(Blaauw and Christen, 2013). Therefore, the results file from BACON does not necessarily give exactly the same age as the calibrated ages at the points from where the samples for radiocarbon analysis were taken. In this way, we calculated different models in order to select a model whose values fall inside the interval of the OxCal v 4.3 calibrated ages at the sampled levels. Every model varied in the accumulation shape, α, which is one of the parameters used in the gamma distribution (Blaauw and Christen, 2011):

$$f(x;\alpha,\beta) = \frac{\beta^{\alpha} x^{\alpha-1} e^{-\beta x}}{\Gamma(\alpha)} \quad \textit{Equation 6.1}$$

Where β is the accumulative mean and x is the random variable.

This distribution is a conjugate distribution in Bayesian statistics, implying that a smaller α will allow more variability in the accumulation rate (sedimentation rate) across the sedimentary sequence (Blaauw and Christen, 2013). Since Franco-Gaviria et al. (2018) did not explain which value of the parameter α was used in the age model for Lake San Lorenzo, we ran different models varying α for applying similar values of α for Lake Esmeralda. Models using α = 0.8 and α = 0.6 gave similar outputs to the model of Franco-Gaviria et al. (2018) (see section 7.1 in chapter 7). For the radiocarbon results from Lake Esmeralda, we ran models with α = 0.2, 0.4, 0.6, 0.8, 1.5, 1.54 and 1.6.The memory strength parameter was left at the default value of four, assuming that the sedimentation rate did not change dramatically from layer to layer.

6.6 Total inorganic and organic carbon content analysis by loss on ignition

Total organic carbon (TOC) and total inorganic carbon (TIC) were measured by the method of loss on ignition, for the sediments of Lake Esmeralda and Lake San Lorenzo, using a methodology adapted from Dean (1974). For sediments from Lake Esmeralda, these analyses were done by Peter G. Atkinson and Annabel Mellor. Loss on ignition is a quick, cheap method to gain estimates of TIC, TOC and TC. However, Santisteban et al. (2004) recommend that loss on ignition data should be used qualitatively due to the effect of sediment composition (predominantly clay mineral concentration) on results. In addition, it must be considered the rehydration of CaO produced at 925°C to $CaCO_3$ at room temperature due to the water present in the atmosphere, which has repercussion in the calculated percentage of inorganic carbonate and residuals. Figure 6.5 explains this method.

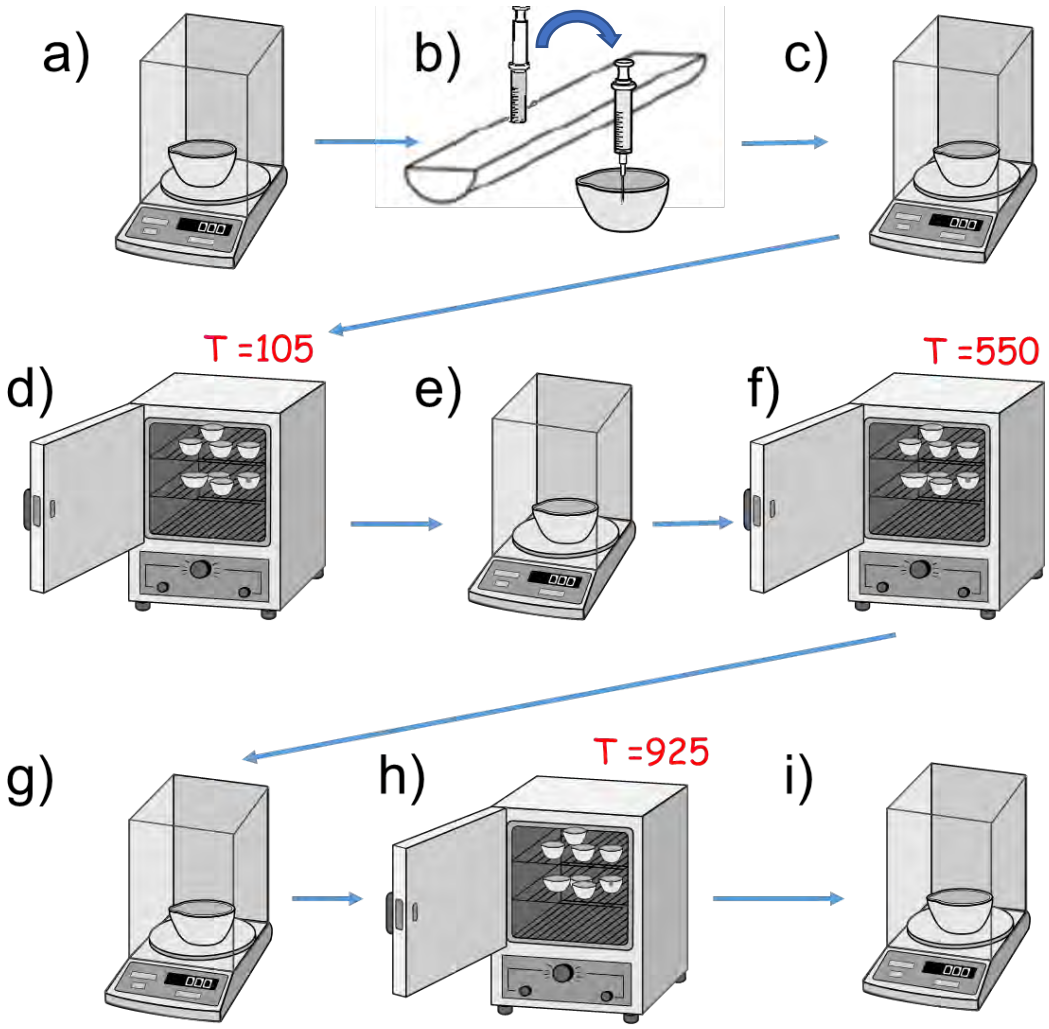

Figure 6.5 Steps in loss on ignition of sediments for obtaining the percentage of total organic carbon and the inorganic total carbon. Most of the samples from Lake Esmeralda were processed in the laboratory for Loss on ignition by the undergraduate students Annabel Mellor and Peter G. Atkinson on the ES-4 and ES-16 cores respectively. The author of this thesis performed the analyses on the samples from Lake San Lorenzo. Samples of approximately 1cm³ were taken every 4 cm from sediments from Lake San Lorenzo and every 2 cm in case of Lake Esmeralda (with the exception of the segment of ES14-4 where samples were taken every 4 cm. a) Pre-weighed dry crucibles b) were filled with samples taken from the core and c) reweighed. d) Sediment filled crucibles were dried for 12 hours in the oven at 105° e) Then crucibles with dry sediment were reweighed. After this, f) crucibles with the dry sample was placed inside the oven at 550°C for 5 hours for taking away the organic content material. g) Crucibles with; organic-free sediment was reweighed. Finally, h) crucibles without organics were placed back in the oven at 925°C for 2 hours to promote the decomposition of carbonates according to the decomposition reaction; $CaCO_3 \rightarrow CaO + CO_2$. *i) After this, the crucible with the sediment remains without organics and water were reweighed. The amount of carbonate needs to be calculated from the amount of CO_2 expelled, assuming that all carbonate is calcium carbonate according to the stoichiometry.*

6.7 Generating Colour and Greyscale records

A greyscale record was developed from the cores collected from Lake Esmeralda for generating a record of the changes in colour and for establishing the number of layers digitally. Four different approaches were used for this purpose.

For three of these approaches, eight drives containing the master sequence of the sediments from Lake Esmeralda (see above) were scanned using an XYZ Multi-Sensor Core Logger, XYZ-MSCL fitted with a Bartington magnetic susceptibility sensor and a Konica Minolta Spectrophotometer at BOSCORF in Southampton (see section 6.9) in order to obtain magnetic susceptibility variations, greyscale variations, reflectance variations in thirteen wavelengths and Munsell colours variations and CIE XYZ colour space variations.

The scan used a step of 5 mm. Greyscale and colour variations are obtained directly from the Munsell colour variations, the reflectance and the XYZ colour space variation. This last methodology gave us the variation of the red, blue and yellow colours in these sediments across the core. Therefore, the scanning gives us a direct greyscale record as well as different colour records extracted from different methodologies.

A fourth way to obtain the variations from greyscale and colours was performed using high-resolution images for every drive in the master sequence. These images were achieved using the same intensity of light provided by a LED in a Geotek Multi-Sensor Core Logger Core Imaging System coupled to a Geoscan IV linesman camera. The scan creates a high-resolution image of 16 bits depth (commonly named XGA High Colour). This image was processed using Matlab© to create a time series based on modifications made to the algorithms proposed by Trauth (2007) (Figure 6.6).

The greyscale record produced from the image has a resolution of 0.01 cm. Therefore, it had a higher resolution in comparison with the records produced using XYZ Multi-Sensor Core Logger.

After getting the greyscale time series from the images, a layer count was calculated based on the first and second derivative criteria, since the borders of the layers correspond to the local minima in the time series for assessing the possibility that the layers were generated annually after comparing with the age of the sediments. Using Matlab©, it was possible to find the position of the boundary of the layers is in the master sequence. Therefore, the thickness of the layers could be measured.

Since the core of Lake San Lorenzo was sampled entirely at 1 cm intervals, after the research of Franco-Gaviria et al. (2018), it was not possible to perform this kind of analysis on it.

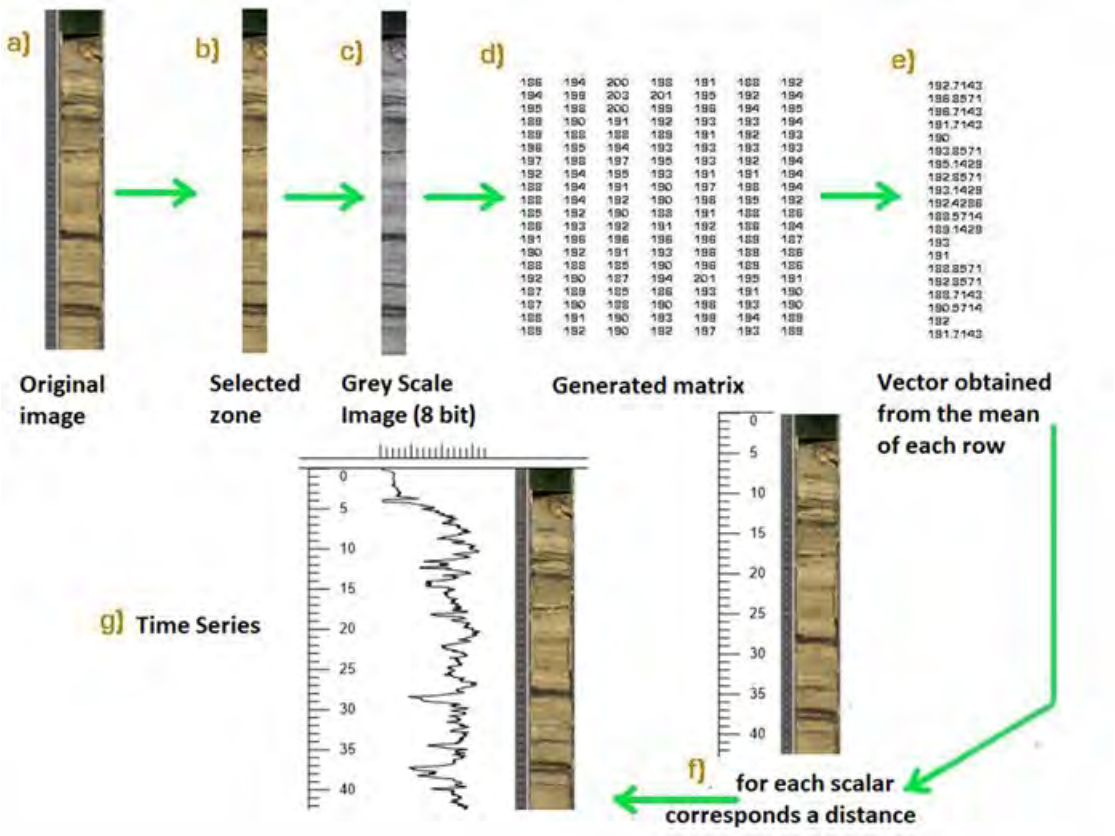

Figure 6.6 Steps used for generating a greyscale and primary colours time series from a) the image obtained in the scanner, then b) the image is first cut to an image of 300 pixels wide. c) In the case of colour images, they were decomposed first into primary colours, red, green and blue (RGB), whilst the colour image was transformed first into a greyscale image. d) Then the image (primary colour or greyscale image) is digitised in a unidimensional matrix. e) An arithmetic mean is obtained for each row, creating a column vector. f) Each scalar in the vector corresponds to a distance. g) Finally, this vector, where each scalar is a function of the distance is a time series.

6.8 Generation of elemental abundances and elemental ratios analysis using XRF core scanning

At the University of Aberystwyth under the supervision of Prof. Sarah J. Davies, the master sequence of the sediments of Lake Esmeralda was scanned using an Itrax core scanner (Cox Analytical Systems) for X-Ray Fluorescence Analysis, which is a non-destructive way for counting elemental abundances along the core. These abundances can be used as environmental proxies (e.g. Haug *et al.* 2003; Metcalfe *et al.* 2010). For instance, elemental chemical ratios, such as Mg/Ca (Cuven et al., 2015), Sr/Ca (Valero-Garcés et al., 1997) can be proxies of the precipitation-evaporation ratio in karst systems. While Zr/Rb ratios could

be a proxy of flood events (Turner et al., 2015) and Ca/Ti trace changes in detrital inputs (Davies et al., 2015)

Since the master sequence comprises eight drives, eight different runs were performed. Before every analysis, the drives were unpacked (Figure 6.7a) and cleaned (Figure 6.7b) to ensure a fresh, flat surface since increased surface roughness could reduce elemental counts (Jarvis, 2012).

After cleaning, every drive was covered (Figure 6.7c) with a thin sheet of transparent polypropylene film (4μm thick) to minimise sediment drying and decay during the analysis due to the intense energy of the beam, as well as to prevent instrument damage from any contact with the sediment (Anderson et al., 2012). Every run was scanned focusing in the intervals constrained by the tie points (Figure 6.7d). In addition, 2 cm were scanned before and after the tie points in order to facilitate the correct assemblage of the data series across the axis of sedimentation. At the same time, an image of the scanned area was obtained. An XR radiograph of the scanned area was also generated.

The analyses were performed using a V= 45 kV, I = 35 mA, exposure time of 100 ms and a resolution of 500 μm. A 4mm wide by 500μm large aperture was selected to focus X-rays onto the sediment. Therefore, a continuous scan of the sedimentary sequence was obtained. A Molybdenum light source was chosen to generate high powered X-rays, which are adequate for most chemical, natural elements (from Al to U), with detection limits as low as 20ppm for some of them (Cuven et al., 2011). Although the scanner also analyses elements of the second and third periods of the Mendeleyev table, the relative variations in their abundance are commonly taken as not reliable (Ravansari et al., 2020). Raw data were displayed as counts per second (cps); this equals the spectral peak area divided by count time in seconds.

Itrax's internal software provides a binary indication of data validity, where surface irregularities (e.g. cracks within the split core) can lead to significant drops in the total number of element counts (kcps) and increased mean, standard error (MSE). Invalid data is generally indicated when the kcps is below 10,000, or the MSE exceeds 5 at every 500μm increment through the sequence. No data was found invalid between tie points.
Since the presence of organic material and water dilutes the detection of the elements (Elbert et al., 2012), variations of these constituents must be taken into account. This interference is perhaps the main reason why an analytical standard is not used for

calculating the concentration of the elements (Boyle et al., 2015). To overcome this problem, geochemists tend to use element ratios and data normalisation. Normalisation also crucially negates the influence of sediment morphology on element counts, so that any variation to counts reflects the geochemical signal (Davies et al., 2015; Kylander et al., 2012). Therefore, the raw data were normalised by total scatter, which is gained through Itrax's detection and addition of coherent and incoherent scatter (inc + coh) (Berntsson et al., 2014; Kylander et al., 2012). Incoherent and coherent scatter are related to the Compton, and Rayleigh scattering of X-ray radiation, respectively and their intensity reflects the organic and water content within the sediment (Davies et al., 2015). In this way, using total scatter acts for normalising minimise the effect of organic/water content and sediment morphology on geochemical signals.

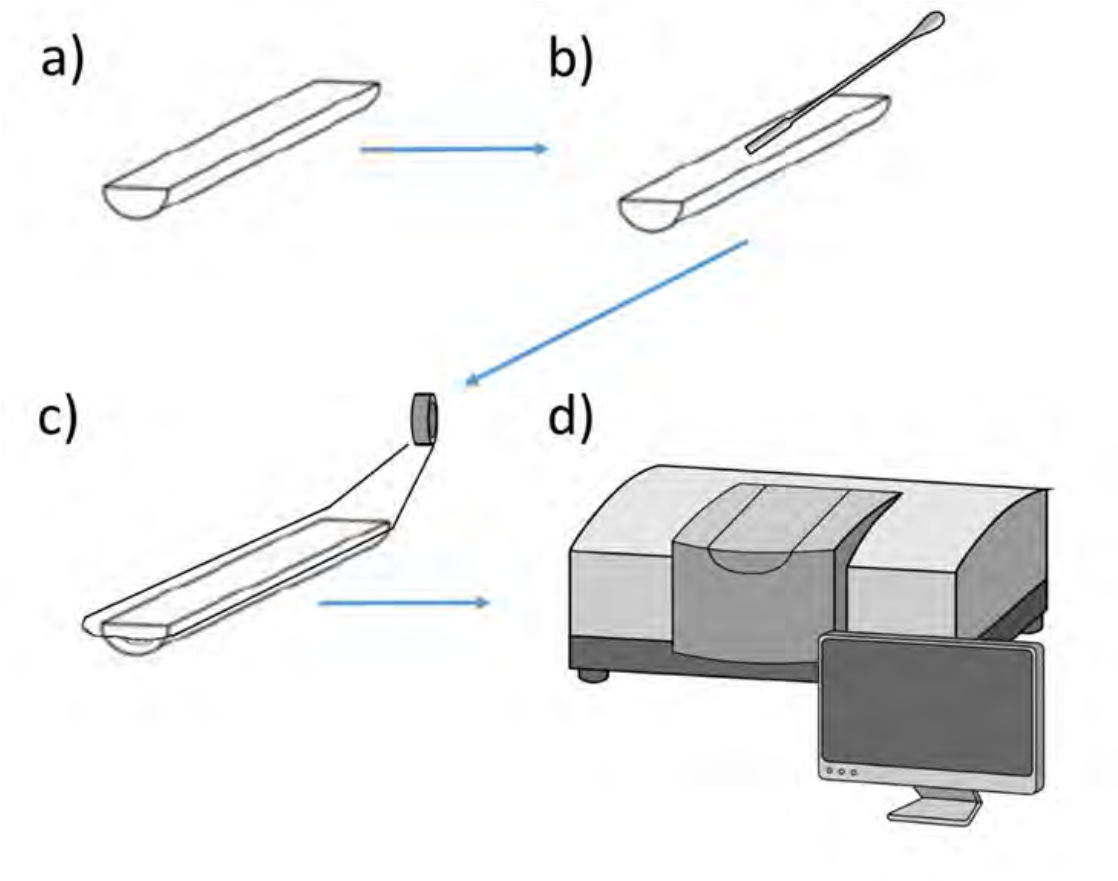

Figure 6.7 Preparation of the core for X-Ray Fluorescence Analysis. a) A drive is uncovered b) the sediment in the drive is cleaned to ensure a flat and smooth surface, c) the sediment in the drive is covered with a film of propylene and d) the drive is positioned inside the Itrax core scanner.

Since the content of organic material and water in the surface of sediments from Lake Esmeralda is relatively low (lower than 20% in most parts of the core and rarely over 40%), the signals were not impacted dramatically after the normalisation. A time series of the

data between the tie points were generated with the normalised abundances, assigning an age based on the age model.

The elemental abundances for the core obtained from Lake San Lorenzo were performed using μ-XRF (instead using a scanner). The subsamples for this analysis were extracted from the core by Franco-Gaviria et al. (2018) at UNAM.

6.9 Density analysis using AGR and LoI

The density record of Chichancanab was vital in establishing the existence of a dry period around the time of the Maya Collapse at the end of the Mesoamerican Classic Period due to the presence of gypsum (Hodell et al., 2005). Therefore, it is desirable to produce density records in our study sites in case abrupt changes might represent important changes in mineralogy. It has to be taken into consideration that the water chemistry of Lake Esmeralda is very different from Chichancanab (Perry et al., 2009, 2002). Therefore, it is unlikely that changes in density in Esmeralda will be directly linked with changes in the precipitation of gypsum. Density records were produced from two different approaches.

In the first approach, eight drives that compose the sedimentary master sequence of Lake Esmeralda were thoroughly scanned using a Geotek Multi-Sensor Core Logger Standard 7.9 (MSCL-S) for attenuated gamma radiation, analysis, AGR (see section 6.7) at BOSCORF (Southampton) in order to obtain the thickness, density and porosity of the bulk sediment (Figure 6.8).

The scan used a step of 5 mm. A previous scan of empty liners of the same material and configuration was conducted as a blank. Some problems arose due to the presence of aluminium foil between the bulk sediments and the liner at segments inside the ES-14 core. The foil could not be removed without disturbing the core.

The second approach involves the production of a density record from the dry weight measured during the Loss on ignition. Since the volume of the sample during this analysis was 1 cm^3, it was possible to calculate the density for every sample based on:

$$\rho = \frac{dry\ weight}{volume}$$ *Equation 6.2*

Where ρ is density, it is essential to highlight, that in contrast to this second approach, the density of the core calculated using AGR considers a wet sample.

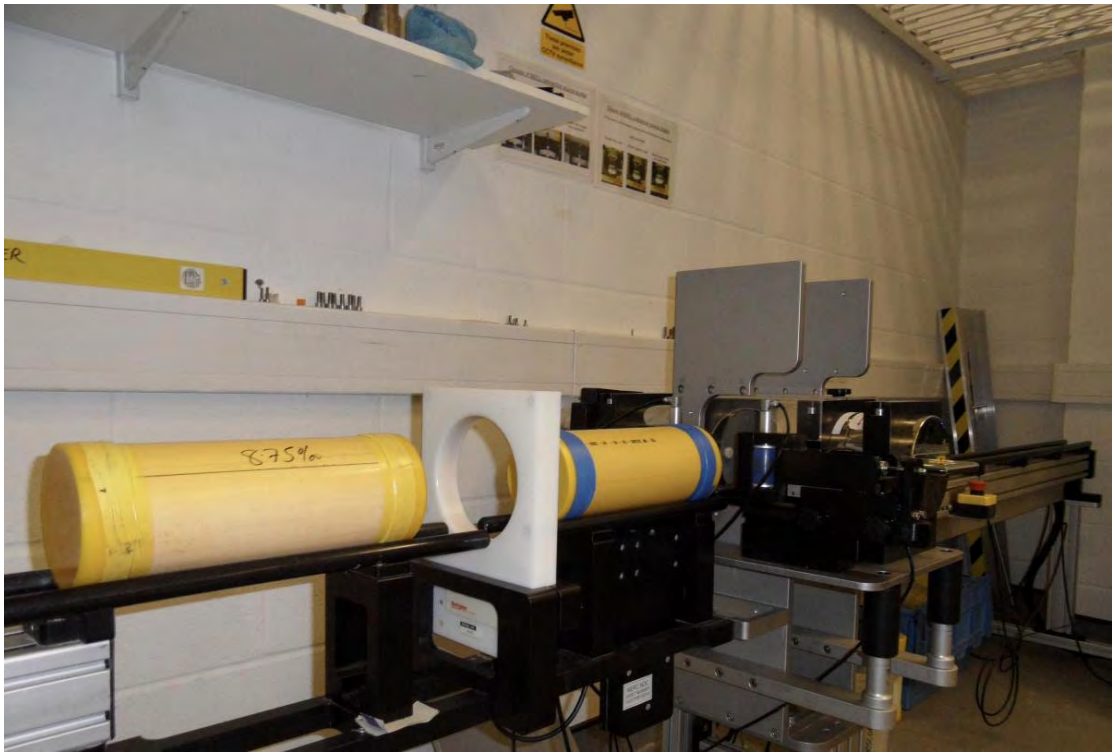

Figure 6.8 Geotek Multi-Sensor Core Logger Standard 7.9 at BOSCORF used for attenuated gamma radiation for measuring the density, thickness and porosity of the cores from Lake Esmeralda. Image taken from https://boscorf.org/instruments/multi-sensor-core-logger-standard.

6.10 Assessment of diagenesis on shells

As a requirement for the isotopic composition of shells, we assessed the possible impact that diagenesis had on the shells, which could interfere in recovering the climatic signal. Phenomena related to diagenesis would be processes like cementation of calcite on the shells, as well as recrystallisation or dissolution of the minerals that make up the shells. As the first step, a series of observations were performed using a scanning electron microscope, SEM, in order to look for structures that could be produced by these phenomena.

A representative specimen of each taxon and site (see table 8.3 in Chapter 3) was observed using a JEOL 6400 SEM in the low vacuum chamber filled with water vapour. The best conditions for recording images were obtained at 80 Pa, a contrast = 40, a bias = 49.5 and a high voltage = 10. Because the analyses were done on samples that were also going to be used for isotope analysis, they were not coated with any material, such as gold or silver, they were just mounted in a carbon base tape (Figure 6.9).

A comparison between the SEM and the high-resolution images obtained in the Olympus SZX10 binocular optical microscope was made, establishing that the major diagenetic

structures could be seen under the optical microscope. Therefore, an assessment of the degree of diagenesis was made for every shell using an Olympus SZX10 binocular optical compound microscope (20x objective magnification) instead of the SEM due to the lower cost of money and time. This assessment uses the idea of quantifying the area covered by diagenetic structures on the shell surface, in a similar way that grains cover a percentage on a matrix. We used grain visual estimation charts for that purpose.

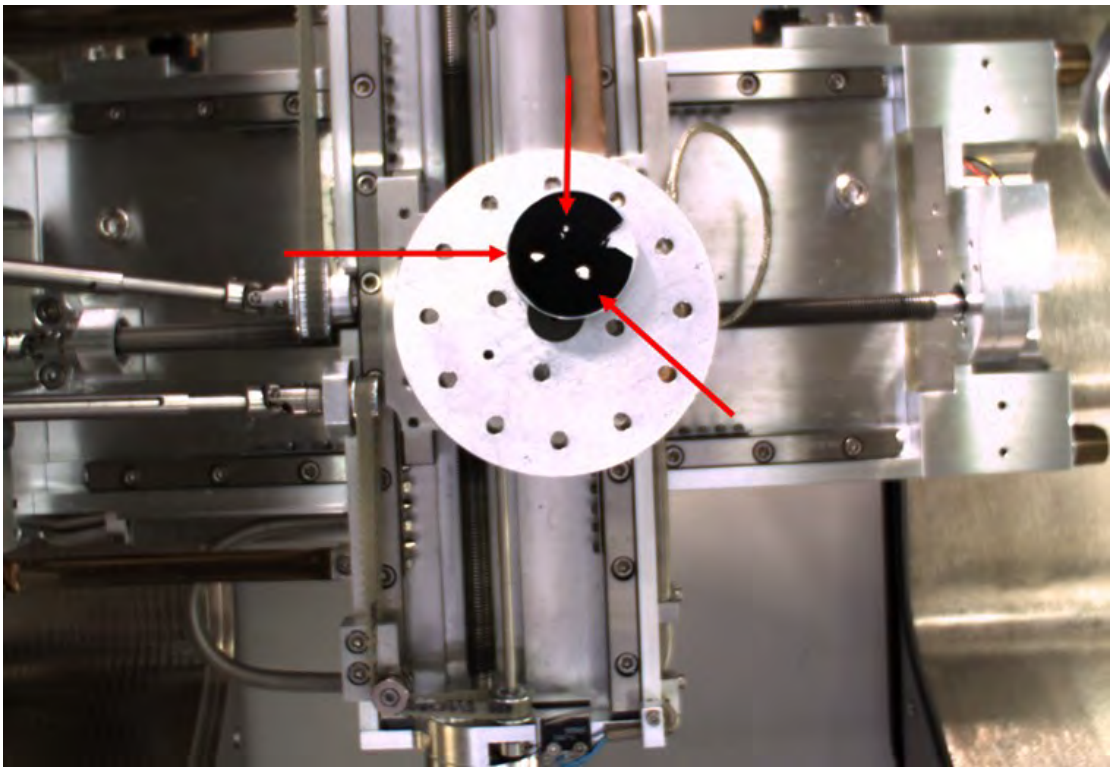

Figure 6.9 Shell specimens fixed in the vacuum chamber for their observation in the Scanning Electronic Microscope. Red arrows point out the shells.

In this way, a percentage of diagenesis was established for the face of the whorl opposite to the aperture, the face of the whorl next to the aperture, and the inside face observed through the aperture. In the end, the total surface covered by diagenetic structures can be calculated considering that each external face contributes to 25 % of the total area, while the inside face contributes 50 % of the total area. The total diagenesis can be expressed in the next equation:

$$\%\, Total\ diagenesis = \%\, D_{(IF)}(0.5) + \%\, D_{(WA)}(0.25) + \%\, D_{(W)}(0.25) \quad \textit{Equation 6.3}$$

where $D_{(IF)}$ is the area covered of diagenetic features in the inner face; $D_{(WA)}$ is the area covered by diagenetic features in the whorl and apex at the same face of the aperture and; $D_{(W)}$ is the area covered by diagenetic features in the whorl and apex on the opposite side to the aperture.

To assess the impact of the diagenesis features on the isotopic signal, a possible correlation between these two variables was calculated. For this purpose, the Pearson's correlation coefficient was calculated in SigmaPlot 13.0.

6.11 Isotope analysis

Analyses of oxygen and carbon stable isotopes were performed for ancient water balance reconstructions on carbonates from bulk sediments previously sieved obtained from Lake Esmeralda and Lake San Lorenzo. In the case of Lake Esmeralda, both sieved sediment and shell isotopes analysis is performed for comparing which method is better for recovering the environmental signal. In the case of Lake San Lorenzo, the lack of micro-subfossils makes the sediment the only possible path for recovering the climatic signal. Samples were taken every 4 cm from the Lake San Lorenzo core and on an average of 10 cm in the case of Lake Esmeralda (since the record was sampled by different people, even distances were not achieved).

Before the isotope analyses on sediments, the bulk sediment was sieved using a mesh size of 250 μm in order to avoid shells of gastropods. Organic material present in the sediments was removed (by oxidation) since organics might interfere with the measurement of the isotopic composition. This removal was performed by Harriet Galley, Nicholas Robinson and Jonathan Dobson for most of the sediments from Lake Esmeralda and by the author in the case of the sediments from Lake Esmeralda corresponding to the period of the last ca. 900 years B. P. and from all the sediments from Lake San Lorenzo. 10 mg of pure carbonates is necessary for every analysis to obtain enough CO_2 for analysis in the mass spectrometer.

The amount required can be estimated based on the Total Inorganic Carbon (TIC) data using the following equation:

$$sample\ required\ (mg) = \frac{1000}{(TIC \times 8.33)}$$ *Equation 6.4*

A sample containing at least 10 mg of pure carbonate was placed in a 200 ml beaker (Figure 6.10a). Approximately 50 ml of 5% NaClO was added (enough to immerse the sample) (Figure 6.10b). The sides of the beaker were also washed with 5% NaClO to ensure complete contact of the sample with the bleaching agent. The beaker was covered with a watch glass and left for 24 hours (Figure 6.10c). After this time, the beaker was filled up to 500 ml with deionised water for washing out the bleaching agent and left until the sample has settled (Figure 6.10d). Once the water was clear, the water was decanted taking care

not to disturb the sediment (Figure 6.10e). After this, the beaker was covered again with deionised water up to the top (500 mL), and I repeated the washing process twice more until reaching a neutral pH (Figure 6.10f).

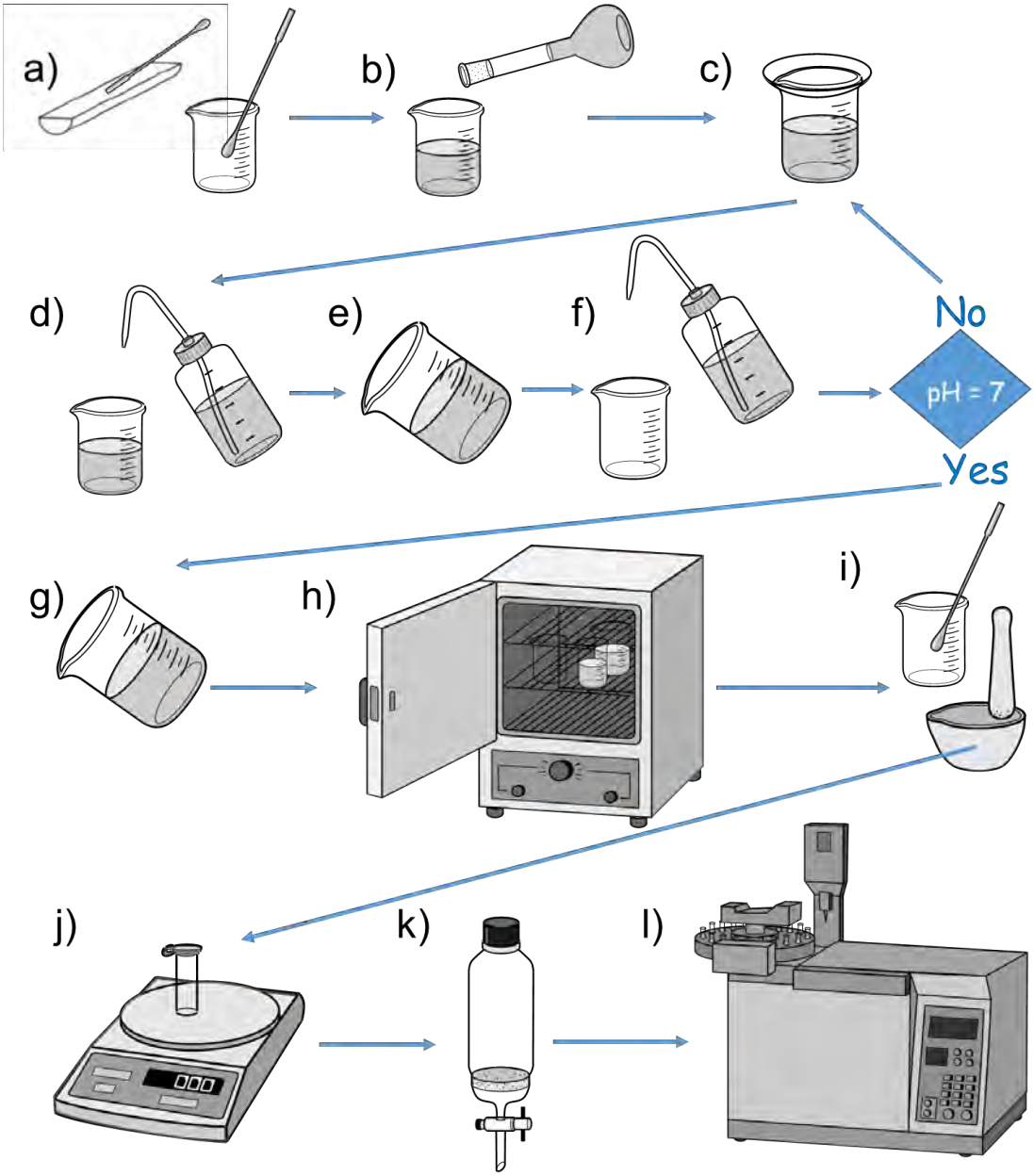

Figure 6.10 Methodology of the oxidation of organics for cleaning carbonates for isotope analysis. Each step is explained in the text.

Once neutral pH was reached, the liquid was decanted, leaving a small amount of water (down to <25 ml) to avoid losing any sediment (Figure 6.10g). Then, the beaker was put inside a drying cabinet and left there for 24 hours at 30°C (Figure 6.10h). When the sample was finally dry, a soft spatula was used to remove the sediment from the bottom of the beaker. Finally, the sediment was ground in an agate mortar (which is better to control the grinding, and practically eliminate any possible contamination from the mortar and pestle

set itself, and it is from a material that does not contain carbonate), to produce a fine powder around 0.2 mm (Figure 6.10i). The sediment was transferred to a vial. Samples were taken to the BGS, for weighing and digestion with H_3PO_4 for extracting CO_2. The isotopic composition of the CO_2 extracted was measured using a GV Isoprime with Multiprep and VG Optima (Figure 6.10j). A duplicate sample was run every ten samples for testing reproducibility. A Middle Cambrian Shale, MCS, used as a standard was also measured every ten samples as well as the Carbon Capture and storage, CCS standard. The analytical error is 0.1 ‰ for both $\delta^{18}O$ and $\delta^{13}C$.

Isotopic analysis on shells was only performed on gastropods of the genus Hydrobiidae founded in sediments of Lake Esmeralda since sediments from Lake San Lorenzo did not have gastropods. After classification (see next section), all modern shells from a specific site and shells from a particular layer were put in a vial (Figure 6.11a), which was put into an ultrasonic bath for 10 minutes (Figure 6.11b). After this, the shells were separated (Figure 6.11c).

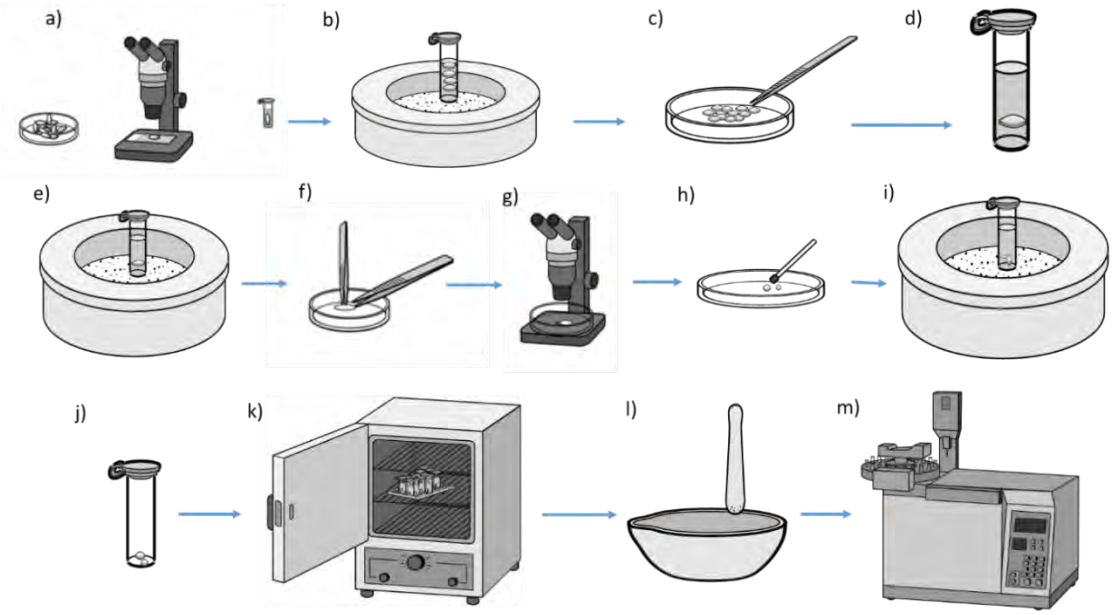

Figure 6.11 *Cleaning protocol for shells for isotope analysis. See full description of the text.*

Each individual shell was then submerged in a vial filled with deionised water (Figure 6.11d) for cleaning to avoid any contaminant that could interfere with the actual isotopic composition of the shell, for instance, charcoal, organic material, plant remains, or crusted cemented calcite. Every vial was put back in an ultrasonic bath covered by distilled water for 2 minutes (Figure 6.11e). After this, every subfossil shell was split, trying to break just the apex of the shell (Figure 6.11f).

In contrast, modern shells were not broken until being observed under the SEM and optical microscopy (see next section). The shell was then observed under the stereomicroscope (Figure 6.11g), and if contaminants were present, such as plant remains, charcoal remains or calcite dust, it was cleaned using a small brush (Figure 6.11h). The split shell was then cleaned again for two minutes inside a vial covered with deionised water in an ultrasonic bath with distilled water for two more minutes Figure 6.11i). After this, the split shell was transferred to a dry vial (Figure 6.11j) and left in an oven for 24 hours at 30°C (Figure 6.11k).

Every shell was sent to the BGS to be plasma ashed to remove any organic material, such as humic acids. Every single shell was then crushed, and ground using an agate mortar since only 10 mg are required, and the average weight of a shell is 50 mg (Figure 6.11l). The ground shells were sent for individual analysis at the BGS.

An aliquot of 30 mg was taken from every ground specimen, although 10 mg were used for each analysis in a GV Isoprime 100 mass-spectrometer with Multiprep (multi preparation system) for analysis of $^{13}C/^{12}C$ and $^{18}O/^{16}O$ (Figure 6.11m). An internal laboratory isotope standard KCM 230119, measured after every three sample analyses, was used to standardise and normalise sample isotope values. The mineral composition of the shell was considered for calculating the appropriate value after fractionation. The precision of the standard analyses was $\leq\pm$ 0.5 ‰. (even 0.1‰).

Six stratigraphic layers were selected from the cores of Lake Esmeralda for picking ten specimens (single shells of *P. coronatus*) (see Table 8.10 in Chapter 8). At the same time, three specific stratigraphic layers were chosen for picking specimens of Hydrobiidae in general. In this way, twenty-five specimens at 20 - 22 cm were collected from drive ES-16-01-I or 20 – 22 cm of master sequence.

Fifteen individuals were picked at 80 – 81 cm from ES-16-01-I (79- 80 cm in the master sequence), and thirteen specimens were obtained at 80 – 84 from drive ES-16-01-I (306.5 – 309.5 cm in the master sequence). The collected gastropods were cleaned using the same methodology used for the modern shells, including the plasma ashing and grinding before their analysis at the BGS using the GV Isoprime mass-spectrometer with Multiprep.

The ten water samples collected at Lake Esmeralda and Chichancanab were used to precipitate carbonate by M. Sc. Ahmad AlShdaifat to obtain isotope values on modern dissolved inorganic carbonate by altering the pH of the solution by adding $BaCl_2$.

Carbonate precipitated from this method was analysed with the same methodology used for carbonates from sieved sediment. Water samples were also used for analysing the isotopic composition of hydrogen (δD) and oxygen ($\delta^{18}O$) using an Isoprime mass-spectrometer with EuroPyrOH (internal precision.1σ(‰) ≤ 0.10 for gas species considering the heavier isotope).

The results of the isotopic composition of the oxygen in waters from Lake Esmeralda and Chichancanab were used to calculate the theoretical value of carbonates precipitated in such waters (see section 8.1 in chapter 8). This calculation is performed based on the equation proposed by Leng & Marshall (2004) for carbonates:

$$T\,°C = 13.8 - 4.58\,(\delta_{Calcite} - \delta_{Water}) + 0.08\,(\delta_{Calcite} - \delta_{Water})^2 \quad \textit{Equation 6.5}$$

This equation is quadratic, therefore, the value of $\delta^{18}O_{Calcite}$ is given by the smaller result of the square root in the following equation, since the other solution does not have a physical meaning.

$$\delta_{Calcite} = \left\{\frac{-(-4.58) \pm ((-4.58)^2 - 4\,(0.08)(13.8 - T°C))^{1/2}}{2(0.08)}\right\} + \delta_{Water} \quad \textit{Equation 6.6}$$

Thus,

$$\delta_{Calcite} = \left\{\frac{-(-4.58) - ((-4.58)^2 - 4\,(0.08)(13.8 - T°C))^{1/2}}{2(0.08)}\right\} + \delta_{Water} \quad \textit{Equation 6.7}$$

This equation 6.7 needs to be modified for calculating the actual value of the isotopic composition of aragonite since aragonite $\delta^{18}O$ values are typically around +0.6 % higher than equivalent calcite (Abell and Williams, 1989). The new equation 6.8 takes into consideration the fractionation during aragonite precipitation (Leng and Marshall, 2004). Taking this into account, the $\delta^{18}O_{Aragonite}$ is given by the equation:

$$\delta_{Aragonite} = 0.6 + \left\{\frac{-(-4.58) \pm (-4.58^2 - 4\,(0.08)(13.8 - T°C))^{1/2}}{2(0.08)}\right\} + \delta_{Water} \quad \textit{Equation 6.8}$$

This equation 6.8 is also applied for calculating the isotope values of the analysed shells, which are composed of aragonite (see section 6.4).

6.12 Analysis of variance of the isotopic composition of single gastropod shells and its comparison to the isotopic signature obtained from sieved sediments.

Based on a study at Lake Chichancanab, Escobar et al., (2010) suggest that the reliability and robustness of the environmental signal acquired from gastropod shells strongly depends on the depositional age (meaning the age of the strata which the gastropods come from) and the number of shells analysed. The robustness of the signals might depend on other factors in different gastropod taxa e. g. age of the gastropod, niche, diet, as well as other variables in different kind of lakes (Leng et al., 1999). To establish the variance in the isotope data obtained from shells, a series of experiments were carried out. The results of these experiments are presented in Chapter 8.

The modern gastropods collected (section 6.1) were washed and sieved in order to separate them from the sediment and organic material in Mexico City. The initial purpose of this collection was to separate the different taxa of gastropods, focusing on the family Hydrobiidae present in Lake Esmeralda, Chichancanab, Chen Ha and Aguada X'Caamal. Shells were taken to the University of Nottingham where they were again washed but using distilled water and dried for 24 hr at 30 °C. The collected Hydrobiidae were classified into four taxa *Aroapyrgus* sp., *Tryonia* sp., *Pyrgophorus coronatus* (smooth form), and *Pyrgophorus coronatus*. (spinose form) according to the morphology of the shell (Dillion, 2006). Sites with fewer than ten Hydrobiidae were not considered for further studies. Every modern shell was then photographed to retain a record of their morphology since this was lost after the analyses.

After the isotopic analyses, a series of statistical tests were performed using SigmaPlot 13.0 on the results of the isotopic analyses to test the null hypothesis that the difference in the $\delta^{18}O$ was due to random sampling and not to a property that could explain the variation, for instance, its membership to a specific genus, lake or locality inside the lake. The samples were divided into sets for comparison in order to answer some specific questions.

In the first comparison, a test of the representative value, e. g. Students t test, and a variance test, e. g. analysis of variance (commonly called ANOVA) was performed comparing the $\delta^{18}O$ between two populations of shells of the same genus; *Aroapyrgus sp., Tryonia sp., P. coronatus* (smooth) or *P. coronatus* (spinose), coming from Chichancanab and Lake Esmeralda respectively. The alternative hypothesis explains the differences in the isotopic signature as a consequence of a different evaporation/rainfall ratio in each lake, meaning different catchments and climates.

The second test involves populations of the same genus and lake, but compared according to the location where they were collected in the same lake. The alternative hypothesis is that there is a difference in the isotopic signature of $\delta^{18}O$ which depends on specific sites within the lake. This comparison was made for populations of *Aroapyrgus sp., Tryonia sp.,* or *P. coronatus* (smooth) in both lakes and *P. coronatus* (spinose) in Chichancanab.

The third test makes a comparison of the differences in the $\delta^{18}O$ between populations of different genera in the same lake (L. Esmeralda or Chicchancanab). The alternative hypothesis explains the different values of $\delta^{18}O$ determined by each taxon. In such a case, the metabolism of the gastropod would perform a selective fractionation of the isotopes.

Similar analyses were carried out for comparing the values of $\delta^{13}C$. The tests used were selected according to criteria for determining if parametric or nonparametric statistics must be applied. Figure 6.12 shows the flow diagram for selecting the test that will compare the values, while Figure 6.13 shows the flow diagram for selecting the variance test.

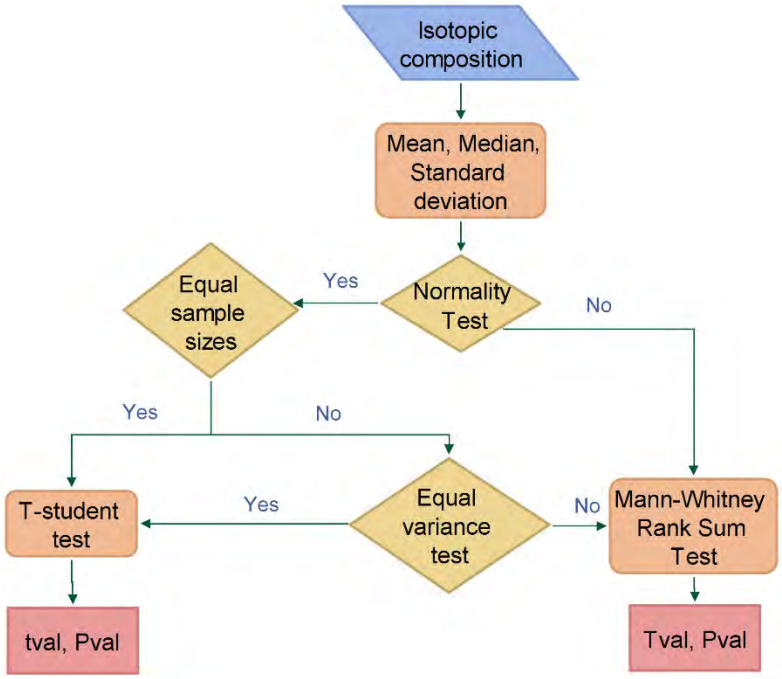

Figure 6.12 Diagram that shows the algorithm for deciding the right test to determine if two sets of data are significantly different from each other based on the normality and variance of the data.

The median (and the mean arithmetic average) were calculated for the isotopic composition values of specimens (shells) from the same stratigraphic layer in order to compare a central value to the isotopic composition of the layer obtained from the analysis of the sieved sediments.

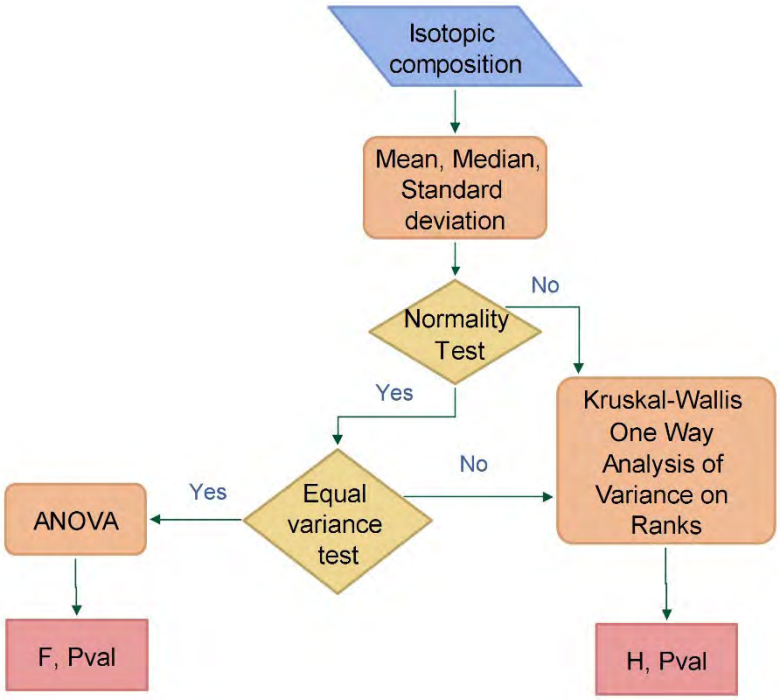

Figure 6.13 Diagram that shows the procedure for choosing the right test to determine the variation between groups of data based on the normality and variance of the groups.

6.13 Calculating the number of shells needed for a representative environmental value

If the isotopic values of a taxon coming from the same lake have satisfied the criteria of normality so that the values have a Student-t distribution, then an optimum sample size can be calculated (Escobar et al., 2010; Holmes, 2008) with the following equation:

$$n = (t\ \frac{s}{E})^2$$ *Equation 5.4*

Where t is the Student's t value for a given level of significance, s is the standard deviation, and E is the acceptable error (Holmes, 2008). The level of significance was fixed at $\alpha = 0.01$ for all the stratigraphic levels of three lakes studied in the Mayab (including Chichancanab). At the same time, the acceptable error was chosen using the variability seen in the complete stratigraphic sequence and set at 10% of the total variability (Escobar et al., 2010). Therefore, I would use these values for specimens from Lake Esmeralda when the normality criteria were met in order to calculate the number of specimens needed to get a reliable value that represents the environmental signal.

6.14 Zonation

A final analysis was performed for establishing the different facies in the environmental story of Lake Esmeralda and Lake San Lorenzo. Zonation has been used for establishing biostratigraphic zones using numerical methods for fifty years in the field of palynology

(Gordon and Birks, 1972). However, the use of numerical methods is not frequently used for establishing stratigraphic zones or facies in Holocene core sediments from lakes in the Maya Cultural Area. The zonation is based on the cluster analyses performed using Matlab®

For Lake San Lorenzo six records were used for the zonation for the last 2800 years B. P., TOC, TIC, residuals from loss on ignition, density, $\delta^{18}O_{Sieved\ sediment}$ and $\delta^{13}C_{Sieved\ sediment}$. (The gaps of isotope data between 1400 to 1100 years B. P. could be overcome by linear interpolation, since there are data at both sides of the gap). At the same time, TOC, TIC, the residual portion of loss on ignition and density records were used for the zonation of the entire time covered by the sedimentary sequence, circa 3400 years B. P. since it is not possible to extrapolate data for the isotope records for the first 600 years of the record (from 3400 to 2800 years B. P.), since only one side of the gap has data. For creating the zonation, records must have data evenly spaced in the time domain. For this purpose, all the records were interpolated, generating time series which had an annual resolution. The time series were used to calculate the Euclidian distance for every point relative to the rest of the points in Matlab® using the algorithms proposed by Trauth (2007). The Euclidian distance is a measurement of the dissimilarity that existed between two samples. We visualised the distances using a hot colourmap calculated from the square form of the Euclidian distances. This hot colourmap represents the Euclidian distances between pairs of samples across the core. The hot colourmap was then used for establishing the zonation, recognising borders between facies when the Euclidian distance between two adjacent samples was ≥ 20. This parameter was selected visually.

The same process for establishing zonation was performed on the sequence from Laguna Esmeralda using Grey-Scale, Colour, Ca, Sr/Ca, TOC, TIC, Residuals of the loss on ignition, density, $\delta^{18}O_{Sieved\ sediment}$ and $\delta^{13}C_{Sieved\ sediment}$ for the 6700 to 1000 years B. P.

6.15 Conclusion

This chapter explains the different methodologies, analyses and algorithms used during this thesis for performing the environmental reconstruction at the sites of Lake Esmeralda in the Mayab and Lake San Lorenzo in the Northern Highlands. Many but not all of these methods were applied to both study sites. In the next three chapters, the results are presented and critically assessed, inferring the meaning of them in the context of environmental change and human interactions as well as connections between them. In addition, the implications of the results will be discussed.

Chapter 7 Environmental History of Lake San Lorenzo.

Photo: The Acropolis of Chinkultic, Lake San Lorenzo is observed behind.

"This is the sign of our word that we will leave behind. Each of us shall first plant an ear of unripe maize in the centre of the house. If they dry up, this is a sign of our death. -They have died,- you will say when they dry up. If then they sprout again, -They are alive,- you will say, our grandmother and our mother. This is the sign of our word that is left with you"

Popol Vuh, 1550.

This chapter presents and discusses the results of the analysis performed on the sediments obtained from Lake San Lorenzo in the Lagunas de Montebello Lake Complex in the highlands of Chiapas. The results are discussed in conjunction with the data generated by Franco-Gaviria et al., (2018). In chapter 5, a description of the site of Lake San Lorenzo was presented as well as the significant outcomes of the research of Franco-Gaviria et al., (2018) using charcoal, pollen, elemental abundances and ratios analyses and Franco-Gaviria et al. (2020) using Cladocera, C/N, Total Nitrogen and Total Phosphorus.

7.1 Age Model

The age model of Lake San Lorenzo is based on four radiocarbon dates, including a post-nuclear bomb date. The age model was constructed using BACON (see section 6.5 in chapter 6) and using the Intcal13 curve for calibration in the case of pre-nuclear era dates. Since the default parameters are described neither in Franco-Gaviria et al., (2018, 2020) nor Franco-Gaviria (2018), a series of calculations were run to reproduce the results of Franco-Gaviria et al. (2018) (see section 6.5 in chapter 6). In this way, $\alpha = 0.6$ (Figure 7.1) and 0.8 were identified as producing the age model published.

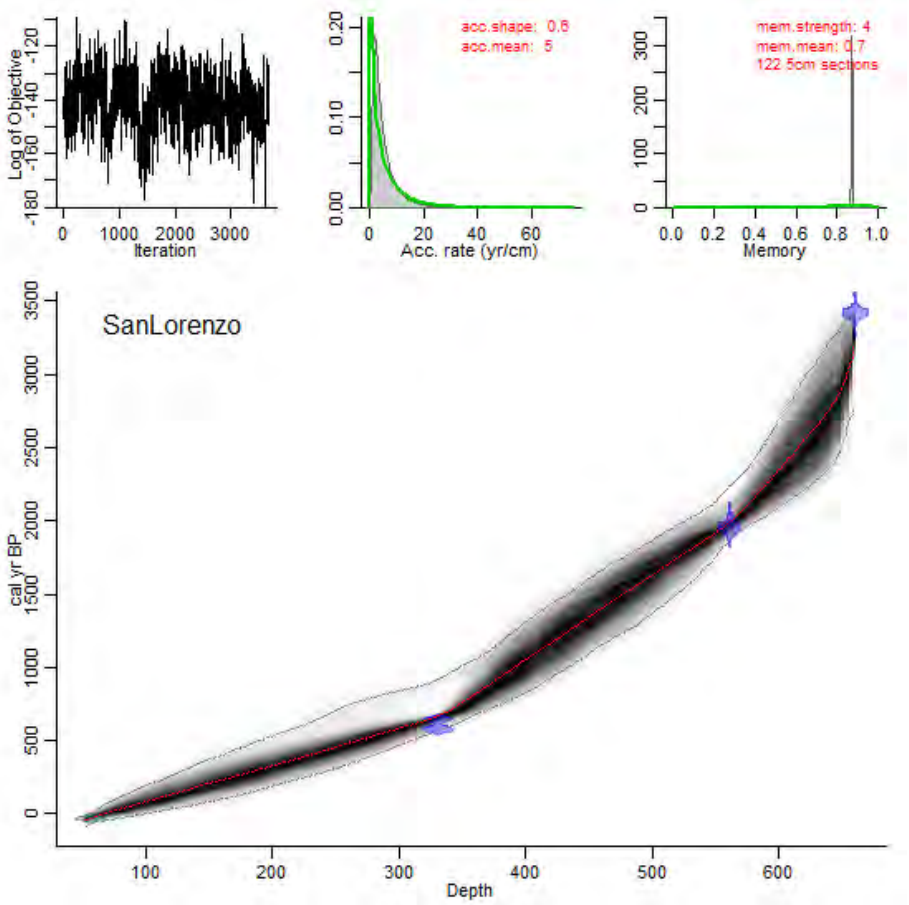

Figure 7.1 Reproduction of the age model of Franco-Gaviria et al. (2018) using an a = 0.6 for the sediments of Lake San Lorenzo.

7.2 Description of the core

Samples used in this thesis were the result of splitting the cores every cm and resampling in small bags which contained at least 1 cm^3 (see section 6.1 in chapter 6). No image of the cores or description of the cores were available beyond those in the previously published papers. The samples in bags were black- brownish silty clays, which did not contain shells of any kind.

Figure 7.1 shows the results of XRD analyses on specific points through the record. Yellow dots in Figure 7.3 indicate the layers that were analysed by XRD. According to the XRD analyses, there are no significant changes in the Bragg pattern between the samples. However, there are changes in the intensity of the peaks between samples, implying variations in the proportion of mineral phases between samples or different preferential orientation in a phase in different samples.

The major phases are an aluminosilicate of tectosilicate structure (precise identification was not possible) and magnesium-calcium carbonates (including calcite). It is not possible to identify which of these phases is predominant based on a low resolution diffractogram of no very crystalline samples. The peak corresponding to the tectosilicate at 42° 2θ is more intense in most of the samples, except in b and e, where the peak at 43° 2θ, which is part of the calcite pattern, is more intense. The pattern with the most intense peaks normally indicates the predominant phase.

However, in this case, the strong intensity of only one peak of the tectosilicate could be an effect of the preferential orientation of the mineral. In a much lower proportion, ferrosilicates, oxides and other aluminosilicates of phyllosilicate structure (clays) can barely be distinguished from noise. The peaks of the tectosilicate do not match with the diffraction signals of montmorillonite argued by Franco-Gaviria (2018, 2020), but it could be the microcline argued by them (although they find this mineral only in what they called the U2, see section 7.7). Other peaks might match with sillimanite, muscovite, melilite, jadeite or pigeonite, which are minerals present in metamorphic or igneous environments (Durán-Calderón et al., 2014).

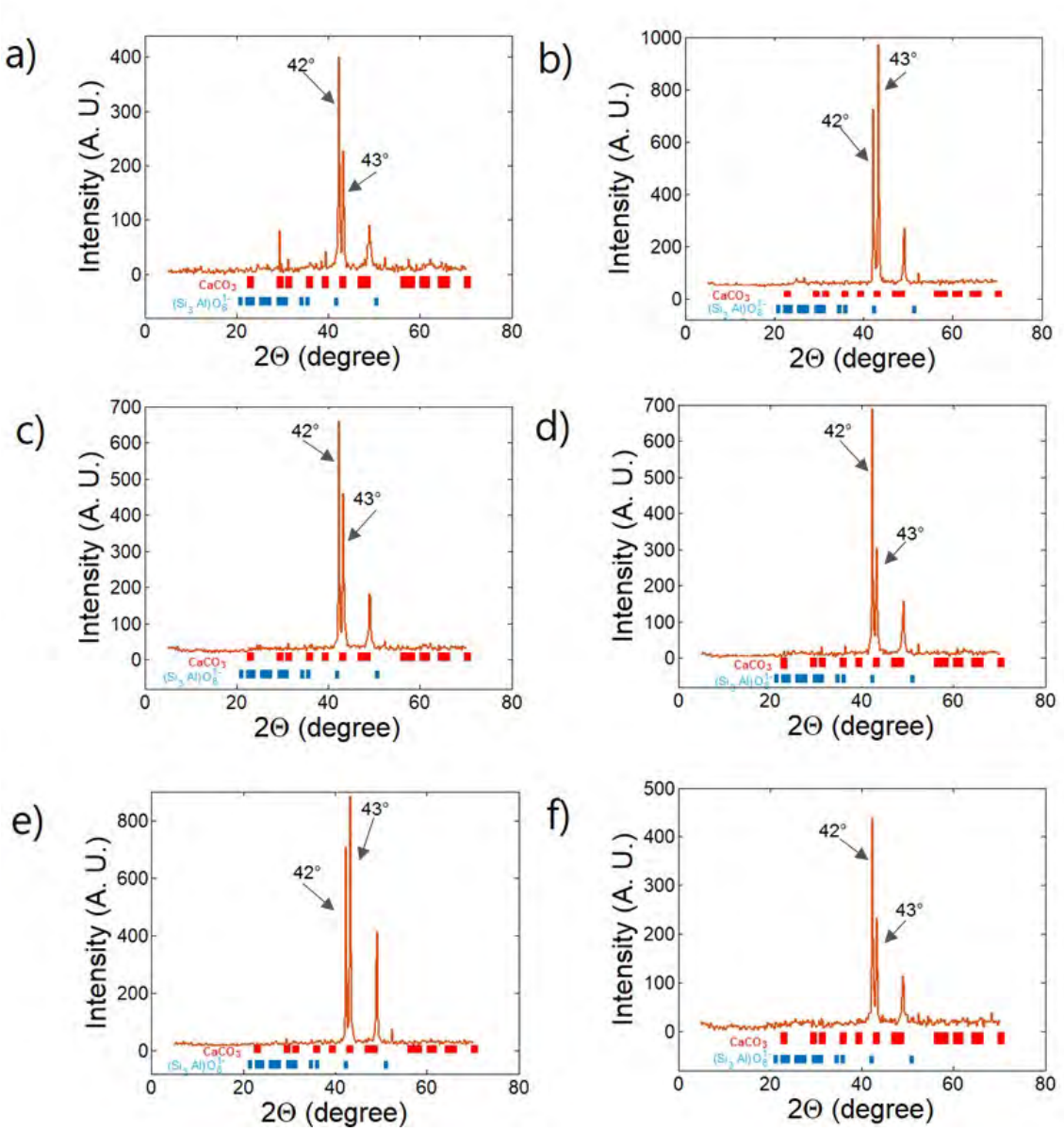

Figure 7.2 X-Ray Diffractogram of samples taken through the sedimentary sequence of Lake San Lorenzo. The diffractogram presented corresponds to a) D1-6; b) D3-9; c)D4-59; d)D6-8; e) D7-3; and f) D7-64 (yellow dots in Figure 7.3).Practically all samples presented two major mineral phases, corresponding to calcite and an aluminosilicate.

Figure 7.2 presents the grain mounts in planar polarised light of samples taken from the highest and the lowest value zones of total inorganic carbon according to the results of the loss on ignition (see below in section 7.4) in order to search silicates, including clays. The same region observed in cross polarised light shows the presence of calcite as the largest grains (Figure 7.2 b). High birefringence minerals were not found. The twinning pattern of microcline was not observed either. Volcanic glass, which could be a candidate for material in the region of Chiapas (Ford and Rose, 1995; Villaseñor and Graham, 2010), was not found. Another candidate, such as biogenic silica, was not observed.

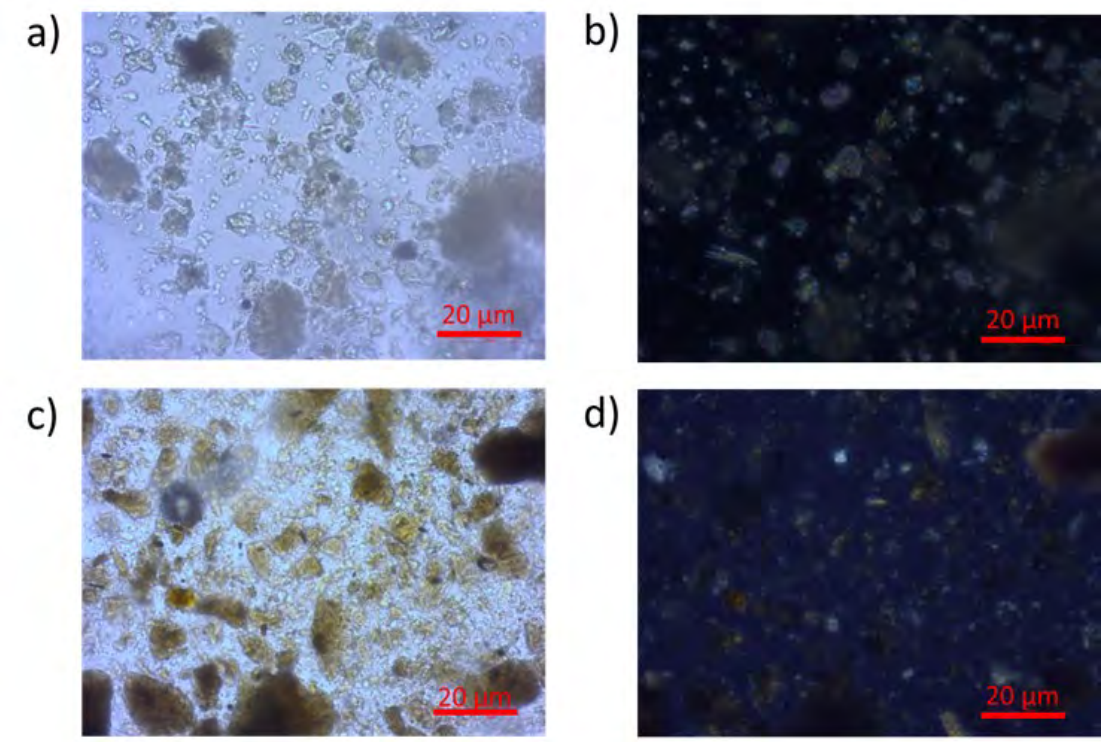

Figure 7.3 Grain Mounts of samples taken from the layer D4-64 at 366 cm (851 years B. P.) in the core from Lake San Lorenzo, which presents high values of carbonate content (53%), observed in the petrographic microscope under a) Planar polarised light, and b) cross polarised light. Grain Mounts of samples taken from the layer D5-26 at 435cm (1253 years B. P.), which presents low values of calcite content (7%), observed under c) Planar polarised light, and d) cross polarised light.

However, the residual of the Loss on Ignition (see section 7.4 below) have a texture and colour similar to terracotta, supporting the statement of Franco-Gaviria (2018) that the residual component is mainly clays. However, interestingly these kinds of minerals, as I said in the previous paragraph, were also barely distinguished from noise in the samples analysed by XRD. Therefore, they might be present as nanocrystals.

7.3 Records produced from Lake San Lorenzo and zonation

Figure 7.3 shows the six proxies developed for this thesis using the sediments of Lake San Lorenzo as well as the zonation (see section 6.14 in chapter 6). In Figure 7.3, the results of the total organic and inorganic carbon are labelled as organics and calcite, respectively. The reason for labelling all inorganic carbon as calcite ($CaCO_3$) is based on the results of XRD analysis (see the previous section) and the comparison with the calcium abundance (see next section). The zonation based on only the records produced from density analysis and the loss on ignition is slightly different from the zonation considering the six proxies. However, we can still observe that facies 1 is a unit with no major differences except for a

small zone around 3000 years B. P. (Figure 7.3). Before explaining the environmental changes recorded, the meaning of every proxy is discussed in the next sections.

7.4 Nature of the TOC, TIC and Residual records.

The organic content changes from 5 % to around 15 % through the record (Figure 7.3). The source of the organic material comes from the phytoplankton (algae), except for the beginning of Facies 6, according to the values lower than 10 in the C/N record developed by Franco-Gaviria et al., (2020). Values between 10 to 20 are interpreted as a mixture of algae and terrestrial material.

Calcite (Total Inorganic Carbon) varies from 4 % to 32 %. Zones, where the amount of calcite is lower than 5% need to be highlighted since they represent a challenge for isotopic analyses as there is not enough calcite in a cubic centimetre to extract CO_2 for analysis (unfortunately, there was no more material available). Zones between 1113 years B. P. (410 cm) to 1403 years B. P. (460 cm) and deeper than 2994 years B. P. (640 cm) present this problem. Finally, the residuals display a variation from 68 % to 94 % across the record. (Figure 7.4). Therefore, the residuals are the principal components of the materials in the dry sediment sequence.

Figure 7.4 also shows the Total Inorganic Carbon record compared with the Ca record obtained by Franco-Gaviria et al., (2018) using XRF. We can observe the resemblance between both records. Therefore, we assume that most of the Ca is in the carbonate.

Figure 7.4 also presents the record generated by the fluctuation in the remaining material amount after the loss on ignition. We suspect that this material is composed mainly of terrigenous sediment. A visual comparison of the Ti record generated by Franco-Gaviria et al., (2018) using XRF and the residuals records shows their resemblance, supporting the terrigenous nature of the remains after loss on ignition. Small differences between these two records might be the result of the differences in the resolution and the nature of the analysis. In the next paragraphs, we assume that the record composed of the residuals of loss on ignition is mainly a proxy of terrigenous input.

Despite the difference in the amplitude of the environmental signal, the calcite and residuals records covary inversely. This could involve two possible scenarios of dependent phenomena. In the first one, a large influx of terrigenous sediment is promoted by more energetic water flow into the lake, which implies high-level water, where calcium or HCO_3 concentration is relatively low, decreasing its possibility of precipitating. In the second one,

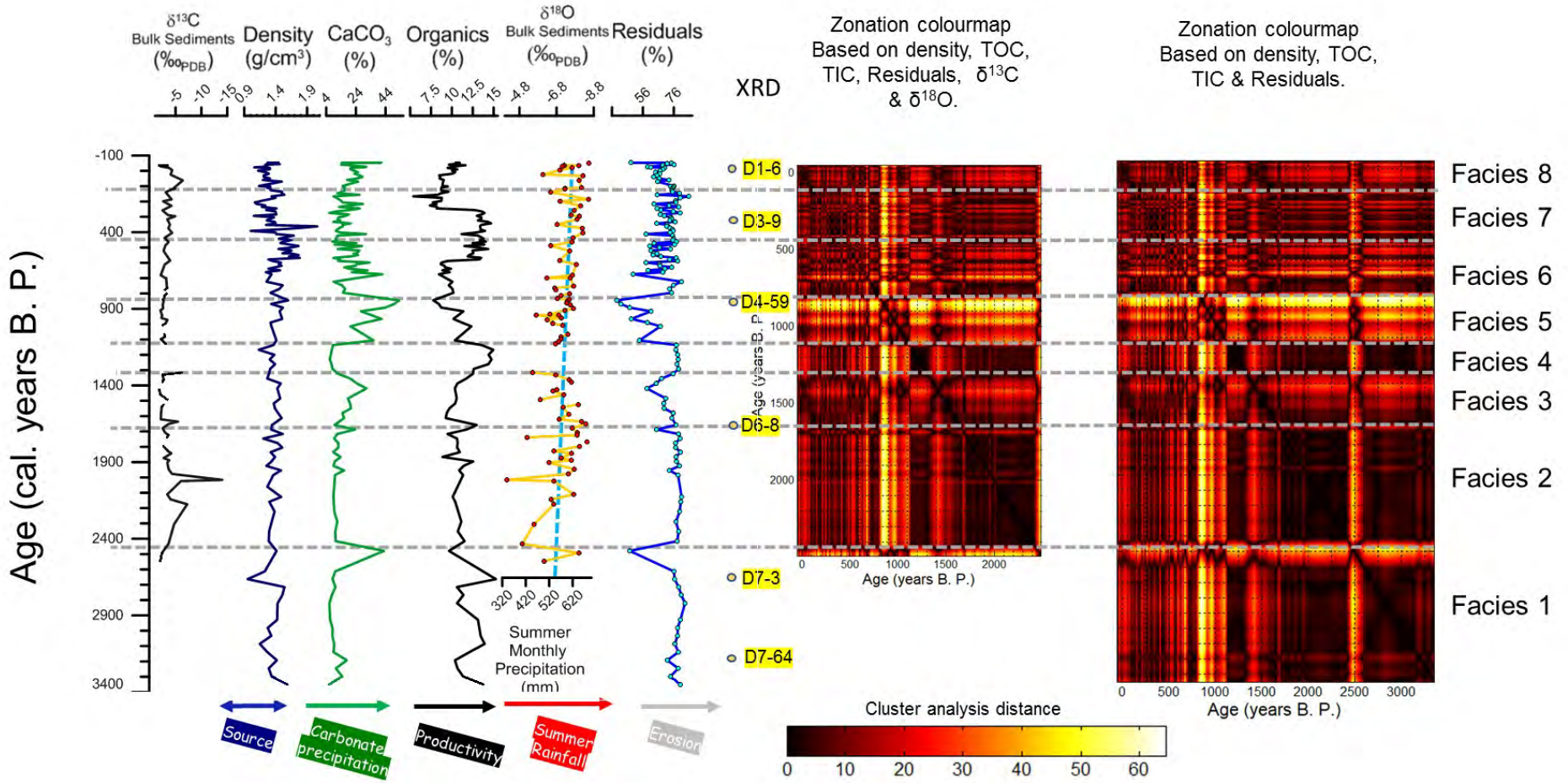

Figure 7.4 Records developed from studying the sediments from Lake San Lorenzo and their zonation considering the density, the proxies developed by Loss on Ignition and the records developed by stable isotope analysis for the last 2500 years B. P., and the density and the proxies develop by Loss on Ignition for the last 3400 years B. P. The yellow dots mark the layers where XRD analysis was performed (see figure 7.1). The dashed blue line through the $\delta^{18}O$ raw values indicates the average of the detrended data.

the intake of terrigenous material increases the acidity of water, changing the chemical equilibrium of the carbonate system, promoting dissolution of carbonates over precipitation. A most parsimonious option might have been that the increased inwash have just diluted the precipitated carbonate in the sediment. But this would have implied a visible change in the sedimentation rate, which is not observed since the stratigraphic layers of this facies are not wider than the layers of the immediately previous facies 3. The time frame between 1414 to 1140 years B. P. (440.5 to 419 cm) is the most prolonged period with a low TIC content and a high amount of terrigenous material simultaneously (Facies 4 in Figure 7.4).

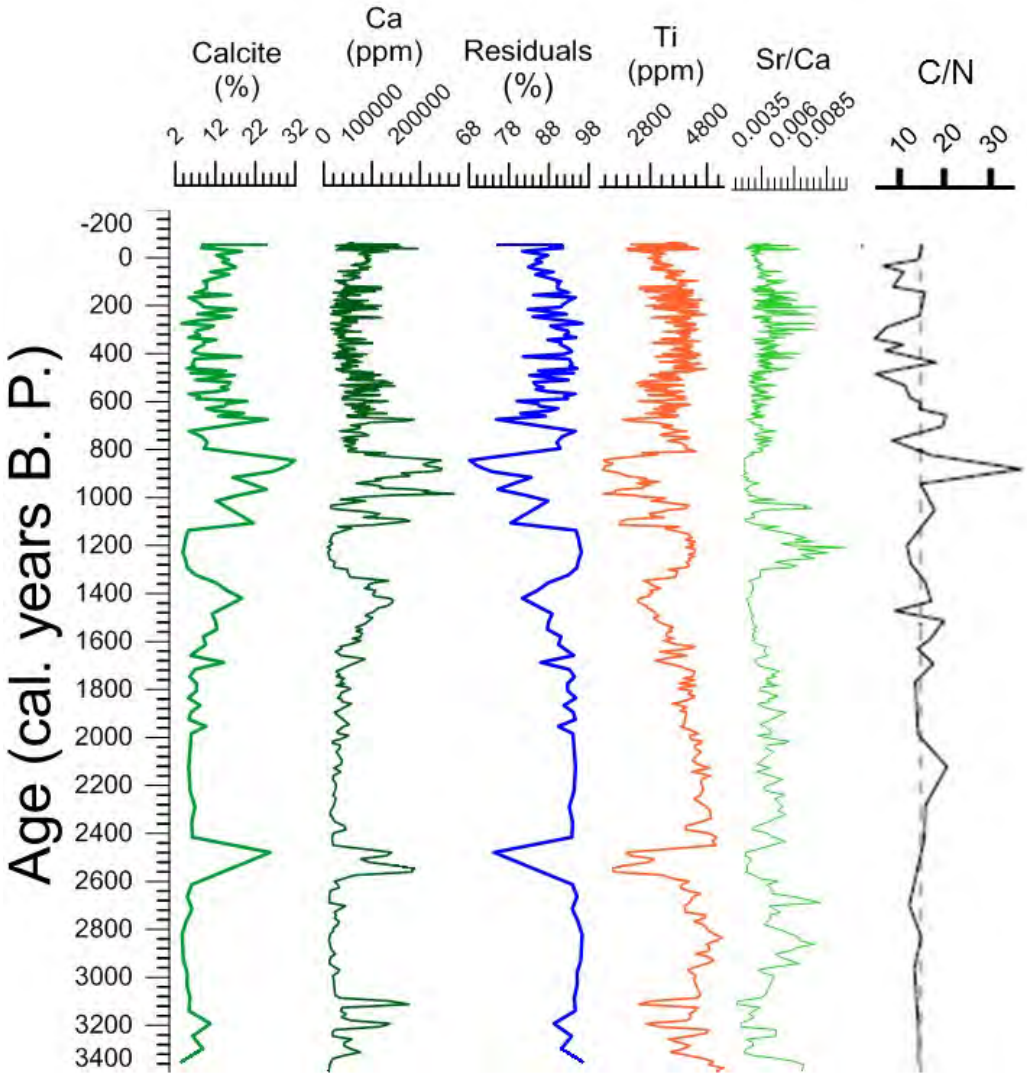

Figure 7.5 Variation in the calcite (Total Inorganic Carbon) and Loss on Ignition percentage residuals compared with the Ca and Ti records, respectively, obtained using XRF by Franco-Gaviria et al., (2018) through the Lake San Lorenzo core. Sr/Ca and C/N analysed by Franco-Gaviria et al., (2020) are also shown. Dashed line in C/N represents the border between phytoplankton and terrestrial organic input.

Figure 7.6 presents the relationship between calcite and titanium for every facies, which shows an inverse linear trend. This kind of trend between both kinds of elements suggests that the origin of calcite in the lake is authigenic, and it is not derived from exogenic sources. Figure 7.5 shows that the inverse trend exists in every facies, indicating that inputs of allogenic Ca are unlikely. In this way, the variation in authigenic calcite in Lake San Lorenzo might be related to diverse processes. It might be produced by fluctuations in water level or by changes in the acidity of water.

Another possibility for changing amounts of carbonate could be variations in CO_2 concentration, either from changes in the intake from the atmosphere or differences in the CO_2 production during algal respiration. Since no ostracods or gastropods were detected in the core, the possibility that carbonate variability is linked to the biogenesis of the shells in these taxa is very low.

Franco-Gaviria et al., (2018), however, interpret the carbonate as biogenic due to changes in CO_2 associated with low lake levels since the Sr/Ca ratio across the record does not show a systematic trend. This would have meant that CO_2 changes in water due to algal productivity could have led to $CaCO_3$ precipitation.

Although Sr is fixed by carbonated organisms, along with Ca (Zaragosi et al., 2006), this is not the only scenario where both carbonates can precipitate inside a lake. Sr tends to co-precipitate with Ca since both cations have similar ionic potential (Bernal and Railsback, 2008; Railsback, 2003).

The inverse linear trend also implies that the oxygen isotopic signature of carbonates can be interpreted as a lake water signal and does not contain the isotopic composition of old carbonates from the surrounding karst (Kelts and Talbot, 1990).

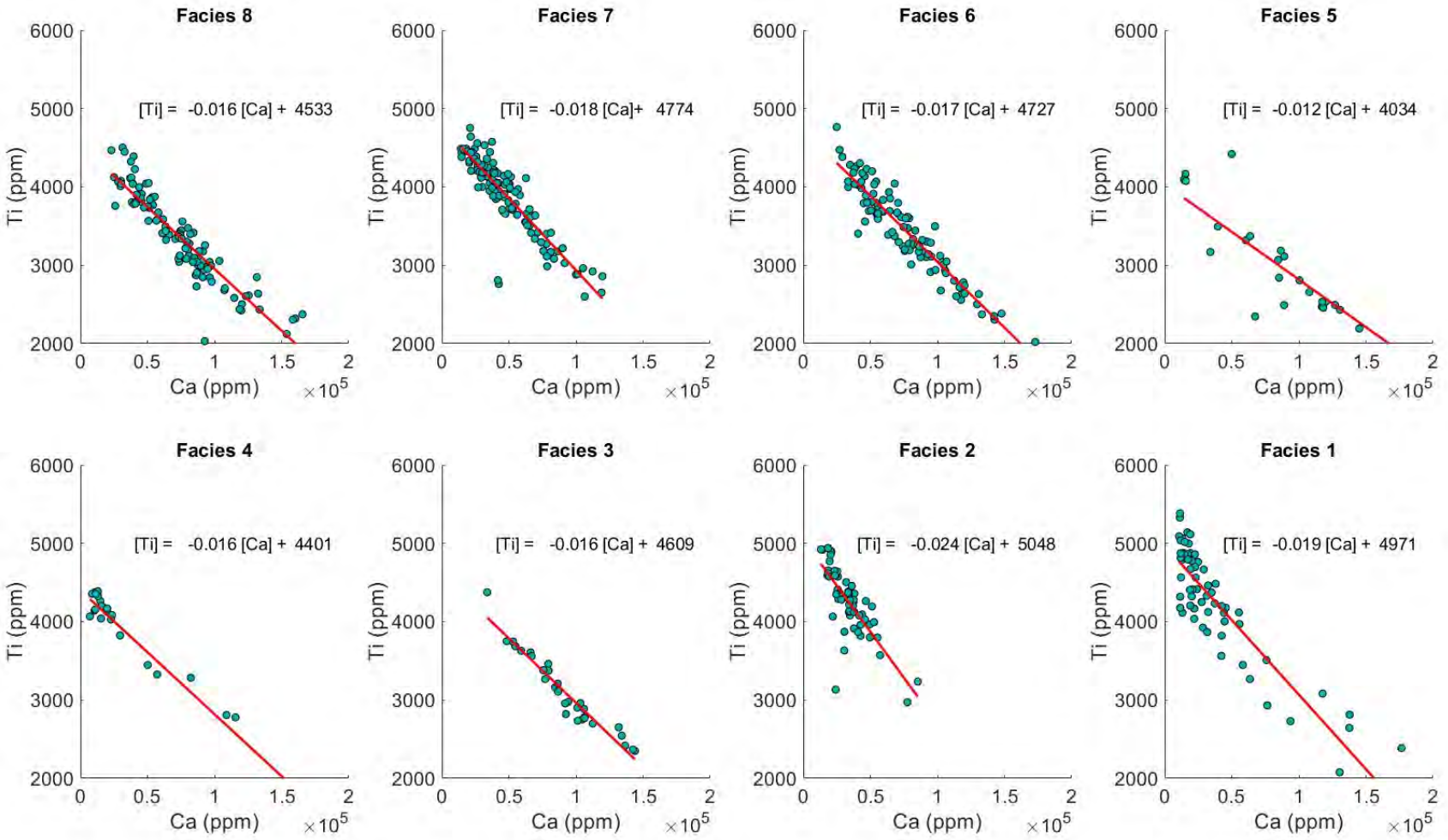

Figure 7.6 Amount of calcium as a function of the amount of titanium present in the core according to the XRF analysis performed by Franco-Gaviria (2018) for every facies of the sedimentary sequence of Lake San Lorenzo. Equations indicate the linear regression model for every facies.

7.5 $\delta^{18}O$ as a proxy of rainfall

Figure 7.6 displays the cross plot of $\delta^{18}O$ and $\delta^{13}C$ of the sieved carbonate sediments from Lake San Lorenzo. The lack of covariation between $\delta^{13}C$ and $\delta^{18}O$ during all the measured record indicates that Lake San Lorenzo was and is an isotopically open system (Li and Ku, 1997; Talbot, 1990). Its water today reflects the meteoric water line signature at that latitude (see Figure 5.8 in section 5.7 in chapter 5), and its waters may have reflected the meteoric line water signature throughout the record.

This open system nature might also suggest that the residence time of water inside the lake is quite short. Since the isotopic signal of rainfall can have significant changes between seasons (Leng and Marshall, 2004), and most of the water entering Lake San Lorenzo comes during the summer rain season (April –September), the isotopic signature in carbonates should reflect the isotopic signature of waters mainly during the summer rainfall season.

For this reason, I argue that the $\delta^{18}O$ is a proxy of the amount of summer rainfall since the $\delta^{18}O$ of waters in this scenario of an open lake depends only on the continental, temperature or amount effect. Since the location of Lagunas de Montebello Lake Complex is too near to both the Pacific and Atlantic Oceans (see section 5.5 in chapter 5) for an important continental effect, and there are no important variations of temperature during the summer (Alcocer et al., 2018), the isotopic ratio is likely given mainly by the amount effect. Water isotope values $\delta^{18}O$ of Lake San Lorenzo fluctuate from -10 to -9 in Lake San Lorenzo (see section 5.7 in chapter 5), which are similar to the isotope values of rainfall in nearby areas in Guatemala, where the dominant control on $\delta^{18}O$ values in time has been shown to be the amount effect (Lachniet and Patterson, 2009).

The gradients of the amount effect (expressed as ‰ per 100 mm of rainfall) is 1.24 ‰ for this area (Lachniet and Patterson, 2009). Assuming that this gradient has not changed, it is possible to estimate the changes in the amount of precipitation across the $\delta^{18}O$ record. In this way, it can be observed that there was a decrease of around 200 mm during dry periods in facies 5 in comparison to the contemporaneous amount of rainfall (*Figure 7.3*).

Values of $\delta^{18}O$ of sieved carbonate in core sediments fluctuate mainly from -8.5‰ to -6‰, which differs from the theoretical values of $\delta^{18}O$ of carbonates (ca. -11.7‰) calculated using a T = 22.5 °C, observed in Lake San Lorenzo (Vera-Franco et al., 2016), and equation

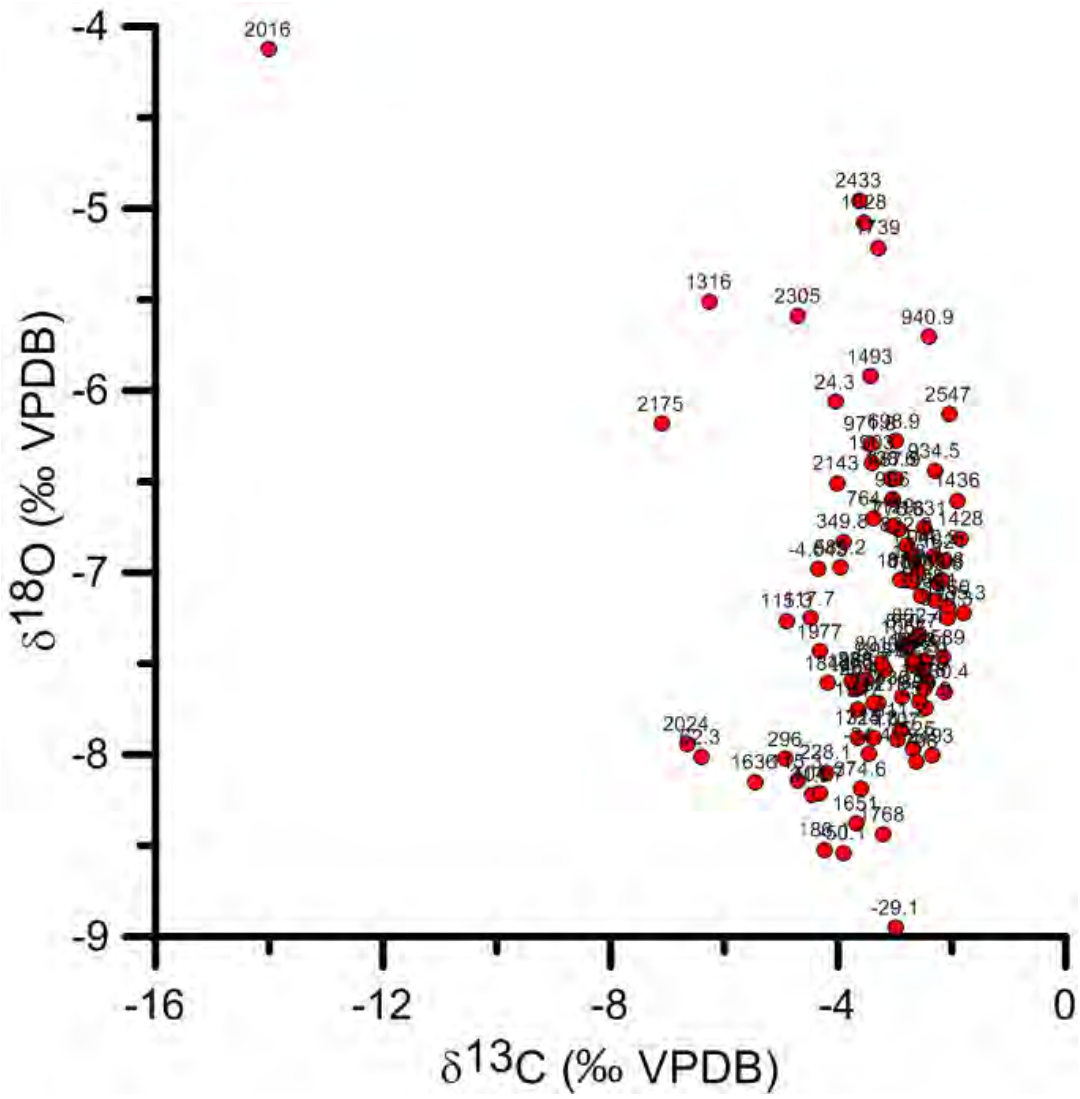

Figure 7.7 Cross plot of $\delta^{18}O$ and $\delta^{13}C$ of the bulk carbonate sediments from Lake San Lorenzo. Numbers indicate the assigned age of every analysed sample.

6.3 (see section 6.11 in chapter 6) from values of lake water isotopes (see section 5.7 in chapter 5).

This might indicate that carbonates do not precipitate in isotope equilibrium, but the calculations are based on minimal monitoring data from different years, and the timing of carbonate precipitation in the lake is unknown.

The oxygen isotope record could be reconstructed for most of the period from 2600 years B. P. to present (Figure 7.3). The lack of enough carbonate was an issue in samples run in layers with an age of 1753, 1541, and 1411 years B. P. The same problem happened in samples found between 1284 to 1159 years B. P. Therefore, we do not have isotope data during this particular period, which is the period of facies 4 (between 1414 to 1140 years B. P.).

$\delta^{13}C$ is difficult to interpret since its variation depends on many variables, including the levels of eutrophication of the lake (Leng and Marshall, 2004). However, despite the value of the outlier, the $\delta^{13}C$ record shows variations (fluctuating most of the time from -4‰ to -2‰), indicating that the source of the dissolved inorganic carbon was practically the same, although it presents slightly more variety during the Classic period (1700 to 850 years B. P) in comparison with the Postclassic (850 to 450 years B. P.), Colonial (429 to 140 years B. P. or 1521 to 1810 A. D.) and Modern periods (1810 A. D. to present). Colonial times also show distinct trends, which will be discussed below.

7.6 Facies

In the next paragraphs, I describe the facies considering the meaning of every proxy or the possible mechanism of positive (or negative) feedback between them (Figure 7.1).

Facies 1 from 3400 to 2400 years B. P., is characterised by a low calcite content (≤ 4 %), while the terrigenous amount (residual of Loss of Ignition) was over 70% during most of this facies. This high percentage implies high erosion at a time of low calcite precipitation. During this period, there is relatively high productivity according to organics, which percentage is over 11 % (when it is under 11 % in most of the facies). The density record has values around 1.4 g/cm^3 when the amount of organic material is high in this facies.

Facies 2 from 2400 to 1620 years B. P. continues to show a high content of terrigenous material and a low percentage of calcite (as in facies 1). Organic content falls under 11 %, meaning a fall in productivity. The $\delta^{13}C$ is quite variable during this facies, ranging between -5‰ to -15‰ (mainly due to an outlier, see later). This might imply that the source of dissolved inorganic carbon changed continuously during this facies. Both $\delta^{13}C$ and $\delta^{18}O$ have an outlier at 2016 years B. P. (remember this is a centre value of an interval of 500 years). This facies was deposited during conditions of relatively high summer rainfall according to the $\delta^{18}O$, although conditions look dry from 2400 to 2150 years B. P. (however, this dry period probably was shorter, but we have a lack of data here, so the resolution was lower). The density record still covaries with the fluctuation in organics.

Facies 3 from 1620 to 1340 years B. P. corresponds to a moment when the calcite increase, reaching a maximum of 31 % around 1420 years B. P., while the erosion into the lake seems to reduce. The productivity of the lake increases after 1620 years B. P., when the organics have their lowest value during the period covered by facies 1 to facies 4. The density record does not fluctuate in the same way as the organics since it also seems to be

affected by changes in the terrigenous and calcite content. The source of organics is algae during the whole facies according to the values, which are lower than 20 in the C/N record developed by Franco-Gaviria et al., 2020. Facies 3 seems to reflect drier conditions compared with facies 2.

Facies 4 was deposited from 1340 to 1130 years B. P. During this facies, the terrigenous amount is 82 %, implying high levels of sediment input, while the total inorganic carbon is maintained at around 6 %. Productivity is the highest in the entire record according to the percentage of organics which is relatively high (around 15%). Despite the relatively high organic content, the density does not reduce dramatically as happens in other facies of the core (e. g. around 2400 years B. P.) probably due to the effect of a high amount of terrigenous input. This facies is also the first when organics and terrigenous inputs have similar tendencies. During this facies, there are no isotope data due to the insufficient amount of calcite (see section 7.4). When I consider only the variables related to the Loss on Ignition, the zonation points out that facies 4 has similar characteristics to facies 1. Unfortunately, we do not know how the rainfall was during facies 4. Since the tendencies in the other proxies do not always covary with $\delta^{18}O$, it is not possible to infer the rainfall conditions in this facies.

Facies 5 (1130 to 800 years B. P.) is characterised by a tendency to minimum values in terrigenous and high values of calcite precipitation, increasing from 35% to 53%, with a minimum value of 20% at 1014 years B. P. During this facies deposition, the conditions seem to be relatively dry, comparable to those that existed during the deposition of facies 3, based on $\delta^{18}O$ (mean value of -7.02 ‰). This facies is the longest and driest period in the record. Similar isotopic values have not been reached since the beginning of facies 2. During this time, the organics tendency is also to minimal values, going from 11.5 to 7.5 %. As a consequence, a slight increase in density is observed. The source of organics is still algae, according to the C/N record developed by Franco-Gaviria et al., (2020).

Facies 6 (800-450 years B. P.) is characterised by relatively high calcite precipitation and low erosion according to the percentage of inorganic calcite and terrigenous material, respectively. The lowest part of this facies (700 to 800 years B. P.) is really different from the top. During this time high summer rainfall amount conditions prevail according to the $\delta^{18}O$ (mean value of -7.15‰, reaching values of -7.7‰ most of the time). The productivity changes from small values (9%) from 800 to 600 years B. P. to relatively high values (14%) in 600 to 500 years B. P. A change in the source of organics is observed according to the

C/N record developed by Franco-Gaviria et al., (2020) at the beginning of this facies. They describe a terrestrial source of organics

Facies 7 (450 to 140 years B. P.) shows relatively low calcite precipitation (≤24 %) while there is a terrigenous percentage over 56 % to 80%. During most of the deposition of this facies, the proportion of organics was relatively high (> 15 %), while there is a trend to reduced density. The $\delta^{18}O$ indicates a period of relatively high summer rainfall amount with values around -8‰ while the $\delta^{13}C$ indicates slight fluctuations from -3.60‰ at 374 years B. P. to 4.47‰ at 110 years B. P.

Facies 8 (140 to -60 years B. P) is characterised by a decrease in erosion and calcite precipitation until ~ 24 years B. P. After this time, the tendencies swap. The productivity increases, but has its highest values in this facies after 20 years B. P. Density values generally stay low, but also increase after 24 years B. P. According to the $\delta^{18}O$ summer rainfall is relatively high (variations from -6.47‰ to -8.54‰). Nevertheless, it has a point of apparently lower rainfall conditions (-6.06‰) at 24 years B. P. The sources of organics are also slightly more diverse than in the previous four facies.

7.7 Comparison with the stages proposed from the pollen and charcoal record.

Figure 7.7 presents a comparison of the different environmental proxies studied in the record from Lake San Lorenzo with the environmental history described by Franco-Gaviria et al., (2018). In addition, we also relate this story with the archaeological and historical record of the Comitan-Chinkultic region since the anthropogenic impact on San Lorenzo was potentially relevant across the record. I will start by comparing with the pollen stages defined by Franco-Gaviria et al., (2018) and the environmental stages defined by Franco-Gaviria et al. (2020) since their stages constrain longer periods of time. For pollen stage 1 (3400 to 2500 years B. P.), Franco-Gaviria et al., (2018) described that Lake San Lorenzo was part of a river, starting to be a depositional environment at 3400 years B. P. based on the abundance and ecology of the algae *Concentrycistis sp.* while *Cyperaceae* pollen suggested a shallow and young lake. This is broadly consistent with the low calcite content

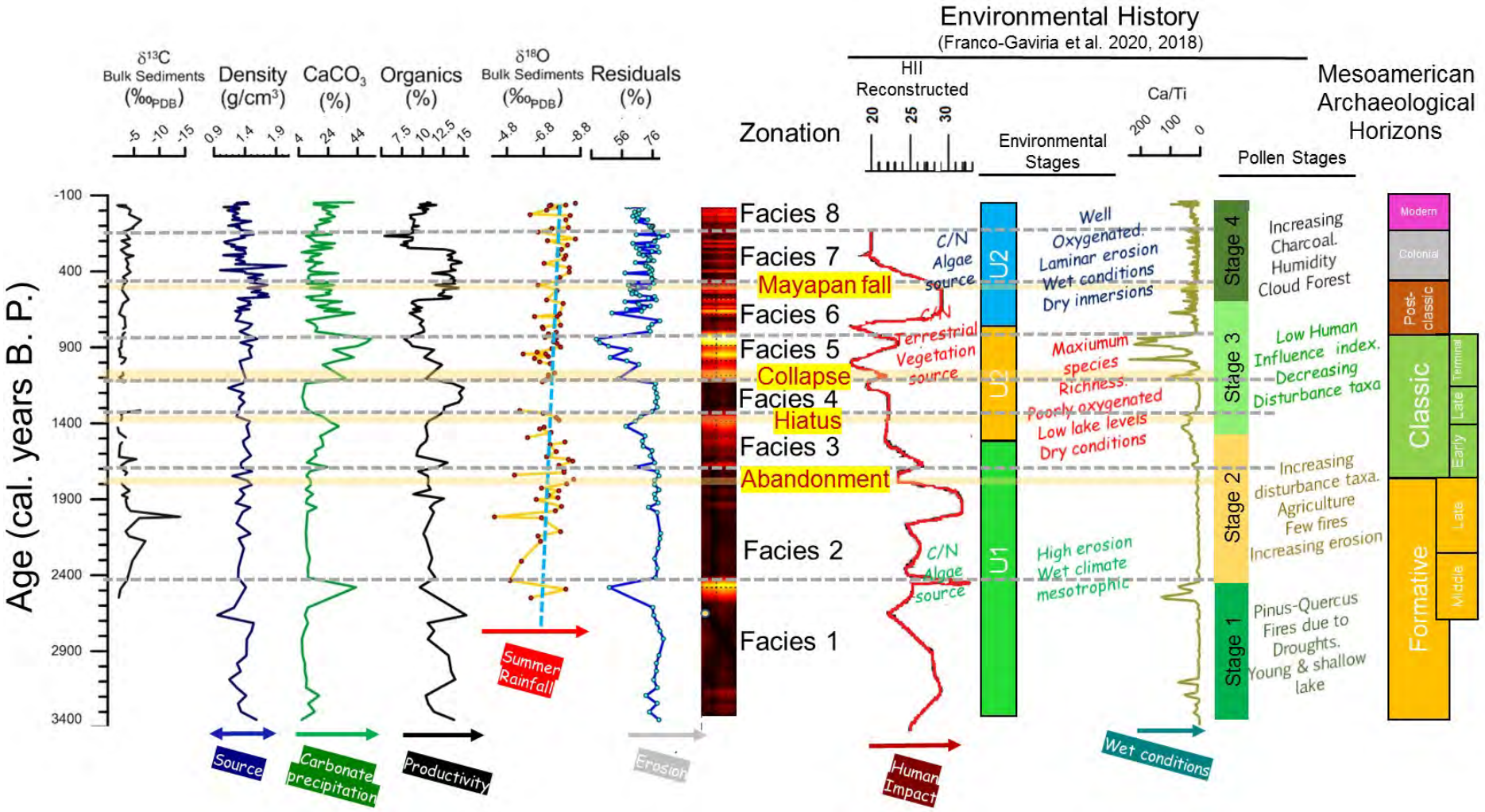

Figure 7.8 Comparison of the records developed from the density analysis, loss on ignition and isotopic analyses of sediments from Lake San Lorenzo and the environmental history, including the Human Impact Index described by Franco-Gaviria et al. (2020, 2018), which shows the different pollen stages based on pollen and charcoal analyses and the environmental stages U1 to U3 based on grain size, elemental ratios and Cladocera. The U2 describes a poorly oxygenated lake based on Mn/Ti; meanwhile, the laminar erosion in U3 is based on Montmorillonite-rich sediment. Critical periods in the cultural history of the Maya are highlighted in yellow

during facies 1 and 2. During stage 1, the pollen record indicates the existence of *Quercus-Pinus* forest until 2400 years B. P. Stage 1 also indicates moderate human impact according to the calculated Human Impact Index, HII by Franco-Gaviria et al., (2018). The high erosion revealed in the percentage of terrigenous content might be explained by this moderate human impact. Unfortunately, the record is not long enough to have a better panorama of how the system functioned without human occupation and how the climatic and ecological conditions were before this.

Franco-Gaviria et al., (2018) described recurrent droughts, based on the titanium record, as drivers of the fluctuations in the charcoal record in stage 1. High concentrations in the charcoal record dominated by small particles would suggest recurring regional fires. For Franco-Gaviria et al., (2018), pollen stage 1 and environmental stage U1 was a dry period based on the charcoal record, emphasising two intense dry periods around 3300 and 2500 based on the Ca/Ti record (Figure 7.7), which was interpreted as a proxy of dry conditions (Franco-Gaviria et al., 2020), as was general for the low latitudes of the northern hemisphere (Haug et al., 2001). This prevalence of drought might imply that erosion was paradoxically higher during a dry period, while the precipitation of calcite was around 5%, being one of the lowest values registered for calcite content in the record. Therefore, this description of a filling shallow lake indicates that the precipitation of calcite is not always primarily driven by changes in the water level. It could be argued that a recently formed and open lake would not have calcite deposition even if the conditions were relatively dry. However, these conditions were maintained for 2000 years during all the U1 stage (Figure 7.7) (Franco-Gaviria et al., 2020), at the end of pollen stage 1, the depth of the lake changed (Franco-Gaviria, 2018). Unfortunately, we have no $\delta^{18}O$ data for this stage to test the dry scenario inferred by Franco-Gaviria et al. (2018) due to the low calcite concentrations.

During stage 2 (2400 to1500 years B. P.), Franco-Gaviria et al. (2018) described an increase in disturbance taxa, e.g. *Ambrosia*, Asteraceae, and Amaranthaceae, implying an enhancement of agriculture (Figure 7.7). They also registered a depletion in the representation of *Pinus* in the pollen record explained by the use of these species by the Maya as a construction material and as a fuel for producing stucco. The charcoal record indicated fewer fires, possibly explained by human management of the forest. During this stage, Franco-Gaviria et al., (2018) calculated a high human impact. They described that the terrigenous input was higher based on the Ti record, explaining this increase in terrigenous influx as relating to a change to more humid conditions. In the $\delta^{18}O$ record, it

is confirmed that this stage receives more summer rainfall, $\delta^{18}O$ mean values of -7.16‰ than the average (dashed blue line). The percentage of terrigenous material is, however, similar from 2400 to 1950 years B. P. to the percentage in pollen stage 1, calcite percentage (TIC) is also similar over this period to pollen stage 1. $\delta^{18}O$ values reached -5.21‰ at the Maya Abandonment. The percentage of terrigenous material starts to reduce from 1950 to 1414 B. P., during facies 3 that is during the Early Classic period. During this period, summer rainfall slightly decreases according to a tendency to more positive values in the $\delta^{18}O$ record, $\delta^{18}O$ mean values of -6.94‰, but reaching values of -6.60‰ at the end of facies 3. These tendencies in facies 3 support the description of Franco-Gaviria et al., (2018). The end of this stage corresponds to the time of the Maya Hiatus (1414 years B. P, see section 2.5., chapter 2), making a transition to drier conditions according to the $\delta^{18}O$ record ($\delta^{18}O$ = -6.70‰). This transition supports the thesis that the Maya Hiatus was driven to some degree by environmental changes. Until 1500 years B. P. the Cladocera assemblage was dominated by littoral-benthic species (Franco-Gaviria et al., 2020).

Pollen Stage 3 (1500 to 600 years B. P.) is described by Franco-Gaviria et al. (2018) as having a low human influence index, including a decrease in disturbance taxa (Figure 7.7). This tendency started at the Maya Hiatus (1414 years B. P.) and continues until the Maya Classic Collapse (1190 to 1140 years B. P.), establishing the modern forest composed of meridional cloud forest after 1200 years B. P. Franco-Gaviria et al. (2018) based on the palynological record and the elemental records suggested that the region was little affected by anthropogenic activities. This idea was supported by the partial abandonment of the Las Margaritas archaeological site, 25 km to the Northwest of Lake San Lorenzo (Álvarez, 1993). However, the nearest centre to Lake San Lorenzo, the Mayan village of Chinkultic, continued to exist until the arrival of Europeans to the region (Borgstede and Mathieu, 2007; Navarrete, 2001). The number of settlements in the Comitan – Chinkultic Region (see Figure 2.9, chapter 2) changes from 11 to 8 during this period, but the density of the population increased (Álvarez, 1993). This increase means that the human impact is more related to the kind of activities performed by humans than the density of the population. From 1500 to 800 years B. P. the Cladocera assemblage is dominated by littoral species, which is associated with drier conditions and lower lake levels (Franco-Gaviria et al., 2020), which is consistent with the scenario described for facies 5.

Pollen stage 4 (from 600 years B. P) is described as a wet period, where the cloud forest is established, having an increase in charcoal (Franco-Gaviria et al., 2018). These wet

conditions, interrupted by occasional droughts (Franco-Gaviria et al., 2020), are confirmed by our $\delta^{18}O$ record, having a mean value of -7.57‰ (slightly lower than the -7.16‰ at stage 2), which confirms the prevalence of a major amount of summer rainfall during this stage. This stage coincides with most of the U3 stage defined by Franco-Gaviria et al., (2020) (Figure 7.7). According to them, in this U3 stage, the organics of the lake came from algal sources according to the C/N record, the erosion was laminar (erosion done layer by layer producing fine grains) according to the elevated ratios in their K/Ti record and the Montmorillonite-rich sediment (Franco-Gaviria et al., 2020). The clay-rich sediment, and the water was well oxygenated according to the low values of their Mn/Ti record and planktonic Cladocera become dominant indicating a substantial deepening and enlargement of the lake (Franco-Gaviria et al., 2020). This is in keeping with a more humid environment described in facies 7 and 8. Environmental variations within stage 4 are not discussed by Franco-Gaviria et al. (2018), describing the complete stage as the same palaeoclimatic unit. During this stage, we have a long period of high organic content from 600 to 250 years B. P. (Figure *7.8*), which coincides with the arrival of the Soctona (an Oto-Mangue ethnic group from Nicaragua, see section 2.5 in chapter 2) and the establishment of a tributary system in the region at 600 years B. P. (Navarrete, 1966). This tributary system might have exerted a social pressure for increasing agriculture in the region. An expansion of agriculture could have increased the input of P and N into the lake, increasing productivity. Unfortunately, the Total Organic Content produced by Franco-Gaviria et al. (2020) has a lower resolution than the record in this thesis, so they did not observe a difference in this record around 600 years B. P. Their P and N record also does not record changes at that time (Franco-Gaviria et al., 2020). However, this can also be related to the lack of resolution.

The Human Impact index reconstructed by Franco-Gaviria et al. (2018) shows relatively high values (up to 30) for 700 to 500 years B. P. (Figure *7.8*), which are similar to the values at the Early Classic (1100 to 1414 years B. P.) when the Total Organic Carbon was high as well as the density of population. Following this argument, the increase in productivity between 600 to 250 years B. P. might have been related to the high human impact (agriculture) due to the relatively high-density population around Lake San Lorenzo. This idea supports an expansion of agriculture related to the arrival of the Soctona. However, the region maintained its high-density population for a century before the period of high productivity, and the high-density population also finished a century before the end of the period of high productivity. The differences in time between the high values of both

records might be explained by the response time (period of resilience) that the environment had before presenting signals of impact during 700 to 600 years B. P. (although significant erosion has been observed at the beginning of a high-density population phase in the Central Maya Lowlands according to Anselmetti et al., (2007)). The input of nutrients might possibly continue after the abandonment of agriculture during 400 to 250 years B. P. However, a higher resolution in the N and P records is required for testing this idea, as well as higher resolution in pollen analysis. The change in the high organic content period from ca. 14 % to 7% and from 30 to 20 units in the HII for 400 to 250 years B. P. (Figure 7.7). might be explained by the changes in the use of land and settlement patterns in the transition from the Soctona Power to the Spanish Crown regime.

Another explanation for the high organic content phase is the drought around 600 years B. P, which would have consequences for lake productivity (Figure 7.7). This dry climatic event is observed in the isotope record of Aguada X'Caamal (Hodell et al., 2005) and coincides with the dismantling of the Mayapan League (see section 2.5 in chapter 2). It is not completely clear how dry conditions might have enhanced the productivity in Lake San Lorenzo during the high organic phase (during and after the dismantling of Mayapan League), but a similar phenomenon is observed in Lake Esmeralda in Central Mayab during the Maya Hiatus, a millennium before (see chapter 9), although in that case the organic material was predominantly allochthonous. Presumably, if the system was more closed, nutrients could have accumulated rather than being flushed through. (It also has to be considered that this high organic phase started in San Lorenzo years before the drought at the time of the Mayapan League). In Lake San Lorenzo, the drought was an event constrained to some years, beginning at 550 years B. P., but humid conditions had returned and prevailed after 400 years B. P., which was not the case at X'Caamal where dry conditions persisted. This opposite trend in San Lorenzo in comparison to X'Caamal, supports the observations at Lake Kail (Guatemala), of contrasting climatic tendencies between the highlands and the lowlands during some periods (Stansell et al., 2020).

The appearance of the Spanish in the area at 400 years B. P. (1650 A. D.) (Figure *7.8*) and the beginning of a new political order coincides with the increase up to 4000 ppm of Ti, as well as a decrease of Ca to its lowest values around 450 B. P. indicating that erosion might be related to new ways of farming introduced in the region or the depopulation of the area leading to a break down in land/soil management (the depopulation of the area was also a parallel consequence of the Conquest process). The $\delta^{18}O$ record of San Lorenzo has a similar trend to Ti around 450 to 500 years B. P. with values that change from -6.48

‰ to -7.63 ‰, supporting a climatic input of the terrigenous fluctuations and calcite precipitation inside the lake.

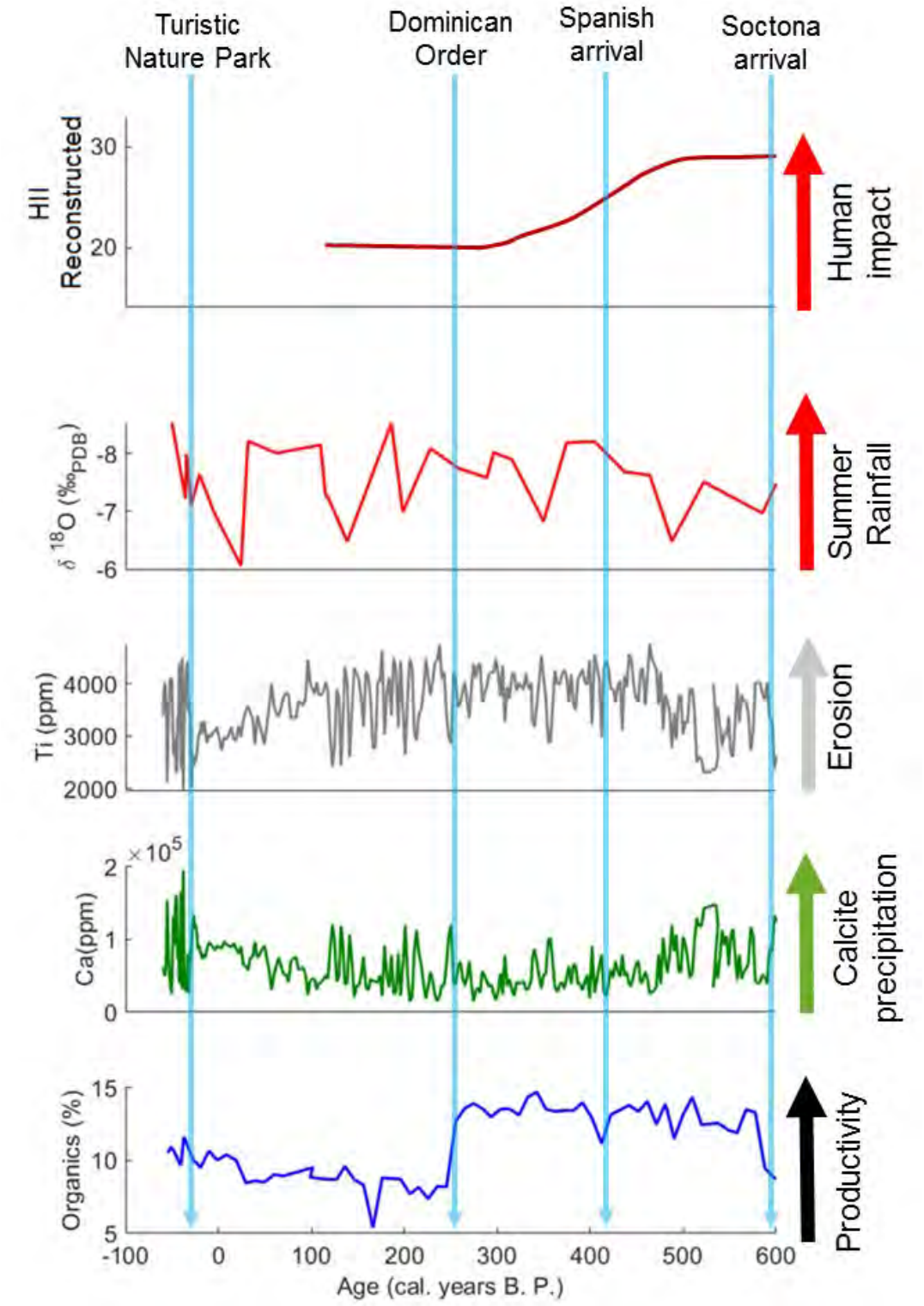

Figure 7.9 Variation of the percentage of organics and the $\delta^{18}O$ in comparison with the Human Index Impact, Ti, and Ca record developed by Franco-Gaviria et al. (2018) during the Colonial and Independence periods. The arrows show relevant historical moments in the existence of Lake San Lorenzo and the Lagunas de Montebello Lake Complex related to changes in land use.

A high proportion of the population of the communities around Lake San Lorenzo, including Chinkultic, migrated to the Comitan-valley, where most of the haciendas (estates imposed by the Spanish crown similar to the Roman latifundium) were located since 1600 A. D. (350 years B. P.) (Zárate-Toledo, 2015). This migration to the Comitan Valley might explain the changes at 400 years B.P. in the records. The change to the lowest value of the HII at 250 years B. P. (1700 A. D.), when the long high organic content period finished, would imply a more prominent abandonment of the population around the lake in the XVIII century. This dynamic of migration into Haciendas is documented by Zarate-Toledo (2015). For instance, in the XVII century A. D. (250 years B. P.), the lands around Lake San Lorenzo started to be a property of the Roman Catholic Dominican Order, which implied a total depopulation of the area (Figure *7.8*).

Without denying the role that anthropogenic impact might have had in the increase of the organics and the high sedimentation rate in the lake during colonial times, it must be highlighted that the system also received more summer rainfall during this time frame according to the $\delta^{18}O$. The fact that the % organics decreased around 250 years B. P., when the population might have emigrated from the surroundings of Lake San Lorenzo, would support the idea of the anthropogenic impact as responsible for the high productivity since the summer rainfall continued increasing.

Around 50 years, B. P., there is a slight increase in organic material. This increase might be related to the establishment of farms near Lake San Lorenzo enhanced by the production of different commercial crops and cattle enhanced by the new agrarian laws associated with the Mexican Revolution of 1910. However, the pattern observed since 50 years B. P. in the organics is similar to the trend in the Ca record and covaries negatively with the Ti records, which might imply that fluctuations in the evaporation-rainfall ratio drive the changes in organic material. However, the record at Lake Balamtetik, also in the Lagunas de Montebello Lake Complex (see Figure 5.6 in chapter 5), indicates high anthropogenic impact due to agrarian activity in the region (Caballero et al., 2020). The high fluctuation in Ti and Ca is the result of the rate of sedimentation, which is the highest during this period. The Ti record reached values up to 4000 ppm since -30 B. P (1980 A. D.)., which coincides with the establishment of the Montebello Lakes complex as a natural protected park (Figure *7.8*). These two issues could be related to the development of intense tourism that the region started to suffer.

The comparison of historical records for the last 600 years with the palaeoenvironmental records obtained from Lake San Lorenzo could help us to elucidate how to interpret the organic productivity of the lake at other times in the 3200-year records of Lake San Lorenzo. However, if this is true, the high % organics in facies 4 might have indicated a substantial anthropogenic impact. In contrast, Franco-Gaviria et al. (2018) found that humans were abandoning the region over these years. The archaeological record, however, supports the persistence of settlements during facies 4. In this case, we have contradictory data that can, unfortunately, not be resolved with the data developed in this research. Our records support the idea that the stages proposed by Franco-Gaviria et al. (2018) can be explained not only by clearance but by variations in rainfall.

7.8 Comparison with other records from the Northern Highlands

Besides Lake San Lorenzo, only four sites have been studied in the Northern Maya Highlands that are over 900 m. a. s. l. Two of these sites, Lake Esmeralda in Chiapas (same name as the lake in the Cochuah Region in Central Mayab, see Chapter 9) and Lake Balamtetik, both at Laguna de Montebello Lake Complex (see Figurer 5.6 in chapter 5), are also in the Montebello Lake Complex, while Lake Kail is 25 km south of Lake San Lorenzo (in Guatemala) (Lake Ocotalito in the Lacandon Forest is the other place, see figure 4.1 in chapter 4). The environmental history reconstructed by Franco-Gaviria et al. (2018) (see the previous section) is also based on the pollen and charcoal record of Lake Esmeralda in Chiapas. The main differences in Lake Esmeralda in Chiapas (mean depth 8 m) are related to its low anthropogenic impact in comparison to San Lorenzo (mean depth 11 m, see section 5.5 in chapter 5) and the presence of allochthonous calcite, which is not present in San Lorenzo (Franco-Gaviria et al., 2018). Even taxa associated with a human occupation like *Z. mays* are absent from Lake Esmeralda in Chiapas. This absence might not only be associated with the lack of human impact on the lake but the fact that Lake San Lorenzo is fed by surface waters; meanwhile, Lake Esmeralda in Chiapas is fed only by underground waters, the first being more exposed to anthropogenic perturbation (Alcocer et al., 2018).

Lake Balamtetik is a short record that is constrained to the second half of the XX century. The record was dated using ^{137}Cs and ^{210} Pb. The record based on diatoms and chemical abundances show the evolution of anthropogenic impact in the sedimentation of this lake (Caballero et al., 2020). The important aspect of this record related to Lake San Lorenzo is the similar high sedimentation rate that exists. In Lake Balamtetik, the sedimentation

rate is 1.4 cm/year, comparable to the 0.9 cm/year at the top of the San Lorenzo core (see section 5.8 in chapter 5).

Figure 7.9 shows a comparison of the proxies of Lake San Lorenzo with the different proxies from Lake Kail. The Kail record (Stansell et al., 2020) has a similar resolution to San Lorenzo. The first difference is the lack of anticovariation between the $CaCO_3$ record and the residuals record in Kail. At the same time, the $CaCO_3$ precipitation at Kail is lower than in San Lorenzo, while the residuals at Kail reached similar values to San Lorenzo between 1700 to 1300 years B. P. The percentage of organics is also higher in Kail than in San Lorenzo, but the land use around Kail seems to have been more intense than at San Lorenzo during the time of Maya occupation of both areas; the Early Mesoamerican Classic Horizon (1700 to 1400 years, B. P.) and the Terminal classic Mesoamerican Horizon (1190 to 850 years B. P). (Stansell et al., 2020).

The $\delta^{18}O$ record based on bulk sediments at Kail is a proxy of the evaporation-precipitation hydrological balance. In contrast to San Lorenzo, which has always been an isotopically open lake, Kail presents transitions from being relatively open hydrologically to behaving like a closed system when lake levels are lower (Stansell et al., 2020). In my opinion, these changes might suggest that the record at Lake Kail is actually a proxy of summer rainfall instead of a proxy of evaporation – rainfall ratio, which is supported by the covariation of both records (see below). This argument is problematic, since it contradicts the explanation given by Stansell et al., (2020) who argue less evaporation for explaining a lower evaporation – precipitation ratio (more humidity) during the last millennium in Lake Kail when the record of precipitation of the stalagmite at Rio Marcos (see figure 10.2 in chapter 10) indicates also a decrease of rainfall for the last millennium (Winter et al., 2020). However, the record at Lake San Lorenzo indicates that the information between stalagmite and lake records in the Maya Highlands has contradictions that are at the moment unsolved (see section 10.5 in chapter 10).

Despite the difference in the meaning of the $\delta^{18}O$, the $\delta^{18}O$ record of Lake San Lorenzo covaries in general with the $\delta^{18}O$ at Kail. Stansell et al. (2020) observed low variability in the Evaporation/Precipitation ratio from 2000 to 1500 years B. P. This time frame coincides with the rainy period observed in San Lorenzo at the end of facies 2 and during facies 3. I propose that the lack of isotope data during facies 4 can be overcome using the $\delta^{18}O$ record at Kail. With this hypothesis in mind, it can be argued that facies 4 presents at least similar summer rainfall amount than facies 3. This scenario would suggest that more

terrigenous material was washed into the lake due to the summer rainfall and less calcite precipitated in a rainy regime. Perhaps the summer rainfall was higher overall, since the percentage of residuals associated with a terrigenous intake was also higher.

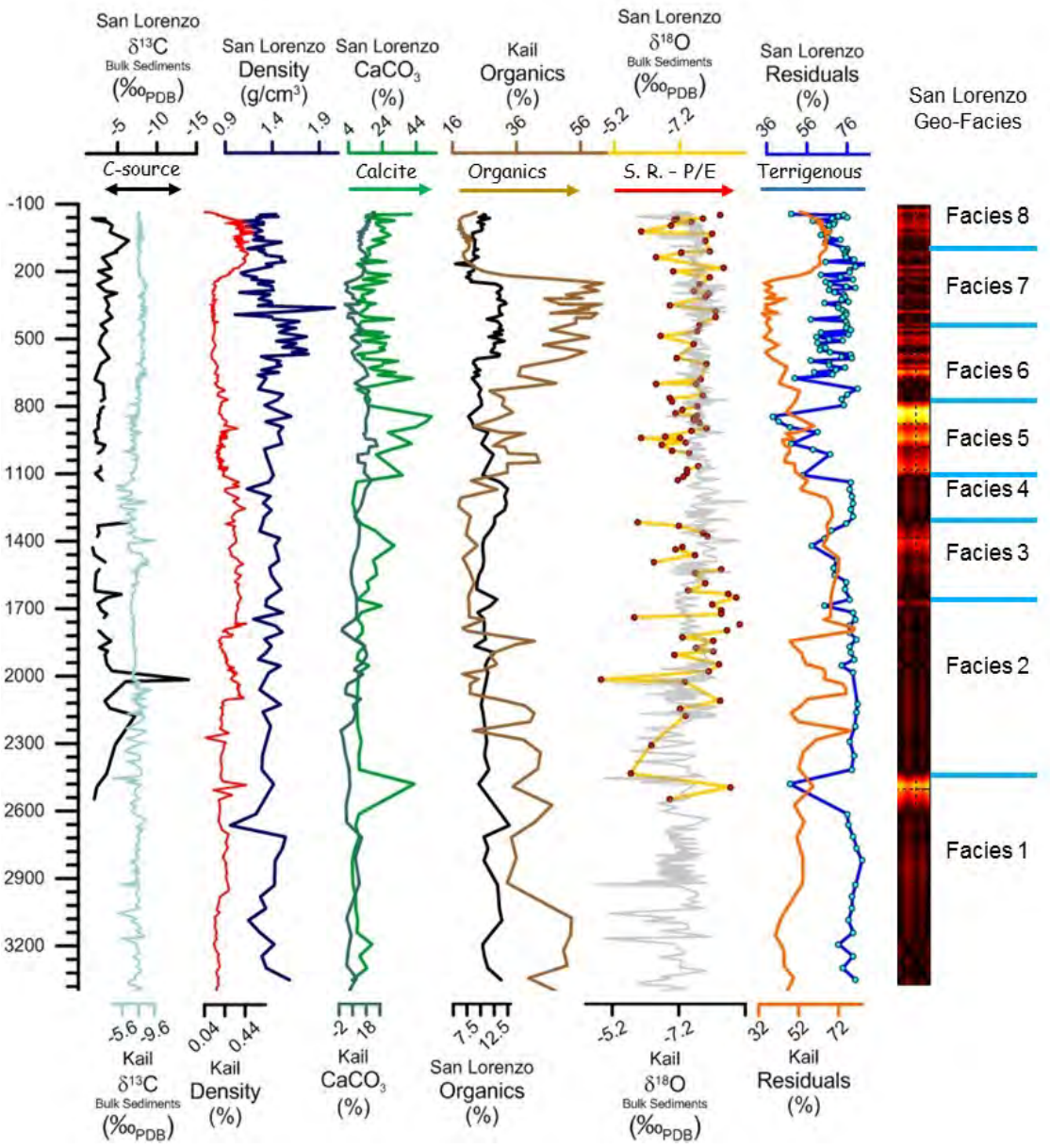

Figure 7.10 Comparison between palaeoenvironmental proxies of Lake San Lorenzo with the proxies from Lake Kail (Guatemala) produced by Stansell et al. (2020). The arrows indicate increases in environmental properties in both records. An exception is the arrow on the $\delta^{18}O$ records, which is a proxy of summer rainfall (S. R.) in Lake San Lorenzo, but a proxy of precipitation- evaporation ratio P/E in Lake Kail. The P/E is normally cited in this thesis as evaporation-rainfall ratio, but on this occasion is named in this way for emphasising the direction of the Effective Rainfall.

This rainfall might have contributed to the forest reexpansion observed by Franco-Gaviria et al. (2018) and the reduction in anthropogenic impact during this time. Stansell et al. (2020) suggest that the Kail records present contrasting precipitation patterns of humidity in comparison with records in the Southern Maya Lowlands after the transition to the Late Holocene at the centennial- millennial scale. For instance, the last millennium has been wet at Kail. This pattern is also present in San Lorenzo.

This contrasting pattern has, however, not always prevailed. As I discussed, facies 5 presented less summer rainfall than any other facies. This was also found for this facies according to the Cladocera assemblage (Franco-Gaviria et al., 2020)(see previous section 7.7). This facies represents the period when the Maya droughts are also observed in the lowlands. In addition, the drought during the destruction of the Mayapan League is also recorded in Lake San Lorenzo. A comparison between our records in the Northern Highlands and Central Mayab in the last chapter of this thesis will contribute to this discussion.

Figure 7.10 shows the $\delta^{18}O$, Ca, Ti records from Lake San Lorenzo in comparison with the Ti record from the Cariaco Basin, which is the iconic record of the movement of the ITCZ and the amount of rainfall derived from it (Haug et al., 2001). The ITCZ has a role in Chiapas since it is practically the only part of Mexico which it affects directly (see chapter 2).

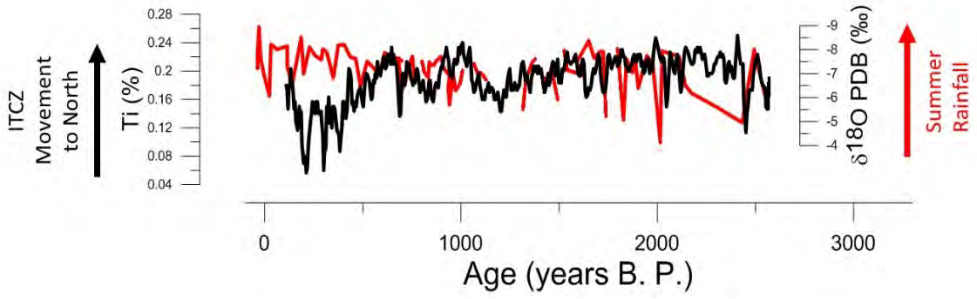

Figure 7.11 Palaeoenvironmental records from Lake San Lorenzo produced by isotope analysis (red) of sieved carbonate sediments in comparison with the percentage of Ti (black time series) of the sediments from the Cariaco basin (Haug et al., 2001).

The similarities in the patterns between the Ti from Cariaco, a proxy of ITCZ movement, and $\delta^{18}O$ records in San Lorenzo, local precipitation response, supports the previous statement arguing that the changes in the $\delta^{18}O$ values of San Lorenzo reflect the summer rainfall. Nevertheless, these changes in summer rainfall are not entirely related to the movement of the ITCZ since the $\delta^{18}O$ record from San Lorenzo presents a different

pattern from the Cariaco Ti record in some periods. For example, the $\delta^{18}O$ of San Lorenzo presents the opposite trend to the Ti record from Cariaco at 2100 years B. P., and 1600 years B. P. The $\delta^{18}O$ from San Lorenzo is also different from the Ti record from Cariaco after 600 years B. P., resembling the same trend followed by the Ti record from San Lorenzo. The similarities in the patterns between the Ti and $\delta^{18}O$ records in San Lorenzo probably means that the changes in sedimentation were driven mainly by changes in the summer rainfall. Therefore, the $\delta^{18}O$ climatic signal shift during the last 600 years might be related to a change either in the nortes dynamics (see section 2.3 in chapter 2) or a drainage water supply from the Grande River, which is consistent with the deepening and enlargement of the lake suggested by the predominant presence of planktonic Cladocera (Franco-Gaviria et al., 2020). This change might also explain in part the increase in the sedimentation rate during this period observed by Franco-Gaviria et al., (2018, 2020).

7.9 Conclusions

In this chapter, I have presented results related to the density, organic, calcite and terrigenous content and the isotope records generated from the sediments of Lake San Lorenzo. We have compared our results with the chemical elements, elemental ratios, Cladocera, charcoal and palynological records generated by Franco-Gaviria et al. (2018). Major findings are:

- It can be observed that the terrigenous input into the lake occurs when the summer rainfall has high values. At the same time, there is less precipitation of calcite when rainy conditions are prevalent. The precipitation of calcite is negatively correlated with the terrigenous input. This might be a dilution effect of the calcite by terrigenous input into the sediments.
- It has been described that the source of the organic material does not present major variations, except for the end of pollen stage U2 defined by Franco-Gaviria et al., (2018) (corresponding to the beginning of Facies 6) when the source was from terrestrial plants and not for algae since the C/N does not reflect significant fluctuations witch exception of the end of that stage (Franco-Gaviria et al., 2020).
- The precipitation changes in the region of Lake San Lorenzo were primarily driven by the movement of the ITCZ.
- Facies 4, between 1414 to 1140 years B. P. marks an important change in human activities, having less impact on the lake and the forest, which coincides with an important climate change to rainy conditions. These changes might also have been

due to the breakdown of trade routes between the Maya cities in the highlands and the city of Teotihuacan in the central highlands, which might have reduced the human activity around Lake San Lorenzo. During facies 5, the time of the Maya Collapse, the region received its lowest amount of summer rainfall. However, the population present at that time is small, inferred by the low anthropogenic impact during the times of the collapse (1140 - 1040 years B. P.) and after that (until ca. 850 years B. P.).

- The record also shows that humans caused a turning point in the environmental history of this region after 600 years B. P. This turning point is driven in part by the arrival of new political relations between the Soctona, Spaniards and the Maya. Nevertheless, this turning point might have also been related to a new climatic pattern influencing humidity besides the movement of the ITCZ. After this time, the region became wetter, in contrast with the lowlands that became drier.
- This study suffered from a lack of a better resolution (due to limited sample availability) and a more precise chronology. It was also limited by the fact that it only covered 3200 years, which is probably the lifetime of Lake San Lorenzo. This issue does not allow a comparison with earlier periods in the Holocene when humans had much less impact on the environment.
- The records from San Lorenzo, which is one of the few sites studied in the highlands of the Maya Cultural Area, alongside the new record from Lake Kail (Stansell et al., 2020), contributes to a more complete picture of the dynamics between humans and the environment in the region. The data from San Lorenzo will be valuable to establish the differences and similarities in the dynamics between the highlands and the lowlands of the Mayab, Belize and the Peten region.
- As usual, we need more study sites in the highlands of the Maya Cultural Zone, not only to complete the picture of the environmental history of the Maya Cultural Zone but to understand the environmental dynamics in Mesoamerica and the tropics in general. In addition, more archaeological projects must be supported in the region, including studies that focus on the Archaic and Early Formative Mesoamerican horizons.

Chapter 8

Preservation of the environmental signal in the isotopic composition of gastropods

Photo: A *P. coronatus* (smooth) shell from Lake Esmeralda observed under SEM.

"… and yet, with the sea-salt they absorb, the solid elements of water which they assimilate, these animalculae produce limestone, and this limestone forms enormous submarine erections, of which the hardness and solidity equal granite. Formerly, at the first periods of creation, nature employing fire, heaved up the land, but now she entrusts to these microscopic creatures the task of replacing this agent…"

L´île mystérieuse, Chapitre XXI. Jules Verne, 1874.

Published carbonate isotope records from the Maya lowlands have relied mainly on the same methodology, based on picking shells of the gastropod *Pyrgophorus* (mainly assumed to be *P. coronatus*) and then combining the individuals (n ≥15) from a single layer to provide a composite sample (Curtis et al., 1996; Hodell et al., 1995, 2005a, 2005b; Wahl et al., 2014). This approach was taken to avoid the impact that in-washed material from the carbonate dominated catchments might have on the analysis of bulk sediment. What has been left relatively unexplored is the variability between individual shells (Escobar et al., 2010) and the impact this might have on the values obtained from a composite sample.

The purpose of this chapter is to attempt to establish a reliable methodology for extracting the climatic signal from carbonates using $\delta^{18}O$ analysis in Yucatan lakes and applying this methodology to the sediments collected from Lake Esmeralda.

Methodologies that involve the use of gastropod shells present some challenges in getting a clear isotopic signal. These challenges are

1. to select a particular taxon of gastropods (see sections 6.1 and 6.12, chapter 6), which will be ubiquitously present in the sedimentary record. As described above, *Pyrgophorus coronatus* has been widely selected for this purpose in different studies of lakes in the Maya Cultural Area. However, some studies have focused on the complete family without distinguishing between genus or species (Whitmore et al., 1996). It would be useful to test the advantages of analysing *P. coronatus* rather than other taxa.
2. to establish how many individual shells need to be analysed to obtain a reliable value for a particular stratigraphic horizon. Escobar et al. (2010) began to investigate this issue, with particular reference to determining the optimum sample size (number of individual shells) needed to obtain reliable reconstructions of low-frequency (decadal/centennial) climate variability. Based on their analysis, they suggested that for $\delta^{18}O$, between 1-43 shells of *P. coronatus* were needed per sample level for Lake Punta Laguna and between 1-45 for the larger and longer residence time Lake Chichancanab.
3. to assess changes in the isotopic composition related to specific locations across the lake. Since several factors can influence the oxygen isotope composition of individual gastropods, including ecology, life history, habitat change and variable $\delta^{18}O$ and temperature of lake water in space and time (Jones et al., 2002). As gastropods can live for just a few months or for more than a year, the isotope record in their shells may reflect seasonal or annual means. In the case of

P. coronatus., this is likely to be an annual value since it is a small gastropod (up to ~5 mm), and its whole shell is used for analysis. *P. coronatus* is a littoral form and detritivore (Dillion, 2006), so in lakes with an extensive littoral area (as in Esmeralda), it might show considerable spatial variability in its isotopic composition. The ecology of *P. coronatus* is also quite poorly known, although it has been widely reported throughout the Caribbean and along the Gulf of Mexico coast from Texas to Venezuela (Covich, 1976), occurring in alkaline and brackish water. It can show striking polymorphism with both smooth and spinous forms.

4. To assess the impact of diagenesis on shells (see section 6.10 in chapter 6), which can affect the isotopic signal by the alteration of the original mineral composition, leading to a false value of the environmental signal.

For these challenges, this chapter presents results of isotope analysis performed on modern shells of different taxa collected in Lake Esmeralda and Lake Chichancanab and in a third lake, Cenote Chen Ha, where sample numbers allowed.

The chapter then explores three different possible methodologies for extracting the isotopic signal from the Lake Esmeralda cores. The possible approaches are to extract the signal from;

- The isotope analysis of a composite of subfossil shells from specimens of a specific taxon of gastropods for particular stratigraphic layers, which will generate a single $\delta^{18}O$ value per layer.
- the median of the $\delta^{18}O$ values obtained from analysing individual subfossil shells from specimens of a specific taxon of gastropods for a particular stratigraphic layer.
- the isotope analysis of the bulk carbonates precipitated in a particular stratigraphic layer, which generates a single $\delta^{18}O$ value per layer.

8.1 Isotopic composition of water from Lake Esmeralda

Figure 8.1 and Table 8.1 show the isotopic composition of water and soluble carbonates (DIC) taken in 2018 from Lake Esmeralda (see Figure 6.1). The isotopic composition of water samples indicates enrichment in deuterium and heavy oxygen (^{18}O) in comparison with the meteoric water line (*Figure 8.1*). The isotopic signatures of the samples collected in 2018 (dark yellow triangles) have similar values to samples collected in the same season (early winter) from 2010 to 2016 (red triangles). The samples collected during the last ten years fall along the local evaporation line.

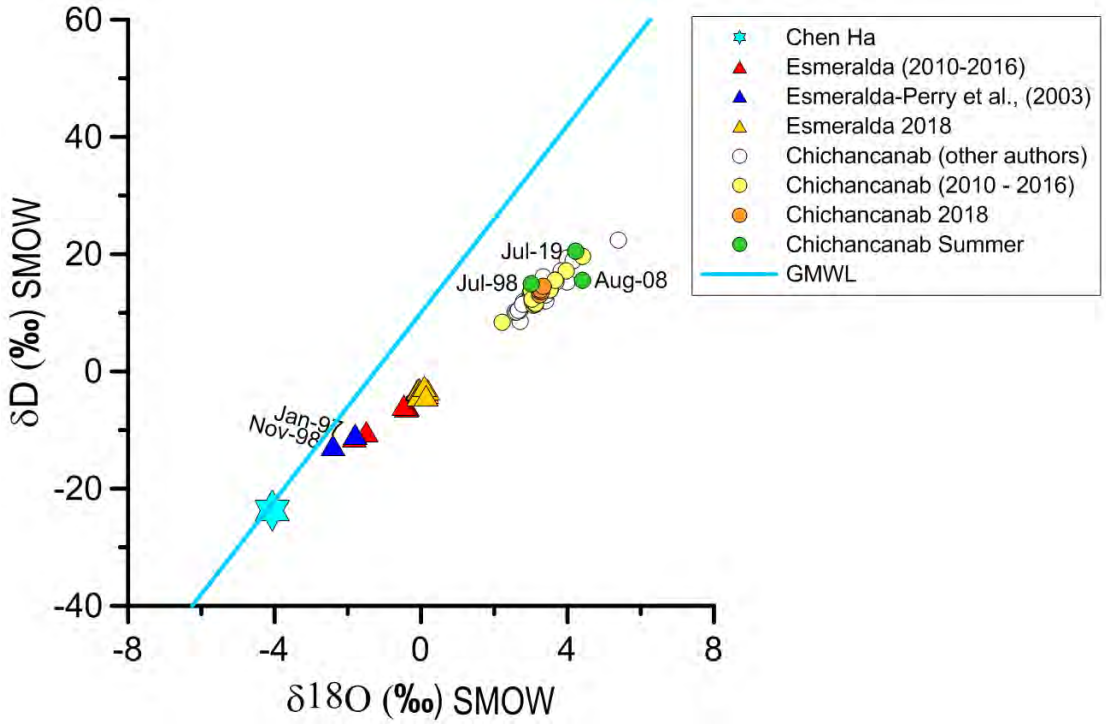

Figure 8.1 Isotopic composition of water samples taken from Lake Esmeralda in January from 2010 to 2016 in comparison with samples taken from Lake Chichancanab from 2010 to 2016 and Cenote Chen Ha. All samples have been collected in winter (January) by undergraduate students from the University of Nottingham under the supervision of Sarah E. Metcalfe, excepting the samples collected at Lake Esmeralda in 2018 collected by the author. The plot also shows the isotopic composition of water samples collected in winter by other authors in Chichancanab (Covich and Stuiver, 1974; Hodell et al., 2012; and Evans et al., 2018) and by Perry et al., (2003) in Esmeralda. Summer samples collected in Chichancanab are taken from Cejudo (unpublished), Douglas et al., (2012) and Perry et al., (2003). The legend in some samples indicate the date of collection (see section 8.8 below).

Figure 8.1 also shows the isotopic composition of samples collected from Chichancanab from 2010 to 2017 (light yellow circles), and samples from 2018 (orange samples). The isotopic values of these samples also fall on the local evaporation line; however, they have more positive values in both isotopic ratios. This isotopic composition implies that Lake Esmeralda is still a relatively hydrologically closed system, with an important degree of evaporation, but it is more open in comparison to Chichancanab. The most parsimonious explanation after considering different water inflows and outflows might be related in some degree to the size of Lake Esmeralda, implying then that the water inflow of both lakes is practically and proportionally the same, which is approximately ten times smaller than Chichancanab and is also shallower (see chapter 4). Therefore, Esmeralda has less volume. It's also likely Esmerelda has more groundwater outflow.

In such conditions, it can be argued that a bigger and deeper lake like Chichancanab have a longer water residence time, where the evaporation provokes a bigger enrichment of ^{18}O.

Following the equation proposed by Leng & Marshall, (2004) the isotopic composition of carbonates that would be precipitated from these waters was calculated from the isotopic signature of the water samples using the temperature measured during the collection, approximately 24.4°C and 30°C for Lake Esmeralda and Chichancanab, respectively. I calculated the values for calcite and aragonite (Table 8.1). A similar calculation was performed for samples collected at Chen Ha, where some snails were also collected. This lake is a more open water body (a sinkhole called a cenote), in the north of the Mayab inside the ring of the cenotes, probably due to its connections with groundwater. In section 8.8, a comparison between the measured isotopic value of shells of Hydrobiidae and the calculated isotopic value of aragonite calculated from water is discussed.

*Table 8.1 Isotopic composition of water and isotopic composition of soluble carbonates (DIC) of samples from Lake Esmeralda and Chichancanab. * Calculated values of $\delta^{18}O$ of precipitated calcite and aragonite in Lake Esmeralda and Chichancanab derived from from Equation 6.7 and Equation 6.8 (see section 6.11 in chapter 6). Values highlighted in yellow indicate the sites that were used for taking shells for isotopic analyses.*

Samples	Depth (cm)	T (°C)	$\delta^{18}O$ Water ($‰_{SMOW}$)	δD ($‰_{SMOW}$)	$\delta^{13}C$ ($‰_{PDB}$)	$*\delta^{18}O_{Calcite}$ ($‰_{PDB}$)	$*\delta^{18}O_{Aragonite}$ ($‰_{PDB}$)
O1	10	24.2	+0.17	-3.7	-8,6	-2.01	-1.41
O2	10	24.1	+0.19	-3.2	-9,6	-1.98	-1.38
O3	10	24.4	+0.08	-3.7	no run	-2.15	-1.55
O4	10	24.3	-0.04	-2.9	-6,3	-2.25	-1.65
O5	10	24.2	-0.02	-3.9	-10,0	-2.21	-1.61
O5D	315	not taken	-0.09	-3.2	-8,0	not analysed	not analysed
O6	10	23.6	-0.07	-3.1	-10,0	-2.14	-1.54
O7	10	24.3	-0.02	-3.2	-8,2	-2.23	-1.63
O8	10	24.2	-0.06	-4.2	-8,1	-2.25	-1.65
O8D	270	not taken	+0.10	-2.6	-11,3	not analysed	not analysed
O9	10	24	+0.14	-4.2	-8,4	-2.01	-1.41
Chichancanab	0	30.452	3.24	13.1	-6,3	-0.19	0.41

Figure 8.2 presents the box and whisker plots that show the variability of $\delta^{18}O$ composition of water samples and the calculated $\delta^{18}O$ signature of aragonite for the lakes Esmeralda, Chichancanab and the cenote Chen Ha. Aragonite is assumed instead of other phases of calcium carbonate due to the composition of the shells (see section 8.3). The calculated isotopic values for aragonite presented a smaller difference between Chichancanab and the other two water bodies in comparison to the isotopic values from water.

This smaller difference is explained by the differences in temperature used for the calculation, while the mean temperatures used for Lake Esmeralda and Chen Ha were 24.4 C and 26.9 ˚C respectively, in Chichancanab the temperature was 30 ˚C. According to the

equation proposed by Leng & Marshall (2004), values can change by 2 ‰ units of $\delta^{18}O$ in a gradient of 10 degrees from 20 to 30 °C and 1‰ of $\delta^{18}O$ in a gradient of 5 °C. A variation of 5 degrees might be achieved by a water body in the Mayab on the same day since the diurnal variation in temperature in the area can be more than 10 °C according to the instrumental records (CONAGUA, 2010a, 2010b).

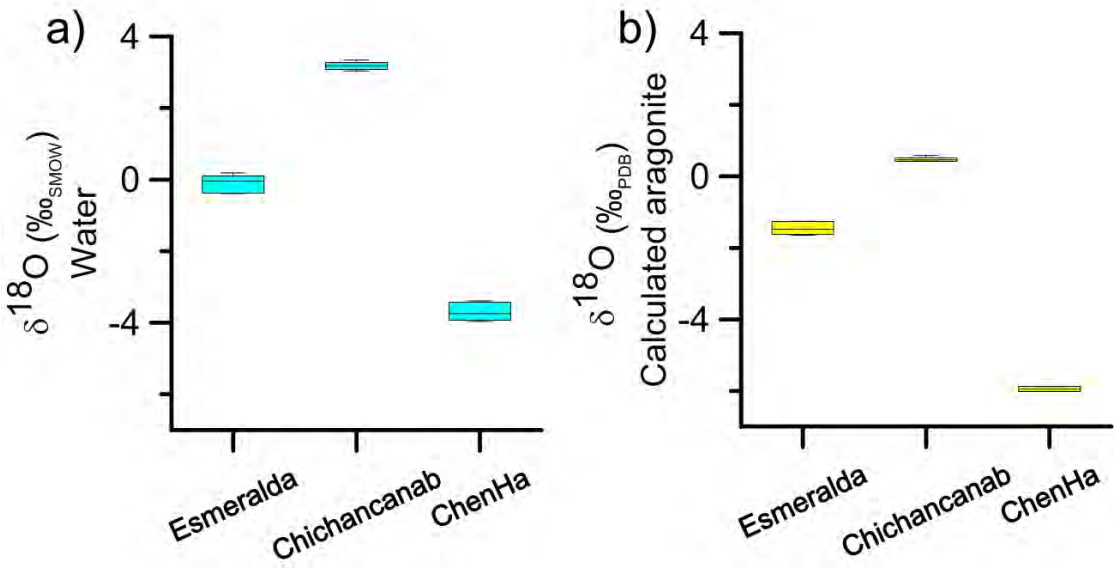

Figure 8.2 a) Box and whisker plot of the isotopic composition of water samples from Esmeralda in comparison with samples from Lake Chichancanab and Cenote Chen Ha. b) Box and whisker plot of the calculated isotopic composition of aragonite from water Esmeralda in comparison with samples from Lake Chichancanab and Cenote Chen Ha.

8.2 Distribution of the shells in the lake and taxa found

Although four sites in Lake Esmeralda were chosen for collecting shells, only two sites had a large number (over 100). All shells were empty, no gastropod was found living inside at the moment of collection. These sites were Esmeralda 6 near the north shore and Esmeralda 9 near the south shore (see Figure 6.1 of chapter 6). Sampling at the other sites, Esmeralda 4 and 7, found around only ten shells at each site. A similar situation happened in Lake Chichancanab, where only two sites Ch1 and Ch4 (see Figure 6.1 in chapter 6) from four had an abundant number of shells (over 50). No gastropod was found inside shells collected in Chichancanab.

After being washed with distilled water and dried for 24 hr at 30 °C, the collected gastropod shells were classified into three taxa *Aroapyrgus* sp., *Tryonia* sp., and *Pyrgophorus coronatus* according to the morphology of the shell (Figure 8.3). This last taxon, *P. coronatus* possess two morphologies (smooth and spinose), which were present at two sites in Chichancanab, and one of the sites in Lake Esmeralda, while only the smooth morphology was present at

Esmeralda site 6. In sensu stricto, the term *Pyrgophorus coronatus* should be constrained for the spinous form of the taxon (Naranjo-Garcia, Personal communication), and the smooth form should be called *Pyrgophorus* sp. according to the phylogeny (Sadava et al., 2011). The taxonomic status of most of the nominal species called "*Pyrgophorus*" is uncertain (Hershler, 1992). For instance, *Pyrgophorus platyrachis* could be an ecophenotype of *P. coronatus* (Andrew et al., 2002).

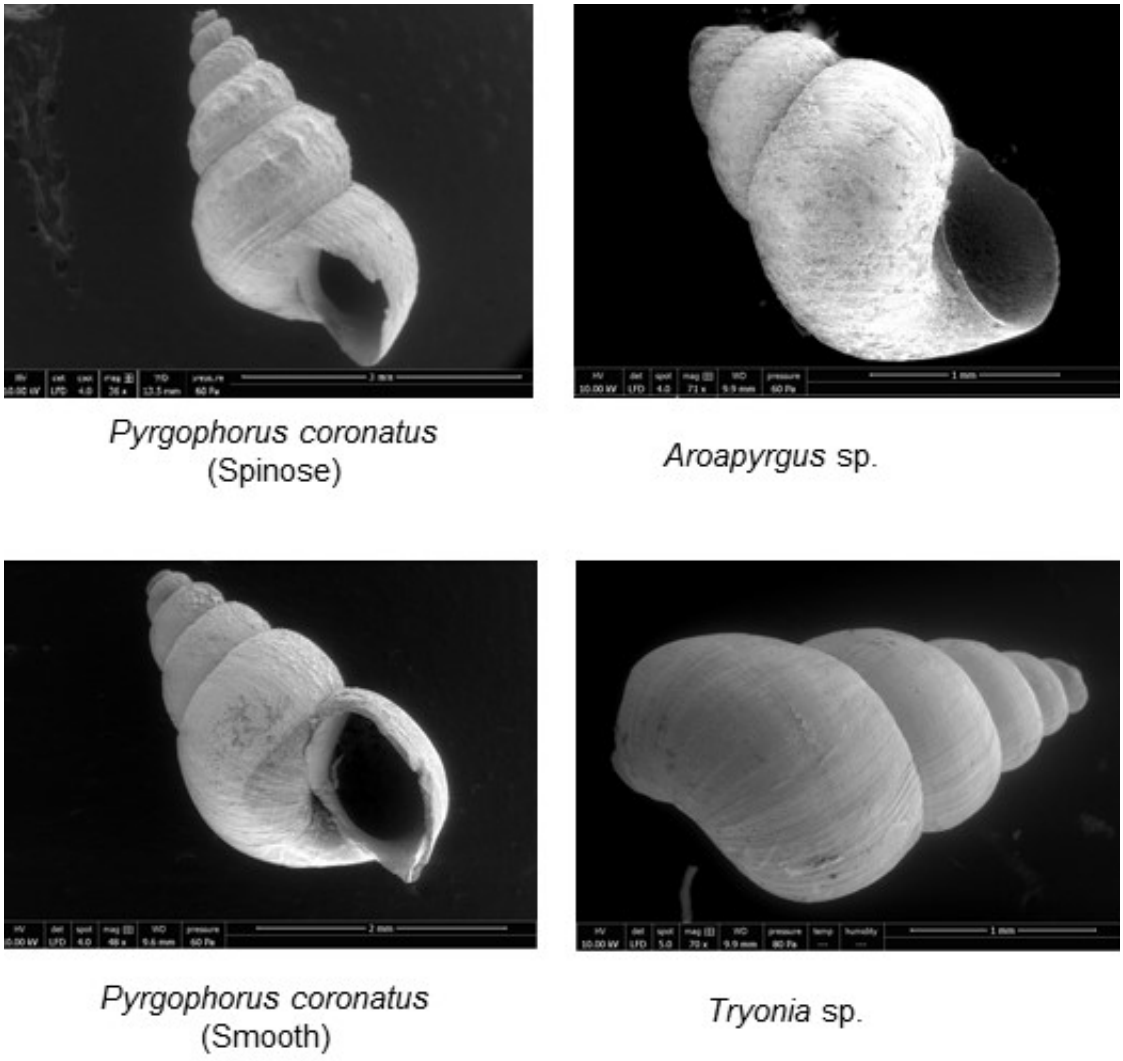

Figure 8.3 Genus of family Hydrobiidae found in Lakes Chichancanab and Esmeralda. In the case of Pyrgophorus coronatus, it was possible to identify the species. Both forms of P. coronatus are classified as different forms of the same species (Covich, 1976; Ditrich et al., 1997).

However, extensive works have implied that both morphologies are the same species (Covich, 1976; Ditrich et al., 1997). This nomenclature has been used in previous palaeoclimate studies in the Maya Cultural Zone, using *P. coronatus* for both morphologies. I decided to continue with this classification, but to separate both morphologies (smooth and spinous) for testing possible variability of the isotopic signal according to morphology.

8.3 Mineral composition of the shells

Figure 8.4 presents some XRD diffractograms obtained for single shells of different taxa. The diffractograms of almost all samples show that the major component of the shells is aragonite (Table 8.2). The presence of other minerals is indistinguishable from background. In the case of samples 17 and 153, (Figure 8.4i & j), the analyses are inconclusive, because the matching algorithm was unable to establish the presence of the aragonite pattern. Since a zero correction of the 2θ cannot solve the problem, I am probably dealing with specimen displacement during the five hours of the XRD analysis.

Table 8.2. Major mineral phase in gastropods collected in Lakes Esmeralda and Chichancanab

Sample	Site	Taxon	Mayor Mineral Phase	Letters in Figure 8.4
17	Chichancanab 1	*Tryonia* sp.	suspected Aragonite	j)
29	Chichancanab 1	*P. coronatus (smooth)*	Aragonite	b)
112	Chichancanab 1	*P. coronatus (spinose)*	Aragonite	c)
122	Esmeralda 6	*Aroapyrgus* sp.	Aragonite	d)
153	Esmeralda 6	*Tryonia* sp.	suspected Aragonite	i)
203	Esmeralda 6	*P. coronatus* (smooth)	Aragonite	e)
209	Esmeralda 6	*P. coronatus* (spinose)	Aragonite	not shown
230	Esmeralda 9	*Aroapyrgus* sp.	Aragonite	g)
259	Esmeralda 9	*Tryonia* sp.	Aragonite	h)
291	Esmeralda 9	*P. coronatus (smooth)*	Aragonite	not shown

Using a visual comparison and arguing the parsimony principle, I postulate that these samples are also composed of aragonite. The lack of coincidence between signals in the experimental diffractogram and the pattern of aragonite might be related to a non homogenous displacement in 2θ. Which means that the sample was not only wrongly positioned (which would be corrected with a zero correction of 2 θ), but it was moving from its position during the analysis. This displacement would be the result of failing to fix the sample properly inside the diffractometer. Remember that this positioning was a challenge (see Figure 6.5 in chapter 6).

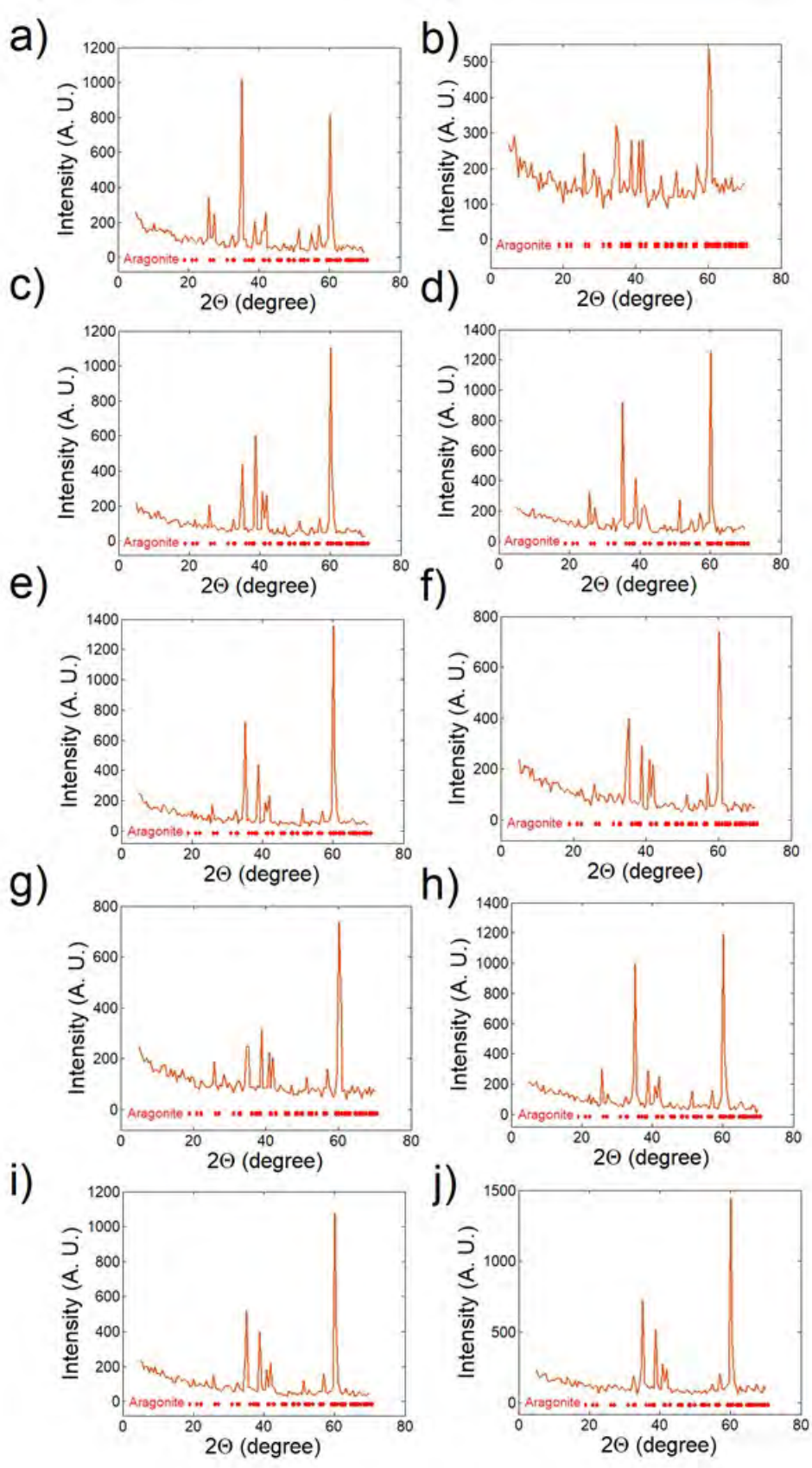

Figure 8.4 XR Diffractograms of the shells of the different taxa found in Chichancanab and Lake Esmeralda. A) 204 P. coronatus, b) 29 P. coronatus, c) 112 P. coronatus, d) 122 P. coronatus, e) 203 Aroapyrgus sp.*, f) 281Aroapyrgus* sp. *g) 230 Aroapyrgus* sp.*, h) 259 Tryonia* sp.*, i) 153 Tryonia* sp.*, and j) 17 Tryonia* sp. *The mineralogy indicates that the shells are composed of aragonite only.*

8.4 Impact of diagenesis on the shells

Some samples of each taxon were observed using Scanning Electron Microscopy, SEM (Table 8.3). Figure 8.5 presents different microstructures possibly produced during diagenesis. These structures might be formed by recrystallisation of aragonite to calcite or by calcite crust cementation on aragonite shells.

Table 8.3 Specimens used for observations in the Scanning Electron Microscopy. The x marks the part of the body observed.

Sample	Site	Taxon	Body whorl	Apex	Aperture	Shell
10	Chichancanab 1	*Aroapyrgus sp.*	x	x		part
16	Chichancanab 1	*Tryonia sp.*	x		x	part
27	Chichancanab 1	*P. coronatus (smooth)*	x	x		complete
49	Chichancanab 1	*P. coronatus (spinose)*	x	x		complete
59	Chichancanab 4	*Aroapyrgus sp.*	x	x	x	complete
71	Chichancanab 4	*Tryonia sp.*	x		x	complete
80	Chichancanab 4	*P. coronatus (smooth)*	x		x	complete
113	Chichancanab 4	*P. coronatus (spinose)*	x		x	complete
123	Esmeralda 6	*P. coronatus (smooth)*	x		x	part
152	Esmeralda 6	*Tryonia sp.*	x		x	part
203	Esmeralda 6	*Aroapyrgus sp.*	x			complete
209	Esmeralda 6	*P. coronatus (spinose)*	x		x	complete
230	Esmeralda 9	*Aroapyrgus sp.*	x		x	complete
237	Esmeralda 9	*Tryonia sp.*	x		x	complete
291	Esmeralda 9	*P. coronatus (smooth)*	x		x	part

Figure 8.6 shows that suspected major diagenetic structures can be observed easily using both the optical microscope and SEM. For this reason, the rest of the samples were observed under the optical microscope to establish their degree of diagenesis (see section 6.10 in chapter 6). Table 8.4 present the percentage of diagenesis features on the surface of each face of the shells based on visual estimation charts (see Chapter 6, section 6.10), as well as the total area covered by such structures calculated from them. Samples highlighted are considered pristine samples due to their low % cover of diagenetic structures, usually less than 5 per cent in the out and inner parts of the shell.

After performing the isotope analyses (see section 8.5), an assessment of the diagenesis on the $\delta^{18}O$ was performed. Figure 8.7 presents the $\delta^{18}O$ of the shells for every taxon collected in Chichancanab and Esmeralda as a function of the area covered by diagenetic structures.

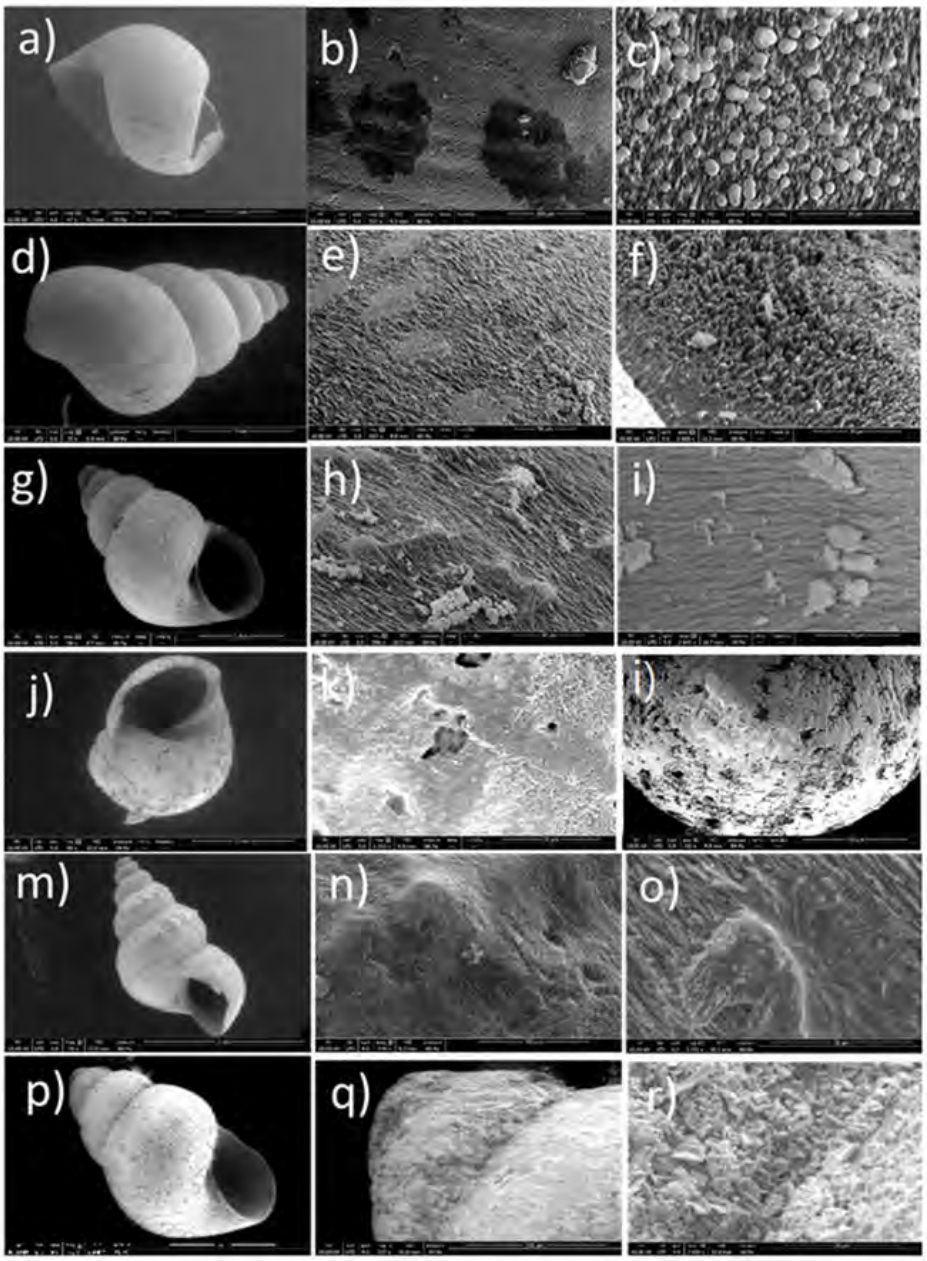

Figure 8.5 Photomicrographs obtained using Scanning Electron Microscopy Visual analyses of diagenetic features on shells. a) Tryonia sp. *18. b) Cemented calcite in Tryonia* sp. *18. c) Tryonia* sp. *16 shows spherulites of calcite over prismatic microstructures. d) P. coronatus (smooth) 27. e) Prismatic microstructures at the body whorl of P. coronatus (smooth) 27. f) Prismatic microstructures at the apex of P. coronatus (smooth) 28. g) P. coronatus (smooth) 291. h) Presence of debris on the prismatic microstructures of aragonite in the body whorl of P. coronatus (smooth) 29. i) Presence of debris on the prismatic microstructures of aragonite in the apex of P. coronatus (smooth). 291 the debris probably came from broken parts of the same shell. j) P. coronatus (smooth) 123. k) and l) another kind of diagenetic pattern is shown on P. coronatus (smooth) 123 where pores can be observed on the tabular aragonite, presumably produced by dissolution. m) Pyrgophorus coronatus (spinose). n) Acicular crystals aggregate in a circular pattern creates the "crone" in Pyrgophorus coronatus (spinose). o) Closer magnification of the last pattern. Despite their contrasting appearance, this pattern is not a product of diagenesis. p) Aroapyrgus* sp. *230 q) another kind of prismatic aggregates on the apex of Aroapyrgus* sp. *r) Closer magnification of the prismatic aggregates on the apex. It is difficult to establish if such a pattern is produced by dissolution, recrystallisation or is primary.*

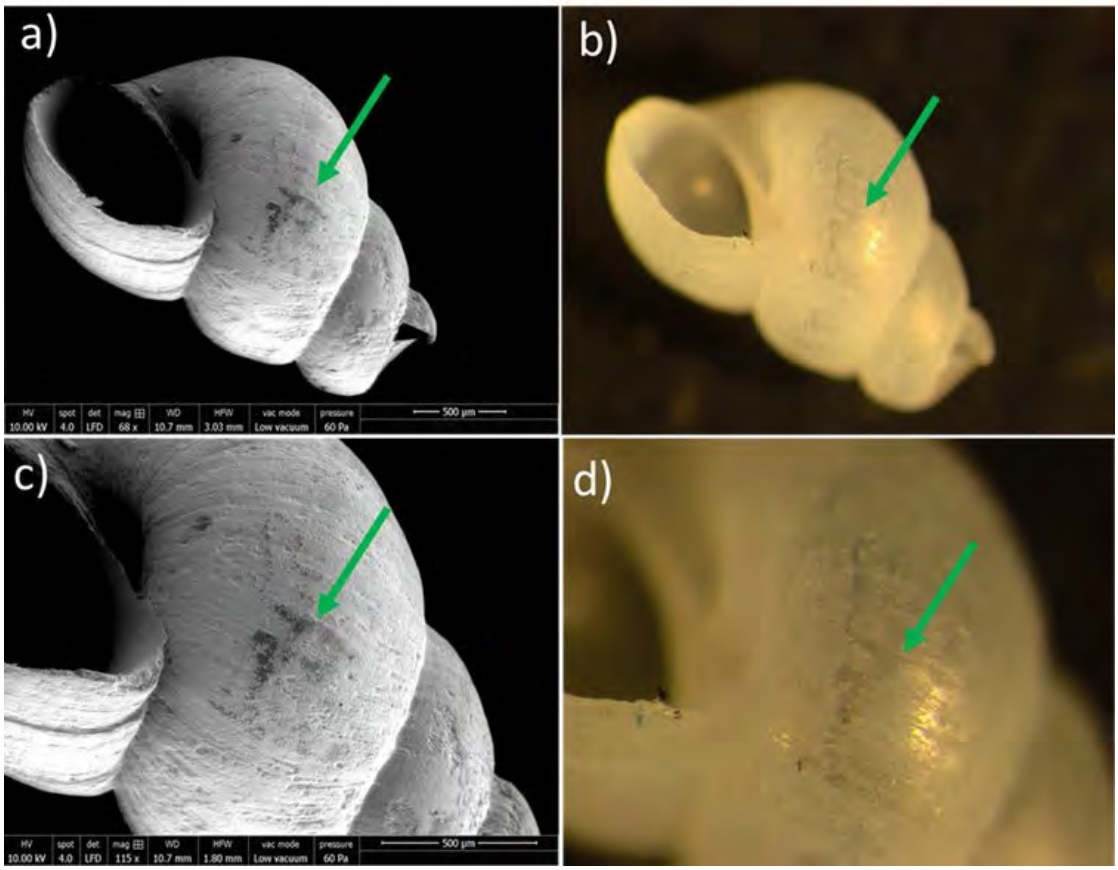

Figure 8.6 Photomicrographs obtained by optical microscopy b) and d) in comparison with the image obtained by Scanning Electron Microscopy a) and c). Green arrows point out possible diagenetic structures. a) Photomicrograph of the whole shell of Pyrgophorus sp. using 60Pa, low vacuum and magnification of 68x at the SEM. b) Photomicrograph of the whole shell of Pyrgophorus sp. observed under an Olympus SZX10 binocular optical microscope. c) Close up of the same shell using a magnification of 115x at the SEM. d) Close up of the same shell using the optical microscope.

The calculated Pearson's correlation coefficient for every taxon is very small, implying a lack of correlation between these two variables. It can be assumed that the isotopic values of the $\delta^{18}O$ are independent of the area covered by diagenetic features. This low impact implies that the diagenetic features might be only superficial and that the bulk structure of the shells remains unaltered. As such, diagenesis features can be in praxis discounted as a potential driver of changes in the down core isotope record. I can assume that, if a subfossil sample from the core is observed with the same percentage of covered area (or even smaller) of diagenetic structures than modern samples, then the diagenesis in these samples will not have an impact on the environmental signal. If this assumption is false, and similar percentage of covered area impacted the environmental signal of the isotopic composition, then I cannot do anything anyway. I do not have a way to test that the diagenesis has gone further even though it covers a similar percentage of area than modern samples, since variations could be still related to the geological age of each subfossil inside the same layer.

Table 8.4 Percentage of diagenetic features on gastropods. Samples marked by yellow are considered pristine.

ID	Site	Age	Surface covered by diagenesis (%)			
		C. E.	Aperture	Whorl next to aperture	Whorl	Total diagenesis considering total surface
Chi-2018-A-10	Chichancanab	2018	2	x	x	2
Chi-2018-P-22	Chichancanab	2018	2	5	2	2.75
Chi-2018-P-24	Chichancanab	2018	25	10	10	17.5
Chi-2018-P-28	Chichancanab	2018	40	2	2	21
Chi-2018-P-34	Chichancanab	2018	2	2	x***	2
Chi-2018-T-35	Chichancanab	2018	10	x	x	10
Chi-2018-P-38	Chichancanab	2018	2	x	x	2
Chi-2018-P-39	Chichancanab	2018	30	x	x	30
Chi-2018-P-40	Chichancanab	2018	10	x	x	10
Chi-2018-A-56	Chichancanab	2018	5	15	15	10
Chi-2018-A-58	Chichancanab	2018	5	5	x	5
Chi-2018-A-59	Chichancanab	2018	50	15	15	32.5
Chi-2018-A-60	Chichancanab	2018	5	x	x	5
Chi-2018-A-62	Chichancanab	2018	40	10	10	25
Chi-2018-A-63	Chichancanab	2018	15	x	x	15
Chi-2018-A-64	Chichancanab	2018	5	5	x	5
Chi-2018-A-66	Chichancanab	2018	40	15	x	27.5
Chi-2018-A-67	Chichancanab	2018	2	2	x	2
Chi-2018-T-68	Chichancanab	2018	25	10	40	25
Chi-2018-T-69	Chichancanab	2018	40	10	10	25
Chi-2018-T-70	Chichancanab	2018	2	2	2	2
Chi-2018-T-71	Chichancanab	2018	5	10	10	7.5
Chi-2018-T-72	Chichancanab	2018	2	2	x	2
Chi-2018-T-73	Chichancanab	2018	10	2	5	6.75
Chi-2018-T-74	Chichancanab	2018	15	2	x	8.5
Chi-2018-P-75	Chichancanab	2018	2	2	x	2
Chi-2018-P-76	Chichancanab	2018	40	2	x	21
Chi-2018-P-78	Chichancanab	2018	5	5	5	5
Chi-2018-P-79	Chichancanab	2018	5	x	x	5
Chi-2018-P-84	Chichancanab	2018	20	5	15	15
Chi-2018-P-85	Chichancanab	2018	5	2	2	3.5
Chi-2018-P-86	Chichancanab	2018	40	15	x	27.5
Chi-2018-P-88	Chichancanab	2018	20	2	2	11
Chi-2018-P-89	Chichancanab	2018	20	5	10	13.75
Chi-2018-P-90	Chichancanab	2018	15	5	2	9.25
Chi-2018-P-91	Chichancanab	2018	25	20	10	20
Chi-2018-PC-112	Chichancanab	2018	10	2	2	6
Chi-2018-PC-113	Chichancanab	2018	25	2	2	13.5
Chi-2018-PC-114	Chichancanab	2018	5	2	5	4.25
Chi-2018-PC-115	Chichancanab	2018	15	10	10	12.5
Chi-2018-PC-116	Chichancanab	2018	20	15	x	20
ES-2018-A-118	Lake Esmeralda	2018	10	10	10	10
ES-2018-A-119	Lake Esmeralda	2018	20	5	5	12.5
ES-2018-A-120	Lake Esmeralda	2018	20	40	20	25
ES-2018-A-121	Lake Esmeralda	2018	20	20	20	20
ES-2018-A-122	Lake Esmeralda	2018	10	10	15	11.25
ES-2018-A-123	Lake Esmeralda	2018	x	x	40	40
ES-2018-A-124	Lake Esmeralda	2018	15	5	15	12.5
ES-2018-A-125	Lake Esmeralda	2018	20	5	5	12.5
ES-2018-A-126	Lake Esmeralda	2018	15	20	20	17.5
ES-2018-A-127	Lake Esmeralda	2018	15	5	5	10
ES-2018-A-128	Lake Esmeralda	2018	15	25	10	16.25
ES-2018-A-129	Lake Esmeralda	2018	2	2	x	2
ES-2018-A-130	Lake Esmeralda	2018	10	10	5	8.75
ES-2018-A-131	Lake Esmeralda	2018	5	15	20	11.25
ES-2018-T-148	Lake Esmeralda	2018	10	5	5	7.5
ES-2018-T-149	Lake Esmeralda	2018	5	5	5	5
ES-2018-T-150	Lake Esmeralda	2018	10	5	5	7.5
ES-2018-T-151	Lake Esmeralda	2018	0	2	5	1.75
ES-2018-T-152	Lake Esmeralda	2018	2	2	x	2
ES-2018-T-153	Lake Esmeralda	2018	10	5	5	7.5

Table 8.4 Continue

ID	Site	Age	Surface covered by diagenesis (%)			
		C. E.	Aperture	Whorl next to aperture	Whorl	Total diagenesis considering total surface
ES-2018-T-155	Lake Esmeralda	2018	20	10	5	13.75
ES-2018-T-156	Lake Esmeralda	2018	15	15	10	13.75
ES-2018-T-157	Lake Esmeralda	2018	20	10	10	15
ES-2018-T-158	Lake Esmeralda	2018	20	15	10	16.25
ES-2018-T-160	Lake Esmeralda	2018	2	10	5	4.75
ES-2018-T-161	Lake Esmeralda	2018	10	10	5	8.75
ES-2018-T-162	Lake Esmeralda	2018	20	15	15	17.5
ES-2018-P-184	Lake Esmeralda	2018	20	20	20	20
ES-2018-P-185	Lake Esmeralda	2018	20	5	10	13.75
ES-2018-P-186	Lake Esmeralda	2018	20	5	10	13.75
ES-2018-P-187	Lake Esmeralda	2018	10	5	5	7.5
ES-2018-P-190	Lake Esmeralda	2018	10	2	2	6
ES-2018-P-193	Lake Esmeralda	2018	2	5	2	2.75
ES-2018-P-194	Lake Esmeralda	2018	5	20	20	12.5
ES-2018-P-197	Lake Esmeralda	2018	5	2	2	3.5
ES-2018-P-200	Lake Esmeralda	2018	2	2	5	2.75
ES-2018-P-201	Lake Esmeralda	2018	2	40	15	14.75
ES-2018-P-202	Lake Esmeralda	2018	5	2	2	3.5
ES-2018-P-203	Lake Esmeralda	2018	2	20	10	8.5
ES-2018-P-204	Lake Esmeralda	2018	5	5	5	5
ES-2018-P-205	Lake Esmeralda	2018	20	5	5	12.5
ES-2018-P-206	Lake Esmeralda	2018	2	5	5	3.5
ES-2018-P-207	Lake Esmeralda	2018	2	2	2	2
ES-2018-PC-208	Lake Esmeralda	2018	10	5	2	6.75
ES-2018-PC-209	Lake Esmeralda	2018	40	40	40	40
ES-2018-PC-210	Lake Esmeralda	2018	2	5	2	2.75
ES-2018-PC-211	Lake Esmeralda	2018	5	2	2	3.5
ES-2018-A-220	Lake Esmeralda	2018	2	5	5	3.5
ES-2018-A-221	Lake Esmeralda	2018	2	5	2	2.75
ES-2018-A-222	Lake Esmeralda	2018	5	15	15	10
ES-2018-A-223	Lake Esmeralda	2018	10	5	5	7.5
ES-2018-A-226	Lake Esmeralda	2018	2	2	2	2
ES-2018-A-227	Lake Esmeralda	2018	2	20	20	11
ES-2018-A-230	Lake Esmeralda	2018	40	40	40	40
ES-2018-A-231	Lake Esmeralda	2018	2	10	5	4.75
ES-2018-A-232	Lake Esmeralda	2018	5	40	40	22.5
ES-2018-A-233	Lake Esmeralda	2018	5	5	2	4.25
ES-2018-A-234	Lake Esmeralda	2018	10	40	40	25
ES-2018-A-235	Lake Esmeralda	2018	2	2	2	2
ES-2018-A-236	Lake Esmeralda	2018	20	15	15	17.5
ES-2018-T-237	Lake Esmeralda	2018	2	5	x	3.5
ES-2018-T-238	Lake Esmeralda	2018	10	40	40	25
ES-2018-T-239	Lake Esmeralda	2018	2	2	15	5.25
ES-2018-T-240	Lake Esmeralda	2018	5	20	20	12.5
ES-2018-T-241	Lake Esmeralda	2018	2	10	10	6
ES-2018-T-242	Lake Esmeralda	2018	2	5	10	4.75
ES-2018-T-243	Lake Esmeralda	2018	2	5	15	6
ES-2018-T-244	Lake Esmeralda	2018	2	20	20	11
ES-2018-T-245	Lake Esmeralda	2018	5	25	40	18.75
ES-2018-T-246	Lake Esmeralda	2018	5	15	15	10
ES-2018-T-248	Lake Esmeralda	2018	10	40	40	25
ES-2018-T-252	Lake Esmeralda	2018	5	15	15	10
ES-2018-T-253	Lake Esmeralda	2018	40	40	50	42.5
ES-2018-T-259	Lake Esmeralda	2018	10	2	10	8
ES-2018-T-261	Lake Esmeralda	2018	20	20	20	20
ES-2018-P-262	Lake Esmeralda	2018	20	20	20	20
ES-2018-P-263	Lake Esmeralda	2018	20	15	25	20
H-2018-T-292	Chen-Ha	2018	5	5	5	5
H-2018-T-294	Chen-Ha	2018	2	2	2	2
H-2018-T-293	Chen-Ha	2018	2	20	20	11
H-2018-A-295	Chen-Ha	2018	25	10	15	18.75
H-2018-A-296	Chen-Ha	2018	5	2	2	3.5

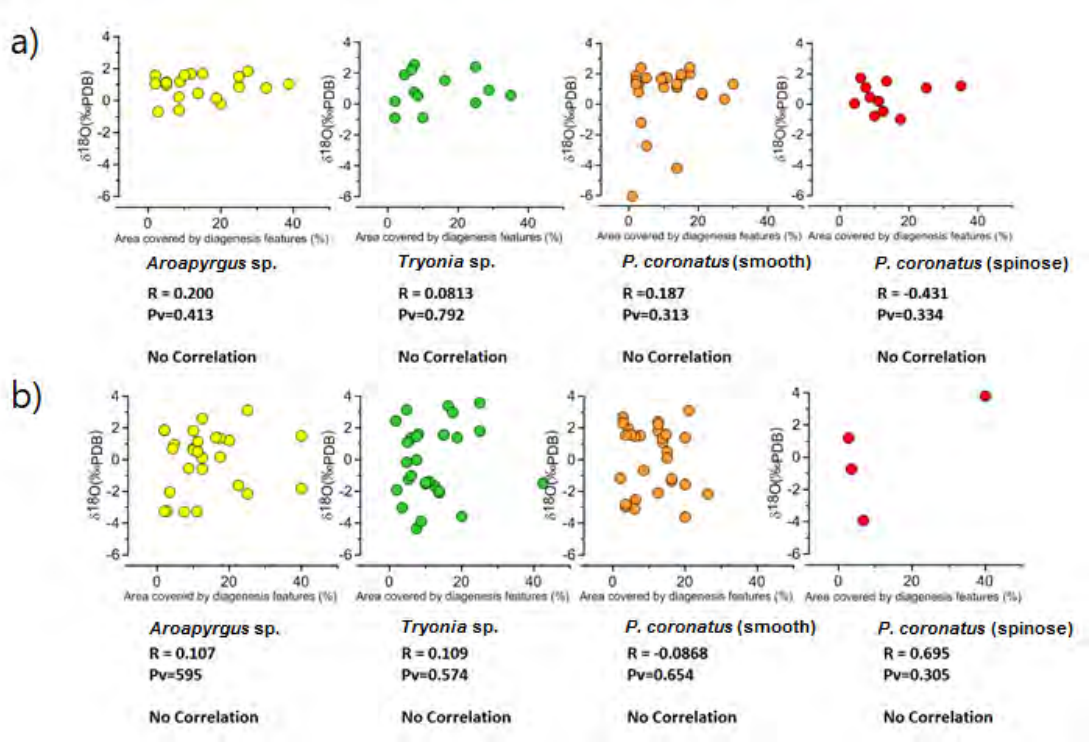

Figure 8.7 a) Oxygen isotopic composition of shells of Hydrobiidae from Chichancanab vs the percentage of the area covered by diagenesis. b) Oxygen isotopic composition of shells of Hydrobiidae from Esmeralda vs the percentage of the area covered by diagenesis.

8.5 Comparison of the isotopic composition of shells between taxa

The normality test (Shapiro-Wilk test) on $\delta^{18}O$ values of Hydrobiidae from Lake Esmeralda (Table 8.5 upper left) failed, showing that the samples do not follow a unimodal (normal) distribution. This can be observed in Figure 8.8b. (In a unimodal distribution the probability of having an experimental value or the frequency of appearance of an experimental value is bigger near a central value; Gonick and Smith, 1993; Trauth, 2007).

Therefore, a non-parametric test of analysis of variance the Kruskal-Wallis test was performed (similar methodology was applied in the next statistical test, when the normality test failed, see appendixes 1-3). In the case of the $\delta^{18}O$ of the shells of Lake Esmeralda, three taxa (*Aroapyrgus* sp, *Tryonia sp. and P. coronatus*) have a distribution that can be described as a bimodal discrete distribution (Figure 8.8b), since the distribution of the values aggregate themselves in two different groups (around two modes or experimental values of high frequency, having the function two humps), having a low probability of having an experimental value near an unique central value (Gonick and Smith, 1993). The samples of the spinose form of *P. coronatus* are just distributed across a range of 8 ‰ units, which is a similar range to the other taxa, having their highest frequencies of values at the extremes of the distribution.

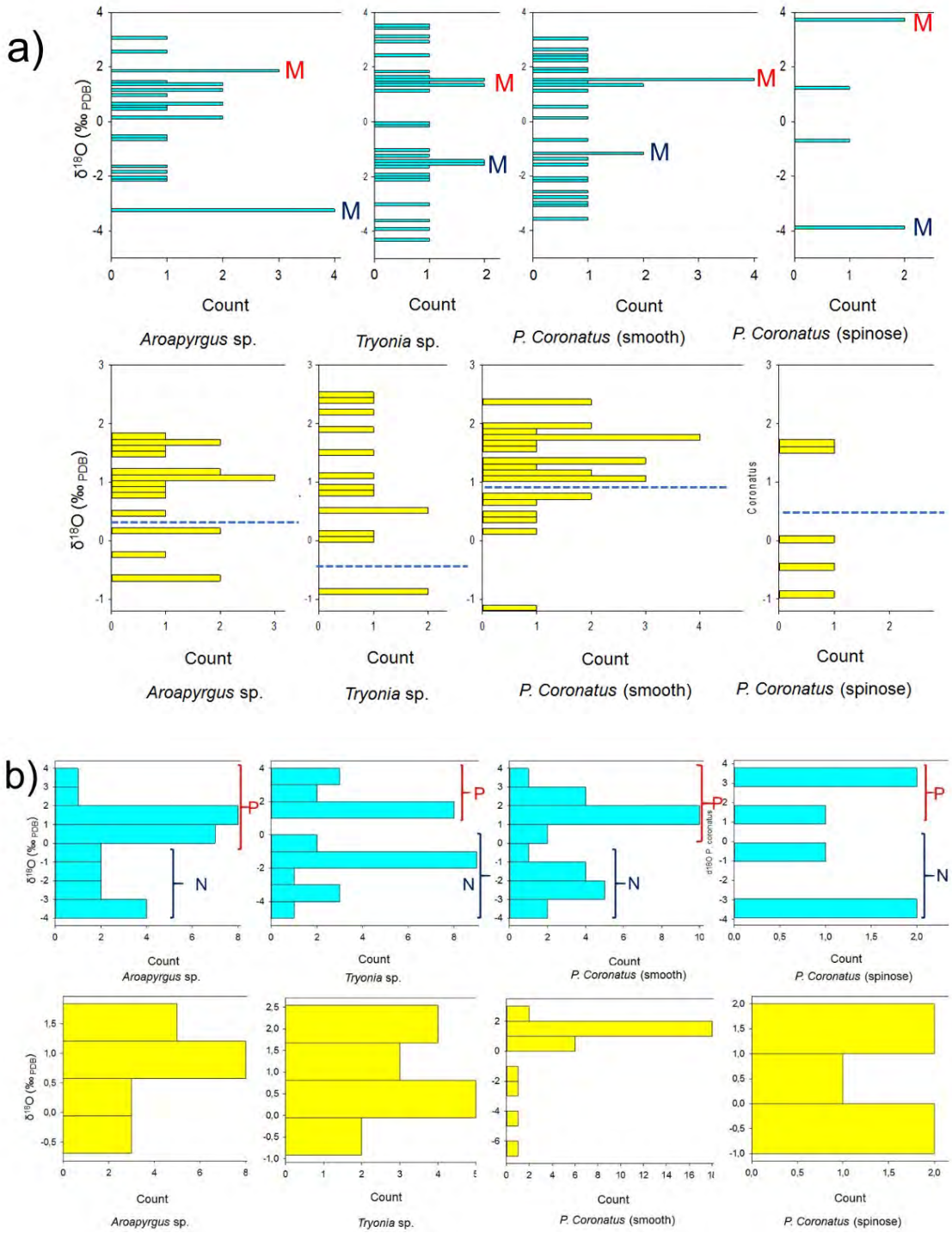

Figure 8.8 a) Distribution of the $\delta^{18}O$ values for every taxon in Lake Esmeralda (blue) and Chichancanab (yellow) considering bins of the size of the analytical error. "M" indicate the mode for subgroup P (M red) and subgroup N (M blue). Dash line defines the artificial border between subgroups P and N in Chichancanab. b) Distribution of the $\delta^{18}O$ values for every taxon in Lake Esmeralda (blue) and Chichancanab (yellow) considering bins of 1 ‰. Red Brackets indicate the bins in the subgroup P, meanwhile blue brackets indicate the bins in the subgroup N in Lake Esmeralda.

Table 8.5 Analysis of variance for the $\delta^{18}O$ of shells from Lake Esmeralda

Statistics test for $\delta^{18}O$ of shells

Normality Test (Shapiro-Wilk)	Alternative test	H (KW)	P (KW)
Failed (P < 0.050)	Kruskal-Wallis One Way Analysis of Variance on Ranks	0.285	0.963

Group Name	N	Mean	Std Dev	SEM	Median	Rank 0.25	Rank 0.75
$\delta^{18}O$ Aroapyrgus sp. Es	27	-0.0121	1.92	0.37	0.607	-1.823	1.388
$\delta^{18}O$ Tryonia sp. Es	29	-0.118	2.3	0.427	-0.168	-1.79	1.588
$\delta^{18}O$ Pyrgophorus sp. Es	29	0.115	2.063	0.383	1.1	-1.832	1.699
$\delta^{18}O$ P coronatus Es	6	0.0308	3.501	1.429	0.232	-3.92	3.781

The fact that there is not a unimodal distribution is problematic, because there is not an actual single central value that can represent all the $\delta^{18}O$ values but two (Figure 8.8). The suggested approach of Escobar et al., (2010) for calculating the optimum number of shells that can reflect the reliability and robustness of the environmental signal (see section 6.12 in chapter 6) is impossible to perform if there is not a unimodal distribution in the $\delta^{18}O$ values.

Since this bimodal distribution (Figure 8.8b) might reflect two different groups of each taxon, (see later explanation), I divided every set (a group of shells of the same taxon from the same lake) artificially into two subsets N (since it is the one with more negative $\delta^{18}O$ values) and P (since it is the one with more positive $\delta^{18}O$ values) according to the closeness of their values to the two local maxima (mode) (indicated by "M" in Figure 8.8a) of the bimodal distribution of the $\delta^{18}O$ values for both kinds of isotopes (Figure 8.8b).

For example, the sets of values of $\delta^{13}C$ of Esmeralda were divided into two subsets (subset P and subset N), each set considers one mode of the two modes of $\delta^{18}O$ values. (To divide according to the values of $\delta^{13}C$ would not be appropriate since it would create a subset constituted by different specimens from the subsets of the $\delta^{18}O$). Then I compared all the artificial subgroups from the same lake that represent the more negative values (all subsets N). Then, the same process was performed for the subset with more positive values (all subsets P).

Figure 8.9 presents the box and whisker diagram of the results of the isotopic analyses done on the different subgroups of the family Hydrobiidae collected from Chichancanab and Lake Esmeralda considering all the specimens collected of the same taxon. It shows that the different taxa have a similar standard deviation for the $\delta^{18}O$ of three taxa, *Aroapyrgus* sp., *Tryonia* sp. and *Pyrgophorus coronatus* (the smooth form), while the standard deviation is larger for the spinouse form of *P. coronatus*. The bigger variability of this group is explained by the small numbers of individuals included, which made it difficult to calculate an appropriate value for the standard deviation. Statistical tests confirm these

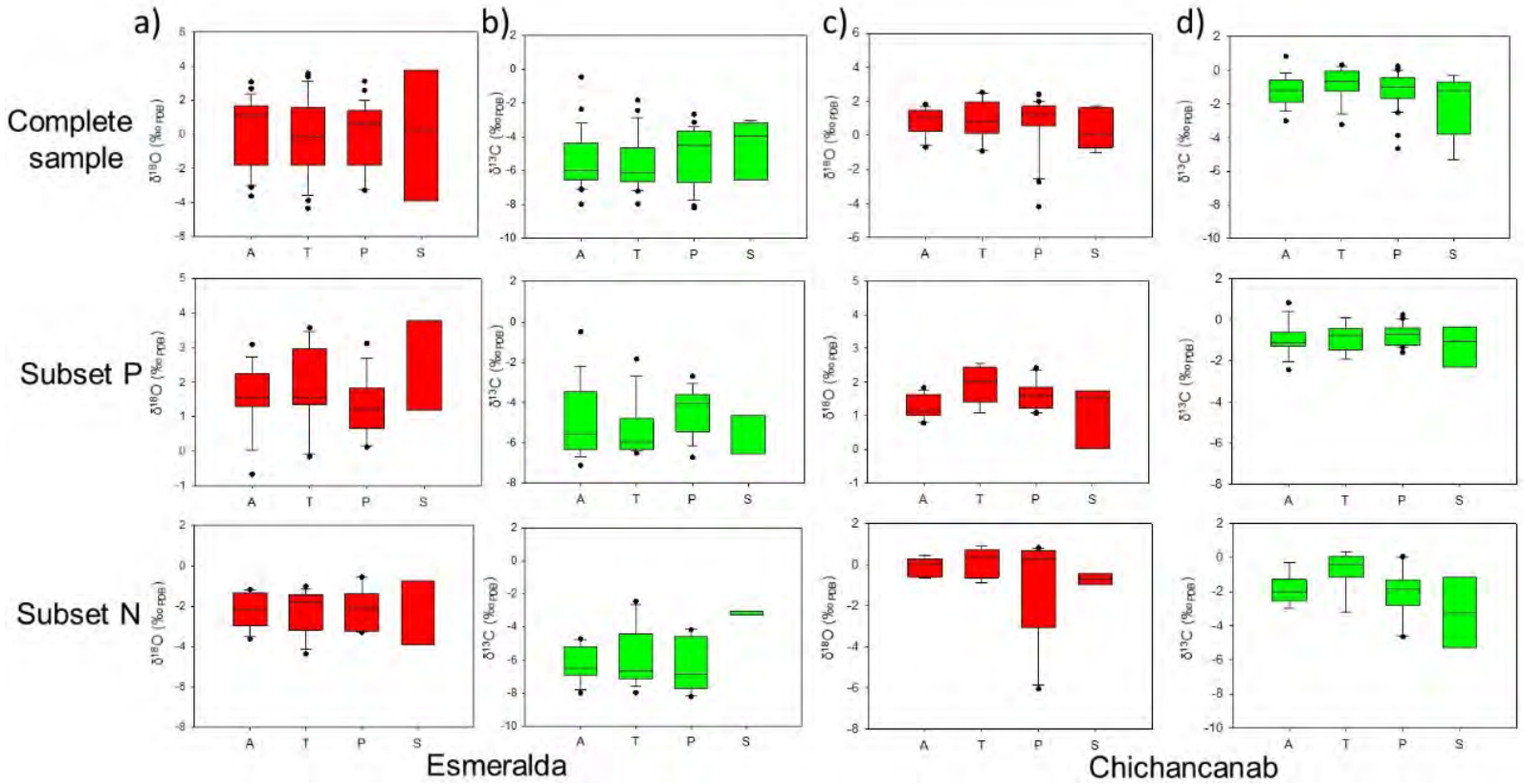

Figure 8.9 Box and box and whisker plot showing a comparison between the taxa collected at Esmeralda and Chichancanab of a) $\delta^{18}O$ at Esmeralda; b) $\delta^{13}C$ at Esmeralda; c) $\delta^{18}O$ at Chichancanab; d) $\delta^{13}C$ at Chichancanab. Every set (complete sample) was divided artificially in two subsets (N and P) according to the proximity of $\delta^{18}O$ values to the nearest highest local value in the bimodal distribution. A = Aroapyrgus sp.*; T = Tryonia* sp.*; P = P. coronatus smooth form and; S = P. coronatus spinose shape. Middle line denotes median; box limits denotes lower and upper quarts; box and whiskers denotes minimum and maximum values. Black points indicate outliers.*

observations. For instance, the analysis of variance points out that the median values between the different subgroups of the genus Hydrobiidae are not different enough to exclude the possibility that the difference is due to random sampling variability; there is no statistically significant difference (P = 0.963) (Table 8.5).

In the case of the Subset N of $\delta^{18}O$ samples of Esmeralda (Figure 8.9a bottom), the box and whisker diagram shows that there is no difference in the standard deviation. Therefore, the statistical test also failed in showing statistically significant differences between these groups. However, among the shells of the subset P of $\delta^{18}O$ in Figure *8.9*a (middle), the smooth form of *P. coronatus* shows values that are statistically significantly different from the other taxa.

Figure 8.9b presents the box and whisker diagram for the values of $\delta^{13}C$ for the shells for the four taxa collected at Esmeralda. Each taxon was divided into two groups according to which range the value of $\delta^{18}O$ fell for creating two subsets (subset P and subset N) with a unimodal distribution in the oxygen isotopes. Each of these unimodal subgroups might be related to a physical variable, such as the isotopic signature in winter or summer.

In the box and whisker plots that considers all the samples for each taxon (Figure 8.9b top), there is not a significative different standard deviation, while the median is very similar for *Aroapyrgus* sp. and *Tryonia* sp., but different for both forms of *P. coronatus*. When all the specimens are considered, the One-way analysis of variance test done on the $\delta^{13}C$ values (Table 8.6) shows that the differences in the median values between the different subgroups of the genus Hydrobiidae are not great enough to exclude the possibility that the difference is due to random sampling variability; there is not a statistically significant difference (P = 0.510).

Table 8.6 Analysis of variance for the $\delta^{18}C$ of shells from Lake Esmeralda

Statistics test for $\delta^{13}C$ of shells

Normality Test (Shapiro-Wilk)	Equal Variance Test (Brown-Forsythe)	F	P
Passed(P = 0.090)	Passed (P =0.941)	0.777	0.51

Group	N	Mean	Std Dev	SEM	Source of Variation	DF	SS	MS
$\delta^{13}C$ Aroapyrgus sp. Es	27	-5.161	1.644	0.316	Between Groups	3	6.202	2.067
$\delta^{13}C$ Tryonia sp. Es	29	-5.568	1.564	0.29	Residual	87	231.399	2.66
$\delta^{13}C$Pyrgophorus sp. Es	29	-5.37	1.68	0.312	Total	90	237.601	
$\delta^{13}C$ P coronatus Es	6	-4.539	1.647	0.672				

When I consider only the shells of subgroup N (Figure 8.9b bottom), the range of the $\delta^{13}C$ values of the subset is also constrained automatically to more negative values (except for the spined form of *P. coronatus*). In the same way, the shells whose $\delta^{18}O$ values fall inside

of the zone nearer to the more positive local maxima in $\delta^{18}O$ (subgroup P in Figure 8.8b middle), have more positive values of $\delta^{13}C$, with the exception again of the spinose form of *P. coronatus*.

In the case of the shells of the subset N (Figure 8.9b bottom*)*, there is no significant difference for *Aroapyrgus* sp., *Tryonia* sp. and *P. coronatus,* but there is a statistical difference of these taxa with the subset N of the spinose form of *P. coronatus*. When I considered the shells of the subset P, there is no statistically significant difference between the four taxa. However, there is a statistically significant difference between both forms of *P. coronatus,* while there is also a difference between the smooth form of *P. coronatus* and the *Tryonia* sp.

Figure 8.9c (top) presents the box and whisker diagram for the $\delta^{18}O$ values of the shells collected from Chichancanab according to the taxa found. The standard deviation of the different taxa is smaller than the standard deviation in Lake Esmeralda. For instance, the standard deviation in Lake Esmeralda is around 4‰, while in Chichancanab, the standard deviation is less than 2‰.

From Figure 8.8, it can be observed that the statistical distribution of the $\delta^{18}O$ values constrained to bins equal to the analytical error of 0.1 ‰ (Figure 8.8a) and constrained to bins of 1‰ (Figure 8.8b) is a unimodal skewed positive distribution in the case of the *Aroapyrgus* sp. and the smooth form of *P. coronatus* for specimens from Chichancanab.

It is also a unimodal skewed negative distribution in the case of *Tryonia.*sp. The number of specimens of the spinose form of *P. coronatus* is again too small to give an idea of the real distribution, although the specimens fall at opposite extremes of the range.

Since there are no bimodal distributions for the $\delta^{18}O$ values in Chichancanab, there are no clear boundaries to divide individual sets of shells into two subgroups, as I did in Lake Esmeralda (Figure 8.8b). However, as an exercise for comparison, I created two subgroups (subset N and subset P), fixing a boundary before a second local maximum counting from positive to negative values (Figure 8.8a line).

When I consider all the shells for every taxon, the analysis of variance (Table 8.7) shows that the differences in the median values between the treatment groups are not great enough to exclude the possibility that the difference is due to random sampling variability; there is not a statistically significant difference (P = 0.340).

The same happens when I consider only the more negative values (subset N), presented according to their proximity to the more negative local maxima. However, the values close

to the mode (subset P) (and therefore to the more positive local maxima) show that the values of *Tryonia* sp. are significantly different from the $\delta^{18}O$ values of the other taxa (Figure 8.9c middle).

Table 8.7 Analysis of variance for the $\delta^{18}O$ of shells from Chichancanab

Normality Test (Shapiro-Wilk)	Alternative test	H (KW)	P (KW)
Failed (P < 0.050)	Kruskal-Wallis One Way Analysis of Variance on Ranks	3.354	0.34

Group Name	N	Mean	Std Dev	SEM	Median	Rank 0.25	Rank 0.75
$\delta^{18}O$ Aroapyrgus Chi	19	0.83	0.756	0.173	1.035	0.217	1.49
$\delta^{18}O$ Tryonia Chi	13	0.898	1.154	0.32	1.035	0.117	2.04
$\delta^{18}O$ Pyrgophorus Chi	26	0.682	2.034	0.399	1.324	0.69	1.76
$\delta^{18}O$ P coronatus Chi	9	0.531	0.92	0.307	0.448	-0.208	1.361

The box and whisker diagram for the values of $\delta^{13}C$ of all the specimens for every taxon (Figure 8.9d top) does not show any significant difference between taxa, which is supported by the analysis of variance (Table 8.8), that found that there are is not a statistically significant difference for rejecting the hypothesis that the differences are due to chances ($P = 0.158$). This is also the case for the comparison between the subsets P created artificially. There is no significant difference between the taxa for subset P in the $\delta^{13}C$ (Figure 8.9d middle). In the case of the subset N, there is a significant difference in the $\delta^{13}C$ values of *Tryonia* sp, compared with the other taxa (Figure 8.9d bottom) while there is no difference between *Aroapyrgus* sp., the *P. coronatus* (spinous form) and *P. coronatus* (smooth form) (Figure 8.9d bottom).

I need to be careful in the comparison between taxa in both lakes since it is evident that I am talking of two different systems. In Lake Esmeralda, the values of $\delta^{18}O$ of each taxon have a bimodal distribution, while in Chichancanab, the distribution is asymmetrical and unimodal. In Lake Esmeralda, the range of values is twice that in Chichancanab, which means that the standard deviation in Lake Esmeralda of every taxon is twice the deviation in Chichancanab.

This more significant standard deviation might be related to the size of the lakes since Chichancanab has an area of circa 8 km^2 against approximately 1 km^2 for Lake Esmeralda. The bimodal distribution present in Lake Esmeralda might be linked to the differences between juvenile against adult specimens, male against female specimens or specimens developed in summer against specimens developed in winter. Such a distribution is not present in Chichancanab, whose water might be isotopically more homogeneous.

Table 8.8 Analysis of variance for the $\delta^{13}C$ of shells from Chichancanab

Normality Test (Shapiro-Wilk)	Alternative test	$H_{(KW)}$	$P_{(KW)}$
Failed (P < 0.050)	Kruskal-Wallis One Way Analysis of Variance on Ranks	5.192	0.158

Group	N	Mean	Std Dev	SEM	Median	Rank 0.25	Rank 0.75
$\delta^{13}C$ Aroapyrgus Chi	19	-1.244	0.909	0.208	-1.203	-1.899	-0.598
$\delta^{13}C$ Tryonia Chi	13	-0.783	0.979	0.272	-0.635	-1.265	0.0128
$\delta^{13}C$Pyrgophorus Chi	26	-1.157	1.097	0.215	-1.037	-1.601	-0.432
$\delta^{13}C$ P coronatus Chi	9	-0.391	1.456	0.485	-0.464	-1.642	0.782

Another aspect to consider is that such a distribution might just reflect the density of sampling effort in the different systems, with far fewer samples from the much larger lake. If the differences between the two groups of the same genus were related to the differences between the gender, since the gender is not associated with the morphology of the shells; (Falniowski, 2018). This would mean that a specific gender would choose a specific niche in the lake (Jones et al., 2002), where water chemistry and isotopic composition are not homogeneous. In contrast, this difference does not exist in Chichancanab, where waters might be more homogenous than Esmeralda (without forgetting the problem of the sample size in Chichancanab), so if the specific niche is filled by a specific gender. The difference would be not evident, since every niche contains isotopically the same kind of water. Another aspect to consider is the ratio of Lake Chichancanab shore to open water.

It has to be highlighted, that the differences between two groups occupying different niches cannot be associated with differences of age, since the morphology of juvenile is distinctive from the morphology of adults (Pilsbry, 1890). Possible differences between juveniles and adult specimens would be reflected in the size and density of the shells (Covich, 1976, 2010). Having this in mind, I collected shells of similar size and presumably similar density. I assumed that translucent shells were less dense than opaque shells, therefore I picked only opaque shells, it is not possible

In a third scenario, it is possible that the gender and age of the Hydrobiidae are not relevant, and the differences in their isotopic composition are due to the differences in the isotopic composition of water between the rainy season and the dry season. In this case, the niches become irrelevant. By parsimony, this would be the elected explanation for the differences since the differences in the isotopic signature of water between seasons impact more open lakes than close lakes.

The fourth scenario would be that each subgroup around a local maximum in the bimodal distribution represents a different time frame. The samples collected from the surface

could be asynchronous. Therefore, they might represent different periods of time separated by several decades. This difference in time frames in samples from the same stratigraphic layer will be discussed in section 8.8.

A fifth possibility is that the bimodal distribution actually does not have a physical meaning, and the isotopic composition is totally random. However, if that were the case, why does this not happen in Chichancanab? Therefore, I believe that this possibility is highly implausible.

The difference in the standard deviation of the taxa between both lakes also implies that Lake Esmeralda is hydrologically more open than Lake Chichancanab, since open lakes are more sensitive to seasonal changes in precipitation $\delta^{18}O$ values (Leng and Marshall, 2004). This basically confirms what it is deduced from the water isotope values.

I can also say that in Chichancanab, this means that the isotopic composition is, in general, the same for the shells of the family Hydrobiidae since the values present a unimodal distribution, which makes it unnecessary to display the sample in two different sets. the isotopic composition is also the same for the shells independently of the genus to which they belong.

In contrast, if the subsets for every taxon in Lake Esmeralda have a physical meaning, e.g. it means that *P. coronatus* (in their smooth form) are significantly different from the other taxa. Nevertheless, if the subsets P and N do not correspond to changes between winter and summer, the values between taxa in Esmeralda are still not significantly different and have a bimodal distribution due to stochastic variables.

8.6 Differences in the isotopic composition at different places in the same lake.

In this section, I present the comparison of the isotopic values obtained from two different sites in the same lake for every taxon. Figure 8.10 shows the cross plot of the isotopic analyses done on shells of the family Hydrobiidae in Lake Chichancanab. It can be observed that the shells have similar values of $\delta^{18}O$ but have entirely different values of $\delta^{13}C$, falling in different 'zones' according to whether they were collected at Site 1 or Site 4 (see Figure 6.1). In the case of the shells of the genera, *Aroapyrgus* sp. and *Tryonia* sp., the isotopic composition of shells is similar for $\delta^{18}O$ but fall in different 'zones' of $\delta^{13}C$ according to where they were collected, while the distribution of the isotopic values is independent of the site for both forms of *P. coronatus*.

Figure 8.10 also displays the box and whisker diagrams comparing the two sites for every taxon. In the case of the oxygen isotopic composition, $\delta^{18}O$, there is no statistically significant difference between the sets of specimens collected from different sites. This result is consistent with the similar value of $\delta^{18}O$ that they have (Figure 8.10a, b, c, d), and supported by the analysis of variance (Appendix 1), which found that that the difference in the median values between the two sites is not great enough to exclude the possibility that the difference is due to random sampling variability.

Nevertheless, in the case of the $\delta^{13}C$, the box and whisker diagrams show that there is no statistically significant difference between the set of specimens of both forms of *P. coronatus* collected in different sites. However, there is a statistically significant difference between shells of *Aroapyrgus* sp. according to which site they were collected from. The same happens for the sets of *Tryonia* sp. Analyses of variance and t-student analyses of $\delta^{13}C$ of taxa collected at different sites inside Chichancanab are presented in Appendix 1 supporting the observations of the box and whisker diagram (Figure 8.10).

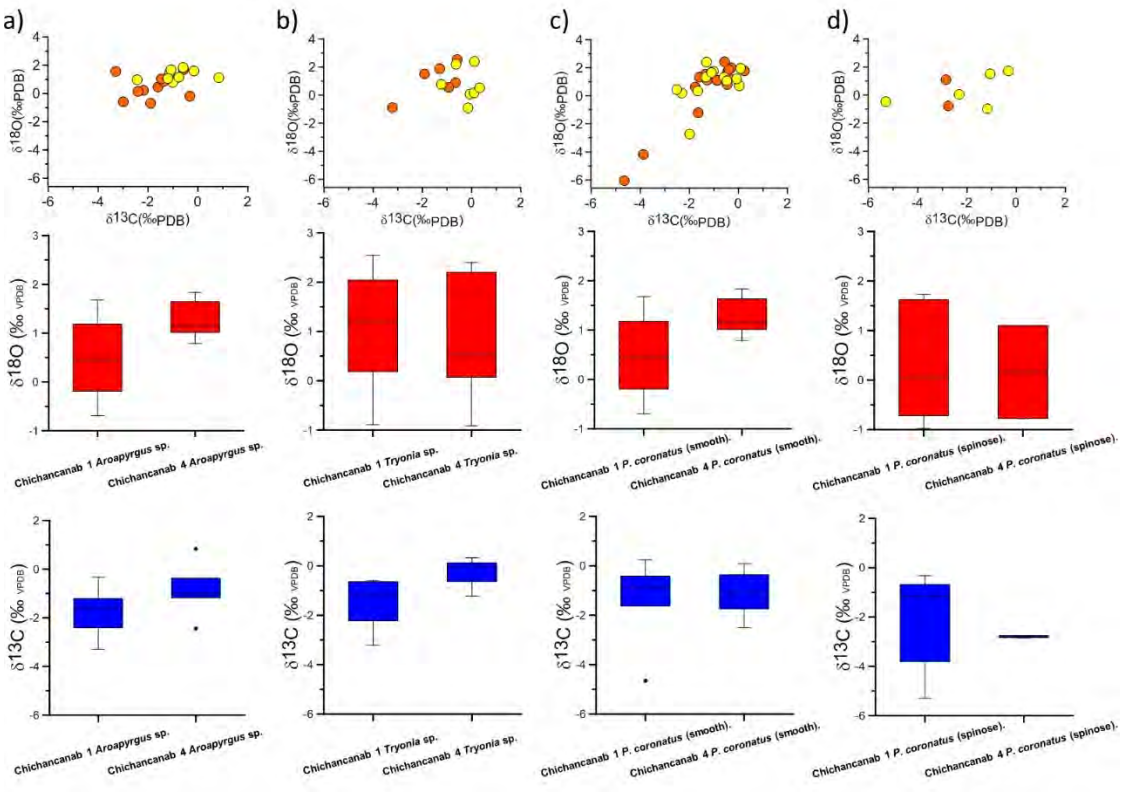

Figure 8.10 Comparison between samples of a) Aroaoyrgus sp.*; b) Tryonia* sp.*; c) P. coronatus (smooth form), and d) P. coronatus (spinose form) taken from different sites at Lake Chichancanab. For every sample taken from a different site inside the lake, the cross isotopic plot $\delta^{18}O$ and $\delta^{13}C$ is presented (upper part), followed by the box and whisker diagram of the $\delta^{18}O$ values of the shells (middle part) and the box and whisker plot of the $\delta^{13}C$ values of the shells. Middle line denotes median; box limits denotes lower and upper quarts; box and whiskers denotes minimum and maximum values. Black points indicate outliers.*

Figure 8.11 presents the results of the isotopic analyses done on shells of the family Hydrobiidae from two different sites in Lake Esmeralda. Site 9 did not contain the spinose form of *P. coronatus*; therefore, it was not possible to make a comparison for this taxon.

It can be observed that the shells of site 6 fall in an area with more positive values of $\delta^{13}C$ than the values of site 9.

The t-student and the analysis of variance showed that the difference in the median values of $\delta^{18}O$ between the two sites at Lake Esmeralda (Appendix 2) is not great enough to exclude the possibility that the difference is due to random sampling variability; there is not a statistically significant difference. This lack of significant difference between specimens according to the sites can be observed in the box and whisker diagrams for each taxon.

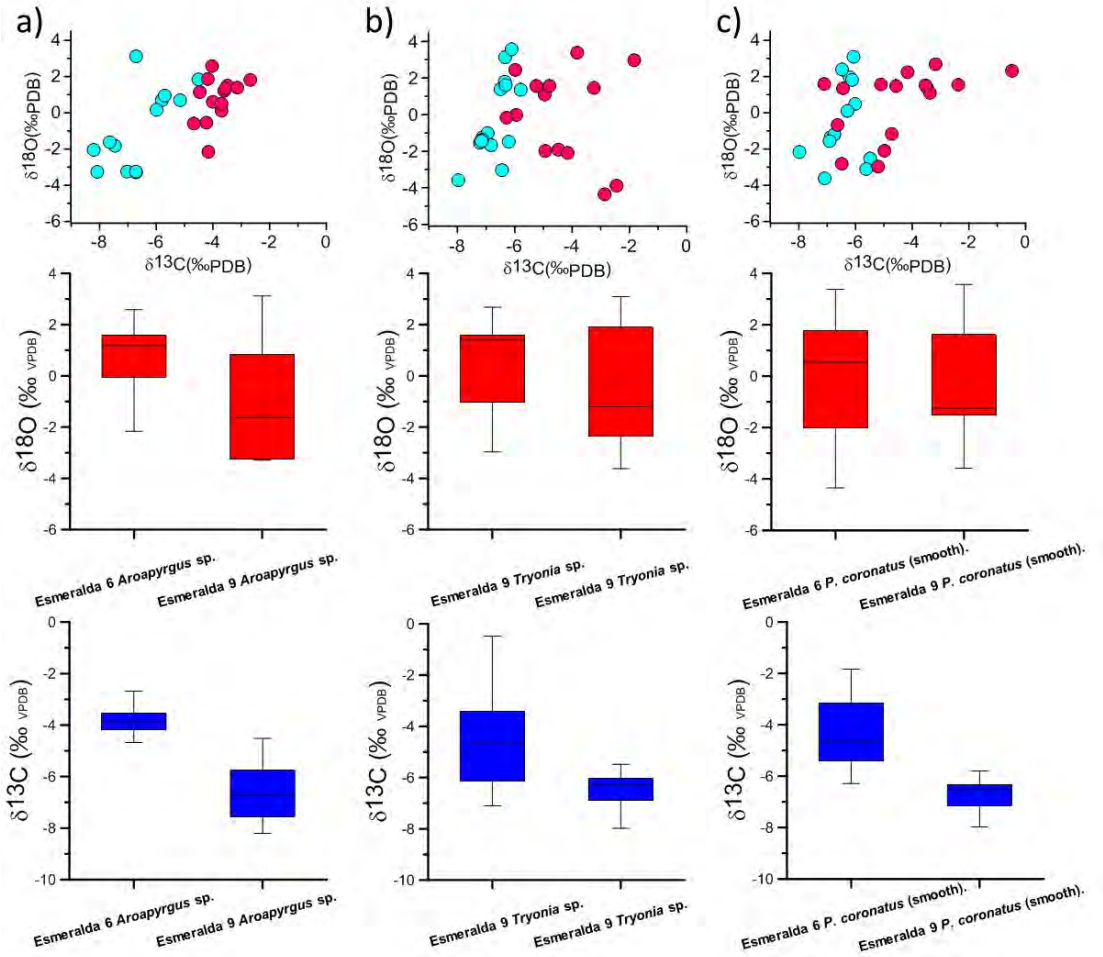

Figure 8.11 Comparison between samples of a) Aroaoyrgus sp.*; b) Tryonia* sp.*; and c) P. coronatus (smooth form) taken from different sites at Lake Esmeralda. For every sample taken from a different site inside the lake, the isotopic cross plot $\delta^{18}O$ and $\delta^{13}C$ is presented (top), followed by the box and whisker diagram of the $\delta^{18}O$ values of the shells (middle) and the box and whisker plot of the $\delta^{13}C$ values of the shells. Middle line denotes median; box limits denotes lower and upper quarts; box and whiskers denotes minimum and maximum values.*

The t-student and the analysis of variance done on the $\delta^{13}C$ values on populations from both sites at Lake Esmeralda (Appendix 2) showed that the difference in the median $\delta^{13}C$ values between the two sites for every taxon is great enough to exclude the possibility that the difference is due to random sampling variability; there is a statistically significant difference between taxa. These differences in $\delta^{13}C$ between the sets collected at different locations inside the lake can be observed in the box and whisker diagrams.

These results mean that the oxygen isotopic composition of the shells collected at Lake Esmeralda is similar regardless of where in the lake they were collected, but shells have a significant different $\delta^{13}C$ signature if they were collected from a different site inside the lake. The tests also show that the bimodal distributions in the $\delta^{18}O$ values occur at both sites. Therefore, based on the data available, the bimodal distribution of all the modern shells collected in Lake Esmeralda is not linked to the possibility that the bimodal distribution had been a mixture of shells collected at different sites inside the same lake since samples collected at the same site inside the lake (e.g. Esmeralda 6) still present the bimodal distribution.

8.7 Differences in the isotopic composition between lakes Esmeralda and Chichancanab

Figure 8.12 presents the cross plot of the isotopic composition of every genus for comparing the differences between Lake Esmeralda and Chichancanab. In Figure 8.12, shells from Chichancanab have more positive values of $\delta^{13}C$ in comparison to the shells of Lake Esmeralda in each taxon. The values of $\delta^{18}O$ of the shells of Chichancanab are constrained to an interval of around 4 ‰ units (except for some outliers in the smooth form of *P. coronatus*), while the $\delta^{18}O$ values of the taxa from Lake Esmeralda cover a range of 10 ‰ units. Unfortunately, the number of shells in cenote Chen Ha was too small to perform statistical analysis.

The t-student and the analysis of variance done on the $\delta^{13}C$ values on populations from both lakes (Appendix 3) showed that there is a statistically significant difference ($P = < 0.001$ see appendix 3), thus the differences in the median values between the groups are more significant than would be expected by chance. Excepting in $\delta^{13}C$ values of *P. coronatus* (spinose) where $P = 0.069$, therefore the differences are not significative (appendix 3). This difference is easily observed in the box and whisker diagrams of the $\delta^{13}C$ of specimens from both lakes for every taxon (Figure 8.12).

In the case of $\delta^{18}O$, the standard deviation is bigger in samples from Lake Esmeralda than in Chichancanab, which is observed in the box and whisker diagrams of $\delta^{18}O$, although

most of the values in Chichancanab are less dispersed and fell around the mode, therefore is a unimodal distribution (Poisson distribution type). The analysis of variance for $\delta^{18}O$ comparing both lakes (Appendix 3) showed that the sample means of the group collected at Esmeralda does not exceed the sample mean of the group collected at Chichancanab by an amount great enough to exclude the possibility that the difference is due to random sampling variability. The hypothesis proposing that the population mean of the group at Chichancanab is equal to the population mean of the group at Esmeralda cannot be rejected. This lack of a statistically significant difference is appreciated in the box and whisker plots, where it can be observed that the median values are very similar (Figure 8.12). Therefore, the variables related to the provenance (either Chichancanab or Lake Esmeralda) of the samples just affects the $\delta^{13}C$.

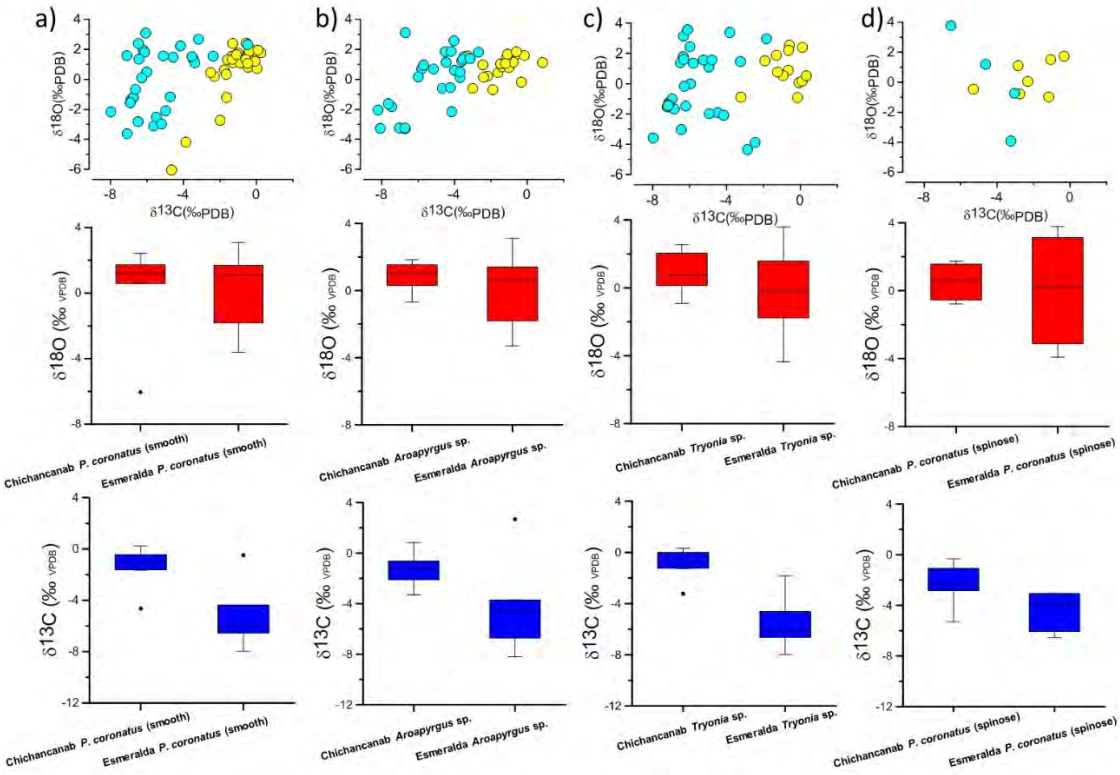

Figure 8.12 Comparison between samples of a) Aroaoyrgus sp.*; b) Tryonia* sp.*; c) P. coronatus (smooth form), and d) P. coronatus (spinose form) taken at Lake Chichancanab and Lake Esmeralda. For each sample taken from a different site inside the lake, the isotopic cross plot $\delta^{18}O$ and $\delta^{13}C$ is presented (upper part), followed by the box and whisker diagram of the $\delta^{18}O$ values of the shells (middle part) and the box and whisker plot of the $\delta^{13}C$ values of the shells. Blue circles represent Esmeralda samples, and yellow circles represent Chichancanab samples in the cross isotopic plot $\delta^{18}O$ and $\delta^{13}C$. Chen Ha samples (black circles) are also shown in the cross isotopic plot $\delta^{18}O$ and $\delta^{13}C$, however it was not possible to perform any statistical analysis on them. Middle line denotes median; box limits denotes lower and upper quarts; box and whiskers denotes minimum and maximum values. Black points indicate outliers.*

8.8 Discussion of the relationship between shell and water isotope values

In this section, a comparison between the calculated $\delta^{18}O$ of aragonite from the isotopic signature of water and the $\delta^{18}O$ of shells is discussed. The calculated mean from the $\delta^{18}O$ values in the sites O1 to O9 for precipitated aragonite is -1.55 ‰ in Esmeralda (Table 8.1) differs from the median $\delta^{18}O$ values for all modern shells picked in this lake (Figure 8.13). However, the median values of the shells of *Aroapyrgus* sp., *Tryonia* sp., and *P. coronatus* that fell around the smaller local minima in the bimodal distribution are similar to the mean calculated values of -1.55‰. This value is actually very similar for *Tryonia* sp. This resemblance might suggest that the subgroup of shells that surround the more negative local maxima in the bimodal distribution (subgroup N) was produced in winter. It can be hypothesised that the other group around the more positive local maxima (subgroup P) was produced in summer. Unfortunately, I was not able to collect water isotope samples in summer from Lake Esmeralda, so I could not have an estimation of the theoretical isotopic value of aragonite for summer. The spatial distribution of $\delta^{18}O$ can be observed in Figure 8.14. Some positive values are present around the edges, probably due to the discharge of water flows in contact with the soil (even though I would expect that such flows would be more enriched in ^{16}O and therefore more negative). Anyway, the difference between the values inside the lake is around 0.24 ‰, which is twice the analytical error.

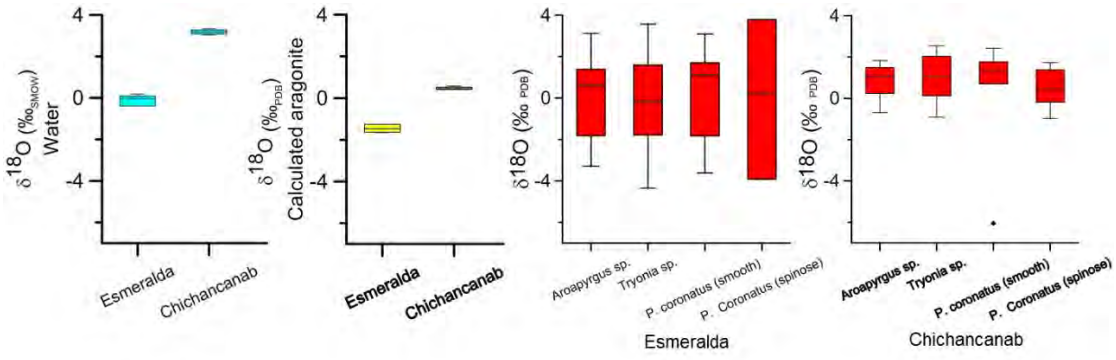

Figure 8.13 Comparison between the calculated composition of aragonite from water and the isotopic composition of shells from different taxa of Hydrobiidae in lakes Esmeralda and Chichancanab. According to the XRD, the mineral composition of shells is aragonite. Middle line denotes median; box limits denotes lower and upper quarts; box and whiskers denotes minimum and maximum values. Black points indicate outliers.

For Chichancanab, the mean calculated values for precipitated aragonite was 0.53‰, which is slightly different from the mean values of the complete set of specimens from every taxon, of 0.83‰, 0.91‰, and 0.69‰ for *Aroapyrgus* sp., *Tryonia* sp. and *P. coronatus* (smooth) respectively (Figure 8.13). The comparison between the median is possible since the

specimens from Chichancanab had a unimodal distribution. In this case, the isotopic composition of the shells would be near the expected isotopic composition of aragonite.

The discrepancies might be due to temperature differences. This match between the theoretical and measured value supports the idea that in Chichancanab, the isotopic value of the shells represents the annual isotopic variation. This match could imply that Chichancanab has a longer residence time and the differences in the isotopic composition of water varies only slightly between summer and winter due to the size of the lake (despite the lack of a bigger sample in a more extensive lake). For instance, measurements show that the differences in the isotopic composition of water in the Lake Petén Itzá between summer and winter are not large (Pérez et al., 2013). But this might not apply to Chichancanab since Peten Itza is a much bigger lake in terms of water volume.

In contrast, Esmeralda, which is a smaller and more open lake, might have a very different water isotopic composition between summer and winter (besides more variability between years as demonstrated in Figure 8.1). This idea is supported by the monitoring of rainfall water collected at the location of Rio Secreto Cave, where differences of 6 ‰ in the isotopic composition between summer and winter between 2014 to 2017 were recorded (Lases-Hernandez et al., 2019). This cave on the Caribbean coast is in the same hydroclimatic region than Chichancanab and Esmeralda. These differences might be exacerbated in the lake because of the predominance of less effective rainfall (evaporation-precipitation ratio) during the dry season in contrast to the rainy season (see figure 5.2 in chapter 5) (CONAGUA, 2010b).

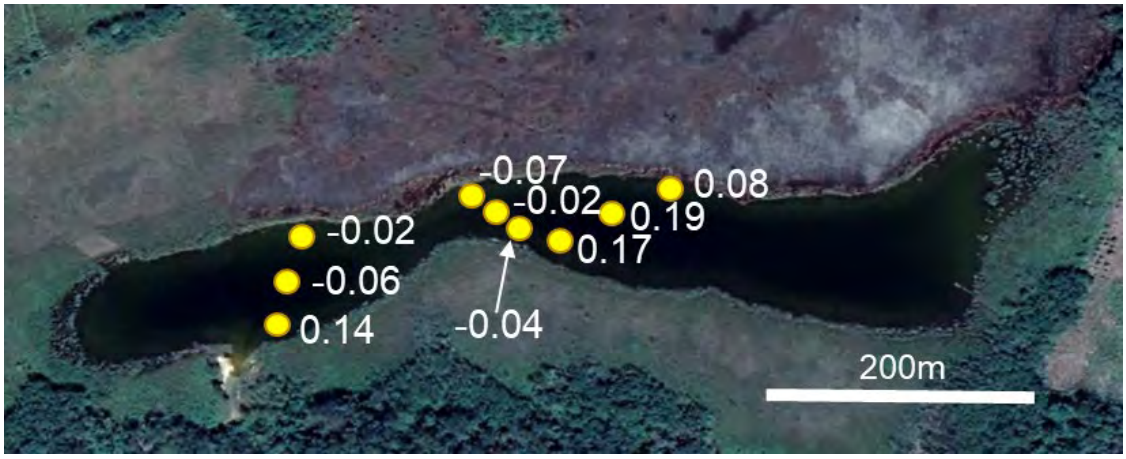

Figure 8.14 Distribution of $\delta^{18}O$ ‰ values of water samples from Lake Esmeralda collected in January 2018.

All this might imply a different isotope composition of precipitation between winter and summer in both lakes, since the isotopic composition depends on the amount of rainfall.

For instance, Cejudo et al., (2020) interpret the $\delta^{18}O$ values of meteoric water samples (from 0.83 to -9.7 ‰) in the Mayab as a result of seasonal variability. Meanwhile, Media-Elizalde et al., (2016b) observed the decrease of values of $\delta^{18}O$ from -1‰ to -8‰ following the increase in precipitation from practically 0 to 400 mm per month in the Riviera Maya in Quintana Roo. Because of its size, Chichancanab does not present a significant variation in the composition of water. This is supported by the isotopic composition of water samples collected in summer (Figure 8.1 green circles) compared with the samples collected in winter (Figure 8.1 white, yellow and orange circles). However, a more open lake like Esmeralda is more sensitive to seasonal changes in precipitation isotope values (Leng and Marshall, 2004).

Escobar et al. (2010) calculated the number of shells needed in every sampled layer of a core from Chichancanab to have a value that represents the actual isotopic composition of carbonates. Their calculations showed a standard deviation similar to the one that I obtained from the modern shells in Chichancanab. Their calculations also implied a unimodal distribution of the isotopic values of the specimens from the same layer.

The condition of normality and therefore of a unimodal distribution was always met in the values of the isotopic signature of the samples collected in Chichancanab. In contrast, such a condition does not exist in Esmeralda. Therefore, it is not possible to calculate the number of shells needed to have a reliable value of the isotopic composition if the bimodal distribution of the isotopic composition of Hydrobiidae's shells indicates two population produced at different seasons during a year. The isotopic analysis of single shells could provide a record of the differences between summer and winter.

It can be argued that individual shells do not only calcify either in summer or winter for having the isotopic signature of only one season. A study in Spain indicates that the span of life of Hydrobiidae is up to 2 years but many live 1.5 years (Drake and Arias, 1995), which indicates that they have lived more under a specific season that under both seasons. In addition, counting of Hydrobiidae in some lakes of Spain shows that there are more Hydrobiidae of a specific taxon during the rainy season in comparison to the dry season (Drake and Arias, 1995). This suggests that most Hydrobiidae survives only a season (6 months), indicating that they developed shells under a specific season, either rainy or dry. Unfortunately, this kind of studies have not been performed in the Mayab, yet. But I argued that this scenario might be also possible for this region.

small in size. Therefore, this scenario in section 8.5 looks to be the better candidate to explain the possible differences between the two subgroups responsible for a bimodal distribution. Unfortunately, as noted previously, I was not able to perform fieldwork in Summer, so I do not have water samples from Summer to test this argument.

While the calculated value of $\delta^{18}O$ of aragonite is more negative than the mean value of the analyses for this genus in Esmeralda, the opposite situation happens in Chichancanab (Figure 8.13). The standard deviation in shells of *Pyrgophorus coronatus* from cores of Chichancanab varied from 0.52 to 1.01 ‰ (Escobar et al., 2010), which is a range lower than the 1.895 obtained in our modern samples. I do not have a convincing explanation for this discrepancy. A possible difference is that the number (39) of modern samples tested is bigger than the number (mean of 14) of tested in every layer by Escobar et al. (2010).

8.9 Isotopic composition of individual shells compared to the isotopic composition of bulk sediment at different levels of the core

Figure 8.15, Figure 8.16 and Figure 8.17 show the cross plots of the isotopic composition of single shells of *P. coronatus* taken from different layers of the Esmeralda core (Table 8. 9). They tend to group in two different regions of the plot in each layer, but there are some layers where they group in only one region of the plot. In this way, the results show that the bimodal distribution of $\delta^{18}O$ of shells per layer (or even multimodal) is maintained in most of the stratigraphic layers.

Table 8.9 Stratigraphic layers selected for analysing single shells.

Type	Taxon	Layer	Up border Depth MS (cm)	Bottom border Depth MS (cm)	Youngest Age	Oldest Age
Interface	*P. coronatus (smooth)*	Modern	0	1	-66	-67
Inner Core	*P. coronatus (smooth)*	ES1601-I 20-22	20	22	453	515
Inner Core	*Hydrobiidae*	ES1601-I 20-22	20	22	453	515
Inner Core	*P. coronatus (smooth)*	ES1601-I 35-36	35	36	919	947
Inner Core	*P. coronatus (smooth)*	ES-16-02-I 70-71	37	38	984	1009
Inner Core	*P. coronatus (smooth)*	ES-16-01-II 41-42	107.5	108;5	2234	2288
Inner Core	*P. coronatus (smooth)*	ES-16-02-I 53-54	119.5	129.5	2863	2906
Inner Core	*P. coronatus (smooth)*	ES-16-02-I 65-66	131.5	132.5	3526	3574
Inner Core	*P. coronatus (smooth)*	ES-16-01-II 73-74	140	141	3914	3957
Inner Core	*Hydrobiidae*	ES1602-I-80-81	147	148	4109	4121
Inner Core	*P. coronatus (smooth)*	ES-16-02-II 57-58	170	171	4345	4356
Inner Core	*P. coronatus (smooth)*	Es-14-3 36.5- 37.5	246.5	247.5	5163	5173
Inner Core	*Hydrobiidae*	ES1601 IV 80-82	307.5	309.5	5826	5850
Inner Core	*P. coronatus (smooth)*	Es-14-4 89 -90	383.5	384.5	6623	6634

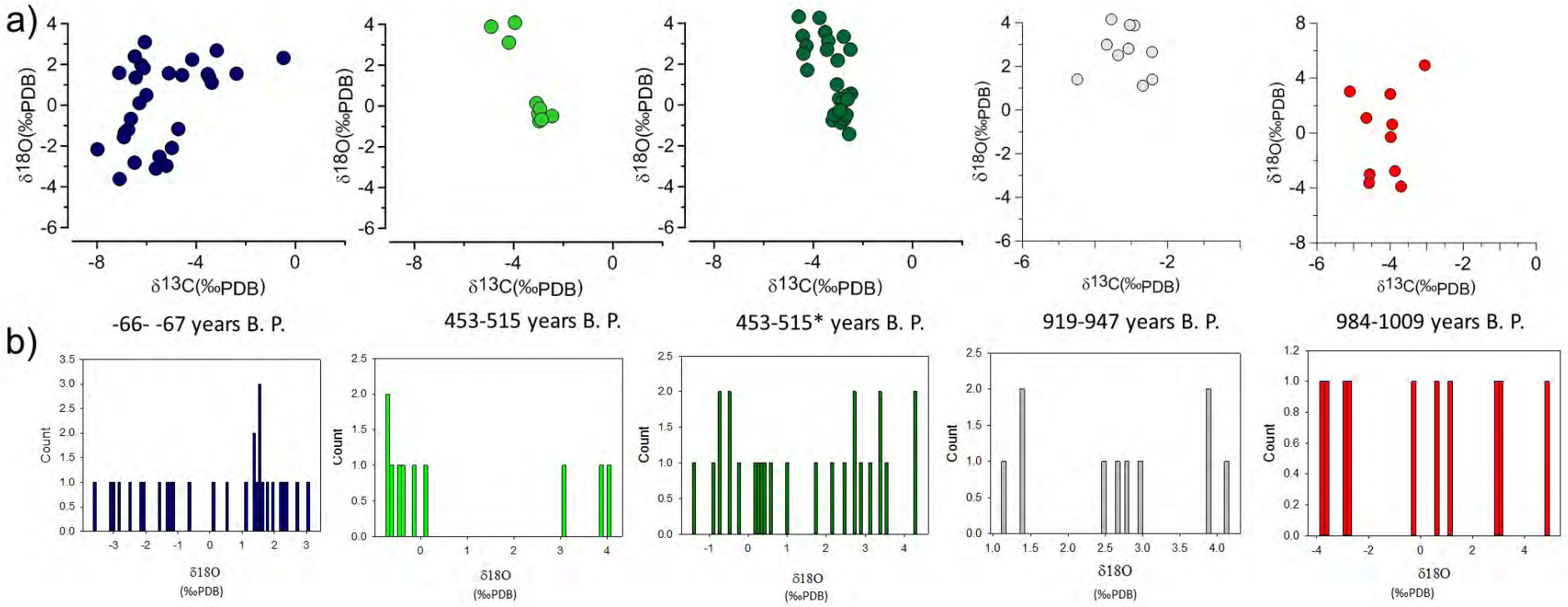

Figure 8.15 a) cross plot of oxygen isotope composition $\delta^{18}O$ and $\delta^{13}C$ of single shells of Pyrgophorus sp. *obtained from stratigraphic layers. Each colour corresponds to shells from a particular layer. b) Histograms presenting the distribution of the oxygen isotopic composition values, the widths of the bins were established based on the analytical uncertainty of the values. The numbers at the centre represent the period covered by 1 cm of sediment at every stratigraphic level. Numbers with an asterisk indicate layers where all kinds of Hydrobbiidae were collected instead of selecting just Pyrgophorus* sp.

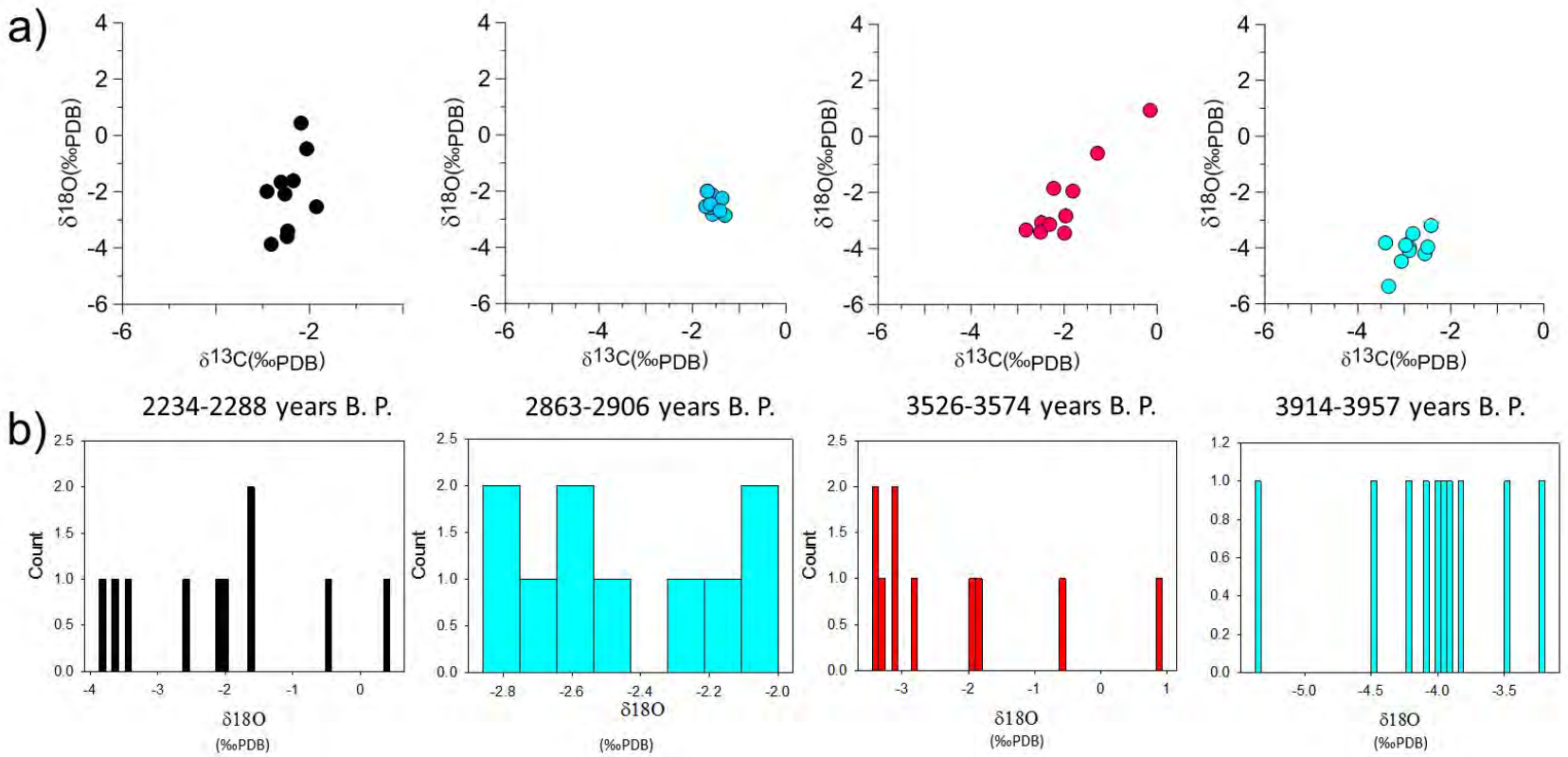

Figure 8.16 *a) cross plot of oxygen isotope composition $\delta^{18}O$ and $\delta^{13}C$ of single shells of Pyrgophorus* sp. *obtained from stratigraphic layers. Each colour corresponds to shells from a particular layer. b) Histograms presenting the distribution of the oxygen isotopic composition values, the widths of the bins were established based on the analytical uncertainty of the values. The numbers at the centre represent the period covered by 1 cm of sediment at every stratigraphic level. Numbers with an asterisk indicate layers where all kinds of Hydrobbiidae were collected instead of selecting just Pyrgophorus* sp.

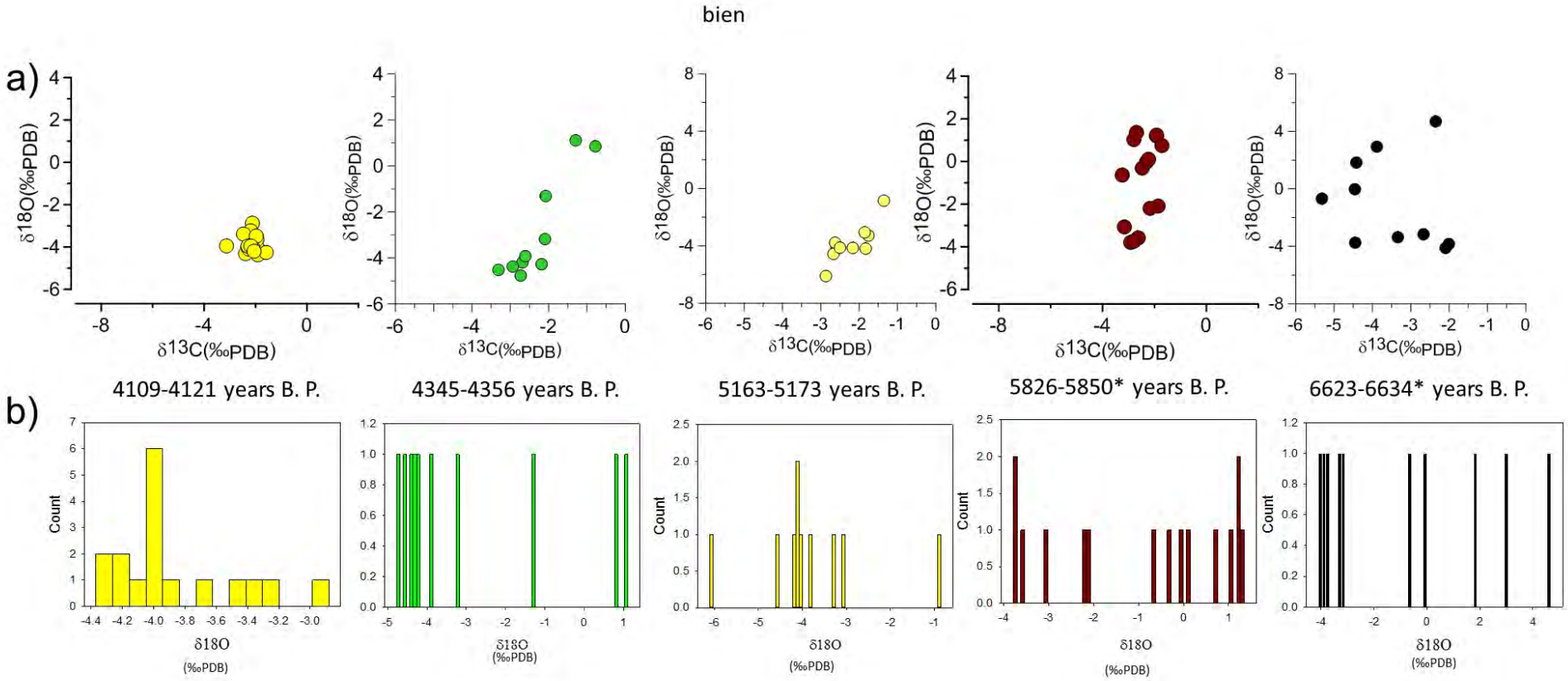

Figure 8.17 *a) cross plot of oxygen isotope composition $\delta^{18}O$ and $\delta^{13}C$ of single shells of Pyrgophorus* sp. *obtained from stratigraphic layers. Each colour corresponds to shells from a particular layer. b) Histograms presenting the distribution of the oxygen isotopic composition values, the widths of the bins were established based on the analytical uncertainty of the values. The numbers at the centre represent the period covered by 1 cm of sediment at every stratigraphic level. Numbers with an asterisk indicate layers where all kinds of Hydrobbiidae were collected instead of selecting just Pyrgophorus* sp.

The intervals between 4109 to 4121 years B. P. (Figure 8.16), 3914 to 3957 years B. P. (Figure 8.16) and between 2863 to 2906 years B. P. (Figure 8.17), however, present unimodal distributions. these unimodal distributions might imply periods when Chichancanab and Lake Esmeralda were connected. Another explanation might be that during these periods, there were no essential differences between the summer and wintertime, which could imply a dry summer or a very rainy winter. A similar scenario would happen for the period between 4109 to 4121 years B. P.

The impact of possible differences in the ages of the shells from the same layer that could explain the bimodal distribution of the samples (see discussion in section 8.4), should also be considered. For instance, in Figure 8.16, the layer with a unimodal distribution between 3914-3957 years B. P. covers a time frame of 43 years. In contrast, other layers at the core; e. g. the layer at 453-515 and the layer 984-1009 years B. P. cover a period of 52 and 25 years, respectively (Figure 8.15). We have to remember that these ages are the median values of the intervals of possible ages assigned as calibrated ages (see section 9.1 in chapter 9). An interval of possible calibrated ages can cover an average of 290 years in the CLAM Model and 903 years in the Bacon Model with $\alpha = 0.6$. Therefore, the calculated time frames of a layer were calculated using central values (median) of the calibrated ages.

In Figure 8.17, the range of the layers with a bimodal distribution is 11 years, while the period covered by the layer with a unimodal distribution is 24 years, which is longer. These observations imply that possible differences in age between the shells are not the leading cause of the bimodal distribution, although this idea cannot be wholly discarded.

Another explanation for the unimodal distribution in the layers between 2863 to 2906 years B. P. (Figure 8.16), 3914 to 3957 years B. P. (Figure 8.16) and between 4109 to 4121 years B. P. might be related to a diagenesis, which would not have shown diagenetic structures on the shells. However, diagenesis is discarded, since the isotopic signature would have changed during the recrystallisation from aragonite to calcite (James and Jones, 2016). This is not consistent with the observation of the coincidence between the median value of the isotopic signature of shells at those levels and the isotopic value of the corresponding bulk carbonate sediment of the surrounding stratigraphic layer (see next paragraphs).

Figure 8.18 shows a comparison between the low-resolution record based on the isotopic composition of bulk sediments and the isotopic composition of single shells (whose distribution has been already discussed above), including their median and mean per stratigraphic layer.

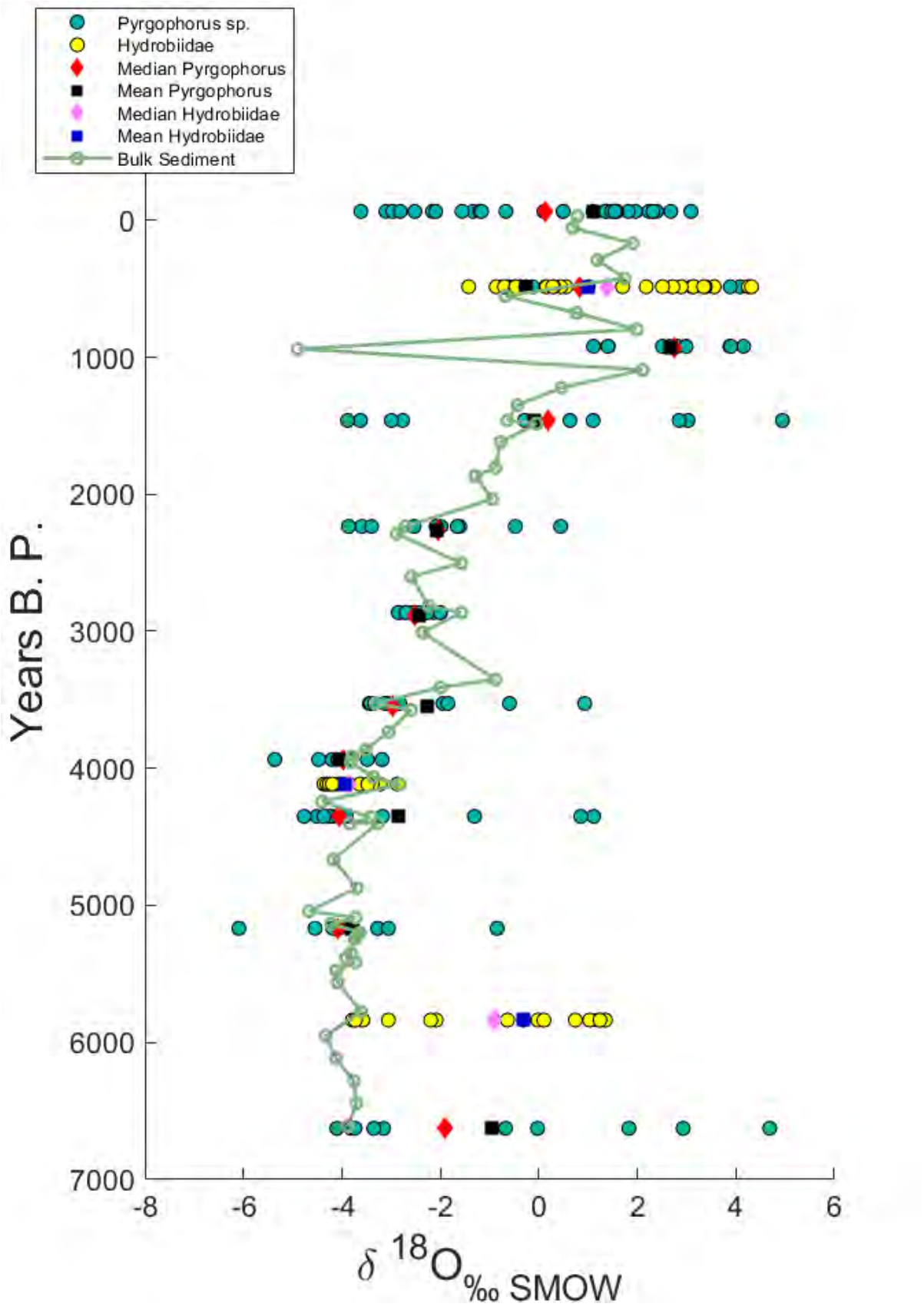

Figure 8.18 Isotopic compositions $\delta^{18}O$ of single shells of Pyrgophorous sp. *from nine levels (or Hydrobiidae in three levels) compared with the low-resolution $\delta^{18}O$ record developed from sieved sediments (< 250µm) sampled every 10 cm in the Esmeralda core sequence. The plot shows the calculated median and means of the isotopic values obtained from single shells from each stratigraphic level studied.*

The median values (red diamonds) are similar in most of the stratigraphic layers to the value of the isotopic composition of the bulk sediment. An exception is the deepest stratigraphic layer analysed between 6623 to 6634 years B. P., where neither the median nor the mean of the composition of single shells coincides with the isotopic signature of the bulk sediment.

Unsurprisingly, the median and the mean are very close and coincide with the value of the bulk sediment in the stratigraphic layer between 3914-3957 years B. P., where the distribution is a unimodal distribution. Another exception happens in a layer between 984 to 1009 years B. P., where the mean of the isotopic composition of the shells (and not the median) is similar to the isotopic composition of the bulk sediments.

The median of a set of data is not sensitive to outliers (Gonick and Smith, 1993). This fact might explain why the isotopic signature of the sediment coincides in most stratigraphic layers with the median of the isotopic composition of shells instead of the mean.

Since the isotopic composition of the individual shells does not have a unimodal distribution in most of the stratigraphic layers, there is no point in performing an analysis of isotopes of a composite of shells from the same layer.

Sensu stricto, a composite of shells should require that we would have the same amount of aragonite from every shell. This is a challenge since the size and density of the shells varies (Covich, 1976, 2010). (This was observed by the author, e.g. differences in density were inferred by differences in the translucent or opaque character of the shells). The isotopic values of the composite would give a value similar to the mean.

After having assessed the differences between the different approaches, I have seen that in the case of Lake Esmeralda, there is no advantage to using single shells over the bulk sediments. Therefore, I will continue to develop the bulk sediment isotope record at a higher resolution.

8.10 Conclusions

The goal of the isotopic analysis in modern shells is to establish the possible differences in the preservation of the environmental signal recorded in shells between Lake Esmeralda and Chichancanab, as well as to develop a strategy to recover that signal from ancient shells in sediments from Lake Esmeralda. The absence of correlation between the presence of diagenetic structures and $\delta^{18}O$ implies that our method for cleaning the shells functions well. It also suggests that the shells do not suffer major diagenesis due to early burial. The

ultrasonic bath with distilled water and the use of plasma ashing, as well as mechanical cleaning when it was needed, was enough to remove contaminants since no major contaminants were observed at the microscope and major outliers in the isotopic analysis were not present. The mineralogical and morphological study of the shells also indicated that it is impossible to establish if the diagenetic structures are the product of dissolution, cementation of allochthonous material or recrystallisation of the aragonite that constitutes the shells initially. Some diagenetic structures indeed remained after cleaning, covering a low proportion of the total area, but they do not look to impact the isotopic signal $\delta^{18}O$.

Provenance from different lakes just affects the $\delta^{13}C$ but not the $\delta^{18}O$, as seen in shells of the different genus of Hydrobiidae, while there is no impact on the isotopic composition of the provenance from different sites in the same lake as tested using the different taxa. This discrepancy between the similar $\delta^{18}O$ of shells of gastropods in both lakes, but a different isotopic composition of water (Figure 8.1) might be related to the big standard deviation that the isotopic values of Hydrobiidae (Figure 8.13) have in Esmeralda. Perhaps a sampling of water during other months might overlap the isotopes values of water of both lakes at some point. In any case, monitoring both lakes during a year would help to resolve this discrepancy.

The use of different genera of the family Hydrobiidae from the same lake also gives similar values in the isotopic composition $\delta^{13}C$ and $\delta^{18}O$, showing that they could be used without distinction for climatic reconstruction when they come from the same stratigraphic layer and from the same lake.

While the isotopic composition of single shells of every taxon in Chichancanab has a unimodal distribution, the composition of the specimens collected in 11 of the 14 stratigraphic layers of Esmeralda presented a bimodal distribution in all taxa. This bimodal distribution implies the existence of two different groups for every taxon over a particular time period (Figure 8.15 to 8.17). The differences within each group could be due to differences in the niche, gender or age of the specimens, the age of the shells, season of the development of the shells (winter or summer) or random process.

Based on the theoretical value of aragonite and knowing by XRD that the shells are composed of aragonite, the subset N of each taxon (with more negative values) in modern samples should have been developed in the winter season because they coincide with the values calculated from water obtained in winter. However, more negative isotope values are associated with a smaller evaporation-rainfall ratio, but this is not the case for the month of January in the Cochuah Region. Figure 5.2 in chapter 5 shows the evaporation-rainfall

ratio at La Presumida meteorological station, the nearest to Lake Esmeralda. It can be observed that the season from January to April presents the months with the highest evaporation-precipitation ratio. Therefore, the N subset could never be developed during winter. This rejects the third scenario of section 8.5. Therefore, I do not have an explanation of the bimodal distribution on shells. However, data of the isotopic composition of water in Lake Esmeralda in summer would still be desirable for resolving any doubt related to the link between the bimodal distribution and seasonal changes in the water composition of the lake, since the lake could still retain the isotopic signature of the previous season (although this retention is highly implausible). This hypothesis would have opened the possibility to know the variations in the isotopic composition between winter and summer, making the gastropods from small and relatively close lakes a resource for knowing interannual variations in a lake.

The high standard deviation in the isotopic signature of Hydrobiidae's shells in Esmeralda compared to Chichancanab is not completely explained by the fact that the lake is more open than Chichancanab, according to the water isotopic composition.

In addition, if the calculated aragonite values do not coincide with the mean values of the complete set and the P subset and their coincidence with the N-subset is by chance, then the precipitation in aragonite might not happen in isotopic equilibrium.

Finally, the existence of a bimodal distribution implies that carrying out isotope analysis on a composite of single shells can be problematic. The coincidence between the median value of the shells with the isotopic composition of the bulk sediment in most of the stratigraphic layers studied indicates that the isotopic composition of bulk sediment in Esmeralda does not reflect the isotopic composition of in-washed sediment from the karst, but actually the lake water isotope values and hence palaeoclimatic conditions. This means that the isotopic composition of the bulk sediments can substitute for the analysis based on shells in Lake Esmeralda.

This page intentionally left blank

Chapter 9 Environmental History of Lake Esmeralda

Photo: Lake Esmeralda in the Cochuah Region

"It took its name from being a fertile territory appropriate for the cultivation of maize and beans. In this way, it was never famine. Therefore, Cochuah means -our food of bread-… The territory of Cochuah was cover by big and dense forest and it was not flat, cause there were rough mountainous hills and small mountains far away from the principal mountains system of Yucatan, they broke the territory at some point, by the location of Lake Chichan Kanab, and next to the kuchkabal of Chetemal. For that side, fordable swamps were found in the dry season, but they were very dangerous in the rain season, and there were many cenotes with unfinished, fresh and pure water whole year."

Historia del descubrimiento y conquista de Yucatán.

Juan Francisco Molina Solís, 1896.

This chapter presents the results related to the analyses performed on sediments collected from Lake Esmeralda and the environmental reconstruction inferred from them. The first section presents the age model. The next three sections describe the different proxies obtained and their interpretation, discussing the issues of recovering an accurate palaeoenvironmental signal. The last sections show the environmental reconstruction and their comparison with other environmental and archaeological records in the region.

9.1 Age Model

The age model is based on the radiocarbon dates obtained on samples of bulk sediments of Lake Esmeralda (Table 9.1) (see section 6.5 in chapter 6). The age of the plant macrofossil Beta-431931 (Table 9.1) is much younger than the ages taken from the bulk sediments (excepting SUERC-75747), therefore it is not in stratigraphic order related to the others. This date was not taken into consideration for the age model.

The radiocarbon dates of the bulk sediment samples were corrected considering the hard water effect since the lake is in a karst environment and the age at the interface is not modern (over 100 pMC). I used the date at the water-sediment interface for correcting, assuming that the correct date should have been -66 years B. P. (the year of the collection of the core). In this way, every radiocarbon age was corrected, by 330 years, the age difference between the assigned conventional age 264 ± 35 and the real age -66 B. P. at the top of the sedimentary sequence. The output model created by CLAM is a piecewise linear model (Figure 9.1). A comparison with the images of the core shows that the dating points SUERC-75751 and SUERC-75752 at 46.25 and 94.75 cm respectively (Figure 9.1 yellow triangle in ES-16-01 core) coincide with changes in the texture, probably resulting in part from changes in the sedimentation rate. However, that is not the case for the fourth dating point (SUERC-75753 at 144.25 cm), where no textural change is easily observed.

Figure 9.2 shows the age model (see section 6.5 in chapter 6) produced using the default value accumulation rate, alpha = 1.54 in BACON (Blaauw and Christen, 2011). It can be observed that the fourth calibrated radiocarbon date, SUERC-75753 did not fall inside the median values of the model with an $\alpha = 1.54$. However, the oldest proposed age at the layer at 144.25 cm just overlaps with the youngest border of the uncertainty of the calibrated ages (red uncertainty bars indicate the interval covered by the calibrated ages at 2σ range error with the highest probability result). In this way, the model $\sigma = 1.54$ indicates that the sedimentation rate would have been the same until 1063 -1333 years B. P. I started to use other smaller values for the alpha accumulation shape parameter, which indicated

Table 9.1 Radiocarbon dates from Lake Esmeralda. Dating was carried out using the Accelerator Mass Spectrometer (AMS) technique at the Natural Environment Research Council (NERC) radiocarbon facility. Calibrated dates were obtained using CLAM. The age at the top of the core is fixed at -66 calibrated years B. P., which is the date of coring.

Publication Code	Nature of sample	Stratigraphic position (cm)	Layer at Core-Drive	^{14}C Enrichment (% Modern ± 1 σ)	Conventional Radiocarbon Age (years B. P. ± 1 σ)	Corrected hard effect Conventional Radiocarbon Age (years B. P. ± 1 σ)	Clam 2σ youngest age (cal. years B. P.)	Clam 2σ oldest age (cal. years B. P.)	OxCal Probablility at 2σ	$\delta^{13}C_{VPDB}$ ‰ (± 0.1)
SUERC-75747	Bulk sediment	0	Water-Core Interface	96.77 ± 0.42	264 ± 35	-66	-66	-66	95	-27
SUERC-75751	Bulk sediment	46.25	Inner core at ES-16-01-I ES-16-02-I	81.64 ± 0.37	1630 ± 37	1300 ± 72	1063	1333	95	-23.5
SUERC-75752	Bulk sediment	94.75	Inner core at ES-16-01-II ES-16-02-I	77.16 ± 0.36	2083 ± 37	1753 ± 72	1530	1829	93.6	-25.9
SUERC-75753	Bulk sediment	144.25	Inner core at ES-16-01-II ES-16-02-II	60.02 ± 0.28	4101 ± 37	3771 ± 72	3972	4359	90.4	-20.8
SUERC-82294	Bulk sediment	387	Inner core at ES-14-4	46.64 ± 0.21	6127 ± 36	5797 ± 71	6438	6749	94.6	-21
Beta-431931	Plant	94.75	Inner core at ES-14-2	no apply	1450 ± 30	no apply	1300	1390	68	-23.8

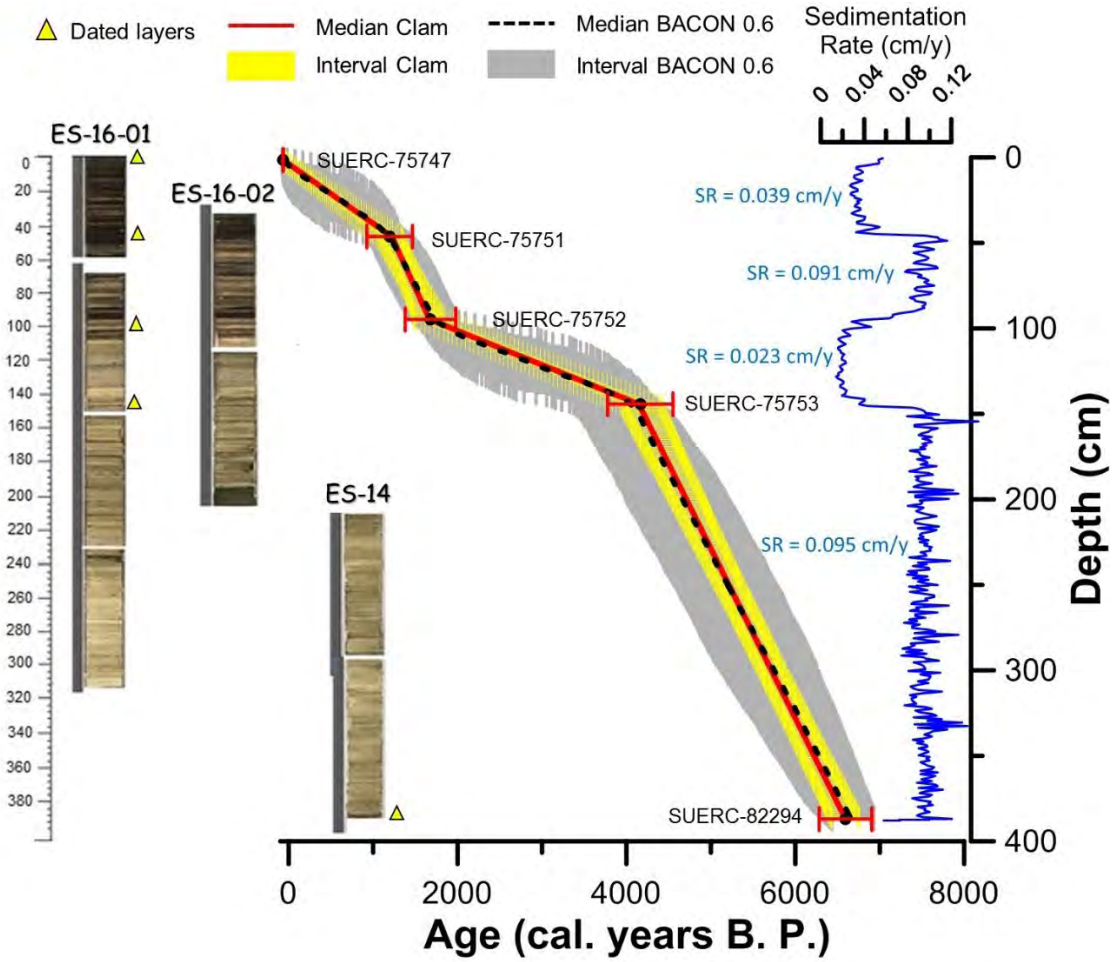

Figure 9.1 Age Model for the sediments from Lake Esmeralda. Left: Stratigraphic correlation between cores ES-14, ES-16-01 and ES-16-02. The yellow triangles indicate the stratigraphic layers where a sample was taken for radiocarbon analysis. Codes for the radiocarbon samples were assigned by the NERC radiocarbon laboratory. Centre: Age model used in this research, calculated using an a = 0.6 in BACON 2.2 in comparison to our model based on CLAM. Both models are shown with the images of the cores and the estimated sedimentation rate. Right: sedimentation rate record calculated from the BACON 0.6 age model.

that abrupt environmental changes could have happened. Different models using different values of α between 1.54 and 0.2 were run. As an example, I present the model produced on BACON using an α = 0.8 (*Figure 9.2*). Its median values fall inside de the interval assigned for the calibrated ages. However, the area of the resulted possible ages cover a more extensive range for most ages (Figure 9.1 cyan area) in comparison to the area of the model at 0.6 Figure 9.1 grey area).

I selected the alpha accumulation shape of 0.6, which produced a model where all the calibrated radiocarbon ages fall inside the median values of the produced model, and the uncertainty of every level was the narrowest (*Figure 9.2*). The BACON model, with the accumulation shape of 0.6 was very similar to the previous model obtained using CLAM (Figure 9.1). However, the range of possible ages for every layer is wider than the interval

assigned by the model produced in CLAM. I have to emphasise that our model in CLAM was our first attempt for an age model, and it was developed previously and independently from the model also developed in CLAM by Bermingham (2020), which used the same radiocarbon ages. For simplicity, I will use the median values of the age model produced in BACON with an α + 0.6 for developing the time series for every proxy at Lake Esmeralda, for being consistent with the BACON Model used in Lake San Lorenzo.

According to the BACON Age Model with α = 0.6, the mean sedimentation rate from 387 cm (SUERC- 82294) to 144.25 cm (SUERC-75753) was 0.095 cm/year, being the highest sedimentation rate for the complete sedimentary sequence (Figure 9.1). The sedimentation rate between 144.25 cm (SUERC-75753) to 94.75 cm (SUERC-75752), in contrast, was the lowest with 0.023 cm/year. The sedimentation rate is 0.091 cm/year between 94.75 cm (SUERC-75752) to 46.25 cm (SUERC75751), which is similar to the sedimentation rate at the bottom. For the interval between 46.25 cm and the top (0 cm), the sedimentation rate is again low, with a mean value of 0.039 cm/year.

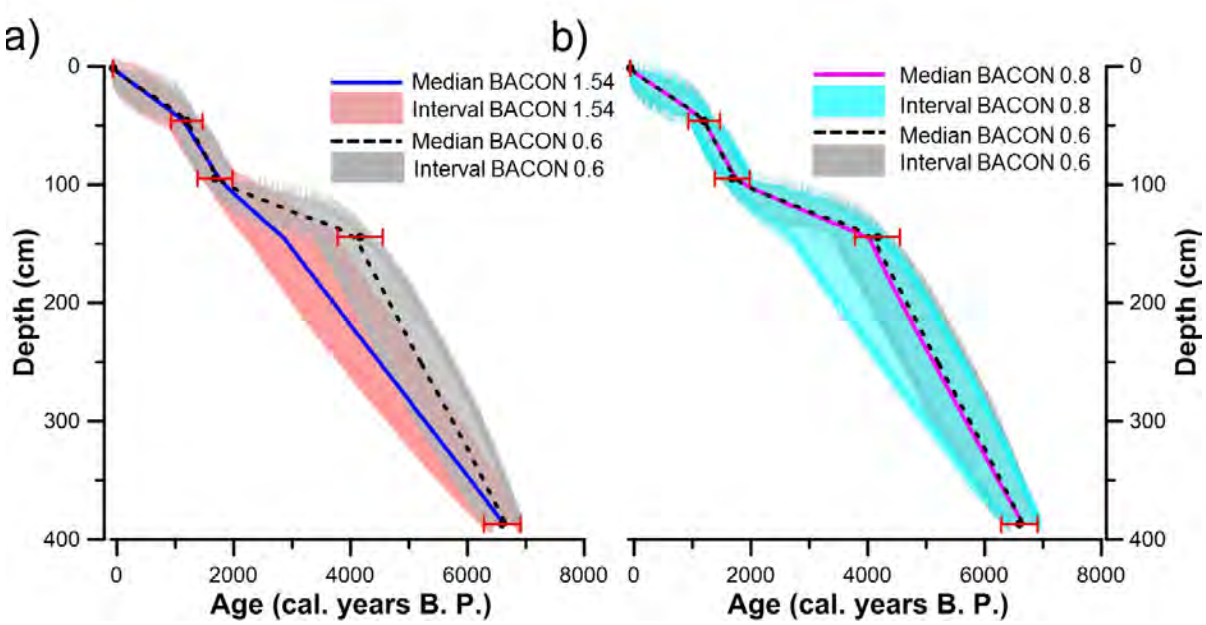

Figure 9.2 Examples of age models generated using different values of a) α = 1.54 and b) α =0.8 within BACON 2.2 in comparison to the model selected of α = 0.6.

9.2 Visual description and mineral composition of the core

The sediment sequence is characterised by high carbonate and low organic percentages from the bottom of the core to around 95 cm (Figure 9.1). The carbonate-rich sediment mostly comprises alternating layers or bands of pale olive (5Y6/3) and pale yellow (5Y7/3) silts, interspersed with <1mm laminations of light grey (5Y7/2), brown (7.5YR4/2) or

reddish black (2.5YR2.5/1) sediment is assumed to be either more organic or being still carbonate but less dense (Figure 9.1).

In the texture and the layer width record (Figures 9.6) there is not a visible change in the point of inflection at 144.25 cm. Meanwhile, visible changes are observed in the inflexion points at 94.75 cm and 46.25 cm. Also, the layer counts, between 387 cm and 0 cm, gave 4106 layers (see section 6.7 in chapter 6), showing that the number of them does not reflect an annual phenomenon or that annual layers have not been developed during some periods. Thus, layers cannot be used for improving the age model. An interesting fact is that there are 1475 layers from 4407years B. P. to -66 years B.P., while there are 2467 layers for the period between 6617 -6755 to 4149 - 4407 years B. P., covering 2468 - 2348 years. So, layers could be annual in the more carbonate-rich part of the core. A second period, where the number of layers is similar to the chronology, occurred between 1256 – 1345 years B. P. and 1691 – 1829 years B. P. where there are 557 layers in 435 – 490 years.

The results of the XRD analysis performed on six samples through the core (see section 6.4 in chapter 6) shows that the principal mineral component is calcite. The XRD analysis at 10 cm from the top (around 150 years B. P.) was the only sample indicating the presence of gypsum (Figure 9.3b). This phase was the second most abundant in that sample. XRD samples could not distinguish other mineral phases in the sample, meaning that besides the organics, the rest of the inorganic material is completely vitreous or is a nanomaterial. As I describe in later sections, more than 10% of the inorganic material would be amorphous or nanomaterial. As we observed in section 8.3 in chapter 8, the shells of modern gastropods are composed of aragonite, which is a different allotropic form of $CaCO_3$. Therefore, the mineral composition of the bulk sediment is different from the gastropods, even though both are composed of $CaCO_3$. I did not analyse the mineral composition of shells collected from inside the core, but since no major diagenetic features were found (see section 8.4 in chapter 8), I assume they are also composed of aragonite.

A Munsell colour record was also obtained every 0.5 cm (see section 6.7 in chapter 6). However, such description is not particularly useful except for describing the transition from more carbonate-rich sediment characterised by a 3.8 Y 6.20/1.70 to more organic sediment characterised by a 9.2 YR 5.0/1.20 (see the transition at 94.75 m in Figure 9.1).

Figure 9.4 presents the different time series obtained from the interaction of the cores with visible light (see section 6.7 in chapter 6). These comparisons point out that analysing using only one light wave or colour is enough for getting a record since the different time series

produced from a particular colour or light wave contains practically the same information (Figure 9.4).

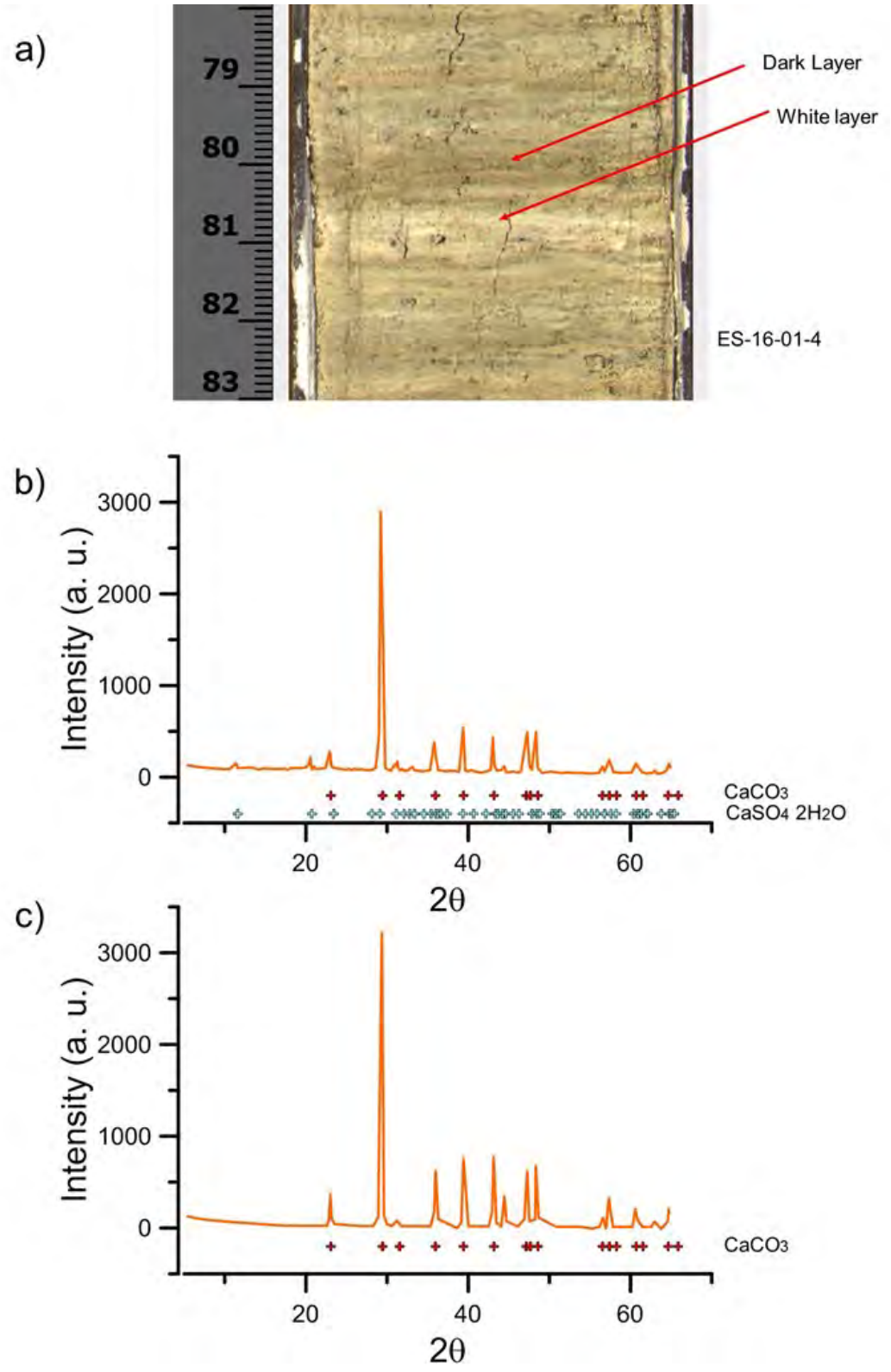

Figure 9.3 Textural and mineralogical composition of sediments. a) A section of drive ES-16-01-4 where the presence of layers can be easily observed. The arrows point out layers that might comprise detrital organic material (dark layer) and pure calcite (white layer). b) The diffractogram shows only the presence of calcite.

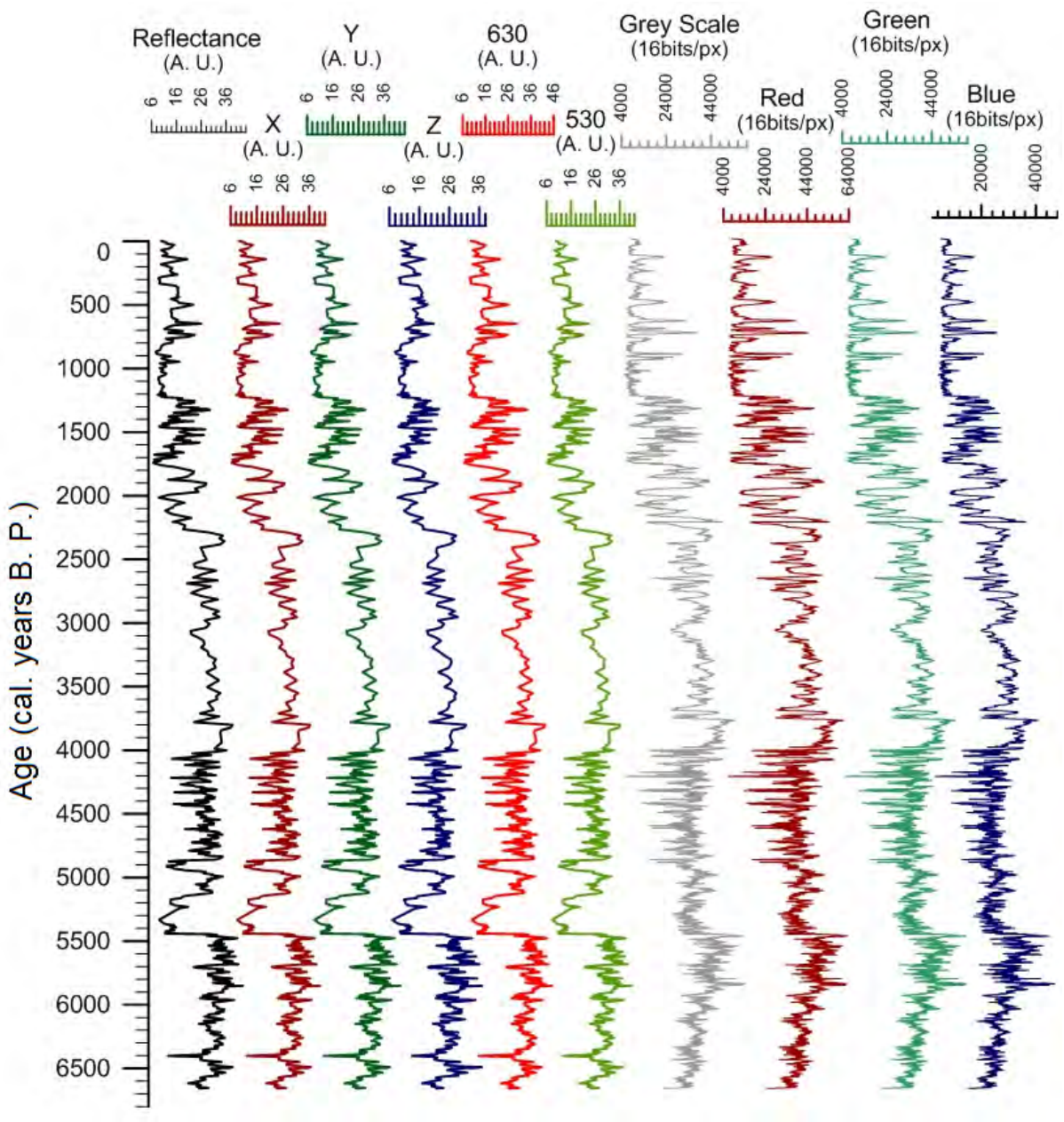

Figure 9.4 Colour and greyscale records plotted against age generated using different methods in the XYZ Multi-Sensor Core Logger in comparison to the colour and greyscale records obtained by the digital processing of the image in Matlab®. The greyscale reflectance X Y Z Colour space and reflectance at 630 nm and 530 nm wavelengths were obtained directly by the XYZ Multi-Sensor Core Logger, XYZ-MSC, having a resolution of 0.5 cm, while the greyscale, red, green and blue proxies were obtained by processing the colour images of the core having a resolution of 0.01 cm, which is the area covered by one pixel (see section 6.7 in chapter 6).

However, the record produced from the interaction with the primary blue colour has smaller magnitudes in its signals. Another situation exists with the Z Colour Space, (representing the primary colour blue), containing less information since the blue colour is not reflected by the yellow segments of most of the core, producing a less noisy time series.

In addition, while these time series obtained directly from the images match with changes in the image, the signal in the time series generated by the XYZ-MSCL had a delay in the collection time. Thus, the signal corresponding to a particular depth does not match with the tone observed on the image at the same depth but coincides with a colour that appeared in a previous depth. This had to be taken into consideration for matching the data of the time series generated by the XYZ-MSCL with other proxies.

Since the resolution and accuracy of the signal is better in the time series obtained using Matlab©, I will use this time-series as proxies of the colour and greyscale instead of the reflectance, greyscale, Munsell colours and CIE XYZ colour space-time series. In particular, I will use the greyscale from the image as a proxy of the changes in colour presented in the record. From this grey time series, the digital count of bands was performed. Besides, the records showing the width of the layers was also obtained from the greyscale record (Figure 9.7).

9.3 Density record

Figure 9.5 shows a comparison between the time series of changes in density based on different methods. The raw data obtained by the AGR present artificial anomalies between the bottom to around 6000 years B. P. and from 5400 to 5000 years B. P. in drives that were covered with aluminium foil (ES14-3 and ES14-4) (see section 6.9 in chapter 6). I tried to overcome this artificial anomaly by adding 0.3 g/cm^3 to the results obtained from ES14 cores, which is the offset due to the presence of aluminium paper. (I will use this corrected record for comparison with other proxies due to the reasons explained in this section). The new time series (Figure 9.5 red density record) still presents an offset from 5500 to 5700 years B. P. Therefore, I added 0.2 g/cm^3 for overcoming this anomalous trend for following the trend of the upper sections. Figure 9.5 blue records). However, no physical explanation during the measurements exists for arguing that the trend in this period is artificial.

Figure 9.5 also shows the results of the density records generated from the data obtained during the measurements of loss on ignition. This density record has similar fluctuating values to the density record obtained from AGR based on the undried sediment. This resemblance makes sense since the sample scanned during the AGR analysis contains still water. However, the trend in the wet density record obtained by loss on ignition increases according to the depth from 2000 years B. P. up to 5100 years B. P. (and then decreases,

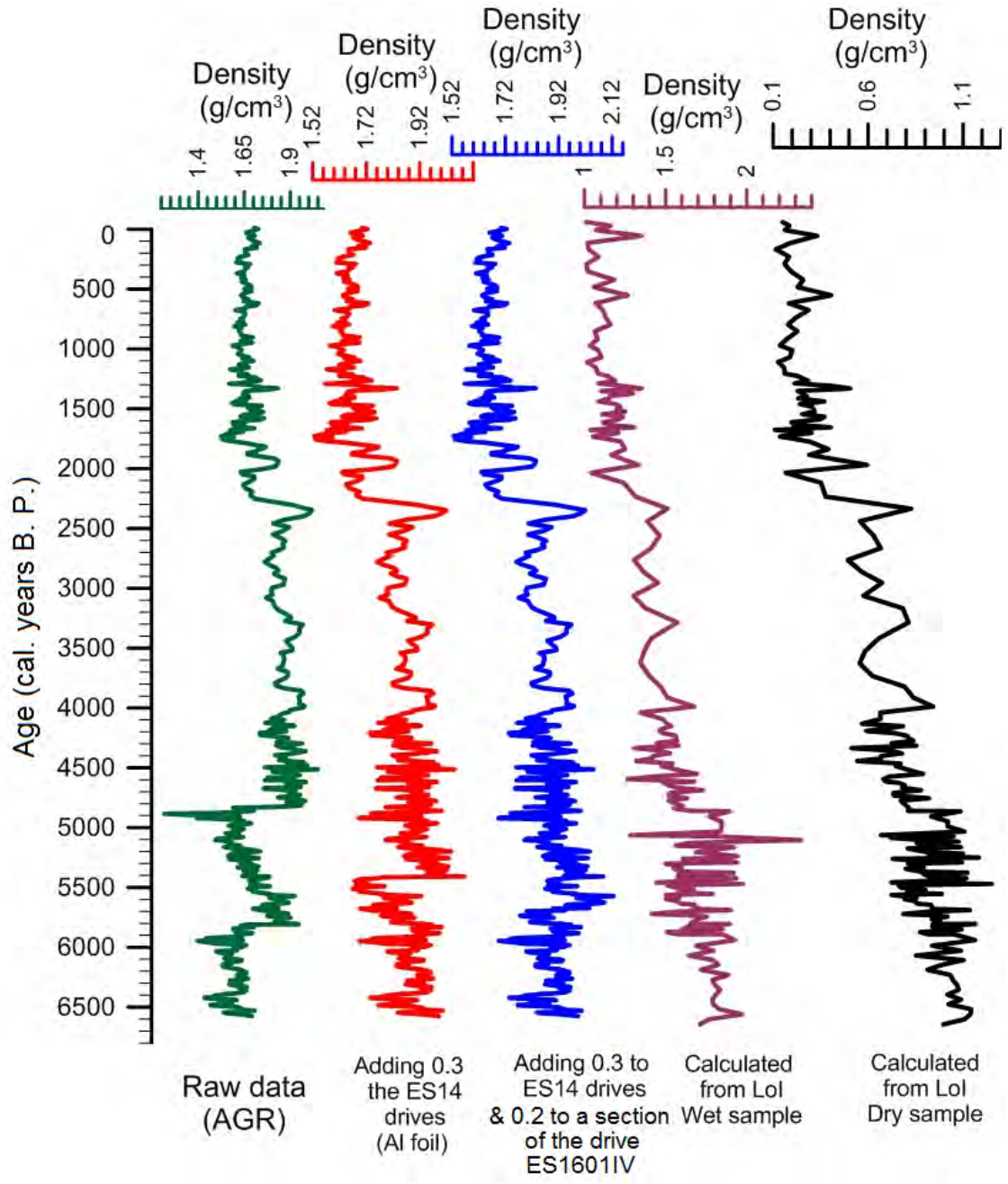

Figure 9.5 Density records plotted against age obtained from sediment cores collected at Lake Esmeralda using AGR in comparison to the wet and dry density record generated by data taken during the loss on ignition. The record generated by AGR was corrected (red line) to overcome interference caused by the aluminium foil.

starting to increase again at 5500 years B. P., reaching a maximum of density at the bottom at 6700 years B. P.), this might reflect the tendency to compaction that sediments suffer due to gravity. This tendency is not registered in the AGR, where gamma radiation scanning is a more superficial phenomenon. The dry density record obtained by loss on ignition (Figure 9.5 black line) density increases with depth in the carbonate reach sediments (from bottom to 2000 years B. P.), possible due to compaction.

The lower density values between 5000 to 5400 years B. P. obtained by AGR, are also present in the density records obtained by loss on ignition, meaning that this particular trend is not artificial. Therefore, the corrected density record obtained by AGR is the record where only the cores with aluminium foil were corrected (Figure 9.5 red records). I will use this corrected record as a proxy of changes in density for future comparisons.

9.4 Elemental abundances, elemental ratio proxies and loss on ignition analysis

Figure 9.6 shows the results of the Total Inorganic Carbon based on loss on ignition (see section 6.6 in chapter 6), which according to the XRD analyses is calcite, $CaCO_3$ (see section 9.2) so labelled as this.

Figure 9.6 also presents the elemental record from the XRF scanner, normalised (see section 6.8 Chapter 6) and filtered from subannual noise for elements that were abundant enough to be distinguished from noise, as well as the elemental ratios Fe/Zr, Ti/Sr, Ca/Sr and K/Sr which might have an environmental meaning.

The Zr and Fe records are both proxies of terrigenous input. However, iron is a soluble element, while zirconium is insoluble. They indicate the presence of allochthonous materials moved by rainfall and runoff. Shifts in this record might indicate changes in source material delivered into the lake (Konfirst et al., 2011). Relatively low values persist across the record, indicating a constant covariation of these elements, implying in general that there has been no diagenesis of the allochthonous material due to the interaction of these sediments with water. Nevertheless, a dramatic change in the Fe/Zr record occurs between 3700 years B. P. and 3000 years B. P., at the time, that the Fe record shows high values. These values might be related to volcanic eruptions since there are not important sources of Fe near the lake, indicating a far source (like the material expelled by a volcano).

Actually, some of these signals coincide with the dates of eruptions (Figure 9.7 left) that occurred very near the Maya Cultural Area, e.g. El Chichon volcano at 3700 and 3100 years B. P. (Macías, 2005), Tacana at 1950 years B. P. (Mora et al., 2013) and El Chichon 1800 ± 70 years B. P. (Macías, 2005). However, there are no additional signals that could support a link between the Fe/Zr and volcanic eruptions, such as tephra layers. Therefore, this link with volcanic eruptions is at the moment highly speculative. In addition, it seems that some of the high signals in the Fe/Zr (at 3600- and 3100-years B. P.) are driven by very low

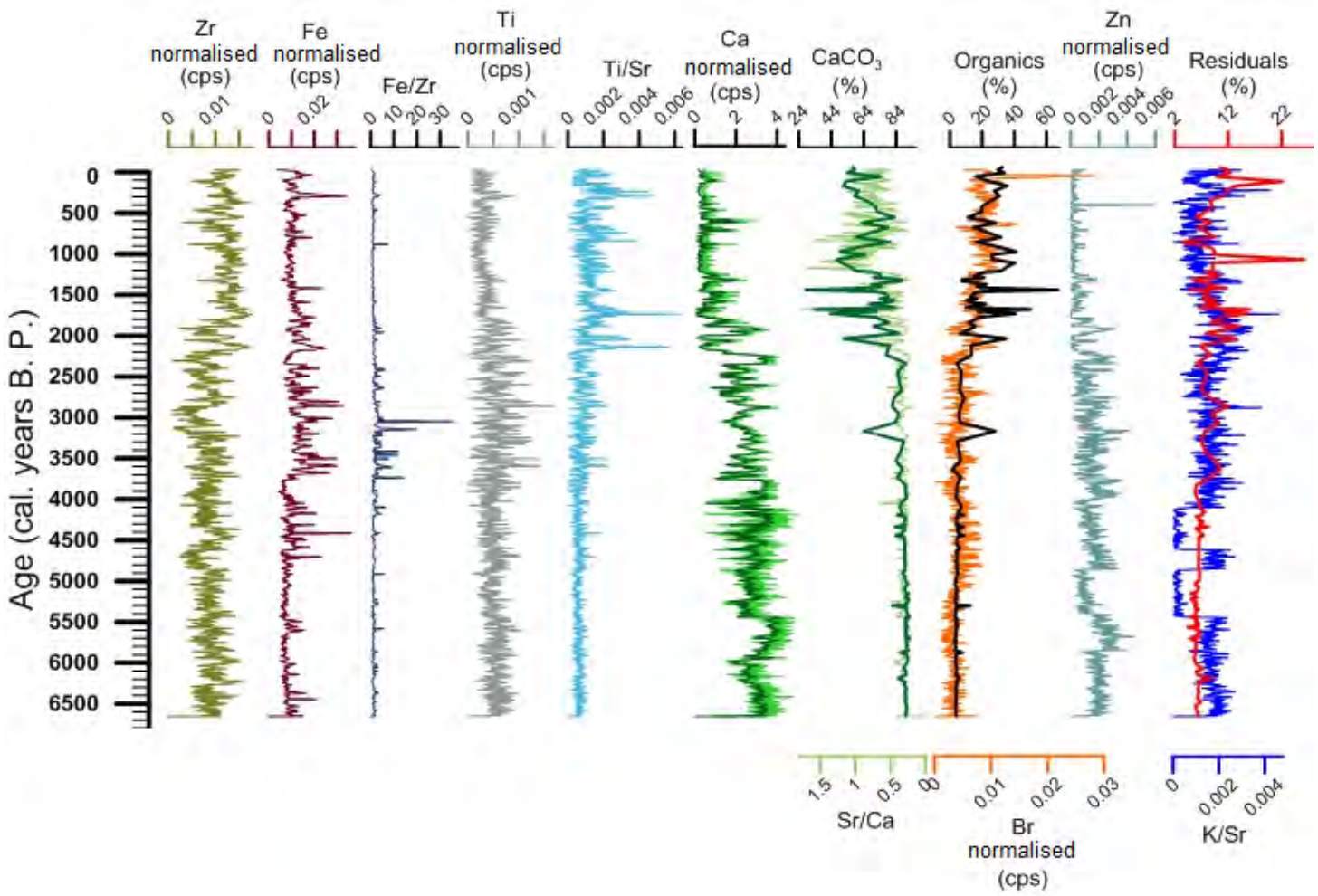

Figure 9.6 Elemental abundances and elemental ratios obtained by the XRF Scanner analysis and the percentage of $CaCO_3$ and organics as well as the residuals obtained by the loss on ignition.Ca abundances record was generated by XRF. Meanwhile, the $CaCO_3$ record refers to the amount of carbonate measured by loss on ignition.

concentrations of Zr, which might indicate some diagenesis of allochthonous material. For these reasons, I will not use the signals of Fe/Zr in Facies 5 and 6 for the description of the environmental history of the Cochuah Region.

The Ti record shows that the presence of this insoluble ion is relatively constant during most of the record, implying little variation in the allochthonous material. This Ti ion has a very low abundance in general. The exception is a phase of high variation between 4000 to 2000 years B. P., which might reflect an occasional minor increase in the input of terrigenous material into the lake. The Ti/Sr record is used as a proxy of terrigenous delivery into the lakes in karst environments (Davies et al., 2015). In this way, the input of terrigenous material is relatively small from the start of the record until 4000 years B.P., when it started to increase. The input of terrigenous material reaches its peak around 2100 years B. P. and after 2000 years B. P. maintains relatively moderate values. The Ti/Sr record resembles the residual of the loss on ignition analysis, implying that the residuals do represent allochthonous material. Both time series match except for signals around 2400, 1100 and 150 years B. P., when the residuals record presents high values contrasting with low values of Ti/Sr, which might be explained by the precipitation of gypsum during those years (see below in this section). The Ti/Sr record anticorrelate with Sr/Ca from 2100 to 1100 years B. P. implying that at least during this period, the apparent reduction in calcium was caused in some degree by a dilution effect due to the input of terrigenous material into the lake.

The differences between the Ti and the Ti/Sr records indicate that the titanium signal is also masked by the presence of organics due to some kind of dilution effect (see later explanation for Ca signal).

Calcium is the only record in Figure 9.6 which is plotted against its filtered (from noise) raw data for the purpose of comparison (dark green and pale green, respectively). This Ca record obtained from XRF is substantially different from the $CaCO_3$ record from loss on ignition (Total Inorganic Carbon), since its values abruptly fall lower than 2 cps for the last 2100 years B. P. At the same time, Ca values (obtained by XRF) fall dramatically to 1/10 of the highest values toward the top. The differences between the $CaCO_3$ and the Ca records (including the discrepancy in their fall after 2000 years B. P) can be explained by the logarithmic correspondence between the intensity of the signal produced in the XRF analysis and the abundance of an element (in this case Ca) according to the Beer-Lambert law in spectroscopy:

$$log_{10}\left(\frac{I}{Io}\right) = elc \quad \text{Equation 9.1}$$

Where I are the intensities, e is an absorption coefficient, l is the longwave of the beam, and c is the concentration of the element.

In this way, small differences in concentration indicate big differences in the intensity of the signal if the concentration of an element is high (Beer et al., 1983). The differences after 3500 years B. P, particularly after 1600 years B. P. between $CaCO_3$ and Ca records probably indicate the presence of carbonates other than calcite. However, the XRD analysis did not detect additional crystalline carbonates. Therefore, this idea is discarded. For this reason, the alternative explanation is that the apparent low concentration at the top of the Ca record is artificial. I will explain this in later paragraphs.

The Sr/Ca negatively covaries with the percentage of $CaCO_3$ (total inorganic carbon). Sr/Ca is frequently used as a proxy of the nature of carbonates, with lower values indicating calcite, while high values can indicate aragonite or magnesium calcite (Davies et al., 2015). High values in Sr/Ca are normally associated with relatively dry conditions (Hodell et al., 2008). A justification of this is based on the prior calcite precipitation model in a karst system, where the calcium carbonate would precipitate in the epikarst before reaching ground waters due to the prevailing dry conditions (Sherwin and Baldini, 2011). Another way to justify the dissolution of Ca and the precipitation of Sr in lakes for explaining the link between Sr/Ca and dry conditions is related to the depletion of CO_2 or Ca from the water fluxes associated with changes in temperature and pressure. Such depletions can be achieved by the common ion effect with gypsum (which tends to precipitate in dry conditions) or by the escape of dissolved CO_2 into the atmosphere (James and Jones, 2015). In this thesis, I will use the Sr/Ca ratio as a proxy of dry conditions.

Zn was one of the few elements whose signal could be differentiated from noise. However, this proxy has been barely used for environmental studies. In Lake Esmeralda, it has a similar trend to the calcium record. Since zinc is an element associated with biological activity, it is possible that it reflects changes in nutrient input into the lake and hence productivity (Reynolds and Hamilton-Taylor, 1992). (In the same way, the nutrient input and productivity may impact the Ca precipitation).

Similar to Zn, S is also used even though the use of XRF for observing variations in this element is not recommended since the mineral structure and matrix effects leads to interferences on measurements when the reference material for calibration and validation

is not very similar to the analyte (Krishna, 2009). Because it had the same problems observed in the Ca record, the S record is used only for the last 1700 years B.P for searching for intense signals that might indicate the presence of gypsum (see section 9.7 below).

Figure 9.6 shows the percentage of total organic carbon superimposed on the bromine record obtained by XRF. The Br record is normally associated with organic material since bromine tends to form covalent bonds with organic molecules (Gilfedder et al., 2011). In this way, the Br record is a proxy of the productivity inside the lake. The percentage of organic material, however, has some peaks, e.g. 3200 and 1450 years B. P. that do not appear in the bromine record, which implies an additional source of organic material from outside the lake, not related to productivity in the lake. Organic material cannot be measured directly by XRF since C has low emission of fluorescence. However, organic material, as well as water, can interfere in recovering the XRF signal related to some elements. This barrier imposed by the organic material might explain the low amount of Ca detected by XRF at the top of the core (see above) and its difference from the $CaCO_3$ (Total Inorganic Carbon) record.

The organic content (based on loss on ignition) is below 5% until 3500 years B. P. and starts to increase after that time. The apparent depletion of Ca abundance (analysed by XRF) starts after 2100 years B. P. when the Total Organic Carbon record reaches around 40%. In the rest of this chapter, when I refer to the organic content, I refer to the organic percentage measured during the Loss of Ignition. It seems that percentages around this value coincide with extremely low intensities in the Ca record, and Ca is an element with lower fluorescence energy. Therefore, the photon emitted by calcium can easily be affected by changes in the density and effective analysed volume (Ravansari et al., 2020). In this way, if the analyte signal originates deeper within the sample, it is less likely to be detected by the instrument because of the narrower range of egression angles capable of incidence upon the instrument's fixed sensor (Ravansari et al., 2020). I will assume that this phenomenon is happening when the percentage of organic material is around 40% and beyond. Therefore, the apparent low concentration at the top of the Ca record is artificial. In addition, the results of XRD analysis of samples in this region do not support the presence of another kind of crystalline carbonate. However, amorphous carbonates different from calcite could be present. Since the presence of organic material could not explain the presence of amorphous material over crystalline carbonates easily, I support by parsimony the idea that the Ca intensity is underestimated when the organic material reaches a proportion of 40%.

Another point to highlight is that the Total Organic Carbon record covaries negatively with the $CaCO_3$ record (Inorganic Carbon Record). This is not always the case (e. g., the correlation of these proxies in Lake San Lorenzo see section 7.4 in chapter 7).

Finally, Figure 9.6 presents the variation of the residuals from the loss on ignition analyses. Besides its resemblance with the Ti/Sr record already discussed, the residuals record has a better covariation with the K/Sr record. An important discrepancy between these two records has to be highlighted since the residuals present important peaks around 1100 and 150 years B. P., which is not observed in the K/Sr record.

In addition, the K/Sr ratio shows artificially low values in the cores ES-14 wrapped in aluminium foil, between 5500 to 5000 years B. P. and 4500 to 4000 years B. P. Since the potassium concentration was low and this element like calcium presents issues with the effective depth of analyses. It can be argued that the aluminium paper influenced the detection of potassium. However, the K/Sr record matches with the K/Sr ratio in the cores ES-16.

K/Sr is, in theory, a proxy of the rainfall in the Mayab according to its lithological characteristics. K abundance in the lake sediments is the result of the in washed material from the surrounding soils or clays (Roy et al., 2018). The K/Ca and K/Sr ratios have been tested as proxies of rainfall, finding a linear correlation between precipitation and K/Ca, but a lack of correlation if the annual rainfall is more than 1400 mm (Roy et al., 2018). Since the calcium record had an excessive depletion at the top, I used the Sr abundance since this element has the same structure as Ca but without an exaggerated depletion at the top. The rainfall at Lake Esmeralda is around 1100 mm, so K/Sr might be a reliable proxy of rainfall.

The covariation between K/Sr and the residuals supports the idea that the residuals are mainly composed of allochthonous material, whose presence in the lake is driven by rainfall. The peaks around 1100 and 150 years B. P. in the residuals might be related to the additional presence of evaporates besides allochthonous material. The signal at 150 years B. P. presented gypsum according to XRD (see section 9.2), so this supports this idea. At the same time, the 1100 years B. P. signal coincides with the last part of the drought signal at the time frame of the Maya Collapse at the end of the Mesoamerican Classic period when the gypsum precipitation was intense in Chichancanab (see section 5.4 in chapter 5). Unfortunately, I am not sure of the exact stratigraphy of XRD samples taken in layers older than 345 years B. P. since these samples were taken by undergraduate students of the

University of Nottingham from core ES-14-II, which could not be correlated into the master sequence (although its assumed position is near from their exact position). In addition, the raw data of these samples was also lost, and I know the only presence of calcite in these samples by their report.

9.5 Geological Facies

The zonation (Figure 9.7) is based on the cluster analysis performed using the abundances of Ca, Ti, Zr, Fe, Sr, Zn, and Br, the K/Sr, Ti/Sr, Sr/Ca ratios, the organics, calcite $CaCO_3$ and terrigenous content (residuals of loss on ignition), the greyscale (section 9.2) and $\delta^{18}O$ and $\delta^{13}C$ (see section 6.14 in chapter 6). The isotope record used is based on the analysis of bulk sediments instead of using shells of gastropods (see section 8.9 in chapter 8). The mean calculated value for the $\delta^{18}O$ of calcite from the isotopic signature of water measured in January 2014, 2016 and 2018 is -2.54‰. This expected value is quite different from the value at the top 0.78‰ of the main core, (assigned age -30 years B. P. or 1980 A. D.), and is similar to values observed at the bottom of the sediment sequence (during facies 1 to 7), when the lake was apparently more hydrologically open than today (see last paragraph in this section). This calculated value is not useful for calibrating the magnitude of the change in the past with respect to present conditions. The calculated value indicates that the isotopic fractionation does not happen in conditions of equilibrium or that the isotopic composition of water in the lake reflects seasonal changes (returning to the argument where the bimodal distribution in gastropod shells represent two distinctive seasons and indicating that the system might retain the isotopic signature of the previous season, see section 8.10 in chapter 8), meanwhile the isotopic signature of sediments reflect the conditions of the whole year (therefore the $\delta^{18}O$ of the sediment coincides with the mean value of the shells). This last possibility can be only rejected when the isotopic composition of water from Lake Esmeralda can be measured in summer (and in months like March and October, when changes of evaporation and rainfall are also distinctive).

The colour map in Figure 9.7 presents 10 facies. Each one can be differentiated from the next phase by a distinctive colour assigned during the cluster analysis. Some facies have the same colour, indicating that palaeoenvironmental conditions were practically the same, e.g. facies 1 and facies3. It can be observed in the colour map that there are two moments when the lake system seems to have a radical change in their environmental conditions at 2100 years B. P. and 1200 years B. P. This creates three distinctive geo-units. The first geo-

unit is composed of facies 1 to facies 7, the second geo-unit is restricted to facies 8, and the third geo-unit is composed of facies 9 and 10.

First Geo-unit

This Geo-unit composed of facies 1 to 7 is seen in the colourmap as the alternation of facies of dark red and black colours, where facies 1, 3, 5 and 7 represent similar environments between them. Meanwhile, facies 2, 4 and 6 are also similar between them. During this geo-unit, the organic material analysed by loss on ignition maintains percentages under 9%. At the same time, the $\delta^{18}O$ record maintains values under -1.5‰, indicating a lake system that is generally more open hydrologically than in present times.

Facies 1 from 6656 to 5900 years B. P. is a period when both O and C isotopes covary, indicating the prevalence of a relatively closed system. During this facies, the $\delta^{18}O$ values around -3.8‰ indicate a low evaporation/rainfall ratio. The rainfall (K/Sr) coincides with the trend of terrigenous input into the lake, around 6 % according to the residuals. Although the $\delta^{18}O$ values indicate a low evaporation-rainfall ratio, the values of K/Sr are similar to the values at the top of the record (with modern rainfall). Therefore, this K/Sr would indicate conditions of rainfall similar to those prevailing during the XX century A. D. However, the $\delta^{18}O$ values at the top of the core(0.4‰) are quite different from the conditions at facies 1 (3.7%). This discrepancy between both records might indicate that Lake Esmeralda was then more hydrologically open than today during this facies or that evaporation was lower in those times. This more hydrologically open system would explain in part the low amounts of residuals (6%) and the relatively low Ti/Sr ratio observed in a rainfall regime that might have a very similar to the modern rainfall regime. The amount of organics is under 4%, implying very low productivity, since the Br and Organics proxies mantains covariation, while the amount of carbonates is around 90%. This high percentage of carbonates is consistent with the precipitation of calcite apparently occurring during this humid period, according to the Ca elemental record. The Sr/Ca record indicates relatively humid conditions. The density record and the greyscale record follow a similar pattern, which is similar to the trend of Ca, reflecting that density and colour are mainly due to changes in the amount of calcite (total inorganic carbon).

Facies 2 from 5900 to 5500 years B. P. is also a time frame of a relatively moderate amount of rainfall (similar to facies 1) according to the K/Sr. At the end of the facies, the $\delta^{18}O$ record implies a relatively lower evaporation/rainfall ratio (-4.09 ‰) around 5662 years

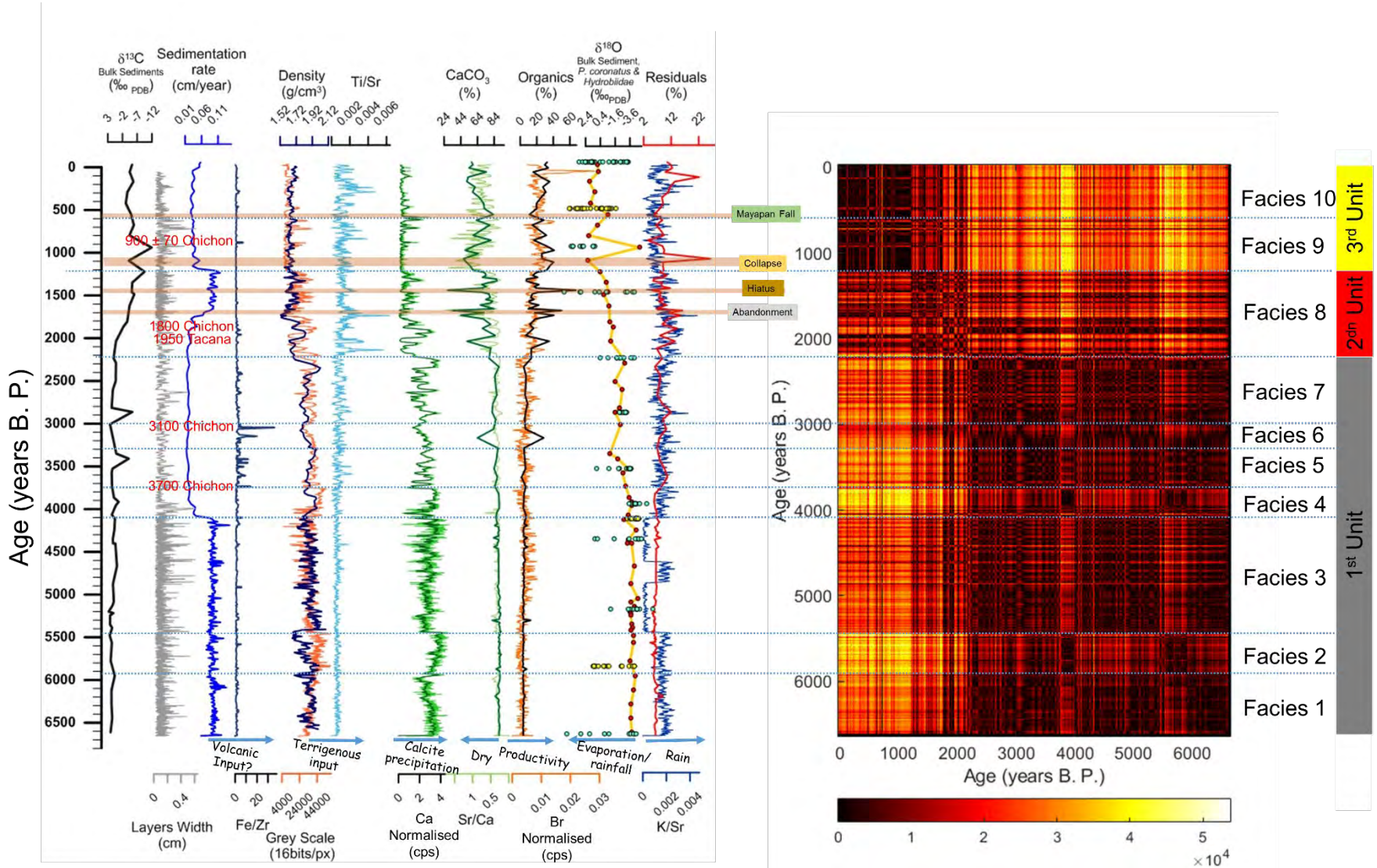

Figure 9.7 Left: Proxies developed from the Lake Esmeralda core and the zonation based on them excepting the density, layer width and sedimentation rate records. Blue circles represent the $\delta^{18}O$ of single shells of P. coronatus whilst yellow circles are the $\delta^{18}O$ of Hydrobiidae, including P. coronatus at that layer. Right: Hot colourmap based on Euclidian distances between pairs of samples across the core during the cluster analysis for establishing the zonation. It can be observed ten different zones in the colour map with different characteristics that correspond to a particular depositional environment (facies).

B. P compared to the previous facies. Although at a lower resolution, the $\delta^{18}O$ continues to follow the trend of the K/Sr record. The rainfall pattern of K/Sr coincides with the trend in the terrigenous input into the lake, around 6 % according to the residuals, which is support by the relatively small Ti/Sr ratio. The amount of organics is still under 4%, implying very low productivity, while the amount of carbonates (calcite) is still around 90%. Precipitation of calcite is still occurring during this humid period. Meanwhile, the Sr/Ca record continues indicating humid conditions. Both isotope records continue covarying in this period indicating the prevalence of a relatively isotopic closed system. The density record and the greyscale record follow a similar pattern, from 5900 to 5800 years B. P. having a similar trend of the Ca abundance obtained by XRF. This record, as well as the density and greyscale, are a key in differentiating this facies from facies 1 and 3. The density decreasesover the rest of the period, which might indicate more porous calcite since this low density appears in one of the two periods with the highest amount of calcium (Ca) in all the record and assuming that most of Ca is associated with the formation of calcite. The fact that there is no increase in organic material supports the presence of more porosities or an aggregate of calcite of low density. Since the colour still has the same trend as the Ca record, then the colour does not necessarily follow the changes in density.

Facies 3 from 5500 to 4100 years B. P. has important gaps in the K/Sr due to the aluminium wrapping in drive ES-14, but between 4900 to 4700 years B. P., fluctuations in K/Sr show values similar to the previous facies. Therefore, I assume a similar rainfall amount for the entire period. This assumption is supported by the $\delta^{18}O$ record (values fluctuate from -4.12‰ to -3.42.‰), indicating a relatively low evaporation/rainfall ratio as in the previous two facies. The terrigenous input into the lake is still around 6 %, according to the residuals. The Ti/Sr ratio in this period support this observation. The organic material stays under 4%, implying very low productivity, while the amount of carbonates is around 90%. This precipitation of carbonates inside the lake seems to occur during this relatively humid period (as previously). The Ca record is the only one that presents important variations during this period. The Sr/Ca record indicates humid conditions for most of the facies changing to a slightly less humid condition after ca. 4400 years B. P. Both O and C isotopes covary during this long period indicating a relatively closed system until the 4200 years B. P., when $\delta^{13}C$ has an opposite trend to $\delta^{18}O$. Facies 3 probably had the same characteristics as facies 1. The density record and the greyscale record follow a similar pattern, which is different to the trend of Ca, reflecting that density and colour are

starting to be also influenced by the input of organics, which start to increase slightly according to the Br record.

In Facies 4 from 4100 to 3750 years B. P., the amount of rainfall (based on K/Sr) starts to decrease slightly in the first half of this period, it starts to increase again after this. In contrast, the $\delta^{18}O$ record (values from -2.83 ‰ to -3.52 ‰) implies a tendency to low evaporation/rainfall ratio (a bit more positive than facies 3), which does not return to the values that existed in the previous facies. This incongruence between the K/Sr and the $\delta^{18}O$ records might indicate summer rains with the same intensity as in facies 3 for the second half of facies 4, but with higher evaporation than the previous facies. Another explanation is a slight change to a more hydrologically open state at the beginning of the facies. The rainfall coincides with the terrigenous input trend, which increases from 6 % to 12 % during facies 4, reaching a minimum of 6 % around 3900 years. B. P., according to the residuals. In contrast, the Ti/Sr ratio slightly increases.

The amount of organics remains under 4%, with a slight increase in the second half of the period implying a continuation of very low productivity. The amount of carbonates decreases to 80% in the first half before recovering to around 90%, following the same pattern as the rain proxy K/Sr. The precipitation of calcite, based on the relative amount of Ca, follows the pattern of the rain proxy K/Sr. The isotope records do not covary during this facies, indicating a change to a more hydrologically open system. The density record and the greyscale record follow a similar pattern again for the first half. These records are influenced as in the last part of facies 3 by the amount of carbonates and organics. The density record has lower values from the second half of facies 4, which might be explained by the increase of terrigenous and decrease of organics at the same time. The decrease in the organics has no major impact on the greyscale record, which continue to have the same tendency as the K/Sr record.

Facies 5 from 3750 to 3300 years B. P. continues with a trend of less rainfall compared to the median values in facies 1 and 2 according to the K/Sr. This rainfall trend is consistent with the change in sedimentation rate from 0.095 cm/year to 0.023 cm/year at 144.25 cm (Figure 9.1). In addition, this rainfall trend is also supported by the trend in the $\delta^{18}O$ record, where the tendency is to a higher evaporation rainfall ratio with the highest value (-0.89 ‰) at 3351 years B. P. The rainfall (K/Sr) still follows the terrigenous input pattern into the lake, which decreases from 12 to 6 % according to the residuals. This change associated with the decrease of terrigenous input is not easily observed in the Ti/Sr ratio, however,

its lowest values also occur around 3300 yeas B. P., implying the minimum sedimentation of terrigenous material into the lake at the moment when the evaporation rainfall ratio reached its maximum values. In contrast, according to the Sr/Ca record, humid conditions still prevailed. The amount of organics slightly increases from 4 to 8%, implying very low productivity, while the amount of carbonates is around 88%.

$\delta^{18}O$ and $\delta^{13}C$ show opposite tendencies indicating that the system might be open, which contrasts with the interpretation of the $\delta^{18}O$ record. However, there are very few data points in each of these facies, therefore it's more likely something else could impact $\delta^{13}C$ or $\delta^{18}O$ data briefly at this scale

The density record and the greyscale record follow a similar pattern, recovering the covariation that existed in the facies at the bottom of the record.

Facies 6 from 3300 to 3000 years B. P. is characterised by a relatively moderate amount of rainfall similar to that during the first half of facies 5, according to the K/Sr. In contrast, the $\delta^{18}O$ record indicates a lower evaporation/rainfall ratio, which might suggest less evaporation at the time of decreasing rainfall, although there is only one data point in this facies.

The residuals record decreases from 10 to 8 %, following the same pattern as the amount of rain (K/Sr). The Ti/Sr ratio in this period also has this trend, indicating a decrease in the input of terrigenous material into the lake as the residuals do. The amount of organics increases, reaching a maximum of around 30 % at 3150 years B. P. before decreasing again. This increase in organic material is not linked to changes in rainfall (K/Sr). The amount of carbonates ($CaCO_3$ record obtained from loss of ignition) negatively covaries with the organics, decaying to its minimum at 64% at 3150 years B. P. This decrease at 3150 years B. P. is also observed in the Ca record obtained by XRF. During this period, the Sr/Ca record does not coincide with the $CaCO_3$ record. Unfortunately, I do not have an explanation for the lack of coincidence between these two records during facies 6. The bromine record also has less variation during this facies in comparison to the organic material record, which might indicate that the increase of organics in the lake was not due to an increase in the productivity of the lake, but a result of exogenous organic material. There is an opposite trend between the isotope records $\delta^{18}O$ and $\delta^{13}C$, reaching -2.36‰ and 2.34‰ respectively. The density record and the greyscale record follow a similar pattern (also similar to the trend in Ca obtained by XRF), reflecting that density and colour are mainly responding to changes in the amount of minerals containing Ca and organics.

Facies 7 from 3000 to 2200 years B. P. is a period of decreasing rainfall in comparison with all the previous facies based on the K/Sr. This tendency starts to be reversed after 2500 years B. P. The $\delta^{18}O$ shows the highest values (an average of -2.60 ‰) since the start of the record (except for the point at 3409 years B. P. with a value of -2.00 ‰). After 2500 years, B. P. trends reverse, with a decrease in the evaporation- precipitation ratio. The rainfall coincides with the terrigenous trend fluctuating from 6 to 14 %, according to the residuals. The lack of congruence between these two records (K/Sr and residuals) in the last three centuries of the deposition of facies 7 can be explained by the lack of resolution in the residuals records. However, the Ti/Sr ratio in this period has similar trends to the residuals, implying that the contribution of terrigenous material into the lake is not always proportional to the amount of rainfall. The amount of organics fluctuates from 6 to 8%, covarying with the Br record, implying very low productivity until 2300 years B. P., when the organics increase toward 14 %, implying an increase in productivity. The percentage of carbonates is around 90% during most of the facies 7 until 2300 years B. P., when it falls to 78 %. This fall also appears in the Ca record. Meanwhile, the Sr/Ca record shows high humidity conditions during the complete facies. $\delta^{18}O$ and $\delta^{13}C$ covary in this facies, except for the point at 2500 years B. P. indicating the prevalence of a relatively closed system. The density record and the greyscale record follow a similar pattern.

Second Geo-unit

This Geo-unit constrained to facies 8 is seen in the colourmap as a transitional geo-unit between the first geo-unit and the third geo-unit, which is observed by the fluctuation of colours, being dark colours representative of conditions similar to those observed in the first geo-unit and light colours (tending to clear red and yellow) representative of conditions similar to the third geo-unit. During this geo-unit, the organic material analysed by loss on ignition maintains percentages not observed before and start to fluctuate. Meanwhile, the $\delta^{18}O$ record start to increase its values, implying that Lake Esmeralda is becoming a more closed hydrological system.

Facies 8 from 2200 to 1200 years B. P., according to the K/Sr, is characterised by a decrease in rainfall from 2150 to 2000 years B. P, continuing with a progressive decrease in the amount of rainfall, with a local increase after the Maya Hiatus. Important decadal periods of minimal rainfall are shown for the Maya abandonment at 1750 years B. P. and the Maya Hiatus at 1438 years B P. (the Maya Hiatus is commonly dated to 1414 years B. P.) in the K/Sr record. During the Maya Abandonment, the residuals record has a tendency

that is contrary to the K/Sr, which is also observed in the Ti/Sr record. This tendency is an anomaly that means a major contribution of terrigenous material in a time of low rainfall. The $\delta^{18}O$ record points out a continuing increase in the evaporation- rainfall ratio, going from - 0.95‰ at the beginning of the facies to 0.46‰ at the end, with small reverse tendencies to decreasing evaporation rainfall around 2000 years B. P. (-1.29‰) and the Maya Hiatus (-0.64‰), having a tendency that is congruent to the K/Sr record. There are no isotope data for the Maya abandonment, since the amount of carbonates per sample of 100 mg was insufficient for being detecting in the isotopes analysis.

The amount of organics increases in general from 4 % to 20 %, with a dramatic increase in organic material around 2000 years B. P., and the time frames covered by the Maya Abandonment (1750 years B. P.) and the Maya Hiatus (1414 years B. P.). Although this increase during the critical moments in the Maya History also appears in the Br record, they have less intensity, indicating that most of the organic material during these events might have come from outside the lake. Precipitation of $CaCO_3$ based on loss on ignition covaries negatively with organics. $CaCO_3$ decreases from 80 % at the beginning of facies 8 to 60% at the end. The $CaCO_3$ percentage falls dramatically around 2000 years B. P., and at times associated with the Maya Abandonment and the Maya Collapse. According to the Sr/Ca, dry conditions increased during this period, having dramatically increased at 2000 years B. P. and during the Maya Abandonment and the Maya Hiatus. According to the Sr/Ca ratio, dry conditions were more intense in the Maya Abandonment than in the Maya Hiatus. This difference is consistent with the argued intensity of droughts described in other records (see chapter 3), even though the amount of organics was weaker in Lake Esmeralda during the Maya Abandonment in contrast to the Maya Hiatus.

$\delta^{18}O$ and $\delta^{13}C$ do not covary in this period indicating a more open system. The $\delta^{13}C$ changes up to 5 ‰, indicating a change of the source of carbon, probably influenced by the increase of productivity (However, productivity itself could just have change the C isotopic signature). The density record and the greyscale record follow a similar pattern, which is starting to be profoundly impacted by the amount of organic material.

Third Geo-unit

This geo-unit composed of facies 9 and 10 is seen in the colourmap as a geo-unit of light colours (tending to clear red and yellow). During this geo-unit, the organic material analysed by loss on ignition maintains relatively high percentages but constant values under

40%. Meanwhile, the $\delta^{18}O$ record maintains positive values (excepting at 530 years B.P., with -0.68‰), in this geo-unit. Lake Esmeralda is a more closed hydrological system in comparison to the preceding geo-units.

Facies 9 from 1200 to 550 years B. P. is, in general, a time frame of decreasing rainfall amount based on the K/Sr, with the period of lowest rainfall happening during the Maya Collapse (1140 to 1040 years B. P.). After 800 years, B. P. the K/Sr indicates a tendency to increasing rainfall. Isotopes covary again in this period indicating the prevalence of a relatively closed system. The $\delta^{18}O$ has a value of 2.11‰ during the Maya Classic Collapse indicating dry conditions; this is the most positive value in the whole record. After this, the $\delta^{18}O$ record has an outlier at 939 years B. P., returning to values that were not observed since facies 2 (-4.90 ‰). This outlier is very probably a spurious signal, even though it was measured twice since it does not coincide with the median and mean value of the *P. coronatus* (Figure 8.18 in chapter 8) at 917-947 years B. P. In addition, the comparison with the $\delta^{18}O$ of *P. coronatus* in Chichancanab (see section 9.7 below) does not show abrupt changes to more humid conditions at that time. The $\delta^{18}O$ has its second-highest value (1.99 ‰), indicating evaporated conditions, before starting to decrease gradually after 800 years B. P., which is consistent with the K/Sr record. The rainfall pattern coincides with the trend in the terrigenous input. The Ti/Sr ratio in this period also follows the same pattern. The percentage of organics has a decreasing tendency in general during the facies, presenting a local maximum (40%) at the time of the Collapse, which probably means an increase in productivity. This percentage of the 40% in organics is one of the highest in the record. After 800 years B. P. the organics return to a percentage of around 20%. Meanwhile, the precipitation of calcite starts to decrease at the beginning of the deposition of these facies, reaching its lowest value (ca. 50 %) in this facies during the Maya Collapse (1140 to 1040 years B. P.), after that it starts to fluctuate, but having an increasing tendency. Sr/Ca has similar tendencies to the $CaCO_3$ record, although this Sr/Ca record is not a good proxy for this zone due to the relatively high percentage of organics. The density record and the greyscale record follow a similar pattern, which is similar to the trend of the organic content, which gives a low density and a dark colour to the records, respectively.

Facies 10 from 550 to -66 years B. P. is a period of an increasing amount of rainfall from 550 years B. P. until 200 years B. P. based on K/Sr. The event at 550 years B. P. coincides with the destruction of the Mayapan League, which is an event linked to a dry period (see section 4.6 in chapter 4). After this, there was a rainfall minimum around 100 years B. P.

before increasing again until the present. The $\delta^{18}O$ record indicates a tendency to a slight decrease of evaporation-rainfall ratio, which persists without significant changes for the first three centuries of the facies deposition (around 1.74‰), and then starts to decrease after 200 years B. P. to 0.69‰. Besides their decreasing tendency, the values of $\delta^{18}O$ indicate a higher evaporation-rainfall ratio than those observed in facies 1 to 8. The rainfall record coincides in general with the pattern of terrigenous input into the lake. However, a major signal around 150 years B. P. is observed in the residuals record, which does not appear in either the K/Sr record or the Ti/Sr record, indicating the presence of another phase not related to terrigenous input. According to the XRD analysis on this sample, the other phase present is gypsum. The presence of gypsum occurs at the same time as a value of 1.90‰ in the $\delta^{18}O$ (the third-highest value in the record) at 167 years B. P. (unfortunately, we do not have a value at 150 years B. P.), indicating evaporated conditions. The amount of organics starts to increase after 550 years B. P. until 115 years B. P., then decreases to a minimum of 100 years B. P. Since 300 years B. P. the bromine record does not follow the same pattern as the organic record, which might indicate the contribution of organic material from outside the lake since the bromine organic carbon ratio Br/C_{org} from the catchment tends to be low due to the low concentration of Br in terrestrial plants (Gilfedder et al., 2011). The peak of Br around 100 years B. P. is also anomalous, since there is not a similar signal in the organics (by loss on ignition proxy). Therefore, it cannot be explained. The precipitation of $CaCO_3$ in the record generated by loss on ignition decreases and increases in the opposite way to the organics record, decreasing from 550 to 115 years B. P. and increasing since then having a local maximum of 74 % at 54 years B.P. O and C isotopes continue to covary in this time frame except for the time around 200 years B.P. The density record and the greyscale record follow a similar pattern, continuing with the same tendency present in facies 9.

In general, the $\delta^{18}O$ record and the K/Sr record covary during the whole sedimentary sequence recording the trends in the hydrocycle. However, the differences in fluctuations in the K/Sr record are not abruptly different between the first and third geo-unit as those in the $\delta^{18}O$ record. This supports the explanation in the first paragraph of this section, arguing that changes in the $\delta^{18}O$ record might be not only driven by the evaporation-rainfall ratio but also by changes in the supply of water by the drainage, making Lake Esmeralda go from a less hydrologically open system in the first geo-unit to a more hydrologically open system in the third geo-unit. The amount of terrigenous material entering the lake generally covaries with the rainfall amount. In this way, a major amount

of rainfall promotes more terrigenous input into the lake while it seems to prevent the precipitation of calcite. This phenomenon can be produced by slight acidification, the increase of ionic strength or the reduction of the concentration of Ca in the water after an increase in water level. It has to be highlighted that the calcite precipitation is only in part driven by the rainfall amount. It is mainly linked to the productivity or organic input of the lake. Sedimentation rates appear to be related to changes in the rainfall amount, at least before organic material makes up an important percentage of the sediments (around 2000 years B. P.). The amount of organics in the lake is a phenomenon partially related to the rainfall. The highest percentage of organics were reached during periods of intense droughts, and were mainly allochtonous (according the discrepancies between the Br and Organics records). The increase in organics after facies 7 also occurred when the lake started to become a more closed system, and the evaporation/rainfall ratio increases to a level never seen before. Variations in productivity have a different pattern from the effective rainfall records.

In the next section, a comparison with the pollen record could help us to determine the potential source of the organic material, confirming or rejecting its apparent autochthonous nature. The pollen record might help us to establish the relationship between the residuals of loss on ignition and the factors that drive inwash into the lake, e.g. the rain or the erosion due to the loss of vegetation cover. Finally, the pollen record is key for determining the human impact in the surroundings of Lake Esmeralda.

9.6 Comparison with the pollen and charcoal record

In the pollen and charcoal analyses presented by Bermingham (2020) using samples from core ES-14 and ES-16-I, the zonation divides the record into different stages. None of the stages based on pollen and charcoal records coincide with the geo-units and geological facies proposed in this thesis (Figure 9.8). However, a comparison of the eleven major taxa used in the analysis with the geological facies shows that upper borders of facies 1, 2, 5 and 9 coincide with changes in all the pollen taxa, except *Z. mays* (Figure 9.8).

The fact that these changes coincide with the geological facies implies that some changes in vegetation are related to changes in rainfall. Meanwhile, changes in the sedimentation inside the lake are partially driven by changes in the ground cover. (Figure 9.8a). I describe this in the next subsections.

It has to be highlighted that arboreal taxa, in particular Moraceae, *Brosimum* and *Maclura,* are considered the main representatives of the original dry broadleaf forests (see section 2.4 in chapter 2) by Bermingham (2020). Taxa like *Bursera* are also considered important components by Bermingham (2020), although they are seen as secondary taxa probably due to their lower contribution to the percentages of pollen. Non arboreal taxa like Asteraceae are shown as disturbance taxa. Meanwhile, *Z. mays* is definitely an indicator of human impact.

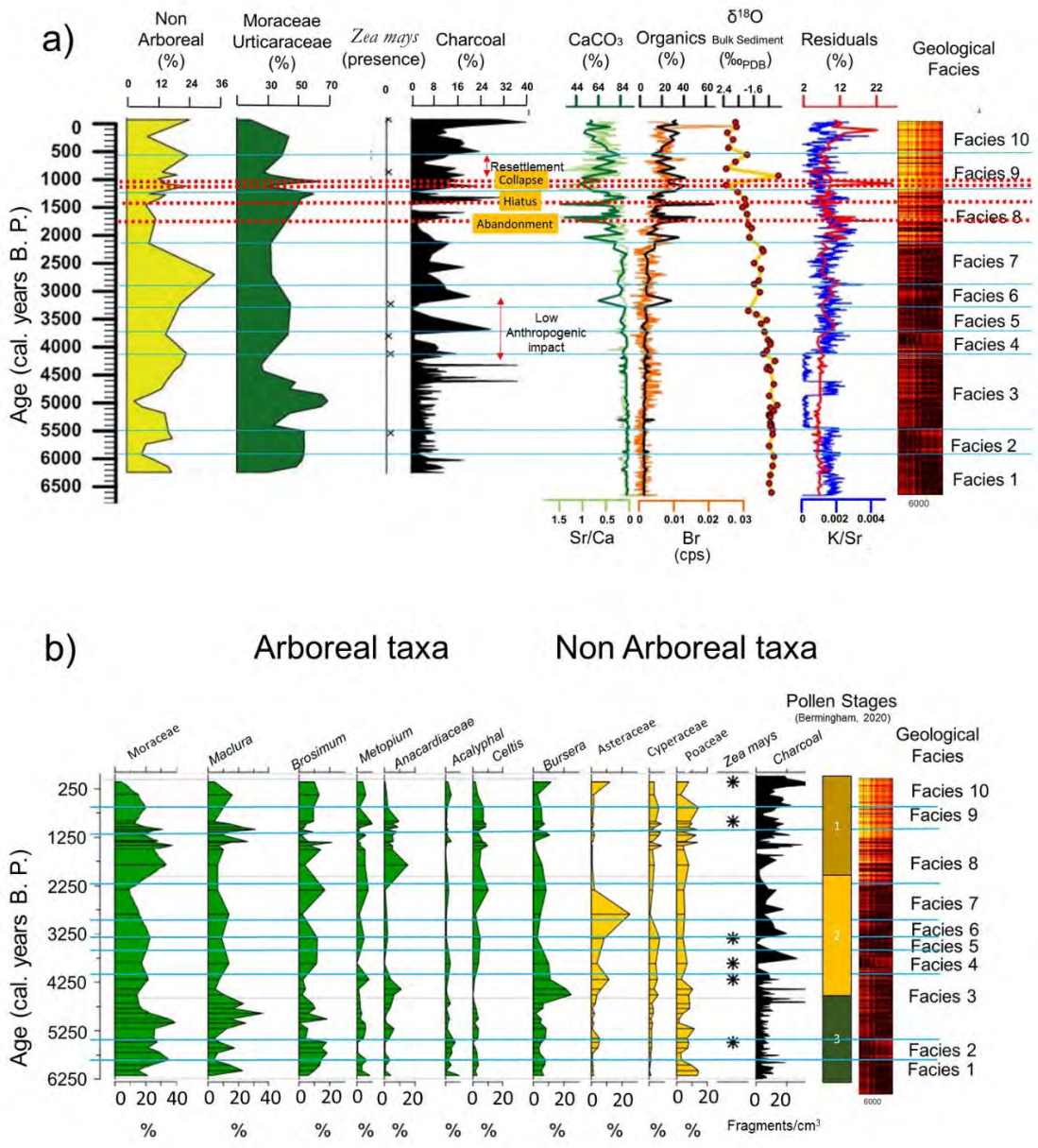

Figure 9.8 Palynological record of Lake Esmeralda developed by Bermingham (2020) in comparison with the records and facies developed in this research for this lake. a) Non arboreal, Moraceae, Z. mays and charcoal abundances compared to records associated with the rainfall amount and productivity records. b) Stages based on most abundant taxa and charcoal from Lake Esmeralda proposed by Bermingham (2020) in comparison to the geological facies proposed in this thesis.

Taxa reflected in the pollen assemblage from sediments or Lake Esmeralda are considered proxies of the local vegetation near this lake due to its size in contrast to the pollen assemblages of bigger lakes like Chichancanab, which are proxies of regional vegetation (Bermingham, 2020). Pollen assemblages of other lakes, including Chichancanab, will not be discussed in this thesis.

The $\delta^{18}O$ record and the pollen record

Changes in the arboreal taxa are not particularly reflected in the $\delta^{18}O$ record during the first geo-unit compared to the third geo-unit of Lake Esmeralda, supporting the idea that the values of the $\delta^{18}O$ in the first geo-unit does not necessarily indicates a prevalent less evaporation-rainfall regime in comparison to the third geo-unit, but also a lake that changed its hydrologically open character through time. (Although, the K/Sr record still indicates less rainfall during geo-unit 3 in comparison to previous geo-units).

Origin of organic material in Lake Esmeralda

An important point to focus on is that the organic material in the lake does not respond to the changes in arboreal taxa but in a small proportion to non arboreal taxa. For example, increments in Asteraceae, particularly during facies 5, 6 and 10, coincides with the increase of organics to over 25%. The increases in organics during facies 8 and 9 might be related to changes in other non arboreal taxa; Cyperaceae and Poaceae, since the trend of these records coincide between them. It also has to be considered that the resolution of data in the pollen record during facies 8, 9 and 10 is higher than the rest of the record. This gives the impression of a lack of variation in previous facies. However, it is true that more variation is also viewed in various of the records developed in this thesis over this time period, e.g. loss on ignition records.

The problem of considering Cyperaceae and Poaceae as partial drivers of the organic material in facies 8 and 9 is that changes in these taxa during the first geo-unit (facies 1 to7) seem to have never impacted the organic record. Percentages in Cyperaceae in facies 8 and 9 are not different from the percentages observed in the first geo-unit, but percentages in Poaceae are slightly superior during facies 8 and 9 compared to previous facies. The problem again is that those increments are ca. 5% higher respect to facies 4 to 7, less than 3% respect to facies 2 and 3 and no different to facies 1. I am incapable of assessing if these percentages are significant enough to stress the system for causing a change since I am not a biologist. A possible explanation of an impact of these taxa during

these facies and not before is that during geo-unit 1, the lake was hydrologically more open. Meanwhile, a more closed character of the lake in facies 8 and 9 might allow that increments in Poaceae impacted easier the amount of organics. A parsimonious explanation would indicate that in a more closed system organic material resulted from the degradation of Poaceae might accumulate easier.

The fact that non arboreal taxa correlate the amount of organics in general sounds logical since these kinds of plant tend to live shorter than arboreal taxa, degrading faster than them and therefore responding also faster to environmental changes. For example, the organic material (organic debris or humic and fulvic acids) of non arboreal taxa after decomposition might have easily been transported into the lake by rain as part of the inwash. In contrast, woody plants might have required more time for the same process. Therefore, changes in the amount of arboreal taxa would not have affected relatively fast changes in the organics, creating a lack of coincidence between both proxies. However, at some points, changes in the arboreal taxa seem to impact also the organic record. For example, the second most intense signals in the organics, which happened during the Maya abandonment, appear when the percentage of arboreal pollen seem to fall to its historical minimum. The strongest signal in the organic record, which occurs during the Maya Hiatus, also coincides with a decrease in the percentage of *Bursera* at that time. This might indicate that some kind of deforestation of the arboreal taxa might have increased the erosion, and therefore, it might have caused more transportation of inwash material. Unfortunately, the data presented in Figure 9.8b taken from Bermigham (2020) does not have sufficient resolution to make a direct visual comparison with the proxies developed in this thesis. Changes at this time scale are also not discussed by Bermingham (2020). Therefore, these apparent coincidences between the decrease of arboreal taxa and the peaks in the organic records at critical moments of the Maya history are not completely confirmed due to the lack of a better presented pollen diagram with a linear chronology (in contrast to a diagram plotted in the depth domain, where dates are indicated aside).

Until now, in this chapter, I have assumed that most organic material is autochthonous in the lake. This assumption takes into consideration the coincidence between the organic record produced by loss on ignition and the Br record. I have also highlighted periods when the lack of correlation between them happened (e.g. facies 6), indicating a source of allochthonous organic material.

This lack of coincidence between these two proxies happens during facies 6 and 10, when high levels in Asteraceae are observed, confirming allochthonous organics since this taxon indicates the loss of ground cover, allowing more erosion that might have enhanced the introduction of allochthonous organic material. Increase in facies 8, which coincide with changes in non arboreal taxa, suggest an external source of organic material. This also might explain why signals in organics are more intense than the signals in Br (Figure 9.7).

This indicates that during facies 8, particularly the increase in organic material during the Maya Abandonment, the Maya Hiatus and the Maya Collapse were not due only to autochthonous production of organic material (observed in Br record), but to the contribution of allochthonous organic material. This is particularly observed during the Maya Hiatus, where the peak in organic material (loss on ignition) is not so intense in the Br record (for example, the intensity of the signal of the Hiatus and the Collapse is practically the same in the Br record, meanwhile in the loss on ignition, the Hiatus is the most intense signal). Therefore, the organic material is produced predominantly inside instead of coming from surroundings during the first geo-unit (with the exception of facies 6, where *Asteraceae* had a role). Meanwhile, there are a combination of sources of organic material from inside and outside the lake in the second and the third geo-units.

Inwash, erosion and the pollen record

As I have discussed in the last paragraph, there are some variations in some taxa that might indicate a larger amount of inwash due to the loss of the ground cover (the loss of arboreal taxa). Besides the dramatic changes in facies 8 during the Maya Abandonment and the Maya Hiatus, changes in arboreal taxa, in particular, *Bursera* and Moraceae, only have an impact on the organics during facies 6. However, in this facies, Moraceae indeed decreases when *Bursera* increases. Facies 6 happens after a period of human impact near the lake (see next subsection), so a scenario similar to that observed in San Lorenzo (see section 7.7 in chapter 7) where erosion increases after the abandonment of agriculture might have happened, even though some of the original taxa, *Bursera* was recovering. Curiously, these increase of inwash due to the loss of ground cover only impact the K/Sr and residuals during facies 6 and only the residuals during the Maya Abandonment.

Other particular periods where there is loss of ground cover due to the loss of arboreal taxa (like the Maya Hiatus) seem not to have repercussions in the K/Sr record or the residuals. This indicates that variations in the K/Sr and the residuals during most of the record are driven mainly by changes in the rainfall. Differences between the K/Sr and the

residuals, as those observed during the Maya Collapse and 150 years B. P. cannot be explained by the loss of ground cover due to the decrease of the percentage of arboreal taxa when the K/Sr indicates periods of less amount of rainfall. It has to be noted that these two proxies of rainfall decrease during the Maya Hiatus, suggesting a dry period when the highest percentage of organics in all the record appears, and this organic material according to the Br record was mostly external and it might be easily transported due to the loss of ground cover according to the percentages of arboreal taxa like *Bursera*. This might indicate a scenario in the Maya Hiatus, where a dry period happened, but major erosion due to the loss of ground cover allows a major contribution of organics from the surroundings of the lake. Even though the rainfall was lower, erosion was capable of contributing more organic material with less rain.

The reasons for the lack of mobility of alkaline ions like K and Sr in a scenario of low flowing water, but more erosion driven by the loss of ground cover, deserves more research that cannot be unfortunately answered with the data obtained in this thesis. Organic material from non arboreal taxa would be moved by the rain as part of the inwash. Their changes in facies 6 and changes in the last three facies appear to be consistent with changes in the residuals, which might imply that these taxa were susceptible to changes in the rainfall. The difference between non arboreal proxies and K/Sr record is mainly due to the major resolution of this last record.

Human impact during the first geo-unit and the pollen record

The charcoal size fraction analysis (Figure 9.8b) suggests only four significant fire events at 5750 years B. P. (in Facies 2) 4650 years B. P (in Facies 3), and 4350 years B. P. (facies 4) and 4250 years B. P. (facies 5)> despite these events, the fire frequency estimated by Bermingham (2020) is no more than two fires for 700 years from the bottom to 1770 years. B. P. (at the middle of facies 8). For pollen stage 3, which includes the rest of facies 8, and facies 9 and 10, the amount of fires increases gradually, having three significant fire events, at 1460, 650 and 200 years B. P. (Bermingham, 2020); the number of events recorded, along with the magnitude of fire events, supports the notion that fire was used as a landscape management tool, but on a smaller scale. It is not clear if this use of fire is argued as a permanent practice during all the record or he implies its use only during the significant fire events.

Zea mays is the principal proxy used for arguing cultivation near Lake Esmeralda (Figure 9.8a) in conjunction with disturbance/openness indicators such as Poaceae*, Cecropia,*

Asteraceae, Chenopodiaceae/Amaranthaceae (Figure 9.8b). The cultivation of maize is seen as a low anthropogenic impact in the lake for the time frame before the Terminal Classic Mesoamerican Period (Bermingham 2020). The first signal of *Z. mays* appears 5450 years B. P. (Figure 9.8a). being an ephemeral event in facies 2. More permanent signals of *Z. mays* appear from 4150 to 3250 years B. P. which coincide with the fire events at facies 3, 4 and 5 (Figure *9.8*a). This coincidence supports the management of the landscape for cultivation during this period since slash and burn is argued as a common practice in the ancient Mesoamerica Milpa system. There is no evidence of cultivation after this, but since *Bursera* and *Brosimum* decrease during this time, the anthropogenic impact is seen as one of the possibilities. However, in this thesis, I observe that changes in these taxa coincide with the changes in rainfall (K/Sr record) and evaporation rainfall ratio ($\delta^{18}O$ record) (Figure 9.8). Therefore, I propose a scenario of no anthropogenic impact in this zone from 3250 years B. P. until the end of the Classic Mesoamerican Period 1050 years B. P., when the Moraceae/Urticaceae taxa start to decrease, and the fire signals increase to 1 fire event per 700 years. As I described in previous subsections, the increase in organics during facies 6 is due to the increase of non arboreal taxa and the loss of ground cover, which might be related to the previous human occupation during the time of the signals of *Z. mays*. However, this erosion could still happen when humans abandoned the area, as apparently happened in Lake San Lorenzo (section 7.7 in chapter 7).

The Maya Collapse and the pollen record

Bermingham (2020) claims that the Maya sites in the Cochuah Region were not abandoned during the Collapse at the End of the Mesoamerican Classic Period. At the same time, he argues that the Terminal drought drove the ancient Maya to intensify strategies around water resources based on the increasing charcoal signal, *Zea mays* and the declining forest abundances.

The decrease of Moraceae/Urticaceae taxa and the charcoal increase starts at 1050 years B. P. at the end of the Maya Collapse and *Zea mays* reappears in the record at 950 years B. P. at the beginning of the Postclassic period defined in this thesis. I established 1140, 1090 and 1040 years B. P. as the periods of droughts based on the Cariaco and speleothem records (see section 3.12 in chapter 3), therefore, the establishment of humans around Esmeralda was practically at the end of the Maya drought period (ca. 1040 years B. P.). Taking these dates into consideration, the argument of "no abandonment" turns in a "post

hoc, ergo propter hoc argument", and therefore, it is problematic, and there may be other factors involved.

The settlement patterns in the region of Lake Esmeralda at the finish of the Terminal Classic Period follow a similar dynamic to the Puuc Region (in the first years of the Maya Collapse in the Terminal Classic) and the Northern Mayab (see section 9.8 below). The Maya Collapse drove an abandonment of the sites in the Southern Lowlands and the Highlands, which apparently enhance migration to the Central and Northern Mayab. In this case, the use of Lake Esmeralda as a water source responds not directly to the drought but to the demographic increasing pressure in the region and the demographic reconfiguration in the Maya cultural Area that happened after the period of droughts. When the signals of cultivation appear in Lake Esmeralda at 950 years B. P, the amount of rainfall (K/Sr) was slightly higher than during the period of the Collapse (but still drier until 900 years B. P.), although not reaching their highest levels reached during facies 8, or the levels in the facies 1 or 2. Also, most of the arboreal taxa recovered or maintained their abundance after 900 years B. P. to the end of the Postclassic period.

In summary, the pollen and charcoal record indicate that the human impact on Lake Esmeralda was scarce (or minimal) and was not permanent since it is not shown in all facies. In addition, many changes in terrestrial vegetation are driven by changes in the hydroclimatic conditions during some periods, e.g. Moraceae and non terrestrial taxa. However, this is not definitive since the quality of the pollen diagram does not allow a direct comparison with the records developed in this thesis, and subcentennial variations are not discussed by Bermingham (2020). Loss of ground cover is shown in some particular moments, which enhanced erosion and a major contribution of organics from outside the lake, supporting the idea that Br is exclusively a record of indigenous organics. One of these periods of loss of ground cover happened during the Maya Hiatus, a dry period according to the K/Sr and residuals record. This might indicate that the loss of ground cover during this critical moment in Maya History was driven mainly by dry conditions and not necessarily by clearance.

9.7 Comparison with Chichancanab records

Figure 9.9 shows the comparison between the palaeoenvironmental proxies obtained from Chichancanab (Douglas et al., 2014; Evans et al., 2018 and Hodell et al., 1995, 2005) and the proxies produced in this research from Lake Esmeralda. The Chichancanab records in Figure 9.9 were produced from cores collected by Hodell et al., (1995, 2005) are in the

middle of Chichancanab at ca. 10 km from Lake Esmeralda (see Figure 6.1 in chapter 6). The core of Chichancanab from where the percentage of carbon was analysed (Covich and Stuiver, 1974) is thought to have been collected at the south part of Chichancanab, at one km from Esmeralda (see Figure 6.1 in chapter 6). It is necessary to consider the proximity to Esmeralda from this organic record. It is possible that the organic content in the middle of Chichancanab might have been different. For this reason and problems with the chronology of this Chichancanab record (see section 5.4 in chapter 5), I do not perform a direct comparison using this proxy.

The stable isotope records

There is, in general, a resemblance between the $\delta^{18}O$ isotope record on *P. coronatus* shells of Chichancanab (Hodell et al., 1995) and the $\delta^{18}O$ isotope record on bulk sediments obtained from Lake Esmeralda, as well as between the percentage of $CaCO_3$ (Hodell et al., 2005) obtained in both lakes. This is also true for the comparison between the K/Sr and Residuals from Lake Esmeralda with the D_{wax} record of Chichancanab (Douglas et al., 2014) and between the grey scale and density records of Esmeralda and the percentage of $CaCO_3$ of Chichancanab (Hodell et al., 2005). The most important difference between both sites is the precipitation of gypsum in Chichancanab, which is clear in its density record (Hodell et al., 2005).

The isotopic records of both lakes display values in a range of 5‰, although Chichancanab tends to have a range with more positive values, confirming the trend seen in water samples (see section 8.1 in Chapter 8), where Chichancanab is a more closed system than Lake Esmeralda.

The apparently greater variability in the $\delta^{18}O$ isotope record on *P. coronatus* shells of Chichancanab (Hodell et al., 1995) is probably related to its higher time resolution (more data per time frame) compared to Lake Esmeralda. Chichancanab and Lake Esmeralda have the same pattern in their $\delta^{18}O$ records during the Middle Holocene (Northgrippian). During the Middle Holocene (Northgrippian), the $\delta^{13}C$ on *P. coronatus* shells of Chichancanab fluctuates 5‰ (-2‰ to 3‰), in the same range as the fluctuations in the bulk sediment of Lake Esmeralda.

Both isotope records have a distinctive pattern in Chichancanab and Esmeralda during the Late Holocene (Meghalayan). The $\delta^{18}O$ record of both lakes has similar patterns from 3000

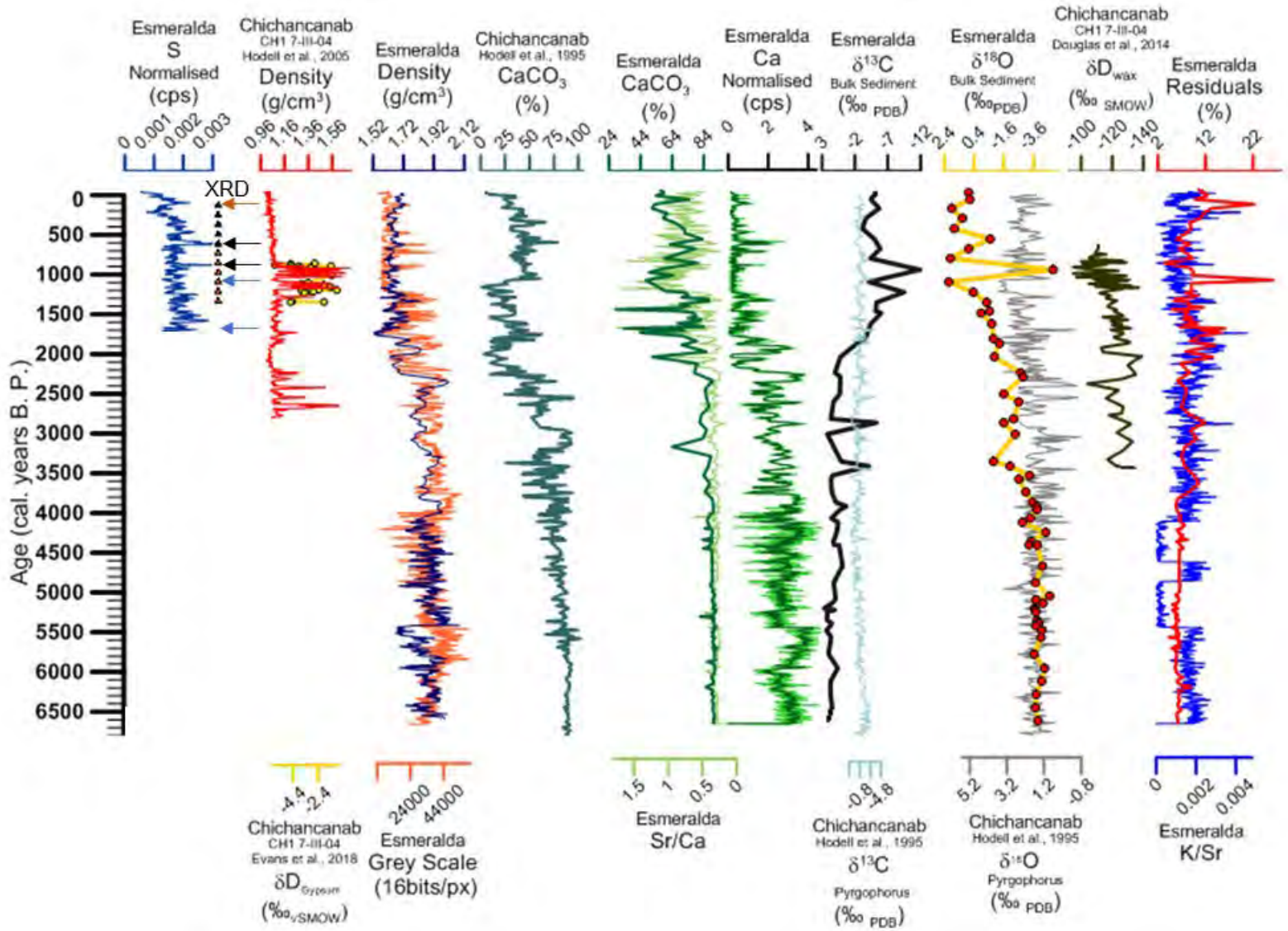

Figure 9.9 Comparison between records developed from sediments collected at Lake Esmeralda with the records developed for Chichancanab by Douglas et al., (2014), Evans et al., (2018) and Hodell et al., (1995, 2005). The S record is shown only for the last 1700 years B. P for seeing intense signals that might be related to sulphate precipitation. Black and orange (stratigraphic position doubted) triangles indicate layers where an XRD analysis was performed. Arrows indicate points where gypsum was searched.

to 2000 years B. P, but thereafter, the $\delta^{18}O$ values in Lake Esmeralda turn more positive, even though they conserve the same trend. This trend means that Lake Esmeralda starts to be a more closed system during the Late Holocene (Meghalayan), while in Chichancanab, this change was slighter.

Around 1000 years B. P., after the Maya Collapse time frame, there is a less dry period in Chichancanab compared to the previous time during the Collapse and the next centuries in the Postclassic period. During this time frame, Lake Esmeralda has an outlier (-4.9‰) in the $\delta^{18}O$ records that would also suggest less dry conditions. However, the previous and next values in Chichancanab are not abruptly different in this particular time as it is in Lake Esmeralda. Therefore, I will still consider this outlier as a spurious signal that cannot be considered for describing the environment. The record based on plant waxes of Chichancanab also has a similar trend to the bulk sediment $\delta^{18}O$ record of Lake Esmeralda (Douglas et al., 2014).

During the Late Holocene (Meghalayan), the $\delta^{13}C$ in Lake Esmeralda decreases up to 5 ‰ units, while the $\delta^{13}C$ values in Chichancanab are more constant. This $\delta^{13}C$ change in Lake Esmeralda might be linked to the sources of carbon and the increase of organic material. Concerning the amount of organic material, Chichancanab also shows a progressive augmentation in organic material, with a similar trend as in Lake Esmeralda (not shown). However, as I described at the beginning of this section, a direct comparison with the organics record in Chichancanab (Covich and Stuiver, 1974) is not possible.

The $CaCO_3$ records

$CaCO_3$ percentage in Chichancanab is interpreted to reflect changes in the hydrologic budget, which were ultimately controlled by changes in the ratio between evaporation and precipitation (Hodell et al., 2005). Calcite percentage obtained by loss on ignition in Chichancanab and the Ca abundance record obtained by XRF in Lake Esmeralda have similar tendencies. Both records become depleted in $CaCO_3$ after 3500 years B. P.

The percentage of $CaCO_3$ in Chichancanab logically resembles also the percentage of calcite obtained by loss on ignition in Lake Esmeralda. It has to be highlighted that the abrupt depletion of $CaCO_3$ in the Esmeralda record at the Maya Abandonment is not observed in Chichancanab. While the depletion at the Maya Hiatus is just slightly recorded in Chichancanab.

The Gypsum

Critical moments in Maya history, including the Maya Collapse (see section 2.7 in chapter 2), are well observed in the density record in Chichancanab (although the Maya Hiatus is slightly registered) with abrupt signals around this time related to gypsum precipitation. In contrast, these abrupt changes in the Chichancanab density record are not clearly registered in the density record of Lake Esmeralda. During these critical moments in Maya History, the Maya abandonment, the Maya Hiatus and the Maya Collapse, Lake Esmeralda has the organic peaks discussed in section 9.5. This amount in organics might suggest that Lake Esmeralda was very shallow during these critical periods in Maya History, becoming perhaps a bog. This idea would be supported by the descriptions of the first Spaniards arriving in the Cochuah Region (Molina-Solís, 1896), although they are not accurate in describing the exact location of their observations. Unfortunately, analysis of subfossil fauna or algae from Lake Esmeralda that could further enlighten us about the lake depth at that time has not yet been undertaken. However, from the pollen and Br analyses, I know that during the Maya Hiatus (1438 years B. P.), most of the organic material in the sediments is allochthonous, and it was probably enhanced by the increased erosion that existed at that point due to the loss of ground cover. This makes the bog scenario unnecessary. In addition, the amount of organic material measured today in Lake Esmeralda is around 40% (Metcalfe, personal communication) and the lake is not a bog.

Table 9.2 shows the results of the water analyses (samples taken in 2018) performed in the southern sites of Lake Esmeralda in comparison with the concentration of dissolved ions in Lake Chichancanab measured by various authors (Covich and Stuiver, 1974; Hodell et al., 1995; Illescas-Pasquel, 1950; Perry et al., 2002). The content of major ions in Lake Esmeralda is lower than in Chichancanab. Inclusive, the results of alkalinity show that Lake Esmeralda has 500 mg/L against 540 mg/L in Chichancanab. Perry et al., (2009) suggested that these differences are related to the surrounding lithology of the lakes. Chichancanab is in contact with a suevite layer produced on the Mesozoic evaporites (called the Evaporite Region), which contributes with sulphate (Perry et al., 2009). In contrast, Lake Esmeralda is not in contact with this layer but still near to it. Other sources of gypsum, like the Cretaceous rocks from the southeastern part Quintana Roo (Gondwe et al., 2010), might have required a more open system with connections to the drainage of this part of the Mayab. However, this connection in the past is still only speculative and definitely did not existed at the time of the collapse, when the hydrological character of

Table 9.2 Concentration of dissolved ions in Lake Esmeralda analysed by ion-exchange chromatography in comparison with similar analyses performed in Chichancanab by various authors (Covich and Stuiver, 1974; Hodell et al., 1995; Illescas-Pasquel, 1950; Perry et al., 2002). The table also shows the solubility of natural salts resulting from the coprecipitation of the analysed ions with their most common conjugate hard-weak acid on Earth surface. The solubility of these salts marks the point of water saturation of these ions related to a specific salt.

Sample	Cl^- (mg/L)	PO_4^{3-} (mg/L)	SO_4^{2-} (mg/L)	Na^+ (mg/L)	K^+(mg/L)	Mg^{2+} (mg/L)	Ca^{2+} (mg/L)
ES-2018-CH9	157	undetected	1180	141	6.85	119	598
ES-2018-CH7	157	0.17	1181	141	6.86	123	600
ES-2018-CH8	157	0.17	1182	141	6.92	123	602
ES-2018-CH8D	157	0.17	1200	141	8.91	120	599
Chichancanab January 2018 (Metcalfe, unpublished data)	240	2.42	2982	153		164	690
Chichancanab March 1996 (Perry et al., 2002)	234		2455	199		201	607
Chichancanab March 1995 (Hodell et al., 1995)	293		2625	210		240	
Chichancanab June 1993 (Hodell et al., 1995)	234		2545	250		257	
Chichancanab 1967 (Covich and Stuiver, 1974)	-		2750-2950	340-400		360-425	
Chichancanab 1950 (Illescas-Pasquel, 1950)	138		2929	105		253	
	NaCl		**$CaSO_4$ 4 H_2O**	**NaCl**		**Magnesite**	**Calcite to Gypsum**
Saturation	357		2500	357		600	14 to 2700

the lake was nearly closed as it is today, according to the $\delta^{18}O$. *Table 9.2* also shows the solubility of some natural salts resulting from the precipitation of these ions for indicating the point of saturation. As it can be observed, the sulphate in Chichancanab is over the value of solubility of gypsum. Therefore, it is oversaturated in gypsum. Meanwhile, the same ion is undersaturated in Lake Esmeralda.

A period in Lake Esmeralda presumably had an oversaturation of sulphates, however. Such a period is around 150 years B. P, which is observed as peaks in the residuals that do not appear in the K/Sr record. The signal at 150 years B. P. has confirmed gypsum presence by XRD. The possibility of a scenario of oversaturated gypsum in Lake Esmeralda would implicate lowering of the water level or an additional source of gypsum.

Additional discrepancies like this observed at 150 years B. P. between the K/Sr and the residuals record would suggest the presence of gypsum, for instance, the signal at 1069 and 1750 years B. P. These signals at 1069 years B. P. has an XRD analysis (although stratigraphy has not been completely confirmed) showing no presence of other minerals besides calcite. The signal at the end of the Maya Abandonment at 1750 years B.P., however, do not have an XRD analysis. From the pollen record, It is known that the loss of ground cover observed by the decrease of *Bursera* during the Maya Abandonment might have enhanced erosion, which might explain the amount of organic material in the lake. However, this is not sufficient for explaining the discrepancies of K/Sr and the residuals at that time.

A view of the upper part of sulphur record obtained by XRF (not entirely reliable because the inherent problem to detect this element accurately by this technique, as well as to present the same problem as the Ca record obtained by XRF in the part of the high percentage of organics in the last 1700 years B. P., where the logarithmic response of the intensity of signals gives very small signals in comparison to the first 5000 years of the record, see section 9.4), shows relatively high signals of S (Figure 9.9 black arrows) comparable to that seen at 150 years B. P (Figure 9.9 red arrow). These signals do not show discrepancies between the K/Sr and residuals, and they do not present gypsum in the XRD. In contrast, points where there are discrepancies between both records (Figure 9.9 blue arrows) do not show signals so intense in the sulphur record, and concerning the signal at 1069 years B. P., the XRD do not show the presence of sulphate minerals. Four samples of XRD (black triangles) and six samples (orange triangles indicating the probable stratigraphic position) do not show the presence of gypsum supporting that the lake was

also unsaturated in gypsum in periods when the lake was reaching its highest hydrologically closed character. Because both analyses, the S analysis by XRF and XRD, are not completely reliable because of problems of detection and problems with the access to raw data, respectively, I cannot take them as definitive proof of the absence of gypsum. However, the presence of gypsum seems highly improbable. They support indeed that discrepancies between the K/Sr indeed and the residuals cannot be explained by the presence of this mineral. Concerning this matter, the cause of discrepancies between both records is still inconclusive.

In summary, the comparison between records from Chichancanab and Esmeralda highlight differences in their catchment, surrounding geochemistry, water chemistry and hydrological open character. All these variables, in addition to their differences in sizes, means that besides their proximity, the term "sister lake" is inaccurate since both systems function as distinctive systems. This comparison opens the question concerning the role of the size of Lake Esmeralda to be more susceptible to change its hydrological open character through time.

9.8 Comparison with Maya History of the Cochuah Region

Lake Esmeralda is in the Southern part of the historic Kuchkabal of the Cochuah Region. The Cochuah Region means in ancient Mayatan literally "our bread food", an accurate translation is "well-fed province that has never found itself in need" (Shaw, 2015a). This name suggests that the region is suitable for agriculture due to the kind of soils in the area despite the relatively small water resources.

Figure 9.10 shows a comparison of the proxies developed in this research with the archaeological and historical data collected in the Cochuah Region. There is no signal of human occupation for the Northgrippian. The first signals of human occupation are the presence of *Z. mays* around Lake Esmeralda in the pollen record (Bermingham, 2020). Contemporary signals of this taxon are observed in the record of Chichancanab (Bermingham, 2020).

Since Chichancanab is the biggest water body in the region, it makes sense that the early occupation has been settled near this lake since the technology these days does not allow better management of water sources, such as channels, wells, or chultunes. However, the water might have still been unpalatable and useless for irrigation at that time.

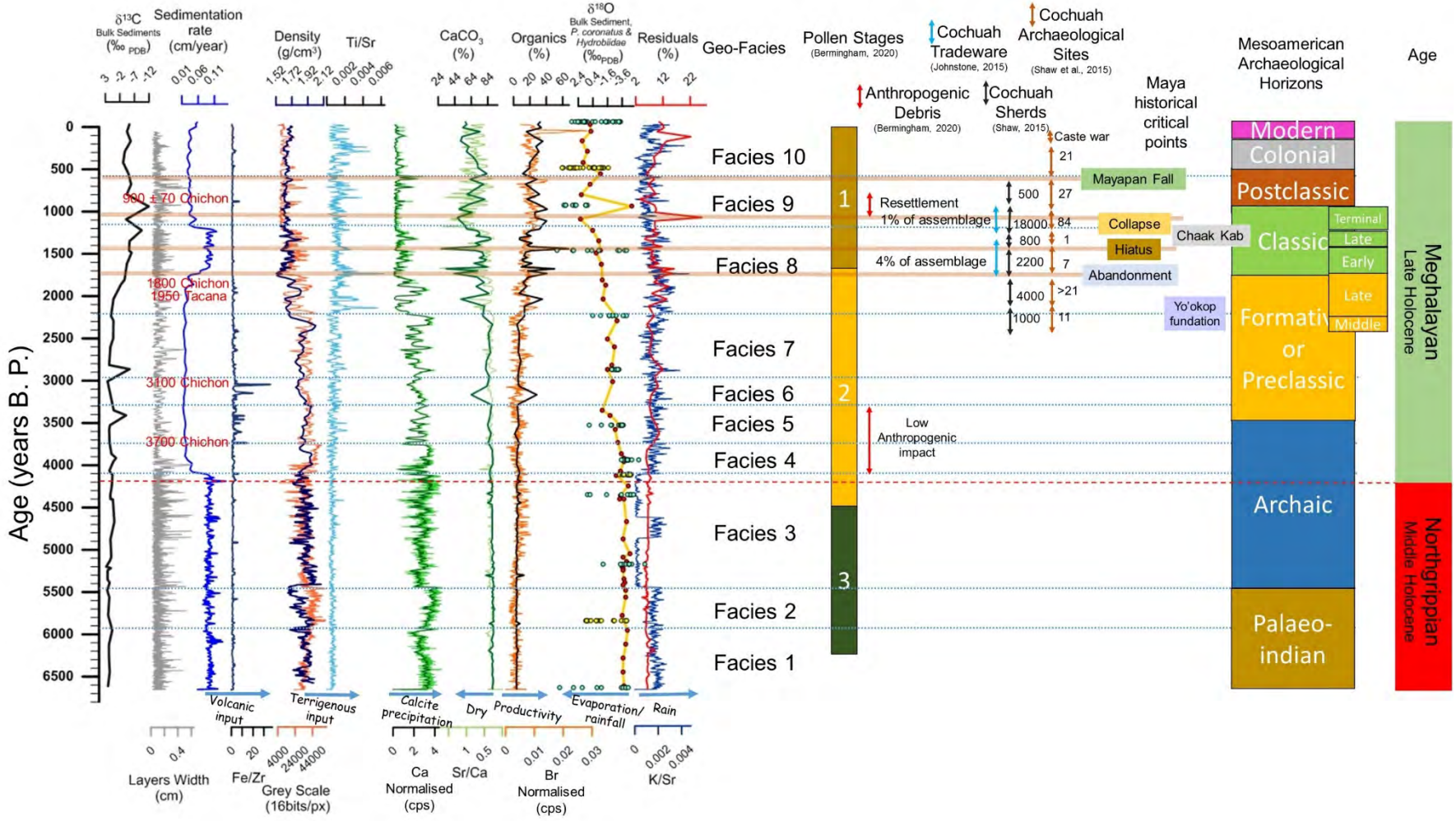

Figure 9.10 Comparison of the environmental history of Lake Esmeralda with the archaeological and historical records of the Cochuah Region. Arrows indicate the time frame of an event. Blue circles represent the $\delta^{18}O$ of single shells of P. coronatus whilst yellow circles are the $\delta^{18}O$ of Hydrobiidae, including P. coronatus in that layer.

This early occupation happened during facies 4 and 5, which are periods of relatively high humidity, although they were drier than previous periods. A change to drier conditions that happened during facies 5 might have driven the end of the occupation in this place.

Another possibility is the change of productivity in Lake Esmeralda in facies 6. Bermingham (2020) suggest a permanent occupation during the rest of pollen stage 2 according to the depletion of some arboreal taxa, but the archaeological finds (performed for 10 years) in the region do not support this. Early occupation based on material culture in the Cochuah Region is found from the Middle Preclassic around 2500 years B. P. Around 11 villages appeared in the region around the Middle Formative, including Yo'ok'op, (20 km east from Lake Esmeralda see Figure 2.9 in chapter 2) which was the settlement with the longest occupation (Shaw, 2015a).

The number of sherds (broken pieces of ceramic material, especially those found on an archaeological site), which is an indirect proxy of human occupation, was around 1000 in the Middle Preclassic (also Middle Forrmative). This occupation coincides with the increase of organics in Lake Esmeralda at the end of facies 7.

The settlements during Middle Formative occupied the north region of the Cochuah region, where the nearest centre Sacalaca was at 20 km from Chichancanab and 30 km from Lake Esmeralda. Sacalaca and Yo'ok'op were the only settlements that had reliable water sources from sinkholes (cenote and aguada) (Shaw, 2015a). At the same time, other villages depended on their ability to store rainfall. This implies a lack of settlements near the biggest sources of water in the Cochuah region; Chichancanab and Lake Esmeralda. This lack might have been related to the productivity of the soils or the presence of wild fauna that might have been existed in Chichancanab and Lake Esmeralda. For example, wild fauna was not only dangerous for human life but sacred in the Maya cosmovision (Vargas-Pacheco and Arias-Ortiz, 2006).

During the Late Preclassic around 2200 years B. P., there was a dramatic increase in the number of sites. At least 21 settlements existed at that time. Around 4000 sherds are found in the archaeological record. Therefore, this was the second most populated period in preeuropean time (Shaw, 2015a).

This high occupation coincides with periods of high productivity at Lake Esmeralda around 2000 years B. P. in a time that was relatively dry after the Maya abandonment, the

Cochuah region decreases its population, having only 7 settlements in the entire early Classic. The number of sherds in the archaeological record is around 2200 (Shaw, 2015a).

It was possible to measure the intensity of trade during this Mesoamerican subhorizon, based on the percentage of finds from other regions, especially the Maya southern Lowlands (Johnstone, 2015). The percentage of finds in the assemblage that was from 'foreign' lands during the Early and Middle Classic was 4%. The early Classic periods happened when Lake Esmeralda was relatively nutrient enriched. If changes in the productivity of the lake were driven by the human occupation in the region, the lake should have lower productivity than in the previous Formative horizon. But the productivity increased even though the population in the region got lower (Shaw, 2015a). Another problem is the lack of evidence of permanent human occupation near the lake and a way to connect changes in productivity with an increase of nutrients derived from agriculture practices at 30 km from the lake. According Leyden (2002) *Z. mays* was present in Chichancanab during the early Classic until the Maya Collapse, inferring agriculture fields 10 km far away from Esmeralda. The record produced by Leyden, (2002) covers a period much shorter than the record produced by Bermingham (2020).

Besides, the possible eutrophication episodes in Lake Esmeralda, when the organic productivity increased dramatically (e.g. during the Maya Abandonment, Maya Hiatus and Maya Collapse) happened in moments when the population in the region might have been really low. In addition, according to my interpretation of the decrease of some arboreal taxa, most of the organic material was not autochthonous but from outside the lake during the Abandonment and the Hiatus. Therefore, a eutrophication episode in the lake does not explain completely the organic input associated with more nutrients generated by the human impact of more population near the lake or in the Cochuah Region.

After the Maya Hiatus, only Yo'ok'op contained a sizable resident population during the Late Classic archaeological horizon. The amount of sherds decreased to around 800 (Shaw, 2015b). At the end of this time, this settlement was ruled by Kaloomte' ix Chaal Kab (Nygard et al., 2015), a rare example of a female ruling cities in ancient Maya society. A female ruler indicated stressing political moments in the region (see Section 3.10, chapter 3). The Cochuah region has maintained a similar evaporation-rainfall ratio since the Late Formative excepting for the Maya Hiatus, which was drier. The productivity in Lake Esmeralda decreases again during the Late Classic period, reaching inclusive levels comparable to the periods without human occupation in the region.

At the Terminal Classic Horizon, the number of settlements increases to around 84. The number of sherds is the highest in history, reaching 18000 (Shaw, 2015a). In contrast, the percentage of assemblage linked to long-distance trade is only 1% (Johnstone, 2015). This decrease in the trade may reflect the disappearance of the trade routes due to the collapse of the payolelo'ob in the Maya Sothern Lowlands (Grube et al., 2012; Grube and Schubert, 2015; Segura, 2017), or it can be an effect of the increasing population, which was capable of providing more goods inside the region (Shaw, 2015b).

In this thesis, I consider that the droughts existed in a period constrained from 1140 to 1040 years B. P., which includes only a century of the Terminal Classic Horizon. The archaeological record in the region, unfortunately, does not have the resolution for establishing if the appearance of these new settlements appears at the beginning of the horizon (1200 years B. P), as a result of the fall of Kak (Calakmul), during the drought at 1140 to 1040 years B. P., or after the droughts when practically all the cities in the Southern Lowlands have disappeared, and the political power of the Peten region had collapsed. Since the pollen record indicates human impact around Lake Esmeralda by the increase of disturbance taxa after 1050 years B. P. and *Zea mays* at 950 years B. P., I support the last possibility. In this way, the Cochuah region had a similar dynamic to the Puuc region.

According to Leyden (2002) native vegetation does not seem to respond much to the droughts, since there was an important decrease of the different taxa, pointing out that this might reflect its resilience to drought, even when the same drought might be really problematic for people. This contrasts with the observations of the pollen in Esmeralda (see section 6.6), but as Bermingham (2020) explains, the pollen record at Chichancanab observed vegetation changes in a regional scale meanwhile the pollen record in Esmeralda observed vegetation changes at the local scale. Therefore, the apparent adaptation of the vegetation to the droughts might have been only happened at some scale. In my opinion, pollen records are not capable to observe decadal changes.

After the time of the Maya droughts after 1040 years B. P., the evaporation rainfall ratio indicates slightly fewer dry periods (ignoring the $\delta^{18}O$ outlier) while the K/Sr rainfall record suggests an amount similar to that existed during the Late Classic period. This short, highly populated time frame might respond to these conditions. In Chichancanab, the $\delta^{18}O$ record also supports a less dry period (Hodell et al., 1995). In its density records, the precipitation of gypsum happened until ca. 900 years B. P. (Hodell et al., 2005) and the δDwax also indicates four recurrent droughts after 1040 Years B. P. until 900 years B. P.

Two strong droughts before 940 years B. P. (Evans, 2013) and two additional small droughts in the next 40 years. This might explain the recovery of some taxa since 900 years B. P. (see previous section 9.7 in this chapter). This recovering also happened at regional scale according the pollen record of Chichancanab (Leyden, 2002).

In the Postclassic horizon after 1200 years B. P., the number of the sites decreased again to around 27, while the number of sherds fell to 27 (Shaw, 2015a). This depopulation happened in a moment when the legends indicate that the region was geo-united as one political entity, in a Kuchkabal (Chilam-Balam, 1966). During this horizon, the evaporation-rainfall ratio decreases, and the K/Sr rainfall record maintains, both indicating humid conditions similar to the one present in the Late and Terminal Classic horizons, except for the time of the Mayan droughts. In this subhorizon, the productivity of the lake continues decreasing.

After the moment of the destruction of the Mayapan League, (including the disintegration of the Kuchkabal of Cochuah), humid conditions similar to those existed in the Early Classic returned. No strong drought is registered for the moment of the destruction of the Mayapan League, however, a fall in the productivity of Lake Esmeralda happened.

Colonial times had a documented decrease in population in Cochuah Region, while the number of sites in the region is 21, including the new Spanish settlements (Shaw, 2015a). This period appears to be the most extended and driest period in the record, while the productivity in the lake increases again.

After independence from Spain, the Cochuah region had a relatively high population since this region was a rebel Maya region during the Caste War (see Section 2.5, chapter 2). The Maya survived and hid here. During this time, the organics in the lake fell again. It is clear that although a relatively high population was maintained, the dynamics of the war did not allow agricultural practices in the way that were performed in pre-colonial times or during the colony. During the XX century, the last century of the record, the Cochuah region had emigrations and immigrations, maintaining a moderate population ca. 36,000 habitants (INEGI, 2010; Shaw, 2015a).

9.9 Conclusion

This chapter deals with the environmental history reconstruction of Lake Esmeralda in the kuchkabal of Cochuah. An age model was created, having corrected for the hard water effect. The fact that anomalous signals in the record coincide with the critical moments in the Maya History such as the Maya Abandonment, the Maya Hiatus or the Maya Collapse suggests that the age model is reliable. The environmental record used different proxies for reconstructing one aspect of environmental history.

Precipitation of $CaCO_3$ and organic deposition in the lake are not entirely linked with changes in the rainfall or evaporation-precipitation ratio ($\delta^{18}O$), but they are related in some way. I have observed that moments of maximum production of organic material and low precipitation of carbonates happened during relatively dry periods. I do not know how these phenomena are connected.

It seems that the loss of ground cover and consequently erosion does not have an effect in the K/Sr record but on residuals during some decadal periods. Therefore, the K/Sr record seems to be an unequivocal record of rainfall variations. This record indicates that the Maya Collapse was a time of hydrological droughts.

The $\delta^{18}O$ record indicates that Lake Esmeralda has become a more hydrologically closed basin across the years, starting to have a change in this matter since 2200 years B. P. This is inferred since the rainfall variation observed in the K/Sr record has not abruptly changed as the $\delta^{18}O$ does during the 6500 years studied. This discrepancy between both records suggests that the big changes between the bottom part and the last 2000 years B. P. in the $\delta^{18}O$ record can be explained by a change in the sources of water, which modified the hydrologically open character of Lake Esmeralda.

Unsurprisingly, both records, the K/Sr and the $\delta^{18}O$ indicate some recurrent droughts across time, including dry periods at the critical moments of the Maya History, including the Maya classic Collapse. The dry period of this event prevailed after the collapse for a century more, which is consistent with was is observed in the density and isotopic records in Chichancanab (Douglas et al., 2016; Evans et al., 2018; Hodell et al., 1995, 2005).

However, the stronger signals associated with droughts during Maya History at critical moments such as the Maya Abandonment (1800 to 1750 years B. P.), the Maya Hiatus (1414 years B. P.) and the Maya Collapse (1190 to 1140 years B. P.) are shown in the percentage of organic material, which present abrupt increase of organic material (ca. 50%,

70% and 40%, respectively) at those times. A high percentage of organics during this period is an allochthonous organic material to the lake enhanced by the loss of ground cover.

The comparison between the palaeoenvironmental records of Lake Esmeralda and the archaeological and historical records enlighten us, suggesting a possible correlation between organic material deposition in the lake and changes in the settlement patterns in the Cochuah region. However, minor anthropogenic impact exists in Lake Esmeralda before and after the XI and XII Century of the C. E.

The mechanism that could link changes in the settlement pattern with the production of organic material in the lake is unknown, taking into consideration that the nearest found settlement and agricultural fields were 30 km away. Closer agricultural fields and settlements could still be discovered in the future, but the pollen records suggest that the human impact was minimal for most of the time in Lake Esmeralda. (agriculture fields existed during Early Classic Horizon at the North of Chichancanab according with Leyden; 2002, but that was not the case at lake Esmeralda according Bermingham; 2020). Nutrients leaching into the lake due to agricultural activity could have increased productivity. It is difficult to imagine a mechanism that could have translated such nutrients from 30 km or beyond. Although, the presence of permeable sediments around the lake suggest that underground waters might have played a role in this since the water table in the region is at 5.2 meters below the mean sea level, and Lake Esmeralda is not a perched aquifer (Gondwe et al., 2010). It has to take into consideration that the highest signals in organics are associated with allochthonous organic material to the lake according the low signal of Br in comparison with the organic percentage, which was enhanced apparently by the loss of ground cover. In this way, at least the allochthonous organic material is driven by the loss of arboreal taxa, which might have been decreased because of the droughts. However, the loss of ground cover happened during sub-centennial periods that cannot still explain most of the increase of organics in other periods, which according to the Br record, were produced inside the lake.

It has to be also considered that the most intense periods of productivity (autochthonous organics) happened during the Maya abandonment and the Maya Collapse. It might have been periods of low agriculture based on the societal challenges observed in most of the Maya villages (Grube and Schubert, 2015). In contrast, the fact that the region was highly populated during the Caste Wars between 150 to 50 years B. P. (1800 to 1900 A. D.), at

the time of minimal agriculture in the Cochuah Region and minimal percentage of carbon (according to loss on ignition) in Lake Esmeralda, would indicate that the agriculture activity would have been responsible for enhancing organic productivity inside the lake. This might explain that the increase of productivity after 1050 years B. P. during the increase of occupation in the Cochuah Region and the observation of *Z. mays* would have enhanced by nutrients derived by agriculture activities. In the end, the response of the drivers of changes in productivity is inconclusive.

Another factor to consider is that the lower charcoal counts might have been an effect of a more hydrologically open lake. More data are needed. For example, a phosphorus or nitrogen content record and a C/N record from Lake Esmeralda and a location of anthroposols in the Cochuah Region would help for tracing the temporal and spatial distribution of nutrients, identifying the sources of them.

In the next chapter, I will summarise the issues related to the significance of environmental history of Lake Esmeralda as well as Lake San Lorenzo presented in chapter 7.

This page intentionally left blank

Chapter 10 Final thoughts and conclusions

Photo: A ceiba Maya holy tree at Uxmal

"The indio cries, Yucalpeten (Mayab,), his cry runs by the cenotes,
his cry runs and it cannot be seen. Because the bad time has arrived;
the bad time of Multundzec, the black time of Multundzec.
The bee from Cuzamil has gone. The deer from Mutulmut has gone.
The burnt flower of Xtabentun has gone with the wind.
Bloody moon, the land is death, the holy land of Itzamatul.
Yucalpeten!, Yucalpeten! All has gone, all has happened".

Yukalpeten, Antonio Mediz Bolio, 1928.

This thesis has dealt with the environmental reconstruction from two lake sites in the Maya Cultural area. One site (Lake San Lorenzo) was in the northern Maya Highlands and the other (Lake Esmeralda) in the central part of the Mayab. The results discussed in previous chapters indicate that both sites had distinctive characteristics even though both experienced a climate change during specific critical moments in Maya History, such as the Maya Hiatus and the Maya Collapse.

Section 1.5 in chapter 1 described how this research had different epistemic levels with their own questions that had to be resolved in order to perform an environmental reconstruction at both sites. A specific answer to the questions for every epistemic level will not be presented in the thesis, but they have been indirectly answered in the previous three chapters (7 to 9). For example, all questions related to the technical level, which dealt with the affordability of a method of analysis or the correct interpretation of a proxy, were answered in the first sections of the previous three chapters.

The final sections of chapter 8 dealt with answers related to the limnological and hydrological system levels. Chapter 7 and 9 also discussed questions related to the hydrological system level (comparing Lake San Lorenzo with Lake Kail (Guatemala) and Balamtetic, and comparing Lake Esmeralda with Chichancanab), and the ecosystem level (when Lake San Lorenzo and Lake Esmeralda were compared with the pollen and charcoal records of Franco-Gaviria et al., 2018 and Bermingham, 2020, respectively).

This chapter presents the conclusions obtained during the study performed on both lakes described in the previous chapters and compares both sites covering the final epistemic levels; the gradient level; the regional level; and the anthropological level. Chapters 8 and 9 have already dealt with the human subregional impact. It has to be highlighted that the initial purpose of this thesis was to make a direct comparison between both sites. However, since most of the records developed in both sites were a proxy of different phenomena, a direct comparison was not possible. Having these issues in mind, a comparison is made to the inferred humidity changes in the environment, in addition, I also compare the responses to humidity of the vegetation, mineralogy, and sedimentation. Figure 10.1 summarises the complexities and overlaps of the research questions, lake and proxy systems investigated in this thesis and is used to structure this concluding chapter.

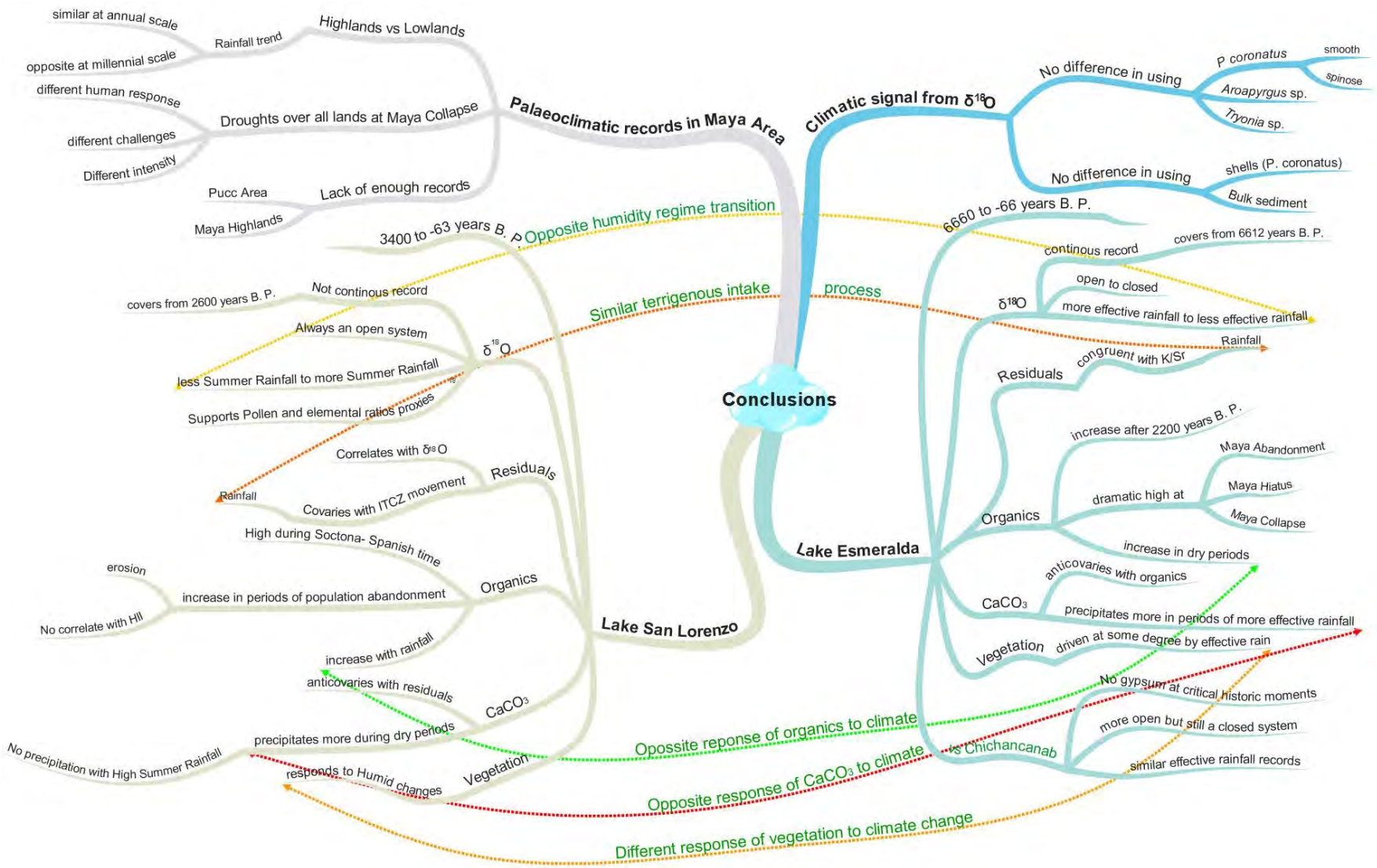

Figure 10.1 Mind map showing the conclusions of this thesis and the connections between them.

10.1 The climatic signal from $\delta^{18}O$ in Lake Esmeralda

In chapter 7, we saw that it was possible to recover the climatic signal from $\delta^{18}O$, which for Lake Esmeralda is a proxy of effective rainfall (evaporation – rainfall ratio). The results showed no difference in using a particular genus of Hydrobiidae (*P. coronatus*, *Aroapyrgus sp.*, or *Tryonia sp.*) for this purpose. However, shells of *P. coronatus* were recommended to be used since they were the most abundant genus. The most important conclusion respecting the $\delta^{18}O$ in Lake Esmeralda was that there was little difference between using shells and bulk carbonate sediments for recovering the environmental signal. Because of the affordability of the analysis, I decided to use the bulk sediment to perform an analysis with a higher resolution.

10.2 Lake Esmeralda vs Lake San Lorenzo

Figure 10.1 (middle and lower area) presents the comparison of the key conclusions obtained from the records collected at Lake Esmeralda in the Cochuah region and Lake San Lorenzo in the Lagunas de Montebello Lake Complex. The next subheadings appearing in green, indicate the comparison between proxies developed for both lakes which give information on a particular process influencing or occurring in the lake. It has to be considered that the record in Lake San Lorenzo covers from 3400 years B. P. to -63 years B. P. (2013) (see figure 7.3 in chapter 7), meanwhile the record at Lake Esmeralda is longer covering from 6660 years B. P. to -66 years B.P (2016) (see section 9.1 in chapter 9).

An opposite humidity regime transition

In Lake San Lorenzo, the $\delta^{18}O$ record was not continuous, presenting some gaps. It covers from 2600 years B. P. to recent years (see section 7.6 in chapter 7). The $\delta^{18}O$ record was continuous in Lake Esmeralda covering the complete stratigraphic sequence (see section 9.5 in chapter 9). The $\delta^{18}O$ record in Lake Esmeralda is a proxy of effective rainfall whilst $\delta^{18}O$ is a proxy of summer rainfall amount in Lake San Lorenzo. Results also showed that Lake Esmeralda changed to become a more closed system in the last 3500. In contrast, Lake San Lorenzo has always been a relatively open system. The $\delta^{18}O$ indicated that the environment near Lake Esmeralda had become drier in the last millennium since the evaporation-rainfall ratio has relatively increased. (Precipitation also decreased according to K/Sr record for the last millennium). Lake San Lorenzo has received relatively more summer rainfall in the same time frame. Although both $\delta^{18}O$ records are proxies of a

different particular phenomenon in each lake, both phenomena are related to the hydroclimate regime.

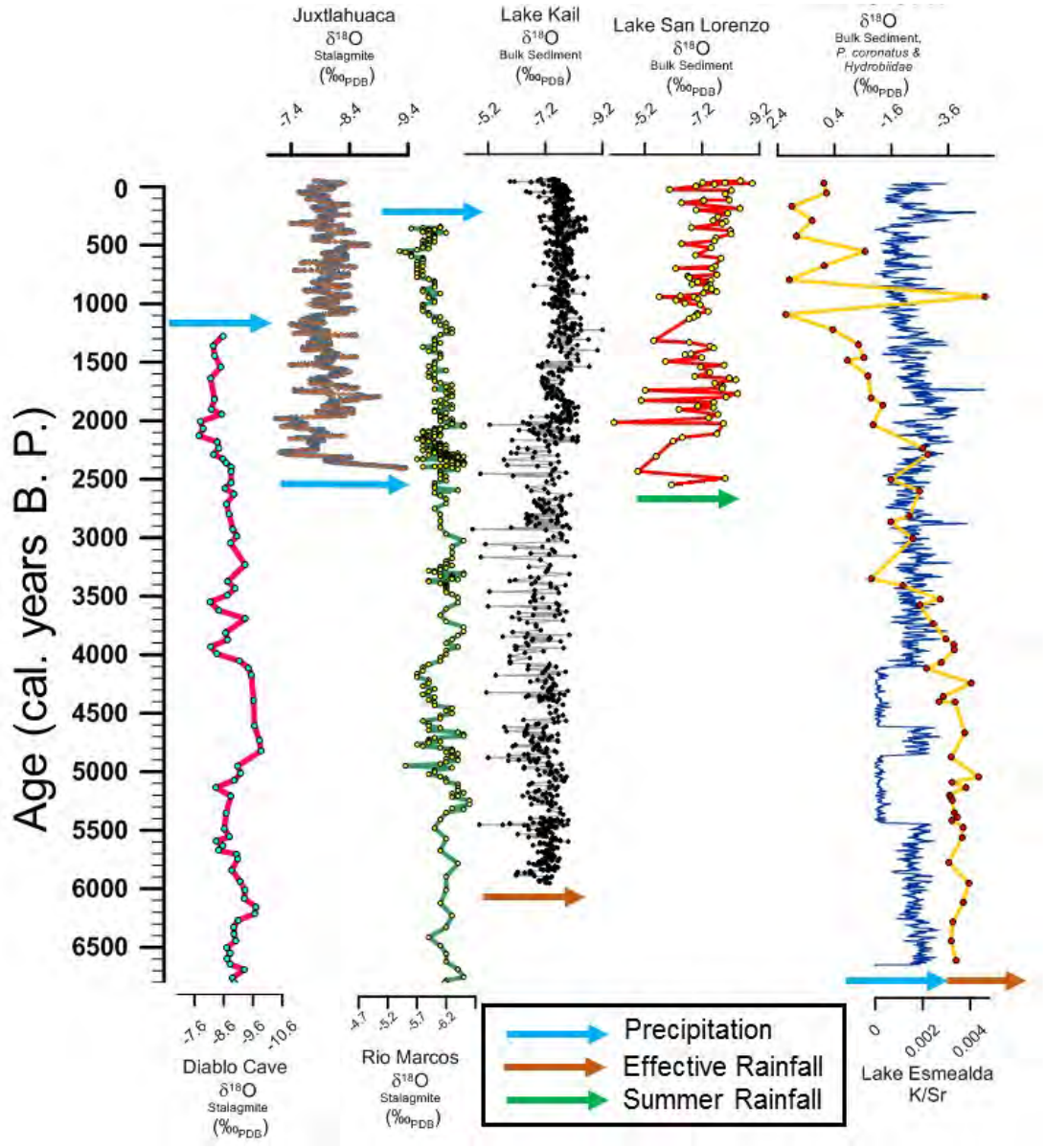

Figure 10.2 Comparison between the stable oxygen isotope records generated in Lake Kail and San Lorenzo in the Maya Highlands and Lake Esmeralda in the Maya Lowlands. The K/Sr record of Lake Esmeralda a proxy of rainfall is also plotted. For comparison records from stalagmites studied in western Mesoamerica are also presented (Juxtlahuaca and Diablo Cave) including the stalagmite record generated at Rio Marcos in the western part of the Maya Cultural Area in the Highlands. Circles indicate the presence of isotope data. Colour in arrows indicates the kind of rainfall assumed for each proxy.

The trends in the $\delta^{18}O$ records from both lakes (Figure 10.2) therefore support the idea observed in the effective rainfall record of Lake Kail that the Highlands had an opposite humidity trend at the millennial-scale compared to the Lowlands (Stansell et al., 2020). However, this opposite trend is explained by a reduction of evaporation at Lake Kail and not by a reduction in meteorological rainfall since the record of precipitation obtained

from the Rio Marcos established a reduction in precipitation (Stansell et al., 2020). In contrast, our study in Lake San Lorenzo indicates that rainfall increased during the last millennium.

A similar terrigenous input process

In Lake Esmeralda, the Loss of Ignition residuals were composed of terrigenous material, washed into the lake by the rain, based on their resemblance to the K/Sr record (see section 9.5 in chapter 9), which is believed to be a proxy of rainfall (Roy et al., 2018). A similar phenomenon happened with the residuals at Lake San Lorenzo, which are also associated with terrigenous material. Although there was not a record of general rainfall in San Lorenzo (such as K/S inputs), the resemblance of its residuals records to the summer rainfall record ($\delta^{18}O$) and the record of the movement of the ITCZ (Cariaco record) indicated that the residual material was also washed into the lake by the rain (see section 7.10 in chapter 7). Even though the amount of residuals in both lakes is driven by rainfall, it would be foolish to use these records as proxies of rainfall per se. In the case of Lake Esmeralda, this is evident in zones where the residuals have an opposite trend to the K/Cl, which might be explained by the presence of gypsum (however it was only tested on the layer at 167 years B. P). In the same way, the amount of residuals in Lake San Lorenzo is also driven by the erosion of the land beside the rainfall. This erosion is related to the human impact in the region (e. g. major erosion of the land happened during periods of abandonment after peaks of the high-density population in Chinkultic, see section 7.7 in chapter 7). These issues with the residuals records in both lakes have to be taken into consideration when comparing both records.

An opposite response of organics to climate

In the case of organics, they appeared to have a different response to climate at each site. However, it looked as if the presence of organic material was mostly not connected with human activity around both sites, even in Lake San Lorenzo, which had an important human population nearby according to the archaeological record (Álvarez, 1993; Navarrete, 2007). In Lake Esmeralda, organic percentage started to increase dramatically after 2200 years B. P., with dramatic increases at the Maya abandonment (1800 to 1750 years B. P.), the Maya Hiatus (1360 years B. P.) and the Maya Collapse (1140-1040 years B. P.). These peaks happened in moments associated with dry periods according to the $\delta^{18}O$ effective rainfall record. Although the increase in organic material 2200 B. P. coincided with the increase of the population in general in the Maya Cultural Area, the

Cochuah Region including the area around Lake Esmeralda were not densely populated before the end of the Maya Collapse (910 B. P.) (see section 9.8 in chapter 9). Therefore, any suggested association of organic material in the lake with human activity would still need to be tested.

In Lake San Lorenzo the organic material was in part enhanced by the summer rainfall amount. The highest abundance of organic material was registered after periods of the dense human population, suggesting that increases in organic material were also driven by the erosion of agricultural land (see section 7.7 in chapter 7). According to the Human Impact Index of the lake (Franco-Gaviria et al., 2018), the first of these abandonments occurred after the Maya Hiatus when the region was abandoned after suffering its most densely populated period. The last of these periods coincided with the arrival of Soctona and then the Spaniards-Tlaxcaltecs to the region (see section 7.7 in chapter 7). This arrival could have led to a decrease in the human population in the region or might have promoted more erosion after imposing new techniques in agriculture. By parsimony, it looks that the high organic production was the result of the erosion of land after the human abandonment during the colonial period.

An opposite response of $CaCO_3$ to climate

A very interesting point was the climatic drivers of $CaCO_3$ precipitation in both lakes. In Lake San Lorenzo, $CaCO_3$ precipitated during dry periods, which is the expected logical tendency, meaning that the precipitation of $CaCO_3$ responded to the water level of the lake (see section 7.4 in chapter4). Therefore, $CaCO_3$ anticovaried with the residuals which would have been washed into the lake by the rainfall. However, in Lake Esmeralda, the $CaCO_3$ precipitated in periods of more effective rainfall (see section 9.5 in chapter 9). The low amount (or lack) of $CaCO_3$ in dry periods could have been explained by some kind of dissolution effect into the organics in the sediment record since organics in Lake Esmeralda increased in dry periods. However, if that was the case, the sedimentation rate would have increased, but the sedimentation rate actually decreased during most of the organic precipitation phase (see section 9.1 in chapter 9). Another explanation is that carbonates actually did not precipitate (or precipitated less) in a bog-scenario since bogs tend to be only cloud-fed deposits (receiving only rainfall). This explanation might be valid for the peaks during the critical moments of the Maya History, but not during the long phase of high organic content and low carbonate precipitation, which is still present in our times (and now Esmeralda is a shallow lake). I have said that the bog scenario was unlikely,

since most of the organics during the critical moments of Maya History was external, mostly in the Maya Hiatus. This indicates that the decrease in precipitation of $CaCO_3$ responded not only to the production of organic material in the lake but to the external organics. Although this supports the dilution of carbonates in the sediments as result of more incoming material, the fact that the sedimentation rate was not faster still casts doubt on a dilution effect for explaining the low carbonate precipitation during these periods. It has to be highlighted that it is also difficult to calculate the sedimentation rate for a specific layer. For now, the data recovered in this thesis were not enough to propose a hypothesis that can explain the observation of less carbonate precipitation during dry periods, but it might be related to the Ca or CO_2 inputs and chemical equilibria of the system.

A different response of vegetation to climate change

In the case of vegetation and its link with climate, the results in Lake Esmeralda indicated that there was partial correspondence between changes in vegetation and the effective rainfall. In contrast, the vegetation in Lake San Lorenzo responded to changes in the summer rainfall amount, (although it also reflected human impact). An example was the generation of the mountain cloud forest in the last 600 years B. P. (see section 7.7 in chapter 7)

Esmeralda in comparison to Chichancanab

One of the motives of this research was to compare two sister lakes, Chichancanab and Esmeralda.

The most evident difference between these lakes was the absence of gypsum in Lake Esmeralda during the dry periods registered on Chichancanab, particularly during the Maya Abandonment and the Maya Collapse (see section 9.7, in chapter 9). However, the peaks of organic material during these periods, as well as the effective rainfall registered in Lake Esmeralda, indicated that those were dry periods, and the absence was related to the different responses of these two lakes to drying, and the undersaturation of gypsum in Esmeralda. A possible dry period according the K/Sr, where gypsum was observed in Lake Esmeralda occurred around 167 years B. P. However, XRD analyses and the sulphur record obtained by XRF in Lake Esmeralda did not have any signal indicating a possible presence of gypsum before 167 years B. P. (see section 9.7, in chapter 9). It is unknown why the gypsum appeared here and not earlier.

Lake Esmeralda is more hydrologically open than Chichancanab today according to the isotopic signature of water. If that was always the case, then this would explain why the signals in the $\delta^{18}O$ of Chichancanab during the droughts at the critical moments of the Maya History are relatively stronger than the signals in the $\delta^{18}O$ of Lake Esmeralda. This hydrologically open state of Esmeralda would also explain why $CaSO_4$ remains undersaturated besides the lower gypsum catchment of this lake.

10.3 Palaeoclimatic data in the Maya Cultural Area

Chapter 4 showed that there were regions in the Maya Cultural Area that do not currently have palaeoclimate records, some of these regions are critical to our understanding of the Maya Collapse, such as the Pucc Region, which became densely populated during the Maya Collapse years. However, the Puuc Region does not have superficial water bodies (see section 3.4 in chapter 3), so practically a palaeoclimatic record based on lake sediments was not possible to obtain. During the time of this research Smyth et al., (2017) obtained a palaeoclimatic record based on a speleothem in this region, which also shows signals of droughts during the Maya Collapse as well as flood events at 1109 and 1105 years B. P. (841 and 845 A. D.). Other regions that possessed a small number of palaeoclimatic records were the Northern and Southern Maya Highlands. When this research started, there were no palaeoclimatic records obtained over 1000 m.a.s.l. excepting for the pollen and charcoal records at San Lorenzo and a different Lake Esmeralda in Chiapas (Franco-Gaviria et al., 2018). The record at Lake Kail (Guatemala) was developed during these years (Stansell et al., 2020).

The meta-analysis, presented in chapter 4, showed a decrease in rainfall or a climate change in the whole Maya Cultural Area during the Maya Collapse. However, this decrease in rainfall, perceived as a drought in the lowlands, had different intensities according to the subregions and was dealt with in different ways by the human population (Hodell et al., 2012; Mueller et al., 2009; Wahl et al., 2014). For example, according to the archaeological records and the pollen records, most sites in the Southern and Central Maya Lowlands were abandoned, but many regions in the central and northern Mayab were repopulated or just remained populated.

The meta-analysis also showed that many, but not all, palaeoenvironmental records had shown signals of a decrease in rainfall or a climate change during the Maya abandonment, the Maya Hiatus or the Fall of the Mayapan League across the complete Maya Cultural Area which indicated the presence of recurrent cyclic drought scenarios, which have been

shown in other sites across Mesoamerica, Oasisamerica and Aridoamerica (Southwest American Archaeological Area) (Hodell, 2001; Lachniet et al., 2012; Metcalfe et al., 2015; Stahle et al., 2011). The meta-analysis confirms the findings for the whole area which suggest that there were effects of droughts, but not everywhere, and in some places worse than others indicating a different sensitivity and response of each site.

The comparison between the records developed in this thesis, the records at Lake Esmeralda at the Cochuah Region and Lake San Lorenzo at the Lagunas de Montebello Lake Complex showed an opposite trend in the rainfall and humidity at the millennial-scale between both lakes (Figure 10.2), which is congruent to the observations and interpretations at Lake Kail (Stansell et al., 2020). However, at a decadal scale, the rainfall tendencies are still similar. For instance, there was a decrease in the summer rainfall during the Maya Abandonment, the Maya hiatus and the Maya Collapse in Lake San Lorenzo, meanwhile was a decrease in effective rainfall at Lake Esmeralda during these critical periods in Maya History (the K/Sr record of rainfall in Esmeralda also indicate a decrease of rainfall in these periods). This may suggest that for the Maya Cultural Area, the drought is due to a decrease in precipitation (a meteorological drought) rather than an increase in evaporation (a hydrological drought). Figure 10.1 upper left shows these conclusions in a mind map.

10.4 Answers at the anthropogenic level

The human drama that the Maya people lived during the development of their civilization from the Preclassic period until the Maya Collapse and the subsequent reconfiguration of their civilization until the arrival of Europeans is studied primarily by anthropology and archaeological sciences. However, environmental reconstruction helps to understand the environmental context that the Maya responded to-, dealt with-, managed and/or adapted to. With the data recovered in this thesis, it is not possible to have definitive answers to the questions asked in the anthropological epistemic level of chapter 1. Nevertheless, they give some points that should be taken into consideration by archaeologists.

A series of droughts existed during the Maya Collapse in Lake Esmeralda, and a decrease in summer rainfall also happened in San Lorenzo. The water in Lake Esmeralda might not have been a source of usable water for humans at this time. Because the archaeological record (Shaw, 2015a, 2015b) and the pollen record developed by Bermingham (2020), it is known that there was no significant human activity in the Esmeralda catchment at the start of the first drought during Maya Collapse (1140 years B. P.). This lack of usable water

probably explains why the Puuc Region (see section 3.4 in chapter 3), which contains chultunes with a capacity of 104 000m^3 in the region for keeping water (Smyth et al., 2017) started to be densely populated since the beginning of the Maya Collapse, but the Cochuah region began to have more settlements only after 1050 years B. P. (a century after the Puuc Region) (Shaw, 2015a, 2015b) with agricultural fields near Esmeralda at that time according to the decrease of Moraceae/Urticaceae and the appearance of *Z. mays* at 950 years B. P. found by Bermingham (2020). Lake Esmeralda has today a capacity of 264000m^3, but with a rainfall reduction of 40% like that observed in Chichancanab during the Maya droughts (Evans et al., 2018), it would have decreased its water level. Even with this low level, the lake might have had more water capacity than the chultunes, but the quality of water might have been not so good as the water stored in chultunes due to the organic content presented during this period. The Cochuah region then was densely populated when the decrease of organic material in Lake Esmeralda happened, which may have provided more usable water.

Settlements close to Lake San Lorenzo already had low-density population values according to the Human Impact Index of Franco-Gaviria et al. (2018) at the start of the first drought during the Maya Collapse (1140 years B. P.). The archaeological record does not have enough resolution to establish if there was some kind of abandonment or reduction of the population as a response to the decreasing summer rainfall observed at that time.

The scenarios presented suggesting water scarcity in Lake Esmeralda and suggesting a reduction of water catchment in Lake San Lorenzo affected the survival of the human population. However, it is not clear if that scarcity or reduction of water catchment made agriculture difficult, or how exactly the scarcity affected human life.

Were the Maya people in harmony with the environment, or were they an early example of irresponsible human impact? This is a very hard question to answer based on the data recovered in this thesis. The Maya at San Lorenzo exerted management of the land-based on the reduction of wildfires during the periods of high population density in the Classic Period (Franco-Gaviria et al., 2018), erosion was also relatively low at this time, in contrast to the high erosion after the abandonment of agriculture resulting from the decrease of population. This impact of the Maya appears to be responsible and conscious, knowing how to manage their resources. The record in Lake Esmeralda cannot help us much with this problem, since the Cochuah region did not appear to have reached at least the levels

of the population presented in the Comitan-Chinkultic Region, excepting for a short period during and after the Maya Collapse.

10.5 Final thoughts

This research had performed an assessment of the palaeoclimatic data recovered in the Maya Cultural Area in particular related to the critical moments of Maya History: the Maya abandonment; the Maya Hiatus; and the Maya Collapse when societal changes occurred, and a reconfiguration of the settlement patterns and the population happened. It has also explored the value of recovering the environmental signal related to humidity from oxygen stable isotopes from shells of the genus Hydrobiidae as obtained from a number of other lakes of the Maya Cultural Area. It established that it was possible to recover the same environmental signal from bulk lake sediments in Lake Esmeralda, but it is probable that such an approach cannot always be extrapolated to other lakes in the area.

Most of all, this thesis makes an environmental reconstruction using a multiproxy approach in Lake Esmeralda and Lake San Lorenzo. This research points out similarities and differences between both lakes concerning their response to changes in the amount of rainfall. Lake Esmeralda tends to become drier (catching less effective rainfall according the $\delta^{18}O$ and meteorological rainfall according the K/Sr) in the last millennium while Lake San Lorenzo has increased its amount of summer rainfall (according the $\delta^{18}O$). The record obtained at Lake Kail by Stansell et al. (2020) supports this if we assume that the correct interpretation of this record is a proxy of summer rainfall instead a record of effective rainfall (see section 7.8 in chapter 7).

Figure 10.2 shows other records that are located in the western highlands of Mesoamerica including the stalagmite record at Rio Marcos. This stalagmite record indicates a tendency to less rainfall during the last millennium similar to the tendency observed in Lake Esmeralda (in particular to the K/Sr) and other lakes in the Mayab. In contrast, the stalagmite record of Juxtlahuaca in Guerrero in Mesoamerica (see figure 2.1 in chapter 2) indicates more rainfall for the last millennium (Lachniet et al., 2017) similar to Lake Kail and Lake San Lorenzo. In addition, the stalagmite record at Diablo Cave (Bernal et al., 2011) also in Guerrero has a trend opposite to the stalagmite of Rey Marcos and similar to the Juxtlahuaca. However, the record at Diablo Cave does not cover the last millennium. Before this comparison, it could have been argued that differences between the Maya lowlands and the highlands might be due to influences of natural phenomena presented in

the Pacific Ocean or in the Atlantic Ocean, such as the ENSO or AMO, but the discrepancy with the record at Rio Marcos casts some doubt on this explanation. The records in Guerrero support the incoming of more rainfall in the western highlands of Mesoamerica as observed in Lake Kail and Lake San Lorenzo in comparison to the previous millennium. The stalagmite at Chillibrillo Cave in Panama has a tendency to more rainfall for the last millennium (Lachniet et al., 2004) in a similar way to most palaeorainfall records in western Mesoamerica. Most of these records are assumed to be influenced by changes in ENSO (Bernal et al., 2011; Lachniet et al., 2017, 2012, 2004). In contrast, Stalagmite record at Yok Balum indicate also less rainfall for the last millennium (see figure 4.10 in chapter 10) which is coherent with its location in the lowlands and near the eastern coast.

In resume, most of these records point out a tendency to more meteorological rainfall in the last millennium in the western Mesoamerican highlands including the Maya Highlands in opposition to what is observed in the Maya Lowlands. The only exception is the record at Rio Marcos, whose climatic dynamics was explained by changes in convective activity favoured by persistent warm sea surface temperatures in the Caribbean Sea in contrast to the influence of the ENSO in the other western stalagmites. The records of Lake San Lorenzo and the interpretation of the record of the Lake Kail as a summer meteorological rainfall proxy as well as their proximity to Rio Marcos might indicate that the explanation for this stalagmite record needs to be reviewed. This is an example of how lake records in open systems are useful in interpreting the works performed on speleothems. More studies are needed in the highlands to support the difference between them and the lowlands observed in this research and the research performed at Lake Kail (Stansell et al., 2020).

The research in this thesis shows that humans were affected to some degree by the decrease of rainfall amount during critical moments of Maya History. This suggests that they took decisions concerning migration and distribution of settlements which took into consideration the access to usable water. This supports the idea that they were not passive to the droughts (Iannone, 2014) and that they were aware of the climatic change under which they lived (Grube and Schubert, 2015).

More data related to past agriculture practices and the location of agriculture fields are needed for the Cochuah Region and the Lagunas de Montebello Lake Complex.

Finally, the archaeological projects at the Cochuah Region and the Chinkultic complex at Montebello need to go further, creating data with higher temporal resolution. These archaeological data must be compared with the data achieved in this thesis as well as future palaeoenvironmental research in both regions. On a regional scale, similar archaeological and palaeoenvironmental projects must be performed in the Maya Cultural Area building bridges between Archaeology and Geosciences, and establishing feedback between them.

The Maya droughts suffered during the time of the Maya Collapse at the end of the Mesoamerican Classic Period changed an entire civilization, its consequences, which we have started to understand impacted and reconfigured all Mesoamerica in practically all fields and had repercussions in the next centuries. This event in the past of the people of the Americas was a wound and a gift, which remembrance has been almost completely erased from the collective memory. But its drama contributed to make us the Belizeans, Guatemalans and Mexicans that we are today in the same way that the European conquest and fight for freedom and equality during the last two centuries did. This thesis is just a small look for recovering a lost memory; a recovered memory, which may help us to understand our present better and act with wisdom.

References

Abell, P.I., Williams, M.A.J., 1989. Oxygen and carbon isotope ratios in gastropod shells as indicators of paleoenvironments in the Afar region of Ethiopia. *Palaeogeogr. Palaeoclimatol. Palaeoecol.* 74, 265–278.

Adams, R.E.W., 1973. The collapse of Maya civilization: A review of previous theories. *Class. Maya collapse* 21–34.

Aimers, J., 2011. Drought and the Maya: The story of artefacts. *Nature* 479, 44.

Aimers, J.J., 2007. What Maya Collapse? Terminal Classic Variation in the Maya Lowlands. *J. Archaeol. Res.* 15, 329–377.

Akers, P.D., Brook, G.A., Railsback, L.B., Liang, F., Iannone, G., Webster, J.W., Reeder, P.P., Cheng, H., Edwards, R.L., 2016. An extended and higher-resolution record of climate and land use from stalagmite MC01 from Macal Chasm, Belize, revealing connections between major dry events, overall climate variability, and Maya sociopolitical changes. Palaeogeogr. Palaeoclimatol. Palaeoecol. 459, 268–288. Alcocer, J., Merino-Ibarra, M., Oseguera, L.A., Escolero, O., 2018. Anthropogenic impacts on tropical karst lakes: "Lagunas de Montebello," Chiapas. *Ecohydrology* 11, 1–13.

Alcocer, J., Oseguera, L.A., Sánchez, G., González, C.G., Martínez, J.R., González, R., 2016. Bathymetric and morphometric surveys of the Montebello Lakes, Chiapas. *J. Limnol.* 75, 56–65.

Álvarez, C., 1993. El patrón de asentamiento en las margaritas, chiapas y su cronología tentativa, in: *VI Simposio de Investigaciones Arqueológicas en Guatemala*. pp. 462–473.

Alvarez, W., Zimmer, C., 1997. *T. Rex and the Crater of Doom*, *Popular science: Paleontology*. Princeton University Press. 185.

Anchukaitis, K.J., Taylor, M.J., Martin-Fernandez, J., Pons, D., Dell, M., Chopp, C., Castellanos, E.J., 2013. Annual chronology and climate response in Abies guatemalensis Rehder (Pinaceae) in Central America. *Holocene* 23, 270–277.

Andersen, M.B., Stirling, C.H., Potter, E.K., Halliday, a. N., 2004. Toward epsilon levels of measurement precision on 234U/ 238U by using MC-ICPMS. *Int. J. Mass Spectrom.* 237, 107–118.

Anderson, N.J., Liversidge, A.C., McGowan, S., Jones, M.D., 2012. Lake and catchment response to Holocene environmental change: Spatial variability along a climate gradient in southwest Greenland. *J. Paleolimnol.* 48, 209–222.

Andrew, S., Heard, R.W., Overstreet, R.M., Foster, J.M., Heard, R.W., Overstreet, R.M., Foster, J.M., 2002. Hydrobiid Snails (Mollusca : Gastropoda: Rissooidea) from St. Andrew Bay, Florida. *Gulf Caribb. Res.* 14, 13–34.

Andrews, A.P., Andrews, E.W., Castellanos, F.R., 2003. The northern Maya collapse and its aftermath. *Anc. Mesoamerica* 14, 151–156.

Anselmetti, F.S., Hodell, D.A., Ariztequi, D., Brenner, M., Rosenmeier, M.F., 2007. Quantification of soil erosion rates related to ancient Maya deforestation. *Geology* 35, 915–918.

Aragón-Moreno, A.A., Islebe, G.A., Roy, P.D., Torrescano-valle, N., Mueller, A.D., 2018. Climate forcings on vegetation of the southeastern Yucatán Peninsula (Mexico) during the middle to late Holocene. *Palaeogeogr. Palaeoclimatol. Palaeoecol.* 495, 214–226.

Aragón-Moreno, A.A., Islebe, G.A., Torrescano-Valle, N., 2012. A ~3800-yr, high-resolution record of vegetation and climate change on the north coast of the Yucatan Peninsula. *Rev. Palaeobot. Palynol.* 178, 35–42.

Aragón-Moreno, A.A., Islebe, G.A., Torrescano-valle, N., Arellano-verdejo, J., 2018. Journal of South American Earth Sciences Middle and late Holocene mangrove dynamics of the Yucatan Peninsula , Mexico. *J. South Am. Earth Sci.* 85, 307–311.

Asmerom, Y., Awe, J., Baldini, J.U.L., Bartlein, P., Culleton, B.J., Ebert, C., Jazwa, C., Macri, M.J., Marwan, N., Polyak, V., Prufer, K.M., Ridley, H.E., Sodemann, H., Winterhalder, B., Haug, G.H., 2012. Supplementary Material for Supporting online material for Development and Disintegration of Maya Political Systems in *Methods* 788, 788–791.

Beach, T., Dunning, N., Luzzadder-Beach, S., Cook, D.E., Lohse, J., 2006. Impacts of the ancient Maya on soils and soil erosion in the central Maya Lowlands. *Catena* 65, 166–178.

Beach, T., Luzzadder-Beach, S., Cook, D., Dunning, N., Kennett, D.J., Krause, S., Terry, R., Trein, D., Valdez, F., 2015. Ancient Maya impacts on the Earth's surface: An Early Anthropocene analog? *Quat. Sci. Rev.* 124, 1–30.

Beach, T., Luzzadder-Beach, S., Dunning, N., Cook, D., 2008. Human and natural impacts on fluvial and karst depressions of the Maya Lowlands. *Geomorphology* 101, 308–331.

Beer, R., Glöckner, W., Letterer, R., 1983. *Chemische Analytik-Kernchemie-Modellvorstellungen.* C.C. Buchners, Bamberg. Deutchland. 173.

Bermingham A. 2020. *Land use strategies of the ancient Maya in seasonally dry tropical forest ecosystems of the Yucatan Peninsula.* PhD Thesis. Northumbria University. UK. 215.

Bernal, J.P., 2003. U-series analysis of weathering minerals by LA-MC-ICP-MS; a new tool for weathering geochronology. *Earth* 27–41.

Bernal, J.P., Beramendi Orosco, L.E., Lugo-Ibarra, K.C., Daesslé, L.W., 2010. Revisión a algunos geocronómetros radiométricos aplicables al Cuaternario. *Bol. la Soc. Geol. Mex.* 62, 305–323.

Bernal, J.P., Lachniet, M., McCulloch, M., Mortimer, G., Morales, P., Cienfuegos, E., 2011. A speleothem record of Holocene climate variability from southwestern Mexico. *Quat. Res.* 75, 104–113.

Bernal, J.P., Railsback, L.B., 2008. Introducción a la Tabla Periódica de los elementos y sus iones para ciencias de la tierra. *Rev. Mex. Ciencias Geol.* 25, 236–246.

Berntsson, A., Rosqvist, G.C., Velle, G., 2014. Late-Holocene temperature and precipitation changes in Vindelfjällen, mid-western Swedish Lapland, inferred from chironomid and geochemical data. *Holocene* 24, 78–92.

Bhattacharya, T., Chiang, J.C.H., Cheng, W. 2017. Ocean-atmosphere dynamics linked to 800-1050 CE dry interval in Mesoamerica. *Quaternary Science Reviews.* 169. 263-277.

Bhattacharya, T., Coats, S. 2020. Atlantic-Pacific gradients drive Last Millennium hydroclimate variability in Mesoamerica. *Geophysical Research Letters* 47(13).

Binford, L.R., 1968. Some Comments on Historical versus Processual Archaeology. *Sowthwestern J. Anthopology* 24, 267–275.

Blaauw, M., 2010. Methods and code for "classical" age-modelling of radiocarbon sequences. *Quat. Geochronol.* 5, 512–518.

Blaauw, M., Christen, J.A., 2013. Bacon manual – v2.2. Tutorial.

Blaauw, M., Christen, J.A., 2011. Flexible paleoclimate age-depth models using an autoregressive gamma process. *Bayesian Anal.* 6, 457–474.

Bolland, N., Shoman, A., 1977. *Land in Belize, 1765-1871*. Mona, Jamaica.

Boremanse, D., 1998. *Hach Winik : the Lacandon Maya of Chiapas, Southern Mexico.* Institute for Mesoamerican Studies, University at Albany, State University of New York, Albany N.Y.

Borgstede, G., Mathieu, J.R., 2007. Defensibility and Settlement Patterns in the Guatemalan Maya Highlands. *Lat. Am. Antiq.* 18, 191–211.

Boyle, J.F., Chiverrell, R.C., Schillereff, D., 2015. Approaches to water content correction and calibration for μXRF core scanning: comparing X-ray scattering with simple regression of elemental concentrations, in: *Micro-XRF Studies of Sediment Cores.* Springer, pp. 373–390.

Braadbaart, F., Poole, I., van Brussel, A.A., 2009. Preservation potential of charcoal in alkaline environments: an experimental approach and implications for the archaeological record. *J. Archaeol. Sci.* 36, 1672–1679.

Bracamonte y Sosa, P., Lizama-Quijano, J., 2003. Marginalidad indígena: una perspectiva histórica de Yucatán. *Desacatos* 83–98.

Bradbury, J.P., Forester, R.M., Bryant, W.A., Covich, a. P., 1990. Paleolimnology of Laguna de Cocos, Albion island, Rio Hondo, Belize, in: Pohl, M.D. (Ed.), *Ancient Maya Wetland Agriculture: Excavations on Albion Island, Northern Belize.* Westview Press,Boulder, pp. 119–154.

Brenner M. 1983. *Paleolimnology of the Maya Region.* PhD Thesis. University of Florida. USA. 249.

Brenner, M., Hodell, D. a, Curtis, J.H., Rosenmeier, M.F., Ariztegui, D., 2003. Paleolimnological Approaches for Inferring Past Climate Change in the Maya Region : Recent Advances and Methodological Limitations, in: Fedick, S., Allen, M., Jimenez-Osornio, J., Gomez-Pompa, A. (Eds.), *The Lowland Maya Area: Three Millennia at the Human-Wildland Interface.* pp. 45–75.

Brenner, M., Rosenmeier, M.F., Hodell, D.A., Curtis, J.H., 2002a. Long-term perspectives on interactions among climate ,. *Holocene* 13, 141–157.

Brenner, M., Rosenmeier, M.F., Hodell, D.A., Curtis, J.H., 2002b. Paleoclima de la región Maya: sintesis del conocimiento basado en registros peleolimnológicos, in: *Los Investigadores de La Cultura Maya.* Universidad Autónoma de Campeche, pp. 248–261.

Brown, A.L., Reinhardt, E.G., van Hengstum, P.J., Pilarczyk, J.E., 2014. A Coastal Yucatan Sinkhole Records Intense Hurricane Events. *J. Coast. Res.* 294, 418–428.

Buckland, P.C., Amorosi, T., Barlow, L.K., Dugmore, A.J., Mayewski, P.A., McGovern, T.H., Ogilvie, A.E.J., Sadler, J.P., Skidmore, P., 1996. Bioarchaeological and climatological evidence for the fate of Norse farmers in medieval Greenland. *Antiquity* 70, 88–96.

Caballero, M., Mora, L., Muñoz, E., Escolero, O., Bonifaz, R., Ruiz, C., Prado, B., 2020. Anthropogenic influence on the sediment chemistry and diatom assemblages of Balamtetik Lake, Chiapas, Mexico. *Environ. Sci. Pollut. Res.* 27, 15935–15943.

Calderón, D.A., Whiling, T.A.L., Guillen, M.L., 2006. *Presencia Zoque*. Universidad de Ciencias y Artes de Chiapas, Tuxtla Gutiérrez.

Calderón, I.D., Fuentes, O.E., Salinas, E.M., Rodríguez, M.C., Romo, G.S., 2014. Cartografía geomorfológica a escala 1 : 50000 del Parque Nacional Lagunas de Montebello , Chiapas (México). *Bol. la Soc. Geol. Mex.* 66, 263–277.

Carrasco, D., 2001. *The Oxford encyclopedia of Mesoamerican cultures : the civilizations of Mexico and Central America*. Oxford University Press, UK.

Carrillo-Bastos, A., Islebe, G.A., Torrescano-Valle, N., 2013. 3800 years of quantitative precipitation reconstruction from the northwest Yucatan peninsula. *PLoS One* 8 (12).

Carrillo-Bastos, A., Islebe, G.A., Torrescano-Valle, N., 2012. Geospatial analysis of pollen records from the Yucat??n peninsula, Mexico. *Veg. Hist. Archaeobot.* 21, 429–437.

Carrillo-Bastos, A., Islebe, G.A., Torrescano-Valle, N., González, N.E., 2010. Holocene vegetation and climate history of central Quintana Roo, Yucatán Península, Mexico. *Rev. Palaeobot. Palynol.* 160, 189–196.

Castro, D., 2010. Variabilidad de los ciclones tropicales que afectan Mexico. *Interciencia* 35, 306–310.

Castro, M.J.T., Schlaepfer, C., Matínez, E., 1975. Estratigrafía y microfacies del Mesozoico de la Sierra Madre del Sur, Chiapas. *Bol. Asoc. Mex. Geol.* Pet. 27, 1–95.

Cejudo, E., 2021. Water Isotope Composition for Yucatan Peninsula. *Unpublished raw data*

Cejudo, E., Acosta-gonzalez, G., Leal-bautista, R.M., Estrada-medina, H., 2020. W ater stable isotopes (δ^2H and δ^{18}O) in the Peninsula of Yucatan ,. *Hydrol. Earth Syst. Sci.* 1–20.

Cervantes-Martìnez, A., Elìas-Gutiéerrez, M., Suárez-Morales, E., 2002. Limnological and morphometrical data of eight karstic systems "cenotes" of the Yucatan Peninsula, Mexico, during the dry season (February-May, 2001). *Hydrobiologia* 482, 167–177.

Charles G, George L. 2010. *Maya Civilization*, Vol. 42. Farmington Hills: Lucent books. Luzent Boo ed. 98.

Chilam-Balam, 1966. *El libro de los libros de Chilam Balam*. FCE, Mexico D. F.

Christopher, R.A., 1976. Morphology and taxonomic status of Pseudoschizaea Thiergart. *Micropaleontology* 22, 143–150.

Clark, J.D., Beyene, Y., WoldeGabriel, G., Hart, W.K., Renne, P.R., Gilbert, H., Defleur, A., Suwa, G., Katoh, S., Ludwig, K.R., Boisserie, J.-R., Asfaw, B., White, T.D., 2003. Stratigraphic, chronological and behavioural contexts of Pleistocene Homo sapiens from Middle Awash, Ethiopia. *Nature* 423, 747–52.

CONAGUA, 2010a. Base de datos climatológica 1950-2010: Estación Dziuche.

CONAGUA, 2010b. Base de datos climatológica 1950-2010: Estación La Presumida.

CONAGUA, 2010c. Base de datos climatológica 1950-2010: Estación Tziscao.

CONAGUA, 2010d. Base de datos climatológica 1950-2010: Estación La Esperanza.

Cook, O.F., 1921. Milpa agriculture: a primitive tropical system. Smithsonian Inst., Washington.

Cooke, W., 1931. Why the Mayan cities of the Petén District , Guatemala , were abandoned. *J. Washingt. Acad. Sci.* 21, 283–287.

Cordero-Oviedo MC. 2015. *Paleopalinología y geoquímica del Lago Esmeralda, Chiapas, México: Una reconstrucción paleoecológica.* Universidad de Costa Rica. MSc. Thesis 71.

Correa-Metrio, A., Bush, M.B., Cabrera, K.R., Sully, S., Brenner, M., Hodell, D.A., Escobar, J., Guilderson, T., 2012. Rapid climate change and no-analog vegetation in lowland Central America during the last 86,000 years. *Quat. Sci. Rev.* 38, 63–75.

Covich, A., 1976. Recent changes in molluscan species diversity of a large tropical lake (Lago de Peten, Guatemala). *Limnol. Oceanogr.* 21, 51–59.

Covich, A., Stuiver, M., 1974. Changes in oxygen 18 as a measure of long-term fluctuations in tropical lake levels and molluscan populations. *Limnol. Oceanogr.* 19, 682–691.

Covich, A.P., 2010. Winning the biodiversity arms race among freshwater gastropods: Competition and coexistence through shell variability and predator avoidance. *Hydrobiologia* 653, 191–215.

Cowgill, U.M., Goulden, C.E., Hutchinson, G.E., 1966. *The History of Laguna de Petenxil.* Connect. Acad. ARTS Sci. XVII, 128.

Cowgill, U.M., Hutchinson, G.E., 1966. Article title La Aguada de Santa Ana Vieja: The History of a Pond in Guatemala. *Arch. für Hidrobiol.* 62, 13–15.

Culbert, T.P., 1973. *The Classic Maya collapse,* Advanced seminar series Santa Fe School of American Research advanced seminar series. University of New Mexico Press, USA.

Culbert, T.P., Rice, D.S., 1990. *Precolumbian Population History in the Maya Lowlands.* University of New Mexico Press, USA.

Curtis J, Brenner M, Hodell DA, Balser RA, Islebe GA, Hooghiemstra H. 1998. A multi-proxy study of Holocene environmental change in the Maya Peten, Lowlands. *J. Paleolimnol.* 19:139–59.

Curtis, J.H., Hodelle, D.A., Brenner, M., Hodell, D.A., Brenner, M., 1996. Climate Variability on the Yucatan Peninsula (Mexico) during the Past 3500 Years, and Implications for Maya Cultural Evolution. *Quat. Res.* 46, 37–47.

Cuven, S., Francus, P., Crémer, J.F., Bérubé, F., 2015. Optimization of Itrax Core Scanner Protocols for the Micro X-Ray Fluorescence Analysis of Finely Laminated Sediment: A Case Study of Lacustrine Varved Sediment from the High Arctic, in: Crowdace, I.W., Rothwell, R.G. (Eds.), *Micro-XRF Studies of Sediment Cores: Applications of a Non-Destructive Tool for the Environmental Sciences.* Springer, pp. 279–303.

Cuven, S., Francus, P., Lamoureux, S., 2011. Mid to Late Holocene hydroclimatic and geochemical records from the varved sediments of East Lake, Cape Bounty, Canadian High Arctic. *Quat. Sci. Rev.* 30, 2651–2665.

Cvitanović, P., 1989. *Universality in chaos : a reprint selection.* Adam Hilger, Copenhagen.

Davies, S.J., Lamb, H.F., Roberts, S.J., 2015. Micro-XRF core scanning in palaeolimnology: recent developments, in: Rothwell, I.W.C.& R.G. (Ed.), *Micro-XRF Studies of Sediment Cores.* Springer, pp. 189–226.

Dean, W.E.J., 1974. Determination of Carbonate and Organic Matter in Calcareous Sediments and Sedimentary Rocks by Loss on Ignition: Comparison With Other Methods. *SEPM J. Sediment. Res.* Vol. 44.

Decker MJ. 2017. Approaches to the environmental history of Late Antiquity, part II: Climate Change and the End of the Roman Empire. *Hist. Compass*. 15(10):e12425.

Deevey, E.S., Brenner, M., Flannery, M.S., Yezdani, G.H., 1980. Lakes Yaxha and Sacnab, Peten, Guatemala: limnology and hydrology. *Arch. Hydrobiol* 57, e460.

Deevey, E.S., Rice, D.S., Rice, P.M., Vaughan, H.H., Brenner, M., Flannery, M.S., 1979. Mayan Urbanism: Impact on a Tropical Karst Environment. *Science*. 206, 298–306.

Deevey, G.B., 1977. A taxonomic and distributional study of the planktonic ostracods collected on three cruises of the Eltanin in the South Pacific and the Antarctic region of the South Pacific, in: *Biology of the Antarctic Seas* VIII. John Wiley & Sons, USA, pp. 43–70.

Demarest, A.A., 2014. The Classic Maya collapse, water, and economic change in Mesoamerica: Critique and alternatives from the wet zone, in: Iannone, G. (Ed.), *The Great Maya Droughts in Cultural Context. University* Press of Colorado, Boulder, Colorado, pp. 177–206.

Demarest, A.A., 2004. *Ancient Maya: The Rise and Fall of a Rainforest civilization.* Cambridge University Press, Cambridge, UK. 373.

Demarest, A.A., 1976. *A critical analysis of Yuri Knorozov's decipherment of the Maya hieroglyphics.* Middle American Research Institute, Tulane University.

deMenocal, P.B., 2001. Cultural Responses to Climate Change During the Late Holocene. *Science*. 292, 667–673.

Diaz-Bolío, J., 1998. *Yucatán en el perfil del tiempo.* UADY, Merida, Yucatán.

Díaz, K.A., Pérez, L., Correa-Metrio, A., Franco-Gaviria, J.F., Echeverría, P., Curtis, J., Brenner, M., 2017. Holocene environmental history of tropical, mid-altitude Lake Ocotalito, México, inferred from ostracodes and non-biological indicators. *Holocene* 27, 1308–1317.

Dillion, R.T., 2006. Feshwater Gastropoda, in: Sturm, C.F., Pearce, T.A., Valdes, A. (Eds.), *The Mollusks: A Guide to Their Study, Collection, and Preservation.* American Malacological Society, Los Angeles, pp. 251–259.

Ditrich, O., Scholz, T., Aguirre-Macedo, L., Vargas-Vazquez, J., 1997. Larval stages of trematodes from freshwaters molluscs of the Yucatan Peninsula, Mexico. *Folia Parasitol. (Praha)*. 44, 109–127.

Domínguez-Vázquez, G., Islebe, G.A., 2008. Protracted drought during the late Holocene in the Lacandon rain forest, Mexico. *Veg. Hist. Archaeobot.* 17, 327–333.

Domínguez-Villar, D., Krklec, K., Pelicon, P., Fairchild, I.J., Cheng, H., Edwards, L.R., 2017. Geochemistry of speleothems affected by aragonite to calcite recrystallization –Potential inheritance from the precursor mineral. *Geochim. Cosmochim. Acta* 200, 310–329.

Douglas, P.M.J., Brenner, M., Curtis, J.H., 2016a. Methods and future directions for paleoclimatology in the Maya Lowlands. *Glob. Planet. Change* 138, 3–24.

Douglas, P.M.J., Demarest, A.A., Brenner, M., Canuto, M.A., 2016b. Impacts of Climate Change on the Collapse of Lowland Maya Civilization. *Annu. Rev. Earth Planet. Sci.* 44, 613–645.

Douglas, P.M.J., Pagani, M., Canuto, M.A., Brenner, M., Hodell, D.A., Eglinton, T.I., Curtis, J.H., 2015. Drought, agricultural adaptation, and sociopolitical collapse in the Maya Lowlands. *Proc. Natl. Acad. Sci.* 112, 5607–5612.

Douglas, P.M.J., Pagani, M., Eglinton, T.I., Brenner, M., Hodell, D.A., Curtis, J.H., Ma, K.F., Breckenridge, A., 2014. Pre-aged plant waxes in tropical lake sediments and their influence on the chronology of molecular paleoclimate proxy records. *Geochim. Cosmochim. Acta* 141, 346–364.

Drake, P., Arias, A.M., 1995. Distribution and production of three hydrobia species (gastropoda: hydrobiidae) in a shallow coastal lagoon in the bay of Cádiz, Spain. *J. Molluscan Stud.* 61, 185–196.

Drew, D., 2015. *The Lost Chronicles Of The Maya Kings.* Hachete, UK. 464.

Dull, R.A.., Southon, J.R.., Sheets, P., 2001. Volcanism , Ecology and Culture : A Reassessment of the Volcán Ilopango TBJ eruption in the Southern Maya. *Lat. Am. Antiq.* 12, 25–44.

Dunning, N., Beach, T., 2000. Stability and instability in Prehispanic Maya landscapes, in: Lentz, D.L. (Ed.), *An Imperfect Balance: Landscape Transformations in the Precolumbian Americas.* Columbia University Press, USA, pp. 179–202.

Dunning, N., Beach, T., Farrell, P., Luzzadder-Beach, S., 1998. Prehispanic Agrosystems and Adaptive Regions in the Maya Lowlands. *Cult. Agric.* 20, 87–101.

Dunning, N., Beach, T., Rue, D., 1997. The Paleoecology and Ancient Settlement of the Petexbatun Region, Guatemala. *Anc. Mesoamerica* 8, 255–266.

Dunning, N., Rue, D.J., Beach, T., Covich, A., Journal, S., Summer, N., Taylor, P., 2017. Human-Environment Interactions in a Tropical Watershed : The Paleoecology of Laguna: Human-Environment Interactions in a Tropical Watershed : The Paleoecology of Laguna Tamarindito , El Peten , Gu. J. F. *Archaeol.* 25, 139–151.

Dunning, N.P., Luzzadder-beach, S., Beach, T., Jones, J.G., Scarborough, V., Culbert, T.P., 2002. Arising from the Bajos: The Evolution of a Neotropical Landscape and the Rise of Maya Civilization. *Ann. Assoc. Am. Geogr.* 92, 267–283.

Durán-Calderón, I., Escolero, O., Muñoz, E., Castillo, M., Silva, G., 2014. Cartografía geomorfológica a escala 1 : 50000 del Parque Nacional Lagunas de Montebello, Chiapas (México). *Boletín la Soc. Geológica Mex.* 66, 263–277.

Eitel, B. et. al., 2006. Holozäner Umweltwandel in der nördlichen Atacama und sein Einfluss auf die Nasca-Kultur (Südperu). *Geogr. Rundschau.* 58, 30–336.

Elbert, J., Grosjean, M., von Gunten, L., Urrutia, R., Fischer, D., Wartenburger, R., Ariztegui, D., Fujak, M., Hamann, Y., 2012. Quantitative high-resolution winter (JJA) precipitation reconstruction from varved sediments of Lago Plomo 47°s, Patagonian Andes, ad 1530-2002. *Holocene* 22, 465–474.

Eroza-Solana, E., 2006. *Lacandones, Pueblos indígenas del México contemporáneo.* Comisión Nacional para el Desarrollo de los Pueblos Indígenas, Mexico City, Mexico.

Escobar, J., Curtis, J.H., Brenner, M., Hodell, D.A., Holmes, J.A., 2010. Isotope measurements of single ostracod valves and gastropod shells for climate reconstruction: Evaluation of within-sample variability and determination of optimum sample size. *J. Paleolimnol.* 43, 921–938.

Evans, N.P., Bauska, T.K., Gázquez-Sánchez, F., Brenner, M., Curtis, J.H., Hodell, D.A., 2018. Quantification of drought during the collapse of the classic Maya civilization. *Science.* 361, 498–501.

Evans, S.D., 2013. Bound in Twine: The History and Ecology of the Henequen-Wheat Complex for Mexico and the American and Canadian Plains, 1880-1950. Texas A&M University Press, USA.

Evans, S.T., Webster, D.L., 2013. *Archaeology of ancient Mexico and Central America : an encyclopedia*, 3rd. ed. Thames & Hudson, USA.624

Fagan, B.M., 2000. *The Little Ice Age: How Climate Made History, 1300-1850*. Basic Books. New York

Fairchild, I.J., Smith, C.L., Baker, A., Fuller, L., Spötl, C., Mattey, D., McDermott, F., 2006. Modification and preservation of environmental signals in speleothems. *Earth-Science Rev.* 75, 105–153.

Falniowski, A., 2018. Species Distinction and Speciation in Hydrobioid Gastropods (Mollusca: Caenogastropoda: Truncatelloidea). *Arch. Zool. Stud.* 1, 1–6.

Faust, B.B., 2001. Maya environmental successes and failures in the Yucatan Peninsula. *Environ. Sci. Policy* 4, 153–169.

Flores, J.S., Vermont-Ricalde, R. minelia, Kantún-Balam, J.M., 2012. *Componentes del Huerto Familiar del Área Maya de la Península de Yucatán.* UADY, Merida.

Ford, A., Clarke, K.C., Raines, G., 2009. Modeling Settlement Patterns of the Late Classic Maya Civilization with Bayesian Methods and Geographic Information Systems. *Ann. Assoc. Am. Geogr.* 99, 496–520.

Ford, A., Hord, S., 2018. Above and below the Maya forest. Science. September, 1313–1315.

Ford, A., Rose, W.I., 1995. Volcanic ash in ancient Maya ceramics of the limestone lowlands: implications for prehistoric volcanic activity in the Guatemala highlands. *J. Volcanol. Geotherm.* Res. 66, 149–162.

Foster, L. V., 2001. *Handbook to Life in the Ancient Maya World.* VB Hermitage, USA.

Franco-Gaviria, F., Correa-Metrio, A., Cordero-Oviedo, C., Lopez-Perez, M., Cardenes-Sandí, G.M., Romero, F.M., 2018. Effects of late Holocene climate variability and anthropogenic stressors on the vegetation of the Maya highlands. *Quat. Sci. Rev.* 189, 76–90.

Franco-Gaviria, F., Correa-Metrio, A., Núñez-Useche, F., Zawisza, E., Caballero, M., Prado, B., Wojewódka, M., Olivares, G., 2020. Millennial-to-centennial scale lake system development in the mountains of tropical Mexico. *Boreas* 49, 363–374.

Franco-Gaviria JF. 2018. *El Holoceno en las montañas de Chiapas: dinámicas ambientales y de la vegetación*. PhD Thesis. UNAM. Mexico. 190.

Frappier, A.B., Pyburn, J., Pinkey-Drobnis, A.D., Wang, X., Corbett, D.R., Dahlin, B.H., 2014. Two millennia of tropical cyclone-induced mud layers in a northern Yucatán stalagmite: Multiple overlapping climatic hazards during the Maya Terminal Classic "megadroughts." *Geophys. Res. Lett.* 41, 5148–5157.

Frappier, A.B., Sahagian, D., Carpenter, S.J., González, L.A., Frappier, B.R., 2007. Stalagmite stable isotope record of recent tropic cyclone events. *Geology* 35, 111–114.

Freidel, D., Schele, L., 1990. *A Forest of Kings: The Untold Story of the Ancient Maya.* Morrow and Company, New York.

Gabriel, J.J., Reinhardt, E.G., van Hengstum, P.J., Beddows, P.A., Peros, M.C., Davidson, D.E., 2009. Palaeoenvironmental evolution of cenote aktun ha (Carwash) on the Yucatan Peninsula, Mexico and its response to holocene sea-level rise. J. Paleolimnol. 42, 199–213.

Gallopin, G.G., 1990. *Water storage technology at Tikal, Guatemala found in Twine: The History and Ecology of the Henequen-Wheat Complex for Mexico and the American and Canadian Plains, 1880-1950.* Texas A&M University Press, USA. 133.

Garcia-Capistran, H., 2019. La montaña sagrada. Aspectos sobre la legitimación del poder en el Clásico maya. *Estud. Cult. Maya* 53, 139–172.

Garcia-de-Miranda, E., Falcon-de-Gyves, Z., 1986. *Atlas: nuevo atlas Porrúa de la República Mexicana.* Editorial Porrúa, Mexico D. F.

García de León, A., 1985. *Resistencia y Utopía. memorial de agravios y crónica de revueltas y profecías acaecidas en la provincia de Chiapas durante los últimos quinientos años de su historia.* Era, Mexico D. F. 200.

Gerardo Aldana, 2007. *The Apotheosis of Janaab ' Pakal Mesoamerican Worlds the Apotheosis of | Amaab P Pakal. University Press of Colorado*, Boulder, Colorado.

Gibbons, A., 1993. How the akkadian empire was hung out to dry. *Science.* 261, 985.

Gilfedder, B.S., Petri, M., Wessels, M., Biester, H., 2011. Bromine species fluxes from Lake Constance's catchment , and a preliminary lake mass balance. *Geochim. Cosmochim. Acta* 75, 3385–3401.

Gill, R.B., 2000. *The Great Maya Droughts: Water, Life, and Death,* 2nd. ed. University of New Mexico Press, USA.

Gill, R.B., Mayewski, P.A., Nyberg, J., Haug, G.H., Peterson, L.C., 2007. Drought and the Maya Collapse. *Anc. Mesoamerica* 18, 283–302.

Gischler, E., Shinn, E.A., Oschmann, W., Fiebig, J., Buster, N.A., 2008. A 1500-Year Holocene Caribbean Climate Archive from the Blue Hole, Lighthouse Reef, Belize. *J. Coast. Res.* 246, 1495–1505.

Gischler, E., Storz, D., 2009. High-resolution windows into Holocene climate using proxy data from Belize corals (Central America). *Palaeobiodiversity and Palaeoenvironments* 89, 211–221.

Gondwe, B.R.N., Lerer, S., Stisen, S., Marín, L., Rebolledo-Vieyra, M., Merediz-Alonso, G., Bauer-Gottwein, P., 2010. Hydrogeology of the south-eastern Yucatan Peninsula: New insights from water level measurements, geochemistry, geophysics and remote sensing. *J. Hydrol.* 389, 1–17.

Gonick, L., Smith, A.W., 1993. *The cartoon guide to statistics*. William Morrow and Company, Inc, USA.

González-José, R., Martínez-Abadías, N., González-Martín, A., Bautista-Martínez, J., Gómez-Valdés, J., Quinto, M., Hernández, M., 2007. Detection of a population replacement at the Classic-Postclassic transition in Mexico. *Proc. R. Soc. B Biol. Sci.* 274, 681–688.

Gordon, A.D., Birks, H.J.B., 1972. Numerical Methods in Quateernary Palaeoecology I. Zonation of pollen diagrams. *New Phytol.* 71, 961–979.

Grube, N., Eggebrecht, E., Seidel, M., 2012. *Maya Gottkönige im Regenwald.* Ullmann Publishing GmbH, Köln.

Grube, N., Schubert, A., 2015. Maya : *Das Rätsel der Königsstädte*. Hirmer, Historisches Museum der Pfalz. Speyer, Germany.

Gulick, S.P.S., Barton, P.J., Christeson, G.L., Morgan, J. V., McDonald, M., Mendoza-Cervantes, K., Pearson, Z.F., Surendra, A., Urrutia-Fucugauchi, J., Vermeesch, P.M., Warner, M.R., 2008. Importance of pre-impact crustal structure for the asymmetry of the Chicxulub impact crater. *Nat. Geosci.* 1, 131–135.

Gunn, J.D., Folan, W.J., Day Jr., J.W., Faust, B.B., Day, J.W., Faust, B.B., 2012. Laguna de Términos/Río Candelaria Core: Conditions of Sustainable Urban Occupation in the Interior of the Yucatán Peninsula. *Estud. Cult. Maya* 39, 67–69.

Gunn, J.D., Folan, W.J., Robichaux, H.R., 1995. A landscape analysis of the candelaria watershed in mexico: Insights into paleoclimates affecting upland horticulture in the southern yucatan peninsula semi-karst. *Geoarchaeology* 10, 3–42.

Gunn, J.D., Foss, J.E., Folan, W.J., Carrasco, M. del R.D., Faust, B.B., 2002. Bajo sediments and the hydraulic system of Calakmul, Campeche, Mexico. *Anc. Mesoamerica* 13, 297–315.

Gutiérrez-Ayala, L.V., Torrescano-Valle, N., Islebe, G.A., 2012. Reconstrucción paleoambiental del holoceno tardío de la reserva los petenes, Península de Yucatán, México. *Rev. Mex. Ciencias Geol.* 29, 749–763.

Guzmán, M.C., 2017. *El manejo del agua a través del tiempo en la Península de Yucatán.* Universidad Autónoma de Yucatán, Centro de Investigaciones Regionales Dr. Hideyo Noguchi Unidad de Ciencias Sociales, Fundacion Gonzalo Rio Arronte, Consejo de Cuenca de la Peninsula de Yucatan, Merida, Yucatán.

Gyles Iannone, 2014. *The Great Maya Droughts in Cultural Context: Case Studies in Resilience and Vulnerability*. University Press of Colorado, USA. 466.

Gyles Iannone, Brett A. Houk, Sonja A. Schwake, 2019. *Ritual, violence, and the fall of the classic maya kings*. University Press of Florida, USA. 378.

Harrison, P.D., 1993. Aspects of Water Management in the Southern Lowlands. *Econ. Asp. Water Manag. Prehispanic New World* 71–119.

Haug, G.H., Günther, D., Peterson, L.C., Sigman, D.M., Hughen, K.A., Aeschlimann, B., 2003. Climate and the Collapse of Maya Civilization. *Science.* 299, 173–175.

Haug, G.H., Günther, D., Sigman, D.M., Hughen, K.A., Aeschlimann, B., 2003. Does climate make History?, *University Potsdam Internal Publication.*

Haug, G.H., Hughen, K.A., Sigman, D.M., Peterson, L.C., Röhl, U., 2001. Southward migration of the intertropical convergence zone through the holocene. *Science.* 293, 1304–1308.

Hernández–García, R., 1973. Paleogeografía del Paleozoico de Chiapas. México *Boletín la Asoc. Mex. Geólogos Pet.* 25, 77–134.

Hershler, R., 1992. A review of the aquatic gastropod subfamily Cochliopinae *(Prosobranchia, Hydrobiidae). Malacological Review.* (Supplement), 5, 1–140.

Higuera-Diaz AE. 1983. *A paleolimnological record of human disturbance in Lakes Atitlan and Ayarza, Guatemala*. MSc Thesis. University of Florida. USA.

Hijmans, R.J., Cameron, S.E., Parra, J.L., Jones, P.G., Jarvis, A., 2005. Very high resolution interpolated climate surfaces for global land areas. *Int. J. Climatol.* 25, 1965–1978.

Hillesheim, M.B., Hodell, D.A., Leyden, B.W., Brenner, M., Curtis, J.H., Anselmetti, F.S., Ariztegui, D., Buck, D.G., Guilderson, T.P., Rosenmeier, M.F., Schnurrenberger, D.W., 2005. Climate change in lowland central America during the late deglacial and early Holocene. *J. Quat. Sci.* 20, 363–376.

Hodell, D., 2011. Drought and the Maya: Maya megadrought? *Nature* 479, 10.

Hodell, D.A., 2001. Solar Forcing of Drought Frequency in the Maya Lowlands. *Science.* 292, 1367–1370.

Hodell, D.A., Anselmetti, F.S., Ariztegui, D., Brenner, M., Curtis, J.H., Gilli, A., Grzesik, D.A., Guilderson, T.J., Müller, A.D., Bush, M.B., Correa-Metrio, A., Escobar, J., Kutterolf, S., 2008. An 85-ka record of climate change in lowland Central America. *Quat. Sci. Rev.* 27, 1152–1165.

Hodell, D.A., Brenner, M., Curtis, J.H., 2007. Climate and cultural history of the Northeastern Yucatan Peninsula, Quintana Roo, Mexico. *Clim. Change* 83, 215–240.

Hodell, D.A., Brenner, M., Curtis, J.H., 2005a. Terminal Classic drought in the northern Maya lowlands inferred from multiple sediment cores in Lake Chichancanab (Mexico). *Quat. Sci. Rev.* 24, 1413–1427.

Hodell, D.A., Brenner, M., Curtis, J.H., Medina-González, R., Ildefonso-Chan Can, E., Albornaz-Pat, A., Guilderson, T.P., 2005b. Climate change on the Yucatan Peninsula during the Little Ice Age. *Quat. Res.* 63, 109–121.

Hodell, D.A., Channeil, J.E.T., Curtis, J.H., Romero, O.E., Röhl, U., 2008. Onset of "Hudson Strait" Heinrich events in the eastern North Atlantic at the end of the middle Pleistocene transition (~640 ka)? *Paleoceanography* 23, 1–16.

Hodell, D. A., Curtis, J.H., Brenner, M.,1995. Possible role of climate in the collapse of Classic Maya civilization. *Nature* 375, 391–375.

Holmes, J.A., 2008. Sample-size implications of the trace-element variability of ostracod shells. *Geochim. Cosmochim. Acta* 72, 2934–2945.

Horta-Puga, G., Carriquiry, J.D., 2012. Coral Ba/Ca molar ratios as a proxy of precipitation in the northern Yucatan Peninsula, Mexico. *Appl. Geochemistry* 27, 1579–1586.

Houston, S.D., Inomata, T., 2009. *The classic Maya*. Cambridge University Press, USA.

Huntington, E., Schuchert, C., Douglass, A.E., Kullmer, C.J., 1914. *The climatic factor as illustrated in arid America*. Carnegie institution of Washington, Washington.

Hurtado-Casas, J.L., 2017. *Apakuway: Llevame dentro de tu corazón*. Global Impresorses E. I. R. L., Cusco, Perú, 112.

Hutchinson, G.E., 1975. *A treatise on limnology / Vol. 1 : Geography, physics, and chemistry. Part 2., Chemistry of lakes*. Wiley-Interscience, USA. 492.

Iannone, G., 2014. *The great Maya droughts in cultural context : case studies in resilience and vulnerability*. University Press of Colorado, USA. 489.

Illescas-Pasquel, F., 1950. Fisicoquimica de las aguas de Yucatan. *Bol. la Soc. Geogr. y Estad.* 205–224.

INEGI, 2010. *México - Censo de Población y Vivienda 2010*. Mexico D. F.

Islebe, G., 2012. Paleoecology of the Yucatan peninsula: palynological evidence of drought during the late Holocene. *Quat. Int.* 279–280, 216–217.

Islebe, G.A., Sanchez, O., 2002. History of Late Holocene vegetation at Quintana Roo, Caribean coast of Mexico. *Plant Ecol.* 160, 187–192.

James, N.P., Jones, B., 2015. Origin of Carbonate Sedimentary Rocks. Wiley, Chichester, UK. 446.

Jamieson, R.A., Baldini, J.U.L., Brett, M.J., Taylor, J., Ridley, H.E., Ottley, C.J., Prufer, K.M., Wassenburg, J.A., Scholz, D., Breitenbach, S.F.M., 2016. Intra- and inter-annual uranium concentration variability in a Belizean stalagmite controlled by prior aragonite precipitation: A new tool for reconstructing hydro-climate using aragonitic speleothems. *Geochim. Cosmochim. Acta* 190, 332–346.

Jarvis, S., 2012. *Optimising, understanding and quantifying Itrax XRF data*. University of Southampton. UK.

Jobbová, E., Helmke, C., Bevan, A., 2018. Ritual responses to drought: An examination of ritual expressions in Classic Maya written sources. *Hum. Ecol.* 46, 759–781.

Johnson, S.A.J., 2013. Translating Maya Hieroglyphs. University of Oklahoma Press, USA. 386.

Johnstone, D., 2015. Ceramic Exchange in the Cochuah Region, in: Justine M. Shaw (Ed.), *The Maya of the Cochuah Region: Archaeological and Ethnographic Perspectives on the Northern Lowlands*. University of New Mexico Press, U. S. A., pp. 41–56.

Jones, J., 1994. Pollen evidence for early settlement and agriculture in Northern Belize. *Palynology* 18, 205–211.

Jones, J.G., 1994. Agriculture in Northern Belize. *Palynology* 18, 205–211.

Jones, M.D., Leng, M.J., Eastwood, W.J., Keen, D.H., Turney, C.S.M., 2002. Interpreting stable-isotope records from freshwater snail-shell carbonate: A Holocene case study from Lake Gölhisar, Turkey. *Holocene* 12, 629–634.

Jones, M.D., Metcalfe, S.E., Davies, S.J., Noren, A., 2015. Late Holocene climate reorganisation and the North American Monsoon. *Quat. Sci. Rev.* 124, 290–295.

Joo-Chang, J.C., Islebe, G.A., Torrescano-Valle, N., 2015. Mangrove history during middle- and late-Holocene in Pacific south-eastern Mexico. *Holocene* 25, 651–662.

Jürgen Schwoerbel HB. 2010. *Einführung in Die Limnologie*. Augsburg: Spektrum akademische verlag. 1st ed. 340.

Kappas, M., 2009. Klimatologie : Klimaforschung im 21. Jahrhundert - Herausforderung für Natur- und Sozialwissenschaften. *Spektrum Akademischer Verlag*, Heidelberg.

Kardashev, N.S., 1964. Transmission of Information by Extraterrestrial Civilizations. *Sov. Astron.* 8, 217.

Kaufman, T., 1976. Archaeological and linguistic correlations in Mayaland and associated areas of Mesoamerica. *World Archaeol.* 8, 101–18.

Kelts, K., Talbot, M., 1990. Lacustrine Carbonates as Geochemical Archives of Environmental Change and Biotic/Abiotic Interactions, in: Tilzer, M.M., Serruya, C. (Eds.), *Large Lakes: Ecological Structure and Functio*n. Springer Berlin Heidelberg, Berlin, Heidelberg, pp. 288–315.

Kenkmann, T., Schönian, F., 2006. Ries and Chicxulub: Impact craters on Earth provide insights for Martian ejecta blankets. *Meteorit. Planet. Sci.* 41, 1587–1603.

Kennett, D., Edwards, L., Cities, T., Yaeger, J., Antonio, S., Cave, Y.B., Hodell, D., 2012. Did Pulses of Climate Change Drive The Rise and Fall of the Maya ? Science. 338, 730–731.

Kennett, D.J., Beach, T.P., 2013. Archeological and environmental lessons for the Anthropocene from the Classic Maya collapse. *Anthropocene* 4, 88–100.

Kennett, D.J., Breitenbach, S.F.M., Aquino, V. V, Asmerom, Y., Awe, J., Baldini, J.U.L., Bartlein, P., Culleton, B.J., Ebert, C., Jazwa, C., Macri, M.J., Marwan, N., Polyak, V., Prufer, K.M., Ridley, H.E., Sodemann, H., Winterhalder, B., Haug, G.H., 2012. Development and disintegration of Maya political systems in response to climate change. *Science.* 338, 788–91.

Kirchhoff, P., 1960. Mesoamerica: sus límites geográficos, composición étnica y caracteres culturales. ENAH, México. 107

Konfirst, M.A., Kuhn, G., Monien, D., Scherer, R.P., 2011. Correlation of Early Pliocene diatomite to low amplitude Milankovitch cycles in the ANDRILL AND-1B drill core. Mar. *Micropaleontol.* 80, 114–124.

Krause, S., Beach, T., Luzzadder-Beach, Cook, D., Islebe, G., Palacios-Fest, M.R., Eshleman, S., Doyle, C., Guderjan, T.H., 2019. Wetland geomorphology and paleoecology near Akab Muclil, Rio Bravo floodplain of the Belize coastal plain. *Geomorphology* 331, 146–159.

Krishna, K., 2009. A Simplified and Rapid Method for the Determination of Sulphur in Kimberlites and Other Geological Samples by WD-XRF Spectrometry. *At. Spectrosc.* 30, 178–183.

Kylander, M.E., Lind, E.M., Wastegård, S., Löwemark, L., 2012. Recommendations for using XRF core scanning as a tool in tephrochronology. *Holocene* 22, 371–375.

Lachniet, M.S., 2015. Are aragonite stalagmites reliable paleoclimate proxies? Tests for oxygen isotope time-series replication and equilibrium. *Bull. Geol. Soc. Am.* 127, 1521–1533.

Lachniet, M.S., Asmerom, Y., Polyak, V., Bernal, J.P., 2017. Two millennia of Mesoamerican monsoon variability driven by Pacific and Atlantic synergistic forcing. *Quat. Sci. Rev.* 155, 100–113.

Lachniet, M.S., Bernal, J.P., Asmerom, Y., Polyak, V., Piperno, D., 2012. A 2400 yr Mesoamerican rainfall reconstruction links climate and cultural change. *Geology* 40, 259–262.

Lachniet, M.S., Burns, S.J., Piperno, D.R., Asmerom, Y., Polyak, V.J., Moy, C.M., Christenson, K., 2004. A 1500-year El Niño/Southern Oscillation and rainfall history for the Isthmus of Panama from speleothem calcite. *J. Geophys. Res. D Atmos.* 109, 1–8.

Lachniet, M.S., Patterson, W.P., 2009. Oxygen isotope values of precipitation and surface waters in northern Central America (Belize and Guatemala) are dominated by temperature and amount effects. *Earth Planet. Sci. Lett.* 284, 435–446.

Lamb, H.H., 1982. *Climate, History and the Modern World*, 1st ed. Roudledge, London. 464.

Lases-Hernandez, F., Medina-Elizalde, M., Burns, S., DeCesare, M., 2019. Long-term monitoring of drip water and groundwater stable isotopic variability in the Yucatán Peninsula: Implications for recharge and speleothem rainfall reconstruction. *Geochim. Cosmochim. Acta* 246, 41–59.

Lechleitner, F.A., McIntyre, C., Jamieson, R.A., Breitenbach, S.F.M., Polyak, V.J., Asmerom, Y., Prufeir, K.M., Culleton, B.J., Kennett, D.J., Baldini, J.U.L., Eglinton, T.I., 2015. Late Holocene 14C variations recorded by a speleothem from Yok Balum Cave, Belize. *Goldschmidt 2014* (January) 2015.

Leng, M.J., Lamb, A.L., Lamb, H.F., Telford, R.J., 1999. Palaeoclimatic implications of isotopic data from modern and early Holocene shells of the freshwater snail Melanoides tuberculata, from lakes in the Ethiopian Rift Valley. *J. Paleolimnol.* 21, 97–106.

Leng, M.J., Marshall, J.D., 2004. Palaeoclimate interpretation of stable isotope data from lake sediment archives. *Quat. Sci. Rev.* 23, 811–831.

Leyden, B.W., 2002. Pollen evidence for climatic variability and cultural disturbance i the Maya Lowlands. Anc. Mesoamerica 13, 85–101. Leyden, B.W., 1987a. Man and Climate in the Maya Lowlands. *Quat. Res.* 414, 407–414.

Leyden, B.W., 1987b. Man and climate in the Maya lowlands. *Quat. Res.* 28, 407–414.

Leyden, B.W., 1984. Guatemalan forest synthesis after Pleistocene aridity. Proc. Natl. Acad. Sci. U. S. A. 81, 4856–4859.

Leyden, B.W., Brenner, M., Dahlin, B.H., 1998. Cultural and Climatic History of Coba, a Lowland Maya City in Quintana Roo, Mexico. *Quat. Res.* 122, 111–122.

Leyden, B.W., Brenner, M., Hodell, D.A., Curtis, J.H., 1993. Late Pleistocene Climate in the Central American Lowlands. *Clim. Chang. Cont. Isot. Rec. Geophys. Monogr.* 78, 165–178.

Li, H.C., Ku, T.L., 1997. $\delta^{13}C$-$\delta^{18}O$ covariance as a paleohydrological indicator for closed-basin lakes. *Palaeogeogr. Palaeoclimatol. Palaeoecol.* 133, 69–80.

Lowe, J.W.G., 1985. *The Dynamics of Apocalypse: A Systems Simulation of the Classic Maya Collapse*. University of New Mexico Press, USA.

Lozano, S., Roy, P.D., Luna-Gonzales, L., Metrio, Y.A.C., Colaboradores:, A., Miranda, M.E.C., Beltrán, J.D.C., Figueroa-Rangel, B.L., Islebe, G.A., González, L.L., Díaz, J.V., 2015. Capítulo 5 Registros Paleoclimàticos, in: *Reporte Mexicano de Cambio Climàtico. Bases Cientìficas. Modelos y Modelaciòn.* Mexico City, Mexico, pp. 113–130.

Lugo-Hubp, J., 1990. El relieve de la republica mexicana. Rev. Mex. Ciencias Geol. 9, 82–111.

Mächtle, B., 2007. *Geomorphologisch-bodenkundliche Untersuchungen zur Rekonstruktion der holozänen Umweltgeschichte in der nördlichen Atacama im Raum Palpa/Südperu.* Heidelberger Geogr. Arb. 123.

Macías, J.L., 2005. Geología e historia eruptiva de algunos de los grandes volcanes activos de México. *Boletín la Soc. Geológica Mex.* 57, 379–424.

Magaña, V., Amador, J.A., Medina, S., Magaña, V., Amador, J.A., Medina, S., 1999. The Midsummer Drought over Mexico and Central America. *J. Clim.* 12, 1577–1588.

Marchant, R., Hooghiemstra, H., Islebe, G., 2004. The Rise and Fall of Peruvian and Central American Civilizations: Interconnections with Holocene Climatic Change - A Necessarily Complex Model. *Monsoon Civiliz.* 351–376.

Martin, S., Grube, N., 2000. *Chronicle of the Maya kings and queens : deciphering the dynasties of the ancient Maya.* Thames & Hudson, USA.

Mayewski, P.A., Rohling, E.E., Stager, J.C., Karlén, W., Maasch, K.A., Meeker, L.D., Meyerson, E.A., Gasse, F., van Kreveld, S., Holmgren, K., Lee-Thorp, J., Rosqvist, G., Rack, F., Staubwasser, M., Schneider, R.R., Steig, E.J., 2004. Holocene climate variability. *Quat. Res.* 62, 243–255.

Mcanany, P.A., Yoffee, N., 2010. Why we question collapse and study human resilience, ecological vulnerability, and the aftermath of empire, in: Mcanany, P.A., Yoffee, N. (Eds.), *Questioning Collape; Human Resilence, Ecological Vulnerability, and the Aftermath of Empire.* Cambridge University Press, New York, pp. 1–17.

McCormick, M., Büntgen, U., Cane, M.A., Cook, E.R., Harper, K., Huybers, P., Litt, T., Manning, S.W., Mayewski, P.A., More, A.F.M., Nicolussi, K., Tegel, W., 2012. Climate change during and after the Roman Empire: Reconstructing the past from scientific and historical evidence. *J. Interdiscip. Hist.* 43, 169–220.

McDougall, I., Brown, F.H., Fleagle, J.G., 2005. Stratigraphic placement and age of modern humans from Kibish, Ethiopia. *Nature* 433, 733–6.

McKillop, H.I., 2004. *The ancient Maya : new perspectives*. Norton & Company, New York.

Medina-Elizalde, M., Burns, S.J., Lea, D.W., Asmerom, Y., von Gunten, L., Polyak, V., Vuille, M., Karmalkar, A., 2010. High resolution stalagmite climate record from the Yucatán Peninsula spanning the Maya terminal classic period. *Earth Planet. Sci.* Lett. 298, 255–262.

Medina-Elizalde, M., Burns, S.J., Polanco-Martínez, J.M., Beach, T., Lases-Hernández, F., Shen, C.C., Wang, H.C., 2016a. High-resolution speleothem record of precipitation from the Yucatan Peninsula spanning the Maya Preclassic Period. Glob. Planet. Change 138, 93–102.

Medina-Elizalde, M., Polanco-Martínez, J.M., Lases-Hernández, F., Bradley, R., Burns, S., 2016b. Testing the "tropical storm" hypothesis of Yucatan Peninsula climate variability during the Maya Terminal Classic Period. *Quat. Res.* 86, 111–119.

Medina-Elizalde and, M., Rohling, E.J., 2012. Collapse of classic Maya civilization related to modest reduction in precipitation. *Science* 335 (6071), 956-959.

Metcalfe, S.E.., 2018. Water Isotope Composition in North Yucatan. *Unpublished raw data.*

Metcalfe, S.E., Barron, J.A., Davies, S.J., 2015. The Holocene history of the North American Monsoon: "known knowns" and "known unknowns" in understanding its spatial and temporal complexity. *Quat. Sci. Rev.* 120, 1–27.

Metcalfe, S.E., Breen, A., Murray, M., Furley, P., Fallick, A., McKenzie, A., 2009. Environmental change in northern Belize since the latest Pleistocene. *J. Quat.Sci.* 24, 627–641.

Metcalfe, S.E., O'Hara, S.L., Caballero, M., Davies, S.J., 2000. Records of Late Pleistocene-Holocene climatic change in Mexico - A review. *Quat. Sci. Rev.* 19, 699–721.

Michels, J.W., 1979. *The Kaminaljuyu Chiefdom, Monograph series on Kaminaljuyu.* Pennsylvania State University Press, USA.

Mills, K., Schillereff, D., Saulnier-Talbot, É., Gell, P., Anderson, N.J., Arnaud, F., Dong, X., Jones, M., McGowan, S., Massaferro, J., Moorhouse, H., Perez, L., Ryves, D.B., 2017. Deciphering long-term records of natural variability and human impact as recorded in lake sediments: a palaeolimnological puzzle. Wiley Interdiscip. *Rev. Water* 4, e1195.

Moholy-Nagy, H., 2003. The Hiatus at Tikal, Guatemala. *Anc. Mesoamerica* 14, 77–83.

Molina-Solís, J.F., 1896. *Historia del descubrimiento y conquista de Yucatán*. Caballero, Merida, Yucatán.

Montero-Serrano, J.C., Bout-Roumazeilles, V., Carlson, A.E., Tribovillard, N., Bory, A., Meunier, G., Sionneau, T., Flower, B.P., Martinez, P., Billy, I., Riboulleau, A., 2011. Contrasting rainfall patterns over North America during the Holocene and Last Interglacial as recorded by sediments of the northern Gulf of Mexico. *Geophys. Res. Lett.* 38, 1–6.

Moorhouse, H.L., McGowan, S., Taranu, Z.E., Gregory-Eaves, I., Leavitt, P.R., Jones, M.D., Barker, P., Brayshaw, S.A., 2018. Regional versus local drivers of water quality in the Windermere catchment, Lake District, United Kingdom: The dominant influence of wastewater pollution over the past 200 years. *Glob. Chang. Biol.* 24, 4009–4022.

Mora, J.C., Gardner, J.E., Macías, J.L., Meriggi, L., Santo, A.P., 2013. Magmatic controls on eruption dynamics of the 1950yrB.P. eruption of San Antonio Volcano, Tacaná Volcanic Complex, Mexico-Guatemala. *J. Volcanol. Geotherm. Res.* 262, 134–152.

Morán Zenteno, D.J., 1988. *Geología de la República Mexicana,* 1st. ed. UNAM-INEGI, Mexico, D. F.

Moreno-Estrada, A., Gignoux, C.R., Fernández-López, J.C., Zakharia, F., Sikora, M., Contreras, A. V., Acuña-Alonzo, V., Sandoval, K., Eng, C., Romero-Hidalgo, S., Ortiz-Tello, P., Robles, V., Kenny, E.E., Nuño-Arana, I., Barquera-Lozano, R., Macín-Pérez, G., Granados-Arriola, J., Huntsman, S., Galanter, J.M., Via, M., Ford, J.G., Chapela, R., Rodriguez-Cintron, W., Rodríguez-Santana, J.R., Romieu, I., Sienra-Monge, J.J., Del Rio Navarro, B., London, S.J., Ruiz-Linares, A., Garcia-Herrera, R., Estrada, K., Hidalgo-Miranda, A., Jimenez-Sanchez, G., Carnevale, A., Soberón, X., Canizales-Quinteros, S., Rangel-Villalobos, H., Silva-Zolezzi, I., Burchard, E.G., Bustamante, C.D., 2014. The genetics of Mexico recapitulates Native American substructure and affects biomedical traits. *Science.* 344, 1280–1285.

Morley, S.G., 1946. The Ancient Maya. Standford University Press, Stanford.

Mortimer, G.E., McCulloch, M.T., Kinsley, L.P.J., Esat, T.M., 2002. High precision 234U-230Th dating using MC-ICP-MS. *Geochim. Cosmochim. Acta.* 66 66, 527.

Mosiño-Alemán, P.A., García-Acosta., E., 1974. *The climate of Mexico.* World Surv. Climatol. 551. 67.

Mueller, A.D., Anselmetti, F.S., Ariztegui, D., Brenner, M., Hillesheim, M.B., Hodell, D.A., Mc Kenzie, J.A., 2008. Human-Climate-Environment interactions in the Maya Lowlands: Evidence from Lake Petén Itzá (Guatemala). *Quat. Res.* 71, 133–141.

Mueller, A.D., Islebe, G.A., Anselmetti, F.S., Ariztegui, D., Brenner, M., Hodell, D.A., Hajdas, I., Hamann, Y., Haug, G.H., Kennett, D.J., 2010. Recovery of the forest ecosystem in the tropical lowlands of northern Guatemala after disintegration of classic Maya polities. *Geology* 38, 523–526.

Mueller, A.D., Islebe, G.A., Hillesheim, M.B., Grzesik, D.A., Anselmetti, F.S., Ariztegui, D., Brenner, M., Curtis, J.H., Hodell, D.A., Venz, K.A., 2009. Climate drying and associated forest decline in the lowlands of northern Guatemala during the late Holocene. *Quat. Res.* 71, 133–141.

Navarrete, C., 2007. El Complejo Escénico De Chinkultic, Chiapas, in: Laporte, J.P., Arroyo, B., Mejía, H. (Eds.), *XX Simposio de Investigaciones Arqueológicas En Guatemala.* Museo Nacional de Arqueología y Etnología, Guatemala, Guatemala, pp. 987–1006.

Navarrete, C., 2001. Arqueología de los Altos Orientales de Chiapas. Arqueol. Mex. 32–37.

Navarrete, C., 1966. *The Chiapanec History and Culture.* Utah, New World Archaeological Foundation, Brigham Young University, USA.

Navarro, A.G., 2008. El Culto De Kukulcán Em *Chichén Itzá : Interaçoes Cult. e Comunidade* 3, 115–131.

Neff, H., Pearsall, D.M., Jones, J.G., Arroyo de Pieters, B., Freidel, D.E., 2006. Climate change and population history in the Pacific Lowlands of Southern Mesoamerica. *Quat. Res.* 65, 390–400.

Newhall, C.G., Paull, C.K., Bradbury, J.P., Higuera-Gundy, A., Poppe, L.J., Self, S., Bonar Sharpless, N., Ziagos, J., 1987. Recent geologic history of lake Atitlán, a caldera lake in western Guatemala. *J. Volcanol. Geotherm. Res.* 33, 81–107.

Newhall, C.G., Self, S., 1982. The volcanic explosivity index (VEI): an estimate of explosive magnitude for historical volcanism. *J. Geophys. Res.* 87, 123–1238.

Nichols, D.L., Pool, C.A., 2012. The Oxford Handbook of Mesoamerican Archaeology. Oxford University Press, UK. 931.

Nooren K, Hoek WZ, Dermody BJ, Galop D, Metcalfe S, Islebe, G., Middelkoop, H. 2018. Climate impact on the development of Pre-Classic Maya civilisation. *Clim. Past.* 14(8):1253–73.

Nooren K. 2017. *Holocene evolution of the Tabasco delta - Mexico*. University of Utrecht. PhD Thesis. 172.

Nygard, T., Spencer, K., Wren, L., 2015. Contemplating Carvings at theFeet of Queen Chaak kab, in: Justine M. Shaw (Ed.), *The Maya of the Cochuah Region: Archaeological and Ethnographic Perspectives on the Northern Lowlands*. University of New Mexico Press, U. S. A., pp. 57–76.

Oseguera, L.A., Alcocer, J., 2015. Concentración y distribución vertical de la clorofila-a fitoplanctónica en los lagos de Montebello, Chiapas, in: *Estado Actual Del Conocimiento Del Ciclo Del Carbono y Sus Interacciones En México: Síntesis a 2015*. Programa Mexicano del Carbono en colaboración con el Centro del Cambio Global y la Sustentabilidad en el Sureste, A.C y el Centro Internacional de Vinculación y Enseñanza de la Universidad Juárez Autónoma de Tabasco, Texcoco, Estado de México, p. 678.

Palemón-Arcos, L., Gómez-Arredondo, C.M., Damas-Llópez, D.A., Chávez-Hernández, G., Gutiérrez-Can, Y., Hernández-Hernández, M.A., Bojórquez, E., Barrera-Lao, F., 2020. Subsoil seismic characterization through Vs30 for future structural assessment of buildings (Ciudad del Carmen , Mexico). *Nat. Hazards Earth Syst. Sci.* 1–24.

Palomino, L.M., García, L.A., Ramos, Y.R., Bonifaz, R., Escolero, O., 2017. Description of Chemical Changes in a Large Karstic System: Montebello, Mexico. *Procedia Earth Planet. Sci.* 17, 829–832.

Paoli Bolio, F.J., 2015. *La Guerra de Castas en Yucatán*. Editorial Dante, Mérida.

Pendergast, D.M., 1986. Stability through Change: Lamanai, Belize, from the ninth to the seventeenth century. Late Lowl. *Maya Civiliz. Class. to Postclassic* 223–249.

Pérez-Ceballos, R., Pacheco-Ávila, J., Euán-Ávila, J.I., Hernández-Arana, H., 2012. Regionalization based on water chemistry and physicochemical traits in the ring of Cenotes, Yucatan, Mexico. *J. Cave Karst Stud.* 74, 90–102.

Perez-Gil, R., 1991. Lacandonia controvertida y amenazada, in: Bolivar, A. (Ed.), *Lacandonia, El Último Refugio*. UNAM, Mexico D. F., pp. 126–137.

Pérez Domínguez, M., Savarino Roggero, F., Ramírez Carrillo, L.A., 2001. *El cultivo de las élites : grupos económcos y políticos en Yucatán en los siglos XIX y XX*. CONACULTA, México D. F.

Pérez, L., Curtis, J., Brenner, M., Hodell, D., Escobar, J., Lozano, S., Schwal, A., 2013. Stable isotope values ($\delta^{18}O$ & $\delta^{13}C$) of multiple ostracode species in a large neotropical lake as indicators of past changes in hydrology. *Quat. Sci. Rev.* 66, 96–111.

Perry, E., Paytan, A., Pedersen, B., Velazquez-Oliman, G., 2009. Groundwater geochemistry of the Yucatan Peninsula, Mexico: Constraints on stratigraphy and hydrogeology. *J. Hydrol.* 367, 27–40.

Perry, E., Velazquesz-Oliman, G., Socki, R., 2003. Hydrogeology of the Yucatán Peninsula. *Limnol. Oceanogr.* 47, 1808–1818.

Perry, E., Velazquez-Oliman, G., Marin, L., 2002. The Hydrogeochemistry of the Karst Aquifer System of the Northern Yucatan Peninsula, Mexico. *Int. Geol. Rev.* 44, 191–221.

Peterson, L.C., Haug, G.H., 2006. 150 Jahre Trockenheit. *Spektrum der Wiss.* Januar 200, 42–48.

Phillips, C., Jones, D.M., 2009. *The illustrated encyclopedia of Aztec & Maya : the history, legend, myth and culture of the ancient native peoples of Mexico and Central America.* Hermes House, China.

Pilsbry, H.A., 1890. Academy of Natural Sciences Land and Fresh-Water Mollusks Collected in Yucatan and Mexico Published by : Academy of Natural Sciences. *Proc. Acad. Nat. Sci. Philadelphia* 43, 310–334.

Pohl, M.D., Pope, K.O., Jones, J.G., Jacob, J.S., Piperno, D.R., Susan, D., Lentz, D.L., Gifford, J. a, Danforth, M.E., Kathryn, J., Latin, S., Antiquity, A., Dec, N., Pohl, M.D., Pope, K., Jones, J.G., Jacob, J.S., Piperno, D.R., Susan, D., Lentz, D.L., Gifford, J. a, Danforth, M.E., Josserand, J.K., 1996. Early Agriculture in the Maya Lowlands *J. Lat. Am. Antiq.* 7, 355–372.

Polk, J.S., van Beynen, P.E., Reeder, P.P., 2007a. Late Holocene environmental reconstruction using cave sediments from Belize. *Quat. Res.* 68, 53–63.

Polk, J.S., van Beynen, P.E., Reeder, P.P., 2007b. Late Holocene environmental reconstruction using cave sediments from Belize. *Quat. Res.* 68, 53–63.

Pollock, A.L., van Beynen, P.E., DeLong, K.L., Polyak, V., Asmerom, Y., Reeder, P.P., 2016. A mid-Holocene paleoprecipitation record from Belize. *Palaeogeogr. Palaeoclimatol. Palaeoecol.* 463, 103–111.

Poppe, L.J., Paull, C.K., Newhall, C.G., Bradbury, J.P., Ziagos, J., 1985. A Geophysical and Geological Study of Laguna de Ayarza, A Guatemalan Caldera lake. J. *Volcanology and Geothermal Research* 25, 125–144.

Primmer N. 2019. *Reconstructing high resolution environmental change from carbonate-rich lakes in Turkey and Mexico using varve microfacies analysis*. PhD Thesis. University of Nottingham. UK. 365.

Railsback LB. 2003. An earth scientist's periodic table of the elements and their ions. *Geology*. 31(9): 737–40

Ramos, E.L., 1975. Geological Summary of the Yucatan Peninsula, in: Nairn, A.E.M., Stehli, F.G (Eds.), *The Gulf of Mexico and the Caribbean*. Springer US, Boston, MA, pp. 257–282.

Ravansari, R., Wilson, S.C., Tighe, M., 2020. Portable X-ray fluorescence for environmental assessment of soils : Not just a point and shoot method. *Environ. Int.* 134, 105250.

Reynolds, G.L., Hamilton-Taylor, J., 1992. The role of planktonic algae in the cycling of Zn and Cu in a productive sof-water lake. *Limnology* 37, 1759–1769.

Rice, D., Rice, M., Deevey, E.S., 1983. El impacto de los mayas en el ambiente tropical de la cuenca de los lagos Yaxha. *Am. Antig.* 43, 1–2.

Rice, M., Rice, D.S., 1984. La época postclásica en la región de los lagos de El Peten central, Guatemala. *Mesoamerica* 5, 334–350.

Rice, P.M., Rice, D.S. (Don S., 2009. *The Kowoj : identity, migration, and geopolitics in late postclassic Petén, Guatemala*. University Press of Colorado, Boulder, Colorado, USA. 458.

Ridley, H.E., 2014. *Recent Central American and low latitude climate variability revealed using speleothem-based rainfall proxy records from southern Belize*. PhD Thesis. University of Durham. 214.

Ridley, H.E., Baldini, J.U.L., Prufer, K.M., Walczak, I.W., Breitenbach, S.F.M., 2015. High-resolution monitoring of Yok Balum Cave, Belize: An investigation of seasonal ventilation regimes and the atmospheric and drip-flow response to a local earthquake. *J. Cave Karst Stud.* 77, 183–199.

Riese B. 2006. *Die Maya : Geschichte - Kultur - Religion*. Beck. 128.

Roberts, N., Allcock, S.L., Arnaud, F., Dean, J.R., Eastwood, W.J., Jones, M.D., Leng, M.J., Metcalfe, S.E., Malet, E., Woodbridge, J., 2016. A tale of two lakes : a multi-proxy comparison of Lateglacial and Holocene environmental change in Cappadocia , Turkey. *J. Quat. Sci.* 31, 348–362.

Roberts N. 1998. *The Holocene: An Environmental History*. Sussex, UK: Wiley. 364.

Roman, S., Palmer, E., Brede, M., 2018. The Dynamics of Human–Environment Interactions in the Collapse of the Classic Maya. *Ecol. Econ.* 146, 312–324.

Rosenmeier, M.F., Brenner, M., Hodell, D.A., Martin, J.B., Curtis, J.H., Binford, M.W., 2016. A model of the 4000-year paleohydrology ($\delta^{18}O$) record from Lake Salpetén, Guatemala. *Glob. Planet. Change* 138, 43–55.

Rosenmeier, M.F., Hodell, D.A., Brenner, M., Curtis, J.H., Guilderson, T.P., 2002a. A 4000-year lacustrine record of environmental change in the southern Maya lowlands, Petén, Guatemala. *Quat. Res.* 57, 183–190.

Rosenmeier, M.F., Hodell, D.A., Brenner, M., Curtis, J.H., Martin, J.B., Anselmetti, F.S., Ariztegui, D., Guilderson, T.P., 2002b. Influence of vegetation change on watershed hydrology: Implications for paleoclimatic interpretation of lacustrine $\delta^{18}O$ records. *J. Paleolimnol.* 27, 117–131.

Roy, P.D., Torrescano-Valle, N., Del Socorro Escarraga-Paredes, D., Vela-Pelaez, A.A., Lozano-Santacruz, R., 2018. Comparison of elemental concentration in near-surface late holocene sediments and precipitation regimes of the yucatán peninsula (Mexico): A preliminary study. *Bol. Geol. y Min.* 129, 693–706.

Ruiz-Suárez, L.G., Núñez, X.C., 2004. *Los gases de efecto invernadero y sus emisiones en México, Cambio climático una visión desde México.* Instituto de Ecología. UNAM, México D. F.

Rushton EAC. 2014. *'Under the shade I flourish': An environmental history of northern Belize over the last three thousand five hundred years*. University of Nottingham. School of Geography. 273.

Ruz, M.H., 1992. *Savia india, floración ladina: apuntes para una historia de las fincas comitecas (siglos XVII y XIX).* CENCA, Mexico. 200.

Sabloff, J.A., 1994. *The New Archaeology and the Ancient Maya.* Henry Holt and Co., USA. 193.

Sabloff, J.A., Willey, G.R., 1967. The Collapse of Maya Civilization in the Southern Lowlands: a consideration of History and Process. *Sowthwestern J. Anthopology* 23, 311–336.

Sadava, D.E., Hillis, D.M., Heller, H.C., Berenbaum, M.R., 2011. *Life : the science of biology.* Sinauer Associates, USA.

Santisteban, J.I., Mediavilla, R., Dabrio, C.J., Lo, E., Castan, S., Zapata, M.B.R., Jose, M., 2004. Loss on ignition: a qualitative or quantitative method for organic matter and carbonate mineral content in sediments? ´. *J. Paleolimnol.* 32, 287–299.

Sapper, K., 1931. Klimaänderungen und das alte Mayareich. *Gerlands Beiträge zur Geophys.* 34, 333–353.

Scarborough, V.L., Gallopin, G.G., 1991. A water storage adaptation in the Maya Lowlands. *Science* 251, 658–662.

Schele, L., Freidel, D.A., 1990. *A forest of kings : the untold story of the ancient Maya.* William Morrow and Company, Inc, New York.

Schönwiese, C., 2013. Klimaänderungen: Daten, Analysen, Prognosen. Springer-Verlag, Deutschland.

Schreg, R., 2009. *Wasser im Karst: Mittelalterlicher Wasserbau und die Interaktion von Mensch und Umwelt.* Gesellschaft für Archäologie des Mittelalters und der Neuzeit 21, 17–30.

Schreg, R., Sirocko, F., 2009. 400 – 500 AD - Völkerwanderung und Umweltkrise: Das Ende des römischen Weltreiches, in: Sirocko, F. (Ed.), *Wetter, Klima, Menschheits-Entwicklung.* Theiss, Stuttgart, pp. 150–153.

Schüpbach, S., Kirchgeorg, T., Colombaroli, D., Beffa, G., Radaelli, M., Kehrwald, N.M., Barbante, C., 2015. Combining charcoal sediment and molecular markers to infer a Holocene fire history in the Maya Lowlands of Petén, Guatemala. *Quat. Sci. Rev.* 115, 123–131.

Sedov, S., Solleiro-Rebolledo, E., Fedick, S.L., Gama-Castro, J., Palacios-Mayorga, S., Vallejo Gómez, E., 2007. Soil genesis in relation to landscape evolution and ancient sustainable land use in the northeastern Yucatan Peninsula, Mexico. *Atti della Soc. Toscana di Sci. Nat. Mem. Ser.* A 112, 115–126.

Segura, A., 2017. *Les Mayas des temps anciens.* Hyères, Great Britain. 349.

Sharer, R., Traxler, L., 2005. *The Ancient Maya,* 6th Edition, 6th ed. Stanford University Press. 931.

Sharpe, A.E., Inomata, T., Triadan, D., Burham, M., MacLellan, J., Munson, J., Pinzón, F., 2020. The maya preclassic to classic transition observed through faunal trends from Ceibal, Guatemala, *PLoS ONE.* Vol. 15. 1-42.

Shaw, J.M., 2015a. The Cochuah Region and the CRAS Project, in: Justine M. Shaw (Ed.), *The Maya of the Cochuah Region: Archaeological and Ethnographic Perspectives on the Northern Lowlands.* University of New Mexico Press, U. S. A., pp. 3–24.

Shaw, J.M., 2015b. The problem of Mobility in Estimating the Extent of terminal Classic populations in the Cochuah Region, in: Justine M. Shaw (Ed.), *The Maya of the Cochuah Region: Archaeological and Ethnographic Perspectives on the Northern Lowlands.* University of New Mexico Press, U. S. A., pp. 117–131.

Sherwin, C.M., Baldini, J.U.L., 2011. Cave air and hydrological controls on prior calcite precipitation and stalagmite growth rates: Implications for palaeoclimate reconstructions using speleothems. *Geochim. Cosmochim. Acta* 75, 3915–3929.

Smyth, M.P., Dunning, N.P., Weaver, E.M., van Beynen, P., Zapata, D.O., 2017. The perfect storm: climate change and ancient Maya response in the Puuc Hills region of Yucatán. *Antiquity* 91, 490–509.

Smyth, M.P., Zubrow, E., Dunning, N.P., Weaver, E.M., Slater, J.E., 2011. Exploratory Research into Arctic Climate Change and Ancient Maya Response: Paleoclimate Reconstruction and Archaeological Investigation at the Puuc Region of Yucatan, Mexico. Washington D. C.

Socki, R.A., Perry, E.C., Romanek, C.S., 2002. Stable isotope systematics of two cenotes from the northern Yucatan Peninsula, Mexico. *Limnol. Oceanogr.* 47, 1808–1818.

Sosa, T.S., Cucina, A., Price, T.D., Burton, J.H., Tiesler, V., 2014. Maya coastal production, exchange, life style, and population mobility: a view from the port of Xcambo, Yucatan, Mexico. *Anc. Mesoamerica* 25, 221–238.

Spinden, H.J., 1928. In Quest of Ruined Cities. *Sci. Am.* 138, 108–111.

Stahle, D.W., Burnette, D.J., Diaz, J.V., Heim, R.R., Fye, F.K., Paredes, J.C., Soto, R.A., Cleaveland, M.K., 2012. Pacific and Atlantic influences on Mesoamerican climate over the past millennium. *Clim. Dyn.* 39, 1431–1446.

Stahle, D.W., Diaz, J.V., Burnette, D.J., Paredes, J.C., Heim, R.R., Fye, F.K., Soto, R.A., Therrell, M.D., Cleaveland, M.K., Stahle, D.K., 2011. Major Mesoamerican droughts of the past millennium. *Geophys. Res. Lett.* 38, 2–5.

Stansell, N.D., Steinman, B.A., Lachniet, M.S., Feller, J., Harvey, W., Fernandez, A., Shea, C.J., Price, B., Coenen, J., Boes, M., Perdziola, S., 2020. A lake sediment stable isotope record of late-middle to late Holocene hydroclimate variability in the western Guatemala highlands. *Earth Planet. Sci. Lett.* 542, 116327.

Stephens, J.L., 1854. *Incidents of Travel in Yucatan : volumes 1 & 2.* Arthur Hall, Virtue and Co, London. UK. 725.

Storey, R., Storey, G.R., 2017. *Rome and the Classic Maya: Comparing the Slow Collapse of Civilizations*. Taylor and Francis, Houston.

Sudrys, R., Berger, R., 1979. Lowland Maya radiocarbon dates and the classic Maya collapse. *Nature* 281, 407.

Thompson, J.E.S., 1966. *The rise and fall of Maya civilization*, 2nd ed, The Civilization of the American Indian. Pimlico, USA.

Thompson, L.G., Davis, M.E., Mosley-Thompson, E., 1994. Glacial records of Global climate: A 1500-year tropical ice core record of climate. *Hum. Ecol.* 22, 83–95.

Tokovinine, A., Dumbarton, 2013. *Place and Identity in Classic Maya Narratives*, Academy of Management Review. Sheridan Books, Inc., Dumbarton Oaks. 149.

Toledo, V.M., 1980. Las llu

vias en Mexico. *Nexos* 32, 10–12.

Torrescano-Valle, N., Islebe, G.A., 2015. Holocene paleoecology, climate history and human influence in the southwestern Yucatan Peninsula. *Rev. Palaeobot. Palynol.* 217, 1–8.

Trauth, M., 2007. *Matlab Recipes for Earth Sciences*. Springer Verlag. Springer-Verlag Berlin Heidelberg, Germany.

Turner, J.N., Jones, A.F., Brewer, P.A., Macklin, M.G., Rassner, S.M., 2015. Micro-XRF Applications in Fluvial Sedimentary Environments of Britain and Ireland: Progress and Prospects, in: Croudace, I.Wr., Rothwell, R.G. (Eds.), *Micro XRF Studies of Sediment Cores*. Springer Link, Keynes UK, pp. 227–265.

Urry, J., 2011. Climate Change and Society, in: *Why the Social Sciences Matter*. Palgrave Macmillan, London, pp. 45–59.

Valero-Garcés, B.L., Laird, K.R., Fritz, S.C., Kelts, K., Ito, E., Grimm, E.C., 1997. Holocene Climate in the Northern Great Plains Inferred from Sediment Stratigraphy, Stable Isotopes, Carbonate Geochemistry, Diatoms, and Pollen at Moon Lake, North Dakota. *Quat. Res.* 48, 359–369.

Van West, C.R., Dean, J.S., 2000. Environmental Characteristics of the a.d. 900–1300 Period in the Central Mesa Verde Region. *KIVA* 66, 19–44.

Vargas-Pacheco, E., Arias-Ortiz, T., 2006. The Crocodile and the Cosmos: Itzamkanac, the Place of the Alligator'S House, *Famsi Report*. California.

Vaughan, H.H., Deevey, E.S., Garrett-Jones, S.E., 1985. Pollen stratigraphy of two cores from the Petén Lake District, in: Pohl, M.D. (Ed.), *Prehistoric Lowland Maya Environment and Subsistence Economy*. Harvard University Press, Cambridge, Massachusetts, pp. 73–89.

Vela-Ramirez, E., Solanes-Carraro, M.C., 2000. Costa Sur. Arqueol. Mex. Atlas del Mex. Prehisp. Especial 5, 60–65.

Velez, M.I., Curtis, J.H., Brenner, M., Escobar, J., Leyden, B.W., Popenoe de Hatch, M., 2011. Environmental and cultural changes in highland Guatemala inferred from Lake Amatitlán sediments. *Geoarchaeology* 26, 346–364.

Vera-Franco, M.N., Hernández-Victoria, P.P., Alcocer, J., Ardiles-Gloria, V., Oseguera, L.A., 2016. Concentración y distribución vertical de la clorofila-a fitoplanctónica en los lagos de Montebello, Chiapas. *Tendencias Investig. en Limnol. Trop. Conc.* 55.

Villaseñor, I., Graham, E., 2010. The use of volcanic materials for the manufacture of pozzolanic plasters in the Maya lowlands: A preliminary report. *J. Archaeol. Sci.* 37, 1339–1347.

Vimeux, F., Sylvestre, F., Khodri, M. (Eds.), 2009. *Past Climate Variability in South America and Surrounding Regions, Developments in Paleoenvironmental Research*. Springer Netherlands, Dordrecht.

Vivo-Escoto, J.A., 1964. Weather and Climate of Mexico and Central america, in: Robert Wauchope, Robert C. West (Eds.), *Handbook of Middle American Indians, Volume 1: Natural Environment and Early*. University of Texas Press, USA, p. 590.

Wahl, D., Anderson, L., Estrada-Belli, F., Tokovinine, A., 2019. Palaeoenvironmental, epigraphic and archaeological evidence of total warfare among the Classic Maya. *Nat. Hum. Behav.* 3, 1049–1054.

Wahl, D., Byrne, R., Anderson, L., 2014. An 8700 year paleoclimate reconstruction from the southern Maya lowlands. *Quat. Sci. Rev.* 103, 19–25.

Wahl, D., Estrada-Belli, F., Anderson, L., 2013. A 3400 year paleolimnological record of prehispanic human-environment interactions in the holmul region of the southern Maya lowlands. Palaeogeogr. Palaeoclimatol. *Palaeoecol.* 379–380, 17–31.

Wahl, D., Hansen, R.D., Byrne, R., Anderson, L., Schreiner, T., 2016. Holocene climate variability and anthropogenic impacts from Lago Paixban , a perennial wetland in Peten , Guatemala. *Glob. Planet. Change* 138, 70–81.

Walsh, M.K., Prufer, K.M., Culleton, B.J., Kennett, D.J., 2014. A late Holocene paleoenvironmental reconstruction from Agua Caliente, southern Belize, linked to regional climate variability and cultural change at the Maya polity of Uxbenká. *Quat. Res.* 82, 38–50.

Wassenaar, L.I., Van Wilgenburg, S.L., Larson, K., Hobson, K.A., 2009. A groundwater isoscape (δD, $\delta^{18}O$) for Mexico. *J. Geochemical Explor.* 102, 123–136.

Waters, M.R., 2019. Late Pleistocene exploration and settlement of the Americas by modern humans. *Science.* 365, 1–9.

Webster, D.L., 2002. *The fall of the ancient Maya : solving the mystery of the Maya collapse.* Thames & Hudson, London. 368.

Webster, J.W., Brook, G.A., Railsback, L.B., Cheng, H., Edwards, R.L., Alexander, C., Reeder, P.P., 2007. Stalagmite evidence from Belize indicating significant droughts at the time of Preclassic Abandonment, the Maya Hiatus, and the Classic Maya collapse. *Palaeogeogr. Palaeoclimatol. Palaeoecol.* 250, 1–17.

Whitmore, T.J., Brenner, M., Curtis, J.H., Dahlin, B.H., Leyden, B.W., 1996. Holocene climatic and human influences on lakes of the Yucatan Peninsula, Mexico: An interdisciplinary, palaeolimnological approach. *Holocene* 6, 273–287.

Wilhelmy, H., 1981. *Welt und Umwelt der Maya. Aufstieg und Untergang einer Hochkultur.* Piper Verlag, München.

Wilk, R.R., 1985. The Ancient Maya and the Political Present. *J. Anthropol. Res.* 41, 307–326.

Winter, A., Zanchettin, D., Lachniet, M., Vieten, R., Pausata, F.S.R., Ljungqvist, F.C., Cheng, H., Edwards, R.L., Miller, T., Rubinetti, S., Rubino, A., Taricco, C., 2020. Initiation of a stable convective hydroclimatic regime in Central America circa 9000 years BP. *Nat. Commun.* 11, 1–8.

Wiseman, F.M., 1985. Agriculture and vegetation dynamics of the Maya collapse in central Peten, Guatemala. Prehist. Lowl. Maya Environ. *Subsist. Econ.* 77, 63–71.

Wright, L.E., White, C.D., Journal, S., June, N., Wright, L.E., White, C.D., 1996. Human Biology in the Classic Maya Collapse : Evidence from Paleopathology and Paleodiet. *J. World Prehistory* 10, 147–198.

Yancheva, G., Nowaczyk, N.R., Mingram, J., Dulski, P., Schettler, G., Negendank, J.F.W., Liu, J., Sigman, D.M., Peterson, L.C., Haug, G.H., 2007. Influence of the intertropical convergence zone on the East Asian monsoon. *Nature* 445, 74–77.

Young, M.N., Leemans, R., Boumans, R.M.J., Costanza, R., de Vries, B.J.M., Finnigan, J., Svedin, U., Young, D.M., 2007. Group Report: Future Scenarios of Human–Environment Systems, in: Costanza, R., Costanza, R., Graumlich, L., Steffen, W. (Eds.), *Sustainability or Collapse? An Integrated History and Future of People on Earth.* MIT Press, Cambridge, Massachusetts, pp. 447–470.

Zaragosi, S., Bourillet, J.-F., Eynaud, F., Toucanne, S., Denhard, B., Van Toer, A., Lanfumey, V., 2006. The impact of the last European deglaciation on the deep-sea turbidite systems of the Celtic-Armorican margin (Bay of Biscay). *Geo-Marine Lett.* 26, 317–329.

Zárate-Toledo, M.A., 2015. *Tierra, bosque y agua en las lagunas de Montebello: procesos espaciales y disputas por los recursos en Ojo de Agua, Chuapas.* PhD Thesis. Centro de Investigaciones y Estudios Superiores en Antropología Social. CONACYT. 183.

Appendix 1

Statistics supporting the differences in the isotopic composition of shells at different sites in Chichancanab

Statistics test for $\delta^{18}O$ of shells from *Pyrgophorus coronatus* (spinose) from Chichancanab

t-test

Normality Test (Shapiro-Wilk): Passed (P = 0.206)
Equal Variance Test (Brown-Forsythe): Passed (P = 0.580)

Group Name	N	Missing	Mean	Std Dev	SEM
Chi S 1 P. coronatus	5	0	0.37	1.201	0.537
Chi S 2 P. coronatus	2	0	0.161	1.328	0.939
Difference	0.209				

t = 0.203 with 5 degrees of freedom.
95 percent two-tailed confidence interval for difference of means: -2.432 to 2.849
Two-tailed P-value = 0.847
One-tailed P-value = 0.424
Power of performed one-tailed test with alpha = 0.050: 0.071

One Way Analysis of Variance

Normality Test (Shapiro-Wilk): Passed (P = 0.206)
Equal Variance Test (Brown-Forsythe): Passed (P = 0.580)

Group Name	N	Missing	Mean	Std Dev	SEM
Chi S 1 P. coronatus	5	0	0.37	1.201	0.537
Chi S 2 P. coronatus	2	0	0.161	1.328	0.939

Source of Variation	DF	SS	MS	F	P
Between Groups	1	0.0622	0.0622	0.0413	0.847
Residual	5	7.537	1.507		
Total	6	7.6			

Power of performed test with alpha = 0.050: --

Statistics test for $\delta^{13}C$ of shells from *Pyrgophorus coronatus* (spinose) from Chichancanab

t-test

Normality Test (Shapiro-Wilk): Passed (P = 0.118)
Equal Variance Test (Brown-Forsythe): Passed (P = 0.318)

Group Name	N	Missing	Mean	Std Dev	SEM
Chi S 1 P. coronatus	5	0	-2.036	1.96	0.876
Chi S 2 P. coronatus	2	0	-2.805	0.0639	0.0452
Difference	0.769				

t = 0.524 with 5 degrees of freedom.
95 percent two-tailed confidence interval for difference of means: -3.001 to 4.539
Two-tailed P-value = 0.622
One-tailed P-value = 0.311
Power of performed two-tailed test with alpha = 0.050: 0.072

One Way Analysis of Variance

Normality Test (Shapiro-Wilk): Passed (P = 0.118)
Equal Variance Test (Brown-Forsythe): Passed (P = 0.318)

Group Name	N	Missing	Mean	Std Dev	SEM
Chi S 1 P. coronatus	5	0	-2.036	1.96	0.876
Chi S 2 P. coronatus	2	0	-2.805	0.0639	0.0452

Source of Variation	DF	SS	MS	F	P
Between Groups	1	0.845	0.845	0.275	0.622
Residual	5	15.365	3.073		
Total	6	16.21			

Power of performed two-tailed test with alpha = 0.050: 0.072

Statistics test for $\delta^{18}O$ of shells from *Pyrgophorus coronatus* (smooth) from Chichancanab

t-test

Normality Test (Shapiro-Wilk): Failed (P < 0.050)
Alternative test: Rank Sum Test begun
Mann-Whitney Rank Sum Test
Data source: Oxygen in Comparison sites isotopes Chichancanab

Group	N	Missing	Median	25%	75%
Pyrgophorus 1	16	0	1.2	0.667	1.766
Pyrgophorus 4	14	0	1.267	0.422	1.73

Mann-Whitney U Statistic= 111.000
T = 216.000 n(small)= 14 n(big)= 16 (P = 0.983)

One Way Analysis of Variance

Normality Test (Shapiro-Wilk): Failed (P < 0.050)
Alternative test: ANOVA on Ranks begun
Kruskal-Wallis One Way Analysis of Variance on Ranks
Data source: Oxygen in Comparison sites isotopes Chichancanab

Group	N	Missing	Median	25%	75%
Pyrgophorus 1	16	0	1.2	0.667	1.766
Pyrgophorus 4	14	0	1.267	0.422	1.73

H = 0.00173 with 1 degrees of freedom. (P = 0.967)

Statistics test for $\delta^{13}C$ of shells from *Pyrgophorus coronatus* (smooth) from Chichancanab

t-test

Normality Test (Shapiro-Wilk): Failed (P < 0.050)
Alternative test: Rank Sum Test begun
Mann-Whitney Rank Sum Test

Group	N	Missing	Median	25%	75%
Pyrgophorus 1	16	0	-0.867	-1.628	-0.407
Pyrgophorus 4	14	0	-1.074	-1.74	-0.375

Mann-Whitney U Statistic= 106.000
T = 211.000 n(small)= 14 n(big)= 16 (P = 0.819)

One Way Analysis of Variance

Normality Test (Shapiro-Wilk): Failed (P < 0.050)
Alternative test: ANOVA on Ranks begun
Kruskal-Wallis One Way Analysis of Variance on Ranks

Group	N	Missing	Median	25%	75%
Pyrgophorus 1	16	0	-0.867	-1.628	-0.407
Pyrgophorus 4	14	0	-1.074	-1.74	-0.375

H = 0.0622 with 1 degrees of freedom. (P = 0.803)

Statistics test for $\delta^{18}O$ of shells from *Aroapyrgus* sp. from Chichancanab

t-test

Normality Test (Shapiro-Wilk): Passed (P = 0.901)
Equal Variance Test (Brown-Forsythe): Failed (P < 0.050)
Alternative test: Rank Sum Test begun
Mann-Whitney Rank Sum Test Sonntag, Juni 02, 2019, 16:14:08
Data source: Oxygen in Comparison sites isotopes Chichancanab

Group	N	Missing	Median	25%	75%
Aroapyrgus 1	11	0	0.453	-0.192	1.179
Aroapyrgus 4	9	0	1.151	1.015	1.638

Mann-Whitney U Statistic= 21.000
T = 123.000 n(small)= 9 n(big)= 11 (P = 0.033)

One Way Analysis of Variance

Normality Test (Shapiro-Wilk): Passed (P = 0.901)
Equal Variance Test (Brown-Forsythe): Failed (P < 0.050)
Alternative test: ANOVA on Ranks begun
Kruskal-Wallis One Way Analysis of Va Sonntag, Juni 02, 2019, 16:14:48
Data source: Oxygen in Comparison sites isotopes Chichancanab

Group	N	Missing	Median	25%	75%
Aroapyrgus 1	11	0	0.453	-0.192	1.179
Aroapyrgus 4	9	0	1.151	1.015	1.638

H = 4.688 with 1 degrees of freedom. (P = 0.030)

To isolate the group or groups that differ from the others use a multiple comparison
All Pairwise Multiple Comparison Procedures (Dunn's Method) :

Comparison	ff of Ran	Q	P	P<0.050
Aroapyrgus 4 vs Aroapyrgus 1	5.758	2.165	0.03	Yes

Statistics test for $\delta^{13}C$ of shells from *Aroapyrgus* sp. from Chichancanab

t-test

Normality Test (Shapiro-Wilk): Passed (P = 0.723)
Equal Variance Test (Brown-Forsythe): Passed (P = 0.639)

Group Name	N	Missing	Mean	Std Dev	SEM
Aroapyrgus 1	11	0	-1.76	0.922	0.278
Aroapyrgus 4	9	0	-0.841	0.879	0.293
Difference	-0.919				

t = -2.262 with 18 degrees of freedom.
95 percent two-tailed confidence interval for difference of means: -1.772 to -0.0655
Two-tailed P-value = 0.0363
One-tailed P-value = 0.0181
Power of performed two-tailed test with alpha = 0.050: 0.572

One Way Analysis of Variance

Normality Test (Shapiro-Wilk): Passed (P = 0.723)
Equal Variance Test (Brown-Forsythe): Passed (P = 0.639)

Group Name	N	Missing	Mean	Std Dev	SEM
Aroapyrgus 1	11	0	-1.76	0.922	0.278
Aroapyrgus 4	9	0	-0.841	0.879	0.293

Source of Variation	DF	SS	MS	F	P
Between Groups	1	4.178	4.178	5.118	0.036
Residual	18	14.694	0.816		
Total	19	18.871			

Power of performed test with alpha = 0.050: 0.484
All Pairwise Multiple Comparison Procedures (Holm-Sidak method):
Overall significance level = 0.05
Comparisons for factor:

Comparison	f of Mea	t	P	P<0.050
Aroapyrgus 4 vs. Aroapyrgus 1	0.919	2.262	0.036	Yes

Statistics test for $\delta^{18}O$ of shells from *Tryonia* sp. from Chichancanab

t-test

Normality Test (Shapiro-Wilk): Passed (P = 0.570)
Equal Variance Test (Brown-Forsythe): Passed (P = 0.797)

Group Name	N	Missing	Mean	Std Dev	SEM
Tryonia 1	6	0	1.078	1.198	0.489
Tryonia 4	7	0	0.744	1.186	0.448
Difference	0.334				

t = 0.504 with 11 degrees of freedom.
95 percent two-tailed confidence interval for difference of means: -1.125 to 1.793
Two-tailed P-value = 0.624
One-tailed P-value = 0.312
Power of performed two-tailed test with alpha = 0.050: 0.075

One Way Analysis of Variance

Normality Test (Shapiro-Wilk): Passed (P = 0.570)
Equal Variance Test (Brown-Forsythe): Passed (P = 0.797)

Group Name	N	Missing	Mean	Std Dev	SEM
Tryonia 1	6	0	1.078	1.198	0.489
Tryonia 4	7	0	0.744	1.186	0.448

Source of Variation	DF	SS	MS	F	P
Between Groups	1	0.36	0.36	0.254	0.624
Residual	11	15.619	1.42		
Total	12	15.979			

Power of performed test with alpha = 0.050: --

Statistics test for $\delta^{13}C$ of shells from *Tryonia* sp. from Chichancanab

t-test

Normality Test (Shapiro-Wilk): Passed (P = 0.093)
Equal Variance Test (Brown-Forsythe): Passed (P = 0.420)

Group Name	N	Missing	Mean	Std Dev	SEM
Tryonia 1	6	0	-1.437	1.001	0.409
Tryonia 4	7	0	-0.223	0.537	0.203
Difference	-1.214				

t = -2.788 with 11 degrees of freedom.
95 percent two-tailed confidence interval for difference of means: -2.173 to -0.256
Two-tailed P-value = 0.0177
One-tailed P-value = 0.00883
Power of performed two-tailed test with alpha = 0.050: 0.719
Power of performed one-tailed test with alpha = 0.050: 0.833

One Way Analysis of Variance

Normality Test (Shapiro-Wilk): Passed (P = 0.093)
Equal Variance Test (Brown-Forsythe): Passed (P = 0.420)

Group Name	N	Missing	Mean	Std Dev	SEM
Tryonia 1	6	0	-1.437	1.001	0.409
Tryonia 4	7	0	-0.223	0.537	0.203

Source of Variation	DF	SS	MS	F	P
Between Groups	1	4.763	4.763	7.771	0.018
Residual	11	6.742	0.613		

Power of performed test with alpha = 0.050: 0.659
All Pairwise Multiple Comparison Procedures (Holm-Sidak method):
Overall significance level = 0.05
Comparisons for factor:

Comparison	Diff of Means	t	P	P<0.050
Tryonia 4 vs. Tryonia 1	1.214	2.788	0.018	Yes

Appendix 2

Statistics supporting the differences in the isotopic composition of shells at different sites in Lake Esmeralda.

Statistics test for $\delta^{18}O$ of shells from *Pyrgophorus* sp. (smooth) from Esmeralda

t-test

Normality Test (Shapiro-Wilk): Passed (P = 0.123)
Equal Variance Test (Brown-Forsythe): Passed (P = 0.213)

Group Name	N	Missing	Mean	Std Dev	SEM
Pyrgophorus 6	16	0	0.564	1.866	0.467
Pyrgophorus 9	13	1	-0.437	2.231	0.619
Difference	1.001				

t = 1.317 with 27 degrees of freedom.
95 percent two-tailed confidence interval for difference of means: -0.559 to 2.561
Two-tailed P-value = 0.199
One-tailed P-value = 0.0995

One Way Analysis of Variance

Normality Test (Shapiro-Wilk): Passed P = 0.123)
Equal Variance Test (Brown-Forsythe): Passed P = 0.213)

Group Name	N	Missing	Mean	Std Dev	SEM
Pyrgophorus 6	16	0	0.564	1.866	0.467
Pyrgophorus 9	14	1	-0.437	2.231	0.619

Source of Variation	DF	SS	MS	F	P
Between Groups	1	7.187	7.187	1.733	0.199
Residual	27	111.95	4.146		
Total	28	119.14			

Power of performed test with alpha = 0.050: 0.131

Statistics test for $\delta^{13}C$ of shells from *Pyrgophorus* sp. (smooth) from Esmeralda

t-test

Normality Test (Shapiro-Wilk): Passed (P = 0.184)
Equal Variance Test (Brown-Forsythe): Failed (P < 0.050)
Alternative test, Rank Sum Test begun
Mann-Whitney Rank Sum Test
Data source: Carbon in Comparison sites isotopes Esmeralda

Group	N	Missing	Median	25%	75%
Pyrgophorus 6	16	0	-4.646	-6.132	-3.401
Pyrgophorus 9	14	1	-6.288	-6.898	-6.043

Mann-Whitney U Statistic= 35.000
T = 126.000 n(small)= 13 n(big)= 16 (P = 0.003)

One Way Analysis of Variance

Normality Test (Shapiro-Wilk): Passed (P = 0.184)
Equal Variance Test (Brown-Forsythe): Failed (P < 0.050)
Alternative test, ANOVA on Ranks begun
Kruskal-Wallis One Way Analysis of Variance on Ranks
Data source: Carbon in Comparison sites isotopes Esmeralda

Group	N	Missing	Median	25%	75%
Pyrgophorus 6	16	0	-4.646	-6.132	-3.401
Pyrgophorus 9	14	1	-6.288	-6.898	-6.043

H = 9.156 with 1 degrees of freedom. (P = 0.002)
All Pairwise Multiple Comparison Procedures (Dunn's Method) :

Comparison	Diff of Ranks	Q	P	P<0.050
Pyrgophorus 6 vs Pyrgophorus 9	9.62	3.026	0.002	Yes

Statistics test for $\delta^{18}O$ of shells from *Aroapyrgus* sp. from Esmeralda

t-test

t-test

Normality Test (Shapiro-Wilk): Passed (P = 0.583)

Equal Variance Test (Brown-Forsythe): Failed (P < 0.050)

Alternative test: Rank Sum Test begun

Mann-Whitney Rank Sum Test

Group	N	Missing	Median	25%	75%
Aroapyrgus 6	14	0	1.175	-0.051	1.579
Aroapyrgus 9	13	0	-1.626	-3.247	0.823

Mann-Whitney U Statistic= 51.000

T = 142.000 n(small)= 13 n(big)= 14 (P = 0.055)

One Way Analysis of Variance

One Way Analysis of Variance

Normality Test (Shapiro-Wilk): Passed (P = 0.583)

Equal Variance Test (Brown-Forsythe): Failed (P < 0.050)

Alternative test: ANOVA on Ranks begun

Kruskal-Wallis One Way Analysis of Variance on Ranks

Group	N	Missing	Median	25%	75%
Aroapyrgus 6	14	0	1.175	-0.051	1.579
Aroapyrgus 9	13	0	-1.626	-3.247	0.823

H = 3.768 with 1 degrees of freedom. (P = 0.052)

Statistics test for $\delta^{13}C$ of shells from *Aroapyrgus* sp. from Esmeralda

t-test

Normality Test (Shapiro-Wilk): Passed (P = 0.931)

Equal Variance Test (Brown-Forsythe): Failed (P < 0.050)

Alternative test: , Rank Sum Test begun

Mann-Whitney Rank Sum Test

Data source: Carbon in Comparison sites isotopes Esmeralda

Group	N	Missing	Median	25%	75%
Aroapyrgus 6	14	0	-3.852	-4.195	-3.531
Aroapyrgus 9	13	0	-6.716	-7.549	-5.753

Mann-Whitney U Statistic= 1.000

T = 92.000 n(small)= 13 n(big)= 14 (P = <0.001)

One Way Analysis of Variance

Normality Test (Shapiro-Wilk): Passed (P = 0.931)

Equal Variance Test (Brown-Forsythe): Failed (P < 0.050)

Alternative test: ANOVA on Ranks begun

Kruskal-Wallis One Way Analysis of Variance on Ranks

Data source: Carbon in Comparison sites isotopes Esmeralda

Group	N	Missing	Median	25%	75%
Aroapyrgus 6	14	0	-3.852	-4.195	-3.531
Aroapyrgus 9	13	0	-6.716	-7.549	-5.753

H = 19.074 with 1 degrees of freedom. (P = <0.001)

All Pairwise Multiple Comparison Procedures (Dunn's Method) :

Comparison	Diff of R	Q	P	P<0.050
Aroapyrgus 6 vs Aroapyrgus 9	13.352	4.367	<0.001	Yes

Statistics test for $\delta^{18}O$ of shells from *Tryonia* sp. from Esmeralda

t-test

Normality Test (Shapiro-Wilk): Passed (P = 0.268)

Equal Variance Test (Brown-Forsythe): Passed (P = 0.719)

Group Name	N	Missing	Mean	Std Dev	SEM
Tryonia 6	14	0	0.0059	2.487	0.665
Tryonia 9	15	0	-0.234	2.192	0.566
Difference	0.24				

t = 0.276 with 27 degrees of freedom.

Two-tailed P-value = 0.784

One-tailed P-value = 0.392

Power of performed two-tailed test with alpha = 0.050: 0.058

Power of performed one-tailed test with alpha = 0.050: 0.085

One Way Analysis of Variance

Normality Test (Shapiro-Wilk): Passed (P = 0.268)

Equal Variance Test (Brown-Forsythe): Passed (P = 0.719)

Group Name	N	Missing	Mean	Std Dev	SEM
Tryonia 6	14	0	0.0059	2.487	0.665
Tryonia 9	15	0	-0.234	2.192	0.566

Source of Variation	DF	SS	MS	F	P
Between Groups	1	0.418	0.418	0.0764	0.784
Residual	27	147.69	5.47		
Total	28	148.11			

Power of performed test with alpha = 0.050: --

Statistics test for $\delta^{13}C$ of shells from *Tryonia* sp. from Esmeralda

t-test

Normality Test (Shapiro-Wilk): Passed (P = 0.660)

Equal Variance Test (Brown-Forsythe): Failed (P < 0.050)

Alternative test: Rank Sum Test begun

Mann-Whitney Rank Sum Test

Group	N	Missing	Median	25%	75%
Tryonia 6	14	0	-4.636	-5.424	-3.148
Tryonia 9	15	0	-6.499	-7.145	-6.322

Mann-Whitney U Statistic= 5.000

T = 310.000 n(small)= 14 n(big)= 15 (P = <0.001)

One Way Analysis of Variance

Normality Test (Shapiro-Wilk): Passed (P = 0.660)

Equal Variance Test (Brown-Forsythe): Failed (P < 0.050)

Alternative test: ANOVA on Ranks begun

Kruskal-Wallis One Way Analysis of Variance on Ranks

Group	N	Missing	Median	25%	75%
Tryonia 6	14	0	-4.636	-5.424	-3.148
Tryonia 9	15	0	-6.499	-7.145	-6.322

H = 19.048 with 1 degrees of freedom. (P = <0.001)

All Pairwise Multiple Comparison Procedures (Dunn's Method) :

Comparison	Diff of Ranks	Q	P	P<0.050
Tryonia 6 vs Tryonia 9	13.81	4.364	<0.001	Yes

Appendix 3

Statistics supporting the differences in the isotopic composition of shells between lakes Esmeralda and Chichancanab.

Statistics test for $\delta^{18}O$ of shells from *Pyrgophorus coronatus* (smooth) from both lakes

t-test

Normality Test (Shapiro-Wilk):	Failed	(P < 0.050)			
Alternative test, Mann-Whitney Rank begun					
Group	**N**	**Missing**	**Median**	**25%**	**75%**
Chichancanab Pyrgophorus sp.	30	0	1.244	0.578	1.732
Esmeralda Pyrgophorus sp.	29	0	1.1	-1.832	1.699
	0.444				
Mann-Whitney U Statistic= 388.000					
T = 823.000 n(small) = 29 n(big) = 30 (P = 0.481)					

One Way Analysis of Variance

Normality Test (Shapiro-Wilk):	Failed	0.050)			
Alternative test	Wallis				
Group	**N**	**g**	**Media**	**25%**	**75%**
Chichancanab Pyrgophorus sp.	30	0	1.244	0.578	1.732
Esmeralda Pyrgophorus sp.	29	0	1.1	-1.832	1.699
H =	with 1				

Statistics test for $\delta^{13}C$ of shells from *Pyrgophorus coronatus* (smooth) from both lakes

t-test

Data source: Carbon in Comparison lakes isotopes ES-Chi1					
Normality Test (Shapiro-Wilk):	Passed	(P = 0.195)			
Equal Variance Test (Brown-Forsythe):	Passed	(P = 0.065)			
Group Name	**N**	**Missing**	**Mean**	**Dev**	**SEM**
Chichancanab Pyrgophorus sp.	30	0	-1.182	1.096	0.2
Esmeralda Pyrgophorus sp.	**29**	0	-5.37	1.68	0.312
Difference	**4.189**				
t = 11.378 with 57 degrees of freedom.					
95 percent two-tailed confidence interval for difference of					
Two-tailed P-value = 2.684E-016					
One-tailed P-value = 1.342E-016					
Power of performed two-tailed test with alpha = 0.050:					
Power of performed one-tailed test with alpha = 0.050:					

One Way Analysis of Variance

Data source: Carbon in					
Normality Test (Shapiro-Wilk):	Passed	(P =			
Equal Variance Test (Brown-	Passed	(P =			
Group Name	**N**	**Missin**	**Mean**	**Std**	**SEM**
Chichancanab Pyrgophorus sp.	30	0	-1.182	1.096	0.2
Esmeralda Pyrgophorus sp.	29	0	-5.37	1.68	0.312
Source of Variation	**DF**	**SS**	**MS**	**F**	**P**
Between Groups	1	258.7	258.7	129.46	<0.001
Residual	57	113.9	1.998		
Total	58	372.59			
Power of performed test with	alpha =				
All Pairwise Multiple Comparison					
Overall significance level = 0.05					
Comparisons for factor:					
Comparison	**Diff of**	**t**	**P**	**P<0.05**	
Chichancanab vs. Esmeralda	4.189	11.378	<0.001	Yes	

Statistics test for $\delta^{18}O$ of shells from *Pyrgophorus coronatus* (spinose) from both lakes

t-test

t-test					
Normality Test (Shapiro-Wilk):	Passed	(P = 0.697)			
Equal Variance Test (Brown-Forsythe):	Passed	(P = 0.063)			
Group Name	**N**	**Missing**	**Mean**	**Std Dev**	**SEM**
Chichancanab Coronatus	6	0	0.525	1.064	0.434
Esmeralda Coronatus	4	0	0.081	3.246	1.623
Difference	0.444				
t = 0.319 with 8 degrees of freedom.					
95 percent two-tailed confidence interval for difference of means: -2.768 to 3.657					
Two-tailed P-value = 0.758					
One-tailed P-value = 0.379					

One Way Analysis of Variance

One Way Analysis of Variance					
Normality Test (Shapiro-Wilk):	Passed	(P = 0.697)			
Equal Variance Test (Brown-Forsythe):	Passed	(P = 0.063)			
Group Name	**N**	**Missing**	**Mean**	**Std Dev**	**SEM**
Chichancanab Coronatus	6	0	0.525	1.064	0.434
Esmeralda Coronatus	4	0	0.081	3.246	1.623

Source of Variation	**DF**	**SS**	**MS**	**F**	**P**
Between Groups	1	0.474	0.474	0.102	0.758
Residual	8	37.264	4.658		
Total	9	37.738			

Statistics test for $\delta^{13}C$ of shells from *Pyrgophorus coronatus* (spinose) from both lakes

t-test

Normality Test (Shapiro-Wilk):	Passed	(P = 0.250)			
Equal Variance Test (Brown-Forsythe):	Passed	(P = 0.785)			
Group Name	**N**	**Missing**	**Mean**	**Std Dev**	**SEM**
Chichancanab Coronatus	7	0	-2.255	1.644	0.621
Esmeralda Coronatus	4	0	-4.364	1.61	0.805
Difference	2.109				
95 percent two-tailed confidence interval for difference of means: -0.206 to 4.424					
Two-tailed P-value = 0.0694					
One-tailed P-value = 0.0347					

One Way Analysis of Variance

Normality Test (Shapiro-Wilk):	Passed	(P = 0.250)			
Equal Variance Test (Brown-Forsythe):	Passed	(P = 0.785)			
Group Name	**N**	**Missing**	**Mean**	**Std Dev**	**SEM**
Chichancanab Coronatus	7	0	-2.255	1.644	0.621
Esmeralda Coronatus	4	0	-4.364	1.61	0.805

Source of Variation	**DF**	**SS**	**MS**	**F**	**P**
Between Groups	1	11.317	11.317	4.246	0.069
Residual	9	23.991	2.666		
Total	10	35.308			

Power of performed test with alpha = 0.050: 0.364

Statistics test for $\delta^{18}O$ of shells from *Aroapyrgus* sp. from both lakes

t-test

t-test

Normality Test (Shapiro-Wilk): Failed (P < 0.050)

Alternative test, Rank Sum Test begun

Mann-Whitney Rank Sum Test

Group	N	Missing	Median	25%	75%
Chichancanab Aroapyrgus	20	0	1.049	0.276	1.546
Esmeralda Aroapyrgus	27	0	0.607	-1.823	1.388

Mann-Whitney U Statistic= 210.000

T = 540.000 n(small)= 20 n(big)= 27 (P = 0.200)

One Way Analysis of Variance

One Way Analysis of Variance

Normality Test (Shapiro-Wilk): Failed (P < 0.050)

Alternative test, ANOVA on Ranks begun

Kruskal-Wallis One Way Analysis of Variance on Ranks

Group	N	Missing	Median	25%	75%
Chichancanab Aroapyrgus	20	0	1.049	0.276	1.546
Esmeralda Aroapyrgus	27	0	0.607	-1.823	1.388

H = 1.667 with 1 degrees of freedom. (P = 0.197)

Statistics test for $\delta^{13}C$ of shells from *Aroapyrgus* sp. from both lakes

t-test

t-test

Normality Test (Shapiro-Wilk): Passed (P = 0.210)

Equal Variance Test (Brown-For Failed (P < 0.050)

Alternative test, Rank Sum Test begun

Mann-Whitney Rank Sum Test

Group	N	Missing	Median	25%	75%
Chichancanab Aroapyrgus	20	0	-1.206	-2.112	-0.64
Esmeralda Aroapyrgus	27	0	-4.514	-6.716	-3.698

Mann-Whitney U Statistic= 3.000

T = 747.000 n(small)= 20 n(big)= 27 (P = <0.001)

One Way Analysis of Variance

One Way Analysis of Variance

Normality Test (Shapiro-Wilk): Passed (P = 0.210)

Equal Variance Test (Brown-Fors Failed (P < 0.050)

Alternative test, ANOVA on Ranks begun

Kruskal-Wallis One Way Analysis of Variance on Ranks

Group	N	Missing	Median	25%	75%
Chichancanab Aroapyrgus	20	0	-1.206	-2.112	-0.64
Esmeralda Aroapyrgus	27	0	-4.514	-6.716	-3.698

H = 33.004 with 1 degrees of freedom. (P = <0.001)

Statistics test for $\delta^{18}O$ of shells from *Tryonia* sp. from both lakes

t-test

t-test

Normality Test (Shapiro-Wilk):	Passed (P =.161))				
Equal Variance Test (Brown-Forsythe):	Passed (P = 0.226))				
Group Name	**N**	**Missing**	**Mean**	**Std Dev**	**SEM**
Chichancanab Tryonia	13	0	-0.783	0.979	0.272
Esmeralda Tryonia	29	0	-5.568	1.564	0.29
Difference	4.785				

t = 10.136 with 40 degrees of freedom.

95 percent two-tailed confidence interval for difference of means: 3.831 to 5.739

Two-tailed P-value = 1.308E-012

One-tailed P-value = 6.539E-013

One Way Analysis of Variance

One Way Analysis of Variance

Normality Test (Shapiro-Wilk):	Passed (P = 0.371)				
Equal Variance Test (Brown-Forsythe):	Passed (P < 0.05)				
Group Name	**N**	**Missing**	**Mean**	**Std Dev**	**SEM**
Chichancanab Tryonia	13	0	0.769	0.117	2.04
Esmeralda Tryonia	29	0	-0.168	-1.79	1.588

H = 2.040 with 1 degrees of freedom. (P = 0.153)

Statistics test for $\delta^{13}C$ of shells from *Tryonia sp.* from both lakes

t-test

t-test

Normality Test (Shapiro-Wilk):	Passed (P = 0.161)				
Equal Variance Test (Brown-Forsythe):	Passed (P = 0.226)				
Group Name	**N**	**Missing**	**Mean**	**Std Dev**	**SEM**
Chichancanab Tryonia	13	0	-0.783	0.979	0.272
Esmeralda Tryonia	29	0	-5.568	1.564	0.29
Difference	4.785				

t = 10.136 with 40 degrees of freedom.

95 percent two-tailed confidence interval for difference of means: 3.831 to 5.739

Two-tailed P-value = 1.308E-012

One-tailed P-value = 6.539E-013

Power of performed two-tailed test with alpha = 0.050: 1.000

Power of performed one-tailed test with alpha = 0.050: 1.000

One Way Analysis of Variance

One Way Analysis of Variance

Normality Test (Shapiro-Wilk):	Passed (P = 0.161)				
Equal Variance Test (Brown-Forsythe):	Passed (P = 0.226)				
Group Name	**N**	**Missing**	**Mean**	**Std Dev**	**SEM**
Chichancanab Tryonia	13	0	-0.783	0.979	0.272
Esmeralda Tryonia	29	0	-5.568	1.564	0.29

Source of Variation	**DF**	**SS**	**MS**	**F**	**P**
Between Groups	1	205.5	205.5	102.73	<0.001
Residual	40	80.015	2		
Total	41	285.51			

Power of performed test with alpha = 0.050: 1.000

All Pairwise Multiple Comparison Procedures (Holm-Sidak method):

Overall significance level = 0.05

Comparisons for factor:

Comparison	Diff of Mt	P	P<0.050
Chichancanab vs. Esmeralda Tr	4.785	10.136 <0.001	Yes